Restore Lagoon Inflow Research (Phase 3) Project Summary

PREPARED BY

Jeff Eble, Austin Fox,
Robert J. Weaver, and Gary A. Zarillo
Florida Institute of Technology
150 West University Boulevard
Melbourne, FL 32091

Jane Caffrey, Wade Jeffrey & Lisa Waidner
University of West Florida

Olivia Escandell
Brevard Zoo

Richard Paperno
Florida Fish and Wildlife Conservation Commission

Matthew Shelton and Marcy Frick
Tetra Tech, Inc.

Jesse Blanchard
Florida International University

Wendy Noke Durden
Hubbs Sea World Research Institute

Edward Phlips
University of Florida

October 2023

Table of Contents

List of Tables

List of Figures

Acknowledgements

The views, statements, findings, conclusions, and recommendations expressed herein are those of the authors and do not necessarily reflect the views of the State of Florida or any of its sub-agencies.

The photographs on the cover were provided by the Florida Tech Principal Investigators on this project.

List of Acronyms and Abbreviations

amoA	Ammonia monooxidase
AOO	Ammonium oxidizing organisms
BRL	Banana River Lagoon
°C	Degrees Celsius
CBA	Choctawhatchee Basin Alliance
Chl-a	Chlorophyll-a
cm	Centimeter
DIN	Dissolved Inorganic Nitrogen
DNRA	Dissimilatory reduction of nitrate to ammonium
DO	Dissolved Oxygen
DON	Dissolved Organic Nitrogen
DOP	Dissolved Organic Phosphorus
EFDC	Environmental Fluid Dynamics Code
ERP	Environmental Resources Permit
FDEP	Florida Department of Environmental Protection
FIM	Fisheries-Independent Monitoring
Florida Tech	Florida Institute of Technology
FWC	Florida Fish and Wildlife Conservation Commission
FWRI	Fish and Wildlife Research Institute
HAB	Harmful Algal Bloom
HEM3D	Hydrodynamic and Eutrophication Three-Dimensional
HSWRI	Hubbs Sea World Research Institute
IRL	Indian River Lagoon
kg	Kilograms
km	Kilometer
LOBO	Land/Ocean Biogeochemical Observatories
m	Meter
m^2/hr	Square Meter per hour
m^3/sec	Cubic Meters Per Second
mg	Milligrams
mg/L	Milligrams Per Liter
mg/L/hr	Milligrams Per Liter Per Hour
N	Nitrogen
NASA	National Aeronautics and Space Administration
NH_4	Ammonium

NOx	Nitrate + Nitrite
nrfA	Nitrite reductase
P	Phosphorus
PO_4	Orthophosphate
ppt	Parts per thousand
PSU	Practical Salinity Unit
qPCR	qualitative Polymerase Chain Reaction
RAI	Request for Additional Information
RMSE	Root mean square errors
rRNA	Ribosomal Ribonucleic Acid
SiO_2	Silica
SJRWMD	St. Johns River Water Management District
SOD	Sediment Oxygen Demand
SoI	Species of Interest
SRP	Soluble Reactive Phosphorus
SRS	Santa Rosa Sound
TDN	Total Dissolved Nitrogen
TDP	Total Dissolved Phosphorus
TN	Total Nitrogen
TP	Total Phosphorus
µM	Micromolar
UME	Unusual Mortalities Event
µmoles/m^2/hr	Micromoles Per Square Meter Per Hour
USACE	U.S. Army Corps of Engineers
UWF	University of West Florida

Executive Summary

More than 50 years of impacts from a growing human population have taken a tragic toll on the Indian River Lagoon (IRL) system. Excessive nutrients and all forms of pollution from human activity flow overland and through groundwater to the lagoon. The seagrasses, clams, and oysters are nearly gone from many regions of the lagoon, displaced by nutrient laden muck, polluted water, and algal blooms. With the loss of most seagrasses, manatees are dying in record numbers as they are unable to find food. Fish populations that survived the 2011 superbloom now struggle to adjust to rapidly changing conditions, and the once popular and economically important Redfish are now closed to harvest in the IRL. Algae that once unnoticeably cycled through the seasons in clear water now cloud the water, as blooms of one dominant species quickly die out only to be replaced by the next dominant species in an unbalanced, sometimes hypoxic or anoxic, high nutrient (eutrophic) system.

Water circulation in the lagoon is restricted on all sides, increasing risk of eutrophication and ecosystem collapse. Previous federal development activity supporting space and defense projects cut off the finger flows of Banana Creek, eliminating the northern connection of the Banana River Lagoon (BRL) to IRL. To the east, natural episodic connections between the coastal ocean and IRL system have been lost with the hardened development of the barrier islands, while the benefits of water circulation through the five maintained inlets are limited by the many causeways that restrict flow north and south. To the west, polluted water that historically largely drained to the St. Johns River now flows to the IRL system, with some improvements from ongoing water farming and wetland restoration projects.

Deliberate and timely restoration of lagoon hydrology can improve water quality and help restore the rapidly deteriorating lagoon ecosystem. Elected officials; local, state, and federal government agencies; and stakeholders in the IRL region are exploring a variety of approaches to help restore the lagoon. The Restore Lagoon Inflow Research project is providing data to help determine the viability of a permanent ocean inflow system as a potential additional tool to stabilize and restore the lagoon.
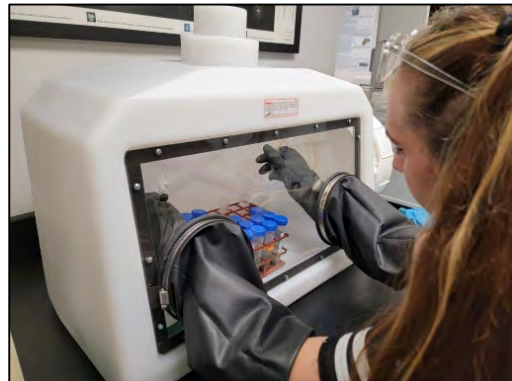
With funding from the Florida Legislature in fiscal year 2020, the Florida Institute of Technology (Florida Tech) completed Phase 1 of a multi-phase research project to explore water quality improvement within the IRL system by enhancing ocean inflows. This first phase gathered baseline data and conducted modeling and experiments on water quality, biological parameters, and hydrologic conditions at candidate locations for a temporary ocean inflow system. The Florida Legislature authorized funding for Phase 2 in fiscal year 2021, which built upon the lessons learned from Phase 1, and focused on planning for construction and implementation of a small-scale, temporary ocean inflow system and the studies required to evaluate its effectiveness. The efforts in Phase 2 included site selection, agency and stakeholder engagement, conceptual engineering and optimization, pre-permitting briefings, expanded ecosystem modeling, and baseline data collection. The Florida Legislature authorized funding for Phase 3 in fiscal year 2023, which included United States Army Corps of Engineers (USACE) Section 404 and Section 408 permits and Florida Environmental Resources Permit (ERP), as well as additional design of the pilot system. Biogeochemical research and modeling efforts proceeded in parallel with

permitting and design in advance of construction and operation of the proposed, temporary pilot inflow system by a state or federal agency.

Phase 1 through 3 results, when combined with findings from the temporary inflow pilot system, will allow for an informed determination of the feasibility and impacts of a potential permanent ocean inflow system.

For Phase 3, the multi-disciplined team of research professionals, supported by community partners, Florida Tech staff, students, and engineering professionals from Tetra Tech, Inc., was expanded to capture data gaps identified in the baseline investigations. The expanded Florida Tech research team included:

- Project Manager – Dr. Jeff Eble
- Engineering – Dr. Robert Weaver and Tetra Tech
- Modeling – Dr. Gary Zarillo
- Geochemistry – Dr. Austin Fox, Dr. Jane Caffrey (University of West Florida [UWF]), Dr. Wade Jeffrey (UWF), and Dr. Lisa Waidner (UWF)
- Biology – Olivia Escandell (Brevard Zoo), Dr. Richard Paperno (Florida Fish and Wildlife Conservation Commission [FWC]) Dr. Jesse Blanchard (Florida International University), Dr. Wendy Noke Durden (Hubbs Sea World Research Institute), and Dr. Edward Phlips (University of Florida)

Project Overview

The multi-phased Restore Lagoon Inflow Research project has included the baseline monitoring, design, permitting, and modeling of a system to provide temporary ocean inflow to IRL to help determine the viability of a permanent ocean inflow system. By improving understanding and management of the IRL system, the implementation of the pilot scale study results will also help to address several actions in the IRL National Estuary Program Comprehensive Conservation and Management Plan, including specifically addressing action Connected Waters-5, which calls for a pilot project to assess the benefits and risks of enhanced ocean exchange with the lagoon.

The pilot system final design was completed in Phase 3, and USACE and state permits were obtained. The permits are transferable to allow any agency to install, operate, and maintain the temporary pumping system. A license has also been prepared by USACE to access the Canaveral Lock property to complete the project. In the next phase, project bid documents will be created, the request for proposals drafted and sent out for bidding, and an award made for construction of the temporary inflow pilot system. The temporary inflow pilot system is expected to be constructed by an agency in accordance with the USACE and ERP permit requirements.

The temporary inflow pilot system is proposed to be operated by a state or federal agency for one year in parallel with continued focused research, monitoring, and modeling. This approach allows for data to be collected on changes due to small-scale ocean inflow at the study site compared to a reference site outside the influence of pumping, to directly assess impacts on focal biological communities and to validate dissolved oxygen (DO), temperature, nutrient, salinity, and chlorophyll-a (Chl-a) model predictions. The temporary pump system established for the project will be decommissioned at the end of the research period, with the piping and pump removed

from the site. The results of the full Restore Lagoon Inflow Research project will be summarized to provide information and analysis to stakeholders and decision-makers on the viability of a permanent ocean inflow system.

Proposed Inflow Site

Based on data collected during Phase 1 and discussions with agencies and stakeholders, Phase 2 identified the northern BRL as the most feasible and cost-effective location of a temporary inflow research site, and design and permitting was completed in Phase 3. BRL is a sub-basin of IRL that lies between Cape Canaveral and Merritt Island and extends from the National Aeronautics and Space Administration (NASA) Kennedy Space Center to Dragon Point. It is poorly flushed with no direct connection to the ocean, which results in long water residence times and increased vulnerability to nutrient accumulation.
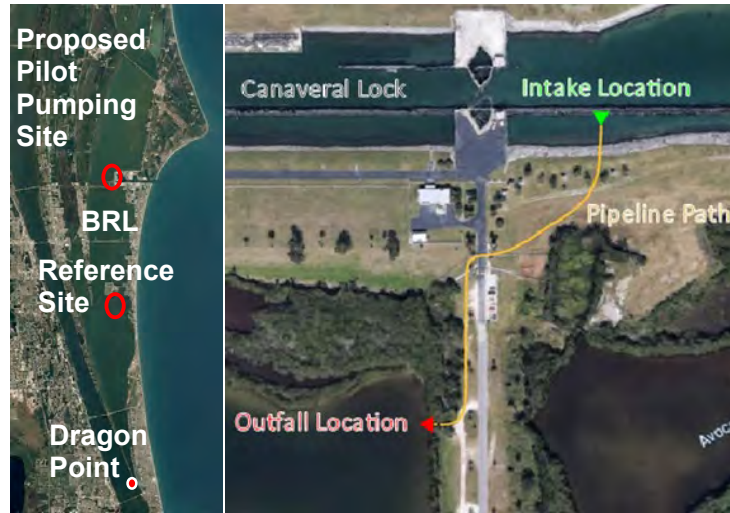
Figure ES-1. Map of the proposed inflow pilot system site

The proposed temporary inflow system installed by an agency would extract water from the ocean side of the Canaveral Lock system and discharge to BRL via the cove to the west of Avocet Lagoon (**Figure ES-1**). A pump station is proposed that pumps a relatively small volume of 0.5 cubic meters per second of seawater through a pipe system above ground to the lagoon. While offshore seawater would be better suited for inflow due to lower nutrient concentrations and more stable dissolved inorganic nitrogen and soluble reactive phosphorus ratio, the data-to-date support a limited test of inflow from Port Canaveral waters, providing a significant cost savings due to the proximity of the waters in Port Canaveral to the IRL. The cove configuration will restrict flow movement from the outfall location and provide a concentration gradient to evaluate changes on water quality, geochemistry, and biology. A reference site in the central BRL was proposed, which was identified through model evaluation and field sampling as comparable to the proposed inflow site and outside the influence of the pilot system. The proposed pilot system configuration was selected to preserve the reference site while minimizing cost and impacts to existing infrastructure, public access, and natural resources.

Data Collection and Modeling

Florida Tech adapted the project approach based on data collected while addressing concerns/questions from stakeholders. Internal project meetings and stakeholder meetings were focused on providing the lowest cost and least invasive approach to implement the temporary inflow pilot system, without sacrificing the validity and quality of the pilot research project.

An IRL Environmental Fluid Dynamics Code model was updated to provide numerical predictions of hydrodynamics, flushing rate, water quality, and phytoplankton concentration with and without enhanced inflow. Model boundary conditions used data from St. Johns River Water Management District and Harbor Branch Oceanographic Institute IRL Observation Network, with watershed

inputs from the Spatial Watershed Iterative Loading model developed by Applied Ecology and internal nutrient loading and groundwater inflow predictions compiled by Florida Tech.

Acoustic Doppler Current Profiler units were deployed in BRL near the Barge Canal, Dragon Point, and Sykes Creek to improve modeling of current directions and velocities. Data on temperature, salinity, DO, and nutrients were also collected with a focus on the proposed temporary inflow pilot system site, internal and external reference sites, and Port Canaveral. Uptake and release (fluxes) of nutrients from sediments and water column were evaluated in the field and using laboratory bench tests of IRL sediments in simulated inflow conditions. During Phase 3, this work was conducted in parallel with sediment microbial assessments with the goal of investigating inflow potential to promote natural nutrient removal through improved bottom water circulation, lower water temperature, and higher and more stable DO concentrations.

In addition, biological data collection efforts for seagrass, drift algae, phytoplankton and harmful algae, benthic infauna, mammals, and fish community continued from Phases 1 and 2. These data improve understanding of the BRL ecosystem, providing biological baselines for comparison to conditions with the proposed temporary inflow pilot system in place to identify effects of enhanced inflow to key species, communities, and habitats. The project also included a comparison of biological and geochemical data near the Destin Harbor inflow site, which has been in operation since 1992.

Highlighted Key Initial Findings

<u>The Restore Lagoon Inflow system is designed, permitted, transferable, and shovel ready.</u>
Thoughtful consideration and design of the study and inflow system is the result of a collaborative approach of the study team and input from federal and state agencies and other stakeholders. A natural cove a short distance from ocean water was selected to confine inflows and allow development of measurable concentration gradients in water quality parameters at relatively low pumping volumes. A similar reference site outside the influence of pilot pumping has also been evaluated to test predicted impacts of inflow on lagoon water quality, nutrient removal, and biology using scientifically sound methods. The design allows for normal operations at the Canaveral Lock site to continue, eliminates the need for dredging, avoids impacts to wetlands, prevents impacts to manatees and other mammals and fish populations, and provides the lowest cost option to achieve the project goals. The design and permits may be transferred for temporary pump implementation by a state or federal agency to evaluate the efficacy of a permanent inflow system.

<u>Inflow would help to buffer against extreme temperatures and salinities</u>.
One major predicted benefit of ocean inflow would be buffering against extreme temperature and salinities that have been attributed to mass mortality events and initiation of the regime shift from a seagrass to algal dominated system. Consistent with events in the IRL, initiation of the Laguna Madre, Texas seagrass to algal regime shift was attributed to extreme low temperatures and perpetuated by subsequent changes in internal nutrient cycling with increased occurrences of hypoxia.

Stabilizing DO and reducing water temperature can improve natural nutrient removal.
Under low oxygen conditions (hypoxia), sediments were found to be a source of dissolved nutrients to overlying water. Inflow is predicted to stabilize DO concentrations (as well as temperature and salinity) and mitigate occurrences of hypoxia, which would improve binding of orthophosphate by sediments, reduce total nitrogen (TN), and promote nutrient ratios that are less favorable for harmful algal bloom (HAB) species. Predicted lower temperatures resulting from the temporary small-scale inflow system are estimated to prevent 1.6 metric tons of TN and 0.7 metric tons of total phosphorus (TP) from entering the lagoon.

Net nutrient reduction is predicted as a result of enhanced inflow.
Models and field data suggest that measurable impacts of inflow rates from 0.5 to 10 cubic meters per second (m^3/sec) will be limited to the northern compartments of the IRL system. This is supported in water quality projections for Sebastian Inlet, which indicate increased water discharge but no detectable change in nutrient concentrations in or near the inlet. The most apparent impact of prescribed pilot inflow rates (0.5 m^3/sec) is in the bottom model water layer in the immediate vicinity of the BRL outfall site, where the DO concentration is predicted to increase. Pilot inflow nutrient improvements are expected to be small but measurable and no large changes in salinity, water temperature, or water quality constituent concentrations are predicted that could produce a significant negative impact during the pilot inflow project.

Water quality determines fish distribution and local population size.
Significant responses were shown to increased inflow by ecologically and recreationally valuable fishes. Model projections indicate local populations of five of eight species of interest would increase and three species would decrease with enhanced inflow. Significant positive and negative associations between local fish population size and Chl-a concentrations were detected and include a decline in nearly all species of interest following the 2011 "superbloom." Species of Interest are likely to be relatively unaffected by net changes to salinity and temperature predicted with inflow; however, negative impacts are expected if rates of change exceed species' response capacity.

Biological baselines allow tracking system response to inflow.
The biological assessments undertaken in Phase 3 and the prior phases provides a solid foundation for understanding the biological state of the BRL. Collaborative efforts between Florida Tech and five partner organizations resulted in diverse datasets, each addressing different biological aspects of the lagoon ecosystem. A significant component was the in-depth assessment of benthic habitats, focusing on the distribution and health of seagrass and other submerged aquatic vegetation. This developing baseline and fish habitat suitability model infrastructure will help ensure that any changes from inflow, positive or negative, can be accurately attributed to intervention and not mistakenly ascribed to pre-existing conditions.

Improvements in the BRL study area were observed.
During the Phase 3 study, minor recovery of seagrasses, reduced nutrient loads, more favorable nitrogen to phosphorus ratios, and stable phytoplankton communities were observed. While these improvements were small, they hold promise for a recovering IRL system, but this recovery is fragile. Estuaries by their nature are subject to changing conditions in nutrients, temperature, salinity, and DO. Long-term recovery relies on the system's resilience at the extreme edges of (and beyond) normal ranges. These improvements in water quality and sea grasses observed in 2023 may be one cold spell, one hurricane, or other extreme event away from being stressed beyond the system resilience and return to severe instability. Ocean inflow may be proven to help regulate temperature, DO, and salinity, thereby reducing the stressors to the system.

1 Introduction and Study Background

1.1 Introduction

The Indian River Lagoon (IRL) is a shallow bar-built estuary that extends 250 kilometers (km) along the central east coast of subtropical Florida, ranging in width from less than 1 km to approximately 9 km (Sigua et al., 2000). IRL is poorly flushed across most of its length, with limited exchange with the ocean occurring through six engineered inlets (from north to south): Ponce de Leon, Port Canaveral, Sebastian, Fort Pierce, St. Lucie, and Jupiter (**Figure 1**). The inlets are directly connected to the ocean except for the Port Canaveral Inlet, which is separated from the lagoon by a lock system. The northern portion of IRL is micro tidal and tidal flushing between sub-basins is negligible (Saberi and Weaver, 2016; Zarillo, 2015). Flushing in IRL is further limited by the presence of causeways connecting the mainland to the barrier islands.
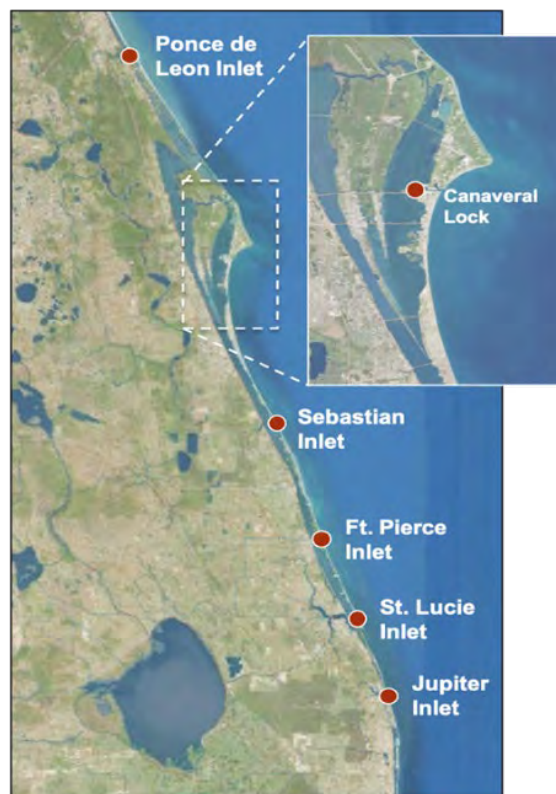
Figure 2. Location of IRL inlets

Historically, and prior to the development of human infrastructure, the IRL system was episodically connected to the coastal ocean through storm produced cuts, over washes, and persistent tidal inlets that migrated alongshore under the net southward wave produced drift of littoral sediments (Zarillo et al., 2013). Cartographic and topographic evidence indicate these features were a re-occurring presence and include evidence of overlapping storm-induced inlet cuts in the Banana River Lagoon (BRL) north of Patrick Air Force Base (Almasi,1985; Stauble, 1988; Brech, 2004). This process, over geological time, resulted in a system of wash over platforms and tidal inlet flood shoals upon which extensive human infrastructure has been built on the barrier islands bounding the east side of IRL (Stauble et al., 1988; Zarillo et al., 2013). Correspondingly, historical development of coastal Florida resulted in a major expansion of the IRL watershed from Brevard County to Martin County due to construction of the canal system and associated water control

structures bringing water formerly destined for the St. Johns River to IRL. Over this same period, existing natural and engineered tidal inlets were stabilized by jetty construction coupled with shore protection projects, which involve repeated beach restoration projects that can have a 50-year planning horizon. This resulted in the prevention of natural tidal inlet migration, episodic storm cuts, and barrier over wash events that reduced the potential for nutrient loading by providing exchanges between the coastal ocean and IRL.

Eutrophication of coastal marine ecosystems has become increasingly common due to enhanced nutrient loading from adjacent watersheds (Brady et al., 2013; Diaz and Rosenberg, 2008). In eutrophic systems, harmful algal bloom (HAB) events contribute to occurrences of hypoxia and anoxia, where even short events can promote loss of ecosystem services including coupled nitrification-denitrification that removes nitrogen (N) from the system as inert N gas and sequestration of phosphorus (P) into sediments. As the eutrophic state progresses, sediment mineralization becomes an important source of nutrients and can sustain eutrophication through the dry season (Cowan and Boynton, 1996; DiDonato et al., 2006; Seitzinger, 1988; Kemp et al., 1990). Extended periods of eutrophication can destabilize the trophic state of an estuary and lead to a shift from seagrass-dominated ecosystems to degraded, algae-dominated systems (DiDonato et al., 2006).

Several decades of increasing anthropogenic impacts have resulted in the lagoon being at risk of ecosystem collapse (Adams et al., 2019). IRL experienced a dramatic shift from a system where benthic aquatic vegetation was expanding to one dominated by planktonic microalgae following an unprecedented algal bloom in 2011 (now referred to as the "superbloom"). The post-2011 IRL is characterized by intense, recurring, and long-lasting algal blooms; widespread loss of seagrasses; and episodic wildlife mortality events. Ongoing blooms of picocyanobacteria, nanoplanktonic chlorophyte, and *Aureoumbra lagunensis* appear to be the "new normal" for the central and northern IRL (IRL National Estuary Program, 2020). As a result of declining water quality, the IRL system lost 58% seagrass habitat from 2009 to 2019 (Morris et al., 2021), which contributed to an increase in marine mammal mortality. The latest Florida Fish and Wildlife Conservation Commission (FWC) data documents 929 manatee deaths in Florida as of August 27, 2021, with deaths more than doubling the five-year average for manatee mortality due in part to IRL seagrass losses and manatee malnourishment and starvation (FWC, 2021).

A multifaceted approach to IRL restoration is underway by multiple state and local government and non-governmental organizations. The Restore Lagoon Inflow Research project seeks to evaluate the efficacy of enhancing ocean inflow to the lagoon as a potential tool for stabilizing and restoring the lagoon ecosystem. This project was inspired by the understanding that restricted circulation is a critical issue, particularly in northern IRL (Smith, 1993; Bilskie at al., 2019). Destin Harbor, Florida, successfully installed a pumping system in 1992 to mitigate a similar issue. Enhanced circulation projects in India (Ghosh et al., 2006), Netherlands (Wijnhoven et al., 2010), New Zealand (Schallenberg et al., 2010), China (Li et al., 2013), Australia (Humphries and Robinson, 1995), Denmark (Peterson, et al., 2008), and Portugal (Lillebo et al., 2005) highlight interest in this approach to combat eutrophication. St. Johns River Water Management District (SJRWMD) initiated a feasibility study for enhanced inflow in 2017 near Port Canaveral, and the Restore Lagoon Inflow Research project evaluated those lessons learned. With improvements to site selection, costs, and potential impacts to infrastructure and lagoon biology, the Restore Lagoon Inflow Research project was designed to directly evaluate the feasibility of enhanced ocean inflow with development of a small-scale, temporary inflow system to be installed by a state or federal agency.

1.2 Objectives

Phase 1 provided essential baseline monitoring and ecosystem modeling for the project. The project team carefully evaluated the parameters required to assess the effectiveness, environmental effects, and limitations of an inflow system. Phase 2 continued to build on these critical datasets that are valuable for the inflow project, as well as the research community and management agencies addressing related questions in IRL and nearshore Atlantic Ocean. The project team adapted the project approach based on data collected while addressing additional concerns/questions from stakeholders. Internal project meetings and stakeholder meetings were focused on providing the lowest cost and least invasive approach to implement the temporary inflow pilot system, without sacrificing the validity and quality of the science produced by the project. Phase 3 included a final system design, refined the modeling efforts, obtained all necessary permits, and continued the baseline geochemical and biological research.

As part of Phase 3 the temporary inflow pilot system design from Phase 2 was developed to a 90% design. The 90% design included the changes discussed in the pre-application meetings with United States Army Corps of Engineers (USACE), Florida Department of Environmental Protection (FDEP), and SJRWMD, as well as incorporated pertinent feedback from other state and federal agencies and stakeholders. The 90% design included the construction drawings for the temporary inflow pilot pumping system, technical and environmental specifications, contingency plan, and opinion of the probable cost of construction. The 90% design was coordinated with USACE and FDEP to obtain the necessary permits. This involves holding additional pre-application meetings, drafting and submitting permit applications, and responding to requests for additional information (RAIs). The permits include USACE Section 404 and 408 permits and FDEP Environmental Resources Permit (ERP). Based on the feedback from the permitting agencies, the 100% design was prepared and submitted as a part of the RAIs. The design and permits may be transferred for temporary pump implementation by a state or federal agency to evaluate the efficacy of a permanent inflow system.

1.3 Study Area

BRL is a sub-basin of IRL that lies between Cape Canaveral and Merritt Island and extends from the National Aeronautics and Space Administration (NASA) Kennedy Space Center to Dragon Point. BRL is poorly flushed with no continuous direct connection to the ocean, which leads to some of the longest residence times in the IRL system. According to the FDEP, it takes approximately two years for water to flush in BRL (FDEP, 2013). The BRL northern section was historically connected to IRL by Banana Creek, which was a series of finger-like channels that were almost completely filled in during the development of NASA Kennedy Space Center. Banana Creek was also periodically connected to the Atlantic Ocean at Pepper Haulover, which was an intermittent storm cut just east of where Launch Complex 39A stands today (USACE, 1882). Prior to development of the barrier island, each IRL basin was subjected to episodic over washing and breaching of the barrier island by storms, as evidenced by numerous relict tidal inlet shoals and expansive wash over sediment fans (Brech, 2004), and was observed in areas of the Mosquito Lagoon in 2022 following Hurricanes Ian and Nicole. This historical inflow would bring in ocean water and enhance circulation in the estuary.

Impacts from declining water quality and increasingly frequent HABs are not evenly distributed across IRL, and the northern IRL and BRL appear to be particularly vulnerable (Badylak and Phlips, 2004; Phlips et al., 2011). Since 2011, large and persistent algal blooms resulted in an unprecedented decline in water clarity, which negatively impacted seagrass growth and distribution (**Figure 2;** Scheidt, 2021a). In BRL, seagrass percent cover dropped drastically from

35% in 2011 to less than 2% in 2012. Additional bloom events, which started in late fall 2015 and persisted into late spring and summer 2016, had a further negative impact. By 2019, seagrasses were absent across most of the region. The previously extensive seagrass beds in BRL provided good forage habitat and safe harbor for Florida Manatee (*Trichechus manatus latirostris*; Provancha and Provancha, 1988; Provancha and Hall, 1991; Lefebvre et al., 2016; Scheidt, 2021b). The catastrophic loss of the once stable manatee seagrass forage in BRL has led to mass starvation events and populations declining to historically low numbers (**Figure 2**). Long-term persistence of manatees in BRL is only possible with restoration of ecosystem integrity and recovery of seagrass foraging habitats (Scheidt, 2021b). In 2022, FWC reported 346 manatee deaths in Brevard County alone, which accounted for nearly half of the record high annual manatee mortality in Florida.
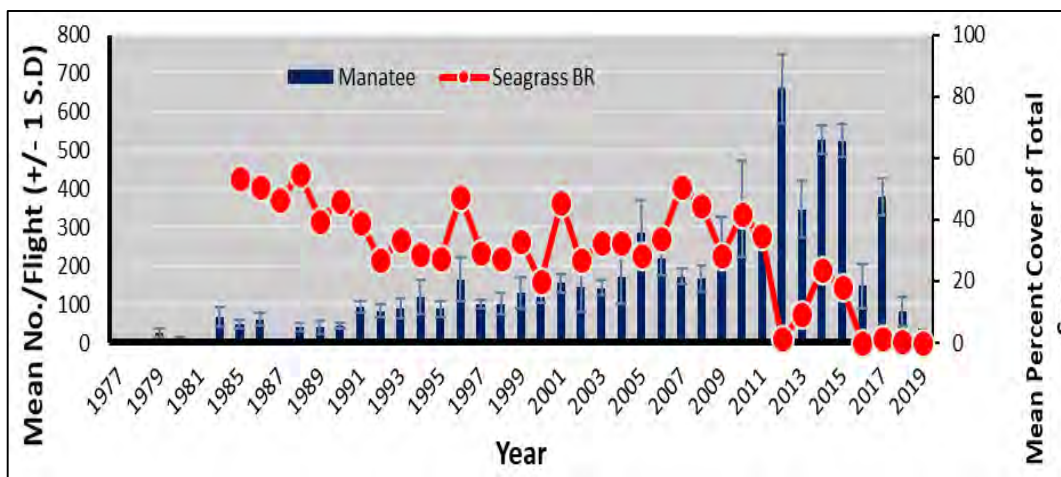
Figure 3. Mean number of manatees (blue bars) per flight from summer aerial surveys and annual mean seagrass percent cover for BRL transects (red line; used with permission from Scheidt, 2021b)

Phase 3 of the Restore Lagoon Inflow Research study built on Phases 1 and 2 efforts to evaluate possible impacts of enhanced circulation in the northern BRL, specifically near the selected inflow site (centered near 28.407, -80.638), and the central BRL evaluated as a reference site where any impacts from a pilot study would be minimized due to geomorphological conditions that limit circulation (centered near 28.287, -80.6100) (**Figure 3**). A natural cove adjacent to Port Canaveral was selected to confine inflow, so that pumping rates for the pilot study could be minimized to reduce installation costs and impacts to the greater IRL system, while still creating water quality concentration gradients that can be monitored and evaluated for their potential to improve ecosystem functions. This approach uses a reference site that was selected based upon model evaluations to identify a location with limited circulation associated with proposed pilot pumping volumes, as well as a comparison of water depth and bottom type similar to the proposed inflow site. The reference site allows for correlation and comparison of data to better evaluate changes strictly due to pumping within the highly variable IRL system.
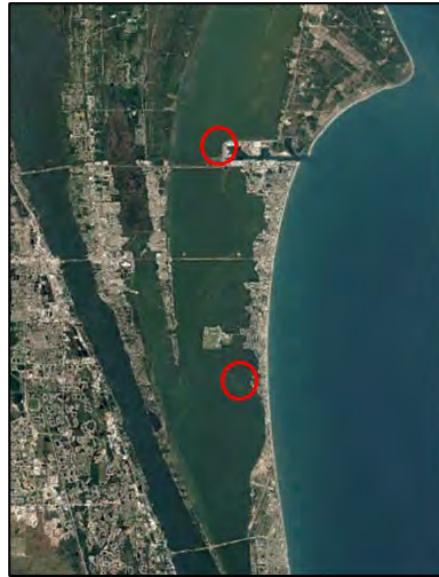
Figure 4. Proposed pilot inflow site in north BRL and reference site in central BRL

1.4 Support for Lagoon Efforts

The Restore Lagoon Inflow Research project builds upon and complements ongoing efforts to better understand the IRL system and identify effective restoration measures. The results will help to determine whether enhanced ocean inflow could be a tool to address declining water quality and ecosystem degradation. In addition, this project is gathering data to help directly address two vital signs and four actions from the IRL National Estuary Program Comprehensive Conservation and Management Plan (2020). The Connected Waters and Watersheds and Hydrology and Hydrodynamics vital signs include the following actions that the study will help to inform:

- Connected Waters-5: Better understand the physical, chemical, and biological implications, benefits, risks, and expected outcomes of enhancing oceanic exchange and develop a pilot project, as appropriate.
- Hydrology-1: Support advancements in hydrological model development, verification, and application.
- Hydrology-2: Apply the best available models to better evaluate connectivity between IRL sub-basins.
- Hydrology-3: Continue evaluation of options to enhance water flow through engineering solutions that have well defined water quality and ecological outcomes.

The engineering design for the Restore Lagoon Inflow Research project builds upon past work by SJRWMD who contracted with CDM Smith, in association with Taylor Engineering, to identify potential locations where enhanced circulation projects would be beneficial. The first phase (CDM Smith et al., 2014) involved a literature review and geographic information system desktop analysis, which identified ten locations for future evaluation. Based on a screening matrix, the top ranked project from this evaluation was a culvert at Port Canaveral (CDM Smith et al., 2015). The third phase developed the conceptual design for a culvert and temporary pump at Port Canaveral at State Road 401 (CDM Smith et al., 2017). As part of the Restore Lagoon Inflow Research project engineering, the exact intake and inflow structures were modified from the proposed design in CDM Smith et al. (2017) to minimize the impact to channel banks and overlying infrastructure. Modifications were also made to provide an outfall location with natural restrictions

to allow for a significantly reduced pumping volume that would still facilitate study of inflow impacts at a smaller scale. This approach greatly reduces the cost and wider reaching impacts of inflow on IRL until a more complete assessment of inflow is evaluated using the pilot system data.

1.5 Coordination

As part of Phase 3, Florida Institute of Technology (Florida Tech) and Tetra Tech continued to consult with key stakeholders and agencies to gather feedback on study design and focused on the permitting efforts with USACE and FDEP. The team closely coordinated with USACE to negotiate the use of USACE lands for the pilot project and navigated through the Section 404 and 408 permitting process. In addition, consultation occurred with FDEP through the ERP process. The project team incorporated lessons learned and design and research comments from Phases 1 and 2 into the final design and permitting packages, which ultimately led to the successful completion of the ERP and USACE Section 404 and 408 permitting.

2   Key Findings: Phase 3

In Phase 3, Florida Tech continued to explore solutions for improving water quality in the lagoon with initiation of a pilot project to investigate the impacts of restoring periodic historical ocean inflows. Phase 3 further developed baseline data and modeling on existing water quality, biological parameters, and hydrologic conditions at the proposed pilot system location. The modeling and engineering proceeded in parallel with biological and water quality monitoring and increase the resolution on the selected pilot project site. The results of the full Restore Lagoon Inflow Research project will provide information and analysis to the lead agency and appropriate decision-makers to help determine the viability of a full-scale, permanent ocean inflow system. The key findings from the project to date are summarized below.

Task 1 Engineering:
- Pilot inflow design includes all project elements, their locations, and principal dimensions.
- USACE Section 404, USACE Section 408, and Florida ERP permits approved.
- Review of similar national and international projects illustrate the benefits of enhancing circulation in enclosed and semi-enclosed estuaries.

Task 2 Hydrologic Modeling:
- To evaluate the potential influence on water quality in a confined BRL compartment, model pilot inflow test cases included no inflow, 0.5 cubic meters per second (m^3/sec) inflow, and 1.0 m^3/sec inflow from Port Canaveral, and 0.5 m^3/sec inflow from the coastal ocean.
- Model error for total nitrogen (TN), total phosphorus (TP), salinity, temperature, and dissolved oxygen (DO) are within an acceptable range.
- No large changes in salinity, water temperature, or water quality constituent concentrations were predicted that could produce a significant negative impact during the pilot inflow project.
- The most apparent impact of prescribed pilot inflow rates is in the bottom model water layer in the immediate vicinity of the BRL outfall site, where the DO concentration is predicted to increase.
- Predicted TN and TP improvements from prescribed pilot inflow rates are small but measurable.

Task 3 Geochemical:
Florida Tech
- Inflow of seawater would help to buffer BRL against extreme temperatures and salinities that have been attributed to mass mortality events and initiation of the regime shift from a seagrass to algal dominated system.
- Consistent with events in the IRL/BRL, initiation of the Laguna Madre, Texas seagrass to algal regime shift was attributed to extreme low temperatures and perpetuated by subsequent changes in internal nutrient cycling with increased occurrences of hypoxia (low DO).
- Minimum winter temperatures in BRL were 3 to 9 degrees Celsius (°C) colder than minimum temperatures in the coastal Atlantic Ocean.
- Since 2017, compared to the coastal Atlantic Ocean, BRL water temperature has averaged 0.5 to 3 °C warmer in the summer and 0.5 to 3°C cooler in the winter.
- Anthropogenic modifications since the early 1900s have likely contributed to lower and less stable salinities by increasing the size of the IRL watershed.
- Salinity in BRL has decreased almost continuously since 2014, reaching a low of 15 to 16 parts per thousand (ppt) which is below the threshold shown to reduce clam and seagrass

- growth and survival. Increased seawater exchange would help to raise salinity, buffer against extremes, and improve habitat quality for these native species.
- Improved water quality with more stable DO would help to disrupt feedback loops that sustain the alternate stable algal regime.
- In BRL, water column respiration accounted for approximately 50% to greater than 80% of the total oxygen consumption (sediments + water) and is a major contributor to variations in DO concentrations and occurrences of hypoxia or anoxia.
- Water column respiration was on average 40% higher in BRL (–0.14 milligrams per liter per hour [mg/L/hr]) compared to the coastal ocean (–0.10 mg/L/hr).
- Inflow and associated mixing would result in lower respiration (oxygen demand), buffering against instances of hypoxia while lowering dissolved nutrient concentrations and favoring types (species) of N and P that are more readily removed through geochemical processes.
- Overall, concentrations of total dissolved nitrogen (TDN), total dissolved phosphorus (TDP) and silica (SiO_2) at the inflow and reference sites were on average 3.3–fold, 1.8–fold and 7.5–fold higher than in Port Canaveral. The relative abundances of organic N and P were 15% and 17% higher, respectively in the BRL than in Port Canaveral and offshore sites.
- The dissolved inorganic nitrogen (DIN) and soluble reactive phosphorus (SRP) ratio (DIN:SRP) in Port Canaveral increased between 2020 and 2023 from an annual median of 22 to 31. The median DIN:SRP ratio in the coastal Atlantic was 20.
- Both the DIN:SRP and TDN:TDP ratios in BRL decreased between 2020 and 2023. Higher ratios are known to promote small, fast-growing algae. Lower ratios observed during 2023 are more consistent with the optimal ratio for some beneficial photosynthesizers including seagrasses that have been recovering in 2023.
- Benthic fluxes of N and P were highly variable, with sandy sediments alternating between a sink and a source of both N and P. Small changes to benthic fluxes have a dramatic impact on N supply or removal from the lagoon. Lower TDN fluxes during Phase 3 compared to Phase 2 support observations for N:P ratios.
- In contrast to variable fluxes observed for sand, muddy "mucky" sediments were a consistent source of N and P to overlying water.
- Significant positive correlations were identified between benthic fluxes of nitrate + nitrite (NO_x), TDN, orthophosphate (PO_4), dissolved organic phosphorus (DOP), and SiO_2 versus sediment temperature.
- Lower summer temperatures in BRL associated with the proposed pilot study were calculated to prevent 1.6 and 0.7 metric tons of N and P from entering the lagoon annually.
- Overall median TDN and TDP fluxes in sandy sediments were –200 ± 381 micro moles (μmoles) N/ square meter per hour (m^2/hr) and 2.7 ± 3.2 μmoles P/m^2/hr, respectively, demonstrating the potential for efficient N removal from sediments when water quality improves.
- The ability of sediments to sorb and sequester P decreased from 133 milligrams (mg) P/kilogram (kg) in a 2001 study to 99 mg P/kg in our 2022 to 2023 study, likely reflecting cumulative impacts of chronic diel and episodic hypoxia.
- A positive P flux is expected with improved water quality and fewer hypoxic events, which would help to preserve the ability of new sediments to sorb and sequester P.
- Collectively, data to date support a limited test of inflow as part of a multifaceted approach to lagoon restoration.

University of West Florida (UWF)
- Aerobic N-cycling microbes were on average nearly five times more abundant in Santa Rosa Sound (SRS) than IRL sediments, indicating the potential for more rapid N removal in SRS sediments than in the IRL.
- Anaerobic ammonia producing microbes that can exacerbate the effects of eutrophication were on average two times more common relative to aerobic N-cycling microbes in the IRL than in the SRS.
- Salinity in the BRL section of IRL normally falls within the known tolerances for two dominant seagrass species, *Halodule wrightii* and *Syringodium filiorme*. Extended periods of high salinity (> 35 ppt) between 2011-2014 and low salinity in the 1990s and following the 2004 hurricane season (< 10 ppt) exceeded ranges for optimal productivity.
- The amount of light available to support seagrass growth is higher in SRS than IRL. Analysis from this study and the literature point to the need to decrease light attenuation (increasing bottom light availability) in IRL to allow seagrasses to recover.
- Despite enhanced inflow, Destin Harbor bottom waters experience episodic hypoxia. High bottom water chlorophyll-a (Chl-a) concentrations indicate substantial nutrients and light availability, which is likely driving water column and sediment decomposition reducing oxygen concentrations in the water column.

Task 4 Biology:
Brevard Zoo
- Total seagrass cover ranged from 0.1% to 3.88% in the vicinity of the northern BRL pilot inflow site and from 0% to 0.5% at southern BRL control sites.
- Seagrass cover increased at north BRL sites from spring 2021 to summer 2023 but no significant change in cover was observed south BRL sites.
- Some sampling locations which once boasted dense seagrass beds, were devoid of seagrass throughout the study period.
- Drift algae and rooted macroalgae (*Caulerpa prolifera*) coverage was seasonal and highest in summer 2023 (15.6% – 24.6%).
- Improvements to water quality in the BRL are necessary to expand seagrass cover and restore this essential benthic habitat.

FWC
- Fish in the proposed inflow area was more diverse than the control site (30 vs. 23 taxa).
- The difference in fish abundance was a result of the greater number of Bay Anchovies (*Anchoa mitchilli*) collected at the inflow sites (n = 29,623) versus the control sites (n = 2,134).

Florida International University
- Temperature and salinity frequency of occurrences for 11 species of interest (SoI) are described for the BRL over a 22-year period using FWC monitoring data.
- Targeted literature reviews are provided for the 11 SoI to describe known temperature and salinity limits.
- Annual spatiotemporal distribution of 11 SoI densities were mapped and rasterized.
- The BRL environment was mapped with respect to salinity, temperature and shoreline type using FWC monitoring data.
- Generated species tolerance data and rasterized occurrence and environmental outputs are critical inputs required to support future habitat suitability modeling.

- Enhanced inflow from an offshore source could potentially mitigate negative impacts from severe heat and cold events, which are expected to become more frequent with human-induced climate change.
- SoI are likely to be relatively unaffected by net changes to salinity and temperature predicted with inflow; however, negative impacts are expected if rates of change exceed species' response capacity.

Hubbs Sea World Research Institute (HSWRI)
- Five vessel-based dolphin surveys were conducted in the Northern IRL (BRL and northern IRL) to assess the nutritional condition of the dolphin community inhabiting the area.
- 77 groups (sightings) were encountered, and 233 distinct dolphins were identified.
- 22,498 images were reviewed to assess nutritional condition. Body index was assessed for 155 marked adult dolphins.
- 93% of dolphins presented in a compromised nutritional condition (68%-underweight, 25%-emaciated).
- Compared to prior evaluations (2013, 2016) the dolphin community appears to be increasingly nutritionally stressed, although the influence of variance between surveys should be considered.

University of Florida
- Phytoplankton composition and biomass at the four sampling sites varied by month.
- The list of dominant species at the four sites over the study period contained many of the same elements. In any given month, Site 1 showed the greatest difference in composition relative to the other three sites, while the other three sites were the most closely aligned.
- In terms of numerical abundance, picoplanktonic cyanobacteria (including spherical forms and *Synechococcus cf* spp.) were always the highest at all four sites, followed by nanoplanktonic eukaryotes (including cryptophytes).
- Diatoms were observed in every sample collected over the study period, but largely at comparatively low biomass levels. Dinoflagellates were often the dominant taxa in terms of biomass in June and July.
- The results of this study provide information helpful for the design of monitoring programs associated with future management efforts aimed at mitigation of HABs.

Additional details on these key findings are presented in **Section 4**, which is a summary of the reports prepared by the Principal Investigators. The Task 1 Engineering report was prepared by Dr. Robert Weaver, and the full report is provided as Appendix A. The Task 2 Hydrologic Modeling report was prepared by Dr. Gary Zarillo and the full report is provided as Appendix B. The Task 3 Geochemistry report was completed in two parts. The Florida Tech portion was prepared by Dr. Austin Fox, and the full report is provided as Appendix C. The UWF portion was prepared by Jane Caffrey, Wade Jeffrey, and Lisa Waidner, and the full report is provided as Appendix D. The Task 4 Biology report was prepared in five parts. The Brevard Zoo portion was prepared by Olivia Escandell, and the full report is provided as Appendix E. The FWC Fish and Wildlife Research Institute (FWRI) portion was prepared by Richard Paperno, and the full report is provided as Appendix F. The Florida International University portion was prepared by Jesse R. Blanchard, and the full report is provided as Appendix G. The HSWRI portion was prepared by Wendy Noke Durden, and the full report is provided as Appendix H. The University of Florida portion was prepared by Edward Phlips, and the full report is provided as Appendix I.

3   Recommendations and Next Steps

The multi-phased, full research project was envisioned to include the baseline monitoring, design, permitting, implementation, and investigation of a system providing temporary ocean inflow to IRL. The results of the full Restore Lagoon Inflow Research project will provide information and analysis to the lead agency and appropriate decision-makers to help determine the viability of a full-scale, permanent ocean inflow system.

3.1   Recommendations

Future phases include preparation of bid specifications, as well as the construction of the temporary inflow pilot system, system operation and maintenance, and a final report of the research project findings.

Once an organization is selected and funded to complete the Restore Lagoon inflow Pilot project, the bid documents will be created, the request for proposals will be drafted and sent out for bidding, and an award will be made for construction of the temporary inflow pilot system. The pilot system will then be constructed in accordance with ERP and USACE permit requirements. The temporary inflow pilot system is proposed to be operated for one year in parallel with continued research monitoring and modeling. This approach allows for data to be collected to identify changes due to small scale ocean inflow at the study site compared to the reference site, directly assessing impacts on focal biological communities and to validate DO, nutrient, and Chl-a predictions. The temporary pump system established for the project will be decommissioned at the end of the research period with the pipe and pump removed from the site. The results of the full Restore Lagoon Inflow Research project will be summarized to provide information and analysis to stakeholders and decision-makers on the viability of a full-scale, permanent ocean inflow system.

3.2   Next Steps

As part of the proposed subsequent phases of the full Restore Lagoon Inflow Research project, specific next steps for each project task are summarized below.

3.2.1   Engineering

The USACE Section 404 and Section 408 and ERP permits provided approval for all project elements and their locations and principal dimensions. The bid package needs to be developed in accordance with the procurement requirements of the organization to be responsible for construction. Once completed the project can be sent out to bid. Engineering oversight of bidding, construction, and operations is an important component of a successful pilot project.

Once construction is completed and the pump is operational, the project moves into the performance and monitoring phase. To fully evaluate the project, it is important to measure the currents both inside the BRL west of the lock and in the port east of the lock. Locations for deployment of two acoustic doppler current profilers are included in the permitting documents. Once deployed, regular monthly servicing, which includes offloading of data, cleaning of the instruments, and battery replacement, will be required. During operations, the engineering team will need to monitor the flow rate and water quality at both the intake and outfall.

Monitoring currents inside the project area and near the intake will aid not only in the understanding of water exchange during the pilot but will also provide a clearer picture of the

hydrodynamics of Canaveral Lock operations. This will assist in understanding the relative contributions of the lock system to lagoon ocean water exchange.

3.2.2 Hydrologic Modeling

Modeling the concept of enhanced inflows has been successful from both the full scale and pilot project perspectives. However, model results clearly indicate that the project would derive significant benefits from more continuous measurements of water quality, as well as salinity and water temperature to enhance model calibration and validation. The minimum temporal resolution water quality measurements would be on a weekly basis combined with high accuracy laboratory analysis of collected water samples. These measurements should begin well in advance of pilot project construction and proceed through the project duration. It is also recommended that in any future phase of this project, field measurement be made to quantify lock flow rates more precisely. Future data collection stations should be consistent with model boundary locations, as well as within the interior of the BRL and Port Canaveral. Well-designed monitoring can provide the basis for accurate and spatially integrated model prediction of pilot project benefits and evaluation of larger inflow rates that may be associated with a full-scale inflow project.

3.2.3 Geochemistry

To date, this project has greatly improved the understanding of nutrient cycling in the IRL system, especially in sandy sediment and in the water column. These data are useful not only to modeling possible impacts of inflow, but for HAB and for generalized nutrient load modeling, especially related to addressing changes to temperature and rainfall associated with changing climatic patterns. Despite knowledge gained during this study, the lagoon is dynamic and with this temporally limited dataset, it is not possible to isolate natural, seasonal patterns from event scale occurrences, something that would be more feasible in the near future if this work is continued to evaluate the pilot project (1 to 2 years). Data to date have demonstrated the importance of processes in sandy sediments and on particles and have yielded wide ranges of values for these critical processes. Phase 3 allowed evaluation of these processes over multiple years coinciding with localized improvements to water quality. Continuing this biogeochemical evaluation would help to resolve event scale variability versus seasonal trends and improve statistical power of trends identified to date. Additional data obtained during the pilot project would improve confidence in extrapolated models. Due to the importance of bottom water DO towards cycling of both N and P, long-term support for this network of quality-controlled bottom water sensors is important. These collective datasets are tools that will help managers select restoration projects based on potential to restore natural cycling of N and P to make efficient use of taxpayer dollars. To continue the specific study of inflow and in response to results to date, the investigation of changes in oxygen and nutrient cycling in sediments would be expended with restored infauna communities. Preliminary data obtained as part of this study indicated that biota influence geochemistry; however, restoring infauna to organic–rich sediments promoted mineralization of organic matter that overshadowed benefits of oxidized surface sediments. The plan would be to repeat and improve these experiments in sandy sediments that are more representative of the lagoon bottom. These next steps should take place before and alongside the proposed pilot inflow project. Overall, data to date support a limited test of inflow as part of a multifaceted approach to lagoon restoration.

3.2.4 Biology

The initial phases of the Restore Lagoon Inflow Research project have included valuable baseline data with a focus on the inflow and reference sites. Continued monitoring before, during, and after the initiation of the pilot pumping project will assist in understanding inflow induced changes in

the IRL system and identify potential changes resulting directly from the pumping project. Seagrass monitoring each season before during and after inflow pumping at the inflow site, adjacent area, and the reference site will be valuable data. Continuing phytoplankton monitoring will provide valuable data for understanding the effects of inflow on the phytoplankton communities and the use of inflow to mitigate HABs. The health of marine mammals in the IRL has been on a steady decline for several years. While the inflow pilot project is not anticipated to have a wide effect on the IRL, continued monitoring of manatees and dolphins will help evaluate the direct affects from pumping on migration, foraging, and refuge habits as well as overall health.

Phase 3 continued development of the infrastructure required to implement habitat suitability modeling to improve predictions of inflow impacts on IRL fishes. Habitat suitability modeling seeks to model species' habitat use based on the complex interactions of the abiotic and biotic factors influencing their spatiotemporal distribution. The major questions to be answered during the pilot project affecting IRL fish species are: What is the anticipated rate of temperature and salinity change? What rate of change can BRL fishes tolerate? How will habitat suitability change under alternative pumping scenarios?

4 Task Summaries

4.1 Engineering (Task 1)

The objectives of the engineering task were to complete a pilot pumping project design and assist in the permitting process. The engineering design and permitting task group developed the pilot system design and worked closely with Tetra Tech, providing them with necessary materials to complete the permits and prepare them for review by the appropriate agencies, including USACE, FWC, and FDEP. These agencies have a regulatory role in approving the pilot project permit applications and early coordination aided in expediting the process. The success of the pilot project is dependent on the approval of the permitting agencies. The following objectives were identified to progress toward the Phase 3 goal:

- Advance the 60% design developed in Phase 2 to the 90% design needed for permit submittal.
- Prepare and submit USACE Section 404, USACE Section 408, and Florida ERP permit applications in close coordination with Tetra Tech.
- Address RAIs from the permitting agencies in an expedited manner.

The Engineering and Design team worked with Restore Lagoon Inflow Task Groups and Tetra Tech to obtain the required data and analysis needed to address the RAIs and draft the responses for Tetra Tech prior to (re)submittal.

4.1.1 Approach

Based on data collected during Phase 1 and discussions with agencies and stakeholders, Phase 2 identified the northern BRL as the most feasible and cost-effective location of a temporary inflow research site. BRL is a sub-basin of IRL that lies between Cape Canaveral and Merritt Island and extends from the NASA Kennedy Space Center to Dragon Point. It is poorly flushed with no direct connection to the ocean, which results in long water residence times and increased vulnerability to nutrient accumulation.

The proposed temporary inflow system would extract water from the port/ocean side of the Canaveral Lock system and discharge to BRL via the cove to the west of Avocet Lagoon (**Figure 4**). A pump station is proposed that pumps a relatively small volume of 0.5 m³/sec of seawater through a pipe system above ground to the lagoon. The cove configuration will restrict flow movement from the outfall location and provide a concentration gradient to evaluate changes on water quality, geochemistry, and biology. The proposed pilot system configuration was selected to preserve the reference site while minimizing cost and impacts to existing infrastructure, public access, and natural resources.

Figure 5: Map of the proposed inflow pilot system site and pipeline path

4.1.2 Results

The Phase 3 Task 1 results include completing the design, submitting permits for the implementation of the pilot pumping system, responding to RAIs from regulatory agencies, and reviewing similar enhanced exchange projects around the globe for guidance on engineering design, management, and anticipated impacts.

4.1.2.1 Design and Permitting

During Phase 3, the focus of Task 1 was to advance the development of the USACE Section 404 and Section 408 and ERP permits, leading to the submission and approval of the permit applications. The Section 404 and Section 408 permits included the approved engineering design of the inflow structure, outflow structure, and pipeline route. These designs contained guidance for telemetry and control of the system and are sensitive to the ability for the pilot project and all associated components to be removed at the end of the one-year study period. The design features based on the temporary nature of the project include a scour pad laid on top of existing ground at the outfall which does not require excavation, timber piles that can be removed and repurposed, and a flow rate that will not induce sediment erosion at the intake.

The inflow structure will consist of a pile supported platform to mount the pipe and the intake side of the pump. The platform will allow access to the intake for maintenance while providing structure to support the pipe and necessary hydraulics. This design is also readily removed at the end of the one-year project duration. To ensure compliance with U.S. Environmental Protection Agency Section 316(b), a new commercially available (and US. Environmental Protection Agency compliant) intake screen designed by Hendrick Screen Supply was selected (**Figure 5**).

Figure 6. Typical drum intake screen per manufacturer Hendrick Supply

The geotextile outfall structure has been designed to eliminate the need for any dredging, excavation, or introduction of rip rap into the outfall area (**Figure 6**). Consulting with geotextile manufacturer Synthnetex, the engineering team was able to design a creative solution to manage stakeholder agency concerns with excavation. The bottom portion of the outfall is designed to be the Synthetex Hydrotex® Articulating Block (or similar product) as a scour mat that will reduce flow velocity and reduce risk of scour at the end of the outfall.
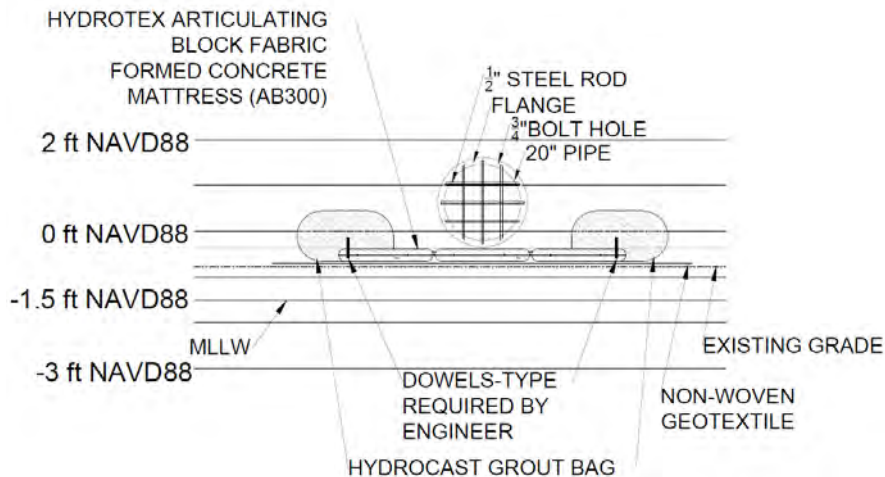
Figure 7. Geotextile outfall structure with manatee exclusion grate (shown on face of pipe)

To provide ongoing monitoring and allow for off-site shutoff, a remote system has been selected to interface with the pump. A system supplied by Allied Pivot Sales will be implemented, which allows operators to remotely turn the pumping system on and off through cellular connection. The system also monitors water temperature, flow rate, and water volume through the pump and stores this information in a cloud-based storage center.

The pipeline must cross the access road to the USACE Canaveral Lock operations facility. It is a requirement that the operations not be impacted. A ramp structure from Bluff Manufacturing was selected that will install on top of the existing roadway and go over the pipeline. During permitting, USACE was concerned about allowing both smaller vehicles and larger trucks access to the site without issue. Consultations with Bluff Manufacturing resulted in a slight redesign of the ramp structure to accommodate a wide range of vehicles.

As the project comes to the end of Phase 3, the USACE Section 404 and Section 408 permits and FDEP ERP have been approved. In that process, the design team received and responded to RAIs from FDEP for the team's ERP application, and USACE for the Section 404 and Section 408 permits. The requested information included details on the exclusion intake screen, new pump selection, geotextile outfall scour protection, and site access and security.

Table 1. Pipe and pump system cost estimate

Structure	Total Cost
Pump	$454,640.00
Ramp	$42,933.00
Inflow	$71,891.15
Outflow	$1,007.30
Subtotal	**$570,471.45**
Contractor Mobilization, Overhead, and Profit (30%)	**$171,141.44**
Contingency (40%)	**$228,188.58**
Total	**$969,801.47**

The estimated cost for the system is just under $1 million dollars based on revised cost estimates for the components in the Phase 3 design (**Table 1**). The costs reflect changes to the pump that resulted in increases from the Phase 2 estimate. These changes are due to the recalculation of total dynamic head which led to the modification of the pump selected for the project. The use of the premanufactured intake screen designed by Hendrick Screen Supply also increased the costs. Post project resale of the intake pump system and pipe to MWI for an estimated $116,000 (MWI pers. comm.) can help to offset the cost of the inflow pilot study.

4.1.2.2 Review of Inflow Projects

Concurrent with the permitting process, a review of existing and historical inflow projects was initiated. Details from inflow sites in Australia, Denmark, the Netherlands, and the USA were collected to review performance and impact on water quality from engineered inflow projects, and a report on the review is currently being prepared.

Each site investigated recorded improvements in water quality, although there was considerable variation in both the extent and rate of improvements. In each case, salinity and DO increased, turbidity reduced, and nutrient levels dropped. These changes often led to a reestablishment of marine flora and fauna, including clams and other benthic fauna known to play an important role in counteracting the effects of excess nutrients.

On example is the Destin Harbor in Desitin, Florida system. Being a Florida project implementing a pump to bring water from the Gulf of Mexico into the enclosed harbor, this system is of particular interest to stakeholders. A permanent pump station was constructed to improve circulation in Destin Harbor (**Figure 7**). The pump system is operated daily from 11:00 pm to 7:00 am in the warmer months and brings in almost 22 million gallons of water from the Gulf of Mexico each night (Burgess, 2020). The system was constructed in two phases and completed in 1992 for a total of $3.3 million.

Figure 8. Destin Harbor aerial map (Google, 2021)

Since the implementation of the pump system, Destin Harbor has maintained Class III surface water quality standards, meaning the basin is safe for fish consumption, able to support recreation, and sustain a healthy population of fish and wildlife. It has also maintained acceptable levels of DO, salinity, and water clarity, and there have been no fish kills (Burgess, 2020).

4.1.3 Conclusions

The design of the proposed pilot scale inflow has been focused on creating a mesocosm in a semi-enclosed basin within the northern BRL. This controlled environment will allow scientists and policy makers to evaluate the benefits of enhancing ocean inflow in the IRL before committing to a full-scale design. The design accounts for the temporary nature of the pilot project, input from the stakeholders and permitting agencies, and the potential need to remotely shut the system down in case of emergency.

With completion of Phase 3, Task 1 achieved:

- Pilot inflow design of all project elements and their locations and principal dimensions.
- USACE Section 404, USACE Section 408, and Florida ERP permits approved.
- Similar national and international projects illustrate the benefits of enhancing circulation in enclosed and semi-enclosed estuaries.

Data from existing inflow projects taken together with work performed by Dr. Zarillo and the Task 2 team as well as Dr. Fox and the Task 3 team support the proposal that enhanced ocean inflow in IRL will buffer regional salinity, temperature, and DO, while also reducing nutrient levels (N and P) and the frequency of HAB outbreaks.

Findings to date indicate that improving water quality in the BRL and IRL by enhancing ocean inflow is both feasible and cost effective. The pilot project is estimated to cost just under $1 million dollars for construction. A structure that would accommodate a full-scale inflow was estimated in Phase 1 to cost approximately $10 million dollars for a weir structure and $60 to $100 million to pump ocean water from offshore using a buried pipe system under the barrier island. To put that into perspective, as of fiscal year 2022/2023 quarter 1, the Brevard County Save Our Indian River Lagoon Plan has allocated or spent nearly $155 million on dredging muck and treatment of the interstitial waters, $50 million on stormwater projects, and $149 million on septic system removal and upgrades in addition to other expenditures (Brevard County, 2023). A permanent managed-flow structure would provide another tool in maintaining a healthy ecosystem in the hydrologically restricted IRL estuary.

4.2 Modeling (Task 2)

The hypothesis of this project states that controlled water exchanges from the coastal ocean into the BRL can be engineered to improved water quality within local compartments of the IRL. A second project hypothesis is that salinity, water temperature, and water level fluctuations generated by an engineered inflow will be small compared to the seasonal fluctuations and event scale fluctuations experienced in the IRL. The Phase 3 model deliverables had a goal to directly support the permit application for implementing temporary pumping of ocean water into the north BRL. Objectives of the modeling task were to:

- Expand the Phase 2 hydrodynamic and water quality model to cover boundary conditions through mid-2022.
- Assemble supporting watershed inputs to mid-2022.
- Establish inflow boundary conditions at Port Canaveral from ongoing water quality monitoring reports compiled by Port Canaveral.
- Update model boundary conditions.
- Refine computational model grid to accommodate inflow locations at Port Canaveral.
- Validate the model based on the existing database of physical and water quality conditions augmented by ongoing measured environmental nutrient and DO data sets.
- Consult with project geochemical team members with respect to nutrient and DO inputs to the water quality model, as well as model calibration.
- Conduct model predictions of water quality conditions in BRL and IRL with and without enhanced inflows at rates prescribed by the pilot project permit.
- Conduct model predictions of water quality conditions in BRL and IRL with and without enhanced inflows at rates that could be associated with a full-scale project.
- Permit directed model runs designated by the Project Team and Tetra Tech designed to anticipate permit requirements.
- Delivery of model predictions of salinity, water temperature, and water quality to support analyses other project team members.
- Update the ongoing archive of all model output data that can be interrogated to provide permit requirements and address RAIs as needed.
- Generate a final report and associated graphics describing the results of environmental and coastal processes modeling.

4.2.1 Approach

The Environmental Fluid Dynamics Code (EFDC)/Hydrodynamic Eutrophication Model Three-Dimensional (HEM3D) coupled hydrodynamic and water quality models were applied to quantity the potential water quality results of the Enhanced Inflow Pilot Project. The intake location of the

project will be a location just to the east of the Canaveral Lock system. The model computational grid area extends from Ponce de Leon Inlet north of the Mosquito Lagoon into the IRL compartments extending to the Fort Pierce Inlet. This multi-parameter finite difference model represents estuarine flow and material transport in three dimensions and has been extensively applied to shallow estuarine environments in Florida and other coastal states. For Phase 3, refinements were made to the model computational grid to resolve the pump inflow area in the BRL on the south side of Port Canaveral. Model boundary conditions were updated to include conditions into mid-2022. The final model runs to test various pumping scenarios covered the period from January 2021 through May 2022.

An update of model verification was also completed consisting of model runs of the previous calibrated model to test model performance for the new time period of model production runs. This process is termed model validation, which consists of model-observation comparisons without any further adjustment of model tuning parameters.

Model production runs consisted of four cases: existing configuration of no enhanced inflows, two inflow cases involving inflows of 0.5 m^3/sec and 1.0 m^3/sec, and hypothetical inflows originating from the coastal ocean that assumed lower nutrient concentrations and higher DO concentrations compared to the ambient water quality of Port Canaveral. The water quality of specified inflows from Port Canaveral were set from monthly data from the ongoing monthly environmental surveys by the Canaveral Port Authority. Model results for each case were compared for predicted changes in salinity, water temperature, DO, and concentrations of water column TN and TP.

4.2.1.1 Grid Refinement

Figure 8 shows the overall extent of the IRL model computational grid, from Ponce de Leon Inlet in the north to just south of Fort Pierce Inlet at the south end. Under Phase 3, additional refinements to the model grid were completed to improve spatial resolution in the BRL at the location of the proposed inflow location to the west of Port Canaveral (**Figure 9**).
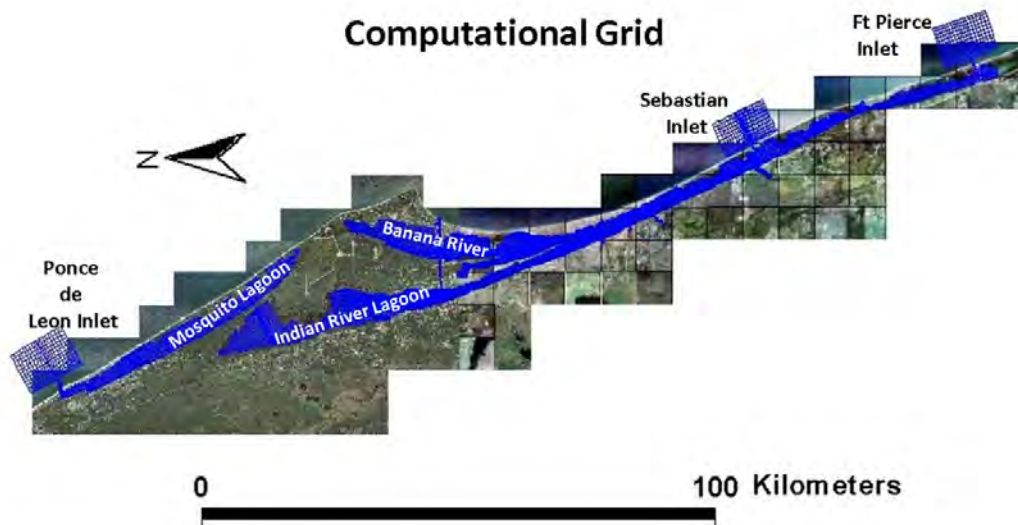
Figure 9. Computational model grid extending from Ponce de Leon Inlet to Fort Pierce Inlet
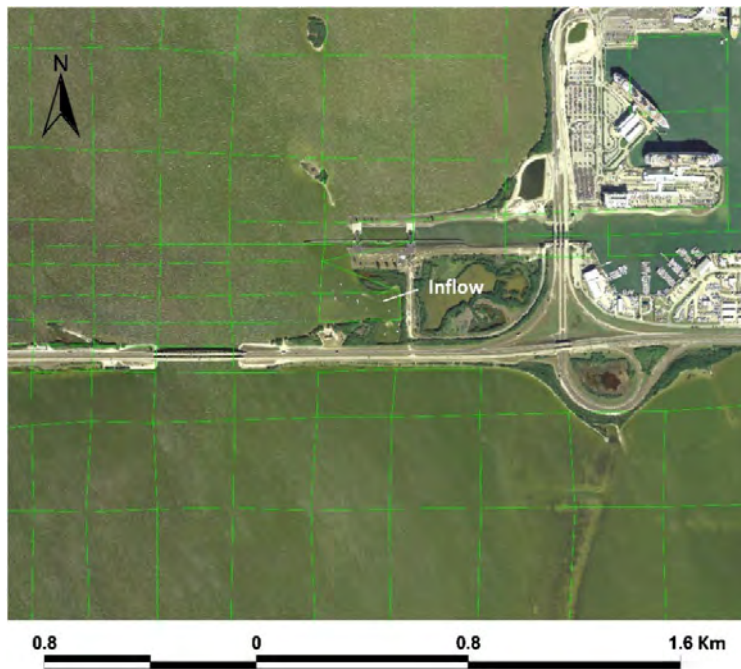
Figure 10. Computational grid refinements in the BRL to accommodate an inflow boundary condition from Port Canaveral

4.2.1.2 Hydrodynamic Model Calibration.

Model calibration results for the IRL model were originally described in Zarillo and Listopad (2016) and updated for an expanded model in Fox et al. (2017) and RLI Phase 2 (Florida Tech 2021). The calibration effort produced predicted water levels having root mean square errors (RMSE) between 5.45 centimeters (cm) (5.5% error) at the Wabasso Bridge USGS station, and 6.1 cm (6.1% error) at the USGS Haulover Canal station (**Figure 10**). Water level calibration is expected to hold for the present model application since model hydrodynamic boundary conditions are from the same sources.
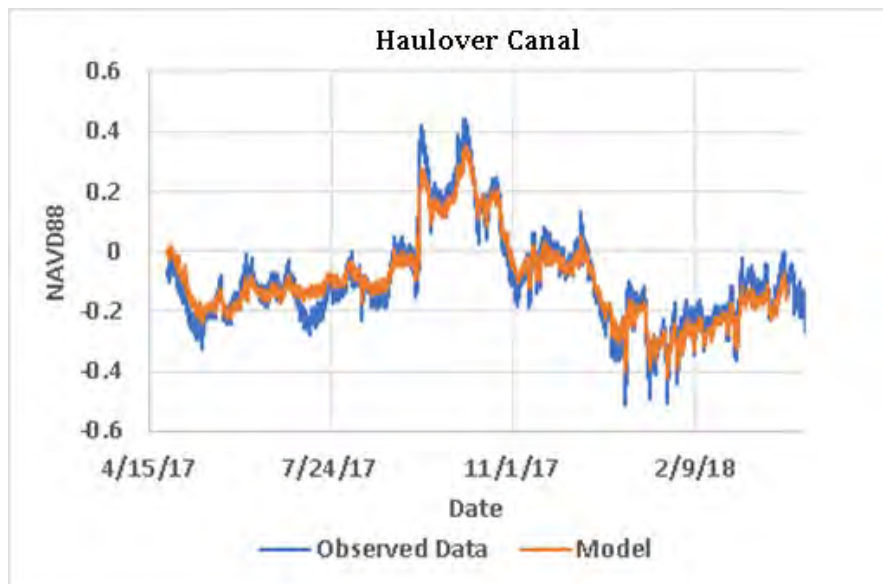
Figure 11. Observed and predicted water levels at Haulover Canal, north Brevard County

Calibration results for salinity and water temperature data were provided by Zarillo & Listopad, 2020 and updated for RLI Phase 2 (Florida Tech 2021). Comparison of predicted salinity values with observed salinity data presented RMSE representing 12% error of 2.7 practical salinity units (PSU) at Florida Atlantic University Harbor Branch Oceanographic Institute's Land/Ocean Biogeochemical Observatories (LOBO) station IRL-SB (**Figure 11**) and 18% error (2.68 ºC) when comparing datasets for temperature (**Figure 12**).
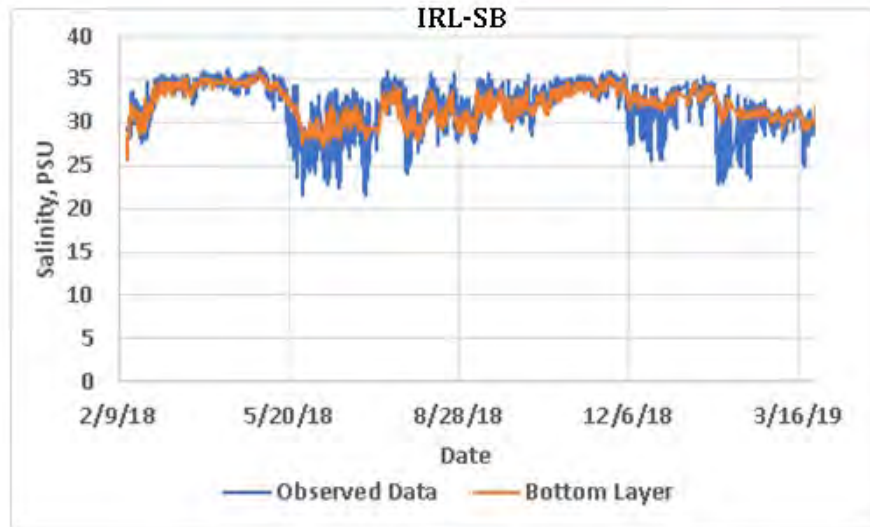
Figure 12. Comparison of observed and model salinity values recorded at LOBO station IRL-SB in the IRL near Sebastian Inlet
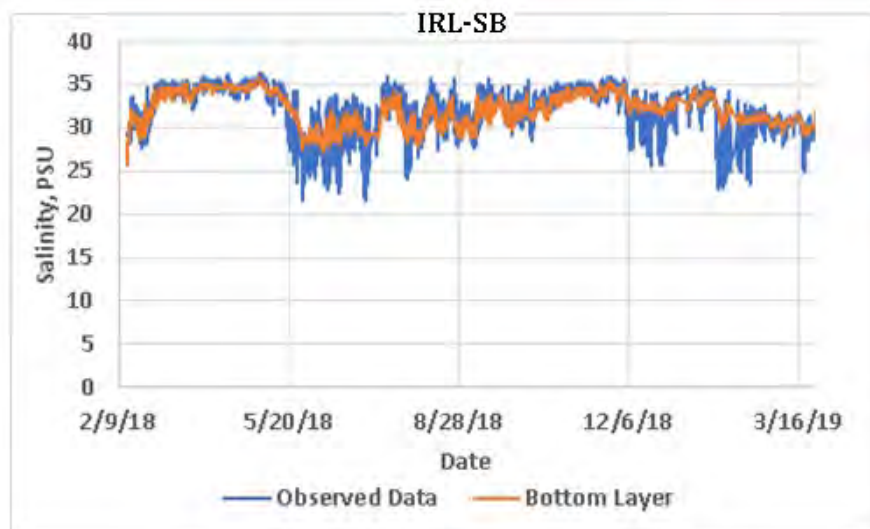
Figure 13. Comparison of observed and model water temperature values recorded at LOBO station IRL-SB near Sebastian Inlet

Verification of the EFDC/HEM3D water quality calculations in the IRL system is an ongoing process. Operation of the water quality model depends on several input files that contain measured data from a variety of sources. However, at this stage of development, predictions of water quality constituent concentrations in the water column align well with measured data.

Chemical species such as PO_4, NOx, and labile and refractory components in the total loads are only estimated. Thus, only model-observation comparisons for TN and TP are considered. DO and chl-a concentrations are also considered at locations where the observed data are deemed to be of good quality along with data from more continuous monitoring stations where statistical comparison are more robust.

4.2.1.3 Model Validation

Under validation, the EFDC model performance was further verified without any adjustments and during a period differing from the calibration period. In this exercise, model performance was validated for the 2021 to 2022 time period of Phase 3. Emphasis was placed on validating model performance in the BRL for major water quality parameters including TN, TP, and DO. Model performance for salinity and water temperature was also validated.

Figure 13 compares measured and model salinity data between January 2021 and May 2022. After an approximate accounting for a 100-day spin-up period, measured and model data agree within a RMSE of 0.53 PSU. Figure 14 compares measured and modeled water temperature at the same IRLB04 location. The comparison results in a RMSE of 1.25 ºC, which for a 21.8 ºC observed temperature range, is equivalent to an error of about 5.7%.
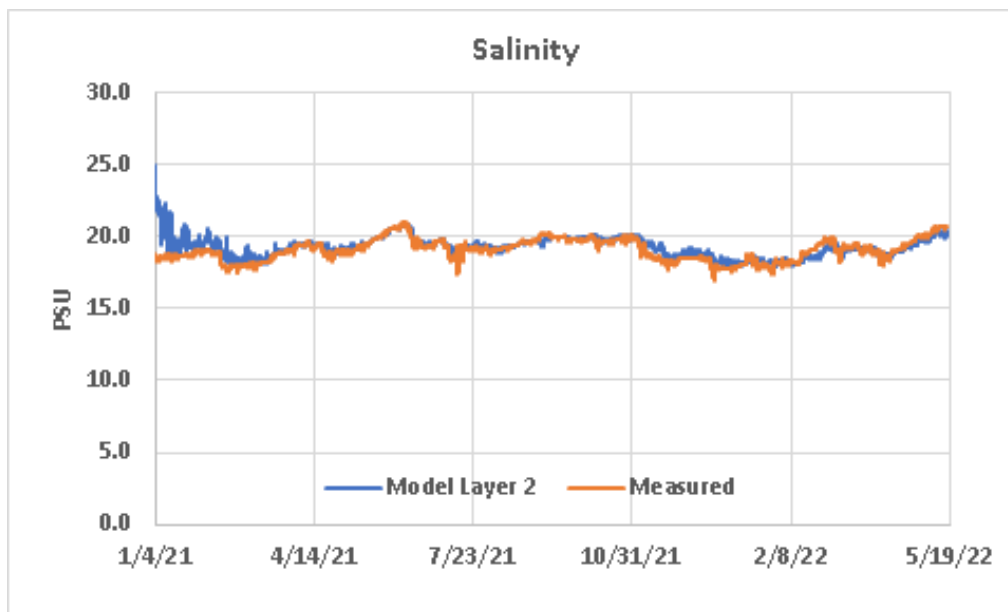
Figure 14. Comparison of measured and model salinity data at Station IRLB04
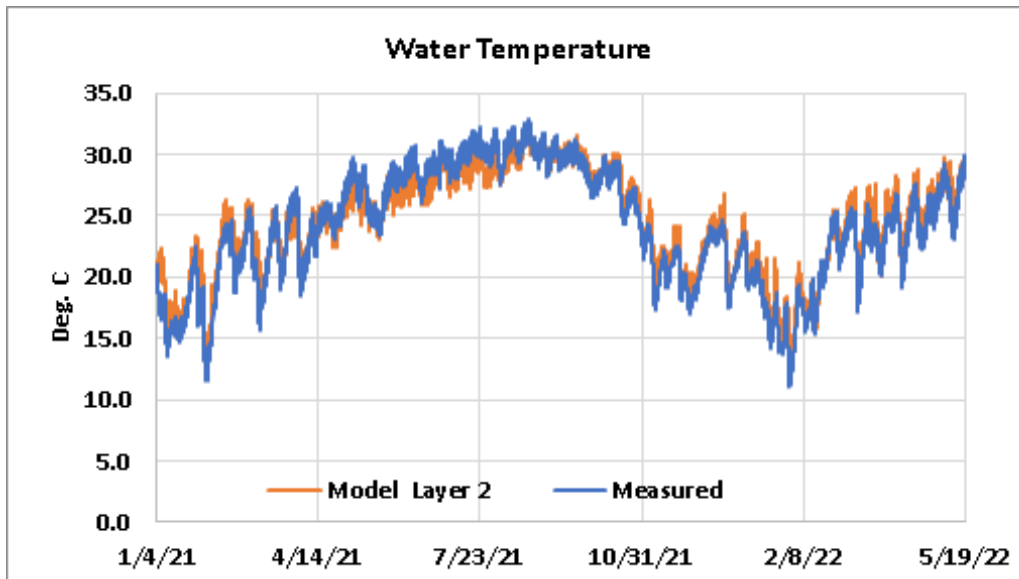
Figure 15. Comparison of measured and model water temperature data at Station IRLB04

In addition to salinity and water temperature, continuous measurements of DO were compared to two available data sets, including Station IRLB04, located 4 km south of Port Canaveral where DO is collected on an hourly basis. If the zero values plotted among the measured data in **Figure 15** are sensor issues rather than good data, the error would be about 13%. This is due to the reduced range of observation values in the RSME/range comparison. In either case, the comparison is very good and in line with the calibration results. The average DO concentration value of measured data is 8.22 milligrams per liter (mg/L) compared to an average of 8.55 mg/L for the model data. Thus, the measured and model DO averages are well within 1 mg/L.
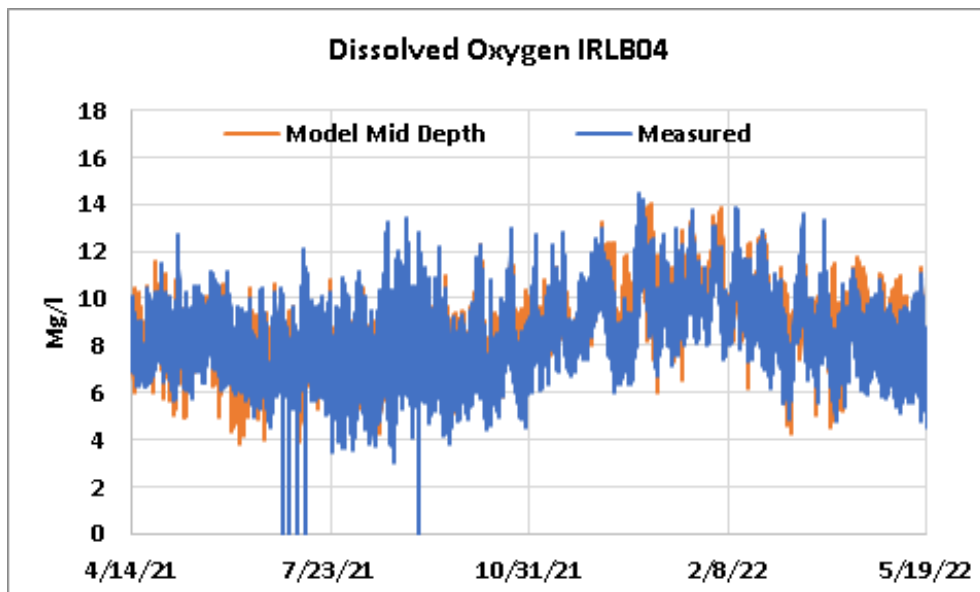
Figure 16. Comparison of measured and model DO data at Station IRLB04

The best comparison of measured TN at Station IRLB04 is with predicted TN in the model surface layer as shown in Figure 16. Here the SJRWMD data collected at monthly intervals and compared

to model data output at 2-day intervals. The average measured and model TN values are very close at 1.07 mg/L and 1.03 mg/L, respectively. This represents a relative error of 3.7% with respect to the average value of the measured and model TN time series.
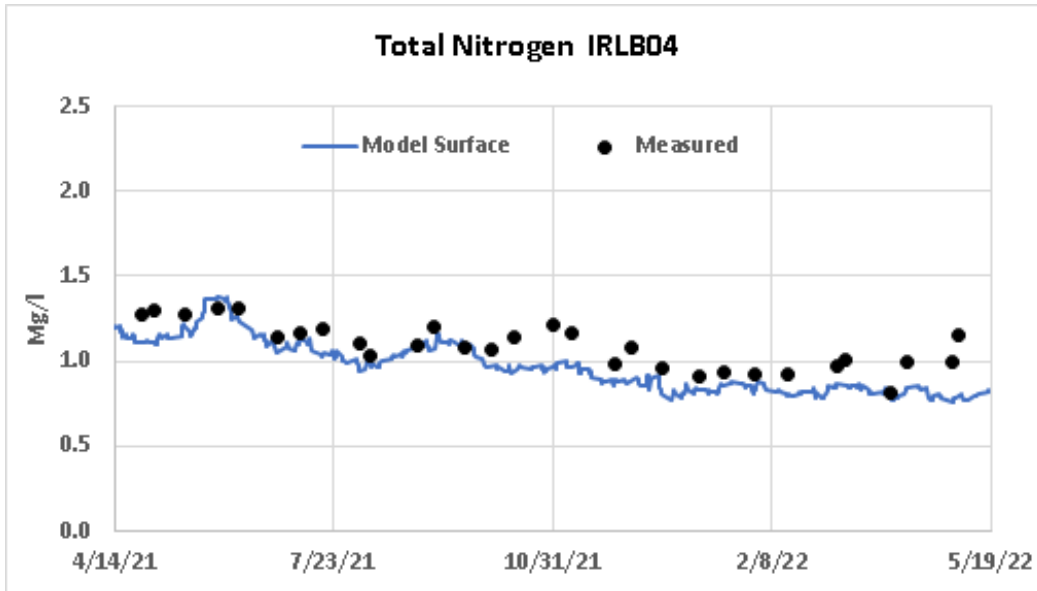
Figure 17. Comparison of measured and model TN data at Station IRLB04

Average TP concentrations closely agree at 0.058 mg/L for the measured data and 0.050 mg/L for average predicted concentration in the model surface layer. The relative error with respect to the measured and model time series average values is 13.9% (**Figure 17**).
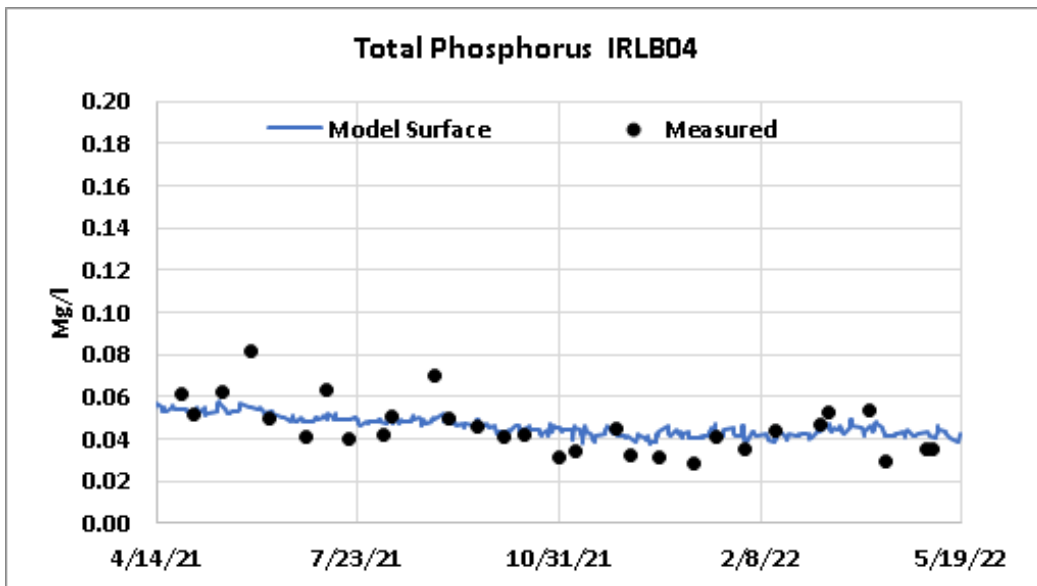
Figure 18. Comparison of measured and model TP data at Station IRLB04

4.2.2 Model Results

The model runs were completed for no inflow and compared to inflow using port water quality parameters with a 0.5 m³/sec and 1.0 m³/sec inflow rate. Additionally, a comparison using ocean water quality data and a flow of 1.0 m³/sec was also used. Results of the model runs are summarized for the vicinity of the inflow area. **Figure 18** shows the location of the model computational cells from which model data were extracted for each case.
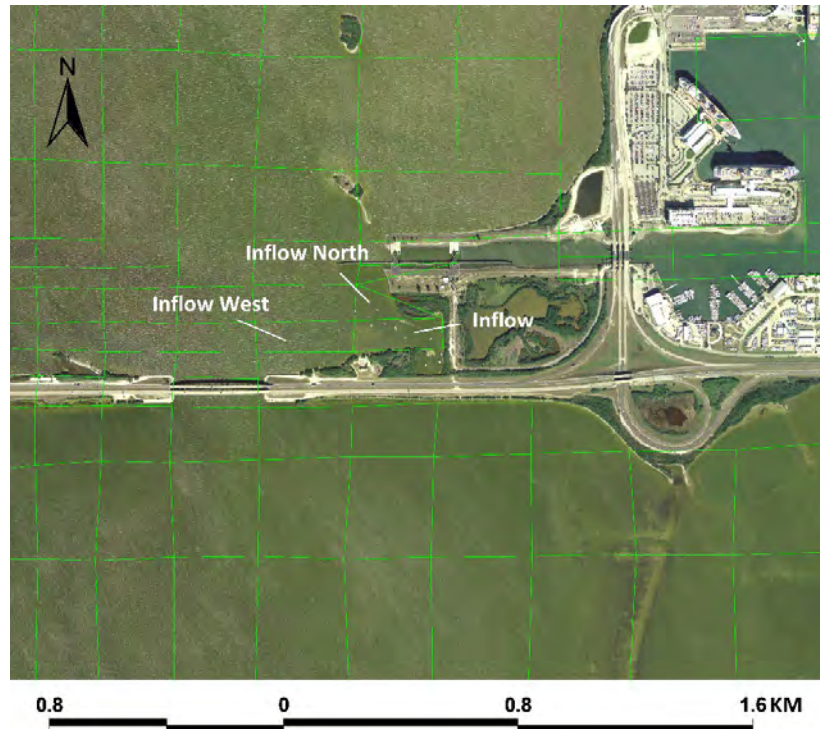
Figure 19. Model cells designated Inflow, Inflow North, and Inflow West from which model data were extracted to compare the results of each model case

4.2.2.1 Salinity

Model results for the test cases are summarized in **Figure 19**. A slight increase in surface to bottom salinity is predicted for the three-monitoring location as shown in **Figure 19**. The maximum predicted increase of 1.71 PSU is seen in the bottom layer of the model cell containing the inflow location. This occurred under the 1.0 m³/sec inflow. The minimum increase in salinity of 0.3 PSU is predicted in the Inflow West cell under the 0.5 m³/sec inflow.
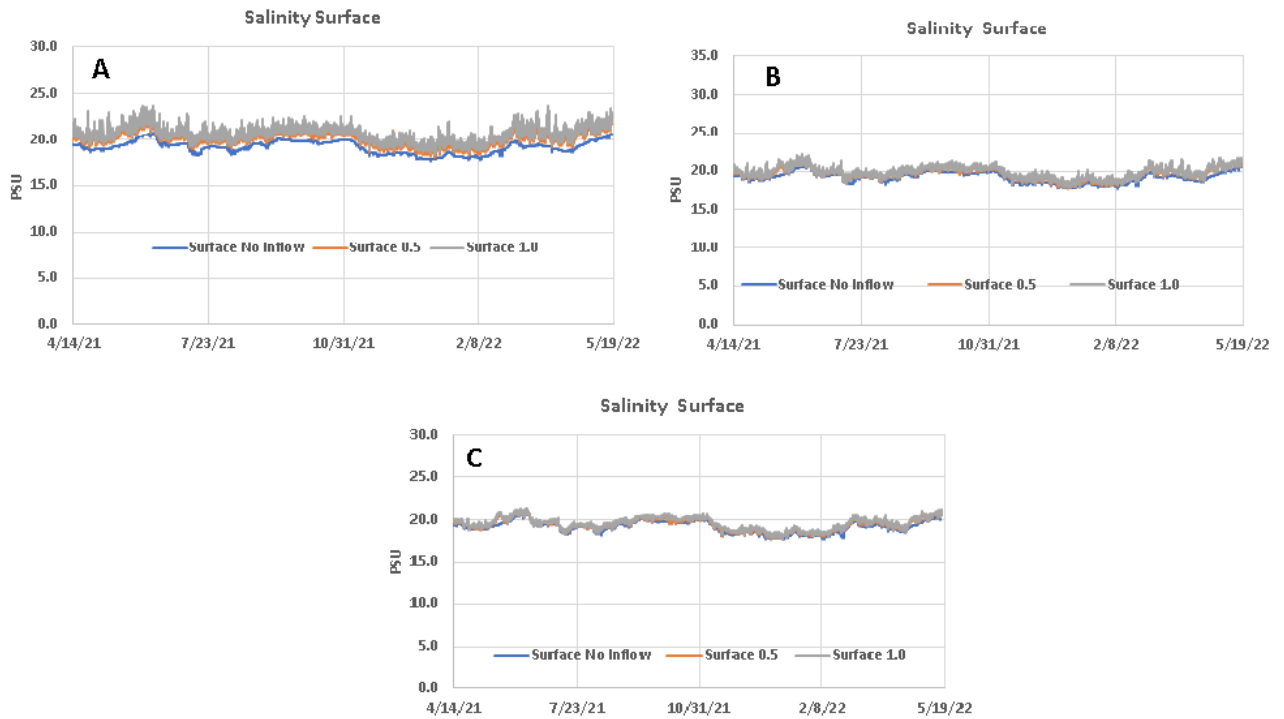
Note: Cell locations shown in Figure 18. Numbers assigned in the legend indicate the inflow rates of 0.5 m³/sec and 1.0 m³/sec.

Figure 20. Salinity predictions in the surface model layer for the Inflow cell (A), Inflow North cell (B), and Inflow West cell (C)

4.2.2.2 Water Temperature

Model test case results for water temperature are best represented in the bottom model layer as shown in **Figure 20**. Inflows of 0.5 m³/sec and 1.0 m³/sec produced slightly higher water temperatures in the surface layer of the model. The seasonal signal of lower winter temperatures is also apparent in **Figure 20**.

Note: Cell locations shown in Figure 18. Numbers assigned in the legend indicate the inflow rates of 0.5 m³/sec and 1.0 m³/sec.

Figure 21. Water tempeature predictions in the surface model layer for the Inflow cell (A), Inflow North cell (B), and Inflow West cell (C)

4.2.2.3   DO

DO predictions are represented in **Figure 21**. The most apparent impact of prescribed inflows is in the bottom model layer where predicted increase in DO concentration is most easily observed in the time series plots. Model predictions followed an expected pattern of higher DO values in the surface model layer and lower concentration in the bottom layer. Higher DO concentrations are also predicted for the winter of 2022.

Differences in DO concentration among the cases were mostly less than 1 mg/L within a model layer. Model results indicate that pilot project inflows are likely to produce measurably higher DO in the vicinity of the inflow. Predicted increase in DO values in the model cells adjacent to the inflow cell are lower, but still measurable in the model results.

Note: Cell locations shown in Figure 18. Numbers assigned in the legend indicate the inflow rates of 0.5 m³/sec and 1.0 m³/sec.

Figure 22. DO predictions in the bottom model layer for the Inflow cell (A), Inflow North cell (B), and Inflow West cell (C)

4.2.2.4 TN

N predictions in the EFDC/HEM3D model can be reported as the individual component of N subspecies or as TN water column concentrations. Since the model calibration and validation results are reported based on comparisons with TN vales measured at SJRWMD monitoring stations, model results are reported as TN. Model results for TN are similar in all model layers and are shown for the surface layer in **Figure 22**. Model predictions indicate a slight decrease in TN concentration with increased pumping. Like the DO predictions, improvements from the hypothetical inflows are small but measurable in the model predictions.
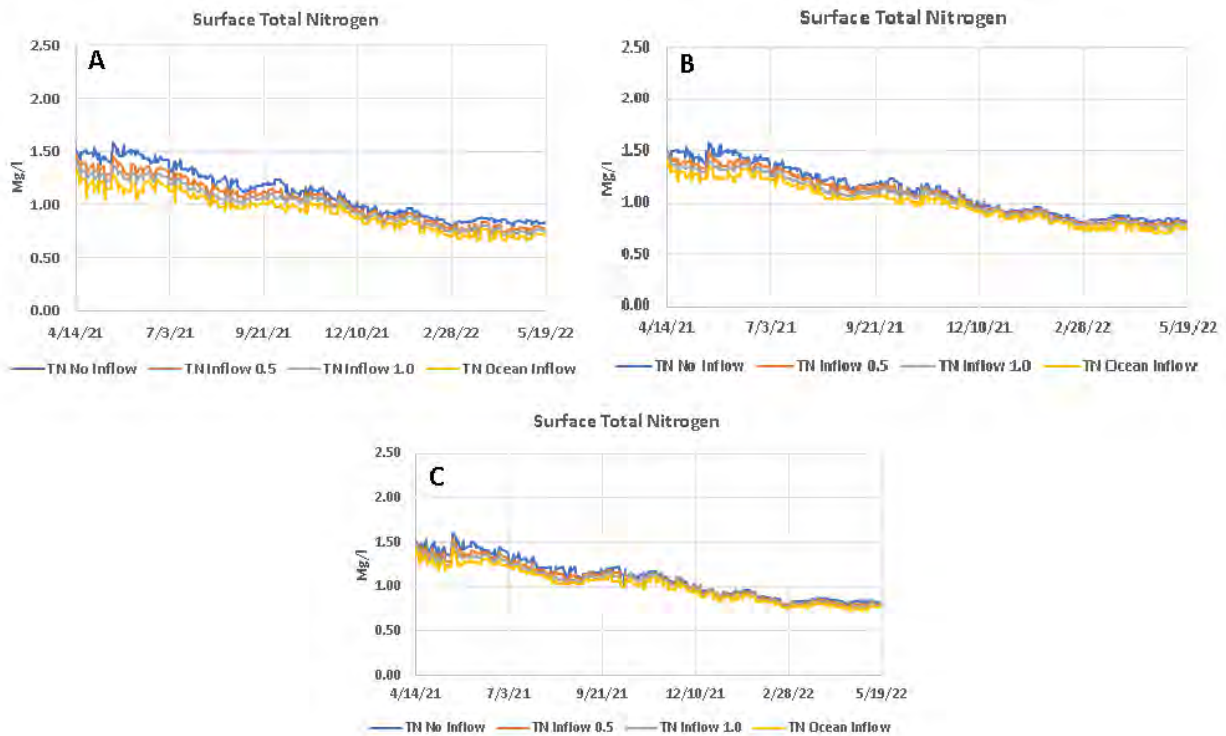
Note: Cell locations shown in Figure 18. Numbers assigned in the legend indicate the inflow rates of 0.5 m³/sec and 1.0 m³/sec.

Figure 23. TN predictions in the bottom model layer for the Inflow cell (A), Inflow North cell (B), and Inflow West cell (C)

4.2.2.5   TP

Like N predictions, P prediction is reported as TP water column concertation in each of the five vertical model layers. Model results for TP concentrations are similar across the model layers as shown for the surface layer in **Figure 23**. Water column concentrations of TP are an order of magnitude lower than precited TN concentration, which is consistent with the comparison of measured and predicted concentration values reported in the model validation section of this report.

Predictions indicate TP concentrations over the water column model layers only vary slightly. However, like the DO and TN predictions, improvements from the hypothetical inflows are small but measurable in the model results. The influence of the hypothermal inflows is traceable through all three monitoring cells, but slightly decrease with distance from the inflow cell as visually apparent in **Figure 23**.
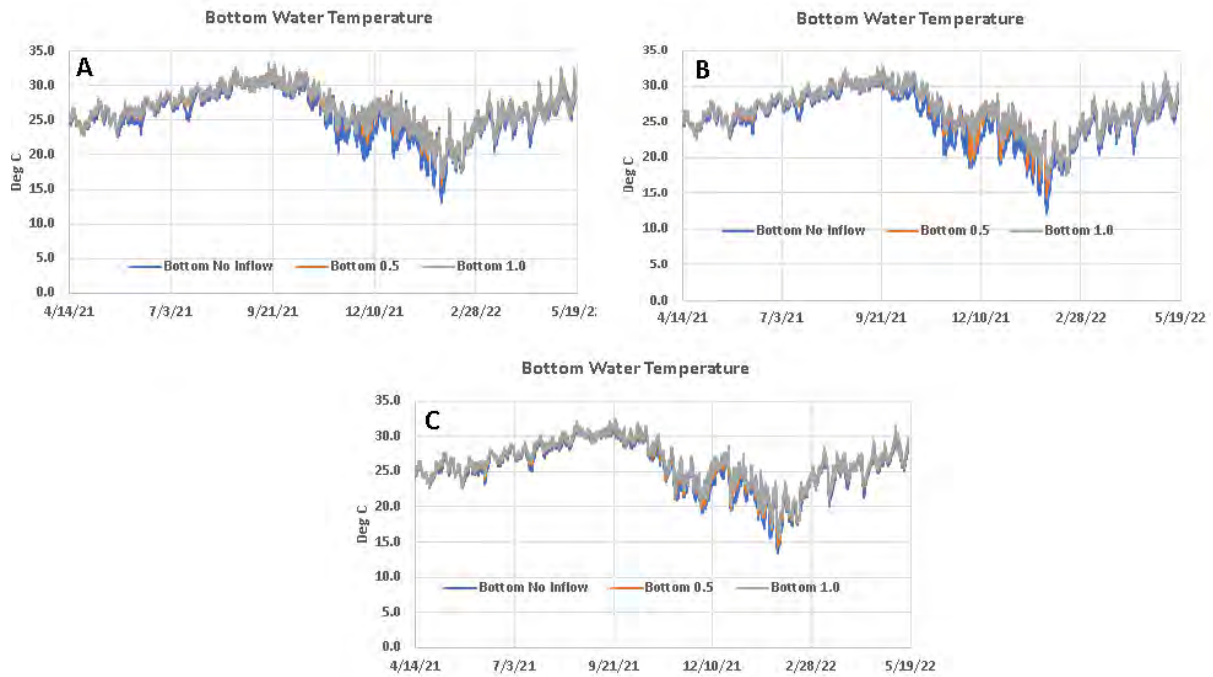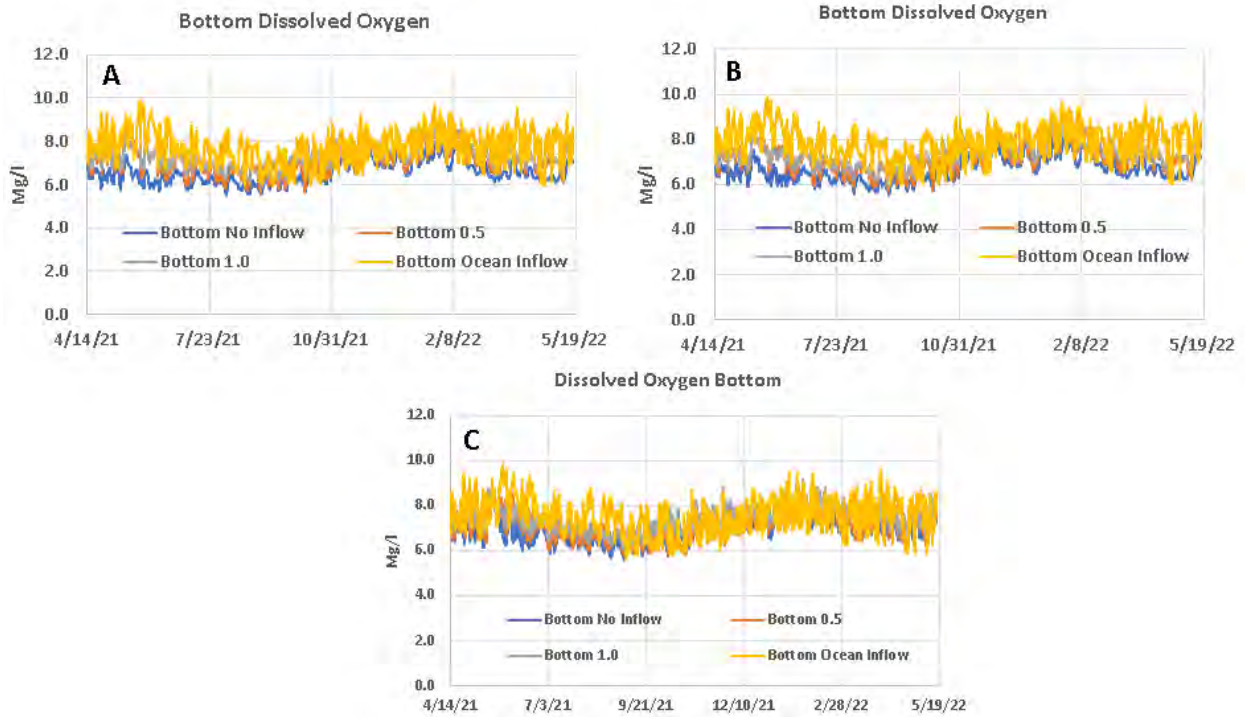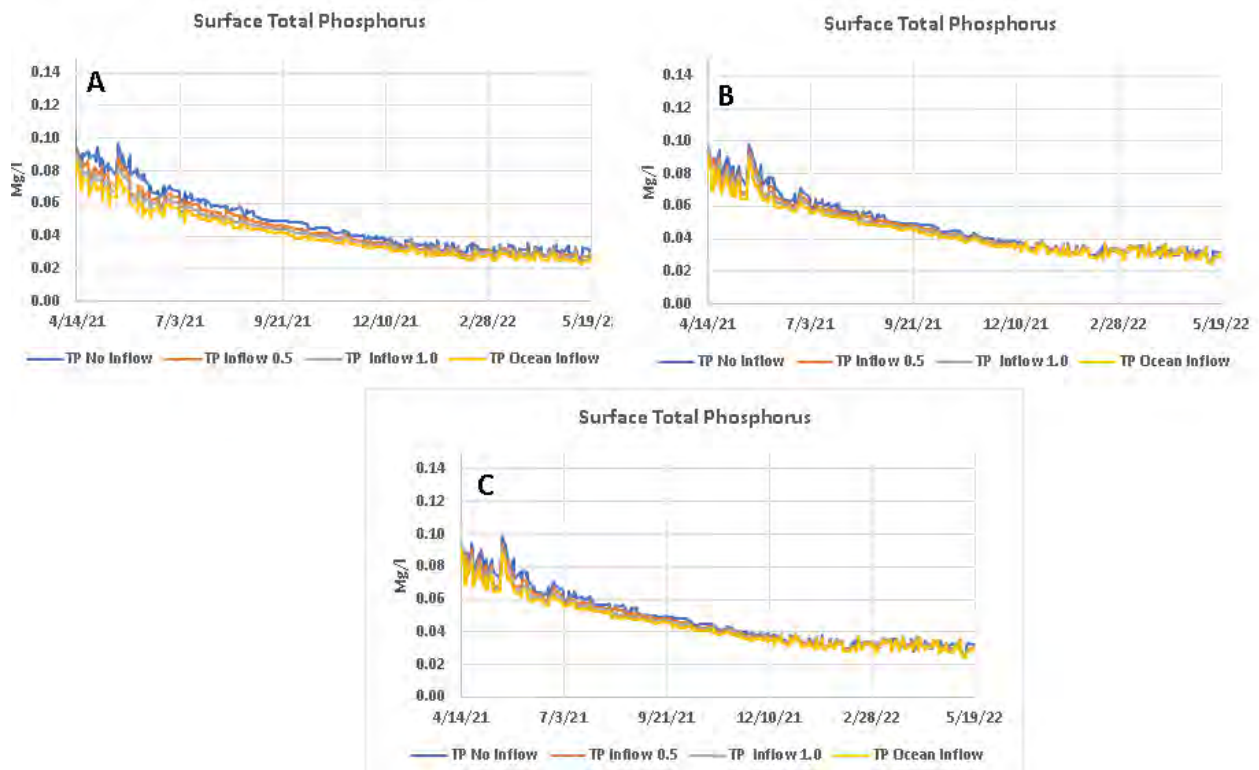
Note: Cell locations shown in Figure 18. Numbers assigned in the legend indicate the inflow rates of 0.5 m³/sec and 1.0 m³/sec.

Figure 24. TP predictions in the bottom model layer for the Inflow cell (A), Inflow North cell (B), and Inflow West cell (C)

4.2.3 Conclusions

Modeling in the Phase 3 project was focused on assessing the potential influence on water quality of a BRL compartment from small inflows rates pumped from an intake located at the west end of Port Canaveral. Thus, the expected impact is small in comparison to the Phase 2 model tests in which inflow pumping rates of up to 10 m³/sec were tested. The overall goal was to verify that small inflow into a confined area of the BRL can be used to assess the potential benefits of much higher inflows rates on the greater BRL. Another goal was to confirm that a pilot project involving lower inflow rates will not have a negative impact on the receiving basin and provide the basis for answering concerns that may arise during the pilot project permitting process.

Model tests produced measurable changes among the test cases, but no large changes in salinity, water temperature, or water quality constituent concentrations were predicted that could produce a significant negative impact during the pilot inflow project. Further, the results of the model cases indicate a slight improvement in water quality within the pilot project test basin under lower inflow rates.

Limitations of the model testing are based on the low temporal resolution of water quality measurement in both the BRL and within Port Canaveral. Since water quality data in the BRL and Port Canaveral can overlap in value, both the modeling and monitoring efforts would benefit from more continuous collection of water quality data.

4.3 Geochemistry (Task 3)

Coastal eutrophication and associated hypoxic events remain one of the greatest challenges facing coastal communities on a global scale (Diaz and Rosenberg, 2008). As the eutrophic state of an estuary progresses, loss of ecosystem services such as coupled nitrification–denitrification and sequestration of P that would, in healthy systems, remove or sequester nutrients, contributes to cascading events and a series of positive feedback loops helping to sustain eutrophication. These changes can lead to non–linear ecosystem level responses to eutrophication sometimes leading to alternate, algal dominated stable states compared to healthy seagrass dominated systems. Such is the case in the IRL, which has been referred as a regime shift that among other things corresponded with an increase in dissolved phosphate concentrations (Phlips et al., 2021). It is possible that restoring historic balances of freshwater and seawater could help restore these services.

Enhanced circulation in the IRL could contribute towards lowering nutrient concentrations that support the onset and proliferation of algal blooms. Another potential benefit would likely be to increase and or stabilize the concentration of DO, yielding enhanced resilience to anoxia and fish kills. The main benefits of decreased respiration and nutrient concentrations, and stabilized DO would likely result from changes to geochemical cycling. Any impacts from direct dilution by seawater would be spatially limited and considered secondary benefits.

Studies were completed by Florida Tech and UWF concurrently, with integrated sampling and analyses where appropriate. Separate reports were prepared.

The Florida Tech study investigated the potential of ocean inflow to decreases nutrient concentrations through (1) sequestration of P in sediments and removal of N via coupled nitrification–denitrification and or anammox, and (2) direct dilution by mixing where nutrients would be discharged to the coastal Atlantic Ocean. This study also investigated how these geochemical removal mechanisms would be altered as a function of changes to temperature, salinity, and DO and began to investigate how secondary impacts related to improved habitat quality may influence nutrient cycling.

The objectives of the Florida Tech geochemistry task were:

- **In–situ nutrient cycling:** Investigate temporal trends for biogeochemical processes (nutrient and oxygen cycling plus temperature and salinity regimes) in sediments and water near the inflow location. During Phase 3, sediments from benthic chambers were collected and sent to UWF for bacterial analysis. This collaborative effort helped to link temporal changes in nutrient cycling to the bacterial communities present and active in lagoon sediments. The collaborative effort helped to distinguish changes related to bacterial versus geochemical processes while providing another quantifiable impact of hypoxia, helping to validate a mechanism by which inflow might improve water quality (e.g., increased abundance of nitrifying bacteria).
- **Laboratory nutrient cycling to quantify potential changes/benefits of inflow:** Laboratory experiments were carried out to determine how changes to DO that could result from inflow N influence the biogeochemical cycling of N, P, and oxygen in lagoon water and sediments. Experiments built upon results from Phases 1 and 2 and added an evaluation of how changes to the ecosystem have impacted the sediments' ability to sequester P over time. In collaboration with UWF, Florida Tech determined if chronic diel or episodic hypoxia impacts nitrifying bacterial communities and thereby nutrient cycling. This next step helped to quantify the sediments' ability to sequester P as diel or episodic

hypoxic events are mitigated by enhanced circulation and provided additional evidence that inflow could promote nitrification an essential step in the N cycle and removal of N from the system.

- **Track potential extent of impacts with focused monitoring:** Datasets for temperature, DO, and salinity in bottom water from select sites were monitored continuously to establish baseline data and trends from which changes associated with a pilot project could be compared. Based on results from Phase 2, existing, spatially limited, monitoring networks (e.g., SJRWMD) with sensors located at mid depths are of limited use towards tracking potential biogeochemical changes associated with a pilot inflow project. In other words, biogeochemical processes that would respond to inflow are focused on the sediment-water interface. Therefore, to track impacts of inflow and provide information to modelers, temperature, salinity, and DO were monitored in key areas. Tracking changes to temperature, salinity, and DO are key to demonstrating feasibility and success of inflow towards improving water and sediment quality. These data showed how processes measured in tasks 1 and 2 impact and apply to broad areas of the lagoon providing a metric to quantify broader impacts on a landscape scale. Continued evaluation of, if, and where data from few existing water quality sensors (approximately 0.5 to 1.0 meter [m]) can be extrapolated to determine conditions in the complete water column (e.g., bottom water). These comparison data help to highlight the importance of diel and episodic hypoxic events focused on the bottom of the lagoon. An understanding of the temporal and spatial extent of hypoxia at the sediment water interface has implications to estuaries around the world while demonstrating how inflow of cool, saline seawater will have the greatest impact at the bottom. This task provided data to modelers allowing them to determine the spatial extent to which mechanisms investigated in tasks 1 and 2 would be altered, thereby enabling a calculation or modeling of the change in nutrient loading based on various inflow volumes using data from the demonstration project.
- **Share data among tasks:** Temporally and spatially resolved data for nutrient cycling in sediments and water are essential for biological and physical modelers. Data from were shared with teams at Florida Tech and UWF at regular intervals throughout the project.

UWF activities in support of the Restore Lagoon Inflow project provide broader interpretation and context for the Phase 2 and 3 project results, specifically those addressing how improved inflow may assist in remediation of the IRL sediment geochemistry. Destin Harbor has been used as a model to design the Restore Lagoon Inflow project, but a detailed examination of the long-term effects of how the pumping system in Destin Harbor affects water quality has not been conducted. UWF goals also included analyses of these data to provide useful information for the Restore Lagoon Inflow project. UWF efforts focused on three major tasks: (1) evaluating existing water quality data from Destin Harbor, (2) assessing fluctuations in communities that affect N cycling and IRL water quality by measuring abundances of key microbial groups performing nitrification and dissimilatory reduction of nitrate to ammonium (DNRA), and (3) evaluating existing IRL water quality monitoring data for conditions outside seagrass tolerances of salinity and DO. For the microbial community work, UWF examined sediments from IRL sites, as well as shallow and deep seagrass reference sites in the Florida Panhandle in SRS to compare with the IRL reference site.

The objectives of the UWF geochemistry task were:

- **Quantify abundance of key N transforming prokaryotes**: Conducted quantitative Polymerase Chain Reaction (qPCR) of sediment samples collected at sediment/water nutrient flux sites in IRL. Samples were collected during monthly IRL benthic chamber deployments. Sediment samples were also analyzed for Chl-a.

- **Assessment of microbial and biogeochemical responses**: Sampling conducted at Florida Panhandle reference sites. Benthic fluxes and porewater nutrients were measured in a shallow seagrass site colonized by *Halodule wrightii* and a deeper site colonized by *Thalassia testudinum*.
- **Review and assessment of existing Destin Harbor water quality data:** Directly compliments the Task 1 effort with field sampling to determine how operation of the Destin pumping system affects water quality.
- **Review salinity and light attenuation key factors limiting seagrass growth and restoration**: Comparison of existing water quality monitoring data in the BRL to tolerances of *Halodule wrightii* and *Syringodium filiforme,* the two dominant species in the IRL.

4.3.1 Florida Tech Approach

4.3.1.1 Sampling and Monitoring

Sediment and water samples were collected from the IRL and SRS using various methods to ensure proper collection, preparation, and preservation of samples for each of the various analyses, as described in the Geotechnical Task 3 reports (Appendices C and D). Water column respiration was measured using benthic chambers deployed in the IRL and SRS. Sediment samples were also collected from sandy sediments to evaluate benthic flux from infauna (**Macoma spp.**), bio irrigation of sediments.

Continuous monitoring for DO was also conducted with sensors located in Port Canaveral (n=1), inflow site (n=3) and reference site (n=2). Additional sensors distributed throughout the BRL and supported by other projects provided a complimentary reference for tracking regional DO patterns.

Building upon efforts from Phases 1 and 2, long–term datasets for temperature and salinity for IRL were obtained and updated for 1987 through July 2023 from sources including SJRWMD and the network of sensors deployed and maintained by Florida Tech. Long term temperature records for the port at Trident Pier were obtained from 2005 to July 2023 (the complete record) from the National Oceanic and Atmospheric Administration's National Data Buoy Center.

4.3.1.2 Water Analysis

Water samples were analyzed as follows:

- Concentrations of ammonium (NH_4), NOx, TDN, PO_4, and TDP were determined for IRL samples.
- Aerobic P sorption/desorption.
- Anaerobic P sorption/desorption.

4.3.1.3 Sediment Analysis

Sediment samples were analyzed as follows:

- Organic matter content was determined using loss on ignition by combusting freeze–dried and desiccated sediments at 550 °C following methods of Heiri et al. (2001).
- Aerobic P sorption/desorption.
- Anaerobic P sorption/desorption.
- Oxygen and nutrient flux.

4.3.2 Florida Tech Results and Discussion

Numerous studies have reported on attempted remediation of eutrophic coastal systems with examples of both successful restoration of ecosystem functions; however, restoration efforts in other areas have been less successful. Overwhelmingly the literature points to the complexity of eutrophication and hypoxia with varied responses to restoration in different systems highlighting the need for system–specific management and remediation that account for both external and internal loading plus physical and ecological processes. In IRL, the importance of these internal changes to ecosystem functioning is underscored by the change to a new stable state, "regime shift" that occurred following the 2011 algal blooms, despite no significant associated change in external loading. Therefore, it is essential to consider how restoration will impact internal processes. For example, direct exchanges of lagoon and seawater provide limited direct benefit as discussed in detail below and as indicated by models; however, small changes to water and sediment quality can alter ecosystem functioning and internal nutrient cycling to yield potentially large benefits at the landscape scale. In addition to subtle geochemical changes that occur over a large spatial and temporal scale, enhanced circulation would certainly help to mitigate extreme temperature of salinity events in IRL thereby helping to mitigate further declines in ecosystem functioning.

4.3.2.1 Temperature

One major benefit of ocean inflow would be buffering against extreme temperature events in IRL and BRL. For example, the "regime shift" in IRL is often causally associated with exceptionally low temperatures, <4 °C, in the lagoon during winter 2009/2010 (Phlips et al., 2021). In addition to buffering extremes, higher temperatures contribute to enhanced internal nutrient loading. Bacterial metabolism increases non–linearly as a function of temperature. As a result, small changes in water temperature can significantly impact rates of bacterial metabolism. On a landscape scale (square kilometers) this can lead to major changes in nutrient cycling and internal loading. For example, IRL benthic fluxes increased by 7% to 10% per °C with cooler temperatures leading to less nutrient recycling and ultimately lower concentrations (Fox and Trefry, 2018; Boynton et al., 2023). Additionally, the solubility of DO changes with temperature and cooler water is more resilient to hypoxic events and fish kills.

Overall, variability in temperature was greater in IRL with more rapid and more extreme changes in response to atmospheric weather patterns. For example, the minimum temperature in BRL near the inflow site was 11.8°C in January 2023 compared to approximately 20°C at Trident Pier in Port Canaveral. On the other end of the spectrum, maximum lagoon temperatures were higher than maximum temperatures in Port Canaveral and the coastal Atlantic Ocean, being on average about 1 to 3°C warmer during summer months.

Based on these data plus long–term datasets, inflow of seawater could help buffer against extreme temperature events that have been associated with deteriorated ecosystem health while also decreasing maximum temperatures during the hottest summer months. For example, pumping during winter months could mitigate extreme cold temperature events such as the 4°C temperatures in winter 2009/2010 when at the same time Port Canaveral reached a minimum of 12.5°. This extreme temperature event, even though short in duration, is often causally associated with a mass mortality of tropical and subtropical species, creating a supply of nutrients ultimately leading to a regime shift (Phlips et al., 2021). A similar cold event in Laguna Madre, Texas during 1989 contributed to a mass mortality event that supplied nutrients spawning algal blooms that persisted for 8 years (Buskey et al., 1996; 1997). In cold environments the opposite has been reported where high temperatures led to mortality of temperate species (e.g., Edwards et al., 2006).

4.3.2.2 Salinity

It has been proposed that remediation of hypoxia and eutrophication can be enhanced by restoration of habitats for filter–feeding bivalves and seagrass beds (e.g., Kemp et al., 2009). In IRL, recent efforts to restore the hard clam *M. Mercinaria* identified low salinity as one of the major challenges towards clam restoration (ROS, 2023). Also, seagrass meadows are reported in IRL and other locations to experience enhanced stress during low salinity events (Morris et al., 2021). With anthropogenic changes to hydrology, the freshwater watershed has increased by 260% since the 1920s with channelized drainage versus sleuths and wetland leading to more rapid and larger inputs of freshwater following rainfall (Osborn, 2016). Increased freshwater inputs were in most cases not balanced by increased exchanges of seawater. Restoring this balance may help buffer against extreme variability and low salinity events.

Overall, during Phases 1 through 3 of this project, salinity was lower in BRL compared to values for Port Canaveral. Near the inflow site lagoon salinity has trended downwards during the project period (Phases 1 through 3 from 2019 to 2023) decreasing from an average of 21.33 during 2020 to an average of 18.4 so far in 2023. This trend for salinity fits a longer–term regional pattern for decreasing salinity in the northern IRL and BRL beginning in about 2014 when salinity was >35.

4.3.2.3 Density

Collectively, data for temperature and salinity were used to determine the density of the two water masses (lagoon and seawater). Despite lower lagoon versus seawater temperatures during winter months, the higher salinity in the Port resulted in a higher density of seawater during the complete study (seawater density 1,018–1,028 kg/m^3 versus lagoon water density 1,007–1,016 kg/m^3). These data indicate that, regardless of mixing, inflow of seawater would preferentially support circulation in bottom water of the lagoon and at the sediment water interface either as a stratified layer of seawater or as a mixed water mass with a higher density than existing water in the BRL.

4.3.2.4 DO

One consistent change in systems that have experienced a "regime shift" is a change in the system's ability to assimilate nutrients without experiencing hypoxia (e.g., Kemp et al., 2009). Increased occurrences and duration of hypoxia promotes recycling versus removal of both N and P creating a series of positive feedbacks that help to sustain eutrophication and an alternate stable state, or "regime." In IRL, high sediment oxygen demand (SOD) for expanding areas of organic rich sediments combined with extreme diurnal oxygen fluctuations promote diel and episodic hypoxia. Inflow of water with lower water column respiration and turbidity could buffer against instances of hypoxia, supporting removal versus recycling of nutrients. This would also support more diverse benthic faunal communities capable of filtering water and bio–irrigating sediments. Increasing the depth of the oxidized surface layer of sediments would contribute to non–linear restoration trajectories with potential benefit beyond direct exchanges.

To assist modeling efforts, long–term datasets for DO concentrations from the IRL and BRL were obtained for surface water from SJRWMD for comparison with bottom water DO sensors. Most existing sensors record DO at fixed depths, often in the middle of the water column, and can miss events that are restricted to the near bottom. For example, sensors referenced in this study had average depths during 2019 to 2023 of approximately 0.5 to 1.5 m (SJRWMD). Overall data for DO from these sensors showed annual trends relatively consistent with variations in DO solubility. During winter months, DO in bottom water at sandy sites typically tracked patters for DO at 0.5 to 1.5 m (SJRWMD); however, during summer months, bottom water DO was often lower and less stable, especially following peaks in DO concentrations (pink line, **Figure 24**).
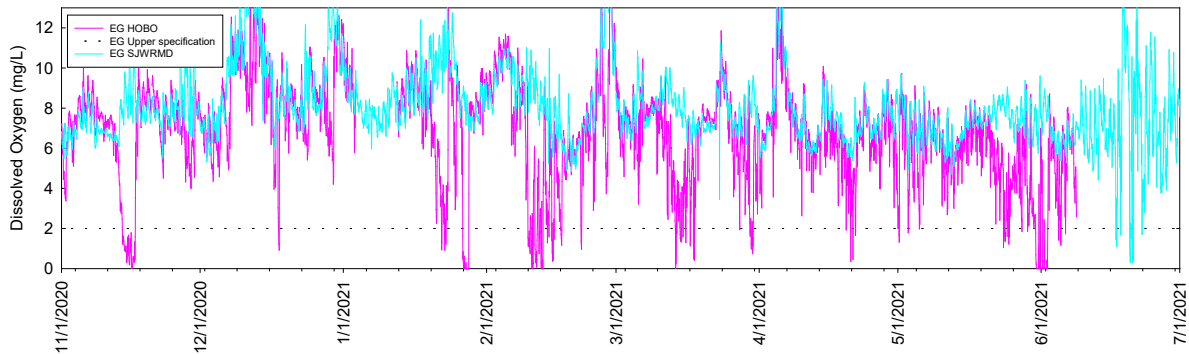
Figure 25. Concentrations of DO (mg/L) in the IRL near Eau Gallie in bottom water (<10 cm above the bottom; cyan line) and at mid–depths ~1–1.5m (pink line) with the dashed black line at 2 mg/L indicating hypoxic conditions

During Phase 1, sensors deployed in the BRL near the reference/control location showed large differences for DO in bottom water overlying mud (muck) versus sand, although the sensors are only about 200–m apart (**Figure 25**). These data are consistent with SOD differences among substrates from –2,400 µmoles/m^2/hr for sandy sites (inflow site) and –4,300 µmoles/m^2/hr for muddy sites (during winter months).
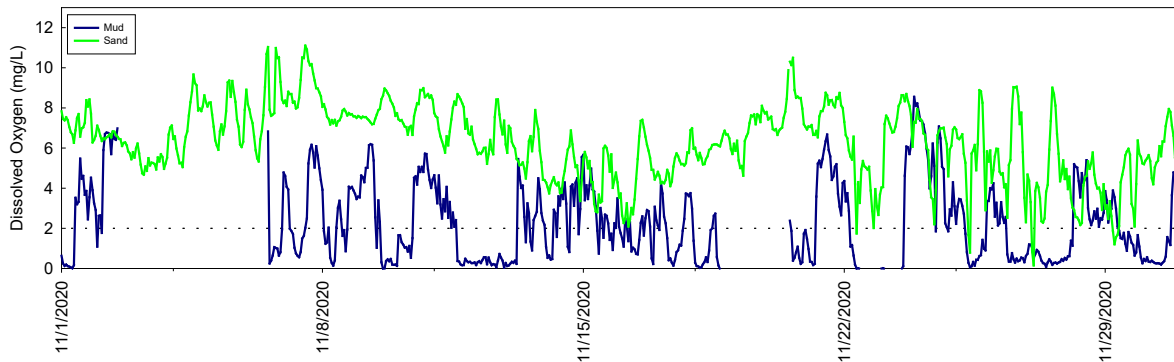
Figure 26. Bottom water DO at sites near the lagoon reference area at sites containing muck (blue line) and sand (green line) with the dashed black line at 2 mg/L indicating hypoxic conditions

4.3.2.5 Dissolved Nutrients

Data obtained between 2020 and 2023 as part of this study (Phases 1, 2, and 3), complement existing long–term datasets for nutrients in IRL and BRL. This study also provides essential new information regarding processes including rates of water column respiration and SOD. Combining long–term nutrient concentrations with new insights into internal processes, we better understand mechanisms and feedback loops that help to sustain nutrient concentrations in the lagoon over time. Through a better understating of these mechanisms, potential impacts of enhanced ocean inflow on nutrient concentrations and cycling were evaluated in the context of changing temperature, salinity, DO and benthic faunal habitat quality.

Nutrients that enter coastal systems including estuaries are removed by either (1) biogeochemical processes, leaving as N gas or through burial in sediments; or (2) discharged into the coastal ocean. Before removal through one of these pathways, nutrients are recycled and reused by algae in the water column. As a result, changes to the rate of removal support variable algal biomass even without a change in external nutrient loading.

To date, most efforts to address eutrophication focus on external loading; however, the ability of an ecosystem to assimilate these external loads is based on removal related to biogeochemical processes combined with rates of discharge to the coastal ocean. For example, a "regime shift" or alternate stable state beginning in 2010 in IRL did not coincide with major changes to external nutrient loading or rainfall. Instead, it occurred with extreme low temperatures during winter 2009/2010 that contributed to a cascade of events that likely altered internal processes, thereby decreasing the system's ability to assimilate external and internal nutrient loads. Looking at historical datasets helps to assess changes to internal processes to better understand what changes have occurred and how lost ecosystem services may recover or be restored. For example, in BRL, TP concentrations were 1.65 times higher between 2010 and 2020, compared to the period between 1997 and 2010 with even larger differences (>2–fold higher) in IRL and Mosquito Lagoon (Philips et al., 2021). As part of Phase 3, investigations were conducted on how changes to sediments likely contribute to enhanced water column concentrations. At the same time, beginning in 2010, no major increase in N concentrations was reported; however, reviewing data for this study, there was likely a shift in N speciation towards organic and reduced forms. For example, pre-2010 NOx accounted for approximately 3% to 5% of TDN decreasing to approximately 1% to 2% after 2010. Both the changes in P concentrations and N speciation could result from a change in the redox environment within the IRL. Similar changes have been observed in other estuaries, again reflecting on Chesapeake Bay where after 1980, the bay experienced hypoxia more readily, despite no major change in external nutrient loading (Kemp et al., 2005).

During Phase 1, nutrient concentrations were evaluated in the coastal ocean and in Port Canaveral as potential sources of inflow water compared to sites throughout the IRL. Overall, the lowest nutrient concentrations were identified 1 to 2 km offshore at the 10–m isobaths (Phase 1 data) with concentrations at 8.0 ± 2.4 µM TDN, 0.15 ± 0.05 µM TDP, and 3 ± 1 µM SiO_2. Concentrations in Port Canaveral, the pilot inflow location averaged 36 ± 12 µM TDN, 0.56 ± 0.22 µM TDP and 9.28 ± 4.86 µM SiO_2, respectively.

Figure 27. Inflow site concentrations of dissolved (a) NH$_4$, (b) NOx, (c) dissolved organic nitrogen (DON), and (d) total dissolved N
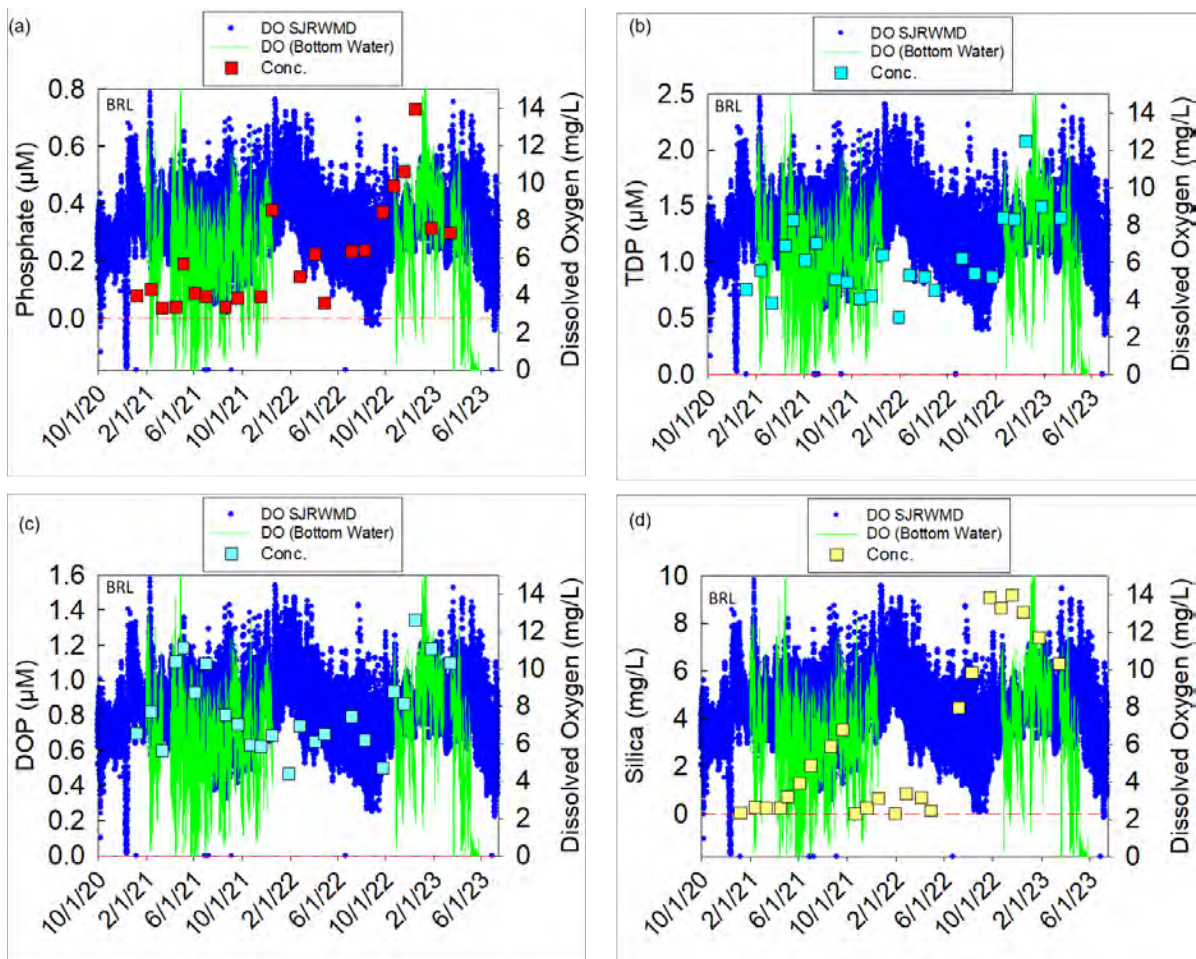
Figure 28. Inflow site concentrations of dissolved (a) phosphate, (b) TDP, (c) DOP, and (d) SiO$_2$

Although total nutrient concentrations are often used as an indicator of the eutrophic state of estuaries, speciation and the relative abundance of bioavailable species of N:P:SiO$_2$ have consistently been shown to contribute to algal community composition, whereby at the same total concentrations, shifts in speciation, and the relative abundance of N:P:SiO$_2$ can favor shifts from beneficial or less harmful photosynthesizers (e.g., seagrasses) to small, fast–growing and harmful species (e.g., *Aureoumbra lagunensis*) or vice versa (e.g., Choudhury and Bhadury 2015). A basis for evaluating N:P ratios originated with Redfield in the 1930s (Redfield 1934) and this traditional N:P ratio at 16:1 has been utilized over decades and, in some cases, expanded to include other macro or micronutrients (e.g., Choudhury and Bhadury 2015).

Ratios of TDN:TDP were higher than values for DIN:SPR. In Port Canaveral, TDN:TDP averaged 82 ± 67 (median 59) relative to 109 ± 38 (median 102) in the lagoon. Since Phase 1 the TDN:TDP ratio has decreased continuously with medians at 139 ± 29 in 2020, 116 ± 6 in 2021, 95 ± 9 in 2022 and 78 ± 2 so far in 2023. This trend reflects the lower TDN concentrations at the inflow site with lower ratios typically associated more beneficial photosynthesizers as discussed below. Ratios of DIN:SRP compared to TDN:TDP reflect the larger fraction of TDN relative to TDP that is present in less bioavailable, organic forms. Traditionally these organic nutrients have not been

considered bioavailable; however, many small bloom–forming algae can use the organic forms of both N and P (Lui et al., 2001). High ratios of TDN:TDP are known to enhance the risk for *Aureoumbra lagunensis* blooms (Lui et al., 2001; DeYoe et al., 2007) whereby, some cyanobacteria and HAB dinoflagellates can store P within their cells helping to promote their taxa when P is otherwise limiting (e.g., Hillebrand et al., 2013; Burford et al., 2014; Willis et al., 2015; Glibert et al., 2012; Accoroni et al., 2015).

Based on global trends plus data from this study and long-term datasets, potential shifts in N:P ratios (DIN:SRP and TDN:TDP and perhaps other N:P ratios) should be considered a component of overall water quality and should be a consideration for modeling and predicting algae blooms and bloom composition (Hillebrand et al., 2013). Based on the importance of N:P ratios towards promoting certain algal groups, restoration efforts, including inflow, should be viewed not only as removing N or P but as regulating the ratio of these elements. Based on long term datasets for water in Port Canaveral or the coastal Atlantic Ocean, inflow water would have both lower concentrations of nutrients and typically lower ratios of both DIN:SRP and TDN:TDP, relative to values in the lagoon.

4.3.2.6 Geochemical Nutrient Cycling (In–situ)

Due to the non–conservative nature of nutrients and strong benthic–pelagic coupling in shallow estuarine systems, modified geochemical processes in sediments and on particles would likely have a greater impact on nutrient concentrations than those resulting from direct export of dissolved nutrients. To address these complex geochemical processes, nutrient and oxygen cycling were investigated in water from Port Canaveral and from the lagoon at the inflow and reference sites and during Phase 2 in laboratory experiments to investigate how changes to temperature, salinity, and DO might influence geochemical nutrient cycling in the water column and sediments.

Water column respiration (dark) in BRL was highly variable and consumed oxygen at an average of –0.14 ± 0.16 mg/L/hr during the complete project, 2020 to 2023. The overall average decreased compared to the average from Phase 2 at 0.19 ± 0.15 mg/L/hr (2020 to 2021). This decrease in water column respiration follows patters of improving water quality and lower nutrients in BRL between 2020 and 2023. In Port Canaveral, water column respiration (dark) during the complete project (2020 to 2023) was approximately 30% lower at 0.10 ± 0.09 mg/L/hr. Overall in BRL, water column respiration (dark) accounted for approximately 50 to >80% of the total respiration (sediments + water) and is a major contributor to variations in DO concentrations and occurrences of hypoxia or anoxia (**Table 2**).

Table 2. Rates of pelagic respiration in the BRL at the inflow site and in Port Canaveral

Year	BRL (mg/L/hr)	Port (mg/L/hr)
All	–0.14 ± 0.16	–0.10 ± 0.09
2023 (Jan–July)	–0.08 ± 0.04	–0.15 ± 0.11*
2022	–0.14 ± 0.21	–0.02 ± 0.03
2021	–0.21 ± 0.13	–0.13 ± 0.06
2020	–	–

As discussed below, recent, short term (2 to 3 years) improvements in water quality coincide with lower water column respiration and benthic fluxes. These small improvements in sediment and water quality help to mitigate instances of hypoxia. Collectively these data demonstrate how small changes either natural or anthropogenic can have large impacts on water quality in IRL system.

Releases of TDN associated with water column respiration in BRL were 4 to 5 times higher than particle fluxes from seawater in Port Canaveral with median TDN values at 1.14 ±1.43 µM/hr and fluxes of NH_4, nitrate, DIN, and DON at –0.02 ± 0.16, 0.9 ± 0.36, 0.78 ± 0.39, and 1.0 ± 1.28, respectively (**Table 3** and **Table 4**). Overall, releases of phosphate from water column respiration were about two times greater in BRL (0.04 ± 0.01 µM/hr) compared to the Port (0.02 ± 0.05 µM/hr). Overall, water column fluxes (dark) were variable; however, ranges were more or less consistent or slightly higher than values reported in previous studies for similar systems (e.g., Ziegler and Benner, 1999). Based on these data, the turnover time for TDN in BRL was approximately 30% shorter than the turnover time in Port Canaveral. In contrast the turnover time for TDP was approximately four times longer in BRL compared to turnover times in seawater from Port Canaveral. These data demonstrate the efficient turnover of N in BRL and less efficient recycling of P helping to maintain the high N:P ratios observed in BRL. The turnover time for NH_4 was positive in BRL (113 hr) and negative (–218 hr) in seawater from Port Canaveral. This distinct difference is consistent with the oxidation of NH_4 to nitrate supported by more stable DO concentrations, lower respiration and less algal recycling in seawater from Port Canaveral collectively supporting a larger fraction of the TDN present as nitrate.

Table 3. Median ± standard error pelagic fluxes of NH_4, NOx, TDN, DIN, DON, PO_4, TDP, DOP, and SiO_2 in µM/hr in BRL

BRL Year	NH_4 (µM/hr)	NOx (µM/hr)	TDN (µM/hr)	DIN (µM/hr)	DON (µM/hr)	PO4 (µM/hr)	TDP (µM/hr)	DOP (µM/hr)	SiO_2 (µM/hr)
All	0.04 ± 0.37	1.2 ± 0.7	4.71 ± 2.07	1.15 ± 0.67	4.54 ± 1.65	0.04 ± 0.01	0.04 ± 0.02	0.00 ± 0.01	–0.25 ± 0.82
2023	0.24 ± 0.07	0.2 ± 0.46	3.45 ± 1.76	0.71 ± 0.46	3.21 ± 1.76	0.04 ± 0.01	0.05 ± 0.02	0.03 ± 0.01	–0.62 ± 1.6
2022	–0.06 ± 0.15	1.47 ± 0.19	1.58 ± 2.05	1.02 ± 0.21	0.82 ± 1.96	0.03 ± 0.01	–0.01 ± 0.02	–0.03 ± 0.02	–1.36 ± 1.9
2021	0.05 ± 0.59	1.1 ± 1.32	9.58 ± 4.54	1.5 ± 1.54	7.87 ± 3.4	0.06 ± 0.02	0.07 ± 0.04	0.01 ± 0.03	0.07 ± 0.6
2020	–5.63 ± 2.83	8.43 ± 4	–4.87 ± 2.76	2.8 ± 1.17	–7.67 ± 3.93	0.07 ± 0.02	–0.05 ± 0.04	–0.12 ± 0.06	–6.27 ± 3.04

Table 4. Median ± standard error water column fluxes of NH_4, NOx, TDN, DIN, DON, PO_4, TDP, DOP, and SiO_2 in µM/hr in Port Canaveral

Port Year	NH_4 (µM/hr)	NOx (µM/hr)	TDN (µM/hr)	DIN (µM/hr)	DON (µM/hr)	PO4 (µM/hr)	TDP (µM/hr)	DOP (µM/hr)	SiO_2 (µM/hr)
All	–0.02 ± 0.16	0.9 ± 0.36	1.14 ± 1.43	0.78 ± 0.39	1 ± 1.28	0.02 ± 0.05	0.06 ± 0.06	0.01 ± 0.02	0 ± 0.34
2023	–0.01 ± 0.21	0.29 ± 0.27	0.77 ± 2.49	0.56 ± 0.4	0.98 ± 2.17	0.01 ± 0.02	0.01 ± 0.04	0 ± 0.03	–0.01 ± 0.82
2022	–0.19 ± 0.16	0.38 ± 0.17	–0.06 ± 0.55	0.67 ± 0.17	–0.79 ± 0.71	0.03 ± 0.22	0.32 ± 0.2	0.01 ± 0.08	0.12 ± 0.16
2021	0.01 ± 0.31	0.95 ± 0.67	2.01 ± 2.39	1.03 ± 0.74	1.38 ± 2.12	0.02 ± 0.04	0.06 ± 0.06	0.04 ± 0.03	0.07 ± 0.07
2020	–	–	–	–	–	–	–	–	–

Overall, data for water column recycling from Phases 2 and 3 of this study indicate that inflow of seawater would bring water with lower rates of dark respiration (approximately 30% lower oxygen consumption) into the BRL, thereby increasing resilience to hypoxia while also decreasing the rate of nutrient recycling in the water column. Because rates of N recycling were 4 to 5 times higher and rates of P recycling were 2 times lower in lagoon water compared to seawater from Port Canaveral, higher N:P ratios were identified for recycling in lagoon water. Based on data from this study, the water column recycling ratio of DIN:SRP for Port water was 30.7 ± 6.4 relative to the DIN:SRP recycling ratio for lagoon water at 15 ± 11.44 in BRL. As expected, ratios for recycling of TDN:TDP were higher at 58.6 ± 17.2 in the Port and 98.7 ± 6.6 in lagoon water during the complete study. These rates were highly variable, responding to changes in water quality. Nevertheless, these recycling ratios act to stabilize ratios of N:P in the water column and followed patterns for ratios observed for the standing stock of nutrients.

Benthic fluxes of N and P from muck are estimated to contribute more than 30% of the annual N and P loading to the IRL (Gao et al., 2009; Tetra Tech, 2023; Fox and Trefry, 2018). These estimates are based only on fluxes from fine–grained, organic–rich sediments locally referred to as "muck." Because sand covers at least 90% of the lagoon bottom, non–trivial fluxes from sand

need to be considered when evaluating the importance of internal nutrient sources and geochemical nutrient cycling within the lagoon. To evaluate the importance of these geochemical processes towards regulating nutrient concentrations in lagoon water, residence times for nutrients were calculated using benthic nutrient fluxes, long–term average nutrient concentrations in lagoon water, and an average lagoon depth of 1.5 m. Data from this study serve as a baseline from which the importance of sandy sediments as both a source and sink of nutrients can be evaluated. Although this study focused on sandy sediments, non–trivial fluxes from muck would be influenced by changes to temperature, salinity, and DO.

Collectively, median ± standard deviation SOD for sandy sediments during Phases 2 and 3 (including data from other projects) was –2,500 ± 1,400 µmoles/m^2/hr (median ± SE 2,400 ± 200 µmoles/m^2/hr, n = 54) for sediment collected at the inflow site. SOD at the inflow location between 2020 and 2023 averaged –2,500 ± 1,500 µmoles/m^2/hr (median = –2,400 ± 200 µmoles/m^2/hr, n = 54). Consistent with trends for concentrations of dissolved nutrients in overlying water, SOD decreased from an average at –2,963 ± 1,174 in 2021 to –2,477 ± 1,677 in 2022 and –2,163 ± 1,194 so far in 2023. Overall, DO concentrations in bottom water and rates of oxygen consumption varied together with lower bottom water DO identified during periods with higher oxygen demand (more negative SOD), except when DO in bottom water approached zero and there was no oxygen to be consumed (i.e., December 2020, **Figure 28**). This pattern is consistent with temperature related trend for (1) DO solubility and (2) bacterial metabolism.
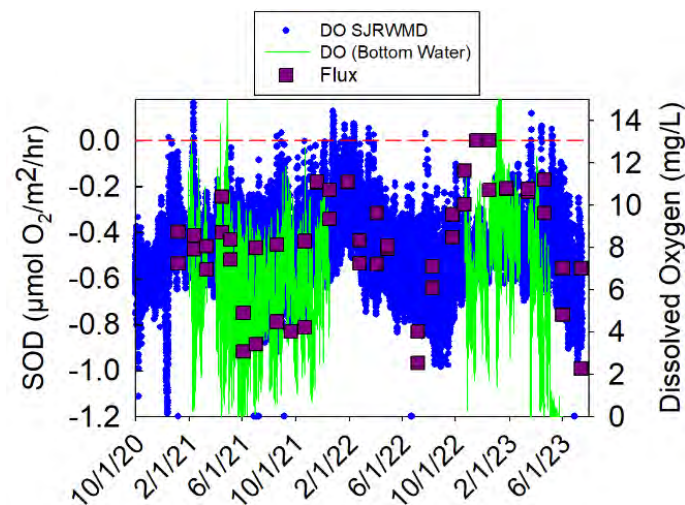
Figure 29. SOD over time at the inflow site. Blue and green lines show DO in mg/L at mid water depth (SJRWMD sensor IRLB04) and in bottom water, respectively

Benthic nutrient and oxygen fluxes plus existing nutrient concentrations in IRL were used to estimate residence (turnover) times for nutrients, based on water column processes and benthic fluxes. Residence times indicate the theoretical amount of time required for all nutrients in the water column to be either re–generated (positive flux) or consumed (negative flux). Despite the importance of benthic–pelagic coupling and short residence times for nutrients in shallow coastal systems, improved water quality that could result from artificial inflow would likely modify geochemical processes, possibly increasing or decreasing benthic fluxes into overlying water and changing residence times for nutrients. To address some of these potential changes, laboratory incubation experiments were carried out for water and sediments to investigate how changes to temperature, salinity, and DO might influence geochemical nutrient cycling in the lagoon. In

addition to geochemical processes, changes to temperature, salinity and DO could influence benthic faunal communities to favor species with different tolerances to hypoxia, or favor species with differing salinity tolerances. Nevertheless, the large fraction of total nutrient cycling that occurs in the water column suggest that direct exchanges of water and particles would likely have large and direct impacts on nutrient cycling in the lagoon.

4.3.2.7 Summary of Laboratory Experiment Results

Water column processes play a major role in overall nutrient recycling; however, no significant correlations were identified between water column nutrient fluxes and changes to temperature, salinity, or DO. Although no changes were observed in response to variations in temperature, salinity, or DO, mixing seawater with differing turnover times into lagoon water would, in and of itself, decrease rates of nutrient recycling in the area of inflow as discussed. During Phase 2, significant positive correlations were identified for NO_x, TDN, PO_4, DOP, and SiO_2 versus sediment temperature, indicating that lower temperature could decrease internal loading (inputs) of these nutrients into the IRL. Significant positive correlations were identified between DO and both DON and TDN; however, after initial releases, significant negative correlations were identified between DON and TDN and DO and a positive correlation between NH_4 and DO.

Overall, N and P responded to changes in temperature and DO, but not salinity. Using equations from statistically significant relationships, quantities of nutrients that could be removed or prevented from entering the lagoon in response to changes in temperature or DO were calculated using data from this study. Because these responses are scalable depending on the magnitude of change to temperature or DO and the area of lagoon that experiences various levels of change (km^2), results are presented per °C and per mg/L per km^2 (**Table 5**).

Table 5. Expected changes to N and P fluxes resulting from an increase in temperature of 1°C and an increase in DO of 1 mg/L

Matrix	Change in N flux / °C	Change in P flux / °C
Water	–	–
Sediment	0.4 tons/km^2/year/°C	0.16 tons/km^2/year/°C
Matrix	**Change in N flux / mg*L^{-1}**	**Change in P flux / mg*L^{-1}**
Water	–	–
Sediment	1.8 tons/km^2/year/mg*L^{-1}	–0.9 µmoles/m^2/hr (0.24 tons/km^2/year/mg*L^{-1})

Using a simple mixing model for temperature, a current residence time for water in the northern lagoon (50% exchange approximately 300 days and complete exchange approximately 2 years, Smith 1993; FDEP 2013), inflow of seawater at 0.5 m^3/sec, and a difference in temperature in the lagoon and in Port Canaveral of (approximately 0.5°C), the average change in lagoon temperature over various spatial scales with inflow (new equilibrium temperatures) was calculated and used to estimate decreases in N and P loading from sandy sediments. Based on these data and calculations, the quantity of nutrients removed via changes to benthic fluxes is expected to be greater than the net quantity of nutrients that would be discharged to the coastal ocean. Additional benefits are expected based on increased DO concentrations; however, these improvements are less easily modeled. Nevertheless, these data suggest that a pilot inflow project would yield net removal of N and P from the combined lagoon–ocean system, where decreased nutrient concentrations resulting from changes to internal cycling are expected to exceed changes to resulting from direct exchanges of water.

In addition to short term changes that would result from lower lagoon temperatures or increased and stabilized DO concentrations, decreased respiration of seawater would mitigate hypoxia and

could prevent future sediments from deteriorating and losing sorption / sequestration capacity for P through the formation of iron sulfide. The 2.6–fold increase in equilibrium P concentrations and 30% decrease in sorption capacity in 2023 compared to 2001 helps to sustain higher benthic P fluxes and concentrations in overlying water.

Overall, laboratory experiments carried out to estimate the potential impacts of pumping on geochemical nutrient cycling showed that potential lower lagoon temperatures and higher DO lead to significant decreases in benthic fluxes for N and P. These observations suggest that geochemical responses to inflow would contribute to decreasing nutrient concentrations within the IRL, mitigating discharges to the coastal ocean. Over the long–term, decreased respiration and settling of algal biomass would help to mitigate hypoxia allowing future sediments to maintain higher sorption / sequestration potential. Data obtained during this study illustrate the importance of DO in the IRL towards regulating fluxes, cycling and sequestration of dissolved nutrients. To track hypoxia and estimate the spatial extent of these processes, beginning with this project, Florida Tech established a network of DO sensors to aid in modeling efforts and to better understand benthic–pelagic coupling in this system.

4.3.3 Florida Tech Summary and Conclusions

A shift in the IRL system from a seagrass dominated stable state to an algal dominated state has been referenced as a "regime" shift beginning in 2010 (Phlips et al., 2021). This sudden shift coincided with the loss of biomass and fish kills associated with extreme low temperatures during winter 2009/2010, reaching <4°C in the IRL. Prior to these events, algal blooms followed general patterns related to external nutrient loading; however, since 2010 occurrences of algal blooms are less predictable based on external factors. Since 2010 internal processes, geochemical nutrient cycling of material already in the system, likely contributes to and fuels subsequent blooms. Similar changes have been reported in other estuaries with systems becoming less able to assimilate external nutrient loads without experiencing hypoxia and amplified effects of eutrophication (e.g., Kemp et al., 2005; Buskey et al., 1996, 1997). Eutrophication driven hypoxia promotes a series of self–reinforcing feedback loops that helps to sustain eutrophication and hypoxia with geochemical processes helping to maintain either stable state or regime.

Historically, few data are available to describe the spatial extent of hypoxia in IRL or BRL; however, data from three phases of this study kicked off a broader monitoring network that has increased understanding of hypoxia in this system, most recently in August 2023 capturing an increase in DO associated with a bloom of *P. bahamense* followed by a crash in the bloom and DO leading to a fish kill that was not captured with other nearby sensors higher in the water column. Based on data from this study, diurnal and episodic bottom water hypoxia events are a regular occurrence in the IRL and BRL. Although most are short in duration (a few days or less) the effects of chronic diel and episodic hypoxia may significantly alter nutrient cycling. Concurrently with the 2010 regime shift, concentrations of dissolved P in IRL increased without any known corresponding increase in external loading (Phlips et al., 2021). This increase in dissolved P is likely related to the chronic impacts of hypoxia, with sulfide produced in anerobic sediments irreversibly binding iron and aluminum oxides. This hypoxia driven, geochemical change in sediment composition has decrease the capacity of sediments to sequester P from 133 mg P/kg of sediments reported in 2001, compared to only 99 mg P/kg of sediments in 2022 to 2023 at the same sites. This and related changes likely contributed to the sudden 1.65 to 2.3–fold increase in dissolved P after major hypoxic events and fish kills that occurred in 2010 (Phlips et al., 2021). In 2023, the average sorption capacity was 99 mg P/kg of sediments compared to 133 mg P/kg of sediments for the same sites in 2001.

With respect to N, chronic impacts of hypoxia or lower DO concentrations would decrease the thickness of the surface oxidizing layer of sediments, decreasing the surface area occupied by nitrifying bacteria (also contributing to increased dissolved P in the water column). This study began to evaluate how changes to habitat quality, such as increased or stabilized temperature, salinity, and DO, may influence bioturbating species, another layer of potential benefits of inflow.

In eutrophic systems, HAB events contribute to occurrences of hypoxia and anoxia, where even short hypoxic or anoxic events can promote loss of ecosystem services including coupled nitrification–denitrification thereby decreasing the removal of N from the system as inert N gas and decreasing the quantity of P that is sequestered in sediments. Loss of these ecosystem services over time and space create positive feedback loops sustaining eutrophication and hypoxia. Distinct differences in the ability of poorly flushed versus well flushed estuaries to cope with eutrophication have been observed throughout the literature, where poorly flushed estuaries with long residence times, like the IRL, more readily retain nutrients to promote algal blooms, loss of seagrass beds, hypoxia, and loss of ecosystem services (Twilley et al., 1999; Defne and Ganju 2015; Kemp et al., 1992; Twilley et al., 1999). Within this conceptual framework, impacts of enhanced inflow of seawater into the IRL were evaluated for its potential to (1) directly decrease nutrient concentrations, (2) promote water column and sediment processes that would help to restore ecosystem services to remove or prevent N and P from entering the lagoon, and (3) buffer against extreme and low salinity and temperature events.

Overall, temperatures in Port Canaveral and the coastal Atlantic Ocean were moderate relative to more variable and extreme temperatures in the lagoon. During winter months water in Port Canaveral experienced fewer extreme cold events and during summer months average temperatures ranged from approximately 0.5 to 3°C higher in BRL. On all occasions, salinity was higher in Port Canaveral than in the lagoon, leading to distinct densities among the lagoon (1,007–1,016 kg/m^3) and Port (1,018–1,028 kg/m^3) water masses. These data indicate that inflow of seawater and a mixed water mass would favor circulation of bottom water, on average raising salinity and helping to stabilize concentrations of DO at the sediment–water interface.

Overall, concentrations of TDN and TDP were lowest at offshore sites (8 ± 2.4 µM TDN, 0.15 ± 0.05 µM TDP); nevertheless, concentrations in Port Canaveral (36 ± 12 µM TDN, 0.56 ± 0.22 µM TDP) were approximately 3–fold 2–fold lower than concentration in the BRL at the inflow site (107 ± 30 µM TDN, 1.2 ± 0.6 µM TDP). This small pilot project would have little impact at the lagoon scale; however, changes at the inflow site would facilitate a scientifically sound scaled study of inflow in a well–defined area while preserving reference/control sites and also mitigating risk of adverse impacts to the broader lagoon. Data from the pilot study could then be used to determine the scale of a full–sized project necessary to achieve desired improvement to water quality.

Biogeochemical responses of the water column and sediments to short term changes in temperature, salinity, DO and infauna were investigated using a combination of field and laboratory experiments. Laboratory experiment also investigated long–term impacts of hypoxia on the sediments ability to sorb and sequester P. Sediment and water column incubations in the field were used to establish current rates of nutrient fluxes and cycling from sandy sediments and water in the lagoon and to serve a baseline to evaluate changes over time.

Despite no significant changes, lower rates of recycling in the proposed inflow water from Port Canaveral and lower N:P ratios (DIN:SRP 34 in the lagoon, 37 in Port Canaveral; TDN:TDP 109 in the lagoon, 82 in Port Canaveral) would, when mixed, help to slow recycling and promote lower N:P ratios in the new, mixed water mass. Lower concentrations and ratios of N:P would help to promote beneficial photosynthesizers. In laboratory incubation experiments, significant positive

correlations were identified between benthic fluxes of NO_x, TDN, PO_4, DOP, and SiO_2 versus sediment temperature. Collectively, these data show that lowering lagoon temperatures, a likely result of inflow, would help to reduce inputs of both N and P to the lagoon. Based on a simple mixing model, the pilot project could prevent 1.6 and 0.7 of N and P from entering the lagoon each year based on lower lagoon temperatures.

Overall, based on laboratory experiments of geochemistry (independent of infauna), no long–term changes in nutrient cycling are expected based on modest changes to salinity that would result from inflow. Nevertheless, stabilized, and higher salinities would favor historically bioturbating and bio irrigating species such as *M. Mercinaria* that help to move oxygen from overlying water into sediments. Therefore, increasing and stabilizing salinity could promote geochemical nutrient cycling though feedback interactions of habitats, food–webs, and biogeochemistry (Kemp et al., 2009). This study began to investigate this relationship in BRL; however, longer term studies in sandy sediments will be required to quantify these complex interactions and potential benefits of inflow.

Finally, in both field measurements and laboratory experiments, low DO promoted release of PO_4 and NH_4, both known to promote HABs. In contrast, higher, stable concentrations of DO promoted removal of PO_4 while also promoting fluxes of nitrate over NH_4, both changes that support beneficial photosynthesizers. Based on these data and trends, lower lagoon temperatures and higher and stabilized bottom water DO expect to result from inflow would support lower nutrient concentrations and ratios promoting species of nutrients that are more favorable to beneficial photosynthesizers.
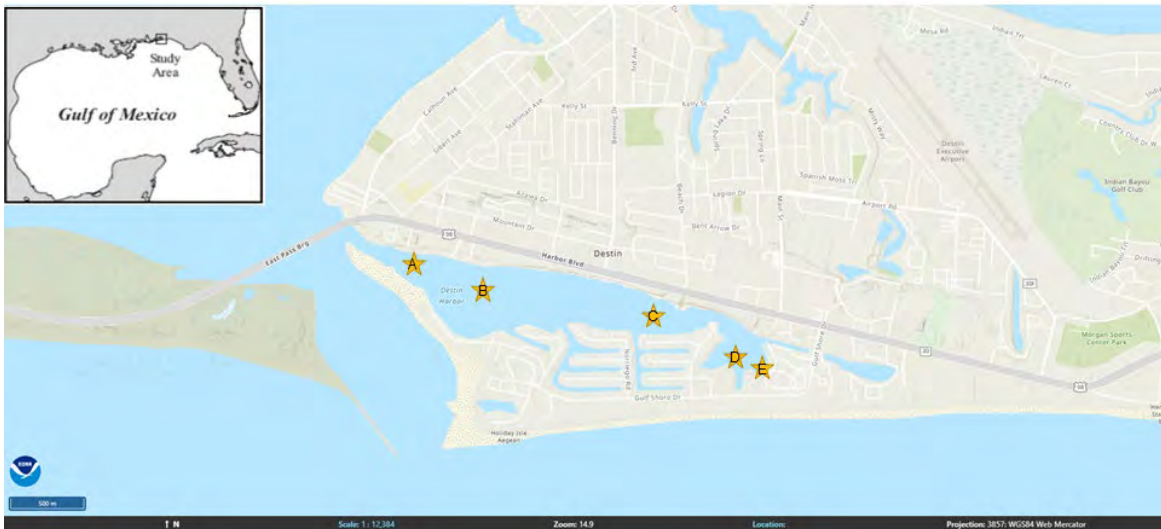
Concentrations of DO in bottom water (<10 cm above the bottom) followed general seasonal patterns observed at mid depths reported by other existing monitoring networks; however, bottom water experienced frequent periods of hypoxia or anoxia, likely due to proximity to sediments responsible for 20 to 50% of the total respiration. These new data are essential towards improving lagoon models used in this study and other generalized nutrient loading or HAB models. Other notable observations from our growing network of bottom water DO sensors was lower concentrations of DO overlying muck deposits relative to concentrations in bottom water overlying directly adjacent sand. On an annual scale, concentrations of DO in Port Canaveral tracked concentrations in lagoon water, both lagoon and seawater varying in response to changes in solubility over time. Despite similarities in long–term trends, diurnal fluctuations in Port Canaveral were much less that those in the lagoon, due mostly to 30% lower rates of dark respiration in Port Canaveral and almost monthly instances of hypoxia observed in lagoon were not observed in Port Canaveral.

4.3.4 UWF Study Area

The primary reference study area was SRS in the Florida Panhandle. SRS is a lagoonal system similar to IRL with a barrier island separating it from the coastal ocean. SRS has a similar morphometry to the BRL segment of the IRL (**Table 6**), but somewhat lower salinity and light attenuation values that are about 1/3 of the IRL. In contrast, Destin Harbor is much smaller, has no seagrasses, and light attenuation about half that of the IRL. SRS still has healthy seagrass beds (Byron et al., 2018) while BRL has seen significant declines (Morris et al., 2018). Grab samples from four locations (**Figure 29**) were collected from Destin Harbor for water quality and sediment characteristics: Chl-a, water, and organic content in October 2022. Two of these locations (sites A and C, **Figure 29**) have been consistently sampled for water quality by FDEP and Choctawhatchee Basin Alliance (CBA).

Table 6. Characteristics of BRL, Destin Harbor, and SRS

Parameter	BRL	Destin Harbor	SRS
Length (km)	62	4	60
Width (km)	2-5	0.05-0.4	0.5-3
Depth (m)	2	~2	2.8
Light attenuation (m^{-1})	1.5	0.84	0.5
Average Salinity	29	25	22
Seagrass species – dominant (other present)	*Halodule wrightii (Syringodium filiorme, Ruppia maritima* and *Halophila sp.)*	none	*Halodule wrightii* and *Thalassia testudinum (Ruppia maritima)*

Note: Site locations: A – DH@ AJ; B – CBA Ft. Walton Beach – 9 & Old Pass Lagoon West; C - CBA Ft. Walton Beach – 10, CBA 10 & Old Pass Lagoon East; D – SC 1C; E – SC 1D.

Figure 30. Location of Destin Harbor sampling locations and inset map showing study area

Figure 31. Location of SRS sampling sites *in Halodule wrightii* (H.w.) bed and *Thalassia testudinum* (T.t.) bed with inset map of study area

4.3.5 UWF Approach

To characterize the dynamics of microbial nutrient cycling, the key N processes of nitrification and DNRA were targeted (**Figure 31**). The two major groups of nitrifiers are NH_4 oxidizing archaea and beta-proteobacteria. Nitrification only occurs when molecular oxygen is present and provides nitrate to denitrifying prokaryotes. This is the dominant pathway removing N in estuaries when water column nitrate concentrations are low as they are in the IRL. Conversely, DNRA is an anaerobic process that recycles N in the system, exacerbating effects of eutrophication. Enumeration of abundances of these key prokaryotes directly relates to benthic chamber and sediment geochemistry measurements collected in the IRL and to the seagrass reference sites in SRS.
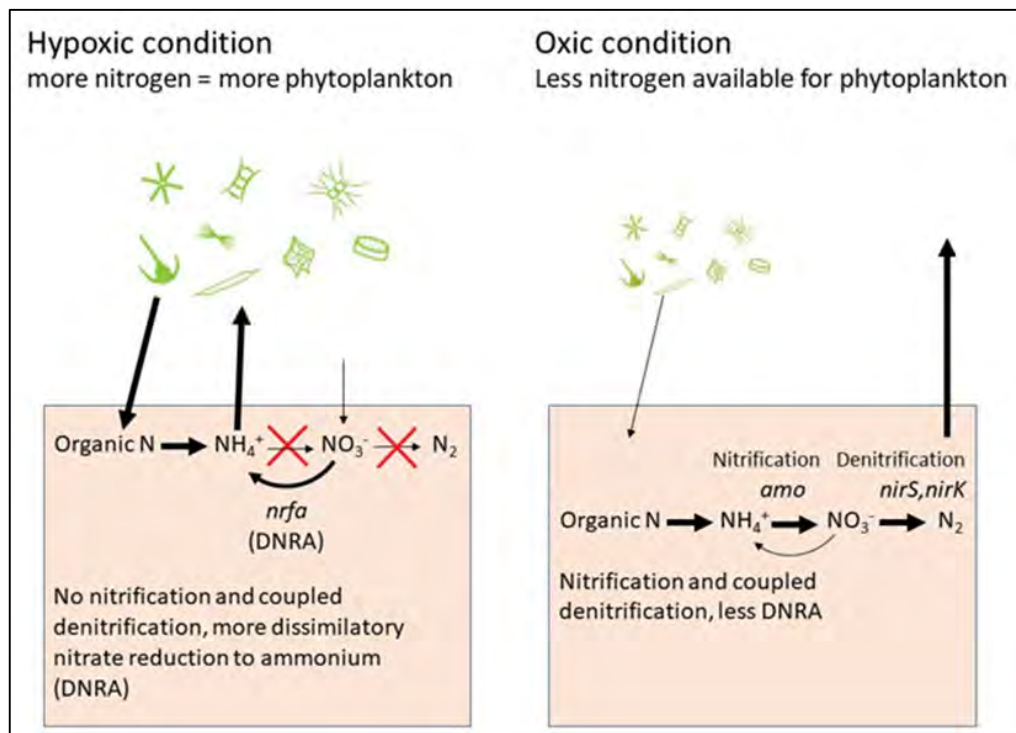
Figure 32. Conceptual model of key N transformation and genes under hypoxic and oxic conditions that are the focus of UWF research activities

Nitrifying prokaryotes were measured with two gene encoding alpha subunit of ammonia monooxidase (*amoA*) targets: archaeal *amoA* and bacterial *amoA*, since the first step, NH_4 oxidation, is often the rate limiting set in the process. Prokaryotes capable of DNRA were enumerated with the gene encoding nitrite reductase (*nrfA*) gene. The relative abundances of these target genes were normalized to total bacteria or total prokaryotes since different sediment types may have different microbial abundances. Total prokaryote abundances were enumerated with prokaryotic ribosomal ribonucleic acid (rRNA) marker genes for bacteria and archaea (BACT1 16S rRNA for Bacteria, Arch-Group I 16S rRNA for Thaumarchaeota 16S rRNA). Polymerase chain reaction conditions for all targets (gene encoding alpha subunit of *amoA* and prokaryote marker genes) were already established at UWF (Babcock et al., 2020), but conditions were again tested and optimized with current qPCR chemistry available for this study's sediment samples. DNRA bacteria enumeration required optimization of *nrfA* qPCR conditions and testing.

Benthic fluxes of nutrients (NH₄, NOx, and DIP) and DO in Florida Panhandle reference sites were measured with sediment domes. During flux experiments, sediments were collected next to domes for qPCR analysis, benthic Chl-a, sediment porewater, water content, and organic content. Benthic flux experiments were done in September, November, and April.

4.3.6 UWF Results

4.3.6.1 Comparison of water quality between Destin Harbor, SRS, and BRL

Plans for a pumping system to improve water quality in Destin Harbor were discussed in the 1988 Destin Harbor Management Plan (Landers-Atkins Planners, Inc., 1987). This report describes an extended fish kill in 1982 and subsequent concerns about poor water quality. A pumping system was installed in 1992 with a goal to have DO levels greater than 5 mg/L (Michael Burgess, City of Destin Engineer, pers. Comm.). According to Mr. Burgess, the pump was run for 8 hours/day at high tide and repairs to this system were required about every 12 to 18 months. Problems with reliability and repairs were noted in 1996 (Lipnicky 1996). In 2004, the system was replaced (NWFDN, 2005). In March 2019, a new schedule of pumping operations was established with pumping for 6 hours every day between March 1 and October 31 on outgoing tides (Burgess, pers. comm). Pumping every other day for several hours occurs between November and April. Between May and November 2021, the pump was out of operation. Additional problems also occurred between July and August 2022.

CBA sampling in Destin Harbor was temporally more comprehensive than the Impaired Waters Rule (IWR) sampling (**Figure 32**). Bottom water DO was often low at CBA FL Walton Beach-10 between May and October. Old Pass E was the same location as the CBA FL Walton Beach-10 site and showed similar patterns. The Old Pass W and CBA Ft Walton Beach 9 sites were at the same location and closer to Destin Pass than Old Pass E. IWR data had lower bottom water DO values in 2013 and 2014 than the CBA sampling (**Figure 32**). There were 198 values out of 446 sampling events that were below the target 5 mg/L between March 1 and October 31 at these two sampling locations. Not surprisingly, in the cooler months between November 1 and February 28, only 26 out of 183 values were less than 5 mg/L.
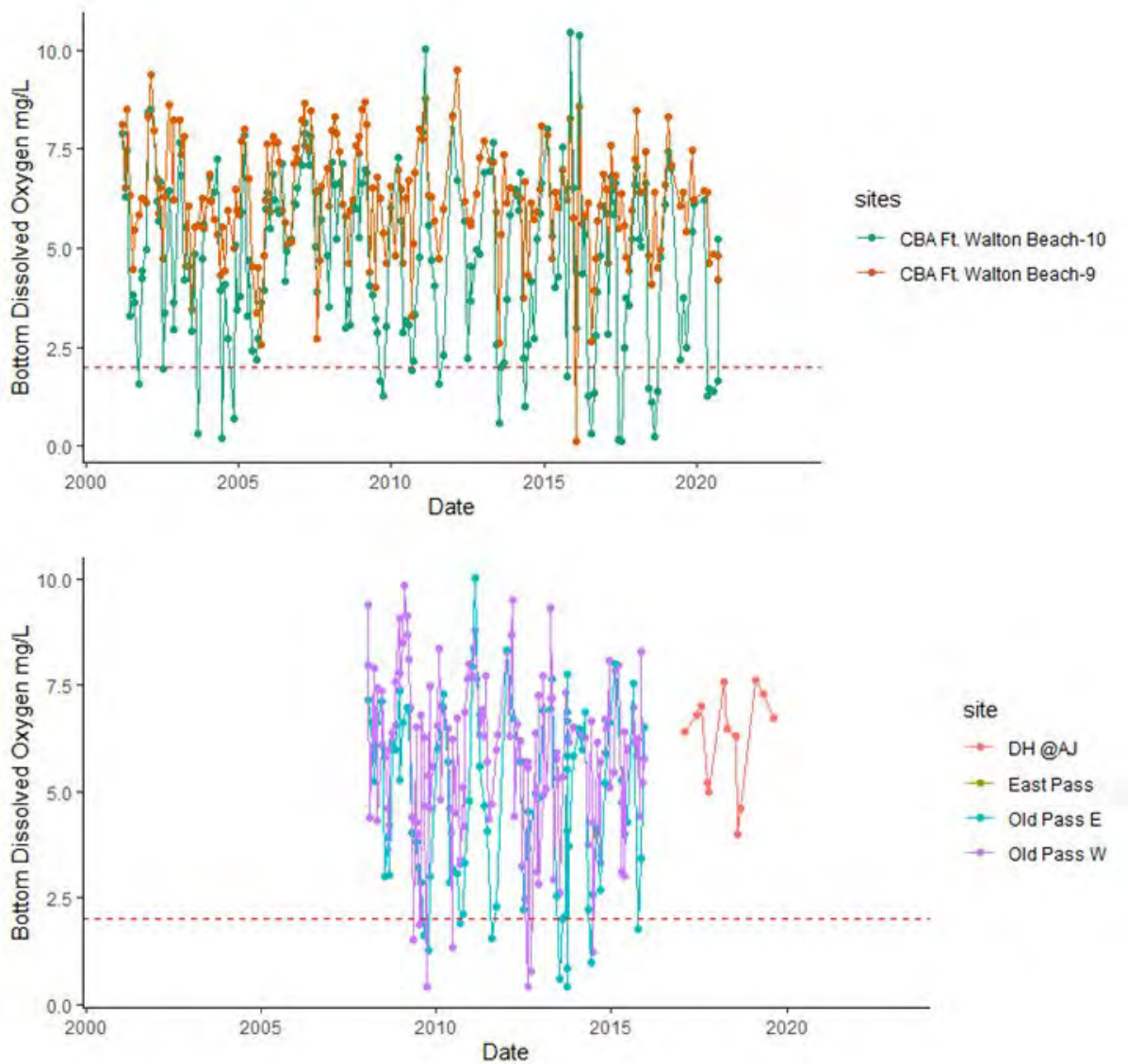
Figure 33. Bottom water DO concentration in Destin Harbor from CBA sampling (upper panel) and IWR database (lower panel)

Sampling by UWF during October 2022 revealed stratification between the surface and bottom layers and the depth of the pycnocline was between 1.5–2 m (**Figure 33**). DO levels were similar between surface and bottom at three of the sampling locations. However, at CBA-10 (the same sample location as CBA FL Walton Beach-10 and Old Pass E), DO concentrations declined below the pycnocline to about 5 mg/L (**Figure 33**). Chl-a fluorescence values, a measure of Chl-a biomass, increased with depth particularly at site CBA-10. Bottom water Chl-a values were also high, 10.4 µg/L, at this site (**Figure 33**). Bottom water NH_4 and DIP concentrations were higher than surface concentrations at this site and SC-1D. Similar patterns were observed in turbidity and TSS concentrations at these two stations. NOx concentrations were at or below detection limits (< 0.2 µM) at all locations. Light attenuation ranged from 0.37 to 0.58 /m with the lowest values near the mouth at site DH@AJ (**Figure 33**).
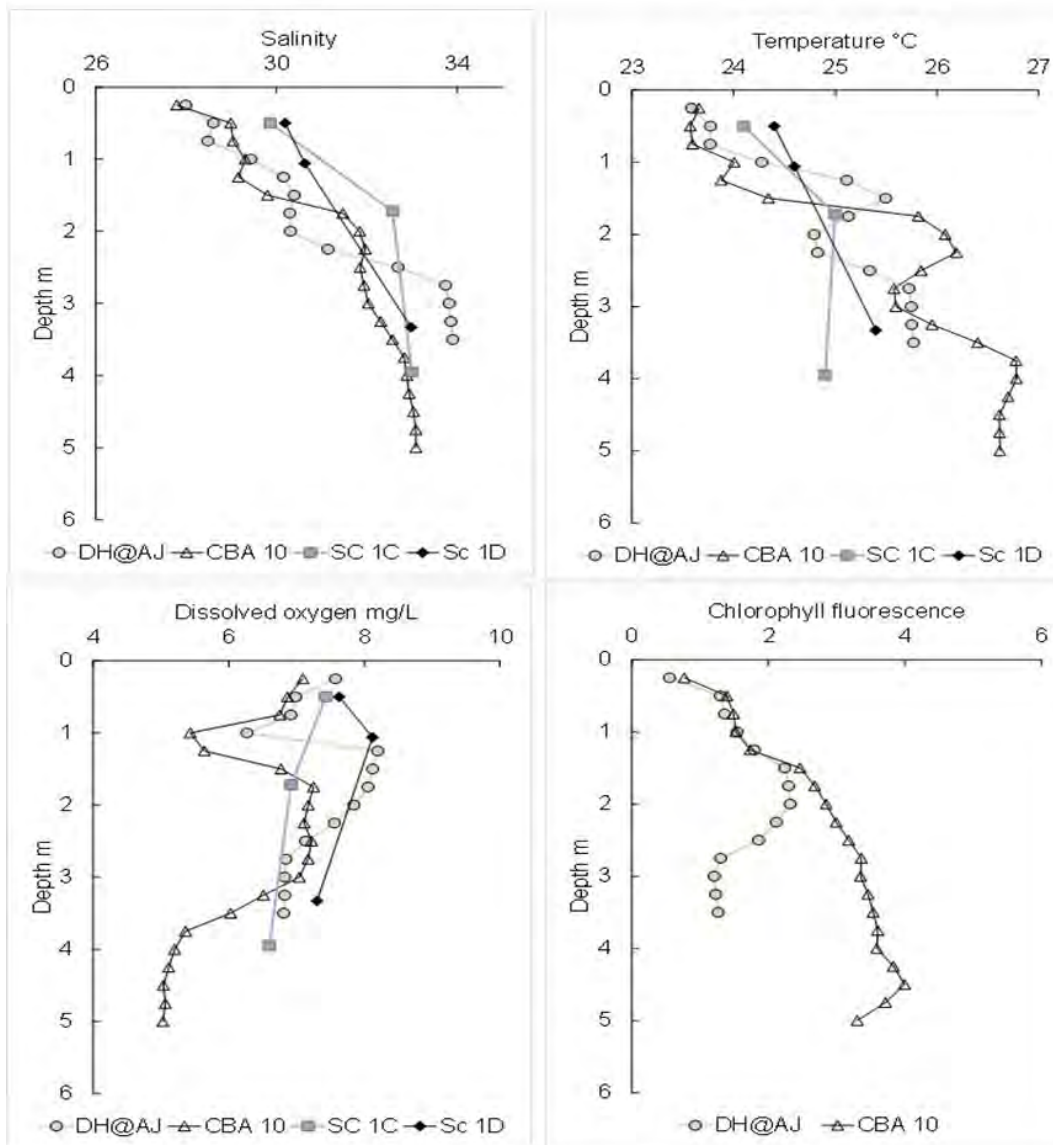
Figure 34. Depth profiles of salinity (upper left), temperature (upper right), DO (bottom left), and Chl-a fluorescence (bottom right) in Destin Harbor in October 2022

Table 7. Water column characteristics from SRS, Destin Harbor and IRL

Location (Layer S-surface, B-bottom)	Date	Salinity	Kd /m	Chl-a µg/L	NOx µM	NH$_4$ µM	DIP µM	TSS mg/L
SRS								
Seagrass (S)	9/21/22	23.7	0.68	2.21	<0.2	0.07	0.16	14.5
Seagrass (S)	11/2/22	26	0.29	0.61	<0.2	0.67	0.27	14.5
Seagrass (S)	4/4/22	24.4	0.45	1.47	0.62	0.52	0.08	11.60
Destin Harbor								
DH @ AJ (S)	10/5/22	29.89	0.37	1.91	<0.2	0.21	0.12	36.00
DH @ AJ (B)	10/5/22	34.62		2.8	<0.2	0.34	<0.05	5.50
CBA-10 (S)	10/5/22	29.55	0.53	1.43	<0.2	0.09	0.16	9

Location (Layer S-surface, B-bottom)	Date	Salinity	Kd /m	Chl-a μg/L	NOx μM	NH$_4$ μM	DIP μM	TSS mg/L
CBA-10 (B)	10/5/22	33.8		10.43	<0.2	0.45	0.42	26.00
SC-1C (S)	10/5/22	29.86	0.43	2.62	<0.2	0.30	0.37	14
SC-1C (B)	10/5/22	32.99		2.52	<0.2	0.61	0.17	17
SC-1D (S)	10/5/22	30.19	0.58	3.52	<0.2	0.13	0.26	5.5
SC-1D (B)	10/5/22	32.98		8.72	<0.2	0.30	0.29	9
IRL								
Slick (S)	3/15/23	18.54	0.62	5.65	<0.2	0.18	0.13	18.00
PCL (S)	3/15/23	18.88	3.27	4.02	<0.2	0.12	0.17	20.00

Salinity in SRS seagrass bed ranged from 19.7 to 26 (**Figure 34**, Bowman in prep.). Periodic low concentrations of DO (<5 mg/L) were observed at night and dawn, while concentration in the afternoon usually exceeded saturation (Bowman in prep., Caffrey, unpublished data). NOx, NH$_4$, and DIP concentrations were often low, less than 1 μM (**Table 7**). Water column Chl-a values ranged from 0.6 to 7.7 μg/L (**Table 7**). Sediments were easily resuspended at this location resulting in TSS concentrations above 60 mg/L (Bowman in prep., Caffrey et al. 2023).

Productivity and survival of seagrasses are influenced by a variety of factors. Salinity, temperature, light availability, and nutrients all interact with each species having different requirements. *Halodule wrightii* is considered a pioneer species with a broad salinity tolerance (normal range of 10 to 35 ppt) and an ability to survive extended periods of 5 ppt (Biber, 2022; Lirman and Cropper, 2003). *Syringodium filiforme* has a narrower range, having higher leaf productivity between 15 and 25 ppt (Lirman and Cropper 2003). Long-term monitoring of salinity in the BRL suggest that salinities are usually within these ranges (**Figure 34**). Salinity outside of the 10 to 25 range occurred in the mid-1990s when some values were below 10 (**Figure 34**). In the early 2010s, there were several years with 6 to 10 months of salinity above 35 (**Figure 34**).

Note: Red dashed lines indicate minimum and maximum salinity tolerances for *H. wrightii*.

Figure 35. Salinity (upper panel) and light attenuation (lower panel) in BRL between January 1987 and April 2022 from SJRWMD (downloaded 8/24/22)

4.3.6.2 Sediment Biogeochemistry

All locations in the Florida Panhandle had sandy, low organic matter sediments (**Table 8**). The depth layers (0-2, 2-4, 4-6 cm) all had similar water and organic matter contents at the shallow

Halodule and deep *Thalassia* sites during each sampling trip (data not shown). Destin Harbor was similar to the two SRS sites in water content but had a much lower organic matter content. This was likely due to the presence of small roots and detritus from the seagrass beds in the SRS samples which were not present in Destin Harbor.

Table 8. Water and organic matter content from sediment samples (0-6 cm)

Note: SRS samples collected in September 2022, November 2022, and April 2023. Destin Harbor samples collected in October 2022. Average + standard error.

Location	Site	Water Content %	Organic Matter Content %
SRS	*T. testudinum* bed	72.7 + 1.0	3.84 + 0.62
SRS	*H. wrightii*	75.8 + 1.5	3.40 + 0.46
Choctawhatchee Bay	Destin Harbor	73.8 + 2.7	0.39 + 0.26

Porewater NH_4 and DIP concentrations were always higher than concentrations in the overlying water. Porewater DIP ranged from 1 to 7 µM, increasing with depth at the *Halodule* site and IRL sites (**Figure 35**). DIP at the *Thalassia* site was similar among depth layers with the highest concentrations in November and lowest in April, which is the start of the growing season. *Halodule* DIP concentrations were also low in April compared to other dates. NH_4 concentrations were highest at IRL sites, increasing from 35 µM in the 0 to 2 cm layer to 60 µM at 4 to 6 cm. Concentrations in the *Halodule* bed were less than 20 µM, similar to those in the *Thalassia* bed except for November at the 2 to 4 cm layer which was 30 µM (**Figure 35**). These values are consistent with previous work in SRS (Presley and Caffrey, 2021; Rothfus, 2022).
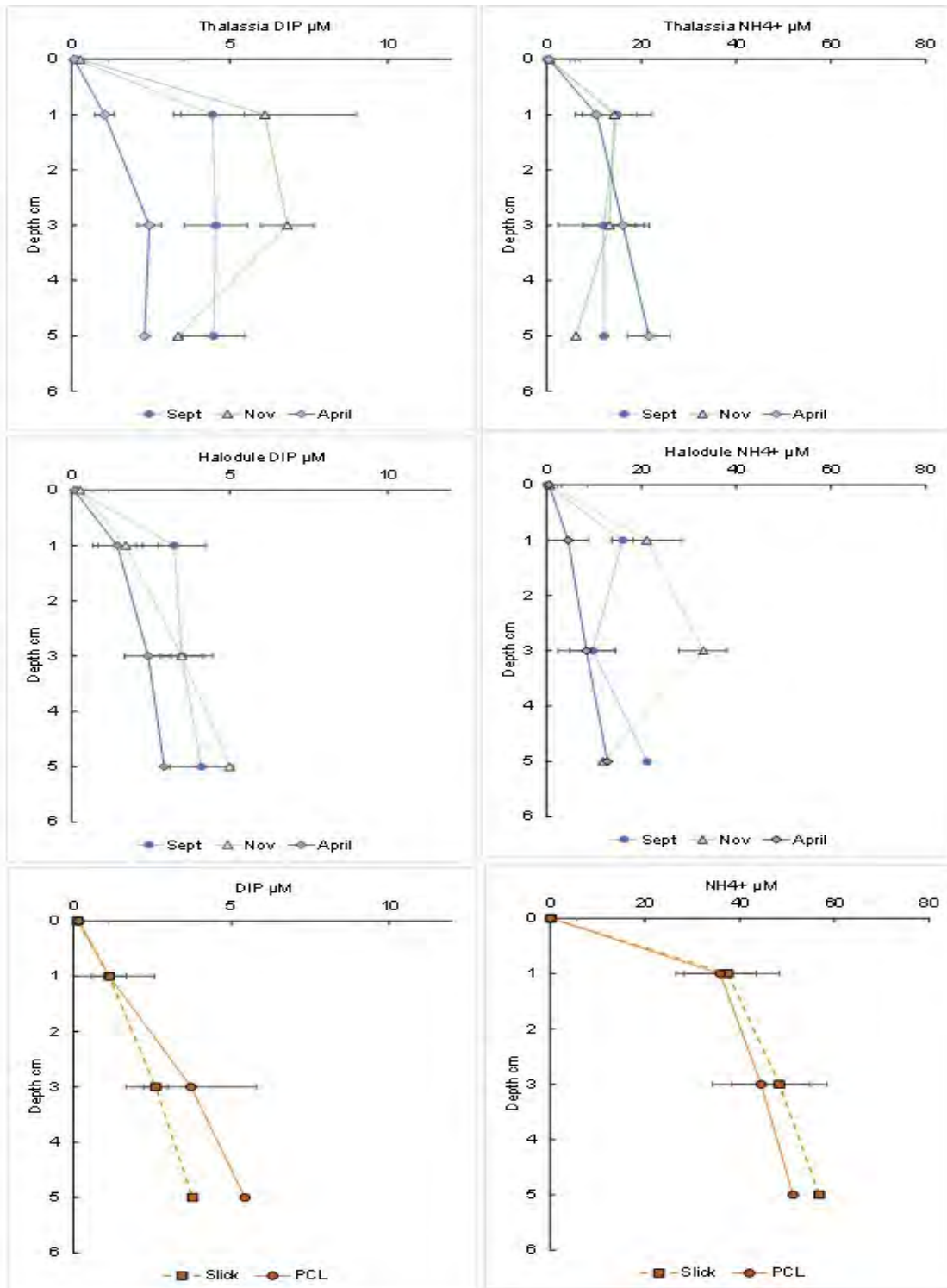
Note: .Value at 0 cm is overlying water value. Mean + Standard Error

Figure 36. Porewater profiles of DIP and NH$_4$ with depth in sediment

Oxygen consumption in SRS ranged from -7,919 to -1,304 µmol/m^2/hr with higher consumption in *Halodule* beds than *Thalassia* (**Figure 36**). These are comparable to the fluxes measured at PCL and Slick in March 2023 (**Table 9**), but lower than those measured in mixed *Halodule* and *Thalassia* beds in Big Lagoon (part of the Pensacola Bay system) in 2011 (Hester et al. 2016). Net community production was also higher in *Halodule* beds than *Thalassia* (**Figure 36**). Higher net community production occurred at the Slick site than the PCL site. Lower light attenuation at Slick could have been responsible for the greater production by benthic microalgae.

NH$_4$ fluxes were higher in dark chambers than light where uptake often occurred, particularly in *Halodule* beds in September. A similar pattern was observed at PCL and Slick sites in March (**Table 9**). At Slick, uptake occurred in both light and dark domes, but those in the dark had lower uptake. This pattern is consistent with nutrient uptake by seagrasses or benthic microalgae. NOx fluxes were very low since concentrations were usually at detection limits. Uptake of NOx in the *Halodule* bed occurred in both September and April. NOx uptake occurred at both IRL sites. DIP fluxes were also near zero except for one high dark chamber value from *Halodule*. There were no consistent differences in NOx or DIP fluxes between light and dark domes from SRS or IRL.

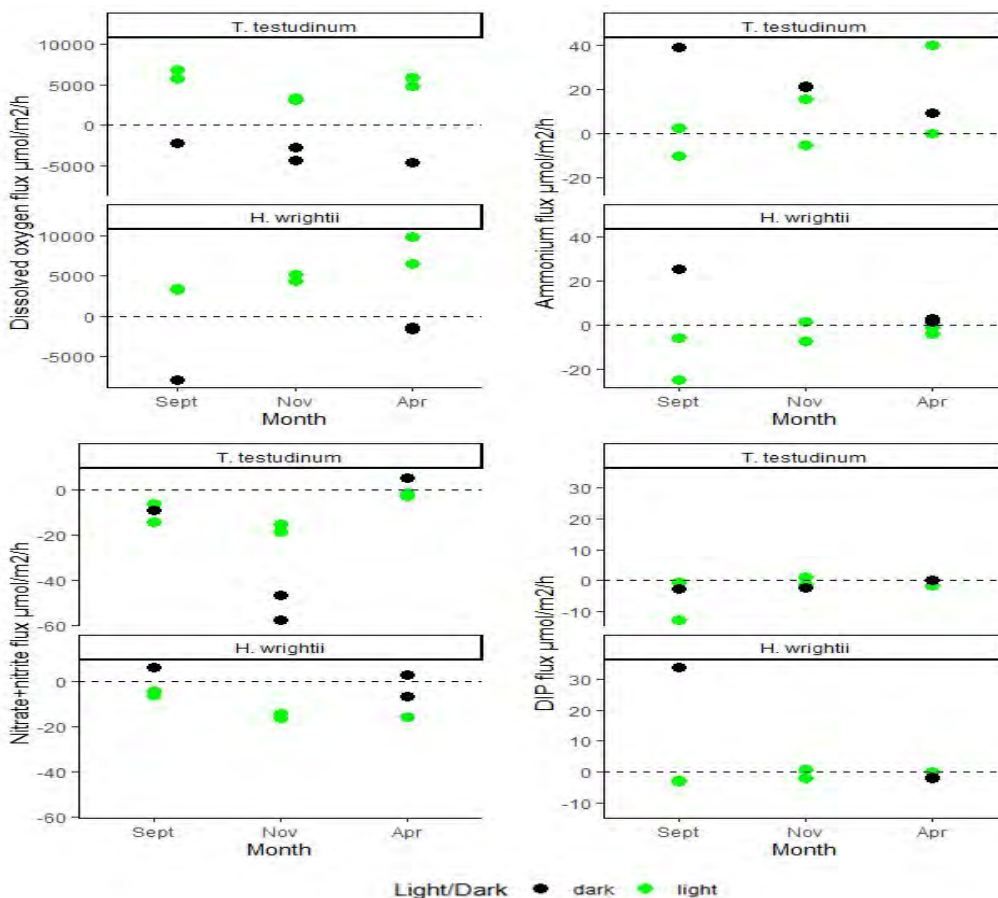**Figure 37. Benthic fluxes of oxygen, NH$_4$, NOx, and DIP in SRS seagrass beds in September 2022, November 2022 and April 2023 from light and dark domes**

Table 9. Benthic fluxes of oxygen, NH$_4$, NOx, and DIP from Slick and PCL in IRL in March 2023

Location	Light/Dark	DO flux (μmol/m^2/hr)	NH4+ flux (μmol/m^2/hr)	NO3-+NO2- flux (μmol/m^2/hr)	DIP flux (μmol/m^2/hr)
Slick	Light	1785 $\pm$ 111	-41.3 $\pm$ 0.7	-6.1 $\pm$ 17.2	-3.0 $\pm$ 16.2
Slick	Dark	-2391 $\pm$ 2527	-23.7 $\pm$ 6.7	-12.2 $\pm$ 8.6	-1.2 $\pm$ 0.0
PCL	Light	160 $\pm$ 133	-0.3 $\pm$ 4.0	-14.8 $\pm$ 20.9	0.0 $\pm$ 5.8
PCL	Dark	-1676 $\pm$ 654	12.1 $\pm$ 4.6	-0.8 $\pm$ 1.0	0.6 $\pm$ 0.6

4.3.6.3 Abundance of Prokaryotes Capable of DNRA and Nitrification

The relative abundances of prokaryotes capable of nitrification, known as ammonium oxidizing organisms (AOO), or capable of DNRA were determined in sediment samples of the IRL study sites and SRS reference site. AOO were enumerated by measuring levels of the *amoA* gene, which encodes the first important enzyme in the nitrification pathway; and DNRA bacteria were enumerated using the *nrfA* gene. Sediments from impacted sites during periods of hypoxia would be expected to contain higher abundances of *nrfA* and conversely, sediments with more oxygen to have higher abundances of *amoA*. In all sediments examined throughout the study, a general pattern of higher DNRA bacteria from the SRS reference sites than from the IRL sites was observed. Additionally, there was also an overall higher abundance of AOO in the SRS sites than in the IRL sediments. There was a seasonal component to changes in abundance of AOO at the Port Canaveral site in the IRL. At all sites overall, there were fewer prokaryotes containing the *amoA* genes than DNRA bacteria. Together, these data suggest both types of prokaryotes with N-cycling functional genes are more abundant in the SRS sediments than in IRL sediments, and N compounds in the SRS sediments may be more rapidly recycled than those in the IRL.

4.3.7 UWF Conclusions

- Methods for quantification of key N transforming microbes were optimized for IRL and SRS sediments.
- Relative abundances of aerobic nitrifying microbes at the Port Canaveral site had a seasonal component, while abundances of anaerobic ammonia producing microbes remained high throughout the year.
- At SRS reference sites, relative abundances of ammonia producing microbes were lowest in late fall/winter, but there was no seasonal pattern in relative abundances of aerobic nitrifying bacteria.
- Aerobic N-cycling microbes were on average nearly five times more abundant in SRS than IRL sediments, indicating more rapid N removal in SRS sediments than in the IRL.
- Anaerobic ammonia producing microbes that can exacerbate the effects of eutrophication were on average two times more common relative to aerobic N-cycling microbes in the IRL than in the SRS.
- Sediment oxygen and nutrient fluxes were similar between SRS and IRL reference sites.
- Salinity in the BRL section of IRL normally falls within the known tolerances for two dominant seagrass species, *Halodule wrightii* and *Syringodium filiorme.* Extended periods of high salinity (> 35 ppt) between 2011-2014 and low salinity in the 1990s and following the 2004 hurricane season (< 10 ppt) exceeded optimal conditions for productivity.
- The amount of light available to support seagrass growth is higher in SRS than IRL. Analysis from this study and the literature point to the need to decrease light attenuation (increasing bottom light availability) in IRL to allow seagrasses to recover.
- Despite enhanced inflow, Destin Harbor bottom waters experience episodic hypoxia likely due to high nutrient loads, water column respiration, and sediment decomposition in this organic poor system. High Chl-a concentrations below the pycnocline indicate substantial

nutrients and light availability, which is likely driving water column and sediment decomposition reducing oxygen concentrations in the water column.

4.4 Biology (Task 4)

The biological studies in Phase 3 expanded upon the biological work from Phases 1 and 2 to create a more robust data set, more complete baseline, and better understanding of the questions to be answered and data gaps to evaluate the efficacy of restoring lagoon inflow. Five organizations worked separately on different biological topics and completed five separate reports. Each report is briefly summarized below.

4.4.1 Brevard Zoo

BRL supports seagrass and rooted macro-algae beds which provide critical habitat to lagoon life. In an effort to establish baseline benthic habitat conditions prior to lagoon inflow piloting, seagrass and other submerged aquatic vegetation were surveyed at sites in the northern and southern BRL during Phases 1 and 2. This effort builds on that work with benthic surveys in the spring and summer of 2023.

Phase 3 sampling locations were selected in two general areas of the IRL: Banana River North and Banana River South. Banana River North sites lay nearest the proposed inflow site at Port Canaveral and Banana River South was chosen to represent baseline controls away from the inflow site. Follow-up surveys were not conducted at an additional site in Vero Beach, sampled during Phase 1 of the project as part of an assessment of candidate inflow sites. Six locations in BRL were sampled during Phase 1, 2, and 3 of the Restore Lagoon Inflow project. Six additional shallow, sandy sites consistent with historic seagrass habitat conditions were selected on the eastern shoreline of the BRL to sample in spring and summer 2023 to improve understanding of changes in benthic cover. At each location, a 100 m long transect was surveyed with standard methods used to evaluate seagrass in the IRL (Virnstein and Morris, 1996; Morris et al., 2001).
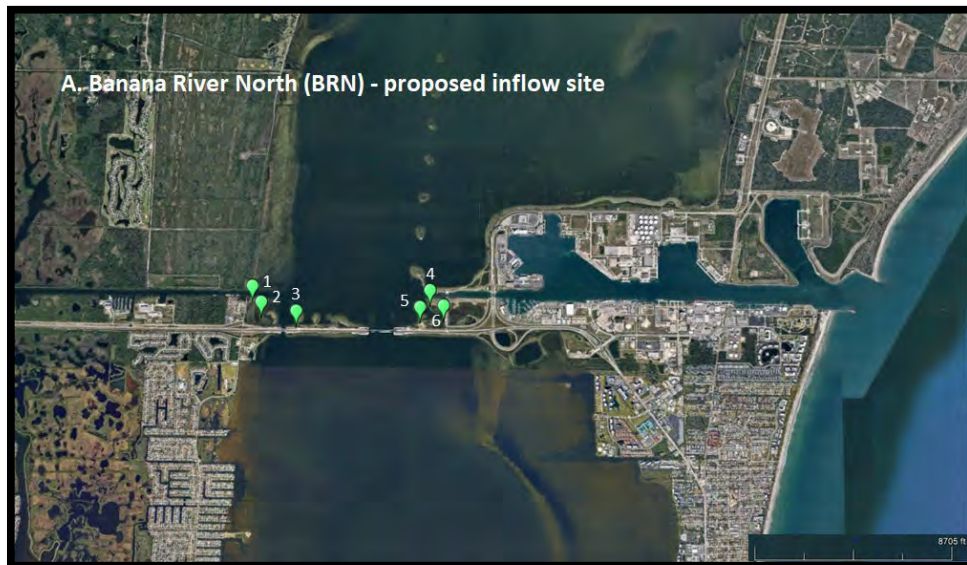

Figure 38. Banana River North submerged aquatic vegetation sampling sites shown in green, numbered 1-6 (n=6)

Figure 39. Banana River South submerged aquatic vegetation sampling sites shown in green, numbered 7-12 (n=6)

4.4.1.1   Submerged Aquatic Vegetation Results for Phase 3

Seagrass presence varied across all sites and when present, was mostly sparse. Two species of seagrass were observed in sampling, Widgeon grass (*Ruppia maritima*) and Cuban shoal grass (*Halodule wrightii*) (**Figure 39**). No seagrass was observed in 2023 at five of the sampling sites: the three sites proximate to the pilot inflow site in Banana River North (transects #4, #5, and #6) and the two southernmost sites in the west portion of Banana River South (transects #11 and #12).
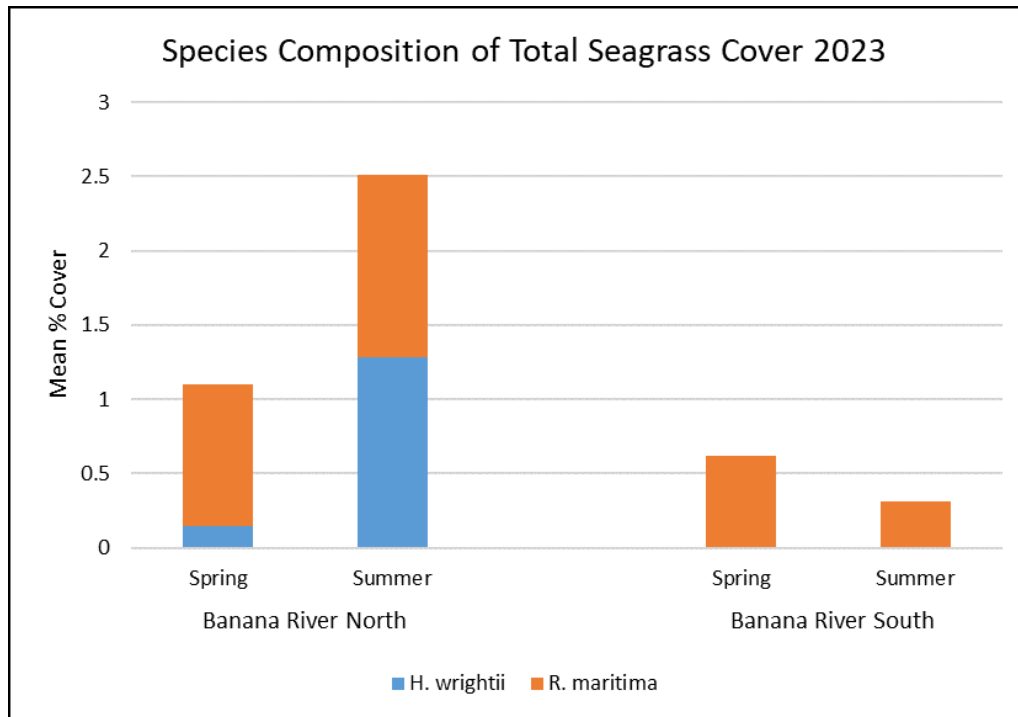
Figure 40. Species composition of mean total visual percent seagrass cover for Banana River North and Banana River South sites spring and summer 2023 for observed species of seagrasses *Ruppia maritima* and *Halodule wrightii*

4.4.1.2   Seagrass Results for Phases 1 through 3

Of the six sites surveyed continuously during all three project phases (transects 1 - 3 and 7 - 9), mean total seagrass cover was highest at Banana River North sites in summer 2023. Total seagrass cover ranged from 0.1% to 3.88% at Banana River North sites and 0% to 0.5% at Banana River South sites (**Figure 13** and **Figure 14**). Banana River North experienced positive growth in mean total seagrass cover from March 2021 to summer 2023. Seagrass cover was consistently low at the Banana River South sites throughout the three phases and did not mimic the growth trend observed at Banana River North sites in the latter half of the project.

Drift algae and *C. prolifera* cover were dynamic throughout the study in both Banana River North and Banana River South. Trends in drift algae cover at Banana River North and Banana River South sites were similar, with peaks in winter 2020 and summer 2021, until summer of 2023 when mean drift algae cover reached its highest point at Banana River South (34.1%) while mean cover in Banana River North stayed relatively low (4.6%). Cycles of *C. prolifera* cover at Banana River North and Banana River South sites did not trend as closely as drift algae cover, reaching peaks in different seasons. The highest mean percent cover of *C. prolifera* occurred in Banana River South sites in spring 2020 (27%).

4.4.1.3   Conclusion

Since 2011, the IRL has lost approximately 58% of seagrass coverage (Morris et al., 2022). These losses are evident in current seagrass conditions of the BRL as seagrass coverage was low at most sampling locations throughout the study. Some sampling locations which once boasted dense seagrass beds, were devoid of seagrass throughout the study period. Additionally, coverage of other submerged aquatic vegetation including drift algae species and rooted macroalgae species *Caulerpa prolifera* were inconsistent and ephemeral through the study.

Without established seagrass beds or stable macroalgae communities, the BRL lacks essential benthic habitat and will continue to suffer from nutrient resuspension as algae and seagrass populations go through cycles of growth and collapse.

In Phase 3, sites in Banana River North exhibited increases in seagrass cover and species composition that may be consistent with signs of recovery of seagrass populations, but water quality conditions remain dynamic in the area. Several months of reduced water clarity brought on by nutrient pollution driven algae blooms could reverse progress. Improvements to water quality in the BRL are necessary to expand seagrass cover and restore benthic habitat.

4.4.2 FWC, Florida Fish and Wildlife Research Institute

The nekton community (free swimming organisms) of the BRL was sampled by the FWC-FWRI Fisheries-Independent Monitoring Program (FIM) between 1990 until 2016 (Tremain and Adams, 1995; Paperno et al., 2016; FWC-FWRI, 2017), after which budgetary restrictions resulted in these efforts being discontinued. As a result of the reduction in effort from this basin, the status of the small-bodied nekton community in the BRL has been largely undocumented over the past several years.

The objective of this sampling project was to provide a current account of nekton abundance and species richness in close proximity of the proposed Restore Lagoon Inflow Project and at a control site approximately 12.5 km south in the BRL (**Figure 40**), that will function as a baseline to evaluate future changes that may occur under pilot project conditions.

Beginning in March 2023 and continuing through June 2023, stratified-random sampling was conducted to provide comprehensive abundance and distribution data on fishes that occur at two sites in the BRL. Sampling events occurred in March, May, and June 2023 and consisted of eight randomly selected 21.3- m seine stations split evenly between the proposed inflow site near Cape Canaveral in the BRL and a control site located approximately 12.5 km south in the BRL (**Figure 40**).
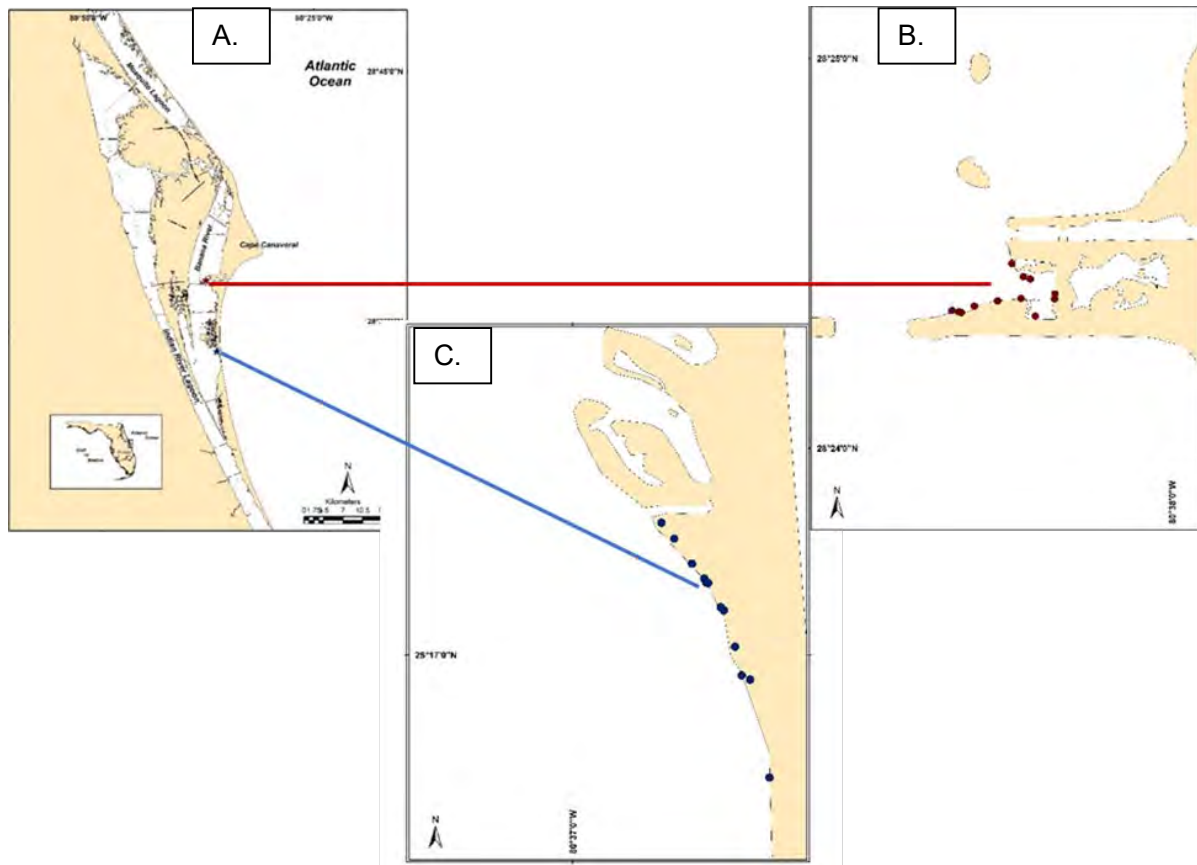
Note: Red circles=21.3-m shore seines at the inflow site; Blue circles = 21.3-m shore seines at the control site.
Figure 41. Map of BRL (A) and location of study sites within BRL (B and C) in Brevard County

4.4.2.1 Stratified-Random Sampling
A total of 33,919 animals, which included 38 taxa of fishes and 3 taxa of selected invertebrates, were collected from 24 BRL stratified-random samples. Bay Anchovy, *Anchoa mitchilli* (n = 31,757) was the most abundant taxon collected, accounting for 93.6% of the total catch. Spot, *Leiostomus xanthurus* (n = 472), *Brevoortia* spp. (n = 287), and *Menidia* spp. (n = 2,409) were the next most abundant taxa collected, accounting for an additional 3.1% of the total catch. Thirteen selected taxa (n = 1,161) composed 3.4% of the total catch. *Leiostomus xanthurus* (n = 472), *Brevoortia* spp. (n = 287), and Atlantic Croaker, *Micropogonias undulatus* (n = 266) were the most abundant selected taxa, representing 88.2% of the selected taxa (3.0% of the total catch).

4.4.2.2 Inflow Sites
A total of 31,557 fishes and selected invertebrates which included 30 taxa of fishes and 3 taxa of selected invertebrates, were collected in 12 samples from this site during the study period. *Anchoa mitchilli* (n = 29,623) was the most numerous species collected, representing 93.9% of the total 21.3-m seine catch at this site. The two next most abundant taxa, *L. xanthurus* (n = 472) and Brevoortia spp. (n = 287) accounted for an additional 2.4% of the total catch at this site. The taxa most frequently caught at the inflow sites were *Eucinostomus* spp. (100% occurrence), followed by *A. mitchilli*, *L. xanthurus*, and *Menidia* spp. (all at 75.0% occurrence).

A total of 13 selected taxa (n=1,158 animals) were collected, representing 3.7% of the total 21.3-m seine catch at the inflow sites. *Leiostomus xanthurus* (n = 472), *Brevoortia* spp. (n = 287), and *M. undulatus* (n = 266) were the most abundant selected taxa, representing 3.2% of the total inflow site catch (88.5% of the selected taxa). The selected taxa most frequently caught at the inflow sites were *L. xanthurus* (75.0% occurrence) and White Mullet, *Mugil curema* (66.7% occurrence).

4.4.2.3 Control Sites

A total of 2,362 animals, which included 23 taxa of fishes and 0 taxa of selected invertebrates, were collected in 12 samples from this site during the study period. *Anchoa mitchilli* (n = 2,134) was the most numerous taxa collected, accounted for 90.4% of the total catch at this site. The two next most abundant taxa, *Menidia* spp. (n = 89) and Rainwater killifish, *Lucania parva* (n = 48), accounted for an additional 5.8% of the catch at this site. The taxa most frequently caught at the control sites were *Menidia* spp. and Goldspotted Killifish, *Floridichthys carpio* (both at 54.5% occurrence).

A total of two selected taxa (n = 4 animals) were collected, representing 0.2% of the total catch at the control sites. Red Drum, *Sciaenops ocellatus* (n = 3) and a single *M. curema* were the only selected taxa collected at control sites.

4.4.2.4 Conclusion

The communities at both sites were found to be typical of historic communities described for the area. The proposed inflow area was more diverse than the control site (30 versus 23 taxa). The difference in overall number of animals collected at each area was a result of the greater number of *A. mitchilli* that were collected at the inflow sites (n = 29,623) versus the control sites (n = 2,134). The collection of fisheries community data in the BRL provide a baseline database from which changes in estuarine health (i.e., loss of seagrass) and restoration efforts may be evaluated for this area of the IRL*.*

4.4.3 Florida International University

For Phase 3, the goal was to investigate thermal and halotolerances, with available data, through complimentary literature review and assessment of twenty-two years of FIM program data to describe the relationships between key SoI, temperature, and salinity. For each species, two guiding questions were explored: (1) What are the known temperature and salinity relationships described in the literature for this species, and (2) What temperatures and salinities is this species typically found in in the BRL?

4.4.3.1 Species Selection

Species selection began with the SoI used in the Restore Lagoon Inflow Phase 2 report: Bay Anchovy, Anchoa mitchilli, Sheepshead, Archosargus probatocephalus, Spotted Seatrout, Cynoscion nebulosus, Pinfish, Lagodon rhomboides, Gray Snapper, Lutjanus griseus, Black Drum, Pogonias cromis, Red Drum, Sciaenops ocellatus and Gulf Pipefish, Syngnathus scovelli. Please see the Restore Lagoon Inflow Phase 2 Final Report section 4.3.1.1 for information on how and why those species were chosen (Blanchard et al., 2021). From here, the 20 most abundant fishes in the BRL as described in the Restore Lagoon Inflow Phase 1 final report (Johnson et al., 2020) were considered, selecting species which have ecological significance not necessarily captured in the previous listing (e.g., trophic position, feeding strategy, life history, etc.). This led to the inclusion of Tidewater Mojarra (*Eucinostomus harengulus*), Spot (*Leiostomus xanthurus*), Thread herring (*Opisthonema oglinum*), and Striped Mullet (*Mugil cephalus*). The Mojarra and Herring are commonly used as baitfish, colloquially called "greenies" and "saw-

bellies." There are active fisheries for them in several regions of the state and both are pelagic low-trophic level predators, with Mojarra primarily targeting small crustaceans (Chi-Espínola et al., 2018) and Herring being more zooplanktivorous ram filter feeders (Finucane and Vaught, 1986; Smith, 1994). Spot are culled recreationally, though mainly for bait, and there are limited commercial fisheries for them around the state. They are smaller bodied, low trophic level, con-familials of the recreationally important drums already in the list (McCall and Fleeger, 1993; Johnson et al., 2013). Striped Mullet are popular baitfish culled by recreational net collections as table fair and bait. They are benthivorous, low trophic level fish that form large schools and have a well-documented migration which provides substantial economic value to Florida (Whitfield et al., 2012). For several of these species, there were other analogous options (e.g., *Eucinostomus gula* instead of *Eucinostomus harengulus*, *Bairdiella chrysoura* instead of *Leiostomus xanthurus*). In such an instance, the "tie" was broken by selecting the more common species in the BRL area, as described in the Phase 1 report (Johnson et al. 2020).

To characterize temperature and salinity envelopes of BRL SoI, for each gear and SoI combination, plots were generated in R Studio depicting SoI annual frequency of occurrence and the raw density at observed temperatures and salinities. The relationship between density and temperature, or salinity, was also calculated and critical statistics provided on the relevant plot. A set of temporally explicit rasters of environmental conditions encountered within the FWC data, regardless of species collected, as well as rasters containing the combination of spatiotemporally explicit occurrences of each SoI with respect to those environmental parameters were also provided in support of habitat suitability model development.

A detailed literature review and integrated summary of each of the selected species thermal and halotolerances is provided in Appendix G. Frequency of occurrence in combination with temperature and salinity data are provided on **Table 10**, **Table 11**, and **Table 12**.

Table 10. Observed abiotic conditions for the BRL and each Sol for each gear type from 1996–2018 in the FWC data

Note: P and Adj R² denote significance of the linear model between fish density and temperature or salinity. NS denotes where the relationship was not statistically significant, and any species-gear combination that had less than 25 observations was left blank to indicate it being data deficient.

Species	Gear	# of fish	Min. Temp.	Max. Temp.	Mean Temp.	P	Adj. R²	Min. Salinity	Max Salinity	Mean Salinity	P	Adj. R²
BRL			6.30	40.00	25.55			0.00	47.80	23.29		
Anchoa mitchilli	20	5040	9.90	34.00	25.51	<=0.001	0.007	0.20	47.80	25.52	NS	NS
	160	3										
	300	249	9.67	32.90	24.59	NS	NS	0.60	36.70	22.21	NS	NS
	301	255	9.90	33.05	24.88	NS	NS	0.60	38.30	27.07	NS	NS
Archosargus probatocephalus	20	1184	9.95	35.00	26.97	0.013	0.004	0.20	47.60	28.66	0.020	0.004
	160	2808	7.10	34.95	25.89	<=0.001	0.013	1.50	43.87	26.20	<=0.001	0.009
	300	92	15.50	32.03	25.72	NS	NS	8.40	36.70	28.29	0.004	0.076
	301	165	11.07	32.75	26.46	NS	NS	0.55	38.67	30.11	NS	NS
Cynoscion nebulosus	20	2637	6.30	40.00	28.20	NS	NS	0.20	35.00	24.95	NS	NS
	160	1440	6.70	34.95	24.32	NS	NS	9.70	42.60	25.16	0.002	0.006
	300	212	13.20	32.77	28.16	NS	NS	0.60	35.63	21.40	NS	NS
	301	135	18.25	33.60	29.27	NS	NS	9.13	39.10	26.92	NS	NS
Eucinostomus harengulus	20	2365	9.00	40.00	26.80	<=0.001	0.022	4.40	46.40	27.35	NS	NS
	160	1893	9.10	34.95	25.88	NS	NS	7.50	43.87	25.87	0.002	0.005
	300	83	13.60	32.77	25.19	0.050	0.040	11.72	39.00	29.17	0.040	0.040
	301	117	11.23	33.20	27.20	NS	NS	1.15	35.40	28.30	NS	NS
Lagodon rhomboides	20	2955	9.10	35.00	25.69	0.040	0.001	9.40	47.80	29.25	0.001	0.003
	160	3135	6.70	34.00	25.94	<=0.001	0.016	7.30	43.87	25.96	<=0.001	0.018
	300	285	12.15	32.90	24.43	0.001	0.007	12.80	37.80	28.81	NS	NS
	301	464	10.40	33.20	24.93	<=0.001	0.010	13.17	38.67	30.00	NS	NS
Leiostomus xanthurus	20	1399	8.50	33.90	22.95	NS	NS	4.80	47.80	28.22	NS	NS
	160	1314	10.00	33.55	26.74	0.001	0.007	10.00	43.87	27.62	<=0.001	0.010
	300	86	13.45	32.50	24.07	NS	NS	12.10	37.80	25.65	NS	NS
	301	114	12.67	32.75	23.92	0.039	0.029	13.23	38.67	30.53	NS	NS
Lutjanus griseus	20	473	12.40	34.80	27.81	0.003	0.017	0.20	43.50	26.91	NS	NS
	160	725	7.50	34.95	27.88	0.029	0.005	1.60	42.60	25.58	<=0.001	0.019

Species	Gear	# of fish	Min. Temp.	Max Temp.	Mean Temp.	P	Adj. R²	Min. Salinity	Max Salinity	Mean Salinity	P	Adj. R²
Mugil cephalus	300	50	18.10	32.77	27.89	NS	NS	12.43	35.55	27.87	NS	NS
	301	153	17.10	33.60	27.75	NS	NS	9.13	36.70	27.23	NS	NS
	20	1379	7.2	37.40	22.47	<=0.001	0.017	4.65	44.10	25.41	NS	NS
	160	4033	6.70	34.95	24.91	NS	NS	1.50	43.87	25.42	<=0.001	0.003
Opisthonema oglinum	300	2										
	301	0										
	20	372	11.50	33.70	28.14	NS	NS	0.20	41.80	27.63	0.046	0.008
	160	512	9.75	33.50	26.51	0.022	0.008	10.00	43.87	26.04	NS	NS
Pogonias cromis	300	0										
	301	1										
	20	115	14.80	33.90	26.44	NS	NS	2.00	42.00	26.58	NS	NS
	160	908	8.85	34.25	25.94	NS	NS	1.50	43.87	26.07	<=0.001	0.026
Sciaenops ocellatus	300											
	301											
	20	1234	7.80	33.55	22.48	NS	NS	2.80	41.70	24.78	NS	NS
	160	2248	7.50	34.25	25.40	0.002	0.004	1.60	43.87	25.26	<=0.001	0.019
Syngnathus scovelli	20	3459	7.40	35.30	24.68	<=0.001	0.010	1.60	47.60	26.11	NS	NS
	160	2										
	300	429	12.70	32.23	24.44	NS	NS	5.28	36.93	23.51	NS	NS
	301	396	10.40	33.20	25.53	NS	NS	12.70	37.10	28.71	NS	NS

Table 11. Frequency of occurrences of each Sol-gear type combination within each temperature bin

Note: Cells with more than 5% of the occurrences are highlighted in light gray, those with less than 5% of the occurrences are blocked in dark gray.

Species	Gear	# of fish	0-5 °C	5-10 °C	10-15 °C	15-20 °C	20-25 °C	25-30 °C	30-35 °C	35-40 °C
Anchoa mitchilli	20	5040	0.00%	0.05%	1.35%	11.30%	30.75%	39.25%	17.30%	0.00%
	160	3								
	300	249	0.00%	0.40%	2.41%	18.47%	28.11%	37.35%	13.25%	0.00%
	301	255	0.00%	0.78%	1.57%	20.39%	23.14%	34.51%	19.61%	0.00%
Archosargus probatocephalus	20	1184	0.00%	0.08%	0.59%	6.59%	22.47%	43.16%	27.11%	0.00%
	160	2808	0.00%	0.11%	1.75%	10.15%	26.35%	40.71%	20.94%	0.00%
	300	92	0.00%	0.00%	0.00%	7.61%	35.87%	41.30%	15.22%	0.00%
	301	165	0.00%	0.00%	0.61%	7.27%	21.82%	52.12%	18.18%	0.00%
Cynoscion nebulosus	20	2637	0.00%	0.08%	0.30%	5.23%	20.40%	47.71%	26.17%	0.11%
	160	1440	0.00%	0.35%	5.56%	18.40%	29.03%	31.32%	15.35%	0.00%
	300	212	0.00%	0.00%	0.94%	10.85%	13.21%	56.13%	18.87%	0.00%
	301	135	0.00%	0.00%	0.00%	2.22%	13.33%	45.93%	38.52%	0.00%
Eucinostomus harengulus	160	1893	0.00%	0.21%	2.38%	10.04%	25.99%	40.20%	21.18%	0.00%
	300	83	0.00%	0.00%	1.20%	16.87%	26.51%	38.55%	16.87%	0.00%
	20	2365	0.00%	0.08%	1.06%	7.15%	23.38%	41.48%	26.77%	0.08%
	301	117	0.00%	0.00%	2.56%	16.24%	20.51%	40.17%	20.51%	0.00%
Lagodon rhomboides	20	2955	0.00%	0.07%	1.52%	12.18%	26.77%	39.76%	19.70%	0.00%
	160	3135	0.00%	0.19%	1.85%	11.20%	23.76%	41.82%	21.18%	0.00%
	300	285	0.00%	0.00%	1.05%	15.79%	39.65%	32.98%	10.53%	0.00%
	301	464	0.00%	0.00%	1.72%	18.10%	30.82%	35.56%	13.79%	0.00%
Leiostomus xanthurus	20	1399	0.00%	0.21%	3.86%	23.95%	37.60%	27.31%	7.08%	0.00%
	160	1314	0.00%	0.08%	0.61%	6.39%	22.68%	48.02%	22.22%	0.00%
	300	86	0.00%	0.00%	2.33%	25.58%	23.26%	38.37%	10.47%	0.00%
	301	114	0.00%	0.00%	1.75%	29.82%	20.18%	31.58%	16.67%	0.00%
Lutjanus griseus	20	473	0.00%	0.00%	1.06%	3.59%	16.07%	49.68%	29.60%	0.00%
	160	725	0.00%	0.14%	0.83%	2.21%	15.86%	48.00%	32.97%	0.00%
	300	50	0.00%	0.00%	0.00%	2.00%	16.00%	64.00%	18.00%	0.00%
	301	153	0.00%	0.00%	0.00%	7.19%	15.03%	44.44%	33.33%	0.00%

Species	Gear	# of fish	0-5 °C	5-10 °C	10-15 °C	15-20 °C	20-25 °C	25-30 °C	30-35 °C	35-40 °C
Mugil cephalus	20	1379	0.00%	0.51%	6.96%	27.56%	32.78%	22.41%	9.72%	0.07%
	160	4033	0.00%	0.22%	2.78%	15.15%	29.51%	35.71%	16.64%	0.00%
	300	2								
	301	0								
Opisthonema oglinum	20	372	0.00%	0.00%	0.54%	1.34%	10.75%	59.41%	27.96%	0.00%
	160	512	0.00%	0.20%	1.56%	5.86%	22.46%	49.61%	20.31%	0.00%
	300	10								
	301	9								
Pogonias cromis	20	115	0.00%	0.00%	0.87%	10.43%	25.22%	38.26%	25.22%	0.00%
	160	908	0.00%	0.11%	1.65%	11.01%	25.22%	40.53%	21.48%	0.00%
	300	0								
	301	1								
Sciaenops ocellatus	20	1234	0.00%	0.49%	4.29%	24.23%	42.63%	24.39%	3.97%	0.00%
	160	2248	0.00%	0.13%	2.49%	12.37%	28.20%	37.94%	18.86%	0.00%
	300	17								
	301	45	0.00%	0.00%	2.22%	40.00%	46.67%	11.11%	0.00%	0.00%
Syngnathus scovelli	20	3459	0.00%	0.14%	2.63%	16.94%	30.90%	33.13%	16.22%	0.03%
	160	2								
	300	429	0.00%	0.00%	3.50%	17.48%	31.47%	34.73%	12.82%	0.00%
	301	396	0.00%	0.00%	1.26%	16.67%	23.23%	38.13%	20.71%	0.00%

Table 12. Frequency of occurrences of each Sol-gear type combination within each salinity bin

Note: Cells with more than 5% of the occurrences are highlighted in light gray, those with less than 5% of the occurrences are blocked in dark gray.

Species	Gear	# of fish	0-5 ppt	5-10 ppt	10-15 ppt	15-20 ppt	20-25 ppt	25-30 ppt	30-35 ppt	35-40 ppt	40-44 ppt	45-50 ppt
Anchoa mitchilli	20	5040	0.20%	0.60%	6.50%	17.60%	23.15%	22.15%	21.00%	7.40%	1.40%	0.00%
	160	3										
	300	249	0.40%	0.40%	20.08%	22.49%	22.09%	15.26%	16.47%	2.81%	0.00%	0.00%
	301	255	0.00%	0.39%	2.75%	9.80%	21.96%	29.02%	31.37%	4.71%	0.00%	0.00%
Archosargus probatocephalus	20	1184	0.17%	0.84%	3.72%	8.70%	15.29%	21.71%	31.25%	15.46%	2.70%	0.17%
	160	2808	0.07%	0.43%	5.41%	15.35%	21.12%	24.93%	22.83%	9.44%	0.43%	0.00%
	300	92	0.00%	1.09%	2.17%	10.87%	10.87%	18.48%	46.74%	9.78%	0.00%	0.00%
	301	165	0.61%	0.00%	1.21%	4.85%	7.27%	24.24%	49.09%	12.73%	0.00%	0.00%
Cynoscion nebulosus	20	2637	0.23%	0.61%	7.24%	18.66%	23.59%	23.25%	18.28%	6.83%	1.33%	0.00%
	160	1440	0.00%	0.21%	4.10%	20.00%	26.32%	25.21%	17.64%	6.18%	0.35%	0.00%
	300	212	0.47%	0.47%	18.87%	30.66%	17.92%	16.04%	13.68%	1.89%	0.00%	0.00%
	301	135	0.00%	1.48%	1.48%	9.63%	24.44%	22.22%	34.81%	5.93%	0.00%	0.00%
Eucinostomus harengulus	20	2365	0.13%	0.51%	4.02%	13.32%	20.68%	24.40%	25.03%	10.19%	1.69%	0.04%
	160	1893	0.00%	0.16%	3.91%	16.90%	25.25%	24.62%	20.66%	8.19%	0.32%	0.00%
	300	83	0.00%	0.00%	9.64%	9.64%	12.05%	21.69%	42.17%	4.82%	0.00%	0.00%
	301	117	0.85%	0.85%	2.56%	3.42%	14.53%	29.91%	43.59%	4.27%	0.00%	0.00%
Lagodon rhomboides	20	2955	0.00%	0.14%	3.38%	8.32%	14.42%	20.95%	33.91%	14.99%	3.72%	0.17%
	160	3135	0.00%	0.19%	3.80%	17.99%	23.13%	23.76%	22.55%	8.20%	0.38%	0.00%
	300	285	0.00%	0.00%	6.32%	7.37%	9.47%	20.00%	45.26%	11.58%	0.00%	0.00%
	301	464	0.00%	0.00%	0.65%	2.80%	12.50%	28.66%	42.46%	12.93%	0.00%	0.00%
Leiostomus xanthurus	20	1399	0.07%	0.21%	4.72%	8.79%	18.66%	22.02%	30.38%	12.22%	2.72%	0.21%
	160	1314	0.00%	0.15%	2.44%	11.19%	20.32%	24.81%	30.44%	10.05%	0.61%	0.00%
	300	86	0.00%	0.00%	17.44%	16.28%	6.98%	15.12%	36.05%	8.14%	0.00%	0.00%
	301	114	0.00%	0.00%	0.88%	1.75%	11.40%	24.56%	46.49%	14.91%	0.00%	0.00%
Lutjanus griseus	20	473	0.42%	0.85%	4.86%	10.99%	18.39%	26.64%	30.02%	6.98%	0.85%	0.00%
	160	725	0.14%	0.69%	4.83%	15.17%	27.03%	24.14%	21.66%	5.93%	0.41%	0.00%
	300	50	0.00%	0.00%	2.00%	10.00%	18.00%	24.00%	44.00%	2.00%	0.00%	0.00%

Restore Lagoon Inflow Research (Phase 3)
Summary Report

Species	Gear	# of fish	0-5 ppt	5-10 ppt	10-15 ppt	15-20 ppt	20-25 ppt	25-30 ppt	30-35 ppt	35-40 ppt	40-44 ppt	45-50 ppt
Mugil cephalus	301	153	0.00%	0.65%	0.65%	9.80%	20.26%	33.99%	31.37%	3.27%	0.00%	0.00%
	20	1379	0.22%	0.65%	7.69%	15.88%	24.22%	21.75%	21.54%	7.03%	1.02%	0.00%
	160	4033	0.05%	0.27%	5.73%	18.35%	24.52%	22.56%	20.31%	7.86%	0.35%	0.00%
	300	2										
Opisthonema oglinum	301	0										
	20	372	0.54%	0.27%	2.15%	8.33%	24.73%	24.46%	24.46%	13.44%	1.61%	0.00%
	160	512	0.00%	0.20%	3.71%	15.43%	23.05%	28.91%	22.46%	5.86%	0.39%	0.00%
	300	10										
Pogonias cromis	301	9										
	20	115	0.87%	0.00%	6.09%	14.78%	21.74%	20.00%	20.00%	15.65%	0.87%	0.00%
	160	908	0.22%	0.88%	4.63%	14.76%	23.79%	24.56%	20.70%	9.91%	0.55%	0.00%
	300	0										
Sciaenops ocellatus	301	1										
	20	1234	0.16%	1.13%	6.48%	19.85%	22.61%	23.50%	21.72%	4.29%	0.24%	0.00%
	160	2248	0.04%	0.31%	6.09%	18.59%	25.09%	23.13%	17.57%	8.67%	0.49%	0.00%
	300	17										
Syngnathus scovelli	301	45	2.22%	2.22%	0.00%	11.11%	31.11%	24.44%	26.67%	2.22%	0.00%	0.00%
	20	3459	0.12%	0.43%	7.55%	16.97%	21.19%	19.57%	21.02%	10.90%	2.17%	0.09%
	160	2										
	300	429	0.00%	0.23%	16.55%	26.34%	12.35%	14.69%	24.48%	5.36%	0.00%	0.00%
	301	396	0.00%	0.00%	1.01%	8.84%	13.38%	28.54%	38.13%	10.10%	0.00%	0.00%

4.4.3.2 Conclusions

Given the vital importance of understanding fish responses to the Restore Lagoon Inflow proposal, this limited and constrained study was developed to: (1) advance understanding of the models produced in Phase 2, and (2) lay the groundwork for that next phase of research: habitat suitability modeling. For this Phase 3 effort, the SoI list was expanded from eight to eleven species to represent a broader ecological context. As this effort is descriptive in nature, no specific conclusions can be reached at this time. Rather, this report provides two valuable deliverables: (1) identification of critical unknowns, which will guide future research questions to be answered during or in advance of any pilot project; and 2) a large portion of the data-infrastructure needed to build species specific habitat suitability models.

This report discusses several critical unknowns with respect to each of the eleven SoI examined. While data on physiological tolerances and habitat use varies among species, there was an emergent recurrent theme in the data gaps.

1) What is the rate of environmental change anticipated by the proposed pumping scenarios?

Estuarine fishes are used to environmental change. It is a normal part of their daily lives in the IRL. They can adapt to changes within their environmental envelopes, and many will emigrate if conditions warrant. However, their adaptive mechanisms take time to respond. If the rate of change exceeds their responsive capacity, it results in quantifiable levels of stress and can result in fish kills similar to what is seen during a HAB induced hypoxia event, cold snap, or heat wave. Inflow pumping ramp-up speeds must be below the level which would induce a fish kill. *To determine what pumping schedule (ramp-up speeds and final pumping rates) are both safe and effective, it will be important to determine the spatially explicit rate of environmental change to be expected under proposed pumping scenarios.*

2) What rate of environmental change can BRL fishes tolerate?

The mechanism behind a fish's adaptive capacity, its efficacy, and their ability to endure stresses to that system are highly species specific. In many cases, they are population specific. For several of the SoI described above, this information is known, or at least can be approximated with a reasonable degree of confidence. However, data gaps exist for the majority of species and the literature review presented above highlighted this need. *To determine a safe pumping schedule, we need to understand the rate of change which can be tolerated by BRL fishes.*

3) How will habitat suitability change in the BRL under each pumping scenario?

At its core, the proposal to increase inflow to the BRL to facilitate biochemical processes to reduce resident pollution levels and restore water quality is an effort to restore the suitability of the BRL habitats to resident species. The Restore Lagoon Inflow Fish Team's efforts to date, including this report, have been building the necessary infrastructure to model habitat suitability changes anticipated in response to each proposed inflow scenario. With this report, we now have the analytical infrastructure necessary to produce these projections. However, we have also learned that the story of how BRL fishes will respond to increased inflow is likely as much behavioral as it is physiological. Some data exist regarding the movement ecology of fishes in the BRL, as summarized in the Phase 2 report, but it is not at the resolution we would need to inform habitat suitability model development. *Moving forward, to improve assessment of inflow impacts to the BRL and IRL overall, we need to better understand the behavioral component of fish responses to changing water quality conditions. This information will inform habitat suitability modeling to*

address the core question regarding the fish response to the Restore Lagoon Inflow proposal:
How will habitat suitability for each SoI change under each pumping scenario?

4.4.4 HSWRI

Evaluating the nutritional condition of free-swimming dolphins can provide valuable information regarding the health of the individuals as well as the population as a whole (Hart et al., 2013; Joblon et al., 2014). Assessing the health of bottlenose dolphins inhabiting the IRL is particularly important as this dolphin stock has been described as an immune compromised population (Bossart et al*.,* 2007) and has been subjected to four Unusual Mortalities Events (UMEs) (2001, 2008, and 2013) including a morbillivirus epidemic (2013–2015) (National Oceanic and Atmospheric Administration 2015). Since seagrass provides critical habitat for prey consumed by estuarine dolphins (Barros and Wells 1998), efforts to improve water quality and restore seagrass habitats could improve the health of the vulnerable IRL dolphin population.

In light of these reoccurring events, establishing baseline information on nutritional condition for the IRL dolphin population is critical to interpreting significant changes during subsequent UMEs. Furthermore, as efforts are made to improve water quality within the region, it will be imperative to have an accurate understanding of dolphin health before and after extensive restorative efforts are employed. The evaluation of lateral photographs of free-swimming bottlenose dolphins can provide consistent data on nutritional condition between seasons or even between years. Previous evaluation of IRL dolphin nutritional condition (2016) indicated that the majority of dolphins in this region (75%) are not in adequate nutritional condition (59% underweight; 16% emaciated). The intent of this study was to collect and utilize images of bottlenose dolphins to evaluate nutritional condition and other indicators of dolphin health (epidermal lesions) for animals inhabiting the northern IRL (northern IRL and BRL).

4.4.4.1 Approach

Dorsal fin image analyses followed established protocols (Mazzoil et al., 2004) and were matched to an existing photo-identification catalog. Matches were accepted only if at least two experienced personnel agreed. To ensure that dolphins were not evaluated twice (unrecognized dolphins resighted), only animals with marked (identifiable) dorsal fins were included in analyses. Likewise, dorsal fins were compared between sub-basins within each complete replicate (northern IRL, BRL) to ensure that animals were only evaluated once. To avoid biasing data with age-related features that may resemble an underweight body condition, calves (including marked calves) were excluded from analyses. A standardized body condition index was used as in prior assessment of IRL dolphins (Fair et al., 2006). All images of each individual (head, body, and peduncle regions) were reviewed to facilitate body condition evaluation. The post-nuchal region is recognized as the key area that loses fat reserves in a nutritionally compromised dolphin and can reliably predict poor body condition (Gryzbek, 2013). However, since movement can temporarily alter the degree of convexity or concavity of a dolphin's post-nuchal fat pad or cause the misleading appearance of fat rolls on the neck, only straight-line body position images were used for scoring. Photographic analyses of body condition of free-swimming dolphins can be subjective and extreme care was taken to be conservative when evaluating photographs. From prior work, it was found that assigning body condition based on one criterion (excluding the post-nuchal depression), may over-estimate the number of dolphins that are underweight. The epaxial musculature and transverse processes are often difficult to evaluate since the animal may be diving or otherwise contorted when exposing the transverse processes, and the epaxial musculature is often obscured by lighting and may appear slightly depressed in some photographs and flat in others. For these reasons, individuals were evaluated conservatively by

using the presence of two or more criteria with an emphasis on the post-nuchal criterion (only acceptable single criterion) to most accurately determine body condition.

Dolphin nutritional condition was binned into ideal, underweight, or emaciated categories and the percentage of each was further evaluated by sub-basin and age class (adult females with and without dependent calves). In circumstances where more than one indicator of body condition was not available, the body condition was scored as could not be determined. Consistent scoring was conducted to enable comparisons with prior evaluations (2008, 2013, and 2016).

Bi-lateral striping was a previously undefined abnormality that has only been documented in the northern and central portion of the IRL (Titcomb et al., 2020). Since the anomaly may be related to significant weight gain/loss (like stretch marks in humans) (Titcomb et al., 2020), each individual was thoroughly evaluated for presence of striping and examined the influence of sub-basin and age class (adults with and without dependent calves).

Epidermal lesions may serve as indicators of cetacean population health and can signify a compromised environment (Van Bressem et al., 2009; Reif et al., 2009; Sanino et al., 2014). The presence and prevalence of epidermal conditions (lesions/anomalies) can provide useful baseline information. Images were thoroughly evaluated for the presence of epidermal disease/anomalies (adjusting contrast/exposure where necessary). If images were not of sufficient quality (poor contrast, lacking excellent focus) or sufficient portions of the animal's body were not exposed during the sighting, epidermal lesions were scored as could not be determined. When epidermal conditions were detected, cases were further grouped based on previously published literature (Harzen and Brunnick, 1997; Bertulli et al., 2012; Sanino et al., 2014; Vilela et al., 2016; Herr et al., 2020) or, in correspondence with prior HSWRI stranding histological evidence (HSWRI unpublished data). Groupings included: (1) pox-like lesions, (2) paracoccidioidomycosis, (3) ulcerated lesions, (4) raised cutaneous lumps, (5) suspected algal sheen, and (6) other unspecified lesions without classification.

4.4.4.2 Results

Between June 19 and June 27, 2023, five vessel-based surveys were conducted over three days to enable two replicate surveys of the northern IRL and BRL. A total of 77 dolphin groups (sightings) were encountered, containing 393 individuals. A total of 194 dolphins were sighted in the BRL and 199 dolphins in the northern IRL. Photographs were sorted by standardized methods, matched to an existing catalog, and evaluated for nutritional condition. A total of 233 identifiable dolphins were identified. **Table 13** presents the results summary of the nutritional conditions observed. **Table 14** provides additional information on the age and presence of calves. **Table 15** provides the epidermal condition results.

We found the overwhelming majority of IRL dolphins presented in decreased nutritional condition (underweight or emaciated; **Table 13**). Female dolphins with dependent calves were more commonly found in poor body condition (emaciated) than adult animals without calves. Prior evaluation of IRL dolphin nutritional condition has shown variance in the number of animals presenting in ideal (2008: 15%; 2013: 31%; 2016: 24%), underweight (2008: 50%; 2013: 64%; 2016: 59%) and emaciated (2008: 35%; 2013: 5%; 2016: 15%) nutritional condition. However, the percentage of animals currently presenting in less-than-ideal condition (93%), was staggering and unprecedented. The prevalence of dolphins that are in poor nutritional condition is concerning. These data will serve as baseline data to evaluate if future mitigation efforts result in improved health of dolphins residing in the northern IRL.

Table 13. Summary of the nutritional condition of IRL dolphins in the northern IRL and BRL during summer 2023 (evaluated by photographic images)

Note: The percentage of each nutritional condition type per sub-basin is presented.

Nutritional Condition	Northern IRL	%	BRL	%	Total	%
Ideal	7	7.95	4	5.97	11	7.10
Underweight	58	65.91	48	71.64	106	68.39
Emaciated	23	26.14	15	22.39	38	24.52
Total number evaluated	**88**		**67**		**155**	

Table 14. Summary of the nutritional condition of IRL dolphins in the northern IRL and BRL during summer 2023 (evaluated by photographic images)

Note: The percentage of each nutritional condition type per age class (adult with and without dependent calves) is presented.

Nutritional Condition	Adult females with Dependent Calves	%	Adults Without Dependent Calves	%	Total	%
Ideal	1	2.86	10	8.33	11	7.10
Underweight	21	60.00	85	70.83	106	68.39
Emaciated	13	37.14	25	20.83	38	24.52
Total number evaluated	**35**		**120**		**155**	

Table 15. Evaluation of the presence of epidermal conditions in dolphins inhabiting the northern IRL during summer 2023

Note: Total evaluated is the number of cases where photographs allowed for a thorough evaluation. Conditions were grouped and the percentage of individuals that exhibited each condition in each sub-basin is presented.

Epidermal Condition	Northern IRL	%	BRL	%	Total	%
Pox-like	58	70.73	44	61.11	102	66.23
Algal sheen	51	62.20	51	70.83	102	66.23
>1 epidermal condition	35	42.68	27	37.50	62	40.26
Paracoccidioidomycosis like	1	1.22	1	1.39	2	1.30
Ulcerated lesions	0	0.00	1	1.39	1	0.65
Raised cutaneous lumps	0	0.00	2	2.78	2	1.30
Other unspecified lesions	5	6.10	1	1.39	6	3.90
Total evaluated	82		72		154	

Table 16. Comparison of IRL dolphin nutritional condition

Note: Evaluation years include UME years (2008 and 2013) and non-UME years (2016 and 2023).

Year of Survey	% Ideal	% Underweight	% Emaciated	Comments
2008	15	50	35	June 2008; *n* = 20 animals evaluated in the northern IRL and BRL (Mazzoil et al., 2008)
2013	31	64	5	August-December 2013; *n* = 337 individuals evaluated in the northern IRL and BRL
2016	25	59	16	August 2016- May 2017; *n* = 340 individuals evaluated in the northern IRL, BRL, and Mosquito Lagoon
2023	7	68	25	June 2023; *n* = 155 individuals evaluated in the northern IRL and BRL

4.4.5 University of Florida

The goal of this study was to examine spatial trends in the composition, abundance and biomass of phytoplankton in the northern BRL. The results of this study provide information helpful for the design of monitoring programs associated with future management efforts aimed at mitigation of HABs. Four sampling sites were selected for the study, each representing key regions within the northern BRL ecosystem.

Water samples were collected monthly from four sites in the northern BRL (**Figure 41**) from February through June 2023. Phytoplankton cells were identified and counted at 400 times and 100 times with a Leica phase contrast inverted microscope.

Picocyanobacteria abundances were determined using a Zeiss Axio compound microscope, using green and blue light excitation (Fahnenstiel & Carrick, 1992; Phlips et al., 1999). Samples were preserved with buffered glutaraldehyde. Subsamples of water were filtered onto 0.2 μm Nucleopore filters and mounted between a microscope slide and cover slip with immersion oil, and picoplankton counted at 1000x magnification.
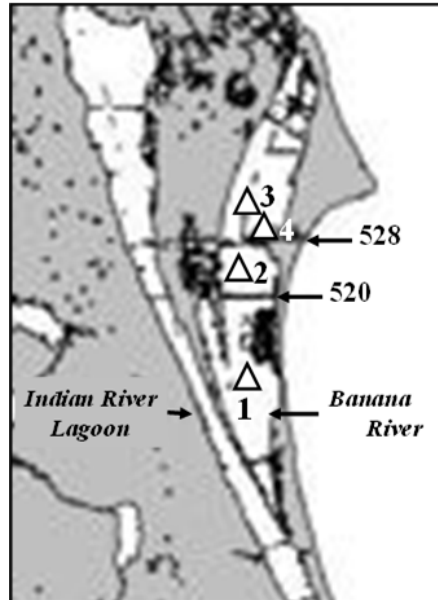
Figure 42. Site map.

4.4.5.1   Results
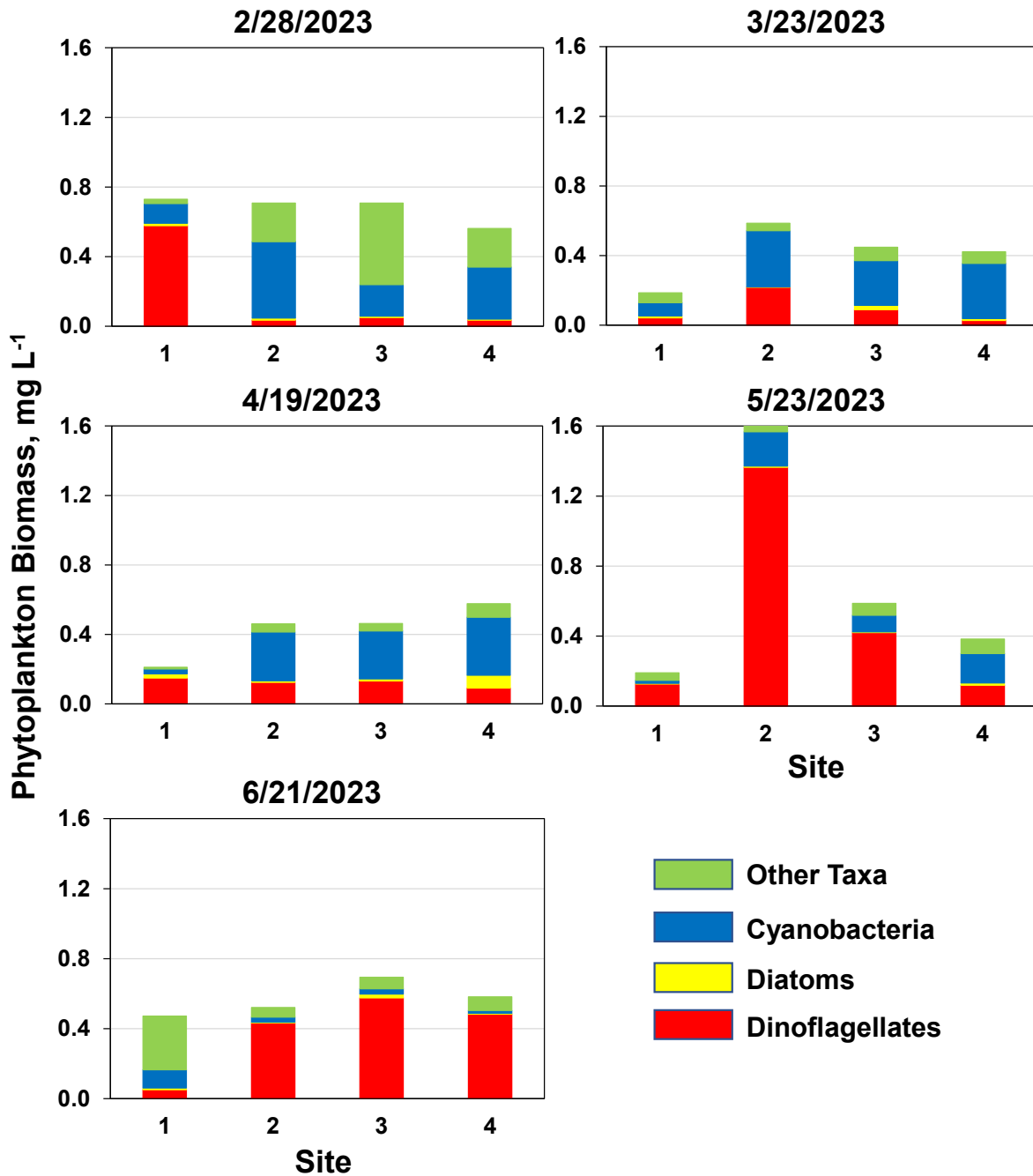
Figure 43. Phytoplankton biomass (mg carbon L-1) at the four sampling sites divided by major phytoplankton group, dinoflagellates (red), diatoms (yellow), cyanobacteria (blue), and other taxa (e.g., cryptophytes, chlorophytes, undefined nanoeukaryotes)

Table 17. Top-20 list of highest biomass observations for individual taxa, including frequency of occurrence in the list, highest biomass observed, and highest cell density

Site 1 - Central Banana River - Buck Pt.			
Species	Freq. in Top-20	Highest Biomass mg carbon/L	Highest Cell Density Cells x 10^3/L
Dinoflagellates			
Pyrodinium bahamense	3	0.085	14.6
Hermesinum adriaticum	1	0.531	1041.0
Gonyaulax polygramma	1	0.055	7.6
Gonyaulax sp.	1	0.032	14.2
Gymnoid sp. (< 15µ)	1	0.030	659.5
Pheopolykrikos hartmannii	1	0.017	1.0
Diatoms			
Rhizosolenia setigera	1	0.023	179.8
Cyanobacteria			
Spherical picocyanobacteria	3	0.107	606805.1
Cyanobium sp. cf	1	0.072	23160.5
Other Taxa			
Nanoplankton (2µ - 5µ)	3	0.059	18862.5
Cryptophyte (>5<15µ)	2	0.047	5123.4
Eutreptia sp (<30µ length)	1	0.196	604.6
Picoeukaryote (≤ 2µ)	1	0.021	43226.0

Site 2 - Between Highway 520 and 528			
Species	Freq. in Top-20	Highest Biomass mg carbon/L	Highest Cell Density Cells x 10^3/L
Dinoflagellates			
Pyrodinium bahamense	3	1.257	214.8
Hermesinum adriaticum	1	0.170	332.7
Peridinium quinquecorne	1	0.064	60.5
Tripos fusus	1	0.029	4.8
Protoperidinium sp.	1	0.016	30.2
Cyanobacteria			
Spherical picocyanobacteria	4	0.388	2204879.2
Cyanobium sp. cf	2	0.120	38600.8
Synechococcus spp.	1	0.038	111170.4
Other Taxa			
Nanoplankton (2µ - 5µ)	3	0.118	38087.3
Cryptophyte (>5<15µ)	2	0.033	3597.1
Picoeukaryote (≤ 2µ)	1	0.102	210084.6

Site 3 - North of Highway 528			
Species	**Freq. in Top-20**	**Highest Biomass mg carbon/L**	**Highest Cell Density Cells x 10^3/L**
Dinoflagellates			
Pyrodinium bahamense	3	0.472	80.6
Peridinium quinquecorne	1	0.032	30.2
Diatoms			
Rhizosolenia setigera	1	0.034	280.0
Cyanobacteria			
Spherical picocyanobacteria	4	0.315	1787990.8
Cyanobium sp. cf	2	0.067	21616.4
Synechococcus spp.	2	0.042	120434.6
Other Taxa			
Nanoplankton (2μ - 5μ)	3	0.156	50178.5
Cryptophyte (>5<15μ)	3	0.047	5123.7
Picoeukaryote (≤ 2μ)	1	0.057	116377.8

Site 4 - Adjacent to Port Canaveral Basin			
Species	**Freq. in Top-20**	**Highest Biomass mg carbon/L**	**Highest Cell Density Cells x 10^3/L**
Dinoflagellates			
Pyrodinium bahamense	3	0.561	95.8
Gonyaulax sp.	1	0.047	20.8
Hermesinum adriaticum	1	0.022	42.6
Gonyaulax polygramma	1	0.017	2.4
Diatoms			
Coscinodiscus sp.	1	0.021	10.0
Cerataulina pelagica	1	0.018	100.8
Cyanobacteria			
Spherical picocyanobacteria	4	0.276	1565649.8
Cyanobium sp. cf	2	0.024	7720.2
Synechococcus spp.	1	0.026	74113.6
Other Taxa			
Cryptophyte (>5<15μ)	3	0.062	6711.1
Nanoplankton (2μ - 5μ)	2	0.457	146901.6

4.4.5.2 Conclusion

In terms of total biomass levels and general phytoplankton group composition, Site 1 was the most distinct from the other three sites, with the lowest total biomass in three of the five sampling months, and significantly different composition in the two other months. The other three sites had generally similar phytoplankton group composition, and total biomass, with the exception of Site 2 in May, which had a bloom (defined as > 1 mg carbon L^{-1}) of the toxic dinoflagellate *P.*

bahamense. Historical records of phytoplankton composition in the BRL, and broader IRL, show that *P. bahamense* has been the most prevalent bloom-forming dinoflagellate in this ecosystem at least since 1997 (Phlips et al. 2010, 2015, 2020, 2021).

The dominant species observed in the four regions over the five-month study period were similar, as illustrated by the Top-20 list of highest biomass values for individual taxa (**Table 17**). In terms of numerical abundance, picoplanktonic cyanobacteria (including spherical forms and *Synechococcus* cf spp.) were always the highest at all four sites throughout the period, followed by nanoplanktonic eukaryotes (including cryptophytes). Picoplanktonic cyanobacteria and nanoplanktonic eukaryotes were also major components of the Top-20 list in terms of biomass at all four sites. Dinoflagellates were the other group prominently represented on the Top-20 list, particularly the HAB species *P. bahamense*. Diatoms were observed in every sample collected over the study period, but largely at comparatively low biomass levels.

The results of this study provide information helpful for the design of monitoring programs associated with future management efforts aimed at mitigation of HABs.

5   References

Abell, G.C. J., A.T. Revill, C. Smith, A.P. Bissett, J.K. Volkman, and S.S. Robert. 2010. Archaeal ammonia oxidizers and nirS–Type denitrifiers dominate sediment nitrifying and denitrifying populations in a subtropical macrotidal estuary. The ISME Journal 4(2):286–300.

Adams, D. H., A. Sebastian, and R. Paperno. 2022. Population decline of Gulf pipefish (Syngnathus scovelli) in a subtropical estuary: ecosystem changes and habitat loss. Marine Biodiversity:52–57.

Adams, D. H., D. M. Tremain, R. Paperno, and C. Sonne. 2019. Florida lagoon at risk of ecosystem collapse. Science 365:991–992.

Adams, G. D., R. T. Leaf, J. C. Ballenger, S. A. Arnott, and C. J. McDonough. 2018. Spatial variability in the growth of Sheepshead (Archosargus probatocephalus) in the Southeast US: Implications for assessment and management. Fisheries Research 206:35–43.

Adriance, J., K. Chapiesky, and J. Isaacs. 2019. Louisiana Black Drum.

Ahlgren, G. (1983). Comparison of methods for estimation of phytoplankton carbon. Arch. Hydrobiologia 98, 489-508.

Alshuth, S., and R. G. Gilmore. 1995. EGG AND EARLY LARVAL CHARACTERISTICS OF POGONIAS CROMIS, BAIRDIELLA CHRYSOURA AND CYNOSCION NEBULOSUS (PISCES: SCIAENIDAE), FROM THE INDIAN RIVER LAGOON, FLORIDA. International Council for the Exploration of the Sea. Conference Manuscript 50.

American Society of Civil Engineers. 2017. Chapter 2: Combinations of Loads. In Minimum design loads and associated criteria for buildings and other structures (ASCE/SEI 7-16) (pp. 7–9). essay.

Anweiler, K. 2013, May. Low-temperature tolerance of juvenile Spotted Seatrout, Cynoscion nebulosus, in South Carolina. Thesis, College of Charleston.

Babcock, K.K., F. Cesbron, W.F. Patterson, S.B. Garner, L.A. Waidner, and J.M. Caffrey. 2020. Changing biogeochemistry and invertebrate community composition at newly deployed artificial reefs in the northeast Gulf of Mexico. Estuaries and Coasts 43:680–92.

Badylak, S., Phlips, E. J., and Mathews, A. L. (2014). Akashiwo sanguinea (Dinophyceae) blooms in a sub-tropical estuary: An alga for all seasons. Plankton Benthos Res. 9. 1-9.

Barros, N.B. and R.S. Wells. 1998. Prey and feeding patterns of resident bottlenose dolphins (Tursiops truncatus) in Sarasota Bay, Florida. Journal of Mammalogy 79:1045–1059.

Bay, B., F. Author, J. C. Leak, E. D. Houde, J. C. Leak1, and E. D. Houde2. 1987. Cohort growth and survival of bay anchovy Anchoa mitchilli larvae in Cohort growth and survival of bay anchovy Anchoa mitchilli larvae in Biscayne Bay Florida. Source: Marine Ecology Progress Series 37:109–122.

Bayly, I. A. E. 1972. SALINITY TOLERANCE AND OSMOTIC BEHAVIOR OF ANIMALS IN ATHALASSIC SALINE AND MARINE HYPERSALINE WATERS.

Bechdel, S.E., M. Mazzoil, E. Murdoch, E.M. Howells, J.S. Reif, S.D. McCulloch et al. 2009. Prevalence and impacts of motorized vessels on bottlenose dolphins (Tursiops truncatus) in the Indian River Lagoon, Florida. Aquatic Mammals; 35(3): 367-37.

Bell, M., and C. McDonough. 2015. Sheepshead, Archosargus probatocephalus.

Benkendorff, K., C Klaas, and M. Kirby. 2022. Water quality in Woolgoolga estuary and valuation of nutrient removal servies by the remnant leaf oyster reef. 2022: Coffs Harbour City Council - Environmental Levy Program.

Bennett, W. A., and F. W. Judd. 1992. Comparison of Methods for Determining Low Temperature Tolerance: Experiments with Pinfish, Lagodon rhomboides. Copeia 1992:1059–1065.

Bechdel, S.E., M. Mazzoil, E. Murdoch, E.M. Howells, J.S. Reif, S.D. McCulloch et al. 2009. Prevalence and impacts of motorized vessels on bottlenose dolphins (Tursiops truncatus) in the Indian River Lagoon, Florida. Aquatic Mammals; 35(3): 367-37.

Bertulli, C.G., A. Cecchetti, M.F. Van Bressem, and K.V. Waerebeek. 2012. Skin disorders in common minke whales and white-beaked dolphins off Iceland, a photographic assessment. Journal of Marine Animals and Their Ecology 5(2): 29-40.

Biber, P. (2022). Prolonged low salinity tolerance in Halodule wrightii Asch. Aquatic Botany, 178, 103498. https://doi.org/10.1016/j.aquabot.2022.103498

Bilecki, Michael S. 2020. "Fire Island National Seashore: A breach in the barrier island at the Otis Pike Fire Island High Dune Wilderness." Parks Stewardship Forum 137-143.

Blanchard, J., J. Eble, K. Johnson, R. Turingan, R. Weaver, G. Zarillo, M. Shelton, and M. Frick. 2021. Restore Lagoon Inflow Research (Phase 2). Melbourne, FL.

Blaylock, R., E. Saillant, A. Apeitos, D. Abrego, P. Cason, and R. Vega. 2021, June 1. The status of spotted seatrout (Cynoscion nebulosus) as a technologically feasible species for U.S. marine aquaculture. Blackwell Publishing Inc.

Bolland, J., and A. Boeticher. 2005. Population Structure and Reproductive Characteristics of the Gulf Pipefish, Syngnathus scovelli, in Mobile Bay, Alabama.

Bossart, G.D. 2007. Emerging diseases in marine mammals: from dolphins to manatees. Microbe, 2: 544-547. doi: 10.1128/microbe.2.544.1

Boucek, R. E., and J. S. Rehage. 2014. Climate extremes drive changes in functional community structure. Global Change Biology 20:1821–31.

Bowman, L.T. in prep. Seasonal variation of epiphyte abundance and nitrogen fixation rates of two seagrass species in the Pensacola Bay System. Master's thesis. University of West Florida.

Boynton, W. R., Ceballos, M. A. C., Bailey, E. M., Hodgkins, C. L. S., Humphrey, J. L., and Testa, J. M. (2017) Oxygen and nutrient exchanges at the sediment–water interface: a Global synthesis and critique of estuarine and coastal data. Estuar. Coasts. doi: 10.1007/s12237–017–0274–5.

Bradford, A.L., D.W. Weller, A.E. Punt, Y.V. Ivashchenko, A.M. Burdin, G.R. Vanblaricom, and R.L. Brownell, Jr. 2012. Leaner leviathans: body condition variation in a critically endangered whale population. Journal of Mammalogy 93:251-266.

Brander, K. 2010. Impacts of climate change on fisheries. Journal of Marine Systems 79:389–402.

Brevard County . 2023. "Save Our Indian River Lagoon Performance Tables – Fiscal Year 22/23 Quarter 1 ." brevardfl.gov. 2 9. Accessed 2023. chrome-extension://efaidnbmnnnibpcajpcglclefindmkaj/https://www.brevardfl.gov/docs/default-source/soirl/oversight-committee/save-our-indian-river-lagoon-performance-table.pdf?sfvrsn=526fff29_5.

Bridges, D. W. 1971, January. The Critical Thermal Maximum of Juvenile Spot Leiostomus xanthurus Lacepede. Thesis, North Carolina State University, Raleigh, North Carolina.

Brown, M., R. Robins, and P. Schofield. 2022. Risk assessment of chanchita Cichlasoma dimerus (Heckel, 1840), a newly identified non-native cichlid fish in Florida. Management of Biological Invasions 13:435–448.

Brown-Peterson, N. J., M. S. Peterson, D. L. Nieland, M. D. Murphy, R. G. Taylor, and J. R. Warren. 2002. Reproductive biology of female spotted seatrout, Cynoscion nebulosus, in the Gulf of Mexico: differences among estuaries? Page Environmental Biology of Fishes.

Burgess, M. 2020. Destin Harbor Pump. https://destin.lifemediagrp.com/destin-harbor-pump-ready-for-the-2020-season/.

Byron Shire Council. 2022. Belongil Creek. https://www.byron.nsw.gov.au/Services/Environment/Coast-and-waterways/Estuaries-and-ICOLLs/Belongil-Creek.

Caffrey, J.M. R. O'Conner, C. Verlinde, B. Albrecht, M. Harvey, and I. Orrantia. 2023. Citizen Science Seagrass Monitoring Report 2022. Center for Environmental Diagnostics and Bioremediation. University of West Florida. https://ircommons.uwf.edu/esploro/outputs/99380176397306600

Caffrey, J.M., N. Bano, K. Kalanetra, and J.T. Hollibaugh. (2007). Ammonia oxidation and ammonia-oxidizing bacteria and archaea from estuaries with differing histories of hypoxia. The ISME Journal, 1(7), 660–662. https://doi.org/10.1038/ismej.2007.79

Cardona, L. 2000. Effects of salinity on the habitat selection and growth performance of Mediterranean flathead grey mullet Mugil cephalus (Osteichthyes, Mugilidae). Estuarine, Coastal and Shelf Science 50:727–737.

Castillo-Rivera, M. 2013. Influence of Rainfall Pattern in the Seasonal Variation of Fish Abundance in a Tropical Estuary with Restricted Marine Communication. Journal of Water Resource and Protection 05:311–319.

Castillo-Rivera, M., G. Moreno, and R. Iniestra. 1994. Spatial, Seasonal, and Diel Variation in Abundance of the Bay Anchovy, Anchoa mitchilli (Teleostei: Engraulidae), in a Tropical Coastal Lagoon of Mexico. Source: The Southwestern Naturalist 39:263–268.

Castro, L. R., and R. K. Cowen. 1991. Environmental factors affecting the early life history of bay anchovy Anchoa mitchilli in Great South Bay, New York. MARINE ECOLOGY PROGRESS SERIES Mar. Ecol. Prog. Ser 76:235–247.

Cavanagh, Damion, Jeremy Visser, Suanne Richards, and Jane Ainsworth. 2015. Review of Environmental Factors: Tallow Creek Entrance Opening - Vol. 1. Brisbane: BMT WBM.

Cesbron, F., M.C. Murrell, M.E. Hagy, W.H. Jeffrey, W.F. Patterson, and J.M. Caffrey. (2019). Patterns in phytoplankton and benthic production on the shallow continental shelf in the northeastern Gulf of Mexico. Continental Shelf Research, 179, 105–114. https://doi.org/10.1016/j.csr.2019.04.003

Chamberlain, G., and K. Strawn. 1977. SUBMERGED CAGE CULTURE OF FISH IN SUPERSATURATED THERMAL EFFLUENT. Proceedings of the annual meeting - World Mariculture Society 8:625–645.

Cheney, B.J., J. Dale, P.M. Thompson, and N.J. Quick. 2022. Spy in the sky: a method to identify pregnant small cetaceans. Remote Sensing in Ecology and Conservation 8: 492-505.

Chi-Espínola, A. A., M. E. Vega-Cendejas, and W. G. Canto-Maza. 2018. Feeding habits of the mojarras (Gerreidae) population in the hyperhaline lagoon system of ría Lagartos, Yucatan, Mexico. Latin American Journal of Aquatic Research 46:810–819.

Christie, A.I., A.P. Colefax, and D. Cagnazzi. 2022. Feasibility of using small UAVs to derive morphometric measurements of Australian snubfin (Orcaella heinsohni) and humpback (Sousa sahulensis) dolphins. Remote Sensing 14: 21

Chung, K. S., and K. Strawn. 1994. What factors influence the thermal tolerance of estuarine animals? Interpretation of multiple regression analyses. Rev. Biol. Trop. 42:365–370.

Colura, R. L. 1974. INDUCED SPAWNING OF THE SPOTTED SEATROUT, Cynoscion nebulosus (CUVIER). Proceedings of the annual meeting - World Mariculture Society 5:319–330.

Coosen, J, PM Meire, JJ Stuart, and J Seys. 1990. "Trophic relationships in brackish Lake Veere: the role of macrophytes." Proceedings of the 24th European Marine Biology Symposium. Aberdeen: Aberdeen University Press. 404-423.

Coutant, C. C. 1985. Striped Bass, Temperature, and Dissolved Oxygen: A Speculative Hypothesis for Environmental Risk. Transactions of the American Fisheries Society 114:31–61.

Craig, S. R., W. H. Neill, and D. M. Gatlin. 1995. Effects of dietary lipid and environmental salinity on growth, body composition, and cold tolerance of juvenile red drum (Sciaenops ocellatus). Fish Physiology and Biochemistry 14:49–61.

Dalton Brown, J. 1972. A COMPARATIVE LIFE HISTORY STUDY OF FOUR SPECIES OF PIPEFISHES (FAMILY SYNGNATHIDAE) IN FLORIDA. Dissertation, University of Florida.

Darcy, G. H. 1985. Synopsis of biological data on Pinfish, Lagodon rhomboides (Pisces: Sparidae). FAO Fisheries Synopsis No. 141. NOAA Technical Report NMFS 23.

David Heil, A. 2017, July 19. Life history, diet, and reproductive dynamics of the sheepshead (Archosargus probatocephalus) in the Northeastern Gulf of Mexico. Master of Science Thesis, Florida State University , Tallahassee, FL.

Dowhan, Joseph, Thomas Halavik, Andrew Milliken, Andrew MacLachlan, Marcianna Caplis, Kelly Lima, and Andrew Zimba. 1997. Significant Habitats and Habitat Complexes of hte New York Bight Watershed. Charleston, Rhode Island: US Fish and Wildlife Service.

Durban, J.W., H. Fearbch, A. Paredes, L.S. Hickmott, and D.J. Le Roi. 2021. Size and body condition of sympatric killer whale ecotypes around the Antarctic Peninsula. Marine Progress Series 677: 209-217.

Durden, W.N., M.K. Stolen, D.H. Adams, and E.D. Stolen. 2007. Mercury and selenium concentrations in stranded bottlenose dolphins from the Indian River Lagoon system, Florida. Bulletin of Marine Science; 81(1): 37-54.

Durden, W.N., J. St. Leger, M. Stolen, T. Mazza, and C. Londono. 2009. Lacaziosis in bottlenose dolphins (Tursiops truncatus) in the Indian River Lagoon, Florida, USA. Journal of Wildlife Diseases, 45: 849-856. doi: 10.7589/0090-3558-45.3.849.

Durden W.N., E. D. Stolen, T. Jablonski, L. Moreland, E. Howells, A. Sleeman, M. Denny, G. Biedenback, M. Mazzoil. 2021. Robust design capture-recapture analysis of abundance and demographic parameters of Indian River Lagoon common bottlenose dolphins (Tursiops truncatus truncatus). PLoS One 16: e0250657.

Dutka-Gianelli, J., and D. J. Murie. 2001. AGE AND GROWTH OF SHEEPSHEAD, ARCHOSARGUS PROBATOCEPHALUS (PISCES: SPARIDAE), FROM THE NORTHWEST COAST OF FLORIDA. Page BULLETIN OF MARINE SCIENCE.

Dutka-Gianelli, J., R. Taylor, E. Nagid, J. Whittington, and K. Johnson. 2011. Habitat Utilization and Resource Partitioning of Apex Predators in Coastal Rivers of Southeast Florida. Page Library.

Eble, J.A, et al. 2021. Restore Lagoon Inflow Research Project Phase 2 Project Summary. Florida Department of Education. https://www.fit.edu/media/site-specific/wwwfitedu/indian-river-lagoon/documents/irlri-research/Final-Phase-2-Final-Project-Report_091521.pdf

Edwards, M., Johns, D. G., Leterme, S. C., Svendsen, E., and Richardson, A. J. (2006). Regional climate change and harmful algal blooms in the north–east Atlantic. Limnol. Oceanogr. 1, 820–829. doi: 10.4319/lo.2006.51.2.0820

Ellis, T. A., J. A. Buckel, J. E. Hightower, and S. J. Poland. 2017. Relating cold tolerance to winterkill for spotted seatrout at its northern latitudinal limits. Journal of Experimental Marine Biology and Ecology 490:42–51.

Environmental Protection Agency (EPA). 1996. The Indian River Lagoon Comprehensive Conservation & Management Plan. www.onelagoon.org/wp-content/uploads/irl_1996_ccmp.pdf. Accessed August 2022.

Ern, R., and A. J. Esbaugh. 2018. Effects of salinity and hypoxia-induced hyperventilation on oxygen consumption and cost of osmoregulation in the estuarine red drum (Sciaenops ocellatus). Comparative Biochemistry and Physiology -Part A : Molecular and Integrative Physiology 222:52–59.

Fair, P.A., J.D. Adams, E. Zolman, S.D. McCulloch, J.D. Goldstein, M.E. Murdoch, R. Varela, L. Hansen, F. Townsend, J. Kucklick, C. Bryan, S. Christopher, R. Pugh, and G.D. Bossart. 2006. Protocols for Conducting Dolphin Capture-Release Health Assessment Studies. NOAA Technical Memorandum NOS NCCOS 49. 83 pp.

Fazio, F., S. Marafioti, F. Arfuso, G. Piccione, and C. Faggio. 2013. Influence of different salinity on haematological and biochemical parameters of the widely cultured mullet, Mugil cephalus. Marine and Freshwater Behaviour and Physiology 46:211–218.

FDEP . 2013. Banana River Lagoon Basin Management Action Plan. Retrieved from https://floridadep.gov/sites/default/files/banana–river–lagoon–bmap.pdf.

FDEP. 2016. Indian River Lagoon Aquatic Preserves System Management Plan. Tallahassee, FL.

FDEP. 2023. DEP 101: Surface Water Quality Standards. March 20. https://floridadep.gov/comm/press-office/content/dep-101-surface-water-quality-standards.

Ferguson, Angus, Danny Wiecek, Michael Hughes, David Hanslow, David Wainwright, and Peter Scanes. 2021. Form and function of NSW intermittently closed and open lakes and lagoons. Parramatta, NSW: Environment, Energy and Science, Department of Planning, Industry and Environment.

Finucane, J. H., and R. N. Vaught. 1986. Species profile of the Atlantic thread herring Opisthonema oglinum (Lesueur 1818). Page NOAA Technical Memorandum NMFS-SEFC-182.

FL.Tech. 2020. Restore Lagoon Inflow Research (Phase 1) Summary Report.

Flaherty-Walia, K. E., R. E. Matheson, and R. Paperno. 2015. Juvenile Spotted Seatrout (Cynoscion nebulosus) Habitat Use in an Eastern Gulf of Mexico Estuary: The Effects of Seagrass Bed Architecture, Seagrass Species Composition, and Varying Degrees of Freshwater Influence. Estuaries and Coasts 38:353–366.

Fox, A.L., Trefry, J.H., Trocine, R.P., Fox, S.L., Voelker, J.E., 2017. Determining the Effectiveness of Muck Removal on Sediment and Water Quality in the Indian River Lagoon. Project Report Submitted to Brevard County Natural Resources Management Department.

Frisbie, C. M. 1961. Young Black Drum, Pogonias cromis, in Tidal Fresh and Brackish Waters, Especially in the Chesapeake and Delaware Bay Areas. Chesapeake Science 2:94.

FWC-FWRI. 2017. Fisheries-Independent Monitoring Program 2016 Data Summary Report. Florida Fish and Wildlife Research Institute. St. Petersburg, Florida.

FWC-FWRI. 2023. Fisheries-Independent Monitoring Program Procedure Manual. Florida Fish and Wildlife Research Institute. St. Petersburg, Florida

Gasparini, J. L., and R. L. Teixeira. (n.d.). REPRODUCTIVE ASPECTS OF THE GULF PIPEFISH, Syngnathus scovelli (TELEOSTEI: SYNGNATHIDAE), FROM SOUTHEASTERN BRAZIL. Page Rev. Brasil. Biol.

Gelwick, F. P., S. Akin, D. A. Arrington, and K. O. Winemiller. 2001. Fish Assemblage Structure in Relation to Environmental Variation in a Texas Gulf Coastal Wetland. Page Estuarine Research Federation Estuaries.

Gobler, Christopher J, Craig S Young, Jennifer Goleski, Alexandra Stevens, Jake Thickman, Ryan B. Wallace, Patrick Curran, et al. 2019. "Accidental ecosystem resotration? Assessing the estuary-wide impacts of a new ocean inlet created by Hurricane Sandy." Estuarine, Coastal and Shelf Science 132-146.

Golden, Z., and B. F. Froeschke. 2023. Comparison of Ecological Niches Between Two Important Recreational and Commercial Fisheries. PhD Dissertation Honors Program, The University of Tampa.

Google. 2021. Google Earth. https://earth.google.com/web/search/old+pass+destin/@30.38769493,-86.50558754,1.60015071a,4146.51368888d,35y,0h,0t,0r/data=CigiJgokCeYi9eA_bT5AEb1v-ShoVz5AGUU1oN1CnVXAlTrQjgUdolXA.

Govonil, J. J., P. B. Ortner, F. Al-yamani, and L. C. Hill. 1986. Selective feeding of spot , Leiostomus xanthurus , and Atlantic croaker , Micropogonias undulatus , larvae in the northern Gulf of Mexico 28:175–183.

Greenwood, M. F. D., R. E. Matheson, R. H. McMichael, and T. C. MacDonald. 2007. Community structure of shoreline nekton in the estuarine portion of the Alafia River, Florida: Differences along a salinity gradient and inflow-related changes. Estuarine, Coastal and Shelf Science 74:223–238.

Gryzbek, M.K. 2013. A visual body condition index for bottlenose dolphins (Tursiops truncatus). Msc. Thesis. University of Florida.

Gunter, G. 1956. A Revised List of Euryhaline Fishes of North and Middle America. Source: The American Midland Naturalist 56:345–354.

Gutierrez, E. M., J. D. Plumlee, D. G. Bolser, B. E. Erisman, and R. J. D. Wells. 2023. Regional Variation in Feeding Patterns of Sheepshead (Archosargus probatocephalus) in the Northwest Gulf of Mexico. Fishes 8.

Hall, L. H. Jr., S. J. Bushong, S. A. Fischer, and J. A. Sullivan. 1989. A synthesis of water quality and contaminants data for the Spot, Leiostomus xanthurus. Shady Side, Maryland.

Hallac, D., J. Kline, J. Sadle, S. Bass, T. Ziegler, and S. Snow. 2010. Preliminary effects of the January 2010 cold weather on flora and fauna in Everglades National Park.

Hare, J. A., M. J. Wuenschel, and M. E. Kimball. 2012. Projecting Range Limits with Coupled Thermal Tolerance - Climate Change Models: An Example Based on Gray Snapper (Lutjanus griseus) along the U.S. East Coast. PLoS ONE 7.

Hart, L.B., D.S. Rotstein, R.S. Wells, J. Allen, A. Barleycorn, B. Balmer, S.M. Lane, T. Speakman, E.S. Zolman, M. Stolen, W. McFee, T.K. Goldstein, and L.H. Schwacke. 2012. Skin lesions on common bottlenose dolphins (Tursiops truncatus) from three sites in the northwest Atlantic, USA. PlosOne, 7(3): e33081.

Hart, L.B., R.S. Wells, and L.H. Schwacke. 2013. Reference ranges for body condition in wild bottlenose dolphins, Tursiops truncatus. Aquatic Biology 18(1): 63-68.

Hartwell, S. I., and D. E. Hoss. 1979. Thermal Shock Resistance of Spot (Leiostomus xanthurus) after Acclimation to Constant or Cycling Temperature. Transactions of the American Fisheries Society 108:397–400.

Harzen, S. and B.J. Brunnick. 1997. Skin disorders in bottlenose dolphins (Tursiops truncatus), resident in the Sado estuary, Portugal. Aquatic Mammals, 21 (1): 59-68.

Helfman, G. S., B. B. Collette, and D. E. Facey. 1997. The Diversity of Fishes. 1st edition. Wiley-Blackwell.

Henriksen, K., J.I. Hansen, and T.H. Blackburn. (1981). Rates of nitrification, distribution of nitrifying bacteria and nitrate fluxes in different types of sediment from Danish waters. Marine Biology, 61, 299–304.

Henry, W. 1803. Experiments on the quantity of gases absorbed by water, at different temperatures, and under different pressures. Philosophical Transactions of the Royal Society of London 93:29–43.

Herr, H., P. Burkhardt-Holm, K. Heyer, U. Siebert, and J. Selling. 2020. Injuries, malformations, and epidermal conditions in cetaceans of the Strait of Gibraltar. Aquatic Mammals, 46(2): 215-235.

Hester, C. M., H.M. Smith, M.E. Head, H. Langsten, S. Linder, E. Manor, J. Norman, L. Sartory, and J.M. Caffrey. (2016). Comparing productivity and biogeochemistry of native and transplanted thalassia testudinum and halodule beaudettei in big Lagoon, Florida, USA. Gulf of Mexico Science, 1, 14–25.

Heiri, O., Lotter, A. F., and Lemcke, G. (2001). Loss on ignition as a method for estimating organic and carbonate content in sediments: reproducibility and comparability of results. J. Paleolimnol. 25, 101–110.

Hodson, R. G., R. G. Fechhelm, and R. J. Monroe. 1961. Upper Temperature Tolerance of Spot, Leiostomus xanthurus, from the Cape Fear River Estuary, North Carolina. Estuaries 4:345–356.

Holmes, R.M., A. Aminot, R. Kérouel, B.A. Hooker and B.J. Peterson. 1999. A simple and precise method for measuring ammonium in marine and freshwater ecosystems. Canadian Journal of Fisheries and Aquatic Sciences 56:1801–1808.

Hornek, R., A. Pommerening-Röser, H-P. Koops, A.H. Farnleitner, N. Kreuzinger, A. Kirschner, and R.L. Mach. (2006). Primers containing universal bases reduce multiple amoA gene specific

DGGE band patterns when analysing the diversity of beta-ammonia oxidizers in the environment. Journal of Microbiological Methods, 66(1), 147–155. https://doi.org/10.1016/j.mimet.2005.11.001

Hotos, G. N., and N. Vlahos. 1998. Salinity tolerance of Mugil cephalus and Chelon labrosus Pisces: Mugilidae fry in experimental conditions. Aquaculture 167:329–338.

Houde, E. D. 1977. Abundance and potential yield of the Atlantic Thread Herring, Opisthonema oglinum, and aspects of its early life history in the Eastern Gulf of Mexico. Fishery Bulletin 75:493–512.

Howells, E., J.S. Reif, M. Mazzoil, M.E. Murdoch, S.E. Bechdel, S. Ziemann, et al. 2008. Using photo-analysis of dolphin mother-calf pairs to determine reproductive rates in the Indian River Lagoon, Florida. Florida Marine Mammal Health Conference III. Marineland, FL, April 22-25

Indian River County. 2016. "Bethel Creek Community Discussion Meeting." Indian River County. https://ircgov.com/Lagoon/Bethel-Creek/Bethel-Workshop-081116.pdf.

IPCC. 2012. Managing the risks of extreme events and disasters to advance climate change adaptation: special report of the intergovernmental panel on climate change. Page (C. B. Field, V. Barros, T. F. Stocker, D. Qin, D. J. Dokken, K. L. Ebi, M. D. Mastrandrea, K. J. Mach, G. K. Plattner, S. K. Allen, M. Tignor, and P. M. Midgley, Eds.). Cambridge University Press, Cambridge, UK & New York, NY, USA.

IPCC. 2018. Special Report on Global Warming of 1.5oC.

IRL 2011 Consortium. 2012. Indian River Lagoon 2011: Superbloom plan of investigation. Prepared by SJRWMD, 27pp.

Joblon, M.J., M.A. Pokras, B. Morse, C.T. Harry, K.S. Rose, S.M. Sharp, M.E. Niemeyer, K.M. Patchett, B. Sharp, and M. Moore. 2014. Body condition scoring system for delphinids based on short-beaked common dolphins (Delphinus delphis). Journal of Marine Animals and their Ecology. 7(2): 5-13.

Johnson, D. R., N. A. Funicelli, and J. A. Bohnsack. 1999. Effectiveness of an Existing Estuarine No-Take Fish Sanctuary within the Kennedy Space Center, Florida. North American Journal of Fisheries Management 19:436–453.

Johnson, J. C., S. Arnott, T. Advisor, B. Roumillat, D. Whitaker, J. Ballenger, C. Mcdonough, and A. T. Mccandless. 2013. QUANTIFICATION OF LIFE HISTORY PARAMETERS IN SOUTH CAROLINA SPOT (Leiostomus xanthurus) at THE GRADUATE SCHOOL OF THE COLLEGE OF CHARLESTON.

Johnson, K. B., R. G. Turingan, J. Eble, J. Shenker, and J. R. Blanchard. 2020. Restore Lagoon Inflow Research Project (Phase 1) Task 2, Biological Monitoring. Melbourne, FL.

Joseph, E. B. 1957. A study of the systematics and life history of the Gulf Pipefish, Syngnathus scovelli (Evermann and Kendall). Doctoral Dissertation, Florida State University.

Jung, S. ;, and E. D. Houde. 2004. Recruitment and spawning-stock biomass distribution of bay anchovy (Anchoa mitchilli) in Chesapeake Bay. Fishery Bulletin 102:63–77.

Kamerosky, A., H. J. Cho, and L. Morris. 2015. Monitoring of the 2011 super algal bloom in Indian River Lagoon, FL, USA, Using MERIS. Remote Sensing 7:1441–1460.

Kesanopoulos, K., G. Tzanakaki, S. Levidiotou, C. Blackwell, J. Kremastinou, J. (2005). Evaluation of touch-down real-time PCR based on SYBR Green I fluorescent dye for the detection of Neisseria meningitidis in clinical samples. FEMS Immunology and Medical Microbiology, 43(3), 419–424. https://doi.org/10.1016/j.femsim.2004.10.011

Khériji, S., M. El Cafsi, W. Masmoudi, J. D. Castell, and M. S. Romdhane. 2003. Salinity and temperature effects on the lipid composition of mullet sea fry (Mugil cephalus, Linne, 1758) *. Aquaculture international 11:571–582.

Kilma, E. F., and D. C. Tabb. 1959. A contribution to the Biology of the Spotted Weakfish, Cynoscion nebulosus, (Cuvier) from northwest Florida, with a Description of the Fishery. Florida Board Conservation Marine Lab Tech. Ser. No. 30.

Kinnear, B. S., and C. M. Fuss Jr. 1971. Thread herring distribution off Florida's West Coast. Fisheries Review 33:27–39.

Komita, Weaver, and Fox. In Prep. "Summary of Inflow Projects."

Krejci, S. E. 2012. HABITAT PREFERENCES AND THE EFFECTS OF SEAGRASS DENSITY ON POPULATION DEMOGRAPHICS AND FEEDING ECOLOGY OF PIPEFISH IN THE INDIAN RIVER LAGOON, FL. Dissertation, Florida Institute of Technology , Melbourne, Fl.

Kucera, C. J., C. K. Faulk, and G. J. Holt. 2002. The effect of parental acclimation to spawning salinity on the survival of larval Cynoscion nebulosus. Journal of Fish Biology 61:726–738.

Kuiter, R. H. 2003. American Gulf Pipefish Sygnathus scovelli. Pages 196–196 Seahorses, Pipefishes and their relatives, a comprehensive guide to Syngnathiformes. Revised Edition.

Kültz, D. 2015, June 1. Physiological mechanisms used by fish to cope with salinity stress. Company of Biologists Ltd.

Landers-Atkins Planners, Inc. (1987). Destin Harbor Management Plan, City of Destin, Florida. September 8, 1987. DER Contract No. CM-176.

Langston, J. N., P. J. Schofield, J. E. Hill, and W. F. Loftus. 2010. Salinity Tolerance of the African Jewelfish Hemichromis letourneuxi, a Non-native Cichlid in South Florida (USA). Copeia 3:475–480.

Lapointe, B. E., L.W. Herren, R.A. Brewton, and P.K. Alderman. (2020). Nutrient over-enrichment and light limitation of seagrass communities in the Indian River Lagoon, an urbanized subtropical estuary. Science of The Total Environment, 699, 134068. https://doi.org/10.1016/j.scitotenv.2019.134068

Lee, K.-S., S.R. Park, and Y.K. Kim. (2007). Effects of irradiance, temperature, and nutrients on growth dynamics of seagrasses: A review. Journal of Experimental Marine Biology and Ecology, 350(1–2), 144–175. https://doi.org/10.1016/j.jembe.2007.06.016

Ley, J. A., C. C. Mcivor, and C. L. Montague. 1999. Fishes in Mangrove Prop-root Habitats of Northeastern Florida Bay: Distinct Assemblages across an Estuarine Gradient. Estuarine, Coastal and Shelf Science 48.

Lirman, D., and W.P. Cropper. (2003). The influence of salinity on seagrass growth, survivorship, and distribution within Biscayne Bay, Florida: Field, experimental, and modeling studies. Estuaries, 26(1), 131–141. https://doi.org/10.1007/BF02691700

Lipnicky, C.D. (1996) Council Ponders Pump System. Northwest Florida Daily News, December 7, 1996. 379494590. U.S. Southeast Newsstream. https://login.ezproxy.lib.uwf.edu/login?url= https://www.proquest.com/newspapers/council-ponders-pump-system/docview/379494590/se-2?accountid=14787

Listopad, C. 2015. Spatial Watershed Iterative Loading (SWIL) Model Methodology Report; Updated for SWIL 3.0. Final Report submitted to Brevard County Natural Resources Management Office by Applied Ecology, Inc.

Livak, K. J., and T.D. Schmittgen. (2001). Analysis of relative gene expression data using real-time quantitative PCR and the 2(-Delta C(T)) Method. Methods (San Diego, Calif.), 25(4), 402–408. https://doi.org/10.1006/meth.2001.1262

Marais, J. F. K. 1978. Routine Oxygen Consumption of Mugil cephalus, Liza dumerili and L. richardsoni at Different Temperatures and Salinities. Marine Biology 50:9–16.

Marcek, B. J., R. W. Brill, and M. C. Fabrizio. 2019. Metabolic scope and hypoxia tolerance of Atlantic croaker (Micropogonias undulatus Linnaeus, 1766) and spot (Leiostomus xanthurus Lacepède, 1802), with insights into the effects of acute temperature change. Journal of Experimental Marine Biology and Ecology 516:150–158.

Massie, J. A., B. A. Strickland, R. O. Santos, J. Hernandez, N. Viadero, R. E. Boucek, H. Willoughby, M. R. Heithaus, and J. S. Rehage. 2020. Going Downriver: Patterns and Cues in Hurricane-Driven Movements of Common Snook in a Subtropical Coastal River. Estuaries and Coasts 43:1158–1173.

Matheson, R. E., and J. D. Mceachran. 1984. Taxonomic Studies of the Eucinostomus argenteus Complex (Pisces: Gerreidae): Preliminary Studies of External Morphology. Copeia 18:893–902.

Matheson, R.E., Jr. 1983. Taxonomic studies of the Eucinostomus argenteus complex (Pisces: Gerreidae). Ph.D. Dissertation, Texas A&M University, College Station. 195 p.

Mazzoil, M., S.D. McCulloch, R.H. Defran, R. H., and E. Murdoch. 2004. Use of digital photography and analysis of dorsal fins for photo-identification of bottlenose dolphins. Aquatic Mammals 30:209-2019.

Mazzoil, M., J.S. Reif, P. Fair, and G.D. Bossart. 2008. 2008 Indian River Lagoon Unusual Mortality Event Report to the Working Group re: Dolphin Body Condition. Technical Report.

McCall, J. N., and J. W. Fleeger. 1993. Recognition and utilization of prey aggregations by juvenile spot (Leiostomus xanthurus Lacepede). Journal of experimental marine biology and ecology 174.1:121–134

McGuire, A., N. Aluru, A. Takemura, R. Weil, J. M. Wilson, and M. M. Vijayan. 2010. Hyperosmotic shock adaptation by cortisol involves upregulation of branchial osmotic stress transcription factor 1 gene expression in Mozambique Tilapia. General and Comparative Endocrinology 165:321–329.

Mcneese, H. C. 2021, May. COMPARISON OF ENDOHELMINTH PARASITES IN BLACK DRUM (POGONIAS CROMIS) AND RED DRUM (SCIAENOPS OCELLATUS) FROM THE SABINE LAKE ESTUARY. Master of Science Thesis, Sam Houston State University.

Merino Contreras, M. de la L. 2018. Aclimatación en cautiverio del sargo Archosargus probatocephalus (Perciformes: Sparidae). Ecosistemas y Recursos Agropecuarios 5:511–521.

Middaugh, D.P., M.J. Hemmer, and Y.L. Rose. 1986. Laboratory spawning cues in Menidia beryllina and Menidia peninsulae (Pisces: Atherinidae) with notes on survival and growth of larvae at different salinities. Environmental Biology of Fishes 15:107-117.

Meagher, E.M., W.A McLellan, A. J. Westgate, R.S. Wells, J.E. Blum, and D.A. Pabst. 2009. Seasonal patterns of heat loss in wild bottlenose dolphins (Tursiops truncatus). Journal of Comparative Physiological Biology 178: 529-543.

Meinhardt, K. A., A. Bertagnolli, M.W. Pannu, S.E. Strand, S.L. Brown, D.A. Stahl. (2015). Evaluation of revised polymerase chain reaction primers for more inclusive quantification of ammonia-oxidizing archaea and bacteria. Environmental Microbiology Reports, 7(2), 354–363. https://doi.org/10.1111/1758-2229.12259

Moody, W. D. 1950. A STUDY OF THE NATURAL HISTORY OF THE SPOTTED TROUT CYNOSCION NEBULOSUS, IN THE CEDAR KEY, FLORIDA, AREA. Quarterly Journal of the Florida Academy of Sciences 12:147–171.

Morris, L. J., L. M. Hall, J. D. Miller, M. A. Lasi, R. H. Chamberlain, R. W. Virnstein, and C. A. Jacoby. 2021. Diversity and distribution of seagrasses as related to salinity, temperature, and availability of light in the Indian River Lagoon, Florida. Source: Florida Scientist 84:119–137.

Morris, L. J., and R. W. Virnstein. 2004. The Demise and Recovery of Seagrass in the Northern Indian River Lagoon, Florida. Page Estuarine Research Federation Estuaries.

Morris, L, L. Hall, R. Chamberlain, and C. Jacoby. (2018). Summary report for the Northern Indian River Lagoon. In Seagrass Integrated Mapping and Monitoring Program. Mapping and Monitoring Report No. 3. Editors. L.A Yarbro and P.R. Carlson Jr. Technical Report 17, Version 3. 2018. Florida Fish and Wildlife Conservation Commission. Fish and Wildlife Research Institute. DOI10.13140/RG.2.2.12366.05445

Morris, L.J., L.M. Hall, C.A. Jacoby, R.H. Chamberlain, M.D. Hanisak, J.D. Miller, and R.W. Virnstein. (2022). Seagrass in a Changing Estuary, the Indian River Lagoon, Florida, United States. Frontiers in Marine Science, 8, 789818. https://doi.org/10.3389/fmars.2021.789818

Mohan, S. B., M. Schmid, M. Jetten, and J. Cole. (2004). Detection and widespread distribution of the nrfA gene encoding nitrite reduction to ammonia, a short circuit in the biological nitrogen cycle that competes with denitrification. FEMS Microbiology Ecology, 49(3), 433–443. https://doi.org/10.1016/j.femsec.2004.04.012

Moser, M. L., and L. R. Gerry. 1989. Differential Effects of Salinity Changes on Two Estuarine Fishes, Leiostomus xanthurus and Micropogonias undulatus.

Moser, M. L., and J. M. Miller. 1994. Effects of salinity fluctuation on routine metabolism of juvenile spot, Leiostomus xanthurus. Journal of Fish Biology 45:335–340.

Moulton, D. L., M. A. Dance, J. A. Williams, M. Z. Sluis, G. W. Stunz, and J. R. Rooker. 2017. Habitat Partitioning and Seasonal Movement of Red Drum and Spotted Seatrout. Estuaries and Coasts 40:905–916.

Murdoch, M.E., J.S. Reif, M. Mazzoil, S.D. McCulloch, P.A. Fair, and G.D. Bossart. Lobomycosis in bottlenose dolphins (Tursiops truncatus) from the Indian River Lagoon, Florida: Estimation of prevalence, temporal trends and spatial distribution. 2008. EcoHealth, 5(3) 289-297; doi: 10.1007/s10393-008-0187-8.

Murphy, M., and R. Taylor. 1989. Reproduction and growth of black drum Pogonias cromis in northeast Florida.

Nielson, Morten Holtegaard, Bjarke Rasmussen, and Flemming Gertz. 2005. "A simple model for water level and stratification in Ringkøbing Fjord, a shallow, artificial estuary." Estuarine, Coastal and Shelf Science 235-248.

Moser, M. L., and L. R. Gerry. 1989. Differential Effects of Salinity Changes on Two Estuarine Fishes, Leiostomus xanthurus and Micropogonias undulatus.

Moser, M. L., and J. M. Miller. 1994. Effects of salinity fluctuation on routine metabolism of juvenile spot, Leiostomus xanthurus. Journal of Fish Biology 45:335–340.

Moulton, D. L., M. A. Dance, J. A. Williams, M. Z. Sluis, G. W. Stunz, and J. R. Rooker. 2017. Habitat Partitioning and Seasonal Movement of Red Drum and Spotted Seatrout. Estuaries and Coasts 40:905–916.

Murphy, M., and R. Taylor. 1989. Reproduction and growth of black drum Pogonias cromis in northeast Florida.

National Oceanic and Atmospheric Administration (NOAA) Fisheries. 2015. Marine mammal stock assessment reports (SARs) by species/stock. Bottlenose dolphin (Tursiops truncatus): Indian River Lagoon estuarine system stock. NOAA Fisheries Office of Protected Resources. https://media.fisheries.noaa.gov/dam-migration/f2015_bodoirl_508.pdf.

Noke, W.D. and D.K. Odell. Interactions between the Indian River Lagoon blue crab fishery and the bottlenose dolphin Tursiops truncatus. Marine Mammal Science, 2002; 18: 819-832.

Northwest Florida Water Management District. 1992. Permit re-application for the Old Pass Lagoon Yater Circulation Facility. Permit Application, Havana, Florida : Northwest Florida Water Management District.

Northwest Florida Daily News (NWFDN). BRIEFS LOCAL" June 3, 2005. 379430140. U.S. Southeast Newsstream.

Ogawa, M., M. W. Moody, R. J. Portier, J. Bell, M. A. Schexnayder, and J. N. Losso. 2003. Biochemical Properties of Black Drum and Sheepshead Seabream Skin Collagen. Journal of Agricultural and Food Chemistry 51:8088–8092.

Olsen, Z. T. 2014. Potential impacts of extreme salinity and surface temperature events on population dynamics of black drum, pogonias cromis, in the upper Laguna Madre, Texas. Gulf of Mexico Science 32:60–68.

Page, L.M., H. Espinosa-Pérez, L.T. Findley, C.R. Gilbert, R.N. Lea, N.E. Mandrak, R.L. Mayden, and J.S. Nelson. 2013. Common and scientific names of fishes from the United States, Canada, and Mexico. Seventh Edition. American Fisheries Society Special Publication 34. 243 pp.

Paperno, R., and R. B. Brodie. 2004. Effects of environmental variables upon the spatial and temporal structure of a fish community in a small, freshwater tributary of the Indian River Lagoon, Florida. Estuarine, Coastal and Shelf Science 61:229–241.

Paperno, R., D.H. Adams, and A.P. Sebastian. 2016. Indian River Lagoon Enhanced Fisheries Monitoring and Phytoplankton Bloom Impact Evaluation. Final Report to the SJRWMD Contract 27574 Prepared by FWC-FWRI, 43 pp.

Parsons, T. R., Y. Maita, and C. M. Lalli. 1984. A manual of chemical and biological methods for seawater analysis. Pergamon Press.

Partridge, C., J. Shardo, and A. Boettcher. 2007. Osmoregulatory role of the brood pouch in the euryhaline Gulf pipefish, Syngnathus scovelli. Comparative Biochemistry and Physiology - A Molecular and Integrative Physiology 147:556–561.

Patetta, N. 2022, April 27. Linking thermal tolerances to estuarine residency of NC fish species. Senior Honors Thesis, The University of North Carolina, Chapel Hill.

Peterson, Jens Kjerulf, Jens Wurgler Hansen, Martha Brogaard Laursen, Preben Clausen, Jacob Carstensen, and Daniel J Conley. 2008. "Regime Shift in a Coastal Marine Ecosystem." Ecological Applications 497-510.

Pettis, H., R. Rolland, P. Hamilton, S. Brault, A. Knowlton, and S. Kraus. 2004. Visual health assessment of North Atlantic right whales (Eubalaena glacialis) using photographs. Canadian Journal of Zoology 82:8-19.

Phlips, E. J., Badylak, S., Christman, M. C., Lasi, M. A. (2010). Climatic trends and temporal patterns of phytoplankton composition, abundance and succession in the Indian River Lagoon, Florida, USA. Estuaries Coasts 33, 498-512.

Phlips, E. J., Badylak, S., Lasi, M., Chamberlain, R., Green, W., Hall, L., et al. (2015). From red tides to green and brown tides: Bloom dynamics in a restricted subtropical lagoon under shifting climatic conditions. Estuaries Coasts 38, 886-904.

Phlips, E. J., Badylak, S., Nelson, N., and Havens, K. (2020). Hurricanes, El Niño and harmful algal blooms in two sub-tropical Florida estuaries: Direct and indirect impacts. Scientific Reports 10, 1910. Doi.org/10.1038/s41598-020-58771-4

Phlips, E. J., Badylak, S., Nelson, N., Hall, L., Jacoby, C., Lasi, M., Lockwood, J., and Miller, J. (2021). Cyclical patterns and a regime shift in the character of phytoplankton blooms in a restricted sub-tropical lagoon, Indian River Lagoon, Florida, USA. Frontiers Mar. Sci. 8:730934. Doi.org/10.3389/fmars.2021.730934

Phlips, E.J., S. Badylak, M.A. Lasi, R. Chamberlain, W.C. Green, L.M. Hall, J.A Hart, J.C. Lockwood, J.D. Miller, L.J. Morris, and J.S. Steward. 2015. From red tides to green and Brown tides: Bloom dynamics in a restricted subtropical lagoon shifting climatic conditions. Estuaries and Coasts 38:886-904.Matheson, R.E., Jr. 1983. Taxonomic studies of the Eucinostomus argenteus complex (Pisces: Gerreidae). Ph.D. Diss., Texas A&M University, College Station, 195 pp.

Port of Los Angeles Engineering Division. 2006. "Inner Cabrillo Beach Water Quality Improvement Project Source Identifications and Mitigation Alternatives." California Water Boards. https://faast.waterboards.ca.gov/attachments/proposal_18975/attachment_61567.pdf.

Potthoff, M. T., and D. M. Allen. 2003. Site fidelity, home range, and tidal migrations of juvenile pinfish, Lagodon rhomboides, in salt marsh creeks. Environmental Biology of Fishes 67:231–240.

Poulakis, G. R., D. A. Blewett, and M. E. Mitchell. 2003. The effects of season and proximity to fringing mangroves on seagrass-associated fish communities in Charlotte Harbor, Florida. Gulf of Mexico Science 21:171–184.

Powell, A. B. ;, M. W. ; Lacroix, and R. T. Cheshire. 2002. An evaluation of Northern Florida Bay as a nursery area for red drum, Sciaenops ocellatus, and other juvenile and small resident fishes. Item Type monograph.

Presley, R., and J.M. Caffrey. (2021). Nitrogen Fixation in Subtropical Seagrass Sediments: Seasonal Patterns in Activity in Santa Rosa Sound, Florida, USA. Journal of Marine Science and Engineering, 9(7), Article 7. https://doi.org/10.3390/jmse9070766

Provancha, M. J., P. A. Schmalzer, and C. R. Hall. 1986. EFFECTS OF THE DECEMBER 1983 AND JANUARY 1985 FREEZING AIR TEMPERATURES ON SELECT AQUATIC POIKILOTHERMS AND PLANT SPECIES OF MERRITT ISLAND, FLORIDA. Source: Florida Scientist 49:199–212.

R Core Team. 2020. The R Stats Package. R Core Team.

Rehage, J. S., and J. R. Blanchard. 2016. What Can We Expect from Climate Change for Species Invasions? Fisheries 41:405–407.

Rehage, J. S., J. R. Blanchard, R. E. Boucek, J. J. Lorenz, and M. Robinson. 2016. Knocking back invasions: variable resistance and resilience to multiple cold spells in native vs nonnative fishes. Ecosphere 7:1–13.

Reif, J.S., M.M. Peden-Adams, T.A. Romano, C.D. Rice, P.A. Fair, and G.D. Bossart. 2009. Immune dysfunction in Atlantic bottlenose dolphins (Tursiops truncatus) with lobomycosis. Medical Mycology 47:125-135.

Reyier, E. A., R. H. Lowers, D. M. Scheidt, and D. H. Adams. 2011. Movement patterns of adult red drum, Sciaenops ocellatus, in shallow Florida lagoons as inferred through autonomous acoustic telemetry. Environmental Biology of Fishes 90:343–360.

Reyier, E. A., D. M. Scheidt, E. D. Stolen, R. H. Lowers, K. G. Holloway-Adkins, and B. J. Ahr. 2020. Residency and dispersal of three sportfish species from a coastal marine reserve: Insights from a regional-scale acoustic telemetry network. Global Ecology and Conservation 23:e01057.

Richards, C. E. 1973. Age, Growth and Distribution of the Black Drum (Pogonias cromis) in Virginia. Transactions of the American Fisheries Society 102:584–590.

Richards, W. J., R. V. Miller, and E. D. Houde. 1974. Egg and larval development of the Atlantic Thread Herring, Opishtonem oglinum. Fishery bulletin 72:1123–1136.

Richards, W. J., and B. J. Palko. 1969. Methods Used to Rear the Thread Herring, Opisthonema oglinum, from Fertilized Eggs. Transactions of the American Fisheries Society 98:527–529.

Riggs, A. F. 1988. The Bohr Effect. Ann. Rev. Physiol 50:181–204.

Rothfus, M. J. (2022). Sediment Biogeochemistry Response to Stingray Bioturbation in Halodule wrightii [M.S., The University of West Florida]. https://www.proquest.com/docview/2705870638/abstract/E5CEF9B91D0B4DD1PQ/1

Rotthauwe, J. H., K.P. Witzel, and W. Liesack. (1997). The ammonia monooxygenase structural gene amoA as a functional marker: Molecular fine-scale analysis of natural ammonia-oxidizing populations. Applied and Environmental Microbiology, 63(12), 4704–4712. https://www.ncbi.nlm.nih.gov/pmc/articles/PMC168793/

Rutherford, E. S., J. T. Tilmant, E. B. Thue, and T. W. Schmidt. 1989. FISHERY HARVEST AND POPULATION DYNAMICS OF SPOTTED SEATROUT , CYNOSCION NEBULOSUS , IN FLORIDA BAY AND ADJACENT WATERS. Bulletin of Marine Science 44:108–125.

Saad, A. M., A. C. Beaumord, and E. P. Caramaschi. 2002. Effects of artificial canal openings on fish community structure of Imboassica Coastal Lagoon, Rio deJaneiro, Brazil. Journal of Coastal Research SI 36:634–639.

Sanino, G.P., M.F. Van Bressem, K. Van Waerebeek, and N. Pozo. 2014. Skin disorders of coastal dolphins at Añihué Reserve, Chilean Patagonia: a matter of concern. Boletin del Museo Nacional de Historia Natural, Chile, 63: 127-157.

Santos, R. O., D. Lirman, S. J. Pittman, and J. E. Serafy. 2018. Spatial patterns of seagrasses and salinity regimes interact to structure marine faunal assemblages in a subtropical bay. Marine Ecology Progress Series 594:21–38.

Santos, R. O., J. S. Rehage, R. Boucek, and J. Osborne. 2016. Shift in recreational fishing catches as a function of an extreme cold event. Ecosphere 7:1–16.

Saucier, M. H., and D. M. Baltz. 1993. Spawning site selection by spotted seatrout, Cynoscion nebulosus, and black drum, Pogonias cromis, in Louisiana. Environmental Biology of Fishes 36:257–272.

Schnetger, B., and C. Lehners. (2014). Determination of nitrate plus nitrite in small volume marine water samples using vanadium(III)chloride as a reduction agent. Marine Chemistry, 160, 91–98. https://doi.org/10.1016/j.marchem.2014.01.010

Schofield, P. J., and D. H. Huge. 2008. Low-temperature tolerance of two non-native fishes (Hoplosternum littorale [Hancock 1828], Cichlasoma bimaculatum [Linnaeus 1758]) established in Florida. Florida Scientist 74:73–83.

Schofield, P. J., and J. L. Kline. 2018. Lower Lethal Temperatures for Nonnative Freshwater Fishes in Everglades National Park, Florida. North American Journal of Fisheries Management.

Schofield, P. J., W. F. Loftus, and M. E. Brown. 2007. Hypoxia tolerance of two centrarchid sunfishes and an introduced cichlid from karstic Everglades wetlands of southern Florida, U.S.A. Journal of Fish Biology 71:87–99.

Schofield, P. J., W. F. Loftus, R. M. Kobza, M. I. Cook, and D. H. Slone. 2010. Tolerance of nonindigenous cichlid fishes (Cichlasoma urophthalmus, Hemichromis letourneuxi) to low temperature: laboratory and field experiments in south Florida. Biological Invasions 12:2441–2457.

Serrano, X., M. Grosell, and J. E. Serafy. 2010. Salinity selection and preference of the grey snapper Lutjanus griseus: Field and laboratory observations. Journal of Fish Biology 76:1592–1608.

Serrano, X. M. 2008, August. Ecophysiology of the Gray Snapper (Lutjanus griseus): Salinity Effects on Abundance, Physiology and Behavior. Master of Science Thesis, University of Miami, Coral Gables, FL.

Serrano, X., J. Serafy, and M. Grosell. 2011. Osmoregulatory capabilities of the gray snapper, Lutjanus griseus: Salinity challenges and field observations. Marine and Freshwater Behaviour and Physiology 44:185–196.

Shelton, et al. 2020. Restore Lagoon Inflow Research Project Phase 1 Project Summary. Florida Department of Education. https://www.fit.edu/media/site-specific/wwwfitedu/indian-river-lagoon/documents/State-of-Florida-Restore-Lagoon-Inflow-Research-Phase-1-Full-Report-2020.pdf

Shervette, V. R., N. Ibarra, and F. Gelwick. 2007. Influences of salinity on growth and survival of juvenile pinfish Lagodon rhomboides (Linnaeus). Environmental Biology of Fishes 78:125–134.

Sicko-Goad, L. M., Schelske, C. L., and Stoermer, E. F. (1984). Estimation of intracellular carbon and silica content of diatoms from natural assemblages using morphometric techniques. Limnol. Oceanogr. 29, 1170-1178.

Sigua, G.C., J.S. Steward, and W.A. Tweedale. 2000. Water quality monitoring and biological integrity assessment in the Indian River Lagoon, Florida: Status, trends and loadings (1988-1994). Environmental Management 25:199-209.

Silverman, M. J. 1979. Biological and Fisheries Data on black drum, Pogonias cromis (Linnaeus).

Smayda, T. J. (1978). "From phytoplankters to biomass" in Phytoplankton Manual, ed. A. Sournia (UNESCO, Paris), 273-279.

Smith, C.J., D.B. Nedwell, L.F. Dong, and A.M. Osborn. 2007. Diversity and abundance of nitrate reductase genes (narG and napA), nitrite reductase genes (nirS and nrfA), and their transcripts in estuarine sediments. Applied and Environmental Microbiology 73(11):3612–22.

Smith, J. W. 1994. Biology and Fishery for Atlantic Thread Herring, Opisthonema oglinum, along the North Carolina Coast. Marine Fisheries Review 56:1–7.

Smith, N.P. 1993. Tidal and nontidal flushing of Florida's Indian River Lagoon. Estuaries 16:739-746.

Smith, N.P. 2001. Seasonal-scale transport patterns in a multi-inlet coastal lagoon. Estuarine Coastal and Shelf Science 52:15-28.

Sogard', S. M., G. V. N. Powell, and J. G. Holmquist. 1989. Utilization by fishes of shallow, seagrass-covered banks in Florida Bay: 1. Species composition and spatial heterogeneity. Environmental Biology of Fishes 24:53–65.

Song, J., R. W. Brill, and J. R. McDowell. 2019. Plasticity in standard and maximum aerobic metabolic rates in two populations of an estuarine dependent teleost, spotted seatrout (Cynoscion nebulosus). Biology 8.

Song, J., and J. R. McDowell. 2021. Comparative transcriptomics of spotted seatrout (Cynoscion nebulosus) populations to cold and heat stress. Ecology and Evolution 11:1352–1367.

Stevens, P. W., M. F. D. Greenwood, and D. A. Blewett. 2013. Fish Assemblages in the Oligohaline Stretch of a Southwest Florida River during Periods of Extreme Freshwater Inflow Variation. Transactions of the American Fisheries Society 142:1644–1658.

Stillman, D. 2023, July 10. Florida ocean temperatures at "downright shocking" levels. The Washington Post.

Stolen, M.K. 1998. Age, growth, and mortality patterns of bottlenose dolphins from the east coast of Florida. Masters thesis. Univ. of Central Florida, Orlando, FL

Stolen, M., W.N. Durden, T. Mazza, N. Barros, and J. St. Leger. 2013. Effects of fishing gear on bottlenose dolphins (Tursiops truncatus) in the Indian River Lagoon system, Florida. Marine Mammal Science, doi: 10.1111/j.1748-7692.2012.00575.x.

Strathmann, R. R. (1967). Estimating the organic carbon content of phytoplankton from cell volume or plasma volume. Limnol. Oceanogr. 12, 411-418.

Sun, J., and Liu, D. (2003). Geometric models for calculating cell biovolume and surface area for phytoplankton. J. Plankton Res. 25, 1331-1346.

Suzuki, M. T., L.T. Taylor, and E.F. DeLong. (2000). Quantitative Analysis of Small-Subunit rRNA Genes in Mixed Microbial Populations via 5′-Nuclease Assays. Applied and Environmental Microbiology, 66(11), 4605–4614. https://doi.org/10.1128/AEM.66.11.4605-4614.2000

Titcomb, E.M., J. Stevens, A. Sleeman, B. Nelson, L. Yrastorza, A,M. Schaefer, G.M. Bossart, J.S. Reif, and M. Mazzoil. 2020. Linear skin markings in common bottlenose dolphins (Tursiops truncatus) from the Indian River Lagoon, Florida. Marine Mammal Science 36:858-870.

Tolley, G. S., A. K. Volety, and M. Savarese. 2005. Influence of salinity on the habitat use of oyster reefs in three Southwest Florida estuaries. Journal of Shellfish Research 24:127–137.

Trefry, J.H., Johnson, K.B., Fox, A.L., and Ma, X. 2019. Optimizing Selection of Sites for Environmental Dredging in the Indian River Lagoon System. Project Report Submitted to Brevard County Natural Resources Management Department.

Tremain, D.M. and D.H. Adams. 1995 Seasonal variation in species diversity, abundance, and composition of fish communities in the northern Indian River Lagoon, Florida. Bulletin of Marine Science 57:171–192.

Tucker, J. W., and P. A. Barbera. 1987. Laboratory Spawning of Sheepshead. The Progressive Fish-Culturist 49:229–230.

Urian, K.W., D.A. Duffield, A.J. Read, R.S. Wells, and E.D. Shell. (1996) Seasonality of reproduction in bottlenose dolphins, Tursiops truncatus. Journal of Mammalogy 77, 394-403

U.S. Army Corps of Engineers. (2001). Unified Facilities Criteria (Ufc): Military harbors and coastal facilities.

U.S. Army Corps of Engineers. (2002). Coastal Engineering Manual.

U.S. Department of Transportation, Federal Highway Administration. (1983). Structural Design Manual for improved inlets and culverts.

Van Bressem, M.F., M.C. De O Santos, and J.F. Oshima. 2009. Skin diseases in Guiana dolphins (Sotalia guianensis) from the Paranagua estuary, Brazil: a possible indicator of a compromised environment. Marine Environmental Research, 67: 63-68.

Vega-Cendejas, M. E., G. Mexicano-Cintora, and A. M. Arce. 1997a. Biology of the thread herring Opisthonema oglinum (Pisces: Clupeidae) from a beach seine fishery of the Campeche Bank, Mexico. Fisheries Research 30:117–126.

Vega-Cendejas, M. E., G. Mexicano-Cintora, and A. M. Arce. 1997b. Biology of the thread herring Opisthonema oglinum (Pisces: Clupeidae) from a beach seine fishery of the Campeche Bank, Mexico. Fisheries Research 30:117–126.

Verity, P., Robertson, C. Y., Tronzo, C. R., Andrews, M. G., Nelson, J. R., and Stieracki, M. E. (1992). Relationships between cell volume and the carbon and nitrogen content of marine photosynthetic nanoplankton. Limnol. Oceanogr. 37, 1434-1446.

Vilela, R., G.D. Bossart, J. St. Leger, L.M. Dalton, J.S. Reif, A.M. Schaefer, P.J. McCarthy, P.A. Fair, and L. Mendoza. 2016. Cutaneous granulomas in dolphins caused by novel uncultivated Paracoccidiodes brasiliensis. Emerging Infectious Diseases, 22(12): 2063-2069.

Virnstein, R.W., Morris, L.J. 1996. Seagrass preservation and restoration: A diagnostic plan for the Indian River Lagoon. SJRWMD, Tech. Memorandum No. 14, Palatka, Florida.

Waidner, L.A., and D.L. Kirchman. 2007. Aerobic anoxygenic phototrophic bacteria attached to particles in turbid waters of the Delaware and Chesapeake estuaries. Applied and Environmental Microbiology 73(12):3936–44.

Ward, B. B. (2008). Nitrification in Marine Systems. In Nitrogen in the Marine Environment, edited by D. C. Capone, D. A. Bronk, M. R. Mulholland, and E. J. Carpenter, 199–261. Amsterdam: Elsevier.

Ward, R., I. R. Blandon, T. L. King, and T. L. Beitinger. 1993. Comparisons of Critical Thermal Maxima and Minima of Juvenile Red Drum (Sciaenops ocellatus) from Texas and North Carolina. Northeast Gulf Science 13.

Weinstein, M. P., and M. P. Walters. 1981. Growth, Survival and Production in Young-of-Year Populations of Leiostomus xanthurus Lacepede Residing in Tidal Creeks. Estuaries 4:185–197.

Welshmeyer, N.A. 1994. Fluorometric analysis of chlorophyll a in the presence of chlorophyll and pheopigments. Limnology and Oceanography 39:1985–1992.

Westerink, J.J., R.A. Luettich and R.L. Kolar, 1996, ADCIRC an advanced finite element model for coastal ocean circulation, Proceedings, The Third Asian Pacific Conference on Computational Mechanics, 16–18 September, Seoul, Korea

White, J. C. JR., and J. W. Angelovic. 1973. Interactions of chromic gamma radiation, salinity, and temperature on the morphology of post-larval Pinfish, Lagodon rhomboides. Pages 199–217 Proceedings of A Workshop on Egg, Larval, and Juvenile Stages of Fish In Atlantic Coast Estuaries.

Whitfield, A. K., J. Panfili, and J. D. Durand. 2012. A global review of the cosmopolitan flathead mullet Mugil cephalus Linnaeus 1758 (Teleostei: Mugilidae), with emphasis on the biology, genetics, ecology and fisheries aspects of this apparent species complex. Reviews in Fish Biology and Fisheries 22:641–681.

Wijnhoven, S, V Escaravage, E Daemen, and H Hummel. 2010. "The decline and restoration of a coastal lagoon (Lake Veere) in the Dutch Delta." Estuar. Coast. 33 1261-1278.

Wise, D. J., and J. R. Tomasso. 1989. Acute Toxicity of Nitrite to Red Drum Sciaenops ocellatus: Effect of Salinity. Journal of the World Aquaculture Society 20:193–198.

Work, K., Havens, K., Sharfstein, B., and East, T. (2005). How important is carbon to planktonic grazers in a turbid, subtropical lake? J. Plankton Res. 27, 357-372.

Wuenschel, M. J., J. A. Hare, M. E. Kimball, and K. W. Able. 2012. Evaluating juvenile thermal tolerance as a constraint on adult range of gray snapper (Lutjanus griseus): A combined laboratory, field and modeling approach. Journal of Experimental Marine Biology and Ecology 436–437:19–27.

Wuenschel, M. J., A. R. Jugovich, and J. A. Hare. 2004. Effect of temperature and salinity on the energetics of juvenile gray snapper (Lutjanus griseus): Implications for nursery habitat value. Journal of Experimental Marine Biology and Ecology 312:333–347.

Ysebaert, Tom, Dirk-jan van der Hoek, Rick Wortelboer, Jeroen W.M. Wijsman, Marijin Tangelder, and Arno Nolte. 2016. "Management options for restoring estuarine dynamics and implications for ecosystems: A quantitative approach for the Southwest Delta in the Netherlands." Ocean & Coastal Management 33-48.

Zarillo, G.A. Listopad, C., 2016. Indian River Lagoon Hydrodynamic and Water Quality Model Quality Assurance Plan: Year 1 Final Report Prepared for Brevard County and the Florida Department of Environmental Protection.

Zarillo, G.A. and Listopad, C. 2020. Hydrologic and Water Quality Model for Management and Forecasting within Brevard County Waters of the Indian River Lagoon. Final Project Report to Brevard County Natural Resources Management Department. 128pp.

Zarillo, G.A. 2021. Development of a Water Quality Model for The Turkey Creek Feasibility Study. Report to Applied Ecology, Inc. 63 p.

Zarillo, G.A. 2022. Impacts of Environmental Muck Dredging 2016-2019. Final Report to Brevard County Dept. of Environmental Management. 60p

Zastrow, C. E., E. D. Houde, and L. G. Morin. 1991. Spawning, fecundity, hatch-date frequency and young-of-the-year growth of bay anchovy Anchoa mitchilli in mid-Chesapeake Bay. Page Source: Marine Ecology Progress Series.

Appendix A   Task 1 – Engineering Report

Restore Lagoon Inflow Research (Phase 3)
Final Report
Task 1: Engineering
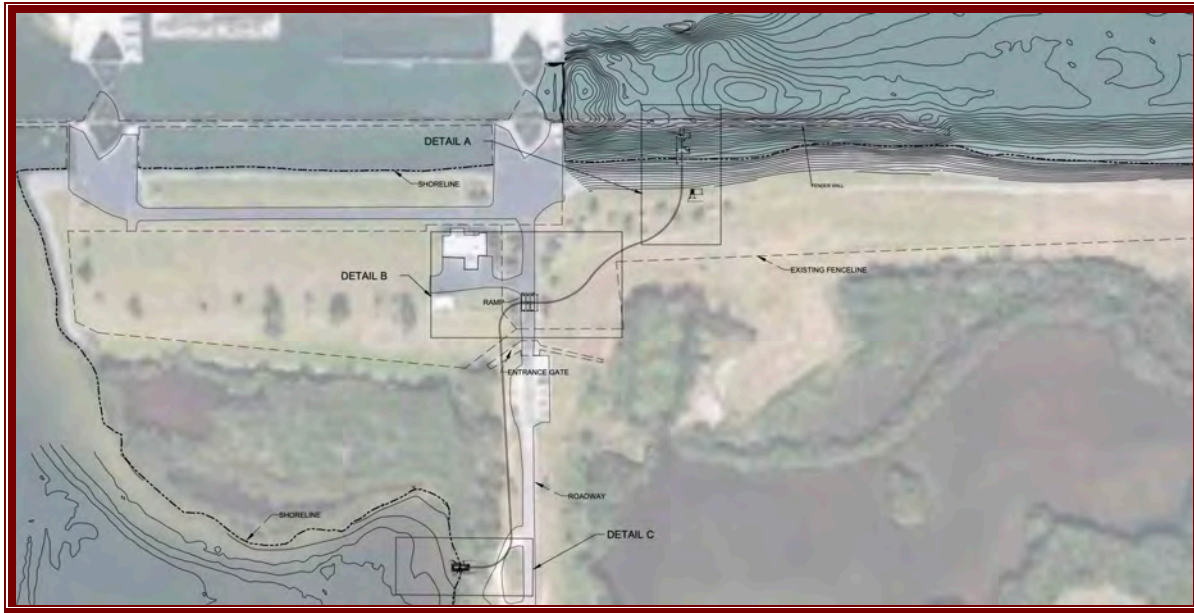
PREPARED FOR

Florida Department of Education
325 W Gaines Street
Tallahassee, FL 32399

PREPARED BY

Robert Weaver
Florida Institute of Technology
150 West University Boulevard
Melbourne, FL 32091

FLORIDA TECH

July 2023

Acknowledgements

Florida Tech Engineering and Design Team would like to acknowledge project partners from Tetra Tech: Engineer Dick Czlapinski, P.E., D.CE., Project Manager Matt Shelton, and Associate Erik Erton.

List of Figures

List of Tables

List of Appendices

List of Acronyms

ASCE	American Society of Civil Engineers
BRL	Banana River Lagoon
D.CE.	Diplomate, Coastal Engineering
DEP	Department of Environmental Protection
DO	Dissolved Oxygen
E.I.T	Engineer in Training
EPA	Environmental Protection Agency
ERP	Environmental Resource Permit
FHWA	Federal Highway Administration
FWC	Florida Fish and Wildlife Conservation Commission
GSA	Graduate Student Assistant
IRL	Indian Rover Lagoon
KSC	Kennedy Space Center
m^3/sec	cubic meters per second
NASA	National Aeronautics and Space Administration
P.E.	Professional Engineer
Ph.D.	Doctor of Philosophy
PI	Principal Investigator
RAI	Request for Additional Information
RLI	Restore Lagoon Inflow
USACE	United States Army Corps of Engineering

Project Staffing (includes part-time and full-time project staff)

Faculty – Robert J. Weaver, Ph.D.   Graduate Assistants–Benjamin Komita, E.I.T

Highlights

- Pilot inflow design completed.
- USACE Section 404, USACE Section 408, and DEP ERP permits approved.
- Similar projects around the globe illustrate the benefits of enhancing circulation in enclosed and semi-enclosed estuaries.

1 Task Summary: Engineering (Task 1)

Enhancing ocean inflow has been shown to improve water quality in enclosed and semi-enclosed estuaries worldwide (Benkendorff et al. 2022, Bilecki 2020, Burgess 2020, Byron Shire Council 2022, Cavanagh, et al. 2015, Coosen, et al. 1990, Dowhan, et al. 1997, Ferguson, et al. 2021, Gobler, et al. 2019, Nielson et al. 2005, Peterson, et al. 2008, Port of Los Angeles Engineering Division 2006, Wijnhoven, et al. 2010, Ysebaert, et al. 2016). Though the mechanisms generating the inflow has varied in the referenced studies, in each case the system shifted toward reduced nutrient load and increased dissolved oxygen (DO). Phase 1 and 2 hydrodynamic modeling and geochemical experiments indicate similar results can be expected for the Indian River Lagoon (IRL). The project goal for Phase 3 was to secure permits and move toward construction and operation of pilot scale pumping system to bring ocean water into the Banana River Lagoon (BRL) in order to validate preliminary findings and evaluate the potential impacts of a full-scale inflow structure.

Once underway, the pilot project will allow researchers to directly assess the feasibility and potential impacts of using enhanced ocean water exchange to improve lagoon water quality in the IRL. An operational pilot project is dependent on multi-agency approval of the concept and design. This approval is achieved through the permitting process. Researchers worked during Phases I and II to develop the pilot design and better understand the current status of the IRL system to establish physical and biological baselines to investigate what the potential impacts may be from enhanced inflow. This effort as well helped to address concerns that permitting agencies had about the potential impacts of the pilot project.

To meet the Phase 3 goal, the engineering design and permitting Task Group consisting of Principal investigator (PI) Weaver and Graduate Student Assistant (GSA) Komita, developed the pilot system design and worked closely with Tetra Tech, providing them with necessary materials to complete the permits and prepare them for review by the appropriate agencies, including the US Army Corps of Engineers (USACE), Florida Fish and Wildlife Commission (FWC), and Florida Department of Environmental Protection (DEP). These agencies have a regulatory role in approving the pilot project permit applications and early coordination aided in expediting the process.

The success of the pilot project is dependent on the approval of the permitting agencies. The following objectives were identified to progress toward the Phase 3 goal.

- Advance the 60% design developed in Phase 2 to the 90% design needed for permit submittal.
    - Design concerns addressed during Phase 3 include finalizing exact location of the project, telemetry and contingency plan for pump control, electrical requirements, site access and security, and geotechnical/environmental specifications.
    - The permitted design includes all project elements and their locations and principal dimensions. With the permitting approved, the remaining work to advance to the 90% design level requires selecting and sizing materials and including connection details.
- Prepare and submit USACE Section 404, USACE Section 408, and Florida Environmental Resource Permit (ERP) permits in close coordination with Tetra Tech.
- Address Requests for Additional Information (RAI's), from the permitting agencies in an expedited manner. RAI's may require:

o Explanations/clarifications of methods, expected impacts, mitigation strategies, design features, etc.
o Modifications to the 90% design.

The engineering design and permitting team worked with Restore Lagoon Inflow (RLI) Task Groups and Tetra Tech to obtain the required data and analysis needed to address the RAI's and draft the responses for Tetra Tech prior to (re)submittal.

1.1 Approach

Based on data collected during Phase 1 and discussions with agencies and stakeholders, Phase 2 identified the northern BRL as the most feasible and cost-effective location of a temporary inflow research site. BRL is a sub-basin of IRL that lies between Cape Canaveral and Merritt Island and extends from the National Aeronautics and Space Administration (NASA) Kennedy Space Center (KSC) to Dragon Point. It is poorly flushed with no direct connection to the ocean, which results in long water residence times and increased vulnerability to nutrient accumulation.

The proposed temporary inflow system would extract water from the port/ocean side of the Canaveral Lock system and discharge to BRL via the cove to the west of Avocet Lagoon (**Figure 1**). A pump station is proposed that pumps a relatively small volume of 0.5 cubic meters per second (m^3/sec) of seawater through a pipe system above ground to the lagoon. The cove configuration will restrict flow movement from the outfall location and provide a concentration gradient to evaluate changes on water quality, geochemistry, and biology. The proposed pilot system configuration was selected to preserve the reference site while minimizing cost and impacts to existing infrastructure, public access, and natural resources.

Figure 1. Map of the proposed inflow pilot system site and pipeline path

1.2 Results

The Phase 3 Task 1 results include completing the design, submitting permits for the implementation of the pilot pumping system, responding to RAI's form regulatory agencies, and reviewing similar enhanced exchange projects around the globe for guidance on engineering design, management, and anticipated impacts.

1.2.1 Design and Permitting

During Phase 3 the focus of Task 1 was to advance the development of the Section 404, Section 408, and ERP permits, leading to the submission and approval of the permit applications. The USACE Section 404 and Section 408 and State ERP permits are provided in Appendix A.3. The Section 404, Section 408, and ERP permits include the approved engineering design of the inflow structure, outflow structure, and pipeline route. These designs contain guidance for telemetry and control of the system and are sensitive to the ability for the pilot project and all associated components to be removed at the end of the one-year study period. The design features based on the temporary nature of the project include a scour pad laid on top of existing ground at the outfall which does not require excavation, timber piles that can be removed and repurposed, and a flow rate that will not induce sediment erosion at the intake.

Design guidelines provided by Tetra Tech include documentation from American Society of Civil Engineers (ASCE) on structure design (ASCE 2017)], USACE Engineer Manuals (USACE 2001, 2002), Department of Defense Uniform Facility Requirement (USACE 2002), and Federal Highway Administration Hydraulic Engineering support (US Department of Transportation 1983). The goal is to ensure 90% and 100% design plans adhere to the strictest of guidelines and anticipate all possible RAI's from the review agencies. The Design Criteria Document contains a detailed listing of the requirements for the engineering design including client, structural (i.e., loads on the structure), regulatory, safety, environmental, operational, maintenance of traffic, and other requirements (see Appendix A1). Together these requirements provide the framework for the 90% design needed for permitting.

Working toward the goal of approved permits, the engineering team worked with Tetra Tech to prepare and submit necessary documents required for Section 404, Section 408, and ERP permits and respond to agency RAI's. Engineering design plans and specifications were advanced from Phase 2 and with agency approval of the permit applications the design can be brought up to the 90% completion status. The engineering team is responsible for finalizing pump selection, intake design including screen specifications, design of the outfall structure, pipe route and diameter, load analysis on support structure, and site access. The finalized location of the pilot project was determined during with the USACE approval of site usage in the Section 408 permit. As a result of pre-permitting meetings spearheaded by Tetra-Tech, structure design was updated taking the suggested modifications into account. Selected design features are provided here with the completed design set included in the Appendix (see Appendix A.2).

The inflow structure will consist of a pile supported platform to mount the pipe and the intake side of the pump. The platform will allow access to the intake for maintenance while providing structure to support the pipe and necessary hydraulics. This design is also readily removed at the end of the one-year project duration. To ensure compliance with United States Environmental Protection Agency (EPA) Section 316(b), a new commercially available (and EPA compliant) intake screen designed by Hendrick Screen Supply was selected (**Figure 2**). This screen will optimize flow into the intake pipe though specially designed holes in the screen as well as minimize biofouling through material selection. The MWI HMF320 Hydraflow Pump made from 316 stainless steel powered by the 2400E electric drive unit with 200 horsepower motor was selected for this project based on the 0.5m3/s flow rate and the updated calculated head losses (42.37 feet) in the pipeline from the intake to the outfall. This selection is a change from the Phase 2 pump. In Phase 2 the total dynamic head was calculated to be only about 20 feet. Updated calculations were made based on intake, pipeline, and outfall modifications, and working with the MWI pump team the updated pump selection was made.

Figure 2. Typical drum intake screen per manufacturer Hendrick Supply

The geotextile outfall structure has been designed to eliminate the need for any dredging, excavation, or introduction of rip rap into the outfall area (**Figure 3**). Consulting with geotextile manufacturer Sythnetex, the engineering team was able to produce a creative solution to manage stakeholder agency concerns with excavation. The bottom portion of the outfall is designed to be the Synthetex Hydrotex® Articulating Block (or similar product) as a scour mat that will reduce flow velocity and reduce risk of scour at the end of the outfall. In the event of erosion or settlement, the articulating block pad can adjust and change to the contour of the ground. Each side of the material features a geotextile curb to ensure that the water flows only on the outfall pad itself and does not flow over the sides, inducing scour. Per National Marine Fisheries guidance, a manatee exclusion screen has been added to the outflow pipe. A simple design of a grate connected directly to the pipeline flange will provide ease of cleaning in event of clogging as well as ease of replacement in cases of damage (**Figure 3**).
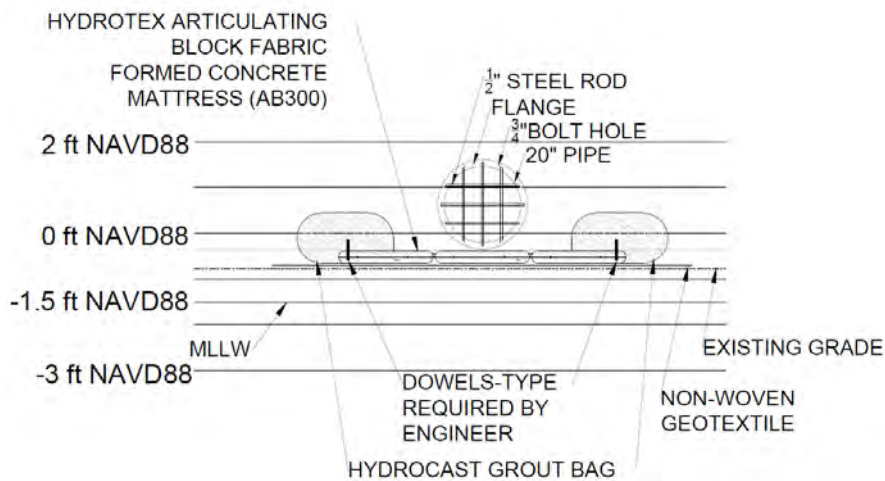
Figure 3. Geotextile outfall structure with manatee exclusion grate (shown on face of pipe)

To provide ongoing monitoring and allow for off-site shutoff, a remote system has been selected to interface with the pump. A system supplied by Allied Pivot Sales will be implemented, which allows operators to remotely turn the pumping system on and off through cellular connection on

a Verizon server as well as monitoring pump status on case of unintentional shutoff. The system also monitors water temperature, flow rate, and water volume through the pump and stores this information in a cloud-based storage center. Once a project sponsor has been identified, the responsibility and communication matrices will be developed with the purpose of determining who is responsible for pump operation, which parties will oversee turning the system off in emergency conditions (hurricane, power outage, flood, etc.), and under what conditions the pump will need to be shutoff.

The pipeline path was modified to remove abrupt 90-degree bends, this modification reduces the head losses and eliminates the need for thrust blocks. The pipeline must cross the access road to the USACE Canaveral Lock operations facility. It is a requirement that the operations not be impacted. A ramp structure from Bluff Manufacturing was selected that will install on top of the existing roadway and go over the pipeline. During RAI, the Corps was concerned about the allowing both smaller vehicles and larger trucks access the site without issue. Consultations with Bluff Manufacturing resulted in a slight redesign of the ramp structure to accommodate a wide range of vehicles.

As the project comes to the end of Phase 3, the USACE Section 404 and 408 permits and the DEP ERP permit have been approved (Appendix A.3). In that process, the design team received and responded to RAI's from the DEP for the team's ERP application, and USACE for the Section 404 and 408 permits. The requested information included details on the exclusion intake screen, new pump selection, geotextile outfall scour protection, and site access and security. The designs developed by Robert Weaver, Ph.D., and Benjamin Komita, EIT, were approved by Tetra Tech Engineer Dick Czlapinski, P.E., D.CE. with review input from Matt Shelton and Erik Erton. The completed plans were submitted and approved. These plans are considered 100% design plans. A completed set of these plans can be found attached to this document as Appendix A.2.

Table 1. Pipe and Pump System Cost Estimate

Structure	Total Cost	
Pump	$	454,640.00
Ramp	$	42,933.00
Inflow	$	71,891.15
Outflow	$	1,007.30
Subtotal	**$**	**570,471.45**
Contractor Mobilization, Overhead, and Profit (30%)	**$**	**171,141.44**
Contingency (40%)	**$**	**228,188.58**
Total	**$**	**969,801.47**

The estimated cost for the system is just under $1 million dollars based on revised cost estimates for the components in the Phase 3 design (**Table 1**). The costs reflect changes to the pump that resulted in increases from the Phase 2 estimate. These changes are due to the recalculation of total dynamic head which led to the modification of the pump selected for the project (MWI HAC316 Hydraflo + Pipeline in Phase 2 combined totaling @ $243,000 2021 vs. the MWI HAC320 Hydraflo + Pipeline for Phase 3 at @ $454,640 2023), and the use of the premanufactured intake screen designed by Hendrick Screen Supply. These two changes in the system design and equipment cost increases from 2021 to 2023 account for the difference in Phase 2 and Phase 3 estimates. Post project resale of the intake pump system and pipe to MWI for an estimated $116,000, based on communications with MWI, can help to offset the cost of the inflow pilot study.

1.2.2 Review of inflow projects

Concurrent with the permitting process, a review of existing and historic inflow projects was initiated. Details from sites around the globe were collected to review performance and impact on water quality from engineered inflow projects. The aim is to project the impact of a large-scale project on the IRL. The manuscript under preparation for submission summarizes enhanced flow projects that have been implemented across the globe including in Australia, Denmark, the Netherlands, and the USA (Komita In Prep). The manuscript takes a close look at several case studies with specific relevance to the situation in the IRL. The paper is meant to serve as an overview of inflow projects globally, with consideration to both natural and artificial inflow systems.

1.2.2.1 Case Study: Destin, FL

In 1992 a permanent pump station was constructed to improve circulation in Destin Harbor (Destin Florida, USA; **Figure 4**). The pump system is operated daily from 11 pm to 7 am in the warmer months and brings in almost 22 million gallons of water from the Gulf of Mexico each night (Burgess 2020).

Figure 4. Destin Harbor Aerial Map (Google 2021)

Originally a natural formation, the harbor formerly served as a connection between the Gulf of Mexico and Choctawhatchee Bay (Landers-Atkins Planners, Inc. 1987). The original inlet, named Old Pass, was closed by a hurricane in 1930 and in 1931 the first mechanically opened channel, East Pass, was constructed. For the next 30 years, the USACE maintained and strengthened this channel with jetties, widening, and dredging (Landers-Atkins Planners, Inc. 1987). Although Destin Harbor remains connected to the Gulf of Mexico via East Pass, natural circulation is restricted and the harbor was poorly flushed, with high residence times especially in the eastern portions of the harbor and in the residential canals (Landers-Atkins Planners, Inc. 1987).

Residential construction booms and infrastructure expansion in the 60's, 70's, and 80's put strain on the stormwater facilities and led to discharges of untreated water into portions of the harbor that already experienced poor circulation. Combined with increased boating activity, water quality within the harbor degraded rapidly, marked by an extended fish kill event in the harbor in the fall of 1982 (Landers-Atkins Planners, Inc. 1987). In 1984, the Northwest Florida Coast Resource Planning and Management Committee was created and charged with creating policies to address development and its effects on the environment, with a subcommittee designated to addressing water quality issues within Destin Harbor. The Destin Harbor Management Plan, written in 1987 by Landers-Atkins Planners, Inc., provided a comprehensive plan recommending the best methods to alleviate the water quality deterioration occurring in the waterbody, and one of the major recommendations was the implementation of the Northwest Florida Water Management District's flushing pipe and pump system (Landers-Atkins Planners, Inc. 1987, Northwest Florida Water Management District 1992) (**Figure 5**).
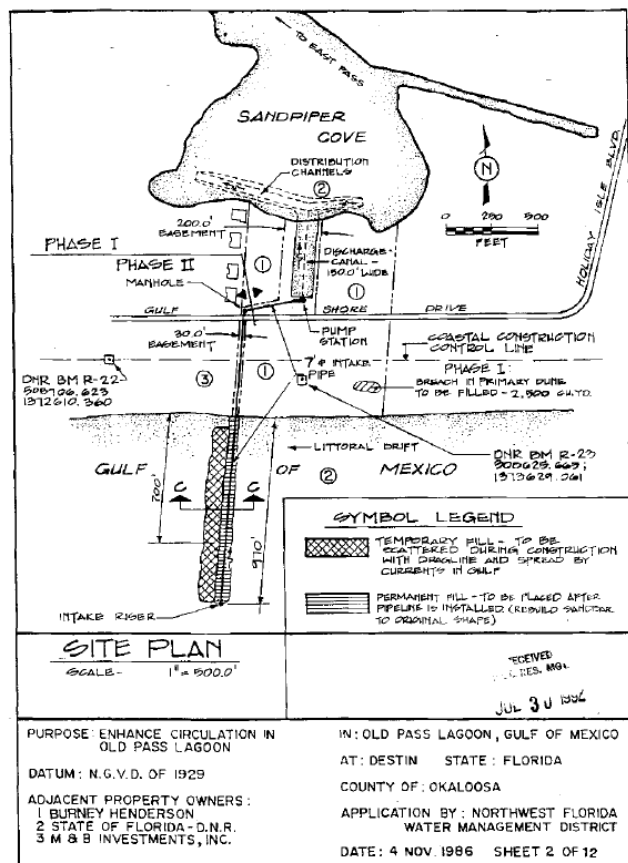
Figure 5. Northwest Florida Water Management District Pipe and Pump Site Plan for Ocean Inflow into Destin Harbor (Northwest Florida Water Management District 1992)

The Destin Harbor Pump Project was constructed in two phases and completed in 1992 for a total of $3.3 million; phase one included the construction of the pump station (**Figure 6**), and phase two included the construction of the Gulf intake structure and related seven foot diameter concrete piping (**Figure 7**) (Indian River County 2016, Northwest Florida Water Management District 1992).

During the warmer months from April to November, the pump system is operated daily during the hours of 11 pm to 7 am, bringing in close to 22 million gallons of low-nutrient water from the Gulf of Mexico every night (Burgess 2020). When the pump is not running, the discharge weir remains open to allow exchange of Gulf water into the Harbor by tidal forcing.

Figure 6. Destin Harbor Pump Project Pump Station (Indian River County 2016)

Figure 7. Destin Harbor Pump Project Gulf Intake (Indian River County 2016)

The implementation of the Destin Harbor Pump Project was seen as a success in its ability to contribute to the improvement of the Harbor's water quality; regular flow of Gulf water allows for greater water circulation inside of the restricted lagoon. Since the implementation of the pump system, the Destin Harbor has maintained Class III Surface Water Quality Standard, meaning the basin is safe for fish consumption and is able to support the recreation and sustain a healthy population of fish and wildlife (FDEP 2023). It has also maintained acceptable levels of dissolved oxygen, salinity, and water clarity, and there have been no additional fish kills (Burgess 2020).

1.3 Conclusion

The design of the proposed pilot scale inflow has been focused on creating a mesocosm in a semi-enclosed basin within the northern Banana River. This controlled environment will allow scientists and policy makers to evaluate the benefits of enhancing ocean inflow in the IRL before committing to a full-scale design. The design accounts for the temporary nature of the pilot project,

input from the stakeholders and permitting agencies, and the potential need to remotely shut the system down in case of emergency.

With completion of Phase 3, Task 1 achieved completion of:

- Pilot inflow design includes all project elements and their locations and principal dimensions.
- USACE Section 404, USACE Section 408, and DEP ERP permits approved.
- Review of similar national and international projects illustrate the benefits of enhancing circulation in enclosed and semi-enclosed estuaries.

Data from existing inflow projects taken together with work performed by Dr. Zarillo and the Task 2 team as well as Dr. Fox and the Task 3 team support the proposal that enhanced ocean inflow in IRL will buffer regional salinity, temperature, and DO, while also reducing nutrient levels (nitrogen and phosphorus) and the frequency of harmful algal bloom outbreaks.

Findings to date indicate that improving water quality in the BR and IRL by enhancing ocean inflow is both feasible and cost effective. The pilot project is estimated to cost just under $1million dollars for construction. A structure that would accommodate a full-scale inflow was estimated in Phase 1 to cost approximately $10 million dollars for a weir structure and $60 to $100 million to pump ocean water from offshore using a buried pipe system under the barrier island. To put that into perspective, as of Fiscal Year 22/23 Quarter 1 the Brevard County Save Our Indian River Lagoon Plan has allocated or spent nearly $155 million on dredging muck and treatment of the interstitial waters, $10 million on building oyster reefs, $50 million on stormwater projects, $25 million on wastewater treatment upgrades, $120 million on septic system removal by sewer extension, and $29 million on septic upgrades in addition to other expenditures, (Brevard County 2023). A permanent managed-flow structure would provide another tool in maintaining a healthy ecosystem in the hydrologically restricted IRL estuary.

1.4 Next Steps

With the approval of the USACE Section 404 and 408 and DEP ERP permits the design can now be brought from the current level up to the 90% and then subsequent 100% design level from construction. With all project elements and their locations and principal dimensions approved in the permitting process, the major details of the elements can be prescribed for the ninety percent design development. These include the plan and sections of the pipeline trestle including beams, stringers, decking, railing materials and sizing and also include more advanced details such as connection and fitting details. With the advancement of the additional design work, the pilot inflow project is ready to finish the pre-construction phase and transition into the construction phase. The bid package needs to be developed. Once completed the project can be sent out to bid. Engineering oversight of bidding, construction, and operations is an important component of a successful pilot project.

Once construction is completed and pump is operational the project moves into the performance and monitoring phase. In order to fully evaluate the project, it is important to measure the currents both inside the Banana River west of the Locks and in the port east of the Locks. Deployment and maintenance of two acoustic doppler current profilers will require permitting of the instrument locations and regular monthly servicing which includes offloading of data,

cleaning of the instruments and, and battery replacement. During operations, the engineering team will need to monitor the flow rate and water quality at both the intake and outfall.

Monitoring currents inside the project area and near the intake will aid not only in the understanding of water exchange during the pilot but will also provide a clearer picture of the hydrodynamics of Canaveral Lock operations. This will assist in understanding the relative contributions of water exchange through the lock to lagoon ocean water exchange.

The pilot project will provide necessary data to allow stakeholders to assess the feasibility of a full-scale inflow project to improve and maintain optimal water quality in the Banana River and northern IRL. An important next step will be to explore full system design options not presented in Phase 1 and compare the costs and benefits of each location and design option.

2 References

American Society of Civil Engineers. 2017. Chapter 2: Combinations of Loads. In Minimum design loads and associated criteria for buildings and other structures (ASCE/SEI 7-16) (pp. 7–9). essay.

Benkendorff, K., C Klaas, and M. Kirby. 2022. *Water quality in Woolgoolga estuary and valuation of nutrient removal servies by the remnant leaf oyster reef.* 2022: Coffs Harbour City Council - Environmental Levy Program.

Bilecki, Michael S. 2020. "Fire Island National Seashore: A breach in the barrier island at the Otis Pike Fire Island High Dune Wilderness." *Parks Stewardship Forum* 137-143.

Brevard County . 2023. "Save Our Indian River Lagoon Performance Tables – Fiscal Year 22/23 Quarter 1 ." *brevardfl.gov.* 2 9. Accessed 2023. chrome-extension://efaidnbmnnnibpcajpcglclefindmkaj/https://www.brevardfl.gov/docs/default-source/soirl/oversight-committee/save-our-indian-river-lagoon-performance-table.pdf?sfvrsn=526fff29_5.

Burgess, M. 2020. *Destin Harbor Pump.* https://destin.lifemediagrp.com/destin-harbor-pump-ready-for-the-2020-season/.

Byron Shire Council. 2022. *Belongil Creek.* https://www.byron.nsw.gov.au/Services/Environment/Coast-and-waterways/Estuaries-and-ICOLLs/Belongil-Creek.

Cavanagh, Damion, Jeremy Visser, Suanne Richards, and Jane Ainsworth. 2015. *Review of Environmental Factors: Tallow Creek Entrance Opening - Vol. 1.* Brisbane: BMT WBM.

Coosen, J, PM Meire, JJ Stuart, and J Seys. 1990. "Trophic relationships in brackish Lake Veere: the role of macrophytes." *Proceedings of the 24th European Marine Biology Symposium.* Aberdeen: Aberdeen University Press. 404-423.

Dowhan, Joseph, Thomas Halavik, Andrew Milliken, Andrew MacLachlan, Marcianna Caplis, Kelly Lima, and Andrew Zimba. 1997. *Significant Habitats and Habitat Complexes of hte New York Bight Watershed.* Charleston, Rhode Island: US Fish and Wildlife Service.

FDEP. 2023. *DEP 101: Surface Water Quality Standards.* March 20. https://floridadep.gov/comm/press-office/content/dep-101-surface-water-quality-standards.

Ferguson, Angus, Danny Wiecek, Michael Hughes, David Hanslow, David Wainwright, and Peter Scanes. 2021. *Form and function of NSW intermittently closed and open lakes and lagoons.* Parramatta, NSW: Environment, Energy and Science, Department of Planning, Industry and Environment.

Gobler, Christopher J, Craig S Young, Jennifer Goleski, Alexandra Stevens, Jake Thickman, Ryan B. Wallace, Patrick Curran, et al. 2019. "Accidental ecosystem resotration? Assessing the estuary-wide impacts of a new ocean inlet created by Hurricane Sandy." *Estuarine, Coastal and Shelf Science* 132-146.

Google. 2021. *Google Earth.* https://earth.google.com/web/search/old+pass+destin/@30.38769493,-86.50558754,1.60015071a,4146.51368888d,35y,0h,0t,0r/data=CigiJgokCeYi9eA_bT5AEb1v-ShoVz5AGUU1oN1CnVXAITrQjgUdolXA.

Indian River County. 2016. "Bethel Creek Community Discussion Meeting." *Indian River County.* https://ircgov.com/Lagoon/Bethel-Creek/Bethel-Workshop-081116.pdf.

Komita, Weaver, and Fox. In Prep. "Summary of Inflow Projects."

Landers-Atkins Planners, Inc. 1987. "Destin Harbor Management Plan." *Coastal Zone Information Center.* https://www.govinfo.gov/content/pkg/CZIC-tc225-d47-d47-1987/html/CZIC-tc225-d47-d47-1987.htm.

Nielson, Morten Holtegaard, Bjarke Rasmussen, and Flemming Gertz. 2005. "A simple model for water level and stratification in Ringkøbing Fjord, a shallow, artificial estuary." *Estuarine, Coastal and Shelf Science* 235-248.

Northwest Florida Water Management District. 1992. *Permit re-application for the Old Pass Lagoon Yater Circulation Facility.* Permit Application, Havana, Florida : Northwest Florida Water Management District.

Peterson, Jens Kjerulf, Jens Wurgler Hansen, Martha Brogaard Laursen, Preben Clausen, Jacob Carstensen, and Daniel J Conley. 2008. "Regime Shift in a Coastal Marine Ecosystem." *Ecological Applications* 497-510.

Port of Los Angeles Engineering Division. 2006. "Inner Cabrillo Beach Water Quality Improvement Project Source Identifications and Mitigation Alternatives." *California Water Boards.* https://faast.waterboards.ca.gov/attachments/proposal_18975/attachment_61567.pdf.

Wijnhoven, S, V Escaravage, E Daemen, and H Hummel. 2010. "The decline and restoration of a coastal lagoon (Lake Veere) in the Dutch Delta." *Estuar. Coast. 33* 1261-1278.

Ysebaert, Tom, Dirk-jan van der Hoek, Rick Wortelboer, Jeroen W.M. Wijsman, Marijin Tangelder, and Arno Nolte. 2016. "Management options for restoring estuarine dynamics and implications for ecosystems: A quantitative approach for the Southwest Delta in the Netherlands." *Ocean & Coastal Management* 33-48.

Appendix

A. 1. Design Criteria Document

Restore Indian River Lagoon Inflow Pilot Project

Design Criteria Document

PREPARED FOR

Florida Department of Education
325 West Gaines Street
Tallahassee, Florida 32399

PREPARED BY

Florida Institute of Technology
150 West University Blvd
Melbourne, FL 32901

Tetra Tech
1353 N Courtney Pkwy.
Suite S
Merritt Island, FL 32953

Discipline	Reviewer	Organization	Review Date	Final Approval Date
Overall Project	Richard Aronson, PhD	FIT		
Overall Project	Jeff Eble, PhD	FIT	13 Jan 23	
Overall Project	Robert Weaver, PhD	FIT	11 Dec 22	
Civil/coastal engineering	Richard Czlapinski, PE	Tetra Tech	9 Dec 22	
Regulatory/permitting	Matt Shelton	Tetra Tech		
Electrical/controls		Tetra Tech		

TABLE OF CONTENTS

LIST OF FIGURES

LIST OF ABBREVIATIONS

AASHTO	American Association of State Highway and Transportation Officials
ASCE	American Society of Civil Engineers
CWA	Clean Water Act
ERP	Environmental Resources Permit
FDEP	Florida Department of Environmental Protection
FEMA	Federal Emergency Management Agency
Florida Tech	Florida Institute of Technology
IRL	Indian River Lagoon
NAVD88	North American Vertical Datum of 1988
USACE	United States Army Corps of Engineers

1.0 BACKGROUND AND PROJECT SUMMARY

Introduction

This Design Criteria Document (DCD) summarizes design criteria and recommendations as part of the Restore Indian River Lagoon Inflow Project. The DCD governs all aspects of the project design and operation. If design changes are required during the project development, then the DCD will be updated, reviewed, and approved by the project stakeholders.

Background

The Indian River Lagoon (IRL) is a lagoon, which is a special type of estuary that is oriented parallel to the coast and characterized by shallow coastal waters with restricted, but free, exchange with the adjacent ocean. This exchange of fresh and saltwater makes estuaries the most productive and fragile coastal ecosystems in the world. The IRL is a microtidal estuary with limited exchange with the ocean through five engineered and stabilized inlets. Exchange within the IRL is further limited by the presence of dozens of earthen causeways constructed across the lagoon. These factors make the IRL a restricted estuary with long residence times and low flushing. The IRL is particularly vulnerable to the accumulation of nutrients that are responsible for eutrophication, harmful algal blooms, and low oxygen (hypoxia).

With funding from the Florida Legislature, the Florida Institute of Technology (Florida Tech) completed Phase 1 of a multi-phase project to explore customized solutions for improving water quality within the IRL by restoring periodic historical ocean inflows. This first phase gathered baseline data and conducted modeling on existing water quality, biological parameters, and hydrologic conditions at candidate locations for a potential temporary inflow pilot system. The Florida Legislature authorized additional funding for Phase 2 of the project, which built on the lessons learned from Phase 1 and focused on creating the foundation for construction and implementation of a small-scale, temporary experimental inflow system and the research required to evaluate its effectiveness. The efforts in this phase included agency and stakeholder engagement, conceptual engineering and optimization, expanded ecosystem modeling, and baseline data collection. The Phase 1 and Phase 2 results, when combined with findings from the temporary inflow pilot system, will allow for an informed determination of the feasibility and impacts of a potential full-scale, permanent system.

Project Description

For Phase 3, the current temporary inflow pilot system design will be developed to a 90% design in coordination with permitting agencies to obtain the necessary permits. The permits include USACE or FDEP Section 404, USACE Section 408, and Florida Environmental Resource Permit. Based on the feedback from the permitting agencies, the 100% design will be prepared. Bio-geochemical research and modeling efforts will proceed in parallel with federal

and state permit processing in advance of the proposed, temporary pilot pumping system to allow informed determination of the feasibility and impacts of a potential permanent ocean inflow system.

<u>Project Location</u>

The proposed temporary inflow system would extract water from the ocean side of the Canaveral Lock system and discharge to the Indian River Lagoon via the cove to the west of Avocet Lagoon, Figure 1.
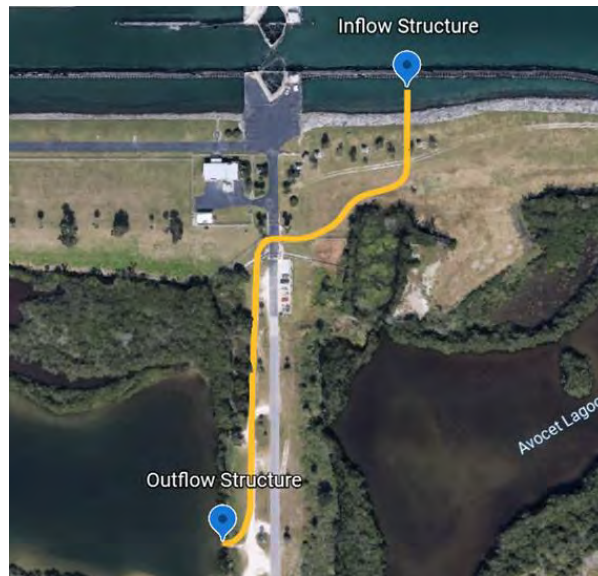
Figure 1: Pipeline Route

The pump and intake will be located on USACE property at Canaveral locks. The pipeline will run through the Canaveral Locks property then turn south following the access road to the outflow location.

2.0 DESIGN CRITERIA

2.1 CLIENT REQUIREMENTS

2.1.1 Project Duration

The pilot project will be in operation for a period of one year. A separate monitoring program will collect data on the performance of the pilot project. These data sets will contribute to the evaluation and proposed design of the full-scale project.

2.1.2 Project Pumping Capacity

The pilot project will have the capacity to continuously pump 0.5 cubic meters per second from the USACE locks basin into the Indian River Lagoon.

2.2 STRUCTURAL REQUIREMENTS

2.2.1 Pumping Loads

The structural components for this project are directly related to the pipeline support structure, carrying water from the inflow in Port Canaveral to the outflow in the adjacent cove as shown on the map, Figure 1. The structure will be designed to withstand maximum flow conditions of 0.5 cubic meters per second with consideration to the momentum changes associated with turns in the pipeline.

2.2.2 Wind Loads

Design for the wind loadings on the pier structure shall be derived as based on the ASCE 7 100 year Mean Recurrence interval. At the project location at Port Canaveral, the 100 year design wind at 10 meters above sea level is 170 mph.

2.2.3 Wave Loads

The design wave loading on the pier structure are based upon maximum possible fetch with associated 100 year winds, while still accounting for limitations from depth. The max fetch length is 440 meters and combined with a 170 mph wind speed, a 4.2 foot wave gets produced. This max wave height will impact the potential scour around the pilings, although the depth of the piles will be deep enough to account for all loads.

2.2.4 Current Loads

The current load is determined based on the max potential wave height. With an estimation of 0.1 knots per foot of wave height, the max current generated in the area behind the fender wall is 0.42 knots.

2.2.5 Flood Level

Since the pipeline will be laying directly on the ground, it is important to consider possible flooding conditions. Almost the entirety of the pipeline structure falls in FEMA Zone X flood level designation, meaning the area is outside the 500-year flood and protected by a levee from the 100-year flood. The intake and outfall locations fall under a FEMA AE flood zone designation, meaning there is less than a 1% chance of annual flooding but a 26% chance of flooding during a 30 year design life. The base flood elevation of the intake is 5' NAVD88 and the base flood elevation for the outfall location is 3' NAVD88, each of which will be designed one foot higher for a factor of safety.

2.2.6 Pile Loads

The depth of piles will need to be determined by soil sampling and geotechnical analysis, ensuring that side friction and bearing capacity far exceed the buoyancy of the timber, the potential uplift forces, and the live and dead loads associated with the pipeline system.

2.3 REGULATORY REQUIREMENTS

There are three significant regulatory permits required: Clean Water Act (CWA) Section 404 Permit, United States Army Corps of Engineers Section 408 Permit, and the Florida Department of Environmental Protection (FDEP) Environmental Resources Permit (ERP).

The CWA 404 permit establishes the program to regulate the discharge of dredged material or fill material, but activities pertaining to water resource projects fall under this permit. Many different agencies are represented as stakeholders under this permit, including the United States Army Corps of Engineers, the United States Environmental Protection Agency, the United States Fish and Wildlife Service, the National Marine Fisheries Service, and, for the sake of this project, the St. Johns Water Management District.

The USACE Section 408 Permit allows any pursuant party to alter a USACE Civil Works Project. The reason for this alteration is because the Port Canaveral lock system is an Army Corps project and the intended pumping station and pipeline will exist on this property. The purpose of the permit is to ensure and authorize that the pursuant activity will not injure public interest or impair the usefulness of the initial USACE project.

The FDEP ERP Program involves the regulation of any activity pertaining to the alteration of surface water flow. The St. Johns Water Management District processes and authorizes all permit applications in conjunction with the FDEP. Since this project involves a seaport and the movement of water from inside Port Canaveral to the adjacent cove, an ERP is required.

2.4 SAFETY REQUIREMENTS

With an industrial pipeline style project, there are many safety requirements that need to be considered. Since the pipeline will originate in the water, it is important to keep both powered and unpowered vessels away from the intake. This will limit damage to the system as well as reduce affect to human life. Proper warning signs and buoys surrounding the intake should be used. Another safety requirement to take into consideration is dealing with high voltage electricity powering the pump. Again, proper warning signs must be posted around the pump and along the power cables carrying the electricity.

2.5 ENVIRONMENTAL REQUIREMENTS

2.5.1 Impingement and Entrainment

Environmental considerations will be taken into account regarding marine life impacts as well as impacts to the surrounding habitat. Specific grates will be identified for use at the inflow structure to reduce entrainment of fish in compliance with EPA Section 316 (b)[1] requirements. The requirement for manatee exclusion grating if the intake screening is Section 316(b) compliant will also be determined. The selected intake screen will be a Drum Passive Intake Screen manufactured by Johnson, which connected to the pipeline through a direct flange mount.

2.5.2 Scour Protection

A specially sized geo-textile pad has been designed at the outflow to reduce erosive impacts to the habitat of Avocet Lagoon. This riprap pad has additional capabilities to catch any organisms

---

[1] Clean Water Act, Section 316 (b), URL: Summary of the Clean Water Act | US EPA

that pass through the pipeline for the purpose of monitoring during implementation of a biological monitoring program.

2.5.3 Treated Timber

The structure design will also consider the selection of proper timber materials for piling, decking, and railings as well as appropriate fasteners. Timber products must be treated with EPA approved wood preservatives to prolong usable life and reduce leaching of preservatives into surrounding soil or water.

The pilings will be 0.8 feet in width by the required length as determined by geotechnical testing.

2.6 OPERATIONAL REQUIREMENTS

2.6.1 Pumping Operations Schedule

Operation of the pumping system is fairly straightforward, with intended use of the pilot project being 24 hours a day for the duration of the project. However, external impacts, such as hurricanes, power outage, or damage to the pipeline system, may affect the project during the one year pilot program and the pump could need to be shut down. A detailed chain of command will be established to determine who makes the final decision, with specific criteria under which the pump will be shut off. It is important under these circumstances that there is clear documentation on the date and time of shut off.

2.6.2. Remote Control System

The pump shall be able to be shut off manually on site as well as remotely through remote connection. The selected shutoff method will utilize the MWI Connect remote monitoring and control system. This control system integrates perfectly into the pump as it is designed by the same manufacturer. The MWI Connect can be operated through a smartphone app, communicating through Wi-Fi and sending alerts to users through SMS and email messages.

2.6.3. Intake Screen Cleaning

The screen used at the intake will be a commercially available screen, specifically the Johnson Manufacturing Drum Passive Intake Screen. This screen utilizes coated material for the purpose of minimizing biofouling in the marine environment. However, the intake screen will require monthly inspection with cleaning of the screen as needed.

2.7 MAINTENANCE OF TRAFFIC REQUIREMENTS

The pipeline shown in Figure 1 represents the initial selection of pipeline pathway. The pipeline will need to pass over the roadway in one location and therefore, a ramp will need to be implemented to allow traffic to continue to operate. This ramp must be able to withstand American Association of State Transportation Officials (AASHTO) H-20 loading for a fully-loaded tractor trailer style vehicle.

2.8 OTHER REQUIREMENTS

Other requirements to the project can be added and addressed as needed throughout the project.

A. 2. RLI Plan Set

VICINITY MAP

Port Canaveral

Scallop Dr
Mullet Rd
Astronaut Blvd

Terminal Dr

NOT TO SCALE

401

A1A

N

80°20'0"W
80°30'0"W
80°40'0"W

28°30'0"N
28°20'0"N

Port Canaveral

FOR REGULATORY REVIEW ONLY - NOT FOR CONSTRUCTION

MARK	DATE	DESCRIPTION	BY
0	08/02/22	VICINITY MAP	EE

INDIAN RIVER LAGOON
RESTORE LAGOON INFLOW RESEARCH
PILOT PROJECT

Project No.:100-WTR-T41008L03
Designed By:
Drawn By:
Checked By:

001

Bar Measures 1 inch.

FOR REGULATORY REVIEW ONLY - NOT FOR CONSTRUCTION

PLAN VIEW (NAVD 88)

INDIAN RIVER LAGOON

RESTORE LAGOON INFLOW RESEARCH
PILOT PROJECT

MARK	DATE	DESCRIPTION		BY

Project No.:104-VIR-H108003
Designed By:
Drawn By:
Checked By:

002

Bar Measures 1 Inch

TETRA TECH
ENGINEERING BUSINESS NO. 2429

www.tetratech.com
201 EAST PINE STREET, SUITE 1000
ORLANDO, FL 32801
PHONE: (407) 839-3955 FAX: (407) 839-3790

FOR REGULATORY REVIEW ONLY - NOT FOR CONSTRUCTION

Datums for 8721604, Trident Pier, Port Canaveral, FL
All figures in feet relative to NAVD88

MSL: -0.95

MLW: -2.66

MHW: 0.75

NAVD88: 0

MHHW: 1.1

MLLW: -2.83

MTL: -0.95

DTL: -0.86

DHQ: 0.35

DLQ: 0.17

MN: 3.4

GT: 3.92

Datums

NOAA/NOS/CO-OPS

ACRONYMS	
MHHW	MEAN HIGH HIGH WATER
MHW	MEAN HIGH WATER
MTL	MEAN TIDE LEVEL
MSL	MEAN SEA LEVEL
DTL	MEAN DIURNAL TIDE LEVEL
MLW	MEAN LOW WATER
MLLW	MEAN LOW LOW WATER
NAVD88	NORTH AMERICAN VERTICAL DATUM 1988
GT	GREAT DIURNAL RANGE
MN	MEAN RANGE OF TIDE
DLQ	MEAN DIURNAL LOW WATER INEQUALITY
DHQ	MEAN DIURNAL HIGH WATER INEQUALITY
NOAA	NATIONAL OCEANIC AND ATMOSPHERIC ADMINISTRATION

Bar Measures 1 inch

Checked By:
Drawn By:
Designed By:
Project No.:100-xITK-2410000.03

INDIAN RIVER LAGOON
RESTORE LAGOON INFLOW RESEARCH PILOT PROJECT

MARK	DATE	DESCRIPTION	BY

TETRA TECH
ENGINEERING BUSINESS NO. 2429
www.tetratech.com
201 EAST PINE STREET, SUITE 1000
ORLANDO, FL 32801
PHONE: (407) 839-3955 FAX: (407) 839-3790

FOR REGULATORY REVIEW ONLY - NOT FOR CONSTRUCTION

NOTE: SCALE: 3/16" = 1'
CONTOURS DISPLAYED AT 1FT CONTOUR INTERVAL

DETAIL B

OVER HEAD
POWER SUPPLY

DETAIL A

DETAIL C

FENCE

SITE PLAN

TETRA TECH
ENGINEERING BUSINESS NO. 2429

www.tetratech.com

201 EAST PINE STREET, SUITE 1000
ORLANDO, FL 32801
PHONE: (407) 839-3955 FAX: (407) 839-3790

INDIAN RIVER LAGOON

RESTORE LAGOON INFLOW RESEARCH
PILOT PROJECT

MARK	DATE	DESCRIPTION	BY

Project No.100-\VTt-Z41000.03

Drawn By:
Designed By:
Checked By:

004

Bar Measures 1 Inch

FOR REGULATORY REVIEW ONLY - NOT FOR CONSTRUCTION

HYDRAULIC PUMP
DISCHARGE PIPE

20.9 ft

20.9 ft

6.7 ft

20" HDPE

HYDRAULIC PUMP
AND INTAKE

HYDRAULIC PUMP
POWER UNIT

5.3 ft

8.5 ft
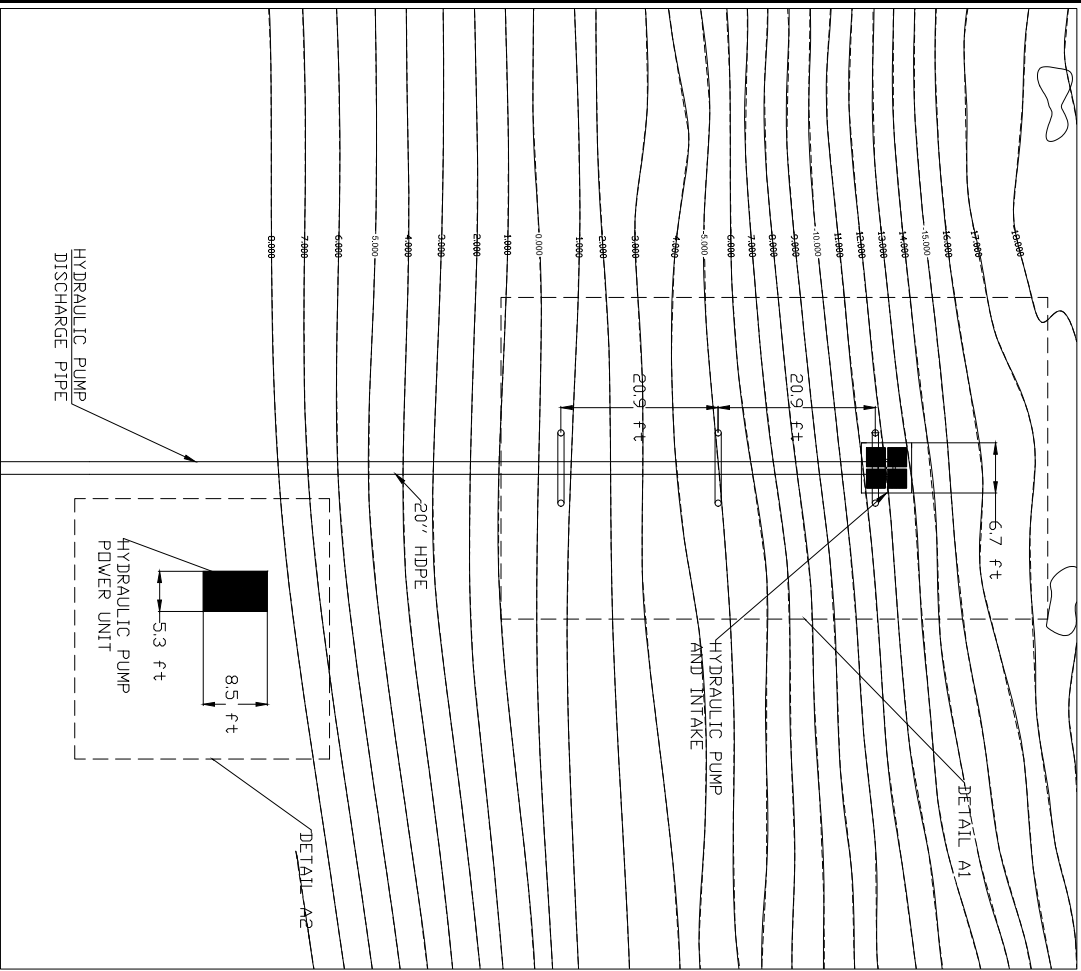
DETAIL A1

DETAIL A2

DETAIL A INTAKE PLAN (NAVD 88)

COORDINATE NAD 83
772774.1897, 1481579.25

FENDER WALL

422 FT

NOTE: POWERLINES NOT REPRESENTED IN
DRAWING FOR CLARITY

DETAIL A1 - INTAKE ELEVATION VIEW

ALIGNMENT PROFILE

FOR REGULATORY REVIEW ONLY - NOT FOR CONSTRUCTION

PIPE ON GRADE

EXISTING GRADE

9.2 ft

SEE DETAIL A3 FOR INTAKE SCREEN DETAILS

0.8 ft

6.4 ft

2.7 ft

20.9 ft

10 INCH TIP TREATED TIMBER PILE (TYP.)

Elevation
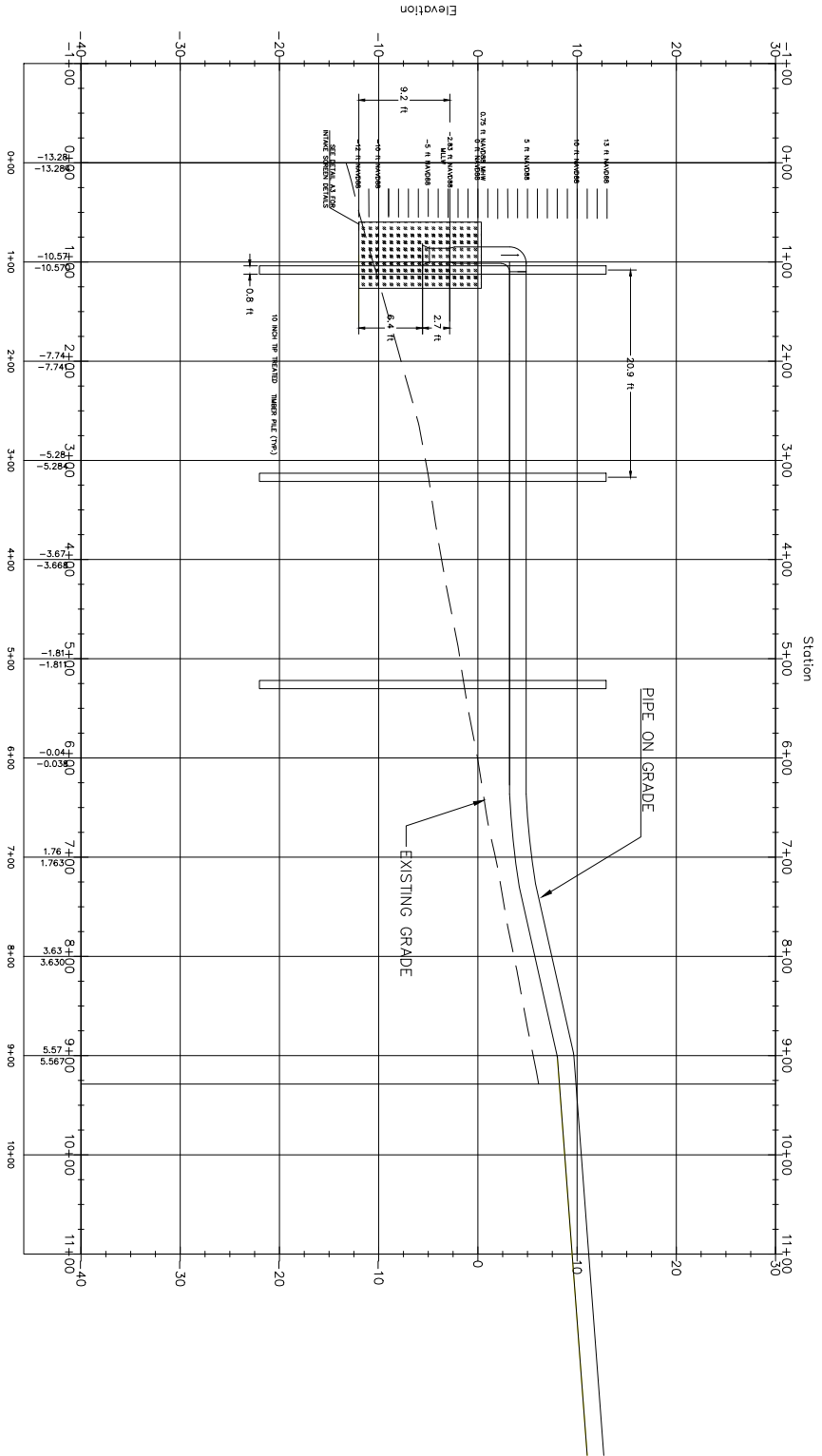
Station

NOTE: DETAIL NOT TO SCALE

INDIAN RIVER LAGOON

RESTORE LAGOON INFLOW RESEARCH PILOT PROJECT

Project No.100-v/T6-Z41000.03

Drawn By:
Designed By:
Checked By:

006

MARK	DATE	DESCRIPTION	BY

TETRA TECH
ENGINEERING BUSINESS NO. 2429
www.tetratech.com
201 EAST PINE STREET, SUITE 1000
ORLANDO, FL 32801
PHONE: (407) 839-3955 FAX: (407) 839-3790

FOR REGULATORY REVIEW ONLY - NOT FOR CONSTRUCTION

PUMP DETAILS:

SINGLE STAGE HYDRAULICALLY
DRIVEN PUMP ELECTRIC POWER UNIT
USING 3 PHASE 460-VOLT POWER 20 IN
ID DISCHARGE PIPE DESIGN FLOW 0.5
CUBIC METERS PER SECOND
SKID-MOUNTED, SELF CONTAINED
UNIT. PUMP SHALL BE MWI HYDRAULIC
UPUMP MODEL HAC 316 OR
APPROVED EQUIVALENT.

DETAIL A2 - PUMP POWER UNIT

INDIAN RIVER LAGOON

RESTORE LAGOON INFLOW RESEARCH
PILOT PROJECT

MARK	DATE	DESCRIPTION	BY

Designed By:
Drawn By:
Checked By:

Project No.100-x\T5-7410000.03

007

Bar Measures 1 inch

TETRA TECH
ENGINEERING BUSINESS NO. 2429
www.tetratech.com
201 EAST PINE STREET, SUITE 1000
ORLANDO, FL 32801
PHONE: (407) 839-3955 FAX: (407) 839-3790

FOR REGULATORY REVIEW ONLY - NOT FOR CONSTRUCTION

Grating 1 in x 4 in with 4 in Aligned to Horizontal Plane

DETAIL A3 — INTAKE SCREEN DETAILS

2.5 ft

2.5 ft

6.7 ft

12.3 ft

INDIAN RIVER LAGOON

RESTORE LAGOON INFLOW RESEARCH
PILOT PROJECT

MARK	DATE	DESCRIPTION	BY

Drawn By:
Designed By:
Checked By:
Project No.100-x/Tt-Z41000/03

008

Bar Measures 1 Inch

TETRA TECH
ENGINEERING BUSINESS NO. 2429

www.tetratech.com

201 EAST PINE STREET, SUITE 1000
ORLANDO, FL 32801
PHONE: (407) 839-3955 FAX: (407) 839-3790

DIMMENSIONS FOR MANATEE GRATE
HAVE BEEN SELECTED ACCORDING TO
FDOT INDEX 280 STANDARDS

2 ft NAVD88

0 ft NAVD88

−1.5 ft NAVD88
MLLW

−3 ft NAVD88

$\frac{1}{2}$" Steel Rod

$\frac{3}{4}$" Bolt Hole

20" Pipe

Flange

Slope 1:1

Filter Fabric

Rip Rap Class 50 (D50 = 0.56 ft)

DETAIL A4 - OUTFALL SCREEN DETAILS

ALL DIMENSIONS +/- ONE INCH

INDIAN RIVER LAGOON

RESTORE LAGOON INFLOW RESEARCH
PILOT PROJECT

MARK DATE DESCRIPTION BY

Project No.100\WTR-T41005.03
Designed By:
Drawn By:
Checked By:

009

Bar Measures 1 inch

Copyright: Tetra Tech

TETRA TECH
ENGINEERING BUSINESS NO. 2429

www.tetratech.com
201 EAST PINE STREET, SUITE 1000
ORLANDO, FL 32801
PHONE: (407) 839-3955 FAX: (407) 839-3790

DETAIL B - PIPELINE ROAD CROSSING

OVERHEAD POWER SUPPLY

Thrust Block

DISCHARGE PIPE

EXISTING ROADWAY

RAMP

1.7 ft

2.1 ft

NOTES:
1. CAPACITY IS 32,000 LB PER AXLE (HS-20 LOADING)
2. DESIGNED AND MANUFACTURED BY BLUFF MANUFACTURING

FOR REGULATORY REVIEW ONLY - NOT FOR CONSTRUCTION

25.0 ft

2.0 ft

1.9 ft

INDIAN RIVER LAGOON

RESTORE LAGOON INFLOW RESEARCH PILOT PROJECT

MARK	DATE	DESCRIPTION	BY

Project No: 100-0477S-14 10093.03

Designed By:

Drawn By:

Checked By:

010

Bar Measures 1 inch

TETRA TECH
ENGINEERING BUSINESS NO. 2429

www.tetratech.com

201 EAST PINE STREET, SUITE 1000
ORLANDO, FL 32801
PHONE: (407) 839-3955 FAX: (407) 839-3790

FOR REGULATORY REVIEW ONLY - NOT FOR CONSTRUCTION

DETAIL C - OUTFLOW

PLAN VIEW

36.0 ft

37.7 ft

5.5 ft

5.0 ft

8.3 ft

Slope 1:1

RIP RAP FP-14 CLASS 1 (D50 = 5-8 INCHES)

THRUST BLOCK

FENCE

SIDE VIEW

2 ft NAVD88

0.75 ft NAVD88

0 ft NAVD88 — MHW

-1.5 ft NAVD88 — MLLW

-3 ft NAVD88

37.7 ft

1.0 ft

Slope 1:1

6.7 ft

0.2 ft

2.3 ft

1.7 ft

Slope 1:1

20 INCH ID DISCHARGE PIPE

FILTER FABRIC

RIP RAP FP-14 CLASS 1 (D50 = 5-8 INCHES)

FOR REGULATORY REVIEW ONLY - NOT FOR CONSTRUCTION

BIOLOGICAL SURVEYS

NOTE: MARINE BIOLOGICAL RESOURCE
SURVEY COMPLETED JUNE 2021

LEGEND

SHOAL GRASS
(LESS THAN 1 M^2)

VEGETATION

✕

BLACK MANGROVE

INDIAN RIVER LAGOON

RESTORE LAGOON INFLOW RESEARCH
PILOT PROJECT

MARK	DATE	DESCRIPTION	BY

Designed By:
Drawn By:
Checked By:

Project No.100-x/TtcT41000.03

012

Bar Measures 1 inch

TETRA TECH
ENGINEERING BUSINESS NO. 2429

www.tetratech.com

201 EAST PINE STREET, SUITE 1000
ORLANDO, FL 32801
PHONE: (407) 839-3955 FAX: (407) 839-3790

Copyright: Tetra Tech

A. 3. Permit Documents

July 21, 2023

Regulatory Division
North Permits Branch
Cocoa Section
SAJ-2022-03034 (NWP-BJC)

Florida Institute of Technology
150 West University Boulevard
Melbourne, Florida 32901
Sent via email: jeble@fit.edu

Dear Applicant:

The U.S. Army Corps of Engineers (Corps) has completed the review of your application for a Department of the Army permit received on 4 October, 2022. Your application was assigned file number SAJ-2022-03034. A review of the information and drawings provided indicates that the proposed work would result in a one year pilot project to determine the effects of a pump inflow project for water quality enhancement of the Banana River. The work consists of the following:

1) Inflow pump in the Canaveral Locks discharging into the Banana River
2) Deployment of seven water quality sensors and two current profilers at the locations depicted in the attached drawings

The activities subject to this permit are authorized pursuant to authorities under Section 10 of the Rivers and Harbors Act of 1899 (33 U.S.C. § 403), **and** Section 404 of the Clean Water Act (33 U.S.C. § 1344). The project site is located at the Canaveral Locks, in Cape Canaveral, Florida, and will be constructed on United States Army Corps of Engineers (USACE) land located in Section 9, Township 24, Range 37 at 1000 Mullet Road in Cape Canaveral, Brevard County, Florida.

Your project, as depicted on the enclosed drawings, is authorized by Nationwide Permit (NWP) 5 (Scientific Measurement Devices). **This verification is valid until March 14, 2026.** In order for this NWP authorization to be valid, you must ensure that the work is performed in accordance with the Nationwide Permit General Conditions, the Jacksonville District Regional Conditions, and the General and Project-Specific Special Conditions listed below. Furthermore, if you commence or are under contract to commence this activity before the date that the relevant NWP is modified or revoked, you will have 12 months from the date of the modification or revocation of the NWP to complete the activity under the present terms and conditions of this NWP. You can

access the U.S. Army Corps of Engineers' (Corps) Jacksonville District's Regulatory Source Book webpage for links to view NWP information at: https://www.saj.usace.army.mil/Missions/Regulatory/Source-Book/. Please be aware this Internet address is case sensitive and should be entered as it appears above. Once there, you will need to select "Nationwide Permits." Among other things, this part of the Source Book contains links to the federal register containing the text of the pertinent NWP authorization and the associated NWP general conditions, as well as separate links to the regional conditions applicable to the pertinent NWP verification.

    You must comply with all of the special and general conditions for NWP-5, including any project-specific conditions included in this letter and all conditions incorporated by reference as described above.

General Conditions:

    1. The time limit for completing the work authorized ends on **March 14, 2026**.

    2. You must maintain the activity authorized by this permit in good condition and in conformance with the terms and conditions of this permit. You are not relieved of this requirement if you abandon the permitted activity, although you may make a good faith transfer to a third party in compliance with General Condition 4 below. Should you wish to cease to maintain the authorized activity, or should you desire to abandon it without a good faith transfer, you must obtain a modification of this permit from this office, which may require restoration of the area.

    3. If you discover any previously unknown historic or archeological remains while accomplishing the activity authorized by this permit, you must immediately notify this office of what you have found. We will initiate the Federal and state coordination required to determine if the remains warrant a recovery effort of if the site is eligible for listing in the National Register of Historic Places.

    4. If you sell the property associated with this permit you must obtain the signature of the new owner on the attached transfer form and forward a copy to this office to validate the transfer of this authorization.

    5. If a conditioned water quality certification has been issued for your project, you must comply with the conditions specified in the certification as special conditions to this permit. For your convenience, a copy of the certification is attached if it contains such conditions

6. You must allow a representative from this office to inspect the authorized activity at any time deemed necessary to ensure that it is being or has been accomplished in accordance with the terms and conditions of your permit.

Project Specific Special Conditions:

The following project specific special conditions are included with this verification:

1. **Reporting Address:** The Permittee shall submit all reports, notifications, documentation, and correspondence required by the general and special conditions of this permit to either (not both) of the following addresses:

    a. For electronic mail (preferred): SAJ-RD-Enforcement@usace.army.mil (not to exceed 15 MB).

    b. For standard mail: U.S. Army Corps of Engineers, Regulatory Division, Enforcement Section, P.O. Box 4970, Jacksonville, FL 32232-0019

    The Permittee shall reference this permit number, SAJ-2022-03034 (NW –BJC), on all submittals.

2. **Commencement Notification:** Within 10 days from the date of initiating the work authorized by this permit, the Permittee shall submit a completed "Commencement Notification" form (attached).

3. **As-Built Certification with X-Y Coordinates:** Within 60 days of completion of the authorized work or at the expiration of the construction window of this permit, whichever occurs first, the Permittee shall submit as-built drawings of the authorized work and complete the enclosed "As-Built Certification by Professional Engineer or Surveyor" form to the Corps (attached). The drawings shall be signed and sealed by a registered professional engineer or a professional land surveyor confirming the actual location of all authorized work/structures with respect to the Federal channel and/or within the Federal easement/license and include the following:

    a. A plan view drawing of the location of the authorized work footprint (as shown on the permit drawings) with an overlay of the work as constructed in the same scale as the attached permit drawings (8½-inch by 11-inch). The drawings shall include the X & Y State Plane coordination points of the most waterward point of the structure. The drawings shall include the dimensions of the structure, location of mean high water line (MHWL),

depth of water (at mean low water) at the waterward end of the structure, and the distance from the waterward end of the structure to the near design edge of the Federal project.

b. A list of any deviations between the work authorized by this permit and the work as constructed. In the event that the completed work deviates, in any manner, from the authorized work, describe on the attached "As-Built Certification by Professional Engineer" form the deviations between the work authorized by this permit and the work as constructed. Clearly indicate on the as-built drawings any deviations that have been listed. Please note that the depiction and/or description of any deviations on the drawings and/or "As-Built Certification by Professional Engineer" form does not constitute approval of any deviations by the Corps.

c. The Department of the Army permit number on all sheets submitted.

d. Within 60 days of completion of the work authorized by this permit, the Permittee shall provide a courtesy copy of the signed and sealed As-Built drawings to the Corps, Engineering Division. Submittals shall be sent either electronically by email at ENPermits.CESAJ@usace.army.mil or by standard mail at Post Office Box 4970, Jacksonville Florida 32232-0019.

4. **Cultural Resources/Historic Properties:**

a. No structure or work shall adversely affect, impact, or disturb properties listed in the *National Register of Historic Places* (NRHP), or those eligible for inclusion in the NRHP.

b. If, during permitted activities, items that may have historic or archaeological origin are observed the Permittee shall immediately cease all activities adjacent to the discovery that may result in the destruction of these resources and shall prevent his/her employees from further removing, or otherwise damaging, such resources. The applicant shall notify both the Florida Department of State, Division of Historical Resources, Compliance Review Section at (850)-245-6333 and the Corps, of the observations within the same business day (8 hours). Examples of submerged historical, archaeological or cultural resources include shipwrecks, shipwreck debris fields (such as steam engine parts, or wood planks and beams), anchors, ballast rock, concreted iron objects, concentrations of coal, prehistoric watercraft (such as log "dugouts"), and other evidence of human

c. Additional cultural resources assessments may be required of the permit area in the case of unanticipated discoveries as referenced in accordance with the above Special Condition and, if deemed necessary by the SHPO or Corps, in accordance with 36 CFR 800 or 33 CFR 325, Appendix C (5). Based on the circumstances of the discovery, equity to all parties, and considerations of the public interest, the Corps may modify, suspend, or revoke the permit in accordance with 33 CFR Part 325.7. Such activity shall not resume on non-federal lands without written authorization from the SHPO for finds under his or her jurisdiction, and from the Corps.

d. In the unlikely event that unmarked human remains are identified on non-federal lands; they will be treated in accordance with Section 872.05 Florida Statutes. All work and ground disturbing activities within a 100-meter diameter of the unmarked human remains shall immediately cease and the Permittee shall immediately notify the medical examiner, Corps, and State Archaeologist within the same business day (8-hours). The Corps shall then notify the appropriate SHPO. Based on the circumstances of the discovery, equity to all parties, and considerations of the public interest, the Corps may modify, suspend, or revoke the permit in accordance with 33 CFR Part 325.7. Such activity shall not resume without written authorization from the SHPO and from the Corps.

5. **Individual Section 408 Approval:** It has been determined that the activities authorized do not impair the usefulness of the Canaveral Locks and are not injurious to the public interest. The Permittee shall adhere to the conditions and limitations referenced in the Section 408 approval memo (attached). All documentation required in the Section 408 approval memo shall be submitted either electronically by email at ENPermits.CESAJ@usace.army.mil or by standard mail at Post Office Box 4970, Jacksonville Florida 32232-0019. For all questions related to the Section 408 approval, contact the Corps, Jacksonville Engineering Division by telephone at 904-232-1604. Engineering Division is the appropriate authority to determine compliance with the terms and conditions of Section 408 approval.

6. **Real Estate Coordination:** The Permittee shall complete coordination for a Department of the Army License with the Corps Real Estate Division SAJ-RE-Consent@usace.army.mil or Post Office Box 4970, Jacksonville, Florida 32232-0019 or by telephone at 904-570-4514. Prior to commencement of construction, the Permittee shall provide a copy of the Corps approved Consent to Easement or Department of the Army License, or correspondence from the Real Estate

Division indicating that neither is required, to the address identified in the **Reporting Address Special Condition**.

7. **Jacksonville District Programmatic Biological Opinion (JAXBO):** Structures and activities authorized under this permit will be constructed and operated in accordance with all applicable PDCs contained in the JAXBO, based on the permitted activity. Johnson's seagrass and its critical habitat were delisted from the Endangered Species Act on May 16, 2022. Therefore, JAXBO PDCs required to minimize adverse effects to Johnson's seagrass and its critical habitat are no longer applicable to any project. Failure to comply with applicable PDCs will constitute noncompliance with this permit. In addition, failure to comply with the applicable PDCs, where a take of listed species occurs, would constitute an unauthorized take. The NMFS is the appropriate authority to determine compliance with the Endangered Species Act. The most current version of JAXBO can be accessed at the Jacksonville District Regulatory Division website in the Endangered Species section of the Sourcebook located at: http://www.saj.usace.army.mil/Missions/Regulatory/SourceBook.aspx

   JAXBO may be subject to revision at any time. The most recent version of the JAXBO must be utilized during the design and construction of the permitted work.

8. **Manatee Conditions:** The Permittee shall comply with the "Standard Manatee Conditions for In-Water Work – 2011" (attached). The most recent version of the Manatee Conditions must be utilized.

This letter of authorization does not include conditions that would prevent the 'take' of a state-listed fish or wildlife species. These species are protected under sec. 379.411, Florida Statutes, and listed under Rule 68A-27, Florida Administrative Code. With regard to fish and wildlife species designated as species of special concern or threatened by the State of Florida, you are responsible for coordinating directly with the Florida Fish and Wildlife Conservation Commission (FWC). You can visit the FWC license and permitting webpage (http://www.myfwc.com/license/wildlife/) for more information, including a list of those fish and wildlife species designated as species of special concern or threatened. The Florida Natural Areas Inventory (http://www.fnai.org/) also maintains updated lists, by county, of documented occurrences of those species.

This letter of authorization does not give absolute Federal authority to perform the work as specified on your application. The proposed work may be subject to local building restrictions mandated by the National Flood Insurance Program. You should contact your local office that issues building permits to determine if your site is located

in a flood-prone area, and if you must comply with the local building requirements mandated by the National Flood Insurance Program.

This letter of authorization does not preclude the necessity to obtain any other Federal, State, or local permits, which may be required.

Thank you for your cooperation with our permit program. The Corps' Jacksonville District Regulatory Division is committed to improving service to our customers. We strive to perform our duty in a friendly and timely manner while working to preserve our environment. We invite you to complete our automated Customer Service Survey at https://regulatory.ops.usace.army.mil/customer-service-survey/. Please be aware this Internet address is case sensitive and you will need to enter it exactly as it appears above. Your input is appreciated – favorable or otherwise.

Should you have any questions related to this NWP verification or have issues accessing the documents referenced in this letter, please contact Brandon J. Conroy at the Cocoa Permits Section at the letter head address, by telephone or by email at brandon.j.conroy@usace.army.mil.

Sincerely,

Brandon J. Conroy, Ph.D.
Senior Project Manager

DEPARTMENT OF THE ARMY PERMIT TRANSFER REQUEST

DA PERMIT NUMBER: SAJ-2022-03034 (NWP-BJC)

    When the structures or work authorized by this permit are still in existence at the time the property is transferred, the terms and conditions of this permit will continue to be binding on the new owner(s) of the property. <u>Although the construction period for works authorized by Department of the Army permits is finite, the permit itself, with its limitations, does not expire.</u>

    To validate the transfer of this permit and the associated responsibilities associated with compliance with its terms and conditions, have the transferee sign and date below and mail to the U.S. Army Corps of Engineers, Enforcement Section, Post Office Box 4970, Jacksonville, FL 32232-0019 or submit via electronic mail to: SAJ-RD-Enforcement@usace.army.mil (not to exceed 15 MB).

_____   _____
(TRANSFEREE-SIGNATURE)   **(SUBDIVISION)**

_____   _____ _____
(DATE)   **(LOT)**   **(BLOCK)**

_____   _____
(NAME-PRINTED)   **(STREET ADDRESS)**

_____

_____
(MAILING ADDRESS)

_____
(CITY, STATE, ZIP CODE)

DEPARTMENT OF THE ARMY PERMIT TRANSFER REQUEST

DA PERMIT NUMBER: SAJ-2022-03034 (NWP-BJC)

When the structures or work authorized by this permit are still in existence at the time the property is transferred, the terms and conditions of this permit will continue to be binding on the new owner(s) of the property. Although the construction period for works authorized by Department of the Army permits is finite, the permit itself, with its limitations, does not expire.

To validate the transfer of this permit and the associated responsibilities associated with compliance with its terms and conditions, have the transferee sign and date below and mail to the U.S. Army Corps of Engineers, Enforcement Section, Post Office Box 4970, Jacksonville, FL 32232-0019 or submit via electronic mail to: SAJ-RD-Enforcement@usace.army.mil (not to exceed 15 MB).

_____   _____
(TRANSFEREE-SIGNATURE)   **(SUBDIVISION)**

_____   _____ _____
(DATE)   **(LOT)**   **(BLOCK)**

                            _____
_____   **(STREET ADDRESS)**
(NAME-PRINTED)

_____

_____
(MAILING ADDRESS)

_____
(CITY, STATE, ZIP CODE)

FOR REGULATORY REVIEW ONLY - NOT FOR CONSTRUCTION

28°20'0"N

28°30'0"N

80°40'0"W

80°30'0"W

80°20'0"W

Port Canaveral

N

VICINITY MAP

A1A

401

Astronaut Blvd

Scallop Dr

Mullet Rd

Grouper Rd

Cruise Terminal Dr

Port Canaveral

INDIAN RIVER LAGOON

RESTORE LAGOON INFLOW RESEARCH
PILOT PROJECT

MARK	DATE	DESCRIPTION	BY

Checked By:

Drawn By:

Designed By:

Project No:100-WTR-41000J3

001

Copyright: Tetra Tech

TETRA TECH
ENGINEERING BUSINESS NO. 2429

www.tetratech.com

201 EAST PINE STREET, SUITE 1000
ORLANDO, FL 32801
PHONE: (407) 839-3955 FAX: (407) 839-3790

FOR REGULATORY REVIEW ONLY - NOT FOR CONSTRUCTION

SURVEY PLAN VIEW (NAVD88)

INDIAN RIVER LAGOON

RESTORE LAGOON INFLOW RESEARCH
PILOT PROJECT

MARK | DATE | DESCRIPTION | | BY

Drawn By:
Designed By:
Checked By:

Project No.100-VITH-47100U03

002

Copyright: Tetra Tech

TETRA TECH
ENGINEERING BUSINESS NO. 2429
www.tetratech.com
201 EAST PINE STREET, SUITE 1000
ORLANDO, FL 32801
PHONE: (407) 839-3955 FAX: (407) 839-3790

FOR REGULATORY REVIEW ONLY - NOT FOR CONSTRUCTION

VERTICAL DATUM

Datums for 8721604, Trident Pier, Port Canaveral, FL
All figures in feet relative to MLLW

MSL: 1.88

NAVD88: 2.83

MHW: 3.58

MHHW: 3.93

MLW: 0.17

MLLW: 0

DTL: 1.97

MTL: 1.88

DHQ: 0.35

DLQ: 0.17

MN: 3.4

GT: 3.92

Datums

NOAA/NOS-CO-OPS

	ACRONYMS
MHHW	MEAN HIGH HIGH WATER
MHW	MEAN HIGH WATER
MTL	MEAN TIDE LEVEL
MSL	MEAN SEA LEVEL
DTL	MEAN DIURNAL TIDE LEVEL
MLW	MEAN LOW WATER
MLLW	MEAN LOW LOW WATER
NAVD88	NORTH AMERICAN VERTICAL DATUM 1988
GT	GREAT DIURNAL RANGE
MN	MEAN RANGE OF TIDE
DLQ	MEAN DIURNAL LOW WATER INEQUALITY
DHQ	MEAN DIURNAL HIGH WATER INEQUALITY
NOAA	NATIONAL OCEANIC AND ATMOSPHERIC ADMINISTRATION

INDIAN RIVER LAGOON

RESTORE LAGOON INFLOW RESEARCH PILOT PROJECT

MARK	DATE	DESCRIPTION	BY

Project No. 100-WTR-41000.03

Designed By:

Drawn By:

Checked By:

003

TETRA TECH
ENGINEERING BUSINESS NO. 2429

www.tetratech.com

201 EAST PINE STREET, SUITE 1000
ORLANDO, FL 32801
PHONE: (407) 839-3955 FAX: (407) 839-3790

Copyright: Tetra Tech

FOR REGULATORY REVIEW ONLY - NOT FOR CONSTRUCTION

NOTE:
1. SCALE 1" = 1'
2. SURVEY COMPLETED BY OCEANSIDE SOLUTIONS ON MARCH 31, 2021
3. CONTOURS DISPLAYED AT 1 FT CONTOUR INTERVAL
4. DURING PIPELINE INSTALLATION, ONLY ONE SEGMENT OF THE FENCE MESH PIPE HAS BEEN PLACED, THE FENCE SECTION WILL BE REPLACED WITH A MINIMUM SECTION OF THE FENCE MESH REMOVED TO ACCOMMODATE THE PIPELINE. THE MESH AROUND THE PIPELINE WILL BE WIRE REINFORCED AS APPROPRIATE TO MAINTAIN THE INTEGRITY OF THE MESH. THE SECTION OF THE FENCE WILL BE REPLACED AFTER THE DECOMMISSIONING OF THE PILOT PROJECT.
5. MINIMUM OVERHEAD POWERLINE CLEARANCE SHALL BE 16 FEET OVER THE ACCESS ROAD.

SITE PLAN

SHORELINE

DETAIL B

OVERHEAD POWER SUPPLY

DETAIL A

SHORELINE

RAMP

ENTRANCE GATE

FENCE

ROADWAY

DETAIL C

POWERLINE

EXISTING FENCELINE

FENDER WALL

FENCE HOLE DETAIL

20" PIPE

6 GAUGE VINYL COATED STEEL WIRE TO BE WEAVED THROUGH FENCE LOOPS AND ENCOMPASSING THE FENCE PENETRATION AND WRAPPING AROUND PIPE

MARK	DATE	DESCRIPTION	BY

INDIAN RIVER LAGOON

RESTORE LAGOON INFLOW RESEARCH PILOT PROJECT

Project No.100-WTR-141008.03
Designed By:
Drawn By:
Checked By:

004

Bar Measures 1 inch

Copyright: Tetra Tech

TETRA TECH
ENGINEERING BUSINESS NO. 2429
www.tetratech.com
201 EAST PINE STREET, SUITE 1000
ORLANDO, FL 32801
PHONE: (407) 839-3955 FAX: (407) 839-3790

FOR REGULATORY REVIEW ONLY - NOT FOR CONSTRUCTION

DETAIL A INTAKE PLAN

Ø2.3 ft
Ø1.7 ft
20.9 ft
20.9 ft
9.3 ft
0.8 ft
0.8 ft
6.7 ft
6.7 ft
3.0 ft

CATWALK

DETAIL A1

ELECTRIC DRIVE UNIT
5.3 ft
8.5 ft
DETAIL A2

CATWALK
ELECTRIC DRIVE UNIT

FENDER WALL

FOR REGULATORY REVIEW ONLY - NOT FOR CONSTRUCTION

DETAIL A1 - INTAKE SIDE VIEW

Elevation

Station

SEE DETAIL A3 FOR INTAKE SCREEN DETAILS

0.75 ft NAVD88 MHW
0 ft NAVD88
-2.83 ft MLW
-5 ft NAVD88
-10 ft NAVD88
-12 ft NAVD88

13 ft NAVD88
10 ft NAVD88
5 ft NAVD88

HENDRICK PASSIVE DRUM INTAKE SCREEN

0.8 ft

10 INCH TIP TREATED TIMBER PILE (TYP.)

20.9 ft

CATWALK

CATWALK RAILING

EXISTING GRADE

PILE DEPTHS TO BE DETERMINED BY RESULTS OF SPT BORING

PIPE ON GRADE

FOR REGULATORY REVIEW ONLY - NOT FOR CONSTRUCTION

DETAIL A2 - PUMP POWER UNIT

PUMP NOTES:
1. MWI HMF320 HYDRAFLO PUMP
2. 2400E ELECTRIC DRIVE UNIT WITH 200HP ELECTRIC MOTOR-SKID CONFIGURATION
3. NEMA 4X STAINLESS AUTO START/STOP CONTROL PANEL WITH FLOATS

MARK	DATE	DESCRIPTION	BY

INDIAN RIVER LAGOON
RESTORE LAGOON INFLOW RESEARCH PILOT PROJECT

Project No:100-WTC-T-100303
Designed By:
Drawn By:
Checked By:

007

TETRA TECH
ENGINEERING BUSINESS NO. 2429
www.tetratech.com
201 EAST PINE STREET, SUITE 1000
ORLANDO, FL 32801
PHONE: (407) 839-3955 FAX: (407) 839-3790

FOR REGULATORY REVIEW ONLY - NOT FOR CONSTRUCTION

DETAIL A3 - INTAKE SCREEN DETAILS

INTERIOR SCREEN
(SEE DETAIL)

48.0 in

30.0 in

84.0 in

Ø48.0 in

Ø30.0 in

DRUM INTAKE SCREEN
TOP VIEW

INTERIOR SPACING DETAIL

SCREEN SPACING IS 0.125". AN INTAKE SPACING OF 0.125" IS MORE RESTRICTIVE THAN THE FWC REQUIRED 6-INCH SPACING BETWEEN GRATES FOR MANATEE PROTECTION.

NOTE:
1. DRUM STYLE INTAKE SCREEN DESIGNED AND MANUFACTURED BY HENDRICK SCREEN SUPPLY COURTESY OF RC BEACH AND ASSOCIATES
2. THE SURFACE WIRE SHALL BE HENDRICK SCREEN SUPPLY CO. NO. 69 WEDGE WIRE. THE SCREEN SLOT OPENING SHALL BE .125". THE OPEN AREA FOR THIS SLOT OPENING SHALL BE 64%. SLOT SIZE SHALL BE CONTROLLED AND CONTINUOUSLY MONITORED DURING MANUFACTURE.
3. THE INTAKE SCREEN CAPACITY SHALL BE 7825 GPM AT A MAXIMUM LOCAL THROUGH SLOT VELOCITY DUE TO WATER REMOVAL NOT TO EXCEED 0.5 FPS AT THE DESIGN FLOW RATE. THE PRESSURE DROP THROUGH THE SURFACE OF THE CLEAN SCREEN SHALL NOT EXCEED 0.1 PSI THE TOTAL PRESSURE DROP THROUGH THE DRUM ASSEMBLY SHALL NOT EXCEED 1.0 FOOT OF WATER.
4. THE SCREEN ASSEMBLY SHALL BE MANUFACTURED OF CORROSION RESISTANT METAL, AISI TYPE 316 STAINLESS STEEL. THE MAIN OUTLET SHALL BE A 36-INCH WITH A PLATE AS REQUIRED FOR CONNECTION TO THE STRUCTURE.

DETAIL A4 - BORING LOCATION

FOR REGULATORY REVIEW ONLY - NOT FOR CONSTRUCTION

PROPOSED BORING LOCATION

ELECTRIC DRIVE UNIT

CATWALK

009

FOR REGULATORY REVIEW ONLY - NOT FOR CONSTRUCTION

DETAIL B - PIPELINE ROAD CROSSING

RAMP

ENTRANCE GATE

NOTE:

1. SCALE 1" = 1'
2. CAPACITY IS 32,000 LBS PER AXLE (HS-20 LOADING)
3. DURING PIPELINE INSTALLATION, ONLY ONE SEGMENT OF THE FENCE WILL BE TEMPORARILY REMOVED. AFTER THE PIPE HAS BEEN PLACED, THE FENCE SECTION WILL BE REPLACED WITH A MINIMUM SECTION OF THE FENCE MESH REMOVED TO ACCOMMODATE THE PIPELINE. THE MESH AROUND THE PIPELINE WILL BE WIRE REINFORCED AS APPROPRIATE TO MAINTAIN THE INTEGRITY OF THE MESH. THE SECTION OF THE FENCE WILL BE REPLACED AFTER THE DECOMMISSIONING OF THE PILOT PROJECT.
4. MINIMUM OVERHEAD POWERLINE CLEARANCE SHALL BE 16 FEET OVER THE ACCESS ROAD.
5. THE RAMP WAS DESIGNED TO ACCEPT PASSENGER CARS AND SEMITRAILERS BASED ON THE DIMENSIONS PUBLISHED IN AASHTO A POLICY ON GEOMETRIC DESIGN OF HIGHWAYS AND STREETS 2018, 7TH EDITION TABLE 2-4.
6. THE TOP OF THE RAMP FEATURES A 37 INCH FLAT SECTION TO ACCOMMODATE RECREATIONAL VEHICLE TRAFFIC.

240 $\frac{5}{8}$ in

60 $\frac{5}{16}$ in

60 in

60 in

60 $\frac{5}{16}$ in

396 $\frac{7}{16}$ in

37 in

25 in

25 in

396 $\frac{7}{16}$ in

INDIAN RIVER LAGOON

RESTORE LAGOON INFLOW RESEARCH PILOT PROJECT

MARK	DATE	DESCRIPTION	BY

Project No.: 100-WTR-T41006183

Designed By:

Drawn By:

Checked By:

Bar Measures 1 inch

010

TETRA TECH
ENGINEERING BUSINESS NO. 2429

www.tetratech.com

201 EAST PINE STREET, SUITE 1000
ORLANDO, FL 32801
PHONE: (407) 839-3955 FAX: (407) 839-3790

FOR REGULATORY REVIEW ONLY - NOT FOR CONSTRUCTION

DETAIL C - OUTFLOW
PLAN VIEW

OAK STAKES

STAKED TURBIDITY BARRIER

HYDROCAST GROUT BAG

HYDROTEX ARTICULATING BLOCK FABRIC FORMED CONCRETE MATTRESS (AB300)

6.0 ft

21.8 ft

2.0 ft

8.0 ft

SIDE VIEW

2 ft NAVD88

0 ft NAVD88

-1.5 ft NAVD88 MLLW

-3 ft NAVD88

TURBIDITY BARRIER

STAKE DRIVEN 24" INTO SEDIMENT WITH 24" ABOVE

HYDROCAST GROUT BAG

20 INCH ID DISCHARGE PIPE

NON WOVEN GEOTEXTILE

EXISTING GRADE APPROXIMATE SLOPE = 1:20

21.8 ft

NOTE:
1. THE STAKED TURBIDITY BARRIER SHALL UTILIZE A BELTED SILT RETENTION FENCE (PRIORITY 1)

INDIAN RIVER LAGOON

RESTORE LAGOON INFLOW RESEARCH PILOT PROJECT

MARK	DATE	DESCRIPTION		BY

Drawn By:
Designed By:
Checked By:

Project No:100-WTS-T41000.03

011

Copyright: Tetra Tech

DETAIL A1 - OUTFALL CROSS SECTION WITH MANATEE SCREEN DETAIL

HYDROTEX ARTICULATING
BLOCK FABRIC
FORMED CONCRETE
MATTRESS (AB300)

2 ft NAVD88

0 ft NAVD88

-1.5 ft NAVD88

-3 ft NAVD88

MLLW

HYDROCAST GROUT BAG

DOWELS-TYPE
REQUIRED BY
ENGINEER

$\frac{1}{2}$" STEEL ROD

$\frac{3}{4}$" FLANGE

"BOLT HOLE

20" PIPE

NON-WOVEN
GEOTEXTILE

EXISTING GRADE

FOR REGULATORY REVIEW ONLY - NOT FOR CONSTRUCTION

NOTE:
1. SCALE 1$\frac{1}{2}$" = 1'
2. DIMENSIONS FOR MANATEE GRATE HAVE BEEN SELECTED
    ACCORDING TO FDOT INDEX 280 STANDARDS

FOR REGULATORY REVIEW ONLY - NOT FOR CONSTRUCTION

NOTE:
1. MARINE BIOLOGICAL RESOURCE SURVEY COMPLETED JUNE 2021

BIOLOGICAL SURVEYS

LEGEND
- SHOAL GRASS (LESS THAN 1 M^2)
- VEGETATION
- BLACK MANGROVE

INDIAN RIVER LAGOON
RESTORE LAGOON INFLOW RESEARCH PILOT PROJECT

MARK | DATE | DESCRIPTION | BY

TETRA TECH
ENGINEERING BUSINESS NO. 2429
www.tetratech.com
201 EAST PINE STREET, SUITE 1000
ORLANDO, FL 32801
PHONE: (407) 839-3955 FAX: (407) 839-3790

013

Copyright: Tetra Tech

Florida Tech SAJ-2022-03034 Proposed Sensor Deployments

Table 1. Summary of proposed water quality sensors and current profilers.

Sensor			Deployment & Service			Location		
code	Type	Parameter measured	Deployed	Secured	Service	Site	Latitude	Longitude
WQ-01	HOBO U-26	Dissolved Oxygen + Temp.	SCUBA	Cement block	Monthly	Port Canaveral	28.4086	-80.6275
WQ-01	HOBO U-24	Conductivity (Salinity)	SCUBA	Cement block	Monthly	Port Canaveral	28.4086	-80.6275
WQ-01	HOBO U-20	Pressure	SCUBA	Cement block	Monthly	Port Canaveral	28.4086	-80.6275
WQ-02	HOBO U-26	Dissolved Oxygen + Temp.	SCUBA	Cement block	Monthly	Inflow	28.4071	-80.6384
WQ-02	HOBO U-24	Conductivity (Salinity)	SCUBA	Cement block	Monthly	Inflow	28.4071	-80.6384
WQ-02	HOBO U-20	Pressure	SCUBA	Cement block	Monthly	Inflow	28.4071	-80.6384
WQ-03	HOBO U-26	Dissolved Oxygen + Temp.	SCUBA	Cement block	Monthly	Inflow	28.4070	-80.6392
WQ-03	HOBO U-24	Conductivity (Salinity)	SCUBA	Cement block	Monthly	Inflow	28.4070	-80.6392
WQ-04	HOBO U-26	Dissolved Oxygen + Temp.	SCUBA	Cement block	Monthly	Inflow	28.4071	-80.6416
WQ-04	HOBO U-24	Conductivity (Salinity)	SCUBA	Cement block	Monthly	Inflow	28.4071	-80.6416
WQ-05	HOBO U-26	Dissolved Oxygen + Temp.	SCUBA	Cement block	Monthly	Inflow	28.4070	-80.6476
WQ-05	HOBO U-24	Conductivity (Salinity)	SCUBA	Cement block	Monthly	Inflow	28.4070	-80.6476
WQ-06	HOBO U-26	Dissolved Oxygen + Temp.	SCUBA	Cement block	Monthly	Reference	28.3131	-80.6329
WQ-06	HOBO U-24	Conductivity (Salinity)	SCUBA	Cement block	Monthly	Reference	28.3131	-80.6329
WQ-07	HOBO U-26	Dissolved Oxygen + Temp.	SCUBA	Cement block	Monthly	Reference	28.2843	-80.6105
WQ-07	HOBO U-24	Conductivity (Salinity)	SCUBA	Cement block	Monthly	Reference	28.2843	-80.6105
ADCP-01	Sontek Argonaut XR	Mean current	Winch	Sandscrews	Monthly	Port Canaveral	28.40901	-80.63729
ADCP-02	Sontek Xargonaut XR	Mean current	Winch	Sandscrews	Monthly	Inflow	28.40765	-80.64104

Figure 1. Map of central and northern Banana River (a) with proposed location of water quality sensors and current profilers. Inset (b) includes proposed sensor locations in Port Canaveral and the inflow site.

CESAJ-EN

MEMORANDUM FOR Chief, Regulatory Division

SUBJECT: Florida Institute of Technology, Restore Lagoon Inflow Research Project, Canaveral Lock, Brevard County, Florida Regulatory File #SAJ-2022-03034.

1. Reference Regulatory email dated 6 February 2023, requesting Engineering Division review the permit package for SAJ-2022-03034 Restore Lagoon Inflow Research Project, Canaveral Lock (2023-0028). The applicant seeks authorization to evaluate water quality, biology, and geochemical effects of providing ocean inflow to the Indian River Lagoon. The intention for this project is to operate the inflow pumping system initially for 24 hours a day, 7 days a week, for 1 year at a flow rate of 0.5 meters/second. The hydraulic pump and intake will be located at the Canaveral Lock behind the navigation fender. The pipe will run onshore at grade with a ramp covering the pipeline at the roadway crossing. The system will have both onsite and remote shut down capability.

2. Engineering Division does not object to the issuance of the permit and approves the request for SAJ-2022-03034 Restore Lagoon Inflow Research Project, Canaveral Locks (2023-0028) as referenced herein as the proposed meets SAJ criteria and will not impact the federal project.

3. Approval of these modifications to the Canaveral Lock Project is in accordance with 33 U.S.C. 408. It also complies with the National Environmental Policy Act as the proposed modifications were previously analyzed in the Department of Army Permit SAJ-2022-03034.

4. The applicant shall comply with Engineering Circular 1165-2-220, dated 10 September 2018, Policy and Procedural Guidance for Processing Requests to Alter U.S. Army Corps of Engineers Civil Works Projects Pursuant to 33 U.S.C. 408, Appendix K, paragraphs 1. to 16. (enclosed) and the time limit for completing the work authorized in Department of Army Permit SAJ-2022-03034. The applicant is responsible for quality control for performance of the work and for ensuring these actions do not interfere with the functioning of the Canaveral Lock Project. Documentation of the completed work must be furnished to USACE within 60 days after completion of the work for our records. This documentation will need to include a certification that the work was completed in accordance with the approved plans and specifications, GPS readings for the limits of the work performed, as-built drawings, and the date the work started and was completed.

5. If you have any questions, please feel free to contact the Engineering Division POC Murika Davis at 904-232-1604 or by email to murika.davis@usace.army.mil.

                                          Laureen A. Borochaner, P.E.
                                          Chief, Engineering Division

APPENDIX K

Standard Terms and Conditions

This appendix includes the standard conditions that must be included in all Section 408 approval notifications, except where marked as optional. Use of optional conditions should be based on scope and scale of the approved activity:

LIMITS OF THE AUTHORIZATION

1. This permission only authorizes you, the requester, to undertake the activity described herein under the authority provided in Section 14 of the Rivers and Harbors Act of 1899, as amended (33 USC 408). This permission does not obviate the need to obtain other federal, state, or local authorizations required by law. This permission does not grant any property rights or exclusive privileges, and you must have appropriate real estate instruments in place prior to construction and/or installation.

2. The time limit for completing the work authorized ends on _____ . If you find that you need more time to complete the authorized activity, submit your request for a time extension to this office for consideration at least one month before the above date is reached. **Addressed in the 408 approval letter or 408 EN Memo.**

3. Without prior written approval of the USACE, you must neither transfer nor assign this permission nor sublet the premises or any part thereof, nor grant any interest, privilege or license whatsoever in connection with this permission. Failure to comply with this condition will constitute noncompliance for which the permission may be revoked immediately by USACE.

4. The requester understands and agrees that, if future operations by the United States require the removal, relocation, or other alteration of the work herein authorized, or if, in the opinion of the Secretary of the Army or an authorized representative, said work will cause unreasonable conditions and/or obstruction of USACE project authorized design, the requester will be required upon due notice from the USACE, to remove, relocate, or alter the structural work or obstructions caused thereby, without expense to the United States. No claim can be made against the United States on account of any such removal or alteration.

INDEMNIFICATION AND HOLD HARMLESS

5. The United States will in no case be liable for:
    a. any damage or injury to the structures or work authorized by this permission that may be caused or result from future operations undertaken by the United States, and no claim or right to compensation will accrue from any damage; or
    b. damage claims associated with any future modification, suspension or revocation of this permission.

6. The United States will not be responsible for damages or injuries which may arise from or be incident to the construction, maintenance, and use of the project requested by you, nor for damages to the property or injuries to your officers, agents, servants, or employees, or others who may be on your premises or project work areas or the federal project(s) rights-of-way. By accepting this permission, you hereby agree to fully defend, **indemnify,** and **hold harmless** the United States and USACE from any and all such claims, subject to any limitations in law.

7. Any damage to the water resources development project or other portions of any federal project(s) resulting from your activities must be repaired at your expense.

REEVALUATION OF PERMISSION

8. The determination that the activity authorized by this permission would not impair the usefulness of the federal project and would not be injurious to the public interest was made in reliance on the information you provided.

9. This office, at its sole discretion, may reevaluate its decision to issue this permission at any time circumstances warrant, which may result in a determination that it is appropriate or necessary to modify or revoke this permission. Circumstances that could require a reevaluation include, but are not limited to, the following:
   a. you fail to comply with the terms and conditions of this permission;
   b. the information provided in support of your application for permission proves to have been inaccurate or incomplete; or
   c. significant new information surfaces which this office did not consider in reaching the original decision that the activity would not impair the usefulness of the water resources development project and would not be injurious to the public interest.

CONDUCT OF WORK UNDER THIS PERMISSION

10. You are responsible for implementing any requirements for mitigation, reasonable and prudent alternatives, or other conditions or requirements imposed as a result of environmental compliance.

11. Work/usage allowed under this permission must proceed in a manner that avoids interference with the inspection, operation, and maintenance of the federal project.

12. In the event of any deficiency in the design or construction of the requested activity, you are solely responsible for taking remedial action to correct the deficiency.

13. The right is reserved to the USACE to enter upon the premises at any time and for any purpose necessary or convenient in connection with government purposes, to make inspections, to operate and/or to make any other use of the lands as may be necessary in connection with government purposes, and you will have no claim for damages on account thereof against the United States or any officer, agent or employee thereof.

14. You must provide copies of pertinent design, construction, and/or usage submittals/documents. USACE may request that survey and photographic documentation of the alteration work and the impacted project area be provided before, during, and after construction and/or installation.

15. You may be required to perform an inspection of the federal project with the USACE, prior to your use of the structure, to document existing conditions.

16. USACE shall not be responsible for the technical sufficiency of the alteration design nor for the construction and/or installation work.

17. (optional, at the discretion of the district) Once permission is granted, you must notify the USACE District at least ( ) days before work/usage is started so that post- permission over sight can be performed by USACE.

18. (optional, at the discretion of the district) You must schedule a final inspection with the USACE within ( ) days after completion of the work/usage.

19. (optional, at the discretion of the district) You must submit a copy of "as-built" drawings within ( ) days of completion of work showing the new work as it relates to identifiable features of the federal project. **Included in the 408 approval letter.**

AS-BUILT CERTIFICATION BY PROFESSIONAL ENGINEER

Submit this form and one set of as-built engineering drawings to the U.S. Army Corps of Engineers, Enforcement Section, P.O. Box 4970, Jacksonville, Florida, 32232-0019. If you have questions regarding this requirement, please contact the Enforcement Branch at 904-232-3131.

1. Department of the Army Permit Number: SAJ-   -   (-   )

2. Permittee Information:

     Name: _____

     Address: _____

                _____

3. Project Site Identification (physical location/address):

_____

_____

_____

4. As-Built Certification: I hereby certify that the authorized work, including any mitigation required by Special Conditions to the permit, has been accomplished in accordance with the Department of the Army permit with any deviations noted below. This determination is based upon on-site observation, scheduled, and conducted by me or by a project representative under my direct supervision. I have enclosed one set of as-built engineering drawings.

_____   _____

Signature of Engineer   Name (*Please type*)

_____   _____

(FL, PR, or VI) Reg. Number   Company Name

_____   _____   _____

City   State   ZIP

        (Affix Seal)

_____   _____

Date   Telephone Number

Date Work Started:_____ Date Work Completed:_____

Identify any deviations from the approved permit drawings and/or special conditions (attach additional pages if necessary):

_____

_____

_____

_____

_____

_____

_____

_____

_____

_____

_____

STANDARD MANATEE CONDITIONS FOR IN-WATER WORK
2011

The permittee shall comply with the following conditions intended to protect manatees from direct project effects:

a. All personnel associated with the project shall be instructed about the presence of manatees and manatee speed zones, and the need to avoid collisions with and injury to manatees. The permittee shall advise all construction personnel that there are civil and criminal penalties for harming, harassing, or killing manatees which are protected under the Marine Mammal Protection Act, the Endangered Species Act, and the Florida Manatee Sanctuary Act.

b. All vessels associated with the construction project shall operate at "Idle Speed/No Wake" at all times while in the immediate area and while in water where the draft of the vessel provides less than a four-foot clearance from the bottom. All vessels will follow routes of deep water whenever possible.

c. Siltation or turbidity barriers shall be made of material in which manatees cannot become entangled, shall be properly secured, and shall be regularly monitored to avoid manatee entanglement or entrapment. Barriers must not impede manatee movement.

d. All on-site project personnel are responsible for observing water-related activities for the presence of manatee(s). All in-water operations, including vessels, must be shutdown if a manatee(s) comes within 50 feet of the operation. Activities will not resume until the manatee(s) has moved beyond the 50-foot radius of the project operation, or until 30 minutes elapses if the manatee(s) has not reappeared within 50 feet of the operation. Animals must not be herded away or harassed into leaving.

e. Any collision with or injury to a manatee shall be reported immediately to the Florida Fish and Wildlife Conservation Commission (FWC) Hotline at 1-888-404-3922. Collision and/or injury should also be reported to the U.S. Fish and Wildlife Service in Jacksonville (1-904-731-3336) for north Florida or in Vero Beach (1-772-562-3909) for south Florida, and emailed to FWC at ImperiledSpecies@myFWC.com.

f. Temporary signs concerning manatees shall be posted prior to and during all in-water project activities. All signs are to be removed by the permittee upon completion of the project. Temporary signs that have already been approved for this use by the FWC must be used. One sign which reads *Caution: Boaters* must be posted. A second sign measuring at least 8½ " by 11" explaining the requirements for "Idle Speed/No Wake" and the shut down of in-water operations must be posted in a location prominently visible to all personnel engaged in water-related activities. These signs can be viewed at http://www.myfwc.com/WILDLIFEHABITATS/manatee_sign_vendors.htm. Questions concerning these signs can be forwarded to the email address listed above.

CAUTION: MANATEE HABITAT

All project vessels

IDLE SPEED / NO WAKE

When a manatee is within 50 feet of work all in-water activities must

SHUT DOWN

Report any collision with or injury to a manatee:

Wildlife Alert:

1-888-404-FWCC(3922)

cell *FWC or #FWC

FLORIDA DEPARTMENT OF
Environmental Protection

CENTRAL DISTRICT OFFICE
3319 MAGUIRE BLVD., SUITE 232
ORLANDO, FLORIDA 32803

Ron DeSantis
Governor

Jeanette Nuñez
Lt. Governor

Shawn Hamilton
Secretary

Permittee/Authorized Entity:	**Landowner:**
Florida Institute of Technology	Canaveral Port Authority
Attn: Dr. Marco Carvalho	Attn: Robert Musser
150 W University Blvd	9001 Charles M Rowland Dr
Melbourne, FL 32901	Cape Canaveral, FL 32920
mcarvalho@fit.edu	bmusser@portcanaveral.com

Restore Lagoon Inflow Pilot Research

Authorized Agent:
Tetra Tech
Attn: Matthew Sheldon
1353 N Courtenay Pkwy
Merritt Island, FL 32953
matt.shelton@tetratech.com

Environmental Resource Permit

State-owned Submerged Lands Authorization –Not Applicable

U.S. Army Corps of Engineers Authorization – SPGP NOT APPROVED

Brevard County
Permit No.: 431679-001-EI

Permit Issuance Date: August 11, 2023
Permit Construction Phase Expiration Date: August 11, 2028

FLORIDA DEPARTMENT OF
Environmental Protection

CENTRAL DISTRICT OFFICE
3319 MAGUIRE BLVD., SUITE 232
ORLANDO, FLORIDA 32803

Environmental Resource Permit

Permittee: Florida Institute of Technology (FIT)
Permit No: 431379-001

PROJECT LOCATION
The activities authorized by this permit are located at 1000 Mullet Rd Cape Canaveral, Florida 32920, in Section 9, Township 24 South, Range 37 East in Brevard County.

PROJECT DESCRIPTION
The permittee is authorized to conduct a pilot research study to evaluate water quality, biology, and biogeochemistry of the Indian River Lagoon, a Class II Waterbody. The pilot study will include the installation of a temporary inflow pump to convey ocean water from the Canaveral Barge Canal to the Banana River Lagoon of the Indian River Lagoon, and an associated 20-inch diameter pipe responsible for the intake and discharge of water to an outfall in a cove west of the Avocet Lagoon. The inflow pumping system will run 24 hours per day for one year with a flow rate of 0.5 m^3/s (cubic meters per seconds). Four instrument stations will be temporarily installed for monitoring purposes. No wetland impacts are associated with the proposed project.

Authorized activities are depicted on the attached exhibits.

AUTHORIZATIONS
Restore Lagoon Inflow Pilot Research

Environmental Resource Permit
The Department has determined that the activity qualifies for an Environmental Resource Permit. Therefore, the Environmental Resource Permit is hereby granted, pursuant to Part IV of Chapter 373, Florida Statutes (F.S.), and Chapter 62-330, Florida Administrative Code (F.A.C.).

Sovereignty Submerged Lands Authorization
As staff to the Board of Trustees of the Internal Improvement Trust Fund (Board of Trustees), the Department has determined the activity is not on submerged lands owned by the State of Florida. Therefore, your project is not subject to the requirements of Chapter 253, F.S., or Rule 18-21, F.A.C.

Federal Authorization
Your proposed activity as outlined in your application and attached drawings **does not qualify** for Federal authorization pursuant to the State Programmatic General Permit VI-R1. **SEPARATE permit(s)** or authorization **will be required** from the U.S. Army Corps of Engineers.

Authority for review - an agreement with the USACOE entitled "Coordination Agreement Between the U. S. Army Corps of Engineers (Jacksonville District) and the Florida Department of Environmental Protection (or Duly Authorized Designee), State Programmatic General Permit", Section 10 of the Rivers and Harbor Act of 1899, and Section 404 of the Clean Water Act

Coastal Zone Management
Issuance of this authorization also constitutes a finding of consistency with Florida's Coastal Zone Management Program, as required by Section 307 of the Coastal Zone Management Act.

Water Quality Certification
This permit also constitutes a water quality certification under Section 401 of the Clean Water Act, 33 U.S.C. 1341.

Other Authorizations
You are advised that authorizations or permits for this activity may be required by other federal, state, regional, or local entities including but not limited to local governments or municipalities. This permit does not relieve you from the requirements to obtain all other required permits or authorizations.

The activity described may be conducted only in accordance with the terms, conditions and attachments contained in this document. Issuance and granting of the permit and authorizations herein do not infer, nor guarantee, nor imply that future permits, authorizations, or modifications will be granted by the Department.

PERMIT CONDITIONS
The activities described must be conducted in accordance with:
- **The Specific Conditions**
- **The General Conditions**
- **The limits, conditions and locations of work shown in the attached drawings**
- **The term limits of this authorization**

You are advised to read and understand these conditions and drawings prior to beginning the authorized activities, and to ensure the work is conducted in conformance with all the terms, conditions, and drawings herein. If you are using a contractor, the contractor also should read and understand these conditions and drawings prior to beginning any activity. Failure to comply with these conditions, including any mitigation requirements, shall be grounds for the Department to revoke the permit and authorization and to take appropriate enforcement action. Operation of the facility is not authorized except when determined to be in conformance with all applicable rules and this permit, as described.

SPECIFIC CONDITIONS - PRIOR TO ANY CONSTRUCTION

1. Prior to initiation of any work authorized by this permit, all wetlands, surface waters, and storm drains, outside the specific limits of construction authorized by this permit shall be protected from erosion, siltation, sedimentation, and/or scouring, including the placement of

staked erosion control devices around the project area and staging area(s) that are located outside of any authorized impact areas.

2. Best management practices for erosion control shall be implemented prior to construction commencement and shall be maintained at all times during construction to prevent siltation and turbid discharges in excess of State water quality standards pursuant to Rule 62-302, F.A.C. Methods shall include, but are not limited to the use of staked hay bales, staked filter cloth, sodding, seeding, staged construction and the installation of turbidity screens around the immediate project site.

SPECIFIC CONDITIONS – CONSTRUCTION ACTIVITIES

3. The project shall comply with applicable state water quality standards, including:
   a. 62-302.500 – minimum criteria for all surface waters at all places and at all times;
   b. 62-302.500 – Surface eaters: general criteria;
   c. 62-302.400 – Class II Waters: Shellfish Propagation or Harvesting

4. The permittee shall report any damage to the Department within 24 hours that occurs to the wetlands not authorized for impacts under this permit. If any damage occurs to wetlands or surface waters as a result of any construction activities, the permittee shall be required to restore the wetland area by re-grading the damaged areas back to the natural preconstruction elevations and planting vegetation of the size, densities, and species that exist in the adjacent areas pursuant to a consent order. The restoration shall be completed within 30 days of completion of the construction and shall be done to the satisfaction of the Department.

5. This permit does not authorize the removal of any vegetation within the jurisdictional area. No dredging, filling, or other construction activity, including the removal of tree stumps and/or vegetative root masses, shall be conducted within the wetlands or surface waters other than that performed within the construction limits authorized in this permit.

6. Storage or stockpiling of tools and materials (i.e., lumber, pilings, debris) within wetlands, along the shoreline, within the littoral zone, or elsewhere within wetlands or other surface waters is prohibited.

7. This permit does not authorize the construction of any additional structures/fill not illustrated on the permit drawings.

SPECIFIC CONDITIONS – CONSTRUCTED ACTIVITY

8. In accordance with 62-330.301(1), F.A.C., the activity authorized to be operated under this permit:
   a. Will not cause adverse water quantity impacts to receiving waters and adjacent lands;
   b. Will not cause adverse flooding to on-site or off-site property;
   c. Will not cause adverse impacts to existing surface water storage and conveyance capabilities;

d. Will not adversely affect the quality of receiving waters such that the state water quality standards set forth in chapters 62-4, 62-302, 62-520, and 62-550, F.A.C., including the antidegradation provisions of paragraphs 62-4.242(1)(a) and (b), F.A.C., subsections 62-4.242(2) and (3), F.A.C., and rule 62-302.300, F.A.C., and any special standards for Outstanding Florida Waters and Outstanding National Resource Waters set forth in subsections 62-4.242(2) and (3), F.A.C.;

e. Will not adversely impact the maintenance of surface or ground water levels or surface water flows established pursuant to section 373.042, F.S.;

f. Will not cause adverse impacts to a Work of the District established pursuant to section 373.086, F.S.;

g. Will be capable, based on generally accepted engineering and scientific principles, of performing and functioning as proposed;

h. Will be conducted by a person with the financial, legal, and administrative capability of ensuring that the activity will be undertaken in accordance with the terms and conditions under this permit;

9. In accordance with 62-330.350(1)(q), F.A.C., if the proposed activity authorized under this permit causes any adverse impacts, the Agency will require the permittee to eliminate the cause, obtain any necessary permit modification, and take any necessary corrective actions to resolve the adverse impacts.

SPECIFIC CONDITIONS – FLORIDA MANATEE

10. The FWC's *Standard Manatee Conditions for In-water Work* (2011; attached) shall be followed for all in-water activity.

11. The Permittee shall install and maintain manatee exclusion devices (such as grating) over any existing or proposed, submerged, or partially submerged pipes or culverts greater than 8 inches, but smaller than 8 feet in diameter that are reasonably accessible to manatees within the bulkhead wall. If horizontal or vertical bars are used, no more than 8-inch gaps on center shall be allowed. Grates shall be in place at the accessible end(s) during all phases of the construction process, and as a final design element to restrict manatee access.

12. The Permittee shall ensure that an observer(s) shall watch for protected marine species (manatees, marine turtles, dolphins, etc.) during all in-water work associated with dredging operations to ensure compliance with the stop work zone required in this authorization. All observers shall have prior on-the-job observation experience (including previous sightings of manatees) during previous dredging work where the activities were similar in nature to this project. The Permittee shall ensure that all observers are given a copy of the permit for the project, including all special conditions, prior to the commencement of construction. FWC guidelines regarding observers can be found at http://www.myfwc.com/wildlifehabitats/managed/manatee/watch-program/.

13. The proposed project location is defined as an Important Manatee Area (IMA) per the U.S. Army Corps of Engineers 2013 Manatee Key. Should dredging operations be needed for this work, the Permittee shall verify that all Protected Marine Species Observers for this work are qualified prior to commencement of construction. An individual may be considered

qualified if previous observational experience is commensurate to the type of work for this project. Commensurate work includes similar types of project activity, similar type of manatee use, and similar potential risk to manatees. Documentation supporting required experience shall be provided when requested through copies of previous project logs and observer reports, copies of the State permit (which would include the type of work and the required conservation conditions), where the nature of the work is similar in nature to this authorization. In addition:

    a. The Permittee shall ensure that all observers are given a copy of the permit for the project, including all special conditions, prior to the commencement of construction. FWC guidelines regarding observers can be found at http://www.myfwc.com/wildlifehabitats/managed/manatee/watch-program/.

    b. All individuals chosen as an observer shall have previously performed the duties of a Protected Marine Species Observer during permitted activities requiring wildlife conservation conditions.

    c. Observers shall not have been found in violation of previous permit conditions relating to the observation of protected marine species (manatees, marine turtles, dolphins, etc.) or found providing inaccurate or false information on the supporting documentation used for verification of previous experience.

    d. The Permittee shall ensure that a final report including names of observers, contact information, protected marine species sightings, and actions taken shall be sent to the FWC at ImperiledSpecies@MyFWC.com, no later than 30 days after (each) event completion.

    e. The Permittee shall ensure that the movement of a work barge and other associated vessels shall be minimized to the greatest extent possible at night.

14. This location is not authorized for night-time clamshell dredging.

15. Blasting is not authorized for this project. If the construction methodology changes in the future to include blasting, a modification to the permit is needed. Specific conditions must address impacts to protected marine species (manatees, marine turtles, dolphins, etc.) if blasting is proposed. Such conditions shall be in the form of an appropriate Blast and Watch Plan, approved by FWC staff, which can be contacted at ImperiledSpecies@MyFWC.com.

16. The Permittee shall develop a Manatee Protection Monitoring Plan prior to commencement of work. The Plan shall describe the use of aerial survey and other best available information, including the survey range, duration, and frequency. The Plan shall also describe how monitoring information will be evaluated to identify any potential effects on manatee behavior. The Plan shall be reviewed and approved by FWC staff, which can be contacted at ImperiledSpecies@MyFWC.com.

SPECIFIC CONDITIONS - OTHER LISTED SPECIES

17. <u>Wading Birds</u>: The potential exists for wading bird nesting activity in the lagoons adjacent to the project site. FWC staff recommends that specific surveys be conducted for wading birds in the adjacent lagoons prior to the commencement of any construction activities. Surveys should be conducted during their breeding season, which extends from March through August. The project site also falls within or adjacent to a reddish egret Core

Foraging Area. Where construction activities are anticipated to occur adjacent to or within waterways, i.e., outflow piping, FWC staff recommends determining if suitable foraging habitat for this species is present within the project footprint. Additional information and guidance for conducting surveys and determining if reddish egret suitable foraging habitat is present can be found in the *Species Conservation Measures and Permitting Guidelines for Little Blue Heron, Reddish Egret, Roseate Spoonbill, Tricolored Heron* found at https://myfwc.com/wildlifehabitats/wildlife/species-guidelines/. If there is evidence of nesting during this period, FWC staff recommends that any wading bird nest sites be buffered by 100 meters (330 feet) to avoid disturbance by human activities. If nesting is discovered after site activities have begun or if maintaining the recommended buffer is not possible, the applicant may contact the FWC staff identified below to discuss potential permitting alternatives. For questions regarding Incidental Take permitting for reddish egret foraging habitat, please contact the FWC Protected Species Permit Coordinator at (850) 921-5990 or WildlifePermit@MyFWC.com.

18. Submerged Aquatic Vegetation: FWC staff recommends that a monitoring plan be developed for the outflow area within the IRL to determine impacts to submerged aquatic vegetation (SAV). Assessments should be completed during the peak growing season of April 1st and October 31st, twice during the first year (spring and fall) and once annually thereafter. Example metrics that may be used during surveys include seagrass shoot counts per unit area, the species present, and the overall areal coverage of seagrasses within the outflow area. Metrics can be monitored either at randomly assigned points along fixed transects or at random fixed quadrat locations at 1% of the project impact area. SAV reconnaissance and surveys should be non-destructive. Additional information and guidance for conducting surveys can be obtained from the Florida Department of Environmental Protection (FDEP) at Guidance on Surveys for Potential Impacts to SAV. FWC staff supports the use of the reference site located approximately 8 miles south in the Banana River for comparison as proposed by the applicant in the *Restore Lagoon Inflow Pilot Research Environmental Resource Permit Permitting Narrative* submitted with the application materials.

19. Temperature Monitoring: If the outflow is much warmer than the ambient water temperature, manatees could find the cove and begin using it as a warm water refuge. FWC staff recommends the applicant create and include in the final report for the pilot study a three-dimensional map of water temperature close to the outflow in early winter when oceanic temperatures are generally warmer than lagoon temperatures during a cold front. The applicant should continue to monitor water temperatures over the course of the winter (November-March) with an array of temperature data loggers, including the outflow temperature as well as collect temperatures manually to map the thermal plume at a finer scale (vertically and horizontally), when outflow temperature is elevated over lagoon temperature and the latter is below 20 degrees Celsius. For further technical assistance regarding temperature monitoring please contact Chip Deutsch at (352) 334-4240 or by email at Charles.Deutsch@MyFWC.com.

20. This permit does not authorize the permittee to cause any adverse impact to or "take" of state listed species and other regulated species of fish and wildlife. Compliance with state laws regulating the take of fish and wildlife is the responsibility of the owner or applicant

associated with this project. Please refer to Chapter 68A-27 of the Florida Administrative Code for definitions of "take" and a list of fish and wildlife species. If listed species are observed onsite, FWC staff are available to provide decision support information or assist in obtaining the appropriate FWC permits. Most marine endangered and threatened species are statutorily protected and a "take" permit cannot be issued. Requests for further information or review can be sent to FWCConservationPlanningServices@MyFWC.com.

SPECIFIC CONDITIONS - CONSTRUCTION COMPLETION

21. Upon final completion of the project and upon reasonable assurance that the project is no longer a potential turbidity source, the permittee will be responsible for the removal of the temporary best management practices and turbidity control devices. All turbidity control devices shall be disposed of in an upland disposal area.

SPECIFIC CONDITIONS – MONITORING/REPORTING REQUIREMENTS

22. Biannual submittals required herein for compliance water quality monitoring reports of total nitrogen (TN), total phosphorus (TP), biological oxygen demand (BOD), and dissolved oxygen (DO) in accordance with 62-302.530, F.A.C. shall be submitted electronically when practicable and shall include the permittee's name and permit number (431679-001). Email submittals shall be sent to DEP_CD@floridadep.gov and CC angelica.sterner@floridadep.gov with a subject line of "Compliance: permit number 431679-001.

GENERAL CONDITIONS FOR INDIVIDUAL PERMITS

The following general conditions are binding on all individual permits issued under this chapter, except where the conditions are not applicable to the authorized activity, or where the conditions must be modified to accommodate project-specific conditions.

1. All activities shall be implemented following the plans, specifications and performance criteria approved by this permit. Any deviations must be authorized in a permit modification in accordance with rule 62-330.315, F.A.C. Any deviations that are not so authorized may subject the permittee to enforcement action and revocation of the permit under chapter 373, F.S.

2. A complete copy of this permit shall be kept at the work site of the permitted activity during the construction phase and shall be available for review at the work site upon request by the Agency staff. The permittee shall require the contractor to review the complete permit prior to beginning construction.

3. Activities shall be conducted in a manner that does not cause or contribute to violations of state water quality standards. Performance-based erosion and sediment control best management practices shall be installed immediately prior to, and be maintained during and after construction as needed, to prevent adverse impacts to the water resources and adjacent lands. Such practices shall be in accordance with the State of Florida Erosion and Sediment Control Designer and Reviewer Manual (Florida Department of Environmental Protection and Florida Department of Transportation, June 2007), and the Florida Stormwater Erosion and Sedimentation Control Inspector's Manual (Florida Department of Environmental Protection, Nonpoint Source

Management Section, Tallahassee, Florida, July 2008), which are both incorporated by reference in subparagraph 62-330.050(9)(b)5., F.A.C., unless a project-specific erosion and sediment control plan is approved or other water quality control measures are required as part of the permit.

4. At least 48 hours prior to beginning the authorized activities, the permittee shall submit to the Agency a fully executed Form 62-330.350(1), "Construction Commencement Notice," (October 1, 2013), (http://www.flrules.org/Gateway/reference.asp?No=Ref-02505), incorporated by reference herein, indicating the expected start and completion dates. A copy of this form may be obtained from the Agency, as described in subsection 62-330.010(5), F.A.C., and shall be submitted electronically or by mail to the Agency. However, for activities involving more than one acre of construction that also require a NPDES stormwater construction general permit, submittal of the Notice of Intent to Use Generic Permit for Stormwater Discharge from Large and Small Construction Activities, DEP Form 62-621.300(4)(b), shall also serve as notice of commencement of construction under this chapter and, in such a case, submittal of Form 62-330.350(1) is not required.

5. Unless the permit is transferred under rule 62-330.340, F.A.C., or transferred to an operating entity under rule 62-330.310, F.A.C., the permittee is liable to comply with the plans, terms, and conditions of the permit for the life of the project or activity.

6. Within 30 days after completing construction of the entire project, or any independent portion of the project, the permittee shall provide the following to the Agency, as applicable:
    a. For an individual, private single-family residential dwelling unit, duplex, triplex, or quadruplex – "Construction Completion and Inspection Certification for Activities Associated with a Private Single-Family Dwelling Unit" [Form 62-330.310(3)]; or
    b. For all other activities – "As-Built Certification and Request for Conversion to Operation Phase" [Form 62-330.310(1)].
    c. If available, an Agency website that fulfills this certification requirement may be used in lieu of the form.

7. If the final operation and maintenance entity is a third party:
    a. Prior to sales of any lot or unit served by the activity and within one year of permit issuance, or within 30 days of as-built certification, whichever comes first, the permittee shall submit, as applicable, a copy of the operation and maintenance documents (see sections 12.3 thru 12.3.4 of Volume I) as filed with the Florida Department of State, Division of Corporations, and a copy of any easement, plat, or deed restriction needed to operate or maintain the project, as recorded with the Clerk of the Court in the County in which the activity is located.
    b. Within 30 days of submittal of the as-built certification, the permittee shall submit "Request for Transfer of Environmental Resource Permit to the Perpetual Operation and Maintenance Entity" [Form 62-330.310(2)] to transfer the permit to the operation and maintenance entity, along with the documentation requested in the form. If available, an Agency website that fulfills this transfer requirement may be used in lieu of the form.

8. The permittee shall notify the Agency in writing of changes required by any other regulatory agency that require changes to the permitted activity, and any required modification of this permit must be obtained prior to implementing the changes.

9. This permit does not:

    a. Convey to the permittee any property rights or privileges, or any other rights or privileges other than those specified herein or in chapter 62-330, F.A.C.;

    b. Convey to the permittee or create in the permittee any interest in real property;

    c. Relieve the permittee from the need to obtain and comply with any other required federal, state, and local authorization, law, rule, or ordinance; or

    d. Authorize any entrance upon or work on property that is not owned, held in easement, or controlled by the permittee.

10. Prior to conducting any activities on state-owned submerged lands or other lands of the state, title to which is vested in the Board of Trustees of the Internal Improvement Trust Fund, the permittee must receive all necessary approvals and authorizations under chapters 253 and 258, F.S. Written authorization that requires formal execution by the Board of Trustees of the Internal Improvement Trust Fund shall not be considered received until it has been fully executed.

11. The permittee shall hold and save the Agency harmless from any and all damages, claims, or liabilities that may arise by reason of the construction, alteration, operation, maintenance, removal, abandonment or use of any project authorized by the permit.

12. The permittee shall notify the Agency in writing:

    a. Immediately if any previously submitted information is discovered to be inaccurate; and

    b. Within 30 days of any conveyance or division of ownership or control of the property or the system, other than conveyance via a long-term lease, and the new owner shall request transfer of the permit in accordance with rule 62-330.340, F.A.C. This does not apply to the sale of lots or units in residential or commercial subdivisions or condominiums where the stormwater management system has been completed and converted to the operation phase.

13. Upon reasonable notice to the permittee, Agency staff with proper identification shall have permission to enter, inspect, sample and test the project or activities to ensure conformity with the plans and specifications authorized in the permit.

14. If prehistoric or historic artifacts, such as pottery or ceramics, projectile points, stone tools, dugout canoes, metal implements, historic building materials, or any other physical remains that could be associated with Native American, early European, or American settlement are encountered at any time within the project site area, the permitted project shall cease all activities involving subsurface disturbance in the vicinity of the discovery. The permittee or other designee shall contact the Florida Department of State, Division of Historical Resources, Compliance Review Section (DHR), at (850)245-6333, as well as the appropriate permitting agency office. Project activities shall not resume without verbal or written authorization from the Division of Historical Resources. If unmarked human remains are encountered, all work shall stop immediately and the proper authorities notified in accordance with section 872.05, F.S. For project activities subject to prior consultation with the DHR and as an alternative to the above requirements, the permittee may follow procedures for unanticipated discoveries as set forth within a cultural resources assessment survey determined complete and sufficient by DHR and included as a specific permit condition herein.

15. Any delineation of the extent of a wetland or other surface water submitted as part of the permit application, including plans or other supporting documentation, shall not be considered binding unless a specific condition of this permit or a formal determination under rule 62-330.201, F.A.C., provides otherwise.

16. The permittee shall provide routine maintenance of all components of the stormwater management system to remove trapped sediments and debris. Removed materials shall be disposed of in a landfill or other uplands in a manner that does not require a permit under chapter 62-330, F.A.C., or cause violations of state water quality standards.

17. This permit is issued based on the applicant's submitted information that reasonably demonstrates that adverse water resource-related impacts will not be caused by the completed permit activity. If any adverse impacts result, the Agency will require the permittee to eliminate the cause, obtain any necessary permit modification, and take any necessary corrective actions to resolve the adverse impacts.

18. A Recorded Notice of Environmental Resource Permit may be recorded in the county public records in accordance with subsection 62-330.090(7), F.A.C. Such notice is not an encumbrance upon the property.

19. In addition to those general conditions in subsection (1), above, the Agency shall impose any additional project-specific special conditions necessary to assure the permitted activities will not be harmful to the water resources, as set forth in rules 62-330.301 and 62-330.302, F.A.C., Volumes I and II, as applicable, and the rules incorporated by reference in this chapter.

NOTICE OF RIGHTS

This action is final and effective on the date filed with the Clerk of the Department unless a petition for an administrative hearing is timely filed under Sections 120.569 and 120.57, F.S., before the deadline for filing a petition. On the filing of a timely and sufficient petition, this action will not be final and effective until further order of the Department. Because the administrative hearing process is designed to formulate final agency action, the subsequent order may modify or take a different position than this action.

Petition for Administrative Hearing
A person whose substantial interests are affected by the Department's action may petition for an administrative proceeding (hearing) under Sections 120.569 and 120.57, F.S. Pursuant to Rules 28-106.201 and 28-106.301, F.A.C., a petition for an administrative hearing must contain the following information:
    (a) The name and address of each agency affected and each agency's file or identification number, if known;
    (b) The name, address, any e-mail address, any facsimile number, and telephone number of the petitioner, if the petitioner is not represented by an attorney or a qualified representative; the name, address, and telephone number of the petitioner's representative, if any, which shall be the address for service purposes during the course of the proceeding; and an explanation of how the petitioner's substantial interests will be affected by the agency determination;
    (c) A statement of when and how the petitioner received notice of the agency decision;

(d) A statement of all disputed issues of material fact. If there are none, the petition must so indicate;

(e) A concise statement of the ultimate facts alleged, including the specific facts that the petitioner contends warrant reversal or modification of the agency's proposed action;

(f) A statement of the specific rules or statutes that the petitioner contends require reversal or modification of the agency's proposed action, including an explanation of how the alleged facts relate to the specific rules or statutes; and

(g) A statement of the relief sought by the petitioner, stating precisely the action that the petitioner wishes the agency to take with respect to the agency's proposed action.

The petition must be filed (received by the Clerk) in the Office of General Counsel of the Department at 3900 Commonwealth Boulevard, Mail Station 35, Tallahassee, Florida 32399-3000, or via electronic correspondence at Agency_Clerk@dep.state.fl.us. Also, a copy of the petition shall be mailed to the applicant at the address indicated above at the time of filing.

Time Period for Filing a Petition

In accordance with Rule 62-110.106(3), F.A.C., petitions for an administrative hearing by the applicant and persons entitled to written notice under Section 120.60(3), F.S., must be filed within 21 days of receipt of this written notice. Petitions filed by any persons other than the applicant, and other than those entitled to written notice under Section 120.60(3), F.S., must be filed within 21 days of publication of the notice or within 21 days of receipt of the written notice, whichever occurs first. You cannot justifiably rely on the finality of this decision unless notice of this decision and the right of substantially affected persons to challenge this decision has been duly published or otherwise provided to all persons substantially affected by the decision. While you are not required to publish notice of this action, you may elect to do so pursuant Rule 62-110.106(10)(a).

The failure to file a petition within the appropriate time period shall constitute a waiver of that person's right to request an administrative determination (hearing) under Sections 120.569 and 120.57, F.S., or to intervene in this proceeding and participate as a party to it. Any subsequent intervention (in a proceeding initiated by another party) will be only at the discretion of the presiding officer upon the filing of a motion in compliance with Rule 28-106.205, F.A.C. If you do not publish notice of this action, this waiver will not apply to persons who have not received written notice of this action.

Extension of Time

Under Rule 62-110.106(4), F.A.C., a person whose substantial interests are affected by the Department's action may also request an extension of time to file a petition for an administrative hearing. The Department may, for good cause shown, grant the request for an extension of time. Requests for extension of time must be filed with the Office of General Counsel of the Department at 3900 Commonwealth Boulevard, Mail Station 35, Tallahassee, Florida 32399-3000, or via electronic correspondence at Agency_Clerk@dep.state.fl.us, before the deadline for filing a petition for an administrative hearing. A timely request for extension of time shall toll the running of the time period for filing a petition until the request is acted upon.

Mediation

Mediation is not available in this proceeding.

FLAWAC Review
The applicant, or any party within the meaning of Section 373.114(1)(a) or 373.4275, F.S., may also seek appellate review of this order before the Land and Water Adjudicatory Commission under Section 373.114(1) or 373.4275, F.S. Requests for review before the Land and Water Adjudicatory Commission must be filed with the Secretary of the Commission and served on the Department within 20 days from the date when this order is filed with the Clerk of the Department.

Judicial Review
Once this decision becomes final, any party to this action has the right to seek judicial review pursuant to Section 120.68, F.S., by filing a Notice of Appeal pursuant to Florida Rules of Appellate Procedure 9.110 and 9.190 with the Clerk of the Department in the Office of General Counsel (Station #35, 3900 Commonwealth Boulevard, Tallahassee, Florida 32399-3000) and by filing a copy of the Notice of Appeal accompanied by the applicable filing fees with the appropriate district court of appeal. The notice must be filed within 30 days from the date this action is filed with the Clerk of the Department.

EXECUTION AND CLERKING
Executed in Orlando, Florida.
STATE OF FLORIDA DEPARTMENT OF ENVIRONMENTAL PROTECTION

Reggie Phillips
Program Administrator
Permitting and Waste Cleanup Program

Attachment(s):

1. Exhibit 1, Project Drawings and Design Specs., 14 pages
2. Standard Manatee Construction Conditions 2011, 2 pages
3. Construction Commencement Notice/Form 62-330.350(1)
4. Request for Transfer to the Perpetual Operation Entity/Form 62-330.310(2)
5. Request to Transfer Permit/Form 62-330.340(1)

CERTIFICATE OF SERVICE
The undersigned duly designated deputy clerk hereby certifies that this document and all attachments were sent on the filing date below to the following listed persons:

Jeffrey Eble, jeble@fit.edu
Brevard County, LeeAnn.McCullough-Wham@brevardfl.gov
ACOE, corpsjaxreg-nc@usace.army.mil
FFWCC, FWCConservationPlanningServices@myfwc.com
DOS, CompliancePermits@dos.state.fl.us
DEO, dcppermits@deo.myflorida.com
Angelica Sterner, FDEP, angelica.sterner@floridadep.gov
Teayann Duclos, FDEP, teayann.duclos@floridadep.gov

FILING AND ACKNOWLEDGMENT
FILED, on this date, pursuant to Section 120.52, F. S., with the designated Department Clerk, receipt of which is hereby acknowledged.

_____   August 11, 2023
Clerk   Date

VICINITY MAP

Port Canaveral

28°20'0"N
28°30'0"N
80°40'0"W
80°30'0"W
80°20'0"W

N

INDIAN RIVER LAGOON
RESTORE LAGOON INFLOW RESEARCH PILOT PROJECT

MARK | DATE | DESCRIPTION | BY

TETRA TECH
ENGINEERING BUSINESS NO. 2429
www.tetratech.com
201 EAST PINE STREET, SUITE 1000
ORLANDO, FL 32801
PHONE: (407) 839-3955 FAX: (407) 839-3790

001

File No: Restore Lagoon Inflow
File No: 43.16779-001-EI
FDEP Page 1 of 14

Copyright: Tetra Tech

NOTES:
1. SCALE 3/8"=1'
2. SURVEY COMPLETED BY OCEANSIDE SOLUTIONS ON MARCH 31, 2021
3. CONTOURS DISPLAYED AT 1-FT CONTOUR INTERVAL

FOR REGULATORY REVIEW ONLY - NOT FOR CONSTRUCTION

SURVEY PLAN VIEW (NAVD88)

INDIAN RIVER LAGOON

RESTORE LAGOON INFLOW RESEARCH
PILOT PROJECT

MARK	DATE	DESCRIPTION	BY

Drawn By:
Designed By:
Checked By:
Project No:00-WTS-41000J3

002

Copyright: Tetra Tech

TETRA TECH
ENGINEERING BUSINESS NO. 2429
www.tetratech.com
201 EAST PINE STREET, SUITE 1000
ORLANDO, FL 32801
PHONE: (407) 839-3955 FAX: (407) 839-3790
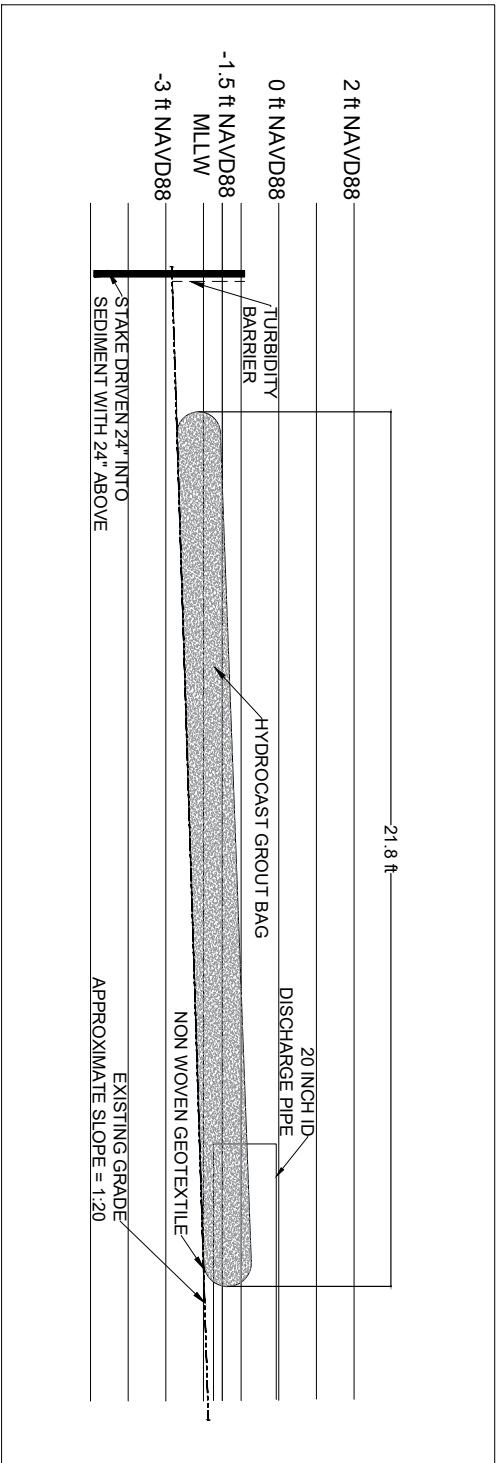
FOR REGULATORY REVIEW ONLY - NOT FOR CONSTRUCTION

VERTICAL DATUM

Datums for 8721604, Trident Pier, Port Canaveral, FL
All figures in feet relative to MLLW

Datums:
- MSL: 1.88
- NAVD88: 2.83
- MHW: 3.58
- MHHW: 3.93
- MLW: 0.17
- MLLW: 0
- MTL: 1.87
- DTL: 1.88
- DHQ: 0.35
- DLQ: 0.17
- MN: 3.4
- GT: 3.92

NOAA / NOS / CO-OPS

MARK	DATE	DESCRIPTION	BY

INDIAN RIVER LAGOON

RESTORE LAGOON INFLOW RESEARCH PILOT PROJECT

Project No:100-xWTt5-r41000/03

Designed By:
Drawn By:
Checked By:

003

TETRA TECH
ENGINEERING BUSINESS NO. 2429
www.tetratech.com
201 EAST PINE STREET, SUITE 1000
ORLANDO, FL 32801
PHONE: (407) 839-3955 FAX: (407) 839-3790

3/30/2023 11:03:16 AM - C:\USERS\BENKO\DOCUMENTS\RLI\RLI PHASE 3 PLAN SET.DWG - BEN KOMITA

FOR REGULATORY REVIEW ONLY - NOT FOR CONSTRUCTION

NOTE:
1. SCALE ¾" = 1'
2. SURVEY COMPLETED BY OCEANSIDE SOLUTIONS ON MARCH 31, 2021
3. CONTOURS DISPLAYED AT 1-FT CONTOUR INTERVAL

SITE PLAN

SHORELINE

DETAIL B

SHORELINE

DETAIL A

RAMP

ENTRANCE GATE

ROADWAY

DETAIL C

EXISTING FENCELINE

FENDER WALL

INDIAN RIVER LAGOON

RESTORE LAGOON INFLOW RESEARCH
PILOT PROJECT

MARK	DATE	DESCRIPTION	BY

Project No:100-WTS-141000.03
Designed By:
Drawn By:
Checked By:

004

Bar Measures 1 inch

TETRA TECH
ENGINEERING BUSINESS NO. 2429
www.tetratech.com
201 EAST PINE STREET, SUITE 1000
ORLANDO, FL 32801
PHONE: (407) 839-3955 FAX: (407) 839-3790

Copyright: Tetra Tech

3/30/2023 11:03:21 AM - C:\USERS\BENKO\DOCUMENTS\RLI\RLI PHASE 3 PLAN SET.DWG - BEN KOMITA

DETAIL A INTAKE PLAN

Ø2.3 ft
Ø1.7 ft

20.9 ft
20.9 ft

9.3 ft

0.8 ft
0.8 ft

6.7 ft
6.7 ft

DETAIL A1

ELECTRIC DRIVE UNIT

5.3 ft

8.5 ft

DETAIL A2

FENDER WALL

INDIAN RIVER LAGOON

RESTORE LAGOON INFLOW RESEARCH
PILOT PROJECT

MARK	DATE	DESCRIPTION	BY

Project No.:30x\HTc-741000.03

Drawn By:
Designed By:
Checked By:

005

Bar Measures 1 inch

Copyright: Tetra Tech

TETRA TECH
ENGINEERING BUSINESS NO. 2429

www.tetratech.com
201 EAST PINE STREET, SUITE 1000
ORLANDO, FL 32801
PHONE: (407) 839-3955 FAX: (407) 839-3790

3/30/2023 11:03:25 AM - C:\USERS\BENKO\DOCUMENTS\RLI\RLI PHASE 3 PLAN SET.DWG - BEN KOMITA

FOR REGULATORY REVIEW ONLY - NOT FOR CONSTRUCTION

DETAIL A1 - INTAKE SIDE VIEW

Elevation

Station

SEE DETAIL A3 FOR
INTAKE SCREEN DETAILS

0.75 ft NAVD88 MHW
0 ft NAVD88
-2.83 ft MLW
-5 ft NAVD88
-10 ft NAVD88
-12 ft NAVD88

5 ft NAVD88
10 ft NAVD88
13 ft NAVD88

HENDRICK PASSIVE
DRUM INTAKE SCREEN

10 INCH TIP
TREATED
TIMBER PILE
(TYP.)

0.8 ft

20.9 ft

PILE DEPTHS TO BE DETERMINED
BY RESULTS OF SPT BORING

EXISTING GRADE

PIPE ON GRADE

INDIAN RIVER LAGOON

RESTORE LAGOON INFLOW RESEARCH
PILOT PROJECT

MARK	DATE	DESCRIPTION	BY

Project No.:30x/Tb-741000.03
Designed By:
Drawn By:
Checked By:

006

Bar Measures 1 inch

Copyright: Tetra Tech

TETRA TECH
ENGINEERING BUSINESS NO. 2429
www.tetratech.com
201 EAST PINE STREET, SUITE 1000
ORLANDO, FL 32801
PHONE: (407) 839-3955 FAX: (407) 839-3790

3/30/2023 11:03:30 AM - C:\USERS\BENKO\DOCUMENTS\RLI\RLI PHASE 3 PLAN SET.DWG - BEN KOMITA

FOR REGULATORY REVIEW ONLY - NOT FOR CONSTRUCTION

DETAIL A2 - PUMP POWER UNIT

PUMP NOTES:
1. MWI HMF320 HYDRAFLO PUMP
2. 2400E ELECTRIC DRIVE UNIT WITH 200HP ELECTRIC MOTOR-SKID CONFIGURATION
3. NEMA 4X STAINLESS AUTO START/STOP CONTROL PANEL WITH FLOATS

	MARK	DATE	DESCRIPTION		BY

INDIAN RIVER LAGOON

RESTORE LAGOON INFLOW RESEARCH PILOT PROJECT

Project No:100-WTG-T41000-03
Designed By:
Drawn By:
Checked By:

007

Copyright: Tetra Tech

TETRA TECH
ENGINEERING BUSINESS NO. 2429
www.tetratech.com
201 EAST PINE STREET, SUITE 1000
ORLANDO, FL 32801
PHONE: (407) 839-3955 FAX: (407) 839-3790

FOR REGULATORY REVIEW ONLY - NOT FOR CONSTRUCTION

DETAIL A3 - INTAKE SCREEN DETAILS

48.0 in

30.0 in

84.0 in

DRUM INTAKE SCREEN
TOP VIEW

Ø48.0 in

Ø30.0 in

NOTE:
1. DRUM STYLE INTAKE SCREEN DESIGNED AND MANUFACTURED BY HENDRICK SCREEN SUPPLY COURTESY OF RC BEACH AND ASSOCIATES.
2. THE SURFACE WIRE SHALL BE HENDRICK SCREEN SUPPLY CO. NO. 69 WEDGE WIRE. THE SCREEN SLOT OPENING SHALL BE .125" THE OPEN AREA FOR THIS SLOT OPENING SHALL BE 64%. SLOT SIZE SHALL BE CONTROLLED AND CONTINUOUSLY MONITORED DURING MANUFACTURE.
3. THE INTAKE SCREEN CAPACITY SHALL BE 7025 GPM AT A MAXIMUM LOCAL THROUGH SLOT VELOCITY DUE TO WATER REMOVAL NOT TO EXCEED 0.5 FPS AT THE DESIGN FLOW RATE. THE PRESSURE DROP THROUGH THE SURFACE OF THE CLEAN SCREEN SHALL NOT EXCEED 0.1 PSI THE TOTAL PRESSURE DROP THROUGH THE DRUM ASSEMBLY SHALL NOT EXCEED 1.0 FOOT OF WATER.
4. THE SCREEN ASSEMBLY SHALL BE MANUFACTURED OF CORROSION RESISTANT METAL, AISI TYPE 316 STAINLESS STEEL. THE MAIN OUTLET SHALL BE A 30-INCH WITH A PLATE AS REQUIRED FOR CONNECTION TO THE STRUCTURE.

FOR REGULATORY REVIEW ONLY - NOT FOR CONSTRUCTION

DETAIL A4 - BORING LOCATION

PROPOSED BORING LOCATION

ELECTRIC DRIVE UNIT

Ø2.3 ft
Ø1.7 ft
Ø3.1 ft

20.9 ft
20.3 ft
0.8 ft
0.8 ft
6.7 ft
6.7 ft

5.3 ft
8.5 ft

NOTE:
1. BORING LOCATION MAY BE MOVED UP TO 25' FROM THE DESIGNATED LOCATION TO ALLOW FOR CLEARANCE FROM IDENTIFIED SUBSURFACE UTILITIES, SURFACE OR SUBSURFACE OBSTRUCTIONS, OR DIRECTION FROM THE USACE.

2. PRIOR TO DRILLING, A SUNSHINE ONE-CALL UTILITY LOCATION REQUEST WILL BE SUBMITTED. A SEPARATE PRIVATE UTILITY LOCATION SERVICE WILL ALSO BE UTILIZED TO IDENTIFY ANY KNOWN SUBSURFACE UTILITIES OR ANOMALIES. IT IS REQUESTED THAT USACE IDENTIFY ANY KNOWN SUBSURFACE UTILITIES IN THE VICINITY OF THE PROPOSED BORING.

3. THE GEOTECHNICAL SPT BORING WILL BE DRILLED USING A PROCEDURE SIMILAR TO THE STANDARD PENETRATION TEST OUTLINED IN ASTM D-1586. THE BORING WILL BE SAMPLED AT 18-INCH INTERVALS TO 10 FEET DEEP AND AT 5-FOOT INTERVALS BELOW 10 FEET. EACH SAMPLE WILL BE REMOVED FROM THE SAMPLER IN THE FIELD AND THEN EXAMINED AND VISUALLY CLASSIFIED BY OUR CREW CHIEF. REPRESENTATIVE PORTIONS WILL BE SEALED AND PACKAGED FOR TRANSPORTATION TO LABORATORY FOR FURTHER ANALYSIS, AS REQUIRED. WATER LEVEL OBSERVATIONS WILL BE MADE IN THE BOREHOLE DURING THE DRILLING OPERATION. UPON COMPLETION OF DRILLING, THE BORING WILL BE GROUTED WITH NEAT GROUT CEMENT.

MARK	DATE	DESCRIPTION	BY

INDIAN RIVER LAGOON

RESTORE LAGOON INFLOW RESEARCH PILOT PROJECT

Project No.:100-WTR-2410003.03
Drawn By:
Designed By:
Checked By:

009

Bar Measures 1 inch

Copyright: Tetra Tech

TETRA TECH
ENGINEERING BUSINESS NO. 2429

www.tetratech.com

201 EAST PINE STREET, SUITE 1000
ORLANDO, FL 32801
PHONE: (407) 839-3955 FAX: (407) 839-3790

3/30/2023 11:03:46 AM - C:\USERS\BENKO\DOCUMENTS\RLI\RLI PHASE 3 PLAN SET.DWG - BEN KOMITA

RAMP

ENTRANCE GATE

20.0 ft

25.4 ft

DETAIL B - PIPELINE ROAD CROSSING

20 ft

25.4 ft

1.9 ft

2 ft

20 ft

NOTE:
1. SCALE 1" = 1'
2. CAPACITY IS 32,000 LBS PER AXLE (HS-20 LOADING)
3. RAMP DESIGNED AND MANUFACTURED BY BLUFF MANUFACTURING

FOR REGULATORY REVIEW ONLY - NOT FOR CONSTRUCTION

MARK	DATE	DESCRIPTION	BY

INDIAN RIVER LAGOON

RESTORE LAGOON INFLOW RESEARCH PILOT PROJECT

Project No:100-NTTS-T410063.03
Designed By:
Drawn By:
Checked By:

Copyright: Tetra Tech

Bar Measures 1 inch

010

3/30/2023 11:03:51 AM - C:\USERS\BENKO\DOCUMENTS\RLI\RLI PHASE 3 PLAN SET.DWG - BEN KOMITA

FOR REGULATORY REVIEW ONLY - NOT FOR CONSTRUCTION

DETAIL C - OUTFLOW
PLAN VIEW

OAK STAKES

STAKED TURBIDITY BARRIER

HYDROCAST GROUT BAG

HYDROTEX ARTICULATING BLOCK FABRIC FORMED CONCRETE MATTRESS (AB300)

6.0 ft

21.8 ft

2.0 ft

8.0 ft

SIDE VIEW

2 ft NAVD88

0 ft NAVD88

-1.5 ft NAVD88 MLLW

-3 ft NAVD88

TURBIDITY BARRIER

STAKE DRIVEN 24" INTO SEDIMENT WITH 24" ABOVE

HYDROCAST GROUT BAG

21.8 ft

20 INCH ID DISCHARGE PIPE

NON WOVEN GEOTEXTILE

EXISTING GRADE APPROXIMATE SLOPE = 1:20

NOTE:
1. THE STAKED TURBIDITY BARRIER SHALL UTILIZE A BELTED SILT RETENTION FENCE (PRIORITY 1)

MARK	DATE	DESCRIPTION		BY

INDIAN RIVER LAGOON

RESTORE LAGOON INFLOW RESEARCH PILOT PROJECT

Drawn By:
Designed By:
Checked By:

Project No: 100-WTS-CF1000.03

011

3/30/2023 11:03:55 AM - C:\USERS\BENKO\DOCUMENTS\RLI\RLI PHASE 3 PLAN SET.DWG - BEN KOMITA

DETAIL A1 - OUTFALL CROSS SECTION WITH MANATEE SCREEN DETAIL

HYDROTEX ARTICULATING BLOCK FABRIC FORMED CONCRETE MATTRESS (AB300)

2 ft NAVD88

0 ft NAVD88

-1.5 ft NAVD88

-3 ft NAVD88

MLLW

HYDROCAST GROUT BAG

DOWELS-TYPE REQUIRED BY ENGINEER

NON-WOVEN GEOTEXTILE

EXISTING GRADE

$\frac{1}{2}$" STEEL ROD

FLANGE

$\frac{3}{4}$"BOLT HOLE

20" PIPE

NOTE:
1. SCALE 1-$\frac{1}{2}$" = 1'
2. DIMENSIONS FOR MANATEE GRATE HAVE BEEN SELECTED ACCORDING TO FOOT INDEX 280 STANDARDS

FOR REGULATORY REVIEW ONLY - NOT FOR CONSTRUCTION

Designed By:
Drawn By:
Checked By:
Project No.:100-WTP-141000.03
INDIAN RIVER LAGOON
RESTORE LAGOON INFLOW RESEARCH PILOT PROJECT
MARK | DATE | DESCRIPTION | BY
012
Copyright: Tetra Tech
TETRA TECH
ENGINEERING BUSINESS NO. 2429
www.tetratech.com
201 EAST PINE STREET, SUITE 1000
ORLANDO, FL 32801
PHONE: (407) 839-3955 FAX: (407) 839-3790

3/30/2023 11:04:01 AM - C:\USERS\BENKO\DOCUMENTS\RLI\RLI PHASE 3 PLAN SET.DWG - BEN KOMITA

NOTE:
1. MARINE BIOLOGICAL RESOURCE SURVEY
COMPLETED JUNE 2021

FOR REGULATORY REVIEW ONLY - NOT FOR CONSTRUCTION

BIOLOGICAL SURVEYS

LEGEND

× SHOAL GRASS (LESS THAN 1 M^2)

VEGETATION

BLACK MANGROVE

INDIAN RIVER LAGOON

RESTORE LAGOON INFLOW RESEARCH PILOT PROJECT

MARK | DATE | DESCRIPTION | BY

Project No:100-WTS-410003/3

Drawn By:
Designed By:
Checked By:

013

TETRA TECH
ENGINEERING BUSINESS NO. 2429
www.tetratech.com
201 EAST PINE STREET, SUITE 1000
ORLANDO, FL 32801
PHONE: (407) 839-3955 FAX: (407) 839-3790

Copyright: Tetra Tech

File No: Restore Lagoon Inflow   File No: 431679-001-EI

STANDARD MANATEE CONDITIONS FOR IN-WATER WORK
2011

The permittee shall comply with the following conditions intended to protect manatees from direct project effects:

a.   All personnel associated with the project shall be instructed about the presence of manatees and manatee speed zones, and the need to avoid collisions with and injury to manatees. The permittee shall advise all construction personnel that there are civil and criminal penalties for harming, harassing, or killing manatees which are protected under the Marine Mammal Protection Act, the Endangered Species Act, and the Florida Manatee Sanctuary Act.

b.   All vessels associated with the construction project shall operate at "Idle Speed/No Wake" at all times while in the immediate area and while in water where the draft of the vessel provides less than a four-foot clearance from the bottom. All vessels will follow routes of deep water whenever possible.

c.   Siltation or turbidity barriers shall be made of material in which manatees cannot become entangled, shall be properly secured, and shall be regularly monitored to avoid manatee entanglement or entrapment. Barriers must not impede manatee movement.

d.   All on-site project personnel are responsible for observing water-related activities for the presence of manatee(s). All in-water operations, including vessels, must be shutdown if a manatee(s) comes within 50 feet of the operation. Activities will not resume until the manatee(s) has moved beyond the 50-foot radius of the project operation, or until 30 minutes elapses if the manatee(s) has not reappeared within 50 feet of the operation. Animals must not be herded away or harassed into leaving.

e.   Any collision with or injury to a manatee shall be reported immediately to the Florida Fish and Wildlife Conservation Commission (FWC) Hotline at 1-888-404-3922. Collision and/or injury should also be reported to the U.S. Fish and Wildlife Service in Jacksonville (1-904-731-3336) for north Florida or Vero Beach (1-772-562-3909) for south Florida, and to FWC at ImperiledSpecies@myFWC.com

f.   Temporary signs concerning manatees shall be posted prior to and during all in-water project activities. All signs are to be removed by the permittee upon completion of the project. Temporary signs that have already been approved for this use by the FWC must be used. One sign which reads *Caution: Boaters* must be posted. A second sign measuring at least 8 ½" by 11" explaining the requirements for "Idle Speed/No Wake" and the shut down of in-water operations must be posted in a location prominently visible to all personnel engaged in water-related activities. These signs can be viewed at MyFWC.com/manatee. Questions concerning these signs can be sent to the email address listed above.

CAUTION: MANATEE HABITAT

IDLE SPEED / NO WAKE

All project vessels

When a manatee is within 50 feet of work all in-water activities must

SHUT DOWN

Report any collision with or injury to a manatee:

Wildlife Alert:

1-888-404-FWCC(3922)

cell *FWC or #FWC

CONSTRUCTION COMMENCEMENT NOTICE

Instructions: In accordance with Chapter 62-330.350(1)(d), F.A.C., complete and submit this form at least 48 hours prior to commencement of activity authorized by permit.

Permit No. _____   Application No. _____

Project
Name _____   Phase _____

Construction of the system authorized by the above referenced Environmental Resource

Permit and Application, is expected to commence on _____ , 20 _____

and will have an estimated completion date of _____ , 20 _____

PLEASE NOTE: If the actual construction commencement date is not known within 30 days of issuance of the permit, District staff should be so notified in writing. As soon as a construction commencement date is known, the permittee shall submit a completed construction commencement notice form.

_____   _____
Permittee's or Authorized Agent's Signature   Company

_____   _____   _____
Print Name   Title   Date

_____   _____
E-mail   Phone Number

Request for Transfer of
Environmental Resource Permit
to the Perpetual Operation and Maintenance Entity

Instructions: Complete this form to transfer ~~to~~ the permit to the operation and maintenance entity. This form can be completed concurrently with, or within 30 days of approval of, the As-Built Certification and Request for Conversion to Operation Phase (Form 62-330.310(1)). Please include all documentation required under Section 12.2.1(b) of Applicant's Handbook Volume I (see checklist below). **Failure to submit the appropriate final documents will result in the permittee remaining liable for operation and maintenance of the permitted activities.**

Permit No.: _____   Application No(s): _____

Project Name: _____   Phase (if applicable): _____

A. Request to Transfer: The permittee requests that the permit be transferred to the legal entity responsible for operation and maintenance (O&M).

By: _____   _____
      Signature of Permittee   Name and Title

      _____   _____
      Company Name   Company Address

      _____   _____
      Phone/email address   City, State, Zip

B. Agreement for System Operation and Maintenance Responsibility: The below-named legal entity agrees to operate and maintain the works or activities in compliance with all permit conditions and provisions of Chapter 62-330, Florida Administrative Code (F.A.C.) and Applicant's Handbook Volumes I and II.

> The operation and maintenance entity does not need to sign this form if it is the same entity that was approved for operation and maintenance in the issued permit.

Authorization for any proposed modification to the permitted activities shall be applied for and obtained prior to conducting such modification.

By: _____   _____
      Signature of Representative of O&M Entity   Name of Entity for O&M

      _____   _____
      Name and Title   Address

      _____   _____
      Email Address   City, State, Zip

      _____   _____
      Phone   Date

Enclosed are the following documents, as applicable:

☐ Copy of recorded transfer of title to the operating entity for the common areas on which the stormwater management system is located (unless dedicated by plat)
☐ Copy of all recorded plats
☐ Copy of recorded declaration of covenants and restrictions, amendments, and associated exhibits
☐ Copy of filed articles of incorporation (if filed before 1995)
☐ ~~A~~ Completed documentation that the operating entity meets the requirements of Section 12.3 of Environmental Resource Permit Applicant's Handbook Volume I. (Note: this is optional, but aids in processing of this request)

Request to Transfer
Environmental Resource Permit

Instructions: To be completed, executed, and submitted by the new owner to the Agency within 30 days after any transfer of ownership or control of the real property where the permitted activity is located.

Use of this form is not required when a valid permit is in the operation and maintenance phase. In such case, the owner must notify the Agency in writing within 30 days of a change in ownership or control of the entire real property, project, or activity covered by the permit. The notification may be by letter or e-mail, or through use of this form, and must be sent to the office that issued the permit. A processing fee is not required for this notice. The permit shall automatically transfer to the new owner or person in control, except in cases of abandonment, revocation, or modification of a permit as provided in Sections 373.426 and 373.429, F.S. (2013). If a permittee fails to provide written notice to the Agency within 30 days of the change in ownership or control, or if the change does not include the entire real property or activity covered by the permit, then the transfer must be requested using this form.

Permit No: Application   Acres to be Transferred:
                               No(s).:

Permitted Project:

Proposed Project Name (if different):

Phase of Project (if applicable):

I hereby notify the Agency that I have acquired ownership or control of the land on which the permitted system is located through the sale or other legal transfer of the land. By signing below, I hereby certify that I have sufficient real property interest or control in the land in accordance with subsection 4.2.3(d) of Applicant's Handbook Volume I; attached is a copy of my title, easement, or other demonstration of ownership or control in the land, including any revised plats, as recorded in the Public Records. I request that the permit be modified to reflect that I agree to be the new permittee. By so doing, I acknowledge that I have examined the permit terms, conditions, and drawings, and agree to accept all rights and obligations as permittee, including agreeing to be liable for compliance with all of the permit terms and conditions, and to be liable for any corrective actions required as a result of any violations of the permit after approval of this modification by the Permitting Agency. Also attached are copies of any recorded restrictive covenants, articles of incorporation, and certificate of incorporation that may have been changed as a result of my assuming ownership or control of the lands. As necessary, I agree to furnish the Agency with demonstration that I have the ability to provide for the operation and maintenance of the system for the duration of the permit in accordance with subsection 12.3 of Applicant's Handbook Volume I.

Name of Proposed Permittee:

Mailing Address:

City: State: Zip:

Telephone: E-mail:

_____   _____
Signature of Proposed Permittee   Date:

_____
Name and Title

Enclosures:

☐ Copy of title, easement, or other demonstration of ownership or control in the land, as recorded in the Public Records

☐ Copy of current plat(s) (if any), as recorded in the Public Records

☐ Copy of current recorded restrictive covenants and articles of incorporation (if any)

☐ Other

Appendix B   Task 2 – Hydrologic Modeling Report

Restore Lagoon Inflow Research (Phase 3)
Final Report
Task 2: Hydrologic Modeling

PREPARED FOR

Florida Department of Education
325 West Gaines Street
Tallahassee, FL 32399

PREPARED BY

Gary Zarillo
Florida Institute of Technology
150 West University Boulevard
Melbourne, FL 32091

FLORIDA TECH

July 2023

Acknowledgements

We would like to thank the following Florida State Legislators, regulatory permitting agencies, and the organizations that have consulted on the project in support of lagoon science. We thank the many students for their dedicated effort and passion that contributed to this.

Project Staffing (includes part-time and full-time project staff)

Faculty – Gary A. Zarillo, Ph.D., P   Graduate Assistant – Ahsan Habib

Highlights

- Phase 3 hydrologic modeling evaluated the potential influence on water quality in a confined Banana River compartment from small inflows rates pumped from an intake located at the west end of Port Canaveral.
- Model error for salinity, temperature and dissolved oxygen are within an acceptable range at 13%, 5.7%, and 9.2%, respectively.
- Model error for total nitrogen and phosphorus at Banana River sampling sites are within acceptable range, respectively differing from observed levels by a range of 0.04-0.05 milligrams per liter (mg/L) and 0.0028-0.003 mg/L.
- Model pilot inflow test cases included no inflow, 0.5 cubic meters per second (m^3/s) inflow, and 1.0m^3/s inflow from Port Canaveral, and 0.5 m^3/s inflow from the coastal ocean.
- No large changes in salinity, water temperature, or water quality constituent concentrations were predicted that could produce a significant negative impact during the pilot inflow project.
- The most apparent impact of prescribed pilot inflow rates is in the bottom model water layer in the immediate vicinity of the Banana River outfall site, where the concentration of dissolved oxygen is predicted to increase.
- Total nitrogen and phosphorus improvements from the hypothetical pilot inflow rates are small but measurable in the model predictions.
- Future modeling and monitoring efforts would benefit from more continuous collection of water quality data for both the Banana River and within Port Canaveral.

Contents

List of Figures

List of Tables

List of Acronyms

ADCIRC	Advanced Circulation
AOS	Weather service automated surface observations system
BRL	Banana River Lagoon
CE-QUAL-ICM	Corps of Engineers Integrated Compartment Water Quality Model
cm	centimeter
deg. °C	Degrees Celsius
DO	Dissolved Oxygen
EFDC	Environmental Fluid Dynamics Code
FDEP	Florida Department of Environmental Protection
FAU-HBOI	Florida Atlantic University Harbor Branch Oceanographic Institute
HEM3D	Hydrodynamic-Eutrophication Model Three-Dimensional
HYCOM	Hybrid Coordinate Model
IRL	Indian River Lagoon
Kg/d	kilograms per day
km	Kilometer
LOBO	Land/Ocean Biogeochemical Observatory

m^3/sec	Cubic Meters Per Second
mg/L	Milligrams Per Liter
NAVD88	North American Vertical Datum of 1988
NOAA	National Oceanic and Atmospheric Administration
POM	particulate organic matter
PSU	practical salinity units
RMSE	Root Mean Square Error
SJRWMD	Saint Johns River Water Management District
SWIL	Spatial Watershed Iterative Loading
TN	Total Nitrogen
TP	Total Phosphorus
µg/L	micrograms per liter
USGS	U.S. Geological Survey

1 Task Summary: Hydrodynamic and Water Quality Model

The hypothesis of this project states that controlled water exchanges from the coastal ocean into the Banana can be engineered to improved water quality within local compartments of the Indian River lagoon (IRL). This hypothesis is consistent with known historical exchanges across the east central Florida coast into the IRL system and the extensive geomorphic evidence for temporary breaches in the barrier island prior to the historical record. A second project hypothesis is that salinity, water temperature, and water level fluctuations generated by an engineered inflow will be small compared to the seasonal fluctuations and event scale fluctuations experienced in the IRL The Phase 3 model deliverables have a goal to directly support the permit application for implementing temporary pumping of ocean water into the north Banana River. The fundamental permit-related question to be answered by modeling in combination with data sets to be collected is also the scientific question: What is the potential impact of enhanced flow on water quality and integrity of the IRL ecosystem?

1.1 Objectives and Tasks

- Expand the Phase II hydrodynamic and water quality model to cover boundary conditions through mid-2022.
- Assemble supporting watershed inputs to mid-2022 .
- Establish inflow boundary conditions at Port Canaveral from ongoing water quality monitoring reports compiled by Port Canaveral.
- Update model boundary conditions.
- Refine computational model grid to accommodate inflow locations at Port Canaveral.
- Model validation based on the existing database of physical and water quality conditions augmented by ongoing measured environmental nutrient data sets and dissolved oxygen data sets.
- Consult with project geochemical team members with respect to nutrient and dissolved oxygen inputs to the water quality model, as well as model calibration.
- Conduct model predictions of water quality conditions in Banana River and IRL with and without enhanced inflows at rates prescribed by the pilot project permit.
- Conduct model predictions of water quality conditions in Banana River and IRL with and without enhanced inflows at rates that could be associated with a full-scale project.
- Permit directed model runs designated by the Project Team and Tetra Tech designed to anticipate permit requirements.
- Delivery of model predictions of salinity, water temperature and water quality to support analyses other project team members.
- Update the ongoing archive of all model output data that can be interrogated to provide permit requirements and address RAIs as needed.
- Generate a final report and associated graphics describing the results of environmental and coastal processes modeling.

1.2 Approach

The Enhanced Fluid Dynamics Code (EFDC)/Hydrodynamic Eutrophication Model Three-Dimensional (HEM3D) coupled hydrodynamic and water quality models were applied to quantity the potential water quality results of the Enhanced Inflow Pilot Project, which will create a temporary inflow to the Banana River from the west compartment of Port Canaveral. The intake location of the project will be a location just to the east of the Port Canaveral Lock system. The U.S. Environmental Protection Agency-supported EFDC/HEM3D includes features and capabilities that make it superior and more applicable to shallow estuarine environments than other models. The model computational grid area extends from Ponce de Leon Inlet north of the Mosquito Lagoon into the IRL compartments extending to the Fort Pierce Inlet. This multi-parameter finite difference model represents estuarine flow and material transport in three dimensions and has been extensively applied to shallow estuarine environments in Florida and other coastal states. For this Phase 3 project refinements were made to the model computational grid to resolve the pump inflow area in the Banana River on the south side of Port Canaveral. Model boundary conditions were updated to include conditions into mid-2022. The final model runs to test various pumping scenarios covered the period from January 2021 through May of 2022.

Updates to the modeling scheme to produce water quality model boundary conditions include updated inputs from Spatial Watershed Iterative Loading (SWIL) model (Listopad, 2015). The SWIL model was developed for Florida Department of Environmental Protection (FDEP) to incorporate more available data, recent conditions, and temporally fine datasets to support predictions of nutrient inflows from the IRL sub-basins. This, in combination with the other benthic flux nutrient boundary conditions, provided by Dr. Austin Fox's team, provide a more complete representation of the IRL nutrient budget and facilitate sensitivity tests based on the proposed enhanced inflows to the Banana River Lagoon (BRL).

An update of model verification was also completed consisting of model runs of the previous calibrated model to test model performance for the new time period of model production runs. This process is termed model validation, which consists of model-observation comparisons without any further adjustment of model tuning parameters.

Model production runs consisted of three cases consisting of the existing configuration of no enhanced inflows, followed by two inflow cases involving inflows of 0.5 m^3/s and 1.0 m^3/s. A final model run includes hypothetical inflows originating from the coastal ocean that assumed lower nutrient concentrations and higher dissolved oxygen concentrations compared to the ambient water quality of Port Canaveral. The water quality of specified inflows from Port Canaveral were set from monthly data from the ongoing monthly environmental surveys by the Canaveral Port Authority. Model results for each case were compared for predicted changes in salinity, water temperature, dissolved oxygen (DO) and concentrations of water column total nitrogen (TN) and total phosphorus (TP).

1.3 Model Setup

1.3.1 Grid Refinement

Figure 1 shows the overall extent of the IRL model computational grid, from Ponce de Leon Inlet in the north to just south of Ft. Pierce Inlet at the south end. The original model grid model grid included 10,123 active computational cells in the horizontal and five layers in the vertical dimension. Layer 1 represents the lower part of the water column and Layer 5 represents the top of the water column. Each layer represents 20% of the water column. Under Phase 3 of the project

additional refinements to the model grid were completed to improve spatial resolution in the Banana River at the location of the proposed inflow location to the west of Port Canaveral (**Figure 2**). The model grid now includes a total of 10,123 computational cells.
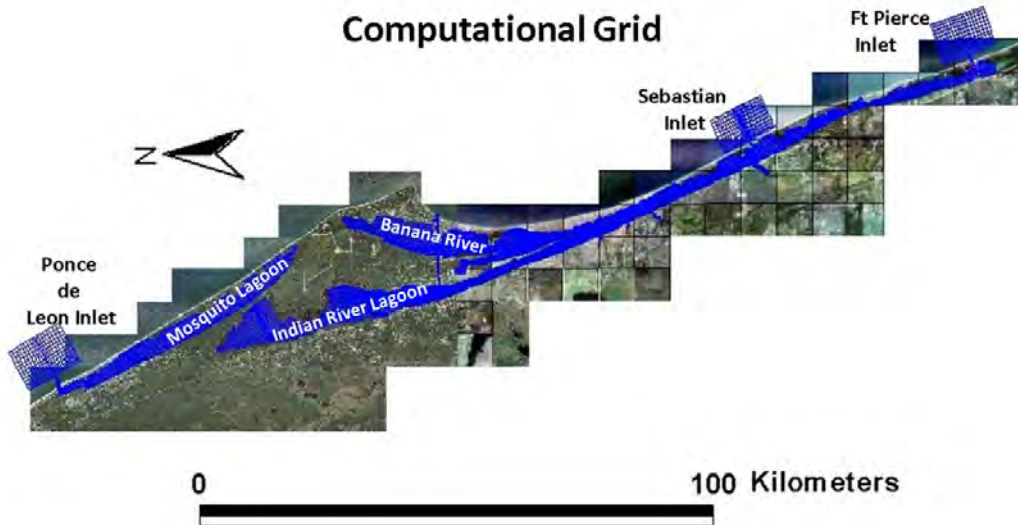

Figure 1. Computational model grid extending from Ponce de Leon Inlet to Ft Pierce Inlet, FL.
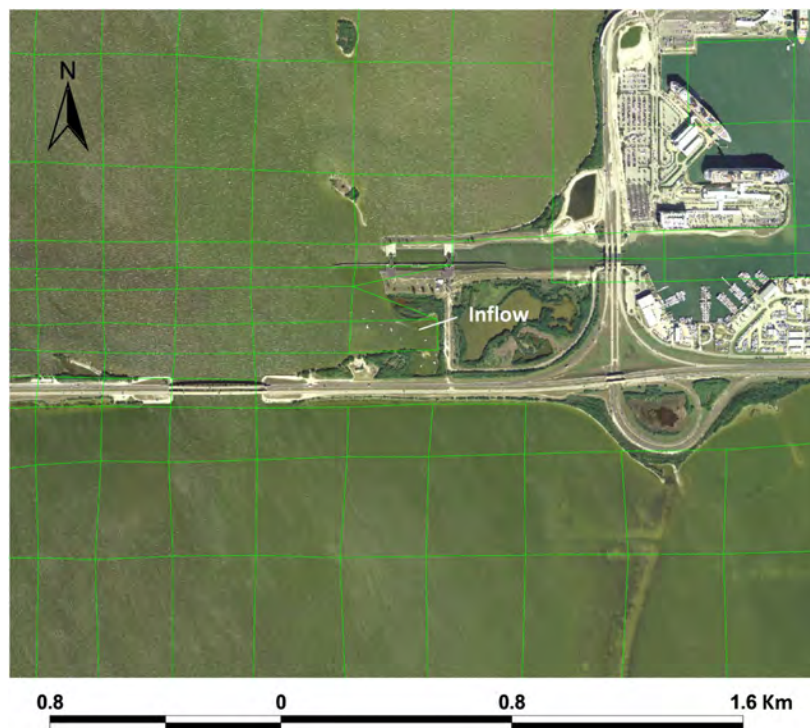

Figure 2. Computational grid refinements in the Banana River to accommodate an inflow boundary condition from Port Canaveral.

1.3.2 Hydrodynamic Boundary Conditions

The model grid includes about two-thirds of the IRL system extending from Ponce de Leon Inlet to Ft. Pierce Inlet. The initial model grid as reports includes all compartments of the IRL system: Mosquito Lagoon, BRL, and the main body of the IRL from Titusville to the vicinity of Ft. Pierce Inlet. In the Cape Canaveral area of the model additional spatial resolution was added to the model grid to conform to the small basin where the pilot project pumping outflow infrastructure will be located. **Figure 2** shows details of model grid refinement and the location of the inflow boundary condition from Port Canaveral.

The major hydrodynamic model input files are listed in **Table 2**. For each of the of the model time series files listed in **Table 2** the complete available data record is loaded in the model boundary input file. Although the available data sets are generally of high quality as they have been quality controlled leveled to North American vertical Datum of 1988 (NAVD88) with respect to water level, they are limited in time span, especially for the model boundaries that extend into the coastal ocean at Ponce de Leon, Sebastian Inlet, and Fort Pierce Inlet.

Table 1. Data providers, data type, and data retrieval sites of data used in the hydrodynamic model setup.

Data Source	Data Type	Data Retrieval Site
St. Johns River Water Management District (SJRWMD)	Water Quality and Meteorologic	http://webapub.sjrwmd.com/agws10/edqt/)
	Hydrologic	http://webapub.sjrwmd.com/agws10/hdsnew/map.html
U.S. geological Survey (USGS)	Hydrologic	https://waterdata.usgs.gov/fl/nwis/rt
Florida Atlantic University Harbor Branch Oceanographic Institute (FAU-HBOI) Land/Ocean Biogeochemical Observatory (LOBO)	Water Quality	http://fau-hboi.loboviz.com/ge/
National Weather Service automated surface observation systems(AOS)	Meteorologic	https://www.weather.gov/

A major input to the air-sea interaction dynamics in the EFDC model is time series of meteorological data provided by the national Weather service automated surface observations system (AOS). Time series of wind velocity, air temperature, precipitation rates, atmospheric pressure, cloud cover and other parameter data are provided by five AOS stations located within the model domain. This allows up to five atmospheric sub-zones to be established within model inputs that will improve the accuracy of model atmospheric forcing (**Figure 3**).

Table 2. Major EFDC input files.

Input File	Description
efdc.inp	Main control file
aser.inp	Atmospheric forcing time-series file.
cell.inp	Horizontal cell type identifier file.
dxdy.inp	File specifying horizontal grid spacing or metrics, depth, bottom elevation, bottom roughness and vegetation classes for either Cartesian or curvilinear orthogonal horizontal grids.
Dye.inp	Initial numerical tracer assigned to selected model cells
lxly.inp	File specifying horizontal cell center coordinates and cell orientations.
Moddydy.inp	File specifying sub-grid cell dimension modification
pser.inp	Water level time series
qser.inp	Volumetric source-sink time-series file. including groundwater (inflow-outflow).
salt.inp	File with initial salinity distribution for cold start, salinity stratified flow simulations.
sser.inp	Salinity time-series file.
temp.inp	File with initial water temperature distribution for cold start, salinity stratified flow simulations.
tser.inp	Temperature time-series file
wser.inp	Wind speed and direction
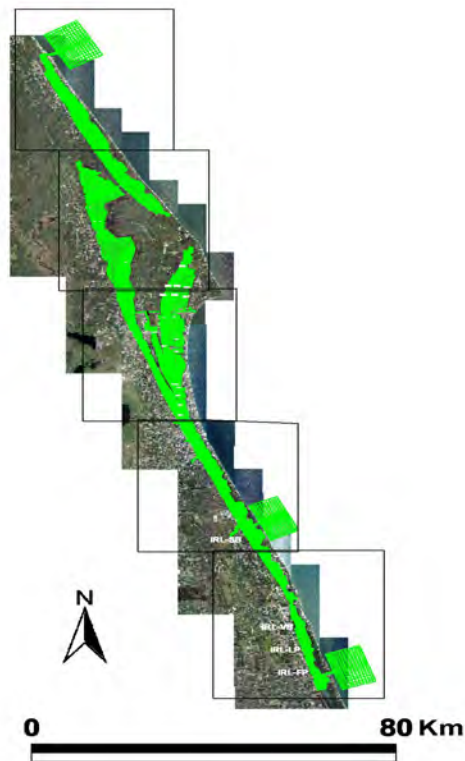
Figure 3. Approximate boundaries of 5 atmospheric forcing zones applied over the model computational grid.

Predicted time series of water elevation specified at model cells in the coastal offshore regions (Ponce de Leon Inlet, Sebastian Inlet, and Fort Pierce Inlet) were provided from the Advanced Circulation (ADCIRC) model, a high-performance, cross-platform numerical ocean circulation model popular in simulating storm surge, tides, and coastal circulation (Westerink et al., 1996). However, since ADCIRC only provides water level time series in the tidal frequency band, lower frequency components that include water level oscillations outside the frequency of the tides were also combined with tidal data. This signal was derived from regional National Oceanic and Atmospheric Administration (NOAA) stations filtered to isolate lower frequency sea level oscillation (**Figure 4**). The lower frequency spectrum includes water level changes due to meteorological forcing and seasonal to interannual sea level shift in the coastal ocean driven by the by the Gulf Stream. Although the complete period of record for each available dataset loaded into the model are generally of high quality as they have been quality controlled, it is important to note they are limited in time span, especially for the model boundaries that extend into the coastal ocean. At each of the open boundary conditions in the nearshore coastal ocean, water level time series covering the 2020 to 2022 model time period were applied to the model cells as shown in **Figure 5** as an example in the Ft. Pierce Inlet area. Similar applications of water level boundary conditions were made at Ponce de Leon and Sebastian Inlets.
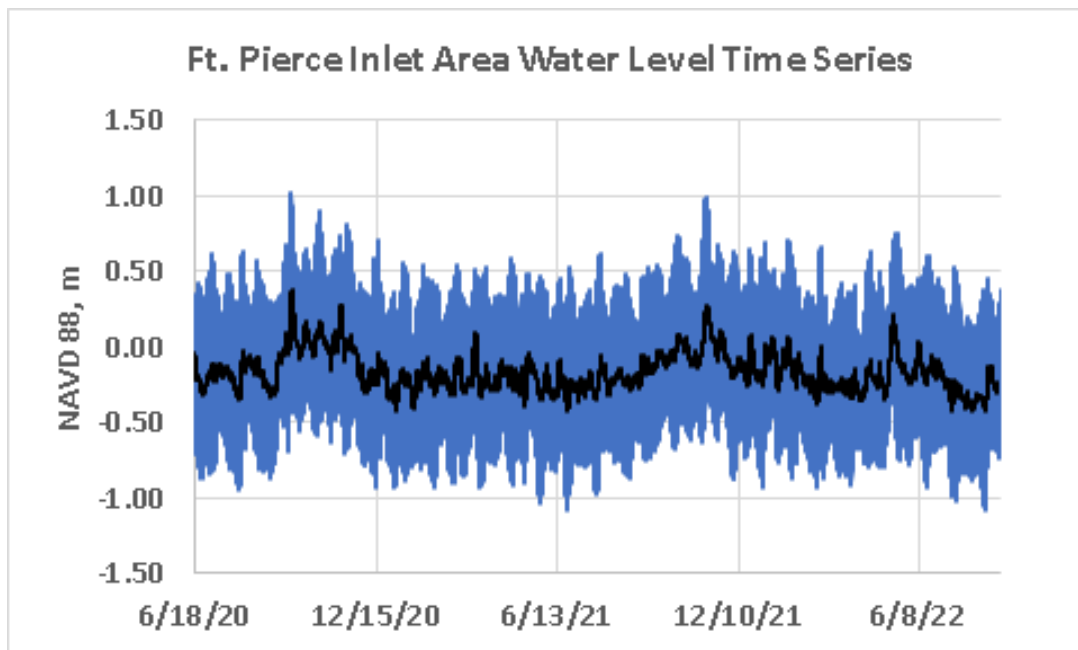
Figure 4. Ft. Pierce area water level time series applied as a model boundary condition solid black line is non tidal sea level.
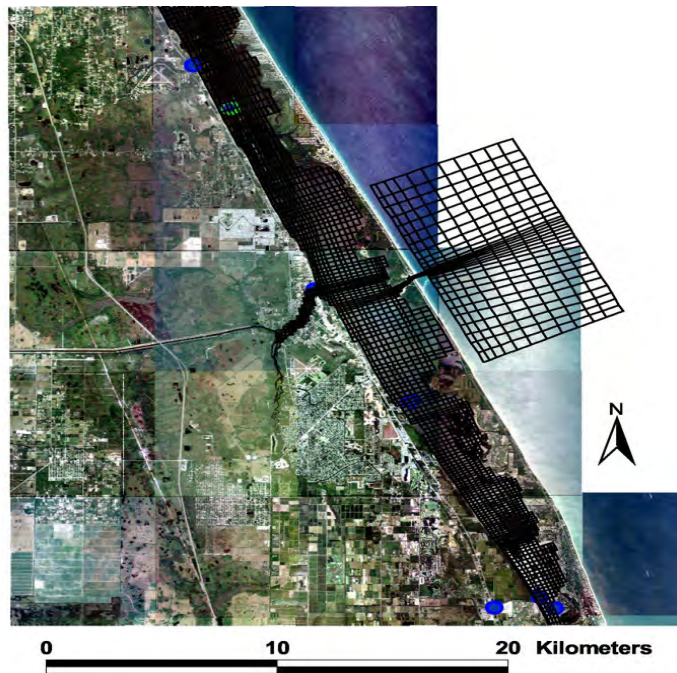
Figure 5. Configuration of the computational model grid in the area of Fort Pierce Inlet, FL.

Salinity and water temperature boundary conditions in the original model setup are described in Zarillo and Listopad (2016). In the present model configuration, salinity, and water temperature time series were assigned to the coastal ocean model boundary cells offshore of Ponce Inlet, Sebastian Inlet, and Ft Pierce Inlet. These data were provided from the archive of model runs maintained by the Hybrid Coordinate Model (HYCOM) Consortium (https://www.hycom.org/). **Figure 6** is an example of salinity and water temperature data provided by HYCOM for offshore model cells at Sebastian Inlet
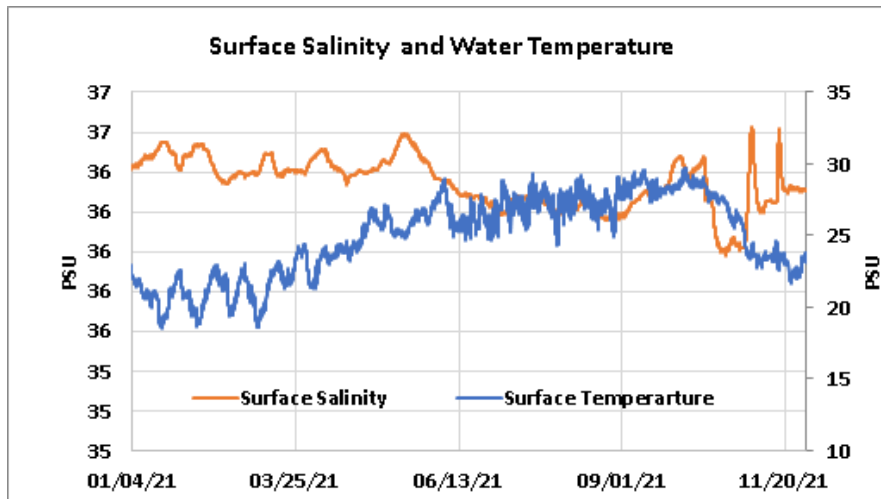
Figure 6. Example of surface salinity and water temperature data provided by the Hybrid Community Ocean Model (HYCOM) for offshore model cells at Sebastian Inlet.

1.3.3 Water Quality Boundary Conditions

Similar to the hydrodynamic portion of the model, water quality data to drive and calibrate the model are derived from existing historical sources, ongoing data collection efforts sponsored by the SJRWMD, and the SWIL model (Listopad, 2015) which produces nutrient loading (TN and TP) values at a subbasin-level throughout the IRL. **Figure 7** presents the locations of water quality monitoring stations in the IRL system maintained by the SJRWMD. To activate the water quality calculations within EFDC/HEM3D, various input files are applied, and controls set in the main water quality control input file (wq3dwq.inp). **Table 4** lists the required files and their function within the model. Similar to the hydrodynamic portion of the model, water quality data to drive and calibrate the model are derived from existing historical sources, on-going data collection effort sponsored by the SJRWMD, and the Spatial Watershed Iterative Loading (SWIL) model (Listopad, 2015) which produces nutrient loading (TN and TP) values at a subbasin-level throughout the IRL. **Figure 8** schematically shows the flow of data into the EFDC/HEM3D model from both the hydrodynamic and water quality input files listed in **Table 2** and **Table 3**.

The water quality parameter concentrations and coefficients controlling the kinetics of the nutrient and sediment cycles were initially set from a review of available water quality data from the IRL and from recent studies of sediment geochemistry by Fox et al. (2017). During the calibration process, kinetics and coefficients for each variable are adjusted to improve the performance of the water quality calculations with respect to measured data. For example, kinetics constants and coefficients for the water column and sediment model input files are adjusted for model calibration and operation using information collected during several years of a project to determine the environmental impacts of muck dredging sponsored by Brevard County (Zarillo and Listopad, 2020).
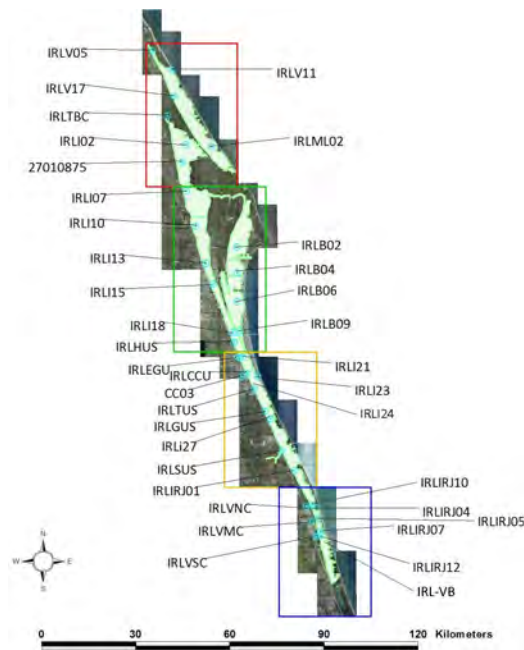
Figure 7. Location of water quality monitoring stations maintained by the SJRWMD.

Table 3. Summary of Major EFDC/HEM3D water quality input files

Model Input File	Description
efdc.inp	Primary controlling input file for EFDC hydrodynamics and water quality transport options
wq3dwc.inp	Kinetics constants/coefficients for the water column
wq3dsd.inp	Kinetics constants and coefficients for the sediment model
cwqsr01-21.inp	Time-series to be applied to model boundary conditions for water quality state variables 1-21
wqpsl.inp	Time-series watershed and point source loads for variables 1-21
BENFN	Time series of the benthic fluxes for the different sediment zones
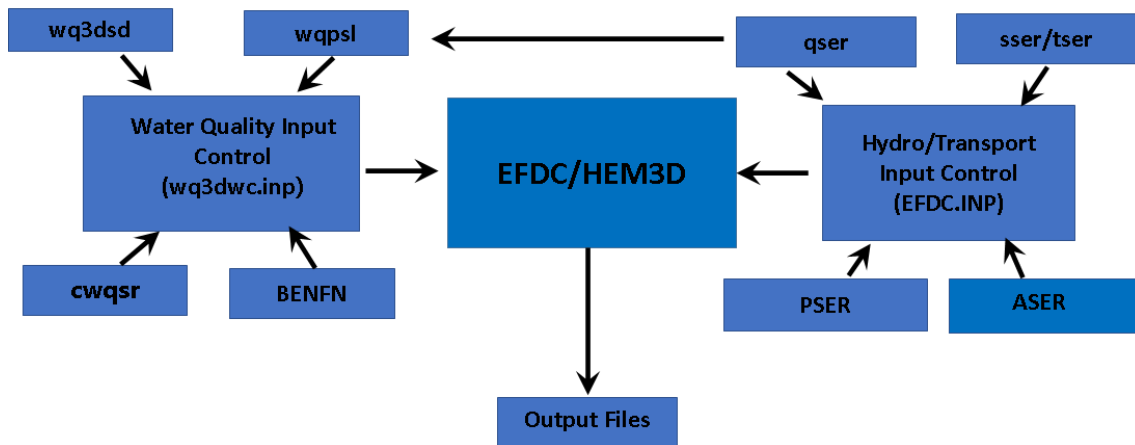
Figure 8. Flow of input data to the EFDC/HEM3 model Table 3and Table 4for definition of input files

The EFDC/HEM3D Sediment Diagenesis model is based on formulations modified from the Chesapeake Bay Corps of Engineers Integrated Compartment Water Quality Model (CE-QUAL-ICM) Model and includes 27 state variables and fluxes. This sediment sub-model as applied within the IRL is a key element in calibrating and running the water quality model. Three basic processes are included in the sediment sub model: 1) depositional flux of particulate organic matter (POM) from water column, 2) diagenesis (decay) of POM in sediments, and 3) flux of substances produced by diagenesis. Benthic sediments are represented by two layers; the upper layer can be oxic or anoxic, whereas the lower layer is always anoxic. The diagenesis model is schematically represented in **Figure 7.** The sediment diagenesis sub model is guided by inputs from files listed in **Table 3** and by the kinetics constants and coefficients in file wq3dsd.inp listed in **Table 3.**
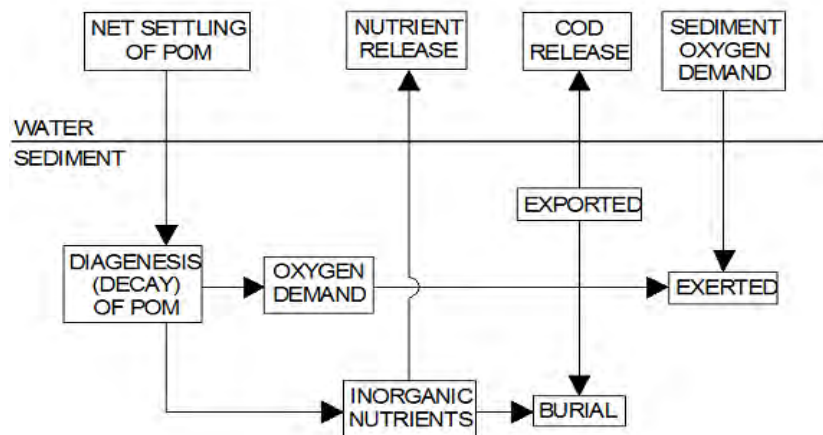
Figure 9. Sediment diagenesis schematic (Tetra Tech, 2007).

1.4 Model Verification

This section presents the results of verifying the model by comparing predictions to measured data at key locations where both modeled and observed data are available. Model predictions of water transport, as well as concentrations of water quality constituents, can be compared for different model layers. Thus, model-observation comparisons are made for selected vertical positions in the water column depending on the best knowledge of where observed data were collected; the modeled data are taken from the grid cell which intersects the station location where the observed data are collected. Model verification has two components including an initial calibration process during which adjustments are made to produce good model -observation companions. The second component is termed model validation consisting of model-observation comparisons without any further adjustments. Model calibration and validation is over the same model domain, but in different time periods. In the following sections the model calibration completed in earlier phase of this project and in separate projects are briefly described followed by additional model-observation comparisons to complete validation and final verification. Throughout the model verification process it is assumed that the impacts of frequency opening and closing the of the Port Canaveral water lock system is implicitly included in measured data used for model-observation companions. The discharge though the locks has not been measured or calculated but given the lock dimensions is likely to be 10 to 20 m^3/s at maximum flow. Among the key factors required to calculate flow, in addition to channel dimensions, are percent hydraulic slope and Manning's coefficient characterizing frictional effects. It is recommended that in any future phase of this project, field measurement be made to quantify lock flow rates more precisely. Over the course of time an assumption of an approximate flow balance between inflow and out flow through the locks can be made to better understand the impact of lock openings on water quality conditions in the Banana River near Port Canaveral and within the Port.

1.4.1 Hydrodynamic Model Calibration.

Model calibration results for the IRL model were originally described in Zarillo and Listopad (2016) and updated for an expanded model Fox et al. (2017). The calibration effort produced predicted water levels having root mean square errors (RMSE) between 5.45 centimeters (cm) (5.5% error) at the Wabasso Bridge USGS station (**Figure 10)** and 6.1 cm (6.1% error) at the USGS Haulover Canal station (**Figure 11**). Water level calibration is expected to hold for the present model

application since model hydrodynamic boundary conditions are from the same sources as described in **Table 1**.
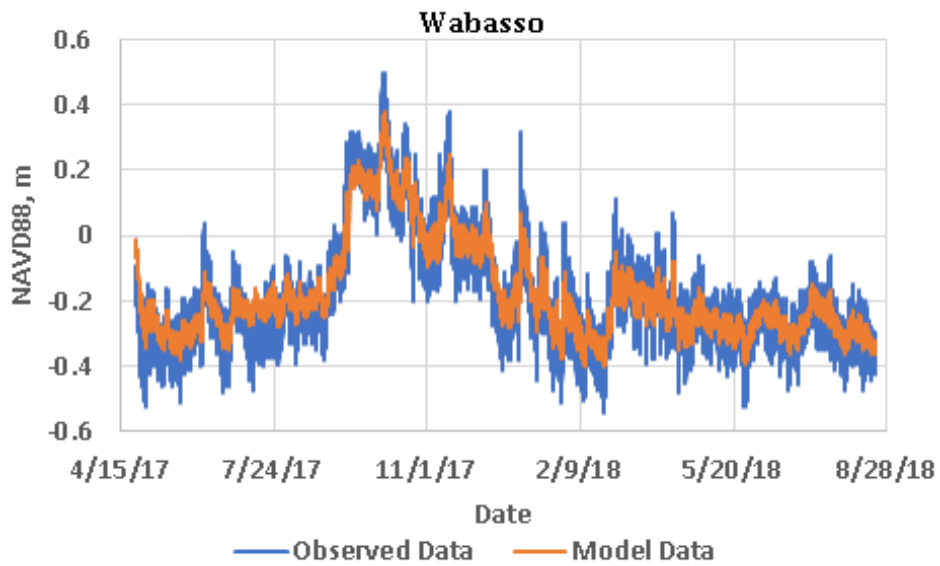

Figure 10. Observed and predicted water levels at Wabasso Bridge, north Indian River County, FL.
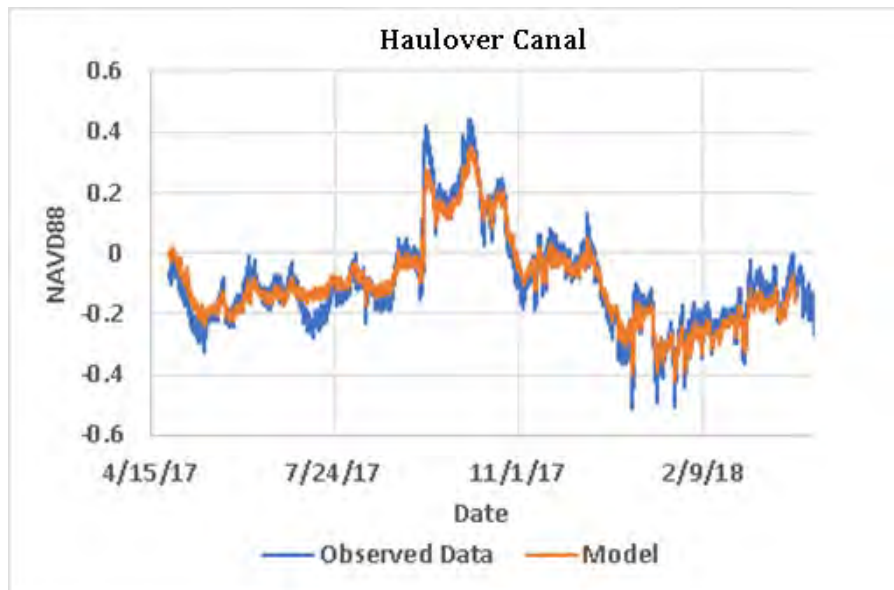

Figure 11. Observed and predicted water levels at Haulover Canal, north Brevard County, FL.

Calibration results for salinity and water temperature data were provided by Zarillo, 2020. Comparison of predicted salinity values with observed salinity data presented RSME representing 12% error of 2.7 practical salinity units (PSU) at FAU-HBOI's LOBO station IRL-SB (**Figure 12**) and 18% error (2.68 degrees Celsius [deg. C]) when comparing datasets for temperature (**Figure 13**).
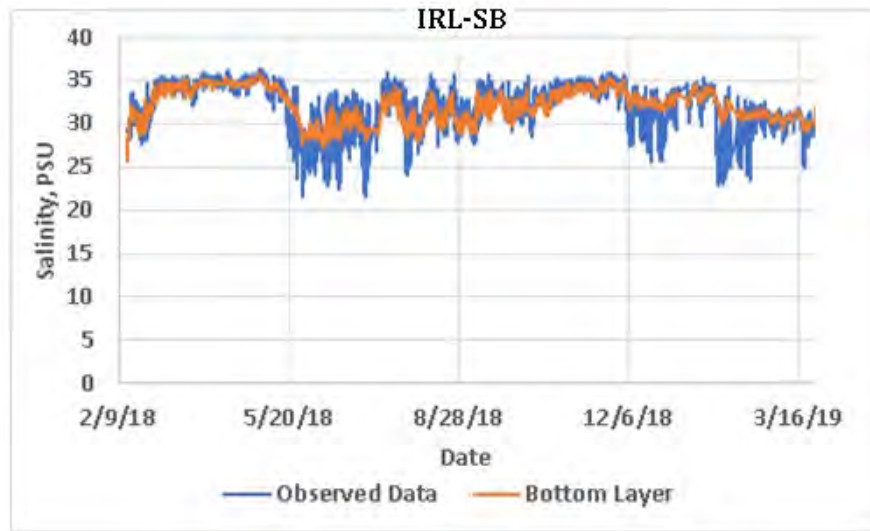
Figure 12. Comparison of observed and model salinity values recorded at LOBO station IRL-SB in the IRL near Sebastian Inlet.
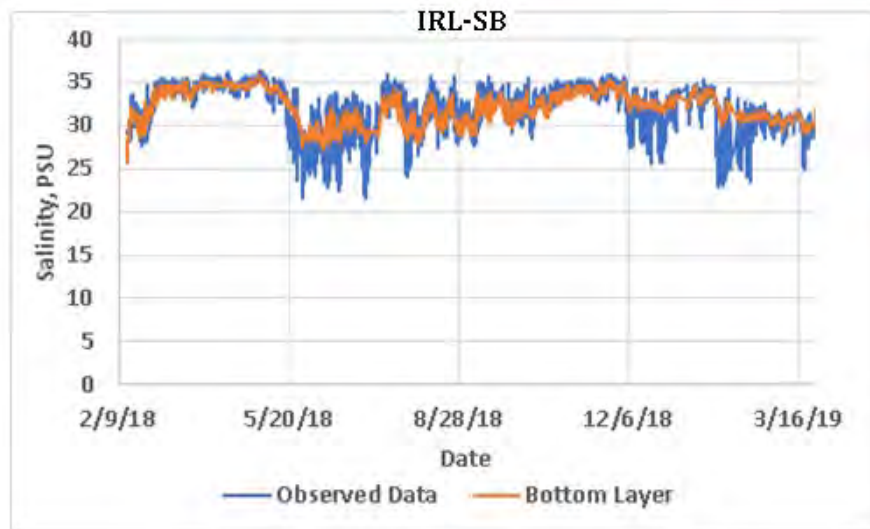
Figure 13. Comparison of observed and model water temperature values recorded at LOBO station IRL-SB near Sebastian Inlet.

1.4.2 Water Quality Model Calibration

Verification of the EFDC/HEM3D water quality calculations in the IRL system is an ongoing process. Operation of the water quality model depends on several input files that contain measured data from a variety of sources. However, at this stage of development, predictions of water quality constituent concentrations in the water column align well with measured data. Chemical species such as phosphate (PO_4^{3-}), nitrate/nitrite (NO_2-NO_3), and labile and refractory components in the total loads are only estimated. Thus, only model-observation comparisons for TN and TP are considered. DO and chlorophyll concentrations are also considered at locations where the observed data are deemed to be of good quality along with data from more continuous monitoring stations where statistical comparison are more robust. In the following sections, graphical comparisons between observed and modeled data are made at various locations. Some of these locations are where observed water quality data (monthly monitoring data) are readily available directly within or near the project area (e.g. nutrients and chlorophyll).

Table 4 presents calibration statistics in terms of RMSE and relative error (RMSE/Range of observed values) for model-observations comparisons. The comparisons are largely at SJRWMD stations in the central and southern parts of the model domain except for IRLB04 which is in the Banana River about 3 kilometers (km) south of Port Canaveral (**Figure 14**). **Figure 15** shows the locations of SJRWMD and HBOI LOBO stations in the central to south portions of the IRL from which monthly or continuous measurements were used to calibration the EFDC model. Details of the model-observation comparisons can be found in Zarillo 2021, 2022.

Table 4. Summary of model-observations comparisons for major water quality constituents (from Zarillo, 2022).

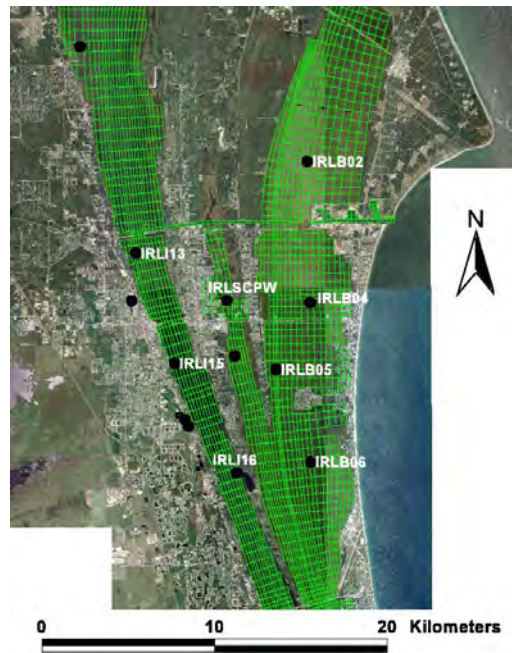| Location	Parameter	RMSE (mg/L)	RSME/Range
IRLI23	TN	0.047	3.9%
IRLI24	TN	0.043	2.9 %
IRLTUS	TN	0.087	6.0%
IRLI23	TP	0.010	6.0%
IRLI24	TP	0.034	17.6%
IRLTUS	TP	0.024	14.3%
IRLTUS	DO	0.42	7.2%
IRLIB04	DO	1.76	12.2%
IRLI21	DO	1.6	11.5%
IRL-VB	DO	1.78	15.5%

Figure 14. Location of SJRWMD water quality monitoring stations in the north-central portion of the Indian River Lagoon and Banana River
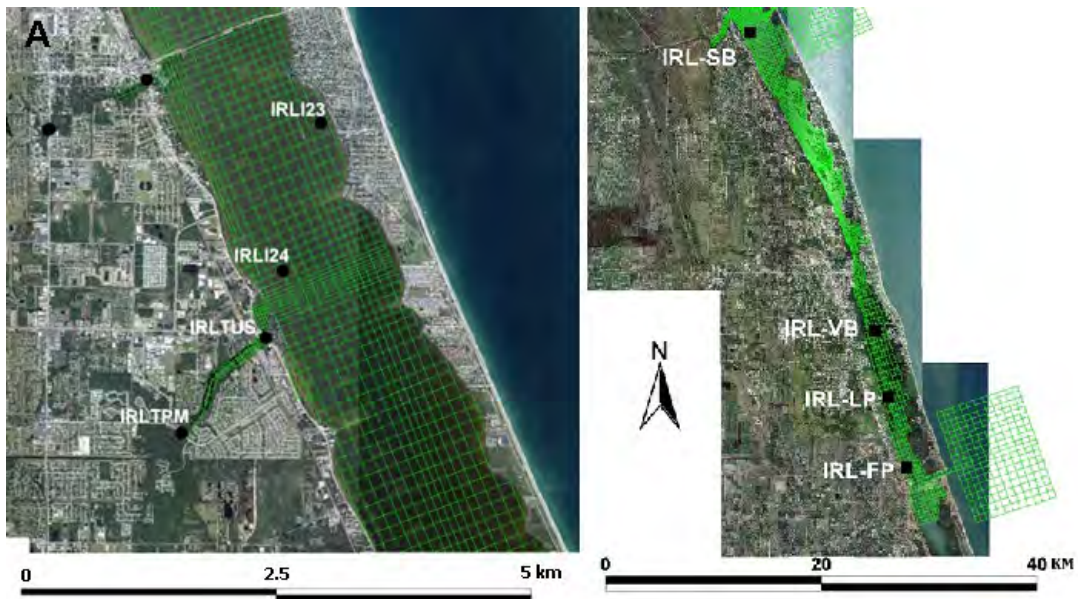

Figure 15. Location of Water quality monitoring station in the central (A) and the south central (B) Indian River Lagoon

1.4.3 Model Validation

Under model validation, the EFDC model performance is further verified without any further model adjustments and during a period differing from the calibration period. In this exercise, model performance is validated for the 2021 to 2022 time period of the Phase 3 Project. Emphasis is placed on validating model performance in the Banana River for major water quality parameters including TN, TP, and DO. Model performance for salinity and water temperature is also validated. Model-observation comparisons are made for the SJRWMD stations IRLB02 and IRLB04, which are nearest to Port Canaveral (**Figure 14**). Observations of salinity, water temperature, dissolved oxygen IRL are continuous at hourly interval, whereas observation at IRLB02 are at monthly intervals. Model-Observations comparisons are made after a 100-day spin up period to allow water quality conditions over the entire model domains to equilibrate with boundary conditions.

Figure 16 compares measured and model salinity data between January 2021 and May 2022. After an approximate accounting for a 100-day spin-up period measured, and model data agrees within a RMSE of 0.53 PSU. Given the narrow range of measured data, within 4 PSU, this corresponds to an error of about 13% which is like the range of 12% to 18% over the calibration period (**Table 4**). **Figure 17** Compares measured and model water temperature at the same IRLB04 location. The comparison results in a RMSE of 1.25 deg. C, which for a 21.8 observed temperature range, is equivalent to an error of about 5.7%.
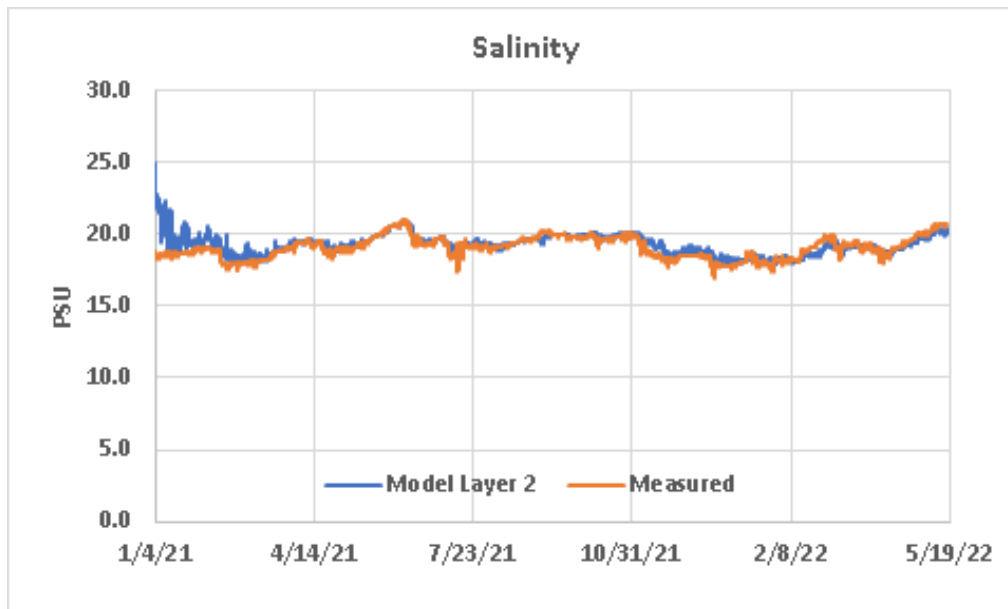
Figure 16. Comparison of measured and model salinity data at Station IRLB04
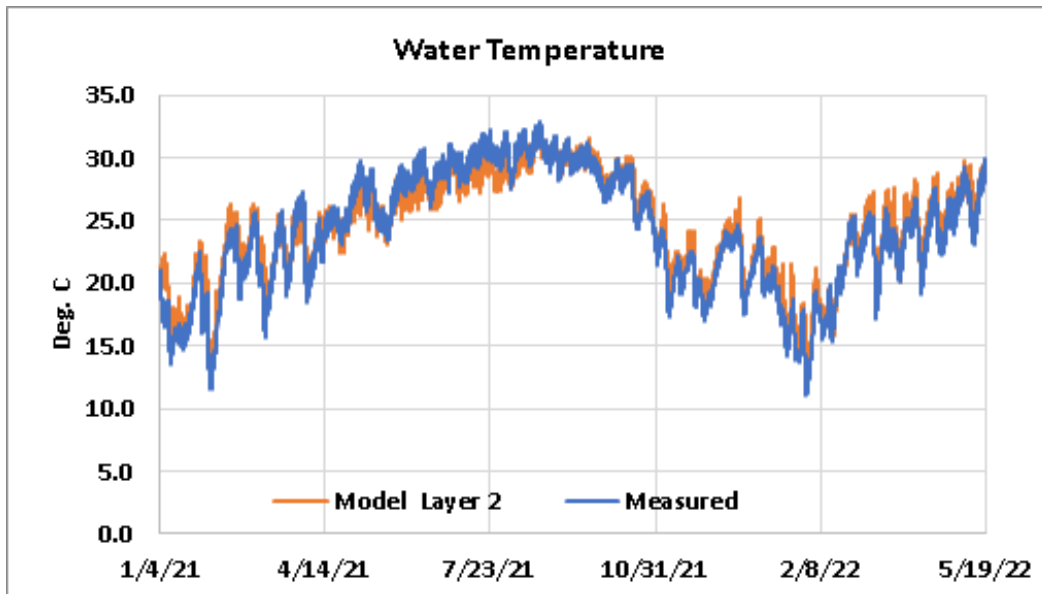
Figure 17. Comparison of measured and model water temperature data at Station IRLB04

In addition to salinity and water temperature, continuous measurements of DO are available at Station IRLB04 on an hourly basis. **Figure 17** compares measured and model DO data at IRLB04. The best comparison is with mid-depth model layer 3 where the RMSE is 1.41 mg/L, which is equivalent to a relative error of about 9.2%. If the zero values plotted among the measured data in **Figure 18** are sensor issues rather than good data, the error would be about 13%. This is due to the reduced range of observation values in the RSME/Range comparison. In either case the comparison is very good and in line with the calibration results at IRLB04 (**Table 4**). The average DO concentration value of measured data is 8.22 mg/L compared to an average of 8.55 mg/L for the model data. Thus, the measured and model DO averages are well within 1 mg/L.
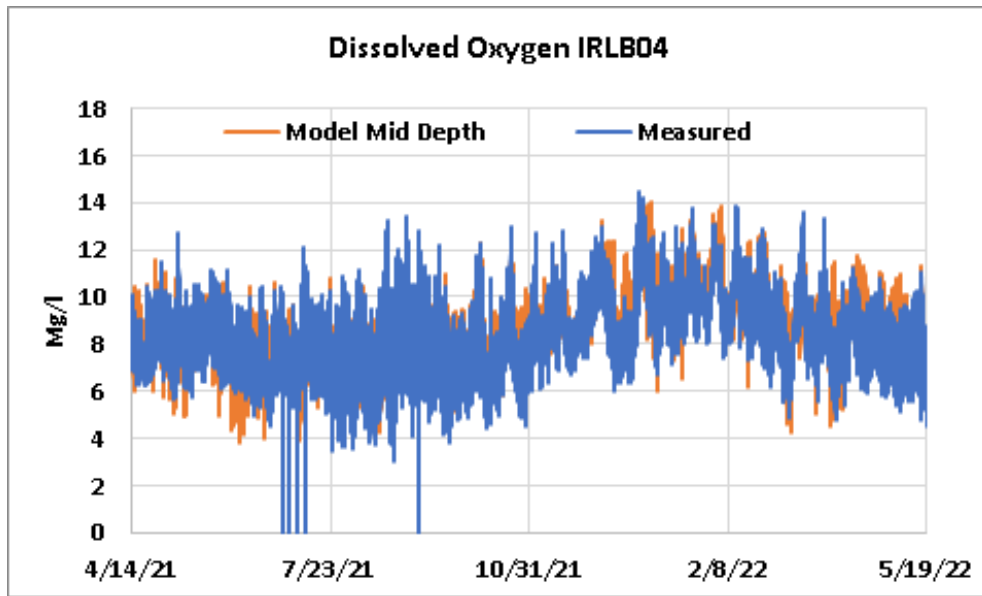
Figure 18. Comparison of measured and model DO data at Station IRLB04

Figure 18 compares measured and model DO data at Station IRLB02 in the Banana River about 4 km north of Port Canaveral in the Banana River (see **Figure 14** for location). The SJRWMD data are collected at monthly intervals and are compared with model data output at 2-day intervals. The measured model comparison is very good in which the measured data average DO value is 6.8 mg/L and the average model DO value is 7.4 mg/L. Like the comparisons at IRLB04, about 4km south ,of the Port, the averaged observation and model DO values are within 1 mg/L. In this case the relative error based of time series average values of observed and model data is 8.8%.
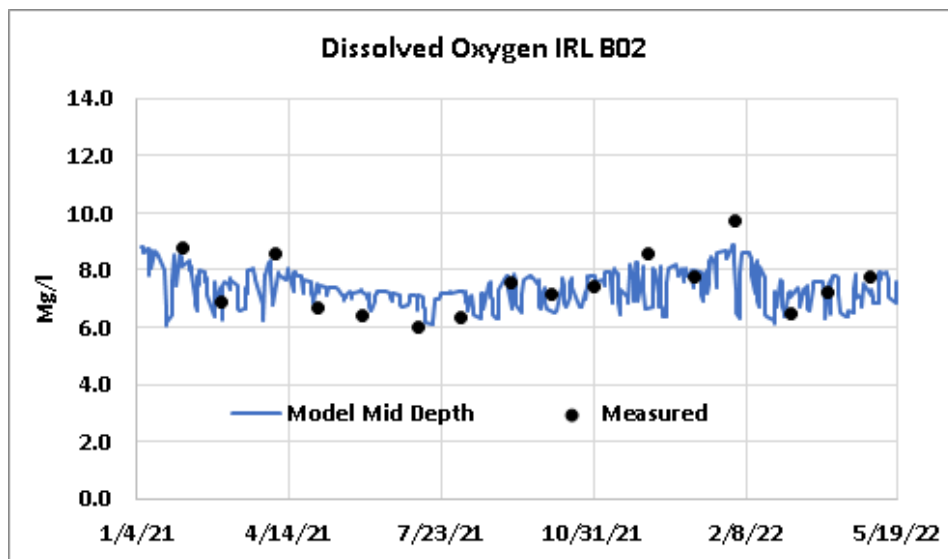
Figure 19. Comparison of measured and model DO data at Station IRLB02

The best comparison of measured TN at Station IRLB04 is with predicted TN in the model surface layer as shown in **Figure 20**. Here the SJRWMD data collected at monthly intervals and compared to model data output at 2-day intervals. The average measured and model TN values are very close at 1.07 mg/L and 1.03 mg/L, respectively. This represents a relative error of 3.7% with respect to the average value of the measured and model DO time series.
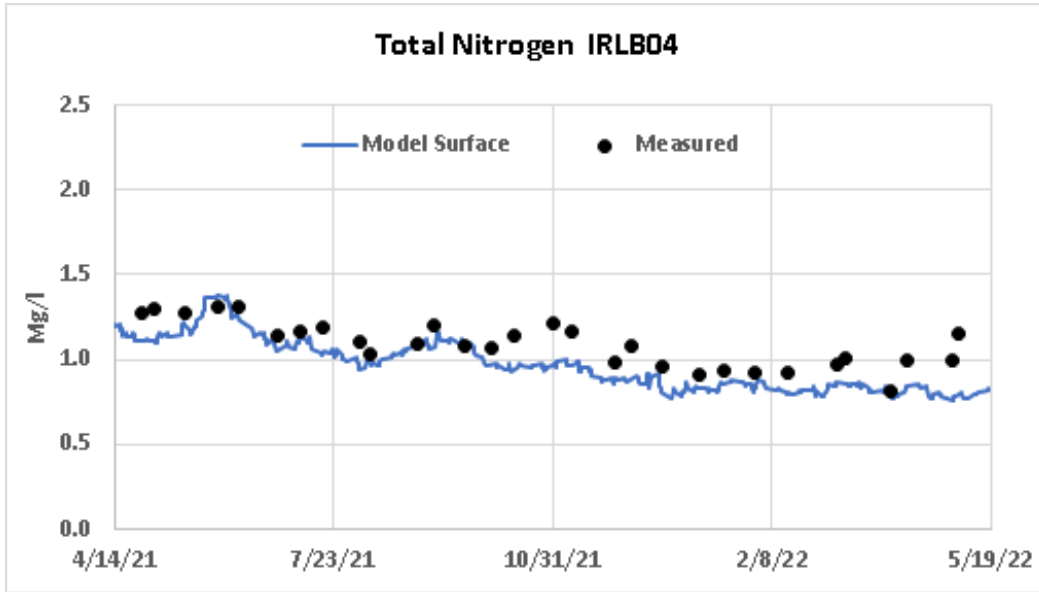
Figure 20. Comparison of measured and model TN data at Station IRLB04

Likewise, the observed and model TN data at station IRLB02 closely correspond as seen in **Figure 21**. Measured data from the SJRWMD is at monthly intervals and the model data are output at 2-day intervals. The average TN concentration of measured data is 1.21 mg/L compared with an average of 1.27 mg/L in the model surface layer representing a relative error of 4.9% with respect to time series average values.
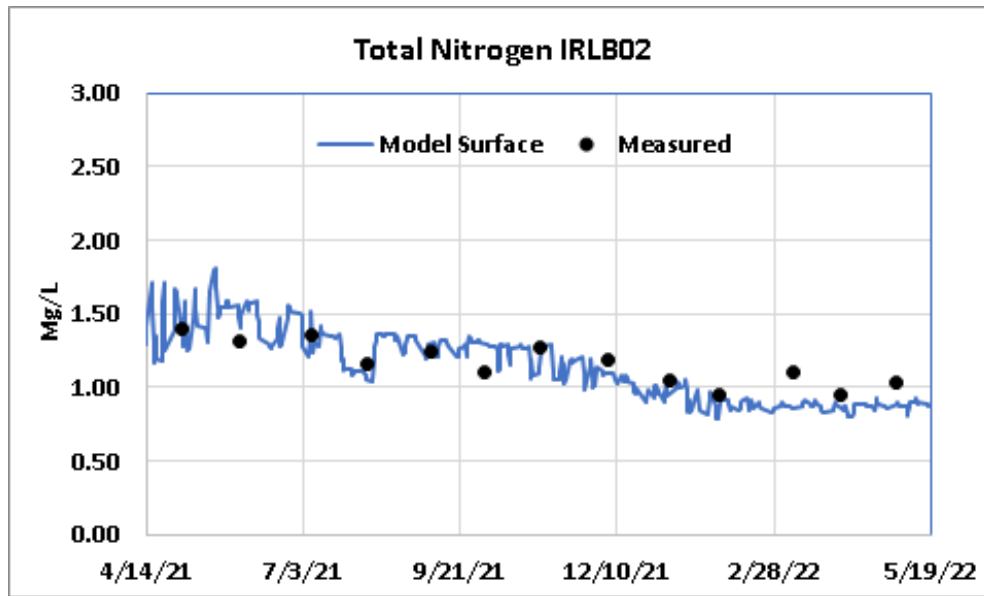
Figure 21. Comparison of measured and model TN data at Station IRLB02

As expected, measured and model TP water column concentration are an order of magnitude lower than TN concentrations. The measured-model TN comparisons at Station IRLB04 is shown in **Figure 22**. Average TP concentration values closely agree at 0.058 mg/L for the measured data and 0.050 mg/L for average predicted concentration in the model surface layer. The relative error with respect to the measured and model time series average values is 13.9%

Measured TP water column concentrations at Station IRLB02 are compared with predicted mode surface layer concentrations in **Figure 23**. Here, the observed and model average TP concentration values over the times series are 0.090 and 0.062 mg/L, respectively corresponding to a relative error of 31%. Although the average values do not correspond as closely as the comparison at Station IRLB04, the model results are considered very good considering the low concentration range and the low temporal resolution of the measured data. Where the model and measured data correspond in time, the difference between observed and predicted concentration is in the range 0.001 to 0.005 mg/L.
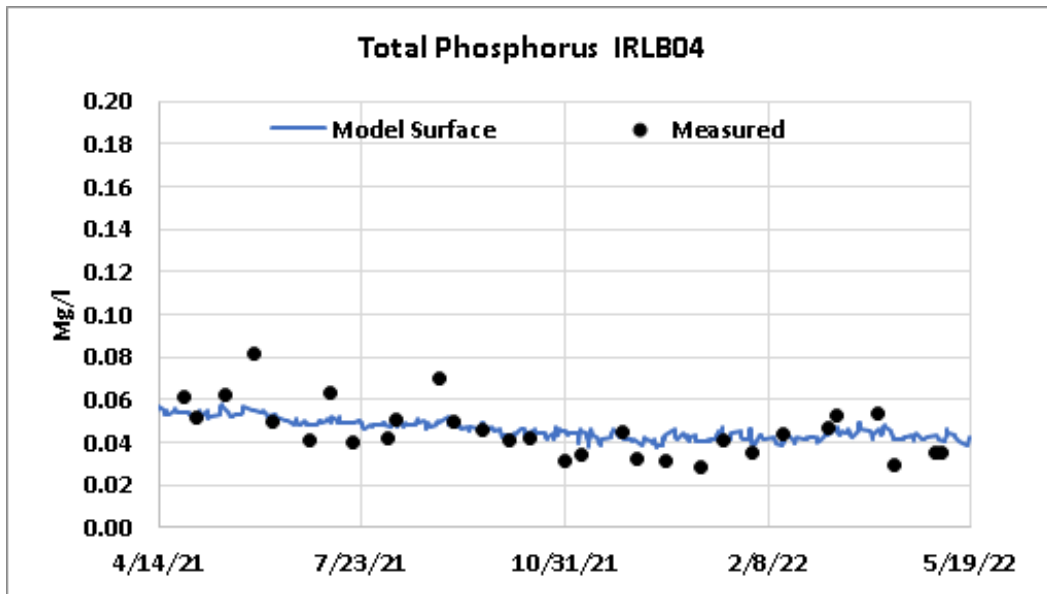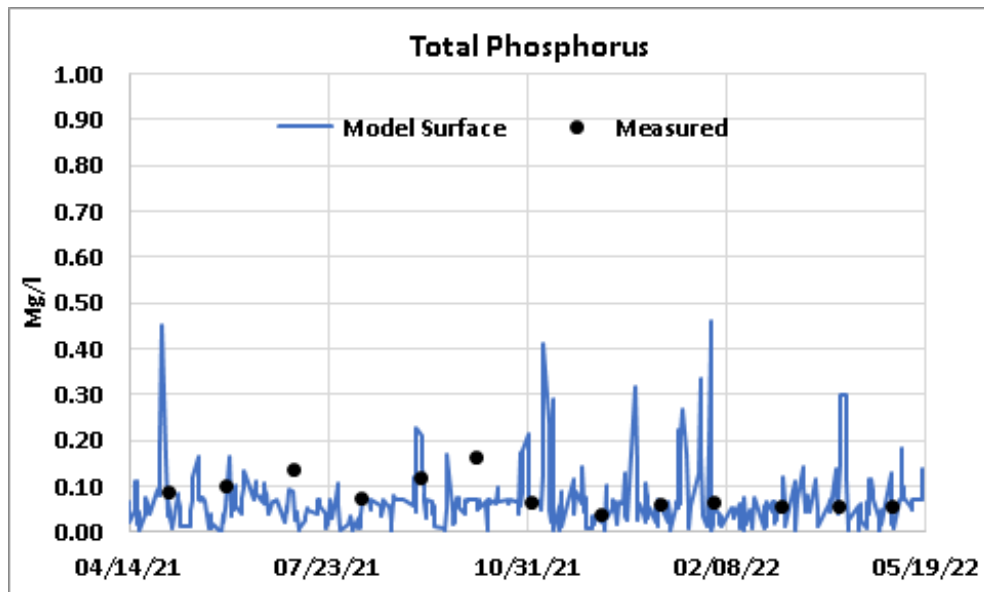
Figure 22. Comparison of measured and model TP data at Station IRLB04
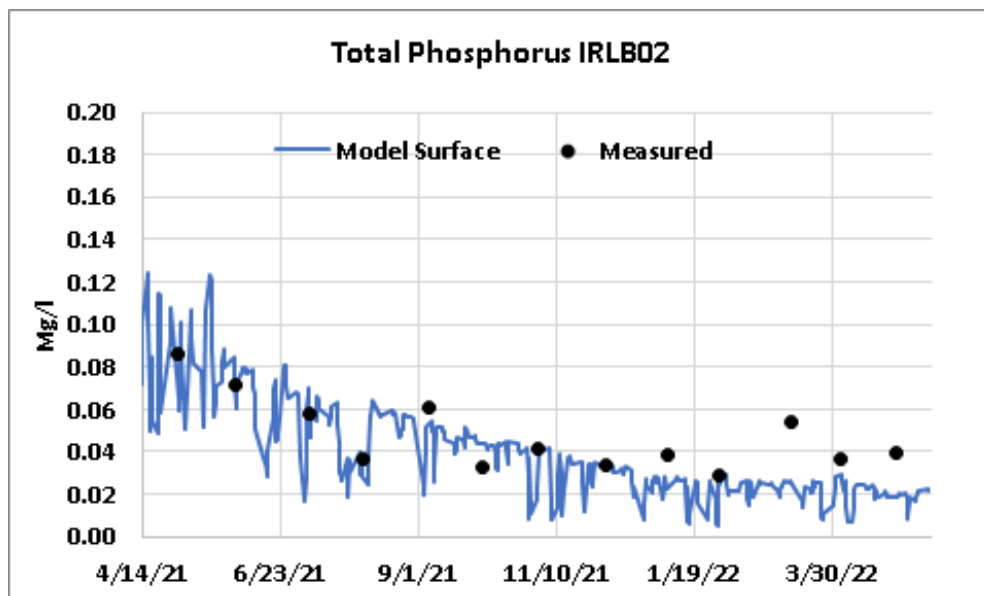
Figure 23. Comparison of measured and model TP data at Station IRLB02

An additional model validation check for water quality performance was made at SJRWMD Station IRLI23 located to the south of Banana River in the central IRL (**Figure 15**). **Figure 22** compares measure and model TP concentrations at Station IRLI23. After allowing for a 100-day spin-up of water quality calculations the observed and model average TP concentration over the times series are 0.083 and 0.069 mg/L, respectively. This corresponds to a relative error of 16.9%. Likewise, the TN comparison at Station IRLI23 is shown in **Figure 25**. Here, the observed and model time series average companion is 0.98 mg/L and 1.26 mg/L respectively and corresponds to a relative error of 28% with respect to the observed and model time series averages.

Temporal variations of model TP and TN concentrations are greater than model predictions in the Banana River. This is thought to be due to influence of freshwater inflows on IRLI23 due the proximity time varying inflows from Turkey Creek and Crane Creek. **Figure 26** compares the model and observed DO data at Station IRLI23. The model predicted time series has an average DO concentration of 7.17 mg/L compared to a 7.14 mg/L average of observed data over the same time period. The relative error of bases on model and observed time series average values is less than 1%.

The water quality data comparison at IRLI23 and many of the other model versus observed water quality comparisons involve different temporal resolution consisting of 2-day intervals for the model data and monthly intervals of the observed data. Thus, model data have more variation in the visual comparisons.

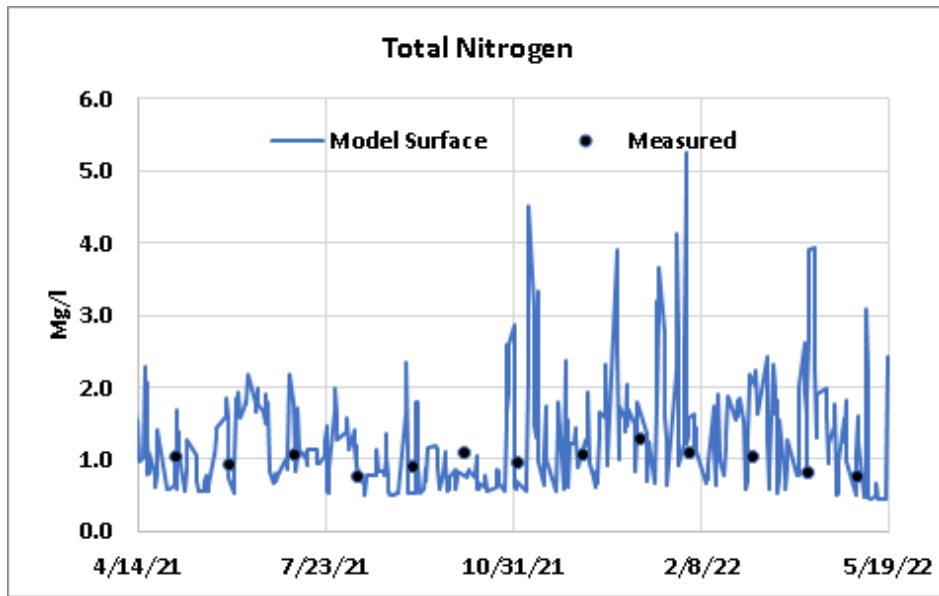**Figure 24. Comparison of measured and model TP data at Station IRLI23**

Figure 25. Comparison of measured and model TN data at Station IRLI23
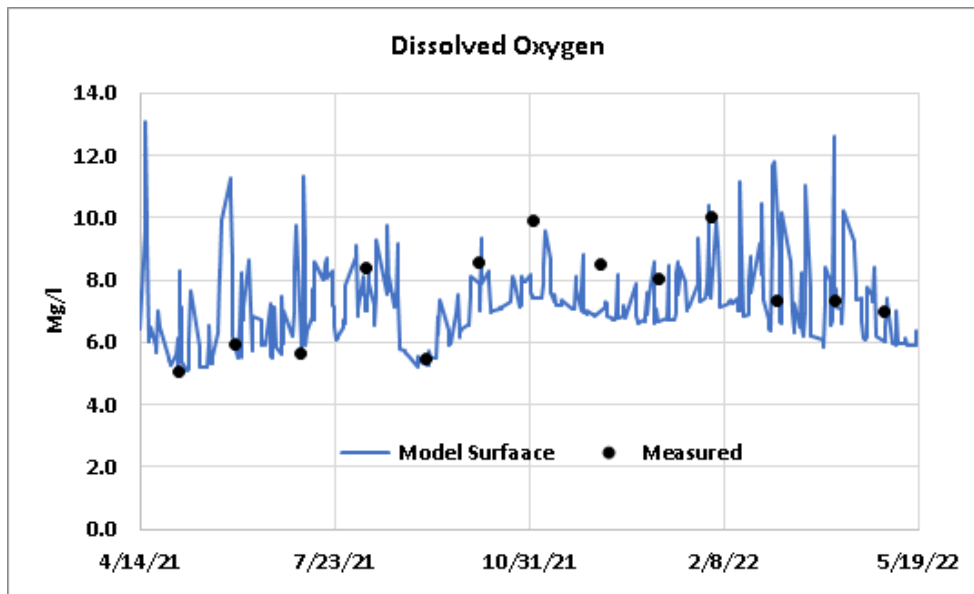

Figure 26. Comparison of measured and model DO data at Station IRLI23

1.5 Model Cases

Model test cases for enhanced inflow are listed in **Table 1**. Case 0 is the existing condition case having no specified enhanced inflow. The model setup in terms of boundary conditions is as described in Section 1.2 of this report. Case 1 involved a hypothetical pilot system inflow pump rate of 0.5 m^3/s from Port Canaveral's western compartment. Under Case 2, the pilot inflow pump rate is increased to 1.0 m^3/s. Under Case 3 the hypothetical source of inflow is shifted to an

unspecified location in the nearby coastal ocean. Case 3 involved a hypothetical 0.5 m³/s ocean inflow to demonstrate relative differences between inflow using port and ocean water sources.

Inflows to the EFDC/HEM3D model domain must be characterized by their water quality. Water quality conditions in Port Canaveral have been monitored at monthly intervals in 2001. These data were provided this project in a series of unpublished Tables and adapted to define water quality constituent concentrations of prescribed inflows. The EFDC model point source inputs are set in terms of kilograms per day in the main water quality input control file and in the point source loading file (WQPSL, inp, see **Table 3)** Thus, for the prescribed inflows, water column concentrations of water quality constituents were converted to loadings in terms of kilograms per day (kg/d) according to a flow rate of either 0.5 m³/s or 1.0 m³/s. Since water quality data from Port Canaveral is collected at monthly intervals, it is of low temporal resolution and limits the temporal resolution of both model input and outputs. Within Port Canaveral water quality data are collected at 7 locations as shown in **Figure 27**. Station P-1 is located just to the east of the Port Canaveral water locks and is essentially at the proposed location of the pump intake for the Inflow Pilot Project.

Table 5. Model run designation.

Model Runs	Case Identification
No Inflow	Case 0
0.5 m³/s Inflow from Port Canaveral	Case 1
1.0 m³/s Inflow from Port Canaveral	Case 2
0.5 m³/s Inflow from Coastal Ocean	Case 3

Figure 27. Location of Port Canaveral water quality monitoring stations.

Figure 28 illustrates nutrient loads assigned to the 0.5 m³/s Inflow from Port Canaveral over the course of the 500-day model production runs. A similar, but higher loading time series was computed for the 1.0 m³/s inflow. Point source loading for the hypothetical ocean inflow case is based on a survey of historical water quality data collected from the nearshore coastal ocean in the vicinity of tidal inlets from Ponce de Leon Inlet to St Lucie Inlet (Applied Ecology, Inc, 2021). Survey results showed that very few data sets are available, which are limited in time and space. **Table 6** summarizes the average values of water quality constituent relevant to the present study. It is noted, that beyond the Port Canaveral outer navigation channel, only 2 data points for DO were collected near Fort Pierce Inlet. Average values in **Table 6** were used to generate average daily constituent loads in terms of kg/d for the Case 3 model run.
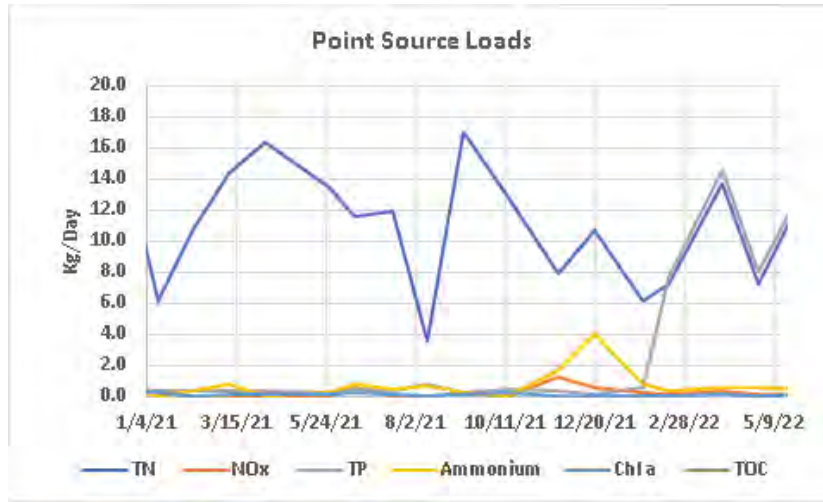
Figure 28. Point source nutrient loads in Kg/day computed from water column concentration and a prescribed inflow rate of 0.5 m³/s

Table 6. Average coastal ocean water quality values

Constituent	Average Data Value
Total Nitrogen	0.19 mg/L
Nitrate/Nitrite	0.0056 mg/L
Total Phosphorus	0.024 mg/L
Dissolved Oxygen	9.2- 9.7 mg/L*
Total Organic Carbon	1.49 mg/L
Ammonium	0.016 mg/L
Chlorophyll a	1.16 µg/l

Fort Pierce Inlet area

1.6 Model Results

Results of the model runs cases described in **Table 5** are summarized for the vicinity of the inflow area. **Figure 29** shows the location of the model computational cells from which model data were extracted for each case. The output cells are termed Inflow, Inflow North, and Inflow West. Model output data from each are examined for changes relative to Case 0, which represents the existing conditions.

Model results showed that changes in constituent concentrations were small for all the cases ranging from near zero to a single or fractional unit value. However, this is to be expected since the prescribed inflows are small and measured data collected by the SJRWMD and the Canaveral Port Authority at the proposed pump intake and the vicinity of the outflow are similar. Global results over the entire model domain are preserved for further analysis if questions arise concerning maximum area of influence for the inflow scenarios. Model results are presented in time series plots comparing the cases along with a set of Tables listing the average water quality constituent concentrations for each test case. Salinity and water temperature are also included along with nutrient and dissolved oxygen comparisons.
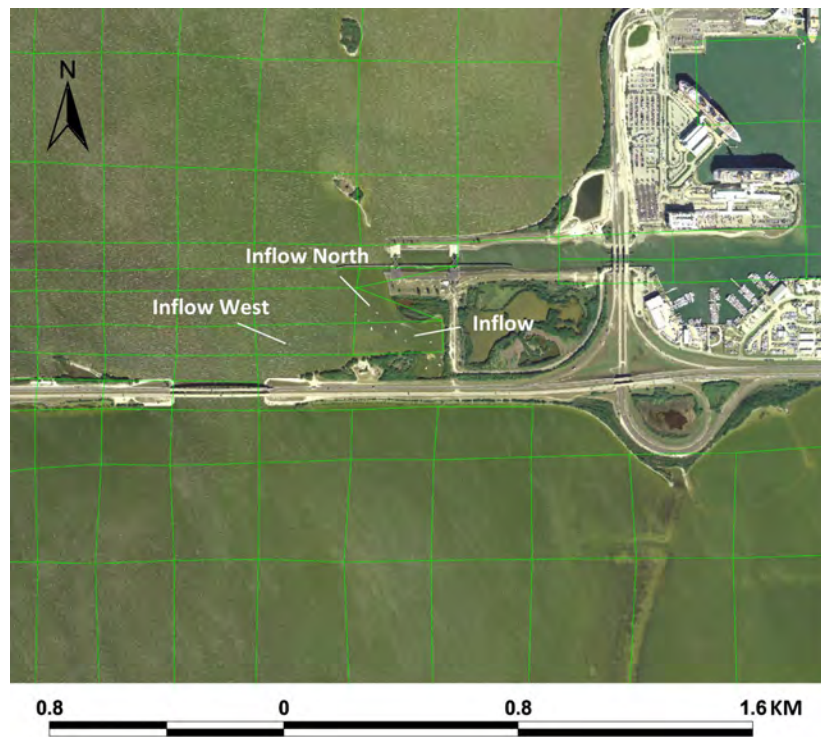
Figure 29. Model Cells designated Inflow, Inflow North and Inflow West from which model data were extracted to compare the results of model cases listed in Table 5

1.6.1 Salinity

Model results for the test cases are summarized in **Figure 30** and in **Table 7** through **Table 9.** A slight increase in surface to bottom salinity is predicted for the three-monitoring location as shown in **Figure 30**. The maximum predicted increase of 1.71 PSU is seen in the bottom layer of the model cell containing the inflow location. This occurred under the Case 2 1.0 m³/s inflow. The minimum increase in salinity of 0.3 PSU is predicted in the Inflow West cell under the Case 2 0.5 m³/s inflow. The Case 3 results for salinity and water temperature are not listed since the prescribed inflow rate and salinity/temperature boundary conditions are identical to Case 1. For Case 3, only the water quality parameters have different values as listed in **Table 6**. The inflows also produced a slight vertical stratification, which is likely results from the increased density of the inflowing water having a salinity value of up to 17 PSU higher than the ambient Banana River salinity.
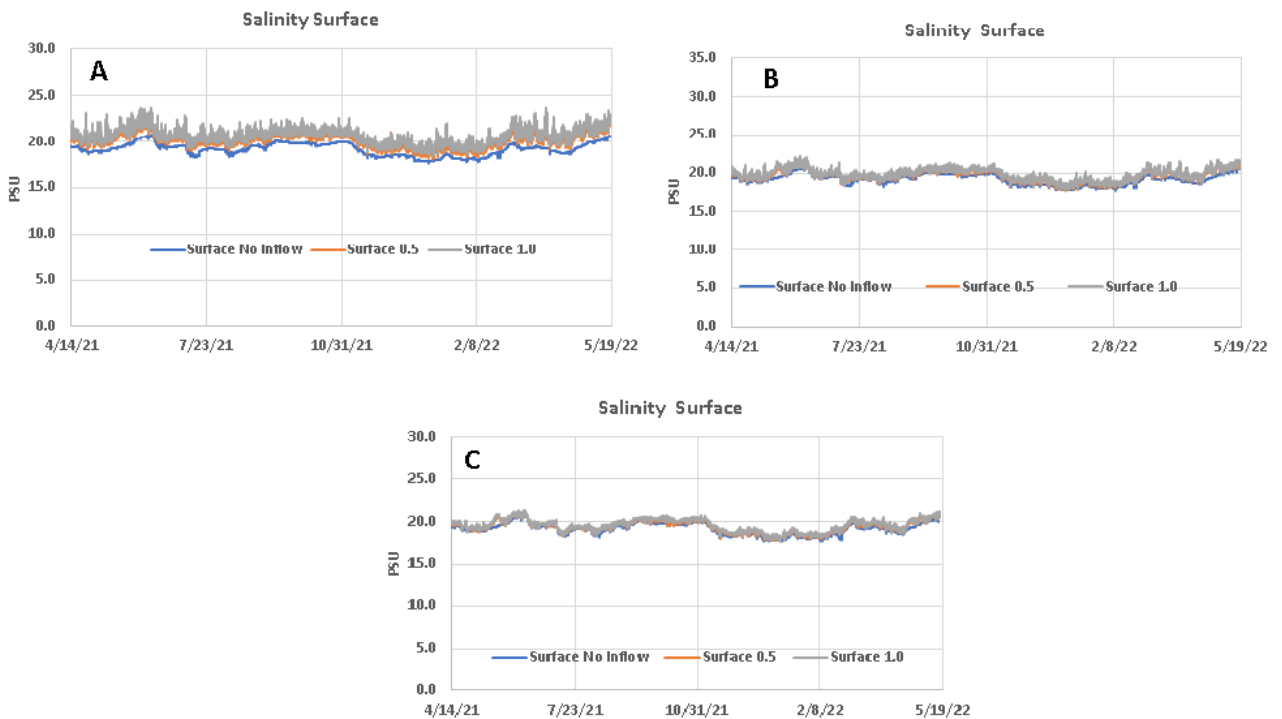
Figure 30. Salinity predictions in the surface model layer for the Inflow cell (A), Inlfow North cell (B) and Inflow West cell (C). Cell locations are shown in Figure 29. Numbers assigned in the legend indicate the inflow rates of 0.5 m³/s and 1.0 m³/s.

Table 7. Predicted average salinity at the inflow cell.
Units are PSU.

Model Case	Bottom	Mid-Depth	Surface
Case 0: No inflow	19.07	19.07	19.07
Case 1: 0.5 m³/s	20.28	20.21	20.09
Case 2: 1.0 m³/s	20.78	20.67	20.48

**Table 8. Predicted average salinity at the inflow-north cell.
Units are PSU.**

Model Case	Bottom	Mid-Depth	Surface
Case 0: No inflow	19.07	19.07	19.07
Case 1: 0.5 m³/s	20.18	19.77	19.58
Case 2: 1.0 m³/s	20.71	20.06	19.75

**Table 9. Predicted average salinity at the inflow-west cell.
Units are PSU.**

Model Case	Bottom	Mid-Depth	Surface
Case 0: No inflow	19.07	19.06	19.06
Case 1: 0.5 m³/s	19.67	19.39	19.36
Case 2: 1.0 m³/s	20.07	19.52	19.47

1.6.2 Water Temperature

Model test case results for water temperature are best represented in the bottom model layer as shown in **Figure 31**. Inflows of 0.5 m³/s and 1.0 m³/s produced slightly higher water temperatures in the surface layer of the model. The seasonal signal of lower winter temperatures is also apparent in **Figure 31**.
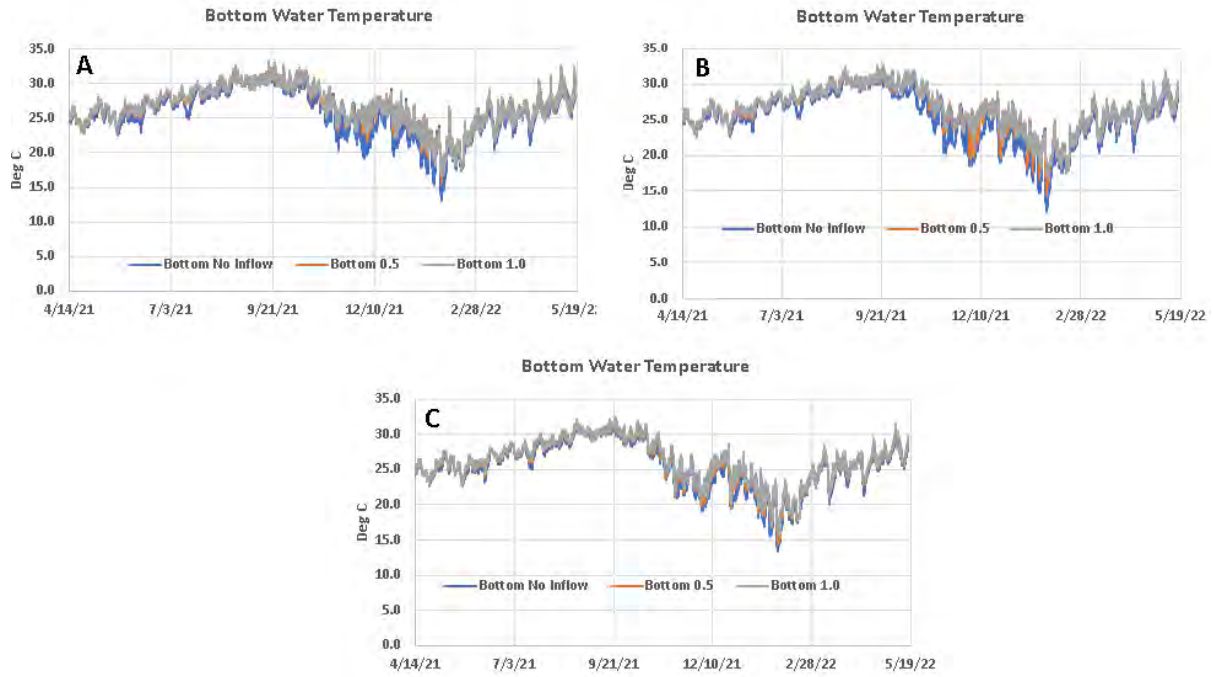
Figure 31. Water tempeature predictions in the surface model layer for the Inflow cell (A), Inlfow North cell (B) and Inflow West cell (C). Cell locations are shown in Figure 31. Numbers assigned in the legend indicate the inflow rates of 0.5 m³/s and 1.0 m³/s.

Average water temperature values produced by the model runs for each test case are listed in **Table 10** through **Table 12**. Temperature increase in the middle and top layers of the model are less than 1 deg. C, whereas as predicted water temperature increase in the bottom layer is on the order of slightly less to slightly more than 1 deg. C.

Table 10. Predicted average water temperature at the inflow cell.
Units are degrees C.

Model Case	Bottom	Mid-Depth	Surface
Case 0: No inflow	24.94	25.41	25.83
Case 1: 0.5 m³/s	25.88	25.96	26.09
Case 2: 1.0 m³/s	25.90	25.94	26.07

Table 11. Predicted average water temperature at the inflow north cell.
Units are degrees C.

Model Case	Bottom	Mid-Depth	Surface
Case 0: No inflow	24.63	25.28	25.77
Case 1: 0.5 m³/s	25.72	25.84	26.10
Case 2: 1.0 m³/s	25.86	25.92	26.15

Table 12. Predicted average water temperature at the inflow north cell.
Units are degrees C.

Model Case	Bottom	Mid-Depth	Surface
Case 0: No inflow	24.74	25.38	25.87
Case 1: 0.5 m³/s	25.36	25.73	26.13
Case 2: 1.0 m³/s	25.59	25.85	26.22

1.6.3 Dissolved Oxygen

DO predictions are represented in **Figure 32**. The most apparent impact of prescribed inflows is in the bottom model layer where predicted increase in DO concentration is most easily observed in the time series plots. Averaged DO values over the model runs are listed in **Table 13**, **Table 14**, and **Table 15** including the results for the Ocean Inflow case. Model predictions followed an expected pattern of higher DO values in the surface model layer and lower concentration in the bottom layer. Higher DO concentrations are also predicted for the winter months of 2022.

Differences in DO concentration among the cases were mostly less than 1 mg/L within a model layer except for the comparison between Case 0 (existing condition) and Case 3, which involved a hypothetical inflow from the coastal ocean where the DO concentration may be on the order of 10 mg/L or higher. The Case 0 to Case 3 comparison in the model bottom layer is an increase of slightly more than 1 mg/ l under the Ocean Inflow case. Overall, the ocean inflow case produced he highest DO concentrations in all model layers even compared to Case 2, which specified a higher inflow rate of 1.0 m³/s. Although the predicted increase in DO concentrations with increasing inflow rates and/or higher DO boundary conditions are small, model results indicate that Pilot Project inflows are likely to produce measurably higher DO in the vicinity of the inflow. Predicted increase in DO values in the model cells adjacent to the inflow cell are lower, but still measurable in the model results.
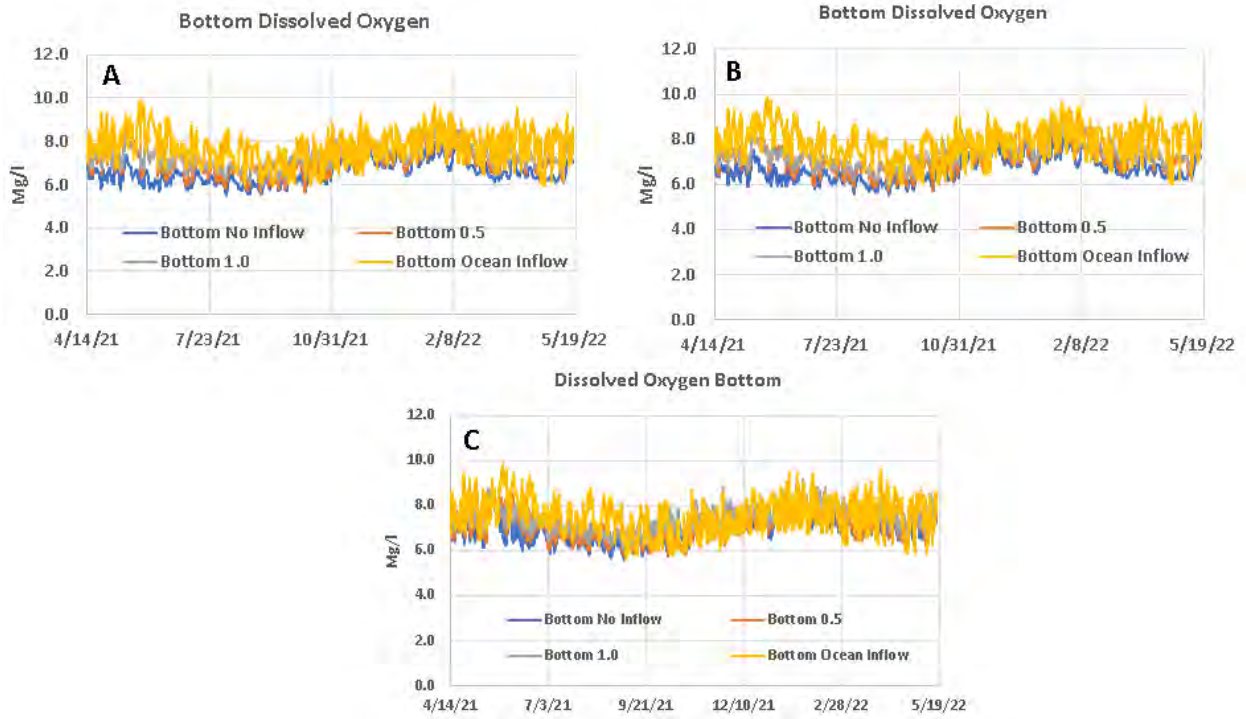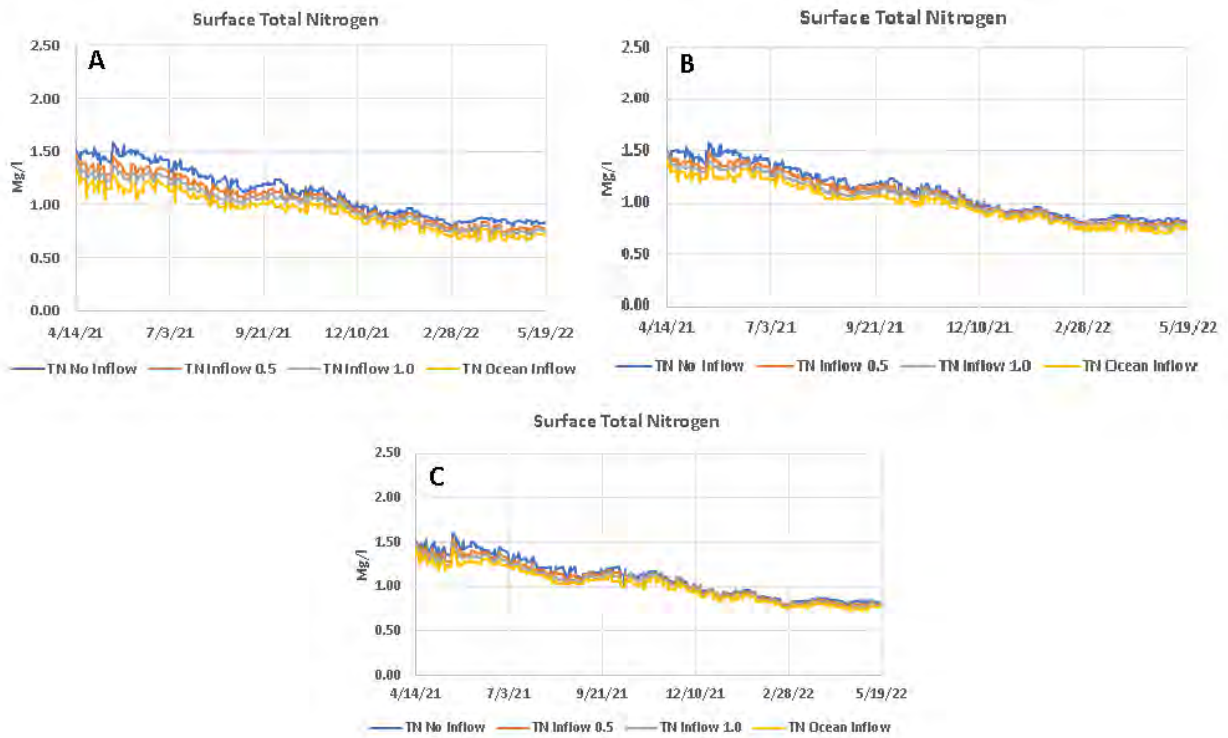
Figure 32. Dissolved predictions in the bottom model layer for the Inflow cell (A), Inlfow North cell (B) and Inflow West cell (C). Cell locations are shown in Figure 29. Numbers assigned in the legend indicate the inflow rates of 0.5 m³/s and 1.0 m³/s.

Table 13. Predicted average DO concentration at the inflow cell.
Units are mg/L.

Model Case	Bottom	Mid-Depth	Surface
Case 0: No inflow	6.58	6.81	7.03
Case 1: 0.5 m³/s	7.20	7.22	7.26
Case 2: 1.0 m³/s	7.35	7.39	7.48
Case 3: 0.5 m³/s Ocean Inflow	7.76	7.77	7.77

**Table 14. Predicted average DO concentration at the inflow north cell.
Units are mg/L.**

| Model Case	Bottom	Mid-Depth	Surface
Case 0: No inflow	6.68	7.19	7.53
Case 1: 0.5 m^3/s	7.23	7.42	7.55
Case 2: 1.0 m^3/s	7.37	7.66	7.87
Case 3: 0.5 m^3/s Ocean Inflow	7.77	7.74	7.90

**Table 15. Predicted average DO concentration at the inflow west cell.
Units are mg/L.**

Model Case	Bottom	Mid-Depth	Surface
Case 0: No inflow	7.02	7.22	7.30
Case 1: 0.5 m^3/s	7.13	7.34	7.45
Case 2: 1.0 m^3/s	7.42	7.49	7.57
Case 3: 0.5 m^3/s Ocean Inflow	7.58	7.60	7.68

1.6.4 Total Nitrogen

Nitrogen predictions in the EFDC/HEM3D model can be reported as the individual component of nitrogen subspecies or as total nitrogen water column concentrations. Since the model calibration and validation results are reported based on comparisons with total nitrogen vales measured at SJRWMD monitoring stations, model results are reported as total nitrogen. Model results for TN are similar an all model layers and are shown for the surface layer in **Figure 33**. The summary of model results for each test case are listed in **Table 16**, **Table 17**, and **Table 18**. Model predictions indicate a slight decrease in TN concentration in a progression from Case 0, the existing condition, through the ocean inflow Case 3. Like the DO predictions, improvements from the hypothetical inflows are small but measurable in the model predictions.

Figure 33. Total nitrogen predictions in the bottom model layer for the Inflow cell (A), Inlfow North cell (B) and Inflow West cell (C). Cell locations are shown in Figure 29 Numbers assigned in the legend indicate the inflow rates of 0.5 m³/s and 1.0 m³/s.

Table 16. Predicted average TN concentration at the inflow cell.
Units are mg/L.

Model Case	Bottom	Mid-Depth	Surface
Case 0: No inflow	1.13	1.13	1.13
Case 1: 0.5 m³/s	1.04	1.15	1.05
Case 2: 1.0 m³/s	0.99	1.10	1.01
Case 3: 0.5 m³/s Ocean Inflow	0.89	1.02	0.95

**Table 17. Predicted average TN concentration at the inflow north cell.
Units are mg/L.**

Model Case	Bottom	Mid-Depth	Surface
Case 0: No inflow	1.14	1.13	1.13
Case 1: 0.5 m^3/s	1.05	1.07	1.09
Case 2: 1.0 m^3/s	1.00	1.04	1.06
Case 3: 0.5 m^3/s Ocean Inflow	0.90	0.97	1.01

**Table 18. Predicted average TN concentration at the inflow west cell.
Units are mg/L.**

Model Case	Bottom	Mid-Depth	Surface
Case 0: No inflow	1.12	1.21	1.12
Case 1: 0.5 m^3/s	1.06	1.17	1.08
Case 2: 1.0 m^3/s	1.02	1.15	1.06
Case 3: 0.5 m^3/s Ocean Inflow	0.97	1.11	1.02

1.6.5 Total Phosphorus

Like nitrogen predictions, phosphorus prediction is reported TP water column concertation in each of the 5 vertical model layers. Model results for TP concentrations are similar across the model layers as shown for the surface layer in **Figure 34**. The summary of model results for each test case are listed in **Table 19, Table 20**, and **Table 21**. Water column concentrations of TP are an order of magnitude lower than precited TN concentration, which is consistent with the comparison of measured and predicted concentration values reported in the model validation section of this report.

Predictions indicate TP concentrations over the water column model layers only vary slightly. However, within each model layer there is a progression of declining TP concentration from Case 0, the existing condition, through the ocean inflow Case 3. Like the DO and TN predictions, improvements from the hypothetical inflows are small but measurable in the model results. The influence of the hypothermal inflows is traceable through all 3 monitoring cells, but slightly decrease with distance from the inflow cell as visually apparent in **Figure 34**.
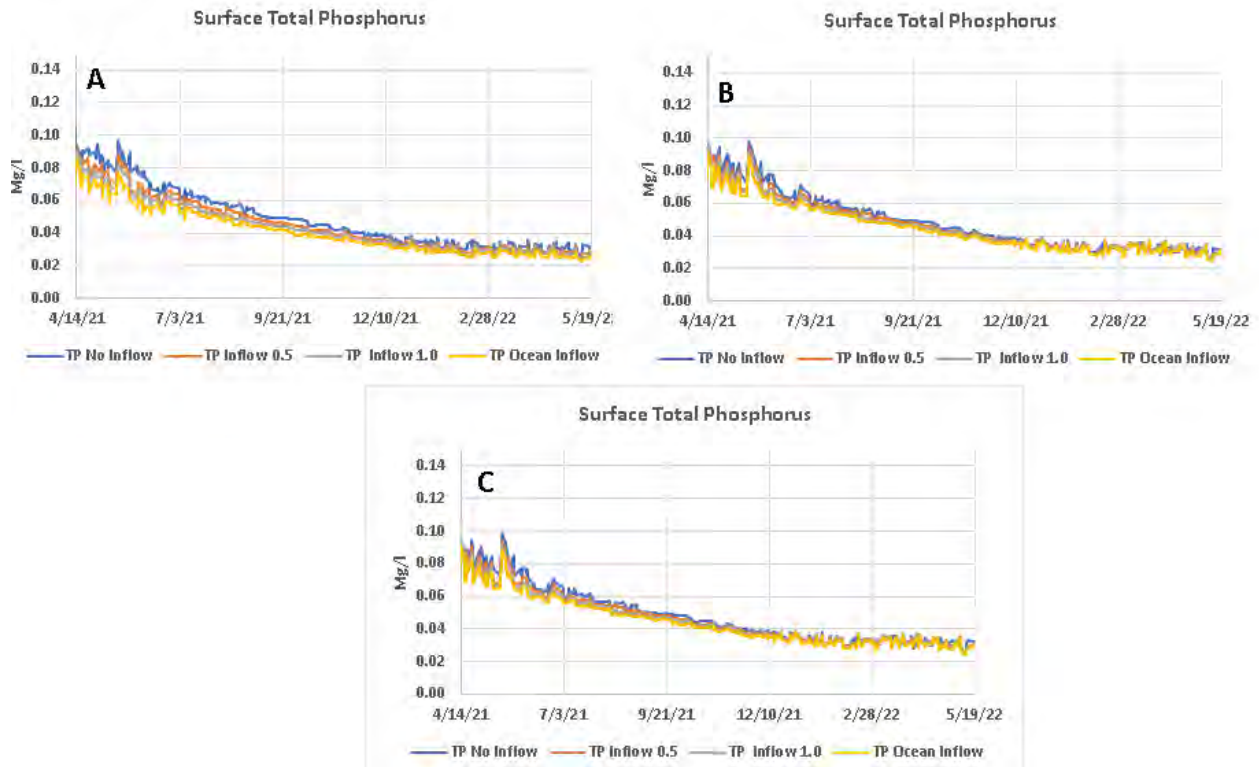
Figure 34. Total phosphorus predictions in the bottom model layer for the Inflow cell (A), Inlfow North cell (B) and Inflow West cell (C). Cell locations are shown in Figure 29. Numbers assigned in the legend indicate the inflow rates of 0.5 m³/s and 1.0 m³/s.

Table 19. Predicted average TP concentration at the inflow cell. Units are mg/L.

Model Case	Bottom	Mid-Depth	Surface
Case 0: No inflow	0.051	0.051	0.051
Case 1: 0.5 m³/s	0.047	0.047	0.047
Case 2: 1.0 m³/s	0.044	0.044	0.045
Case 3: 0.5 m³/s Ocean Inflow	0.040	0.041	0.042

Table 20. Predicted average TP concentration at the inflow north cell.
Units are mg/L.

Model Case	Bottom	Mid-Depth	Surface
Case 0: No inflow	0.051	0.050	0.050
Case 1: 0.5 m^3/s	0.048	0.049	0.048
Case 2: 1.0 m^3/s	0.046	0.047	0.047
Case 3: 0.5 m^3/s Ocean Inflow	0.044	0.046	0.046

Table 21. Predicted average TP concentration at the inflow west cell.
Units are mg/L.

Model Case	Bottom	Mid-Depth	Surface
Case 0: No inflow	0.051	0.050	0.050
Case 1: 0.5 m^3/s	0.048	0.049	0.048
Case 2: 1.0 m^3/s	0.046	0.047	0.047
Case 3: 0.5 m^3/s Ocean Inflow	0.044	0.046	0.046

1.7 Conclusions

Modelling in the Phase 3 project is focused on assessing the potential influence on water quality of a small Banana River compartment from small inflows rates pumped from an intake located at the west end of Port Canaveral. Thus, the expected impact is small in comparison to the Phase 2 model tests in which inflow pumping rates of up to 10 m^3/s were tested. The overall goal is to verify that small inflow into a confined area of the Banana River can be used to assess the potential benefits of much higher inflows rates on the greater Banana River compartment of the IRL. Another goal is to confirm that a pilot project involving lower inflow rates will not have a negative impact on the receiving basin and provide the basis for answering and concerns that may arise during the Pilot Project permitting process.

It is concluded that the goals of the model testing designed around the Pilot Project have been reached. Model tests produced measurable changes among the test cases, but no large changes in salinity, water temperature, or water quality constituent concentrations were predicted that could produce a significant negative impact during the pilot inflow project. Further, the results of the model cases indicate slight improvement in water quality within the pilot project test basin under lower inflow rates.

Limitations of the model testing are based on the low temporal resolution of water quality measurement in both the Banana River and within Port Canaveral. Since water quality data in

the Banana River and Port Canaveral can overlap in value, both the modeling and monitoring efforts would benefit from more continuous collection of water quality data.

1.8 Next Steps

Modeling the concept of enhanced inflows has been successful from both the full scale and pilot project perspectives. However, model results clearly indicate that the project would derive significant benefits from more continuous measurements of water quality, as well as salinity and water temperature to enhance model calibration and validation. The minimum temporal resolution water quality measurements would be on a weekly basis combined with high accuracy laboratory analysis of collected water samples. These measurements should begin well in advance of pilot project construction and proceed through the project duration. It is also recommended that in any future phase of this project, field measurement be made to quantify lock flow rates more precisely. Future data collection stations should be consistent with model boundary locations, well as within the interior of the Banana River and Port Canaveral. Well-designed monitoring can provide the basis for accurate and spatially integrated model prediction of pilot project benefits and evaluation of larger inflow rates that may be associated with a full-scale inflow project.

2 References

Fox, A.L., Trefry, J.H., Trocine, R.P., Fox, S.L., Voelker, J.E., 2017. Determining the Effectiveness of Muck Removal on Sediment and Water Quality in the Indian River Lagoon. Project Report Submitted to Brevard County Natural Resources Management Department.

Listopad, C. 2015. Spatial Watershed Iterative Loading (SWIL) Model Methodology Report; Updated for SWIL 3.0. Final Report submitted to Brevard County Natural Resources Management Office by Applied Ecology, Inc.

Westerink, J.J., R.A. Luettich and R.L. Kolar, 1996, ADCIRC an advanced finite element model for coastal ocean circulation, Proceedings, The Third Asian Pacific Conference on Computational Mechanics, 16-18 September, Seoul, Korea.

Zarillo, G.A. and Listopad, C. 2020. Hydrologic and Water Quality Model for Management and Forecasting within Brevard County Waters of the Indian River Lagoon. Final Project Report to Brevard County Natural Resources Management Department. 128pp.

Zarillo, G.A. Listopad, C., 2016. Indian River Lagoon Hydrodynamic and Water Quality Model Quality Assurance Plan: Year 1 Final Report Prepared for Brevard County and the Florida Department of Environmental Protection

Zarillo, G.A. 2021. Development of a Water Quality Model for The Turkey Creek Feasibility Study. Report to Applied Ecology, Inc. 63 p.

Zarillo, G.A. 2022. Impacts of Environmental Muck Dredging 2016-2019. Final Report to Brevard County Dept. of Environmental Management. 60p

Appendix C   Task 3 – Florida Tech Geochemistry Report

Restore Lagoon Inflow Research (Phase 3)
Final Report
Task #3: Geochemistry
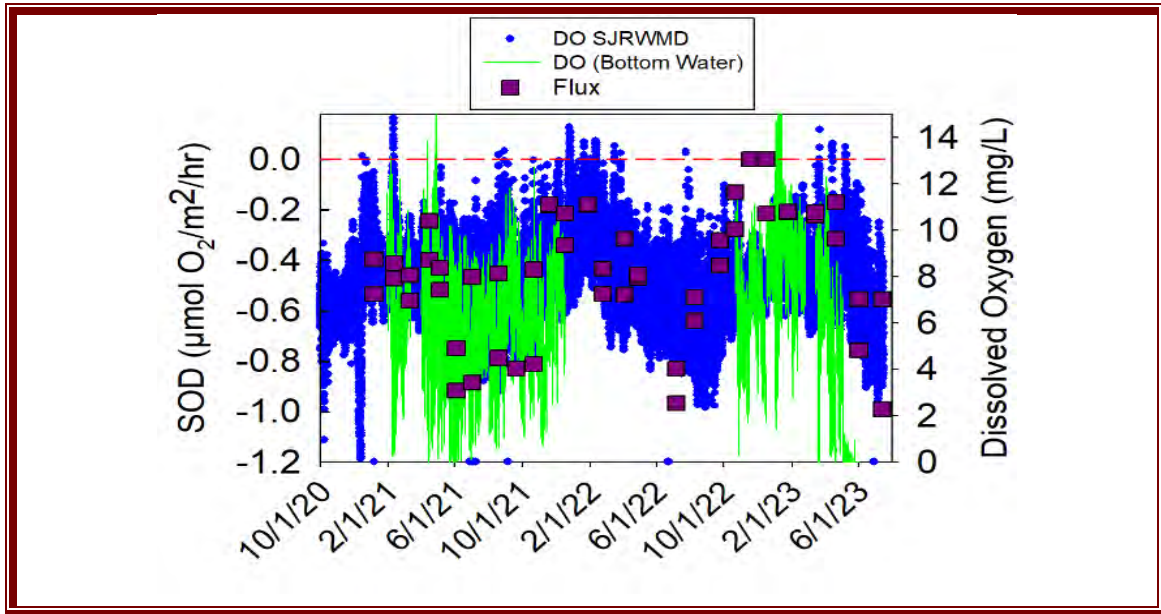
PREPARED FOR

Florida Department of Education
325 West Gaines Street
Tallahassee, FL 32399

PREPARED BY

Austin Fox, Rebecca English, Hope Leonard
Florida Institute of Technology
150 West University Boulevard
Melbourne, FL 32091

FLORIDA TECH

August 2023

Acknowledgements (Geochemistry)

Project Staffing (includes part–time and full–time project staff

Faculty – Dr. Austin Fox
Non–faculty–Stacey Fox
Graduate Assistants – Hope Leonard
College Roll – Rebecca English, Mary MacDonald

Highlights

- Inflow of seawater from port Canaveral or the coastal ocean would help to buffer Banana River Lagoon (BRL) against extreme temperatures and salinities that have been attributed to mass mortality events and initiation of the regime shift from a seagrass to algal dominated system.

- Similar seagrass to algal regime shifts in other estuaries, including Laguna Madre, Texas and Chesapeake Bay, have been attributed to changes in internal nutrient cycling with increased occurrences of hypoxia (low dissolved oxygen [DO]). Consistent with events in the Indian River lagoon (IRL)/BRL, initiation of the Laguna Madre regime shift was attributed to extreme low temperatures.

- Minimum winter temperatures based on hourly sampling in BRL were 3 to 9 degrees Celsius (°C) colder than minimum temperatures in the coastal Atlantic ocean, with monthly averages between 0.5 and 3°C cooler in BRL during winter months.

- Since 2017, summer BRL water temperature has averaged 0.5 to 3 °C warmer (monthly average) compared to the coastal Atlantic Ocean.

- Anthropogenic modifications since the early 1900s have likely contributed to lower and less stable salinities by increasing the size of the IRL watershed.

- Salinity in BRL has decreased almost continuously since 2014, reaching a low of 15 to 16 parts per thousand (ppt) during Phase 3 of this study. Stress from salinities below 23 ppt for seagrasses and below 20 ppt for hard clams have been shown to affect growth and survival. Increased seawater exchange would help to raise salinity, buffer against extremes, and improve habitat quality for these native species.

- Improved water quality with more stable DO would help to disrupt feedback loops that sustain the alternate stable algal regime.

- In BRL, water column respiration accounted for approximately 50 to greater than 80% of the total oxygen consumption (sediments + water) and is a major contributor to variations in DO concentrations and occurrences of hypoxia or anoxia.

- Water column respiration was on average 40% higher in BRL (–0.14 milligrams per liter per hour [mg/L/hr]) compared to the coastal ocean (–0.10 mg/L/hr).

- Inflow and associated mixing would result in lower respiration (oxygen demand), buffering against instances of hypoxia while lowering dissolved nutrient concentrations and favoring types (species) of nitrogen and phosphorus that are more readily removed through geochemical processes.

- Overall, concentrations of total dissolved nitrogen (TDN), total dissolved phosphorus (TDP) and silica (SiO_2) at the inflow and reference sites were on average 3.3–fold, 1.8–fold and 7.5–fold higher than in Port Canaveral. The relative abundances of organic nitrogen and phosphorus were 15% and 17% higher, respectively in the BRL than in Port Canaveral and offshore sites.

- The dissolved inorganic nitrogen (DIN) and soluble reactive phosphorus (SRP) ratio (DIN:SRP) in Port Canaveral increased between 2020 and 2023 from an annual median of 22 to 31. The median DIN:SRP ratio in the coastal Atlantic was 20.

- Both the DIN:SRP and TDN:TDP ratios in BRL decreased between 2020 and 2023 with medians at 47 ± 14 and 139 ± 29, respectively in 2020 compared to 15 ± 7 and 78 ± 2 in 2023. Higher ratios are known to promote small, fast-growing algae.

- The lower nitrogen (N):phosphorus (P) ratios observed during 2023 are also more consistent with the optimal ratio for some beneficial photosynthesizers including seagrasses that have been recovering in 2023.

- Benthic fluxes of N and P were highly variable, with sandy sediments alternating between a sink and a source of both nitrogen and phosphorus. Small changes to benthic fluxes have a dramatic impact on nitrogen supply or removal from the lagoon. Lower TDN fluxes during Phase 3 compared to Phase 2 support observations for N:P ratios.

- In contrast to variable fluxes observed for sand, muddy "mucky" sediments were a consistent source of N and P to overlying water.

- Significant positive correlations were identified between benthic fluxes of nitrate + nitrite (NO_x), TDN, phosphate (PO_4), dissolved organic phosphorus (DOP), and SiO_2 versus sediment temperature.

- Lower summer temperatures in BRL associated with the proposed pilot study (0.5 cubic meters per second [m^3/sec] inflow rate) were calculated to prevent 1.6 and 0.7 metric tons of N and P from entering the lagoon each year.

- Overall median TDN and TDP fluxes in sandy sediments were –200 ± 381 micro moles (µmoles) N/ square meter per hour (m^2/hr) and 2.7 ± 3.2 µmoles P/m^2/hr, respectively. These data demonstrate the potential for efficient removal of nitrogen from sediments when water quality improves.

- The ability of sediments to sorb and sequester phosphorus decreased from 133 milligrams (mg) P/kilogram (kg) in a 2001 study to 99 mg P/kg in our 2022 to 2023 study, likely reflecting cumulative impacts of chronic diel and episodic hypoxia.

- A positive flux for phosphorus is expected with improved water quality and fewer hypoxic events, which would help to preserve the ability of new sediments to sorb and sequester phosphorus.

- Collectively, data to date support a limited test of inflow as part of a multifaceted approach to lagoon restoration.

Table of Contents

List of Figures

List of Tables

List of Acronyms

BMAP	Basin management Action Plan
BRL	Banana River Lagoon
°C	Degrees Celsius
cm	Centimeter
DIN	Dissolved Inorganic Nitrogen

DIP	Dissolved Inorganic Phosphorus
DO	Dissolved Oxygen
DON	Dissolved Organic Nitrogen
DOP	Dissolved Organic Phosphorus
ENSO	El Niño-Southern Oscillation
EPC	Equilibrium P Concentration
FDEP	Florida Department of Environmental Protection
Florida Tech	Florida Institute of Technology
HAB	Harmful Algal Bloom
IRL	Indian River Lagoon
kg	Kilogram
kg/m^3	Kilograms Per Cubic Meter
km	Kilometer
L	Liter
LOI	Loss on Ignition
m	Meter
m^2	Square Meter
m^3/sec	Cubic Meters Per Second
mg	Milligram
mg/L	Milligrams Per Liter
mg/L/hr	Milligrams Per Liter Per Hour
mL	Milliliter
N	Nitrogen
NDBC	National Data Buoy Center
NH_4	Ammonium
NOAA	National Oceanic and Atmospheric Administration
NOx	Nitrate + Nitrite
OM	Organic Matter
ORP	Oxidation Reduction Potential
P	Phosphorus
PO_4	Phosphate
ppt	Parts Per Thousand
PSU	Practical Salinity Unit
PVC	Polyvinyl Chloride
rpm	Rotations Per Minute
SCUBA	Self–Contained Underwater Breathing Apparatus
SiO_2	Silica
SJRWMD	St. Johns River Water Management District
SOD	Sediment Oxygen Demand
SRP	Soluble Reactive Phosphorus
TDN	Total Dissolved Nitrogen

TDP	Total Dissolved Phosphorus
TMDL	Total Maximum Daily Load
UWF	University of West Florida
μm	Micrometer
μM	Micromolar
μmoles/m2/hr	Micromoles Per Square Meter Per Hour

1 Task Summary: Geochemistry (Task 3)

1.1 Background

Coastal eutrophication and associated hypoxic events remain one of the greatest challenges facing coastal communities on a global scale (Diaz and Rosenberg, 2008). With unique bathymetry, geomorphologies, and tidal flushing times, each coastal system experiences different response and restoration trajectories; however, some broad characterizations can be applied (Twilley et al., 1999). For example, Distinct differences in the ability of poorly–flushed versus well–flushed estuaries to cope with eutrophication have been consistently reported where poorly–flushed estuaries with long residence times more readily retain nutrients to promote algal blooms, loss of seagrass beds, hypoxia, and corresponding loss of ecosystem services (Twilley et al., 1999; Defne and Ganju 2015; Kemp et al., 1992; Twilley et al., 1999; Phlips et al., 2014). Consistent with previous studies, long residence times for water have been reported as one of the primary drivers of harmful algal blooms in IRL (Phlips et al., 2014). In contrast, well–flushed estuaries with short residence times have greater resilience to the impacts of eutrophication (Defne and Ganju 2015).

As the eutrophic state of an estuary progresses, loss of ecosystem services such as coupled nitrification–denitrification and sequestration of phosphorus that would in healthy systems remove or sequester nutrients, contributes to cascading events and a series of positive feedback loops helping to sustain eutrophication. These changes can lead to non–linear ecosystem level responses to eutrophication sometimes leading to alternate, algal dominated stable states compared to healthy seagrass dominated systems. In IRL this has been referred as a regime shift that among other things corresponded with an increase in dissolved phosphate concentrations (Phlips et al., 2021). Analogous changes to ecosystem level responses to eutrophication have been observed in other eutrophic estuaries including Laguna Madre, Texas and Chesapeake Bay. As a result, restoration efforts that disrupt the positive feedback mechanisms have been shown to yield non–linear restoration trajectories (Harris et al., 2015; Kemp et al., 2009). It is possible that restoring historic balances of freshwater and seawater could help restore these services.

Because in many cases algal biomass is correlated with nutrient loading, management strategies often address external loading (e.g., Phlips et al., 2014; Kemp et al., 2005). For example, basin management action plans (BMAPs) and total maximum daily loads (TMDL), used in Florida, limit loading that municipalities can contribute to watersheds; however, few management strategies address internal loading or restoration of ecosystem services. Historically, focusing on external loading has likely helped to mitigate algal blooms because peaks in phytoplankton biomass followed increased external loading, including in IRL and BRL (e.g., Phlips et al., 2014). Unfortunately, long term ecosystem responses to external pressures are often nonlinear and after about 2010, blooms in IRL and BRL are less predictable based on external loading. We hypothesize that this change is due to degradation of key ecologic processes sensitive to the effects of eutrophication and hypoxia.

For example, in the absence of significant or abrupt changes in external loading, an approximately 2–fold increase in the standing stock of TDP has been observed in IRL and BRL since 2010 (Phlips et al., 2021). Such shifts for IRL were consistent with altered internal cycling, losses of submerged aquatic vegetation, and increased phytoplankton biomass, most notably during a 2011 mass mortality event (Phlips et al., 2014; Morris et al., 2022). Since then, algal blooms have been more frequent, but less predictable relative to external loading. Over time algal blooms have likely become an important source of sediment organic matter (OM) and benthic nutrient fluxes (Lemley et al., 2021). Ultimately, sediments and internal processes support a larger fraction of

the total primary productivity as the eutrophic state progresses and management strategies must address both internal and external nutrient loading. Altered sediment biogeochemistry can result in more efficient recycling and less uptake and removal by sediments and these processes are sensitive to small changes in water quality. For example, both nitrogen concentrations and hypoxia increased in Chesapeake Bay from 1950 till about 1980; however, instances of hypoxia become more severe after about 1980, despite no appreciable increase in nitrogen loading (Kemp et al., 2005). This change in the system's ability to assimilate nutrients without experiencing adverse impacts was attributed to loss of key ecosystem functions and feedback loops.
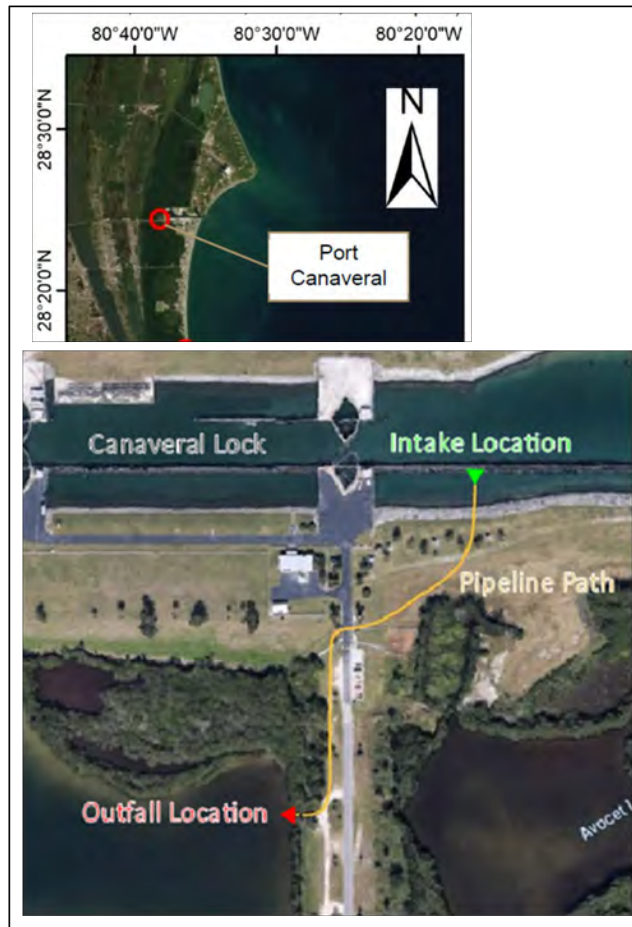
Figure 1. Map of proposed inflow pilot system site and pipeline path

Enhanced circulation in the IRL could contribute towards lowering nutrient concentrations that support the onset and proliferation of algal blooms. Another potential benefit would likely be to increase and or stabilize the concentration of DO, yielding enhanced resilience to anoxia and fish kills. The main benefits of decreased respiration and nutrient concentrations, and stabilized DO would likely result from changes to geochemical cycling. Any impacts from direct dilution by seawater would be spatially limited and considered secondary benefits. This study investigated the potential of ocean inflow to decreases nutrient concentrations through (1) sequestration of P in sediments and removal of N via coupled nitrification–denitrification and or anammox and (2) direct dilution by mixing where nutrients would be discharged to the coastal Atlantic Ocean. This study also investigated how these geochemical removal mechanisms would be altered as a

function of changes to temperature, salinity, dissolved oxygen and began to investigate how secondary impacts related to improved habitat quality may influence nutrient cycling. Preparing for a pilot study, this study built upon previous efforts establishing baseline data and techniques for monitoring temperature, salinity, DO, water–level, nutrient concentrations, pelagic respiration, and benthic fluxes at the inflow location. Data from this investigation are available to modelers to better predict changes to nutrient and DO concentrations and ratios under various pumping scenarios. This new dataset will also help modelers and managers to better predict how changes to temperature, salinity, and/or DO influence water quality in the IRL. These changes could result from a changing climate with impacts to temperature or precipitation (salinity) in the region or from anthropogenic intervention and engineered solutions.

1.2 Study Area

The IRL is a shallow (<5 meter [m]), bar–built, lagoon–type estuary that extends 250 kilometers (km) along the central east coast of subtropical Florida and ranges in width from <1 to approximately 9 km (Sigua et al., 2000; **Figure 1**). In the past decade, water quality in the IRL has declined with more severe and more frequent harmful algal blooms (IRL coalition; Tetra Tech 2016). The IRL is poorly flushed with 140 km between the Sebastian and Ponce de Leon inlets. The northern portion of the IRL is micro tidal and tidal flushing is negligible (Smith 1993) where tides are of only minor significance toward flushing (Smith 1993). Based on rainfall and low–frequency coastal water level variations, the 50% renewal time for water in the northern and central IRL sections ranges from approximately 100 to 300 days with a 100% exchange approximately every two years (Smith 1993; Florida Department of Environmental Protection [FDEP] 2013).

This study was carried out to evaluate possible impacts of enhanced circulation in the BRL with an emphasis at two primary locations: (1) North Banana River, considered as a likely inflow site (centered near 28.407, –80.638); and (2) Central Banana River, evaluated as a reference area where any impacts of inflow would be minimized due to geomorphological conditions that limit circulation (centered near 28.287, –80.6100). The North Banana River site was selected as a test location based on several factors. For example, the embayment provides a well–defined area for the test where the impacts of pumping could be tracked as inflow water mixed westward into the lagoon. A well–defined treatment area representing the lagoon for a scaled pilot–project minimizes risk that impacts are undetectable due to mixing. The control area was selected based on evaluation of models to identify candidate locations with limited circulation associated with proposed pumping volumes, followed by a comparison of water depth and bottom type at candidate sites versus the proposed inflow location (North Banana River) (**Figure 1**). Sampling sites inside the IRL and BRL were selected using a stratified, random approach to ensure that data are scientifically and statistically sound and can be extrapolated to a larger area (e.g., White et al., 1992). Seawater samples were also collected from within Port Canaveral as this is the most likely source of sweater for the proposed inflow project based on logistical considerations identified during Phase 1 of this study.

1.3 Task 3: Biogeochemistry (Objectives)

The objectives of this geochemical evaluation were as follows:

- **In–situ nutrient cycling:** Investigate temporal trends for biogeochemical processes (nutrient and oxygen cycling plus temperature and salinity regimes) in sediments and water near the inflow location. During Phase III, sediments from benthic chambers were collected and sent to the University of West Florida (UWF) for bacterial analysis. This

collaborative effort helped to link temporal changes in nutrient cycling to the bacterial communities present and active in lagoon sediments. The collaborative effort helped to distinguish changes related to bacterial versus geochemical processes while providing another quantifiable impact of hypoxia, helping to validate a mechanism by which inflow might improve water quality (e.g., increased abundance of nitrifying bacteria).

- **Laboratory nutrient cycling to quantify potential changes / benefits of inflow:** Laboratory experiments were carried out to determine how changes to dissolved oxygen that could result from inflow nitrogen influence the biogeochemical cycling of nitrogen, phosphorus and oxygen in lagoon water and sediments. Experiments built upon results from Phases 1 and 2 and added an evaluation of how changes to the ecosystem have impacted the sediments' ability to sequester phosphorus over time. In collaboration with UWF we determined if chronic diel or episodic hypoxia impacts nitrifying bacterial communities and thereby nutrient cycling. This next step helped to quantify the sediments' ability to sequester phosphorus as diel or episodic hypoxic events are mitigated by enhanced circulation and provided additional evidence that inflow could promote nitrification an essential step in the nitrogen cycle and removal of nitrogen from the system.

- **Track potential extent of impacts with focused monitoring:** Datasets for temperature, DO plus salinity in bottom water from select sites were monitored continuously to establish baseline data and trends from which changes associated with a pilot project could be compared. Based on results from Phase II, existing, spatially limited, monitoring networks (e.g., St. Johns River Water Management District [SJRWMD]) with sensors located at mid depths are of limited use towards tracking potential biogeochemical changes associated with a pilot inflow project. In other words, biogeochemical processes that would respond to inflow are focused at the sediment water interface. Therefore, in order to track impacts of inflow and provide information to modelers, we monitored temperature, salinity, and DO in key areas. Tracking changes to temperature, salinity, and DO are key to demonstrating feasibility and the success of inflow towards improving water and sediment quality. These data showed how processes measured in tasks 1 and 2 impact and apply to broad areas of the lagoon providing a metric to quantify broader impacts on a landscape scale. We continued evaluation of, if and where data from few existing water quality sensors (approximately 0.5 to 1.0 meter [m]) can be extrapolated to determine conditions in the complete water column (e.g., bottom water). These comparison data will help to highlight the importance of diel and episodic hypoxic events focused at the bottom of the lagoon. An understanding of the temporal and spatial extent of hypoxia at the sediment water interface has implications to estuaries around the world while demonstrating how inflow of cool, saline seawater will have the greatest impact at the bottom. This task provided data to modelers allowing them to determine the spatial extent to which mechanisms investigated in tasks 1 and 2 would be altered, thereby enabling a calculation or modeling of the change in nutrient loading based on various inflow volumes using data from the demonstration project.

- **Share data among tasks**. Temporally and spatially resolved data for nutrient cycling in sediments and water is essential for biological and physical modelers; data from tasks 1, 2, and 3 were shared with teams at Florida Tech and UWF at regular intervals throughout the project.

2 Methods

2.1.1 Water Sampling

Discrete water samples were collected using either a 1.7-liter (L) horizontal Niskin water sampler (General Oceanics) that was tripped at targeted depths using a weighted messenger or directly from chambers using acid washed 60–milliliter (mL) syringes. Water samples were filtered immediately after collection using Whatman 0.45 micrometer (µm) polypropylene syringe filters. All water samples were transported to the laboratory in a cooler on ice (4 degrees Celsius [°C]) in the dark. Once in the laboratory, samples were stored in the refrigerator until analysis. If analysis was not to be carried out immediately, samples were frozen at –20°C for up to 28 days.

2.1.2 Sediment Sampling

Sediment samples for laboratory experiments were obtained using a 0.1 square meter (m^2) Ekman Grab that was lowered slowly from an anchored boat until it hit the bottom. Any standing water was siphoned off prior to sample collection. Triplicate samples were obtained with three separate deployments of the grab. From each grab an approximately 3 centimeter (cm) layer of surface sediments was subsampled using a clean spoon and placed in an approximately 55 mL polycarbonate vial that was then sealed with parafilm and stored on ice at 4°C, in the dark for transport to the laboratory. Sediment samples were obtained from within benthic chambers using a sediment scoop, placed into approximately 55 mL polycarbonate vials, sealed with parafilm and stored in the dark, on ice at 4°C for transport to the laboratory. Once in the laboratory samples were weighed and stored in a freezer at –20°C (no defrost cycle) until analysis or until transfer to UWF.

Sediment samples from Santa Rosa Sound were collected using either syringe cores or polycarbonate cores (5 cm inside diameter). The top 2 cm from syringe cores were extruded in the field after removing overlying water into whirl pack bags. There were stored on ice at 4°C, in the dark for transport to the laboratory where they were frozen until extraction for deoxyribonucleic acid. Polycarbonate cores were stored in a cooler and extruded in the laboratory for chlorophyll a analysis, water or organic matter content.

2.1.3 Water Column Respiration, Sediment Oxygen Demand (SOD), and Nutrient Fluxes (in–situ)

Methods used in this study were developed following guidelines in Boynton et al. (2018) and used in both IRL and West Florida deployments. Darkened, benthic (sediment) and "blank" chambers were used to determine fluxes of DO (sediment oxygen demand [SOD]) and nutrients from sediments and from suspended particles (water column respiration). Blank chambers containing HOBO U26 Dissolved Oxygen data loggers (IRL) or miniDOT oxygen sensors (West Florida) and mechanical stirrers were rinsed and then filled with bottom water (**Figure 2a**).
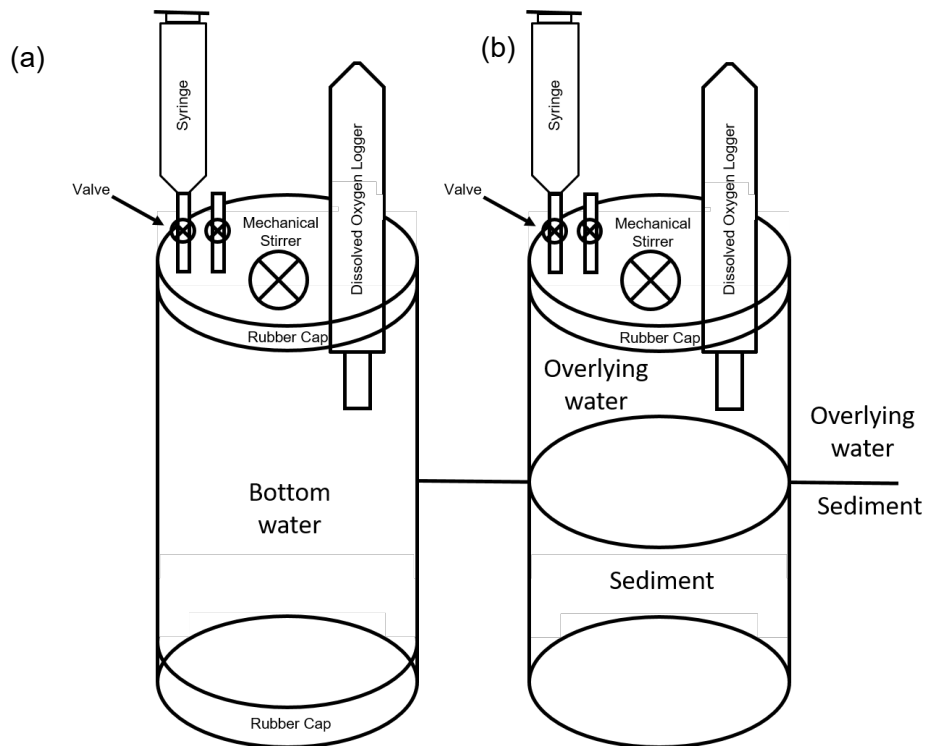
**Figure 2. Schematic diagram of the (a) blank and (b) benthic chambers used
to determine water column respiration, SOD, and nutrient fluxes.
Chambers are darkened to prevent photosynthesis.**

Benthic chambers were pushed vertically into sediments without side–to–side movement to avoid creating channels that would allow water exchanges. Chambers were pushed at least 10 cm into the sediments to prevent burrowing organisms from creating channels that would allow exchange of water with the outside environment. The height of each chamber was recorded to calculate the total volume of water in each chamber (e.g., Boynton et al., 2018). Once inserted, chambers were left open to the water column for 2 to 5 minutes to allow particles and sediments to settle and allow water to be exchanged with undisturbed bottom water. Before sealing each chamber, water samples were obtained from inside the chamber and immediately filtered using Whatman 0.45 µm polypropylene syringe filters. Chambers were then sealed with lids containing mechanical stirrers to keep the water well–mixed and to prevent buildup of a concentration gradient in a boundary layer at the sediment–water interface. Stirrers were designed and deployed to mix the overlying water without causing sediment resuspension. HOBO U26 Dissolved Oxygen data loggers were mounted through an airtight seal in the lid of each chamber (**Figure 2b**). The rate of decline of the DO within the chamber was measured over a 1.5 to 2–hour period for sand and for 20 to 45 minutes for mud. In West Florida, an additional set of water samples was collected from the deployed domes after 4 hours. Chambers were kept in the shade at a constant in–situ temperature for the duration of the incubation. At the end of each deployment, a syringe was attached to a valve on the top of the chamber and a 60 mL water sample for nutrient analysis was extracted and immediately filtered and stored on ice. At the end of each deployment, Water quality parameters were recorded with a YSI multimeter, light levels were measured at depth using LiCor 4PI quantum sensor, and duplicate sediment samples are obtained from inside each sediment chamber, placed in polycarbonate vials (approximately 55 mL) and sealed with parafilm. Sediment

samples were placed in a cooler on ice at 4°C for transport to the laboratory. Upon return to the laboratory, sediments samples are weighed and placed in a freezer at –20°C.

2.1.4 Infaunas impact on nutrient fluxes (ex–situ)

Intact sediment cores were collected via scuba diver from a deposit of fine–grained, organic–rich sediments centered at 28°04'57.8"N 80°35'54.3"W. The 9.5 cm diameter cores were pushed approximately 20 cm into sediments and sealed with approximately 10 cm (700 mL) of overlying water. Cores were returned to the laboratory and placed in temperature–controlled water baths set to 25°C to match the average lagoon temperature. Sediment cores were aerated using standard aquarium diffusers and overlying water was exchanged using calibrated peristaltic pumps. Pump rates were adjusted in each core to achieve an 8–hour residence time for overlying water during the acclimatization period.

Infauna were collected from sandy sediments immediately adjacent to the organic–rich deposit where intact cores were collected. Infauna were collected following methods outlined in Raz–Guzman & Grizzle, 2001. Infauna samples were collected using 0.1 m^2 Ekman Grab that was lowered slowly from an anchored boat until it hit the bottom. Grab samples were sieved through a 0.5mm screen to remove sediment. Infauna were returned to the lab and placed in an aquarium containing water and sediment from the collection site and maintained at 25°C.

Following a 5–day acclimatization period, sediment from the infauna tank were sieved (0.5 mm) to obtain live *Macoma sp*. for addition to experimental cores. Three unaltered cores were used as control. In three replicate, 50 individual *Macoma sp*. were added. To another 3 cores, 100 individuals were added. Following a 5–day acclimatization period with infauna burrowing into cores the pump rate was increased to achieve a 2-hour residence time. After at least 5 residence times 60 mL water samples were obtained from each core and from the influent water to determine nutrient fluxes using this flow–through system. Water samples were immediate filtered through Whatman 0.45 µm polypropylene syringe filters. Filtered samples were stored in the fridge until analysis.

2.1.5 Continuous water quality monitoring (DO)

Continuous monitoring of bottom water DO was carried out using Onset HOBO U26 DO data loggers. Loggers deployed in polyvinyl chloride (PVC) housings equipped with copper based antifouling guards to promote reliable datasets collected over the targeted 14- to 30-day deployment periods. Sensor housings were designed to keep sensor faces within 10 cm of the bottom with development during Phase 1 of this project. Sensors were lab calibrated immediately before each deployment and field data was validated at the beginning and end of each deployment by comparison with data obtained using a calibrated YSI ProDSS (Yellow Springs Instruments) data sonde or a separate, calibrated, HOBO U26 datalogger. Results are reported in milligrams per liter (mg/L) and hypoxia has been defined as DO less than 2 mg/L.

2.1.6 Nutrient and Water Analyses

Concentrations of ammonium (NH_4), nitrate + nitrite (NOx), TDN, ortho–phosphate (PO_4) and TDP were determined for IRL samples using a SEAL AA3 HR Continuous Segmented Flow Autoanalyzer following manufacturer's methods. The NIST–traceable Dionex 5–Anion Standard was analyzed as a reference standard with each batch of samples to ensure accuracy; values were consistently within the 95% confidence interval for the prepared standard. Analytical precision (relative standard deviation) for lab duplicates was <3% for nutrient analyses. In West Florida, chlorophyll *a* from filters and sediments was determined using Welshmeyer (1994), nitrate

plus nitrite were analyzed using Schnetger and Lehners (2014), ammonium was analyzed using Holmes et al. (1999), and nitrite and dissolved inorganic phosphorus (DIP) were analyzed using Parsons et al. (1984).

2.1.7 Sediment Analyses

Vials containing wet sediments were weighed, sealed with parafilm and placed in a Freezer at –20°C until frozen. Frozen sediments were placed into a Labconco, FreeZone 6 system and freeze–dried to a constant weight (>72 hours). Dried sediments were homogenized and powdered using a SPEX Model 8000 Mixer/Mill. The water content of sediments was determined based on the difference in mass between wet and dry sediments (% water = [wet weight – dry weight] *100%). Organic matter content was determined using Loss on Ignition (LOI) by combusting freeze–dried and desiccated sediments at 550°C following methods of Heiri et al. (2001).

2.1.8 Aerobic phosphorus sorption / desorption

Sediment and water were collected from eight sites located between Fort Pierce and Scottsmoor for phosphorus sorption experiments (**Table 1.**). These sites were selected in an effort to revisit sites sampled before the 2011 algal blooms and the associated regime shift (Pant and Reddy, 2001; Phlips et al., 2021). Revisiting these sites provided an opportunity to investigate potential long–term changes that result from the cumulative effects of hypoxia over time. At each site, 3 sediment samples (field replicates) were collected with 3 separate grabs (0.1 m^2 Ekman grab) and 3 L of bottom water were collected to carry out phosphorus sorption experiments. In the lab, each of the three samples were processed with lagoon water spiked with 10 different concentrations of phosphorus for both aerobic and anaerobic conditions. Spikes were followed by desorption experiments for a total of 960 (8x120) water samples and 24 (8x3) sediment samples.

Table 1. Station ID, latitude and longitude for samples collected for phosphorus sorption experiments.

Station ID	Latitude	Longitude
1	27°31.544'	–80°20.131'
2	27°41.455'	–80°23.354'
3	27°51.476'	–80°29.011'
4	27°58.576'	–80°31.842'
5	28°03.285'	–80°34.577'
6	28°08.188'	–80°36.927'
7	28°27.769'	–80°43.600'
8	28°35.386'	–80°44.753'
9	28°43.710'	–80°49.354'

Upon return to the laboratory, wet sediments were homogenized (mixed thoroughly using a plastic spoon) and sieved through a 0.5 cm screen to remove large particles and shell fragments. Ten–gram aliquots of each sieved and homogenized sediment sample were placed into 10 separate (30 total aerobic per site) acid washed and dried 50–mL centrifuge tubes with an 11th aliquot placed into an approximately 55 mL polycarbonate vial for degermation of water and organic matter contents. To each centrifuge tube, 18 mL of filtered lagoon (bottom) water was added with 2 mL of varying concentration solution containing phosphorus such that the total concentration in each centrifuge tube (20 mL) contained 0, 0.1, 0.2, 0.5, 1, 2, 5, 10, 25 and 50 mg/L of dissolved

phosphorus. The 30 samples were placed on a mechanical shaker and shaken for 24–hours. After 24–hours, samples were removed and centrifuged at 3000 rotations per minute (rpm) for 7 minutes to separate water from pelletized sediments. Water from each tube was carefully poured off and immediately filtered using Whatman 0.45 μm polypropylene syringe filters. Filtered water samples were placed in a refrigerator until analysis for dissolved nutrients to determine the quantity of phosphorus sorbed onto aerobic sediments.
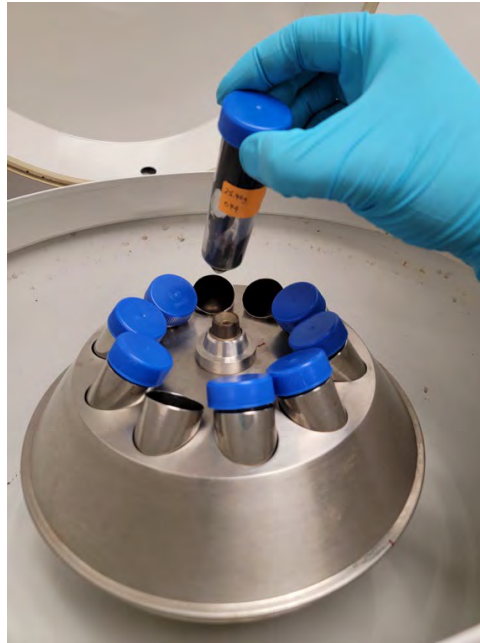
Figure 3. fifty–mL centrifuge tubes containing phosphorus spiked
sediment slurries are loaded into a centrifuge.

Following sorption experiments, an additional 20–mL of filtered lagoon (bottom) water was added to centrifuge tubes containing pelletized sediments (30 total). Centrifuge tubes containing sediments and filtered lagoon water were placed back onto the mechanical shaker and shaken for an additional 24–hours. After the second 24–hours of shaking, samples were removed and centrifuged to separate water. Water from each tube was immediately filtered using Whatman 0.45 μm polypropylene syringe filters. Filtered water samples were placed in a refrigerator until analysis for dissolved nutrients to determine the quantity of phosphorus that had been desorbed into lagoon water following sorption in the previous 24–hour period.

2.1.9 Anaerobic phosphorus sorption / desorption

Coinciding with aerobic experiments, 10–gram aliquots of each sieved and homogenized sediment sample were placed into 10 additional 50–mL centrifuge tubes (30 total anaerobic per site). Centrifuge tubes were sealed into a glove box containing a 100% N_2 atmosphere. To each tube, 18 mL of filtered lagoon water was added, the sediment slurry was purged with N_2, and centrifuge tubes were sealed and removed from the glove–box and placed into a temperature-controlled water bath at 25°C for a 4–week incubation period. Each week, centrifuge tubes were returned to the N_2 glove–box and were purged again with N_2 gas in order to ensure an anaerobic environment was maintained. After purging, samples were sealed and returned to the water bath.
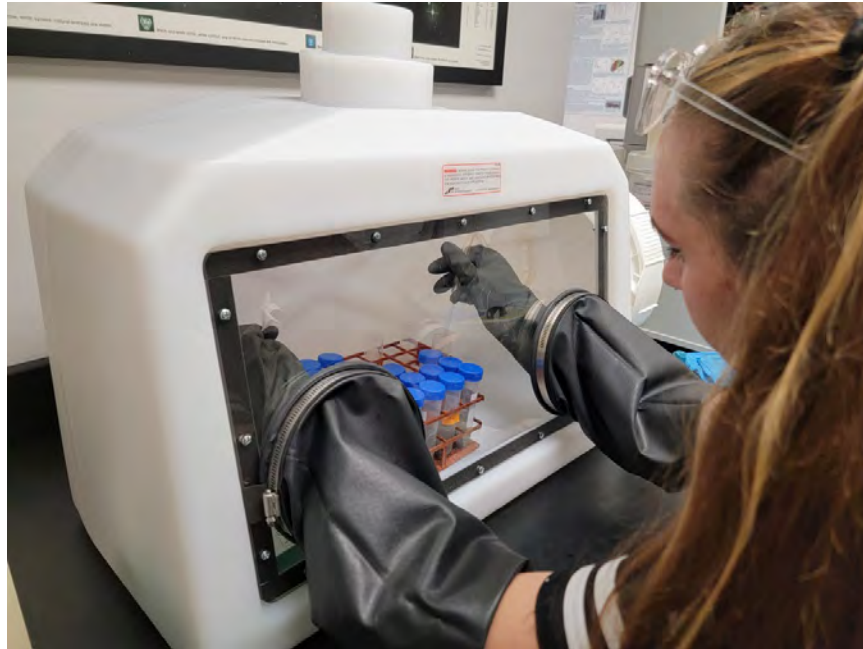
Figure 4. Undergraduate researcher, Rebecca English purges sediment slurries with N2 in a nitrogen glove–box for anaerobic phosphorus sorption experiments.

Following the 4–week incubation period 2 mL of N_2 purged solutions containing varying concentrations of phosphorus were added to each sample such that the total concentration in each centrifuge tube (20 mL) contained 0, 0.1, 0.2, 0.5, 1, 2, 5, 10, 25 and 50 mg/L of dissolved phosphorus in a completely anaerobic environment. At this point, the samples were placed on a mechanical shaker and the sorption and desorption experiments carried out on aerobic sediments were repeated, with the samples being purged with N_2 gas after the sorption experiment to maintain the anaerobic environment for the desorption experiment.

2.1.10 Phosphorus sorption calculations

Data from phosphorus sorption experiments were processed in MS Excel. Sediment P sorption maxima (Smax) and bonding energy constants (K) were estimated using the modified Langmuir equation using S' and S0 (Pant and Reddy, 2001):

$$Ct/S = 1/(k × Smax) + Ct/Smax \qquad \textbf{Eq. 1.}$$

where:

S = S' + S0 = total amount of P sorbed to sediments (mg kg–1);
S' = amount of added P sorbed to sediments (mg kg–1);
S0 = amount of native P originally sorbed to sediments (mg kg–1);
Smax = P sorption maximum (mg kg–1);
Ct = Solution P concentration after 24 hour equilibration (mg L–1);
k = a constant related to P bonding energy (L mg–1);

S0 and EPC (equilibrium P concentration (mg L–1)) were estimated using a least–square fit of the Langmuir isotherm model at low concentrations (Dari et al., 2015; **Figure 5**). The EPC is the P concentration at which there is no net adsorption or desorption and is estimated as the x–

intercept of the least–square best fit trendline. S0 is the amount of P initially held by the sediments before the experiments and is estimated as the y–intercept of the trendline.
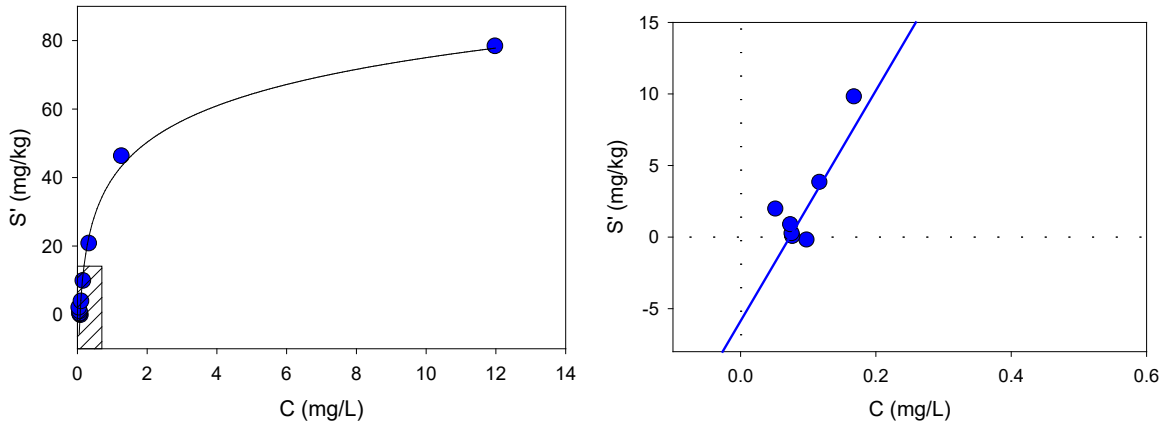
Figure 5. S' (amount retained by sediments; mg/kg) versus C (solution concentration; mg/L) at site 8 replicate 1 (aerobic). (a) complete dataset and (b) zoomed in to show X and Y intercepts used to determine S_0 (innate amount sorbed to sediments) and EPC (equilibrium concentration).

2.1.11 Oxygen and Nutrient Flux Calculations

Sediment oxygen demand was determined by subtracting the water column respiration (milligrams per liter per hour [mg/L/hr]) values for "blank" chambers from values obtained from benthic chambers (Ziegler and Benner 1999). The total rate of oxygen utilization by sediments, accounting for the volume in the benthic chamber [DO used by sediments (mg/L/hr) times the volume of the benthic chamber (L), calculated using the height of the chamber above the sediments] was divided by the surface area of sediment to yield values for SOD. Values for SOD are reported in micromoles per square meter per hour (μmoles/m^2/hr).

Benthic nutrient fluxes were determined from benthic and blank chambers by subtracting initial nutrient concentrations (micromolar [μM]) from final concentrations for both benthic and blank chambers. The changes in concentrations (μM) were then divided by the elapsed time (hours) of each incubation to yield rates in μM/hr. The rate of nutrient production/utilization in blank chambers was then subtracted from the rate calculated for benthic chambers, to determine the production/utilization by sediments and particles independently. The rate (μM/hour) for the benthic chamber was then multiplied by the volume of the chamber, calculated using the height of the chamber above the sediments, to yield the amount of nutrients produced/used by sediments in the chamber per hour (μmoles/hr). This value was divided by the surface area of sediments in the chamber to yield a flux in μmoles/m^2/hr consistent with units used in the literature (e.g., Boynton et al., 2018). A similar approach was used to determine nutrient fluxes from laboratory incubations; however, Phase III laboratory incubations utilized a flow–through system with elapsed time determined by flowrates through each chamber. Nutrient fluxes were evaluated against the rate of oxygen utilization to ensure that linear nutrient production/utilization could be assumed. If the chamber went anaerobic during the deployment or oxygen utilization was non–linear, nutrient fluxes were flagged and not included in data interpretation.
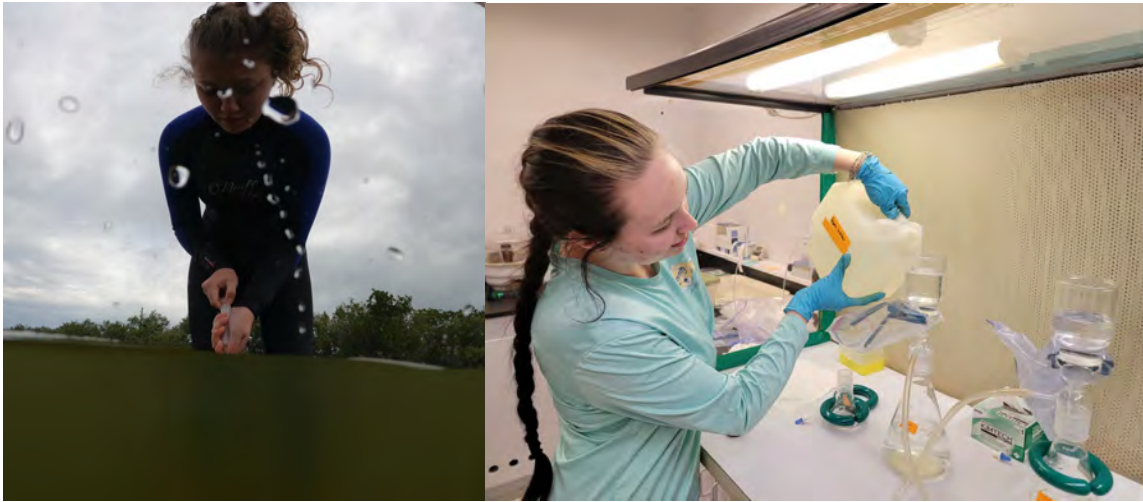
Figure 6. (Left) Marcy MacDonald (student) collecting water samples from a benthic chamber deployed at Slick 520. (Right) Rebecca English (student) filter water for phosphorus sorption experiments.

3 Results and Discussion

3.1 Context and purpose

Numerous studies have reported on attempted remediation of eutrophic coastal systems with examples of both successful restoration of ecosystem functions; however, restoration efforts in other areas have been less successful. Overwhelmingly the literature points to the complexity of eutrophication and hypoxia with varied responses to restoration in different systems highlighting the need for system–specific management and remediation that account for both external and internal loading plus physical and ecological processes. Within each system, fundamental features such as bathymetry, circulation and stratification modulate dissolved oxygen and have often been the focus of restoration and modeling; however, ecological responses and disruption of feedback process that change the trophic structure, habitat quality or biogeochemical cycles can lead to non–linear response trajectories (Kemp et al., 2009; Harris et al., 2005). In IRL the importance of these internal changes to ecosystem functioning is underscored by the change to a new stable state, "regime shift" that occurred following the 2011 algal blooms, despite no significant associated change in external loading. Therefore, it is essential to consider how restoration will impact internal processes. For example, direct exchanges of lagoon and seawater provide limited direct benefit as discussed in detail below and as indicated by models; however, small changes to water and sediment quality can alter ecosystem functioning and internal nutrient cycling to yield potentially large benefits at the landscape scale. In addition to subtle geochemical changes that occur over a large spatial and temporal scale, enhanced circulation would certainly help to mitigate extreme temperature of salinity events in IRL thereby helping to mitigate further declines in ecosystem functioning.

Brief summaries related to changes in temperature, salinity and DO preface our results and discussion below.

Temperature:

One major benefit of ocean inflow would be buffering against extreme temperature events in IRL and BRL. For example, the "regime shift" in IRL is often causally associated with exceptionally low temperatures, <4°C, in the lagoon during winter 2009/2010 (Phlips et al., 2021). In addition to buffering extremes, higher temperatures contribute to enhanced internal nutrient loading. Bacterial metabolism increases non–linearly as a function of temperature. As a result, small changes in water temperature can significantly impact rates of bacterial metabolism. On a landscape scale (square kilometers) this can lead to major changes in nutrient cycling and internal loading. For example, In IRL benthic fluxes increased by 7 to 10% per °C with cooler temperatures leading to less nutrient recycling and ultimately lower concentrations (Fox and Trefry, 2018; Boynton et al., 2023). Additionally, the solubility of dissolved oxygen changes with temperature and cooler water is more resilient to hypoxic events and fish kills.

Dissolved Oxygen:

One consistent change in systems that have experienced a "regime shift" is a change in the system's ability to assimilate nutrients without experiencing hypoxia (e.g, Kemp et al., 2009). Increased occurrences and duration of hypoxia promotes recycling versus removal of both nitrogen and phosphorus creating a series of positive feedbacks that help to sustain eutrophication and an alternate stable state, or "regime." In IRL, high sediment oxygen demand for expanding areas of organic rich sediments combined with extreme diurnal oxygen fluctuations promote diel and episodic hypoxia. Inflow of water with lower water column respiration and turbidity could buffer against instances of hypoxia, supporting removal versus recycling of nutrients. This would also support more diverse benthic faunal communities capable of filtering water and bio–irrigating sediments. Increasing the depth of the oxidized surface layer of sediments would contribute to non–linear restoration trajectories with potential benefit beyond direct exchanges.

Salinity:

It has been proposed that remediation of hypoxia and eutrophication can be enhanced by restoration of habitats for filter–feeding bivalves and seagrass beds (e.g., Kemp et al., 2009). In IRL, recent efforts to restore the hard clam *M. Mercinaria* identified low salinity as one of the major challenges towards clam restoration (ROS, 2023). Also, seagrass meadows are reported in IRL and other locations to experience enhanced stress during low salinity events (Morris et al., 2021). With anthropogenic changes to hydrology, the freshwater watershed has increased by 260% since the 1920s with channelized drainage versus sleuths and wetland leading to more rapid and larger inputs of freshwater following rainfall (Osborn, 2016). Increased freshwater inputs were in most cases not balanced by increased exchanges of seawater. Restoring this balance may help buffer against extreme variability and low salinity events.

3.2 Temperature, Salinity and Density

Building upon efforts from Phase 1 and 2, long–term datasets for temperature and salinity for IRL were obtained and updated for 1987 through July 2023 from sources including SJRWMD and the network of sensors deployed and maintained by Florida Institute of Technology (Florida Tech). Long term temperature records for the port at Trident Pier were obtained from 2005 to July 2023 (the complete record) from the National Oceanic and Atmospheric Administration's (NOAA) National Data Buoy Center (NDBC). Consistent with the past few years, the annual average

lagoon temperature was approximately 25°C and followed seasonal patterns with a range of approximately 21°C, with a minimums at 11 to 12°C typically reported during February, to a maximum of 32 to 33°C typically reported during August and September (e.g., **Table 2**, **Table 3**). Temperatures of seawater in Port Canaveral followed similar seasonal patterns, yet with a smaller range. Minimum temperatures during winter were higher, typically at approximately 18°C and maximum temperatures during summer were slightly lower than those in IRL at 30 to 31°C (e.g., **Figure 7, Table 2, Table 3**). Overall, variability in temperature was greater in IRL with more rapid and more extreme changes in response to atmospheric weather patterns.
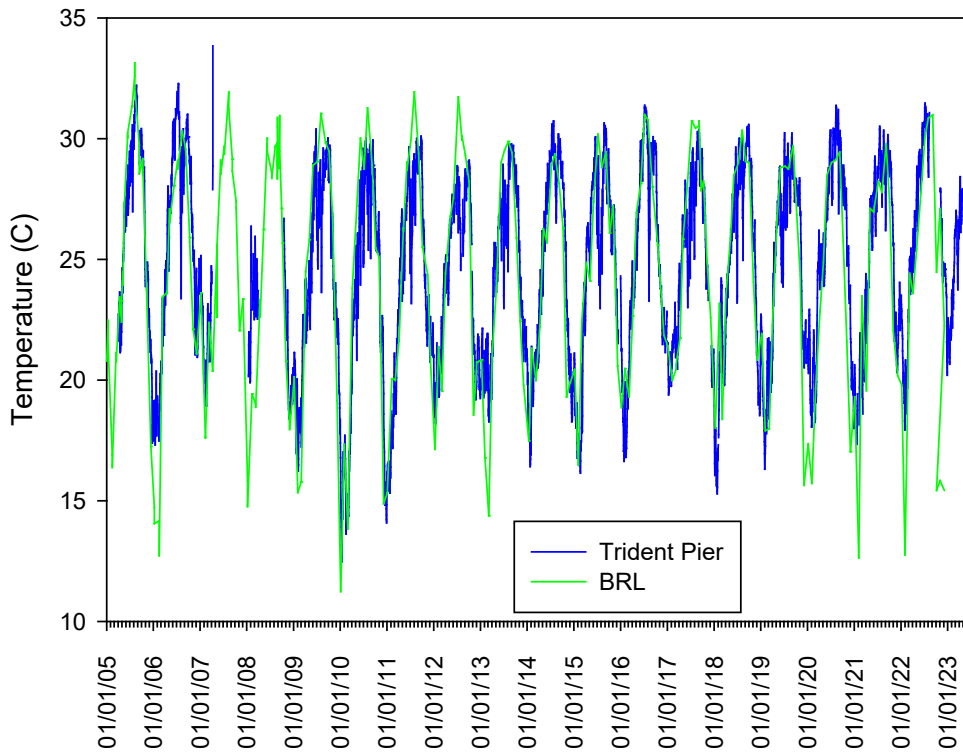
Figure 7. Temperature between 2005 and 2023 in port Canaveral at Trident pier and in BRL at IRLB02. Trident pier data from NOAA NDBC and BRL data from SJRWMD.
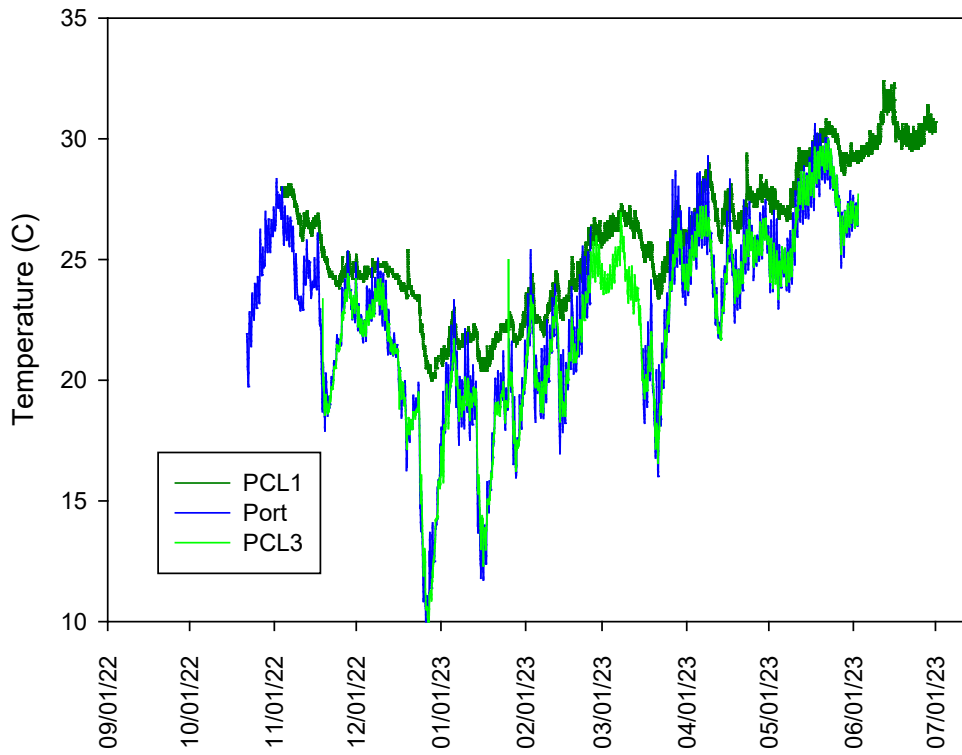
Figure 8. Temperature in BRL in the area of inflow and in Port Canaveral (Port), at the inflow site (PCL1) and along a transect towards the open lagoon (PCL3).

For example, during winter 2020 to 2021 (Phase 2), the lowest temperature recorded near the proposed inflow location in the lagoon was 12.1°C (12/26/2020), compared to 17.1°C in Port Canaveral. In winter 2021 to 2022 the minimum lagoon temperature was 12.7°C compared to 17.9°C in Port Canaveral and in winter 2022 to 2023 the minimum temperature in BRL near the inflow site was 11.8°C in January 2023 compared to approximately 20°C at Trident pier in Port Canaveral (**Figure 7**). Based on these data plus long–term datasets, pumping during winter months could bring warmer water into the lagoon from the ocean. Although warmer water could contribute to increase bacterial activity and nutrient cycling as discussed in **section 3.5.3.1** below, managed pumping could help to mitigate extreme cold temperature events in IRL such as the 4°C temperatures in winter 2009/2010 when at the same time port Canaveral reached a minimum of 12.5°. This extreme temperature event in IRL, even though short in duration is often causally associated with a mass mortality of tropical and subtropical species, creating a supply of nutrients ultimately leading to a regime shift (Phlips et al., 2021). A similar cold event in Laguna Madre, Texas during 1989 contributed to a mass mortality event that supplied nutrients spawning algal blooms that persisted for 8 years (Buskey et al., 1996; 1997). In cold environments the opposite has been reported where high temperatures led to mortality of temperate species (e.g., Edwards et al., 2006).

On the other end of the spectrum, maximum lagoon temperatures were higher than maximum temperatures in Port Canaveral and the coastal Atlantic Ocean. For example, the maximum temperature during summer 2022 (August) at 32.9°C, was 1.5°C higher than the maximum of 31.4°C in Port Canaveral. So far in 2023 the maximum lagoon temperature 33.7°C was 2.1°C

higher than 31.6°C in Port Canaveral. Overall average monthly lagoon temperatures were approximately 1 to 3°C warmer during summer months. During 2023 lagoon temperatures have remained below ocean temperatures likely related to El Niño-Southern Oscillation (ENSO) patterns and increase rainfall and cool freshwater inputs during this El Nino year. Overall, inflow of seawater could help buffer against extreme temperature events that have been associated with deteriorated ecosystem health while also decreasing maximum temperatures during the hottest summer months.

Table 2. Minimum temperature (°C) in Port Canaveral and in BRL in the area of inflow (2017–2023).

Location	2010	2017	2018	2019	2020	2021	2022	2023	Source
Trident Pier	12.5	19.4	15.3	16.3	18.0	17.3	17.9	20.6	Ndbc.noaa.gov
Banana River	<4	13.9	9.2	13.1	10.2	11.7	9.8	11.8	sjrwmd.com/data/water–quality/

Table 3. Maximum temperature (°C) in Port Canaveral and in BRL in the area of inflow (2017–2023)

Location	2017	2018	2019	2020	2021	2022	2023	Source
Trident Pier	30.3	30.6	30.2	31.3	30.5	31.4	31.6	Ndbc.noaa.gov
Banana River	32.9	32.4	32.7	33.1	32.9	32.9	33.7	sjrwmd.com/data/water–quality/

Overall, during Phases 1 through 3 of this project, salinity was lower in BRL compared to values for Port Canaveral. For example, during 2019–2023, salinity in BRL ranged from 15.2–25.5 practical salinity units (PSU) and, as expected, salinity in the lagoon was lower than the range of salinities obtained for seawater in Port Canaveral at 27 to 34 PSU (**Figure 9**). Vertical profiles for salinity in seawater from the proposed inflow location (Port Canaveral) showed a salinity gradient with the lowest salinities in surface water at 27 to 32 PSU, increasing with depth to 30 to 34 PSU (**Figure 9**). In BRL at both the inflow and reference/control locations, salinity was typically well mixed in the range of 15 to 20 PSU (**Figure 10, Figure 11**). In both port Canaveral and BRL temperature was often 0.5 to 2°C cooler in bottom water. DO measured in the late afternoon was typically in the range of 90 to 120% saturation in both Port Canaveral and the BRL. In many cases DO decreased slightly in bottom water; however, daytime photosynthesis and mixing are likely responsible for these trends observed in discrete vertical profiles. Variations in dissolved oxygen over time that result from water column respiration and sediment oxygen demand are discussed in detail below.
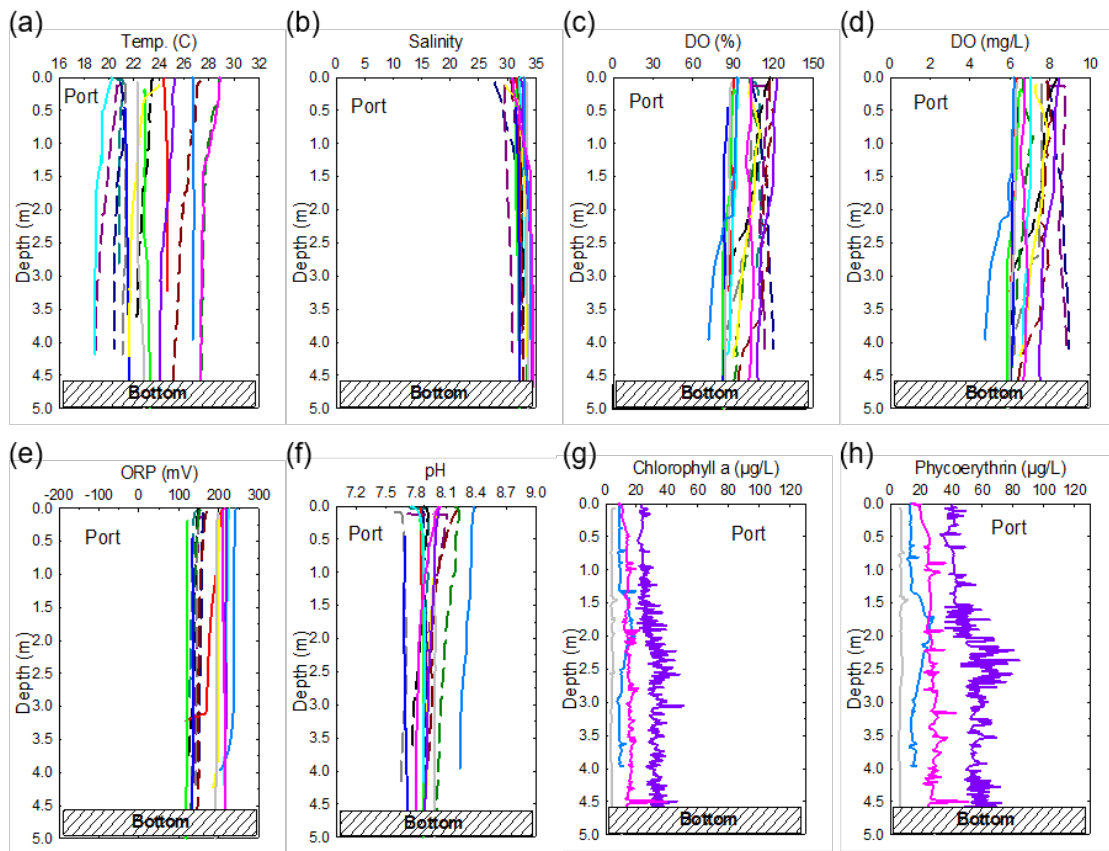
Figure 9. Vertical profiles for (a) temperature, (b) salinity, (c) dissolved oxygen (%), (d) dissolved oxygen (mg/L), (e) oxidation reduction potential, (f) pH, (g) chlorophyll a and (h) phycoerythrin in Port Canaveral during discrete approximately monthly sampling events during Phases 1 through 3.
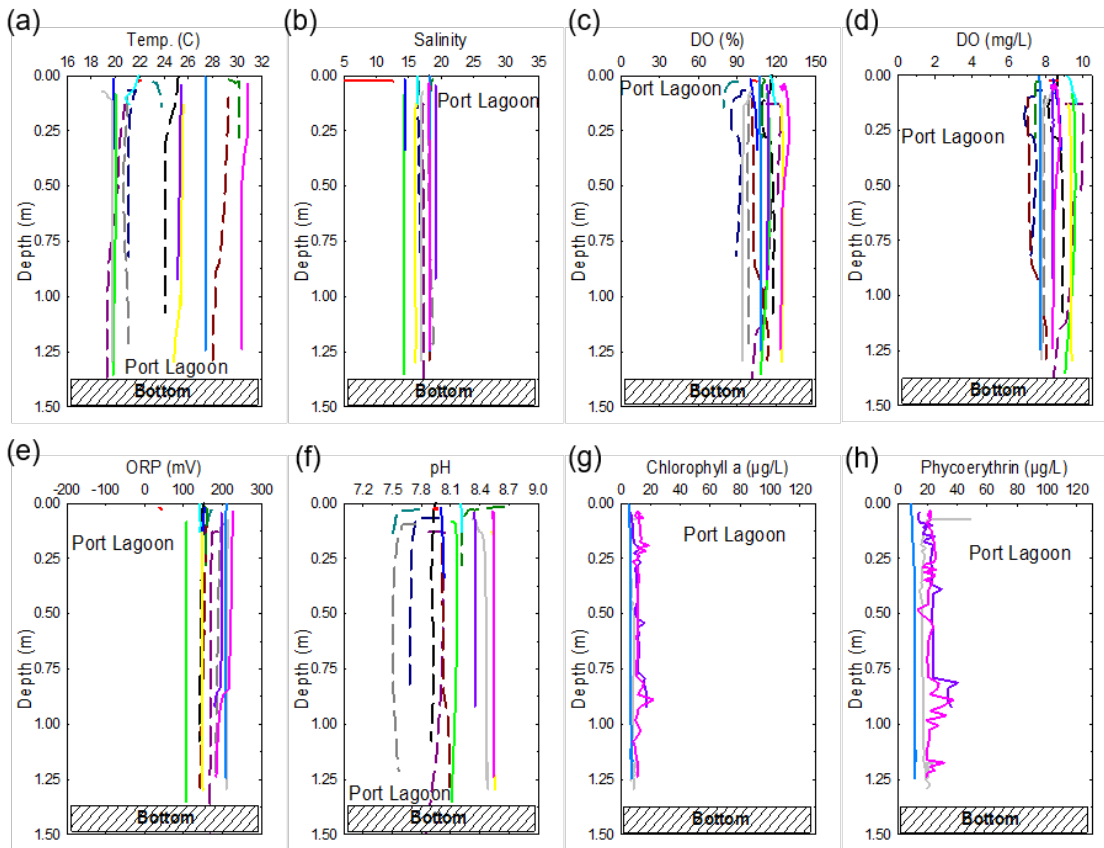
Figure 10. Vertical profiles for (a) temperature, (b) salinity, (c) dissolved oxygen (%), (d) dissolved oxygen (mg/L), (e) oxidation reduction potential, (f) pH, (g) chlorophyll a and (h) phycoerythrin in the Banana River Lagoon at the proposed inflow location during discrete sampling events.
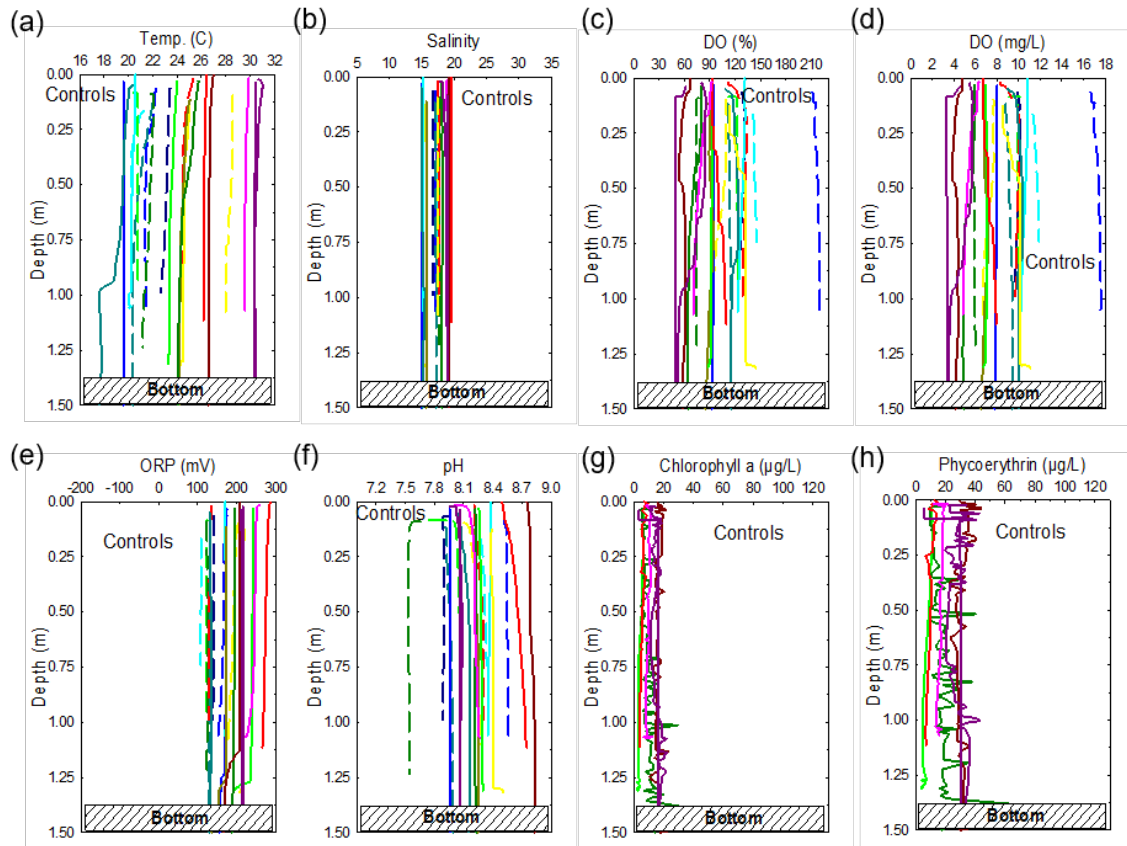
Figure 11. Vertical profiles for (a) temperature, (b) salinity, (c) dissolved oxygen (%), (d) dissolved oxygen (mg/L), (e) oxidation reduction potential, (f) pH, (g) chlorophyll a and (h) phycoerythrin in the reference / control area during discrete sampling events.

In BRL near the inflow site (IRLB04) salinity has trended downwards during the project period (Phases 1–3 during 2019–2023) decreasing from an average of 21.33 during 2020 to an average of 18.4 so far in 2023 with minimum values between 15 and 16 in November and December 2022 (**Figure 12**). This trend for salinity fits a longer–term regional pattern for decreasing salinity beginning in about 2014 when salinity was >35 (

Figure 13). Previous studies have found a relationship between climatic patterns, the ENSO and trends for salinity (Philips et al., 2014). For example, periods of increasing salinity between approximately 1984 and 1991, then again from approximately 1996 to 2001 and most recently between approximately 2006 and 2011 occurred predominantly during periods of La Nina with reduced rainfall. During these periods, salinity increased from approximately 20 to 28, approximately 14 to 31 and approximately 15 to 35, respectively. During each period of increasing salinity, brief El Nino events and associated rainfall slowed the rise in salinity but were not enough to reverse the trend (e.g., a dip in salinity during 2009 in

Figure 13). Between 2011 and 2014 salinity was relatively stable following annual trends for rainfall; however, since 2014 salinity has decreased to approximately 15 to 19 PSU most recently in July 2023. It is interesting that this most recent trend has occurred during predominantly La Nina. Although there is a relationship between lagoon salinity and ENSO, it's not simple and there is no direct correlation between ENSO index and lagoon salinity, mostly because ENSO and associated changes to rainfall patterns impact the trajectory rather than the absolute salinity value (**Figure 14a**). With 2023 entering an El Nino cycle, IRL salinity is likely to drop further. Based on

these data, enhanced exchanges of sweater would help to buffer against salinity extremes and low salinity events in BRL. Although we often consider recent history, ecosystems often respond slowly to external stressors and restoration should consider long term changes and impacts.
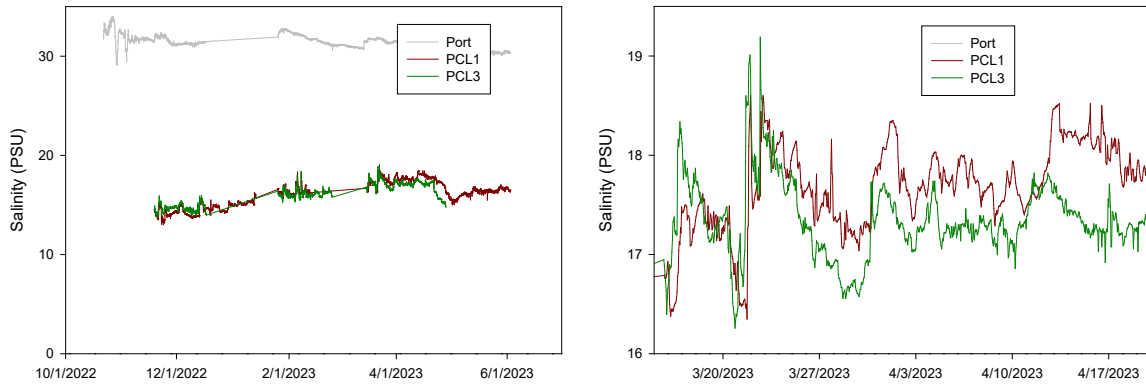
Figure 12. Salinity in port Canaveral (Port) and in BRL at the inflow site (PCL1) and along a transect towards the open lagoon (PCL3).
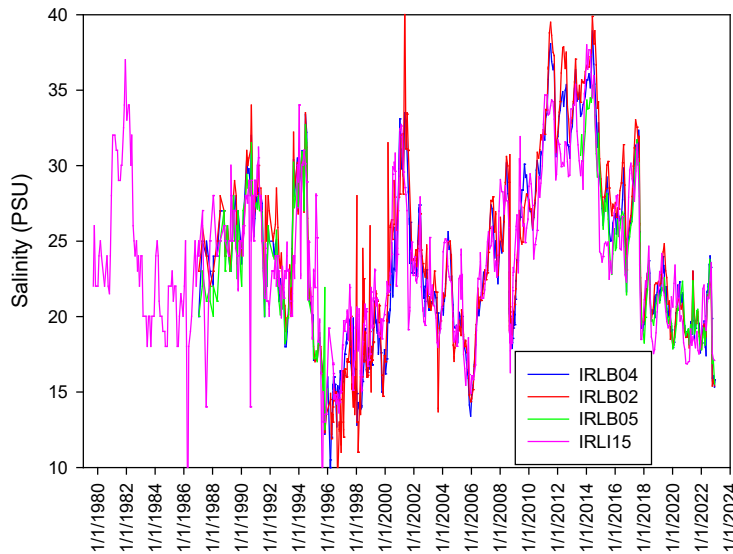
Figure 13. Salinity in the IRL and BRL between 1980 and 2023. Sites are SJRWMD monthly monitoring locations, 2 in BRL and 2 in NIRL.
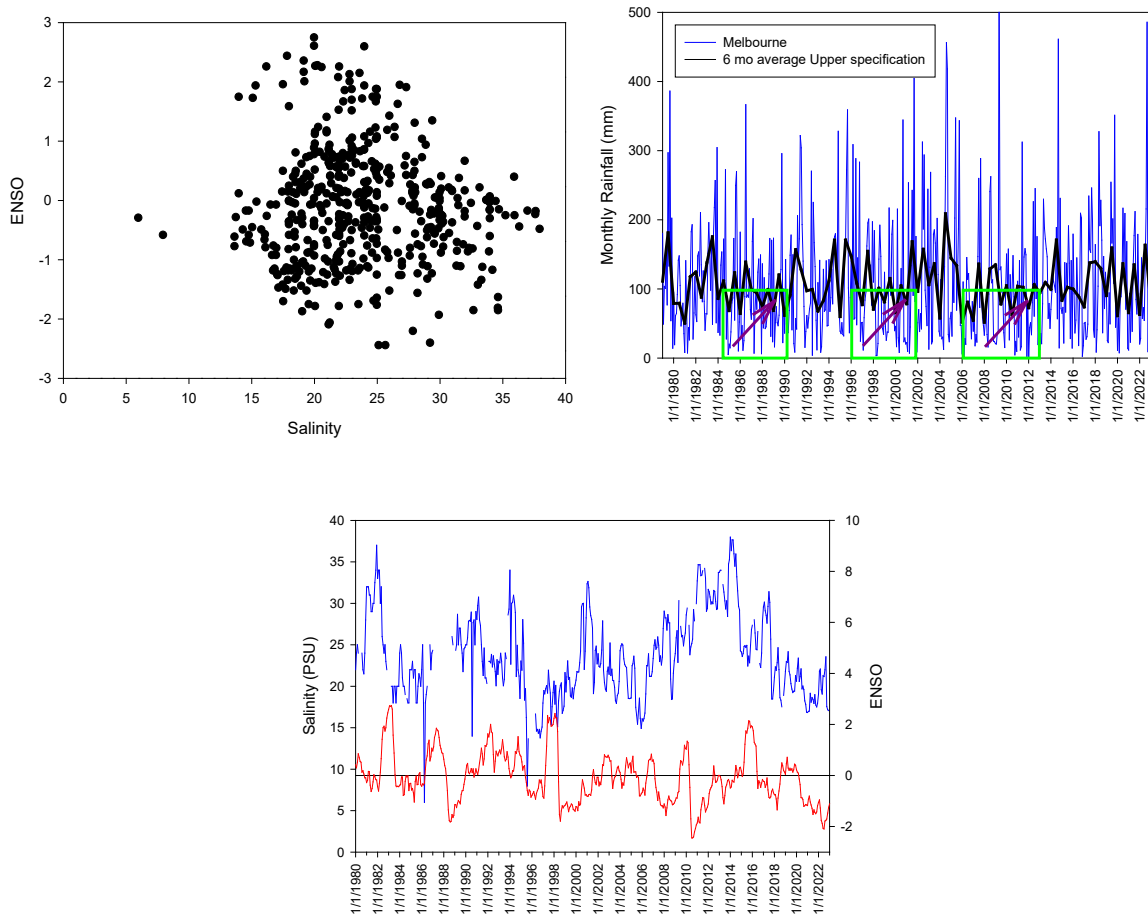
Figure 14. (a) ENSO index versus salinity. (b) monthly rainfall in mm; green boxes highlight predominantly La Nina Periods with below average rainfall associated with increasing salinity in (c). (c) salinity (blue) and ENSO index (red) between 1980 and 2023.

In 1956, a publication in the quarterly journal of the Florida Academy of Sciences identified increasing freshwater discharge as a major threat to the IRL that could change the faunal community structure (Chew, 1956). It is likely that the quantitative, recorded history of IRL salinity reflects major anthropogenic changes to lagoon hydrology starting in the 1920s. For example, in the central and north IRL Ten–Mile ridge was breached in 1922 to drain the natural wetland to the St. Johns River for agricultural use. This process diverted stormwater from the St. Johns River into Turkey Creek and the IRL. Around the same time, in 1923 the Okeechobee waterway was completed to the south. Overall, these changes increased the size of the watershed to the IRL system from an estimated 558,000 acres to 1,460,000 acres, a 260% increase in the size of the watershed, mostly since the 1920s (Osborn, 2016). Although several inlets were stabilized and cut around the same time, the increased freshwater supply likely exceeded additional mixing with seawater that would help to balance these hydrological changes, especially in the northern IRL and BRL.

The average annual rainfall in Melbourne between 1980 and 2022 was 1,300 millimeters equating to >7000 m^3 of water per acre per year. Using a back of the envelope calculation, the increase in

the size of the watershed would bring an additional 6.5 billion cubic meters of freshwater into the IRL watershed each year. Certainly not all of this ends up in the lagoon as a result of evaporation and groundwater recharge; however, this is >5 fold more water than contained in the entire IRL and 2.6–times more than would have entered the lagoon prior to anthropogenic modifications to the watershed. Confounding this increased volume, channelization brings this water to the lagoon more quickly after rainfall opposed to a slow meandering through historical wetlands and sloughs (Osborn 2016). This channelization increased the rate at which salinity varied following rainfall and the 260% increase in the size of the watershed has likely contributed to an overall lower salinity.

Efforts to address freshwater runoff have occurred with most efforts focused on decreasing nutrient and particle loading using stormwater treatment. Other projects, however, have begun to address inputs of freshwater. In 2017 a project was completed to return a portion of C1 canal, Turkey Creek drainage back to the upper St. Johns River (SJRWMD.com). More recently SJRWMD kicked off a project to divert 7 million gallons per day of baseflow from Crane Creek (M1 canal) back to the Saint Johns River (SJRWMD.com/projects/#crane–creek). Redivision of the C1 canal has produced a distinct decrease in freshwater discharge after rainfall (**Figure 15.**). In addition to providing stormwater treatment to address nutrient pollution, the C1 redivision addresses the increased size of the IRL watershed and demonstrates the value of restoring historical freshwater–seawater balance in IRL.
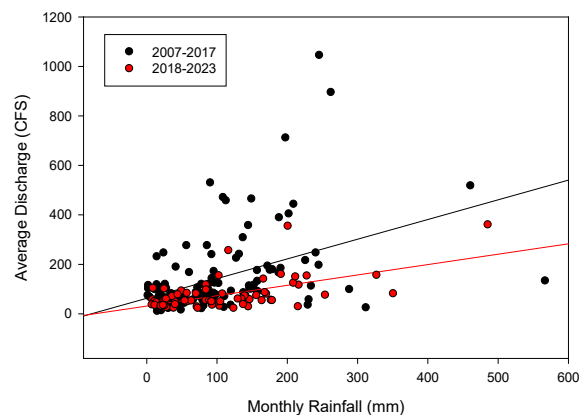
Figure 15. average monthly discharge in cubic feet per second (CFS) of the C1 canal (Turkey Creek) versus average monthly rainfall in mm. Red dots show data after the completion of the C1 redivision project.

These projects begin to address the increase in the size of the IRL watershed since the early 1900s. Another method to address impacts to salinity from increased freshwater runoff (a combination of a larger watershed plus more impermeable surfaces) would be matching increased freshwater inputs with seawater exchanges. Although few if any empirical data are available for salinity in the lagoon before these major changes to the hydrology, anecdotal accounts reference salinities greater than the ocean providing a limited frame of reference. If historical accounts are used as a basis for restoration, modifications to hydrology including enhanced ocean inflow should certainly be considered.

With impacts from both anthropogenic changes to lagoon hydrology combined with climatic variations, low salinity has been attributed to stress and mortality of filter feeders and seagrasses.

Although declining water quality is more complicated than just salinity, salinity is certainly one important variable. In a recent publication, Morris et al. (2021) reported that lagoon seagrasses are stressed by salinity less than 23 PSU. Similarly, in Laguna Madre, decreased abundance of seagrasses (*H. wrightii*) followed decreased salinity resulting from natural climatic variations (Quammen and Onuf, 1993). In 2002, Hanisak (2002) reported that BRL seagrasses experienced die–offs during a 1994 low salinity event. With respect to filter feeders, in a 1985, commercial clammers reported a 10 to 20% die off commercially viable filter feeders after the opening of flood control structures and decreased salinity (Busby, 1985). More recently, a study conducted at Brevard Zoo and Florida Tech identified salinity as a major variable controlling clam survival with low salinity associated with increased mortality of the hard clam *M. mercenaria* (ROS, 2023; Vargas, 2022). These data are consistent with previous studies showing decreased survival or growth of hard clams at lower salinities (e.g., Bergquist et al., 2008).

Changing water quality in IRL and other estuaries is certainly more complicated just salinity. Nevertheless, filter feeders and seagrasses contribute towards feedback loops that help to sustain stable states. Losses or gains of these functional groups can have non–linear impacts to ecosystem functioning. For example, in IRL, restored clam beds had significantly less sediment sulfide compared to directly adjacent sediments (ROS, 2023). These preliminary data demonstrate the potential for restoration of habitats to promote improved sediment quality that is linked to sequestration of nitrogen and phosphorus as discussed in detail below. With low salinity identified as a major stressor to these organisms, the potential for enhanced ocean inflow to increase and stabilized salinity should be considered as a potential benefit, especially in a historical perspective.

Using data for temperature and salinity, the density of water was calculated as an indication of the likelihood of mixing or the degree of stratification that could occur if seawater were to be pumped into the system. Overall, consistent with lower salinity in the lagoon versus the Port, the density of water in BRL was approximately 1,012 kilograms per cubic meter (kg/m^3) (average), 1.3% less dense than typical seawater at 1,025 kg/m^3. This seemingly small difference in density is enough to maintain discrete stratified layers and is greater than differences in density identified among existing layers observed during this study. For example, during Phase 1, discrete surface and bottom layers were identified at offshore sites based on temperature alone (salinity was well mixed) with densities of 1,022.9 kg/m^3 and 1,023.2 kg/m^3 for surface and bottom water respectively, a difference of only 0.03%.

Collectively, data for temperature and salinity were used to determine the density of the two water masses (lagoon and seawater). Despite lower lagoon versus seawater temperatures during winter months, the higher salinity in the Port resulted in a higher density of seawater during the complete study (seawater density 1,018 to 1,028 kg/m^3 versus lagoon water density 1,007 to 1,016 kg/m^3. These data indicate that, regardless of mixing, inflow of seawater would preferentially support circulation in bottom water of the lagoon and at the sediment water interface either as a stratified layer of seawater or as a mixed water mass with a higher density than existing water in the BRL.

Regardless the degree of mixing, any inflow of seawater would help mitigate extreme temperature and salinity and variability in the lagoon. Overall producing slightly cooler lagoon water during summer months and potentially, warmer water during winter months that could buffer against extreme cold events. Salinity would increase slightly and stabilize in the area of inflow as discussed in the corresponding modeling section of the final report.

Trends for salinity represent what can be expected based on the conservative properties of seawater. Although temperature is conservative, the shallow lagoon plus dark water and

sediments are subject to more rapid heating relative to seawater, where changes to lagoon temperature may not behave conservatively. Other variables that, together with temperature and salinity, collectively describe water quality would likely experience less predictable variations as a result of inflow. For example, clearer and lower turbidity seawater typically has more stable DO. The following sections discuss how changes to the conservative properties of seawater could influence other variables. For example, a predictable quantity of nutrients (N and P) would be pumped into the lagoon via inflow and another quantity would be discharged through inlets into the coastal ocean. Simple calculations can describe a "conservative" approach to nutrients in the lagoon, and a simple estimate of the decrease in nutrient concentrations can be made. However, this approach fails to account for the non–conservative nature of nutrient geochemistry that this report addresses. For example, the standing stock of nutrients in the lagoon is based on an existing homeostasis between freshwater inputs including rainfall, tributaries, and groundwater, plus in–situ N fixation and denitrification, evaporation, point sources, legacy loads, algal and bacterial biomass and cycling, existing water quality, as well as other processes. This study addresses these non–conservative processes by studying in the field and in the laboratory how geochemical nutrient cycling responds to changes in temperature, salinity and DO, variables likely to change in response to inflow. The ability to model geochemical responses to these variables is essential not only to evaluating the impacts of enhanced ocean inflow, but these data can be used to assist in modeling how the lagoon will respond to changes in temperature and rainfall associated with climatic changes over time.

3.3 Dissolved Nutrients

3.3.1 Concentrations and Speciation

Data obtained between 2020 and 2023 as part of this study (Phases 1, 2 and 3), complement existing long–term datasets for nutrients in IRL and BRL. This study also provides essential new information regarding processes including rates of water column respiration and sediment oxygen demand. Combining long–term nutrient concentrations with new insights into internal processes, we better understand mechanisms and feedback loops that help to sustain nutrient concentrations in the lagoon over time. Through a better understating of these mechanisms, potential impacts of enhanced ocean inflow on nutrient concentrations and cycling were evaluated in the context of changing temperature, salinity, DO and benthic faunal habitat quality. Nutrients that enter coastal systems including estuaries are removed by either (1) biogeochemical processes, leaving as N_2 gas or through burial in sediments or through (2) discharged into the coastal ocean. Before removal through one of these pathways, nutrients are recycled and reused by algae in the water column. As a result, changes to the rate of removal support variable algal biomass even without a change in external nutrient loading.

To date, most efforts to address eutrophication focus on external loading; however, the ability of an ecosystem to assimilate these external loads, is based on removal related to biogeochemical processes combined with rates of discharge to the coastal ocean. For example, a "regime shift" or alternate stable state beginning in 2010 in IRL did not coincide with major changes to external nutrient loading or rainfall, but extreme low temperatures during winter 2009/2010 contributed to a cascade of events that likely altered internal processes, thereby decreasing the system's ability to assimilate external and internal nutrient loads. Looking at historical datasets we can begin to assess changes to internal processes to better understand what changes have occurred and how lost ecosystem services may recover or be restored. For example, in BRL, TP concentrations were 1.65 times higher between 2010 and 2020, compared to the period between 1997 and 2010 with even larger differences (>2–fold higher) in IRL and Mosquito Lagoon (Philips et al., 2021). As part of this investigation (Phase 3) we investigated how changes to sediments likely contribute

to enhanced water column concentrations. At the same time, beginning in 2010, no major increase in nitrogen concentrations was reported; however, reviewing data for this study, there was likely a shift in nitrogen speciation towards organic and reduced forms. For example, pre 2010 NOx accounted for approximately 3 to 5% of TDN decreasing to approximately 1 to 2% after 2010. Both the changes in phosphorus concentrations and nitrogen speciation could result from a change in the redox environment within the IRL. Similar changes have been observed in other estuaries, again reflecting on Chesapeake Bay where after 1980, the bay experienced hypoxia more readily, despite no major change in external nutrient loading (Kemp et al., 2005).

During Phase 1, nutrient concentrations were evaluated in the coastal ocean and in Port Canaveral as potential sources of inflow water compared to sites throughout the IRL. Overall, the lowest nutrient concentrations were identified 1 to 2 km offshore at the 10–m isobaths (Phase 1 data) with concentrations at 8.0 ± 2.4 µM TDN, 0.15 ± 0.05 µM TDP, and 3 ± 1 µM SiO_2. Concentrations in Port Canaveral, the pilot inflow location averaged 36 ± 12 µM TDN, 0.56 ± 0.22 µM TDP and 9.28 ± 4.86 µM SiO_2, respectively.

Figure 16. Inflow site concentrations of dissolved (a) ammonium, (b) nitrate plus nitrite, (c) dissolved organic nitrogen and (d) total dissolved nitrogen.
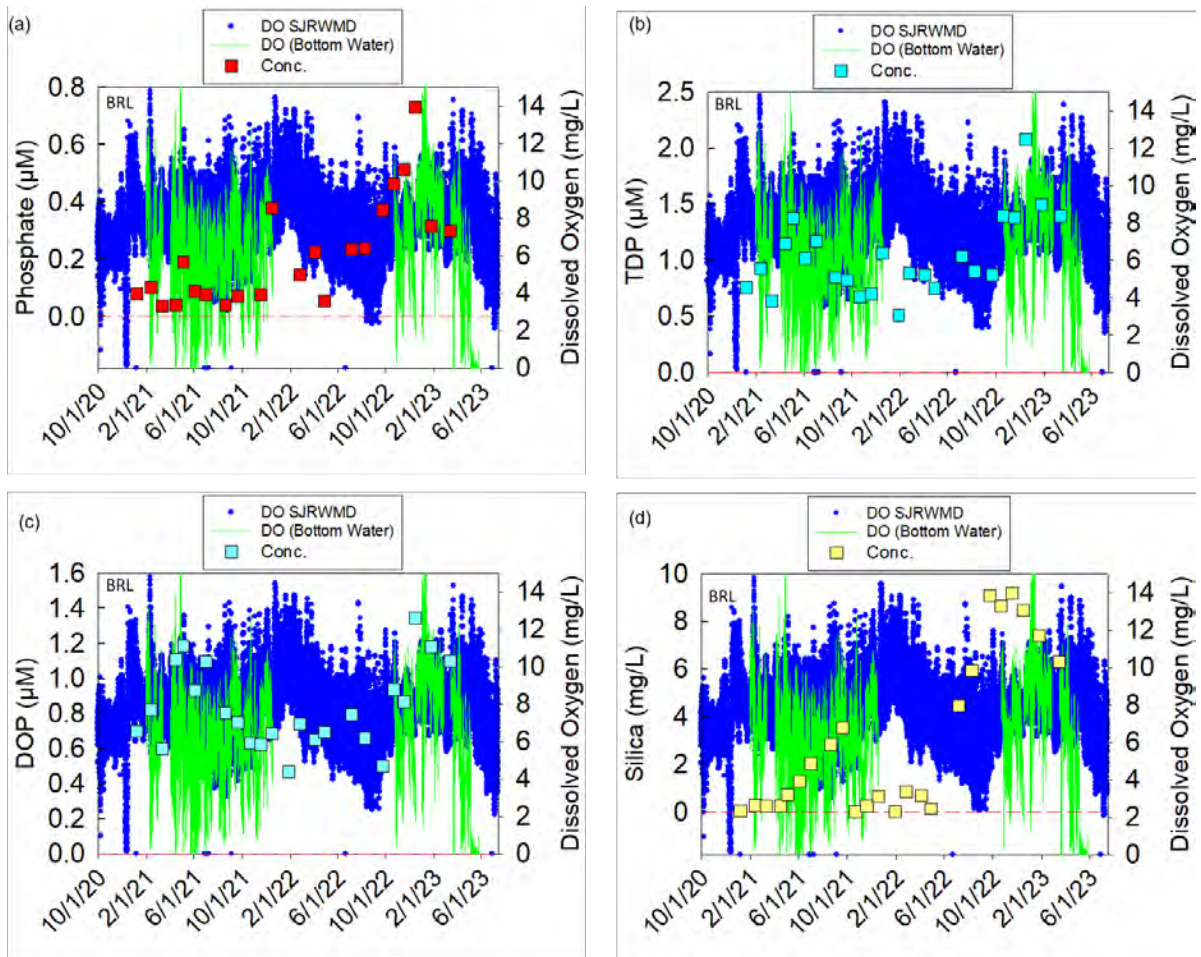
Figure 17. Inflow site concentrations of dissolved (a) phosphate, (b) total dissolved phosphorus, (c) dissolved organic phosphorus and (d) silica.

Concentrations of dissolved nutrients in BRL were more variable compared to values for seawater, as shown using both discrete sampling events during this study (Phases 1 through 3) and long–term datasets (**Figure 16, Figure 17**). Despite variability, trends for increases and decreases in nutrient concentrations over time tracked one another at the lagoon inflow and lagoon reference sites, suggesting that without treatment, these sites follow the same regional trends and that these sites are reasonable for future comparisons during the pilot study. Overall, during this study (2020 to 2023), median ± standard error TDN, TDP, and SiO_2 at lagoon inflow site were 105 ± 3 µM, 0.97 ± 0.06 µM, and 33 ± 8 µM, respectively. During Phase 3 (2022 to 2023), TDN, TDP and SiO_2 in BRL averaged 104 ± 3.3, 1.1 ± 0.1 and 92 ± 11, respectively and in Port Canaveral during the same period, median TDN, TDP and SiO2 were 31.7 ± 3.5, 0.60 ± 0.07 and 12.3 ± 1.4 µM. During Phase 3 concentrations of TDN, TDP and SiO_2 in the lagoon were 3.3–fold, 1.8–fold and 7.5–fold higher than values for seawater from Port Canaveral. In the last report (Phase 2 final report), concentrations of TDN, TDP and SiO_2 at the inflow location were 3–fold, 2–fold, and 6–fold higher, respectively, than values for seawater from Port Canaveral.

Table 4. Concentrations of (Median ± standard error) ammonium, nitrate, total dissolved nitrogen (TDN), organic nitrogen (DON), phosphate, total dissolved phosphorus and silica in the BRL and port Canaveral during the complete study (Phases 1–3) and in the coastal ocean during Phase 1.

Site	NH$_4$ (µM)	NOx (µM)	TDN (µM)	DIN (µM)	DON (µM)	PO$_4$ (µM)	TDP (µM)	DOP (µM)	SiO$_4$ (µM)
Inflow	4.5 ± 7.98	0.41 ± 0.24	107 ± 30	4.87 ± 8.12	102.35 ± 29.59	0.25 ± 0.22	1.18 ± 0.59	0.94 ± 0.43	53 ± 53
Port	4.36 ± 3.08	1.57 ± 1.41	36.18 ± 11.77	5.93 ± 4.3	30.25 ± 13.66	0.2 ± 0.14	0.56 ± 0.22	0.36 ± 0.2	9.28 ± 4.86
Offshore	0.9 ± 0.2	0.3 ± 0.1	8 ± 2.4	1.2 ± 0.3	6.8 ± 2.4	0.06 ± 0.02	0.15 ± 0.05	0.09 ± 0.04	3 ± 1

Differences in TDN and TDP concentrations between Port Canaveral and BRL were accompanied by differences nutrient speciation. In Port Canaveral, NH$_4$, NOx, and organic N accounted for, on average, 14%, 5%, and 81% of the TDN, respectively. Data from N speciation in Port Canaveral were consistent with data for the coastal Atlantic Ocean obtained during Phase 1 at 15% NH$_4$, less than 4% NOx, and 81% organic N. In the lagoon, a larger fraction of the TDN was present as organic N, with NH$_4$, NOx, and organic N accounting for, on average, 4%, less than 0.5%, and 96% of the TDN, respectively. These data were consistent with trends observed for long–term datasets in the IRL (e.g., SJRWMD). Higher concentrations of NH$_4$, especially relative to NOx, are known to stimulate blooms of *Aureoumbra lagunensis* and other small–fast growing and harmful algal species and large fractions of the TDN present as organic N indicate rapid recycling (e.g., Liu et al., 2001).
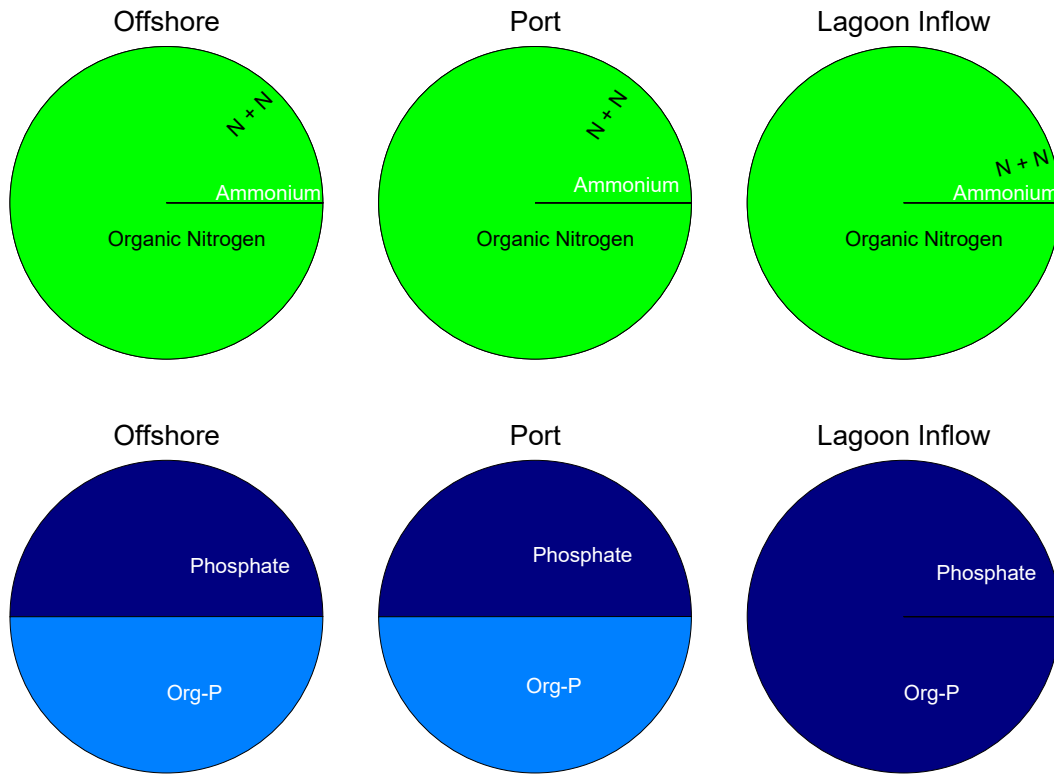
Figure 18. Pie diagrams showing the percent NH$_4$, percent NO$_x$, and percent organic N plus the percent PO$_4$ and percent organic P in the water column (a,d) offshore in the coastal Atlantic ocean (Phase 1) (b,e) Port Canaveral and (c,f) BRL at the proposed inflow location.

Overall, PO$_4$ and organic P accounted for 37% and 63% of the TDP in Port Canaveral (38% and 62% of the TDP at offshore sites during Phase 1) relative to 20% and 80% in the open lagoon Differences in speciation among locations influence bioavailability and provides insights into biogeochemical processes as discussed below. Although concentrations of dissolved nutrients were higher in port Canaveral compared to the coastal Atlantic Ocean, speciation was similar and different from speciation in BRL.

3.3.2 DIN:DIP, TDN:TDP Ratios

Although total nutrient concentrations are often used as an indicator of the eutrophic state of estuaries, speciation and the relative abundance of bioavailable species of N:P:SiO$_2$ have consistently been shown to contribute to algal community composition, whereby at the same total concentrations, shifts in speciation, and the relative abundance of N:P:SiO$_2$ can favor shifts from beneficial or less harmful photosynthesizers (e.g., seagrasses) to small, fast–growing and harmful species (e.g., *Aureoumbra lagunensis*) or vice versa (e.g., Choudhury and Bhadury 2015). A basis for evaluating N:P ratios originated with Redfield in the 1930s (Redfield 1934) and this traditional N:P ratio at 16:1 has been utilized over decades and, in some cases, expanded to include other macro or micronutrients (e.g., Choudhury and Bhadury 2015). For example, many studies now include SiO$_2$ due to its importance for diatom growth. P is used as cellular energetic currency and in ribosomal ribonucleic acid. N and SiO$_2$ are utilized as structural components of hard parts (SiO$_2$ tests) and proteins whereby changes to N:P and N:SiO$_2$ ratios can promote one species versus

another based on differences in metabolic and growth requirements (Harris 1986). Ratios have classically focused on nutrient species that are readily bioavailable, in other words: NH_4 + NOx (DIN) versus PO_4 (SRP). More recently, several species of harmful algae, including *Aureoumbra lagunensis,* the brown tide species in the IRL, have been identified to use organic N and organic P (Liu et al., 2001). In addition to the ability to use organic N and organic P, species such as *Aureoumbra lagunensis* are not able to use nitrate, complicating interpretations of water quality based on N:P. To provide a more complete picture, data are presented here for both DIN:SRP and TDN:TDP.

Overall, (2020 to 2023) DIN:SRP ratios varied among sample locations; DIN:SRP in Port Canaveral averaged 37 ± 24 (median 31), slightly higher than ratios during the Phase 2 (median 22), ratios identified offshore during Phase 1 (offshore DIN:SRP = 20) and with ratios previously identified for the coastal Atlantic Ocean (Kent et al. 2001, Martiny et al., 2014). During the complete study (phases 1 through 3), the average DIN:SRP ratio was 34 ± 48 (median 15 ± 7 SE) for lagoon water. The ratio for lagoon water during Phase 3 at 11 ± 13 (median 5 ± 3) was lower than the ratio during Phase 2 with an average at 45 ± 56 (median 47 ± 14 SE). Ratios during Phases 2 and 3 were both higher than the ratio during Phase 1. The difference was at least partially explained by sampling at northern sites during Phases 2 and 3. During Phase 1 higher N:P ratios in the northern lagoon were consistent with a trend identified during Phase 1 with lower ratios closer to Sebastian inlet and supported by results from Lapointe et al. (2020) showing a similar north–south pattern for the N:P ratios in seagrasses. Despite north–south trends that Lapointe et al. (2020) identified for seagrasses (beneficial photosynthesizers) each species in their study had a relatively narrow range of N:P (*S. filiforme*, *T. testudinum* and *H. wrightii*) and large differences in N:P have been shown to drive change in the composition of photosynthesizers (e.g., seagrasses versus algae, Hillebrand et al., 2013). Differences between Phase 2 and Phase 3 in the same region reflect changes to respiration and benthic fluxes discussed below, where inorganic nitrogen fluxes were lower, but phosphate fluxes were higher during Phase 3 compared to Phases 1 and 2. This notable shift in N:P ratios occurred in the absence of inflow; however, an N:P ratio more closely matching that of seawater is one of the potential benefits of inflow and inflow could help to sustain the lower N:P ratios over time.

Ratios of TDN:TDP were higher than values for DIN:SPR discussed above. In Port Canaveral, TDN:TDP averaged 82 ± 67 (median 59) relative to 109 ± 38 (median 102) in the lagoon. Since Phase 1 the TDN:TDP ratio has decreased continuously with medians at 139 ± 29 in 2020, 116 ± 6 in 2021, 95 ± 9 in 2022 and 78 ± 2 so far in 2023. This trend reflects the lower TDN concentrations at the inflow site with lower ratios typically associated more beneficial photosynthesizers as discussed below. Ratios of DIN:SRP compared to TDN:TDP reflect the larger fraction of TDN relative to TDP that is present in less bioavailable, organic forms. Traditionally these organic nutrients have not been considered bioavailable; however, many small bloom–forming algae can utilize the organic forms of both N and P (Lui et al., 2001). High ratios of TDN:TDP are known to enhance the risk for *Aureoumbra lagunensis* blooms (Lui et al., 2001; DeYoe et al., 2007) whereby, some cyanobacteria and harmful algal bloom (HAB) dinoflagellates can store P within their cells helping to promote their taxa when P is otherwise limiting (e.g., Hillebrand et al., 2013; Burford et al., 2014; Willis et al., 2015; Glibert et al., 2012; Accoroni et al., 2015).

In effort to understand functional reasons behind the Redfield ratio, other studies have identified optimal N:P_opt (molar) ratios (where limitation switches from N to P) for different groups of algae. For example, Hillebrand et al. (2013) reported the lowest N:P_opt for diatoms at 14.9 increasing to 15.1 for dinoflagellates, 25.8 for cyanobacteria, and 27.0 for chlorophytes. At high N:P ratios, diatoms, which would generally be considered as fast–growing, can be outcompeted by species,

such as dinoflagellates, cyanobacteria, and chlorophytes, that have a higher optimal N:P ratios and are more frequently HAB–forming (Phlips et. al., 2010). In the lagoon, high N:P ratios are preferred by HAB species such as *Pyrodinium bahamense var. bahamense, Aureoumbra lagunensis* and *Akashiwo sanguinea*, which are commonly encountered in the northern IRL where muck and organic–rich sediments are prominent (e.g., Foster et al., 2018;

Figure 19). Muck further promotes the dominance of HAB species by preferentially releasing ammonium, the preferred form of nitrogen of many harmful phytoplankton species, including *Pyrodinium bahamense var. bahamense (e.g., Lui et al., 2001).*
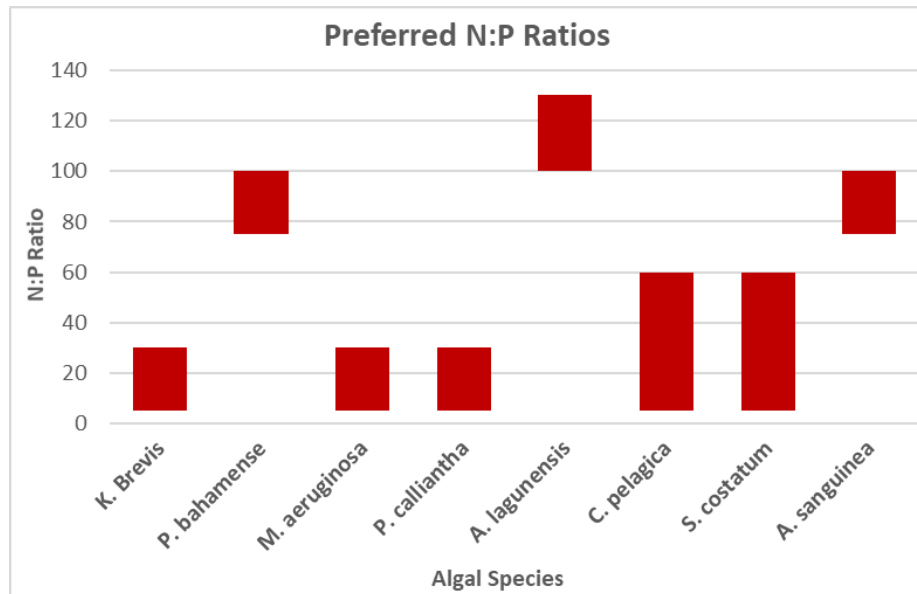
Figure 19. Preferred N:P ratios of selected algal species found in the IRL: ***K. brevis*** **(Vargo et. al, 2008),** ***P. bahamense*** **(Azanza et. al., 2004),** ***M. aeruginosa*** **(Smith et. al., 1983),** ***P. calliantha*** **(Guo et. al.),** ***A. lagunensis*** **(Liu et. al., 2001),** ***C. pelagica*** **(Hauss et. al., 2012),** ***S. constatum*** **(Maso and Garces, 2006), and** ***A. sanguinea*** **(Chen et. al., 2019)**

Based on global trends plus data from this study and long-term datasets, potential shifts in N:P ratios (DIN:SRP and TDN:TDP and perhaps other N:P ratios) should be considered a component of overall water quality and should be a consideration for modeling and predicting algae blooms and bloom composition (Hillebrand et al., 2013). Based on the importance of N:P ratios towards promoting certain algal groups, restoration efforts, including inflow, should be viewed not only as removing N or P but as regulating the ratio of these elements. Based on long term datasets for water in Port Canaveral or the coastal Atlantic Ocean, inflow water would have both lower concentrations of nutrients and typically lower ratios of both DIN:SRP and TDN:TDP, relative to values in the lagoon.

3.4 Geochemical Nutrient Cycling (In–situ)

Due to the non–conservative nature of nutrients and strong benthic–pelagic coupling in shallow estuarine systems, modified geochemical processes in sediments and on particles would likely have a greater impact on nutrient concentrations than those resulting from direct export of dissolved nutrients. To address these complex geochemical processes, nutrient and oxygen cycling were investigated in water from Port Canaveral and from the lagoon at the inflow and

reference sites and during Phase 2 in laboratory experiments to investigate how changes to temperature, salinity, and DO might influence geochemical nutrient cycling in the water column and sediments. Results from these investigations are presented here first in **Section 3.4.1** discussing water column cycling and then in **Section 3.4.4** discussing sediment processes.

3.4.1 In–situ Water Column Processes

Water column respiration (dark) in BRL was highly variable and consumed oxygen at an average of –0.14 ± 0.16 mg/L/hr during the complete project, 2020 to 2023 (**Figure 20, Table 5)**. The overall average decreased compared to the average from Phase 2 at 0.19 ± 0.15 mg/L/hr (2020 to 2021). This decrease in water column respiration follows patters of improving water quality and lower nutrients in BRL between 2020 and 2023. In Port Canaveral, water column respiration (dark) during the complete project (2020 to 2023) was approximately 30% lower at 0.10 ± 0.09 mg/L/hr (**Figure 20. **).

Overall in BRL, water column respiration (dark) accounted for approximately 50 to >80% of the total respiration (sediments + water) and is a major contributor to variations in DO concentrations and occurrences of hypoxia or anoxia (**Table 6. **). These data fit well within a range of data (12 to 87%) from a review of coastal systems around the globe (Boynton et al., 2018). The importance of water column processes are captured by our continuous dissolved oxygen data at the proposed inflow location and in Port Canaveral, where high rates of SOD and water column respiration lead to large diurnal fluctuations in DO concentrations in the lagoon, with lower magnitude diurnal fluctuations in seawater from Port Canaveral. Lower respiration in seawater from port Canaveral buffers this water against instances of hypoxia and major variations in dissolved nutrient concentrations and speciation discussed below.
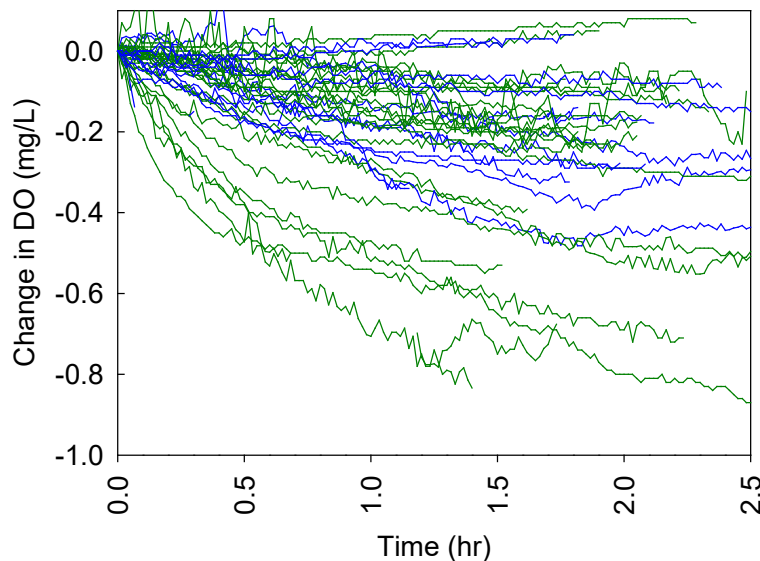
Figure 20. Change in DO over time average ± SD for water incubated in the dark at in–situ conditions. Blue are seawater sample from Port Canaveral and Green are Lagoon samples from the inflow site.

Table 5. Rates of pelagic respiration in the BRL at the inflow site and in Port Canaveral.

Year	BRL (mg/L/hr)	Port (mg/L/hr)
All	−0.14 ± 0.16	−0.10 ± 0.09
2023 (Jan–July)	−0.08 ± 0.04	−0.15 ± 0.11*
2022	−0.14 ± 0.21	−0.02 ± 0.03
2021	−0.21 ± 0.13	−0.13 ± 0.06
2020	−	−

Table 6. Rates of pelagic respiration and SOD and the relative importance of sediments towards total respiration for varying water depths (per 1m^2 of lagoon). Calculated using average rates of water column respiration (−0.14 mg/L/hr) and SOD (~2500 µmoles/m^2/hr = ~80 mg/m^2/hr) from sandy sediment.

Depth	DO consumed by sed (mg/m^2/hr)	Water volume / m^2 (L)	DO consumed by water (mg/hr)*	% consumed by sediments	% consumed by water
0.5	80	500	70	53	47
1.0	80	1,000	140	36	64
1.5	80	1,500	210	28	72
2.0	80	2,000	280	22	78
2.5	80	2,500	350	19	81

Water column respiration (dark conditions) is accompanied by increased nutrient cycling or recycling (particle fluxes). Incubations carried out under dark conditions show how respiration and decomposition of particles in the water column influence dissolved nutrient concentrations. Previous studies have shown that these dark processes are relatively well matched, but opposite during light experiments to maintain nutrient concentrations over time (Ziegler and Benner, 1999). In that context, results presented here should be viewed as an indication of recycling efficiency and how exchanges of particles during inflow may influence concentrations of dissolved nutrients over time. In other words, a combination of water column and sediment processes combined with rates of input and removal help to maintain nutrient concentrations and ratios over time. As discussed below, recent, short term (2 to 3 years) improvements in water quality coincide with lower water column respiration and benthic fluxes. These small improvements in sediment and water quality help to mitigate instances of hypoxia. Collectively these data demonstrate how small changes either natural or anthropogenic can have large impacts on water quality in IRL system.

Overall in BRL (2020 to 2023), TDN, NH$_4$, nitrate, DIN and organic N (dark conditions) increased by (median ± standard error) 4.71 ± 2.07 µM/hr, 0.04 ± 0.37 µM/hr, 1.2 ± 0.7 µM/hr and 4.54 ± 1.65 µM/hr, respectively due to water column processes (**Table 7** and **Figure 21**). Releases of TDN associated with water column respiration in BRL were 4–5 times higher than particle fluxes from seawater in Port Canaveral with median TDN values at 1.14 ±1.43 µM/hr and fluxes of NH4, nitrate, DIN and organic N at −0.02 ± 0.16, 0.9 ± 0.36, 0.78 ± 0.39 and 1.0 ± 1.28, respectively (**Table 7**). Overall, releases of phosphate from water column respiration were about 2 times greater in BRL (0.04 ± 0.01 µM/hr) compared to the port (0.02 ± 0.05 µM/hr). Overall, water column fluxes (dark) were variable; however, ranges were more or less consistent or slightly higher than values reported in previous studies for similar systems (e.g., Ziegler and Benner 1999). Based on these data, the turnover time for TDN in BRL was approximately 30% shorter than the turnover time in Port Canaveral. In contrast the turnover time for TDP was approximately. 4 times longer in BRL compared to turnover times in seawater from Port Canaveral (). These data demonstrate the efficient turnover of nitrogen in BRL and less efficient recycling of P helping to maintain the high N:P ratios observed in BRL (). The turnover time for ammonium was positive in BRL (113 hr) and negative (−218 hr) in seawater from Port Canaveral. This distinct difference is consistent with the oxidation of ammonium to nitrate supported by more stable DO concentrations,

lower respiration and less algal recycling in seawater from Port Canaveral collectively supporting a larger fraction of the TDN present as nitrate.

Table 7. Median ± standard error pelagic fluxes of ammonium (NH4), nitrate + nitrite (NOx), total dissolved nitrogen (TDN), dissolved inorganic nitrogen (DIN), dissolved organic nitrogen (DON), phosphate (PO4), total dissolved phosphorus (TDP), dissolved organic phosphorus (DOP) and silica in µM/hr in the Banana River Lagoon (BRL).

BRL Year	Ammonium (µM/hr)	NOx (µM/hr)	TDN (µM/hr)	DIN (µM/hr)	DON (µM/hr)	PO4 (µM/hr)	TDP (µM/hr)	DOP (µM/hr)	Silica (µM/hr)
All	0.04 ± 0.37	1.2 ± 0.7	4.71 ± 2.07	1.15 ± 0.67	4.54 ± 1.65	0.04 ± 0.01	0.04 ± 0.02	0.00 ± 0.01	−0.25 ± 0.82
2023	0.24 ± 0.07	0.2 ± 0.46	3.45 ± 1.76	0.71 ± 0.46	3.21 ± 1.76	0.04 ± 0.01	0.05 ± 0.02	0.03 ± 0.01	−0.62 ± 1.6
2022	−0.06 ± 0.15	1.47 ± 0.19	1.58 ± 2.05	1.02 ± 0.21	0.82 ± 1.96	0.03 ± 0.01	−0.01 ± 0.02	−0.03 ± 0.02	−1.36 ± 1.9
2021	0.05 ± 0.59	1.1 ± 1.32	9.58 ± 4.54	1.5 ± 1.54	7.87 ± 3.4	0.06 ± 0.02	0.07 ± 0.04	0.01 ± 0.03	0.07 ± 0.6
2020	−5.63 ± 2.83	8.43 ± 4	−4.87 ± 2.76	2.8 ± 1.17	−7.67 ± 3.93	0.07 ± 0.02	−0.05 ± 0.04	−0.12 ± 0.06	−6.27 ± 3.04

Table 8. Median ± standard error water column fluxes of ammonium (NH4), nitrate + nitrite (NOx), total dissolved nitrogen (TDN), dissolved inorganic nitrogen (DIN), dissolved organic nitrogen (DON), phosphate (PO4), total dissolved phosphorus (TDP), dissolved organic phosphorus (DOP) and silica in µM/hr in Port Canaveral.

Port Year	Ammonium (µM/hr)	NOx (µM/hr)	TDN (µM/hr)	DIN (µM/hr)	DON (µM/hr)	PO4 (µM/hr)	TDP (µM/hr)	DOP (µM/hr)	Silica (µM/hr)
All	−0.02 ± 0.16	0.9 ± 0.36	1.14 ± 1.43	0.78 ± 0.39	1 ± 1.28	0.02 ± 0.05	0.06 ± 0.06	0.01 ± 0.02	0 ± 0.34
2023	−0.01 ± 0.21	0.29 ± 0.27	0.77 ± 2.49	0.56 ± 0.4	0.98 ± 2.17	0.01 ± 0.02	0.01 ± 0.04	0 ± 0.03	−0.01 ± 0.82
2022	−0.19 ± 0.16	0.38 ± 0.17	−0.06 ± 0.55	0.67 ± 0.17	−0.79 ± 0.71	0.03 ± 0.22	0.32 ± 0.2	0.01 ± 0.08	0.12 ± 0.16
2021	0.01 ± 0.31	0.95 ± 0.67	2.01 ± 2.39	1.03 ± 0.74	1.38 ± 2.12	0.02 ± 0.04	0.06 ± 0.06	0.04 ± 0.03	0.07 ± 0.07
2020	–	–	–	–	–	–	–	–	–

Table 9. Turnover time in hours for N and P in Port Canaveral and BRL

	NH$_4$	NOx	DIN	Org–N	TDN	PO$_4$	TDP	DOP
Port Canaveral	−218	1.7	7.6	30	32	10	9.3	36
BRL	113	0.3	4.2	23	23	6.3	39	–
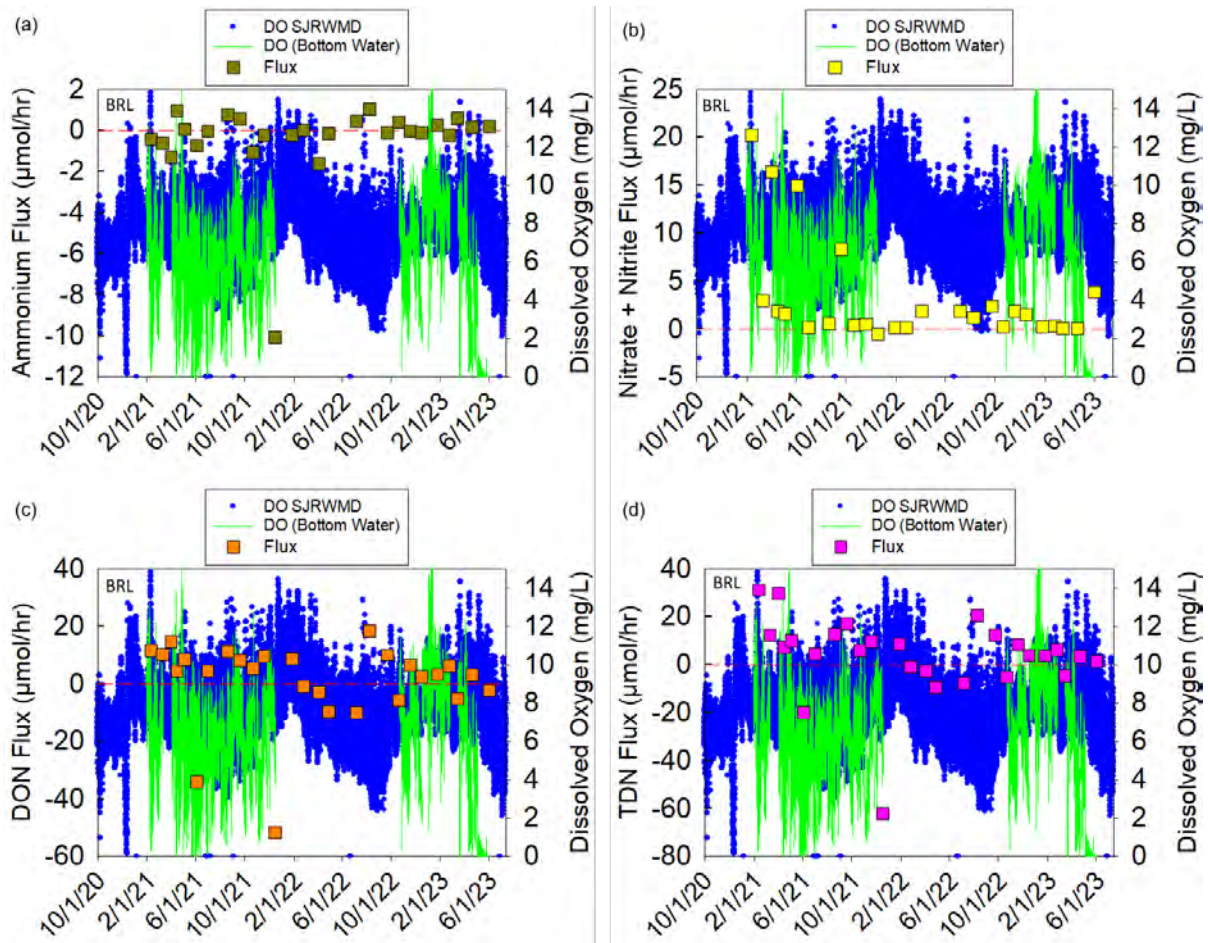
Figure 21. Water column fluxes of (a) NH4, (b) NOx, (c) DON and (d) TDN. Note: Green and blue dotted lines show DO in the region at mid water depths (SJRWMD site IRLB04) and in bottom water at the inflow site.
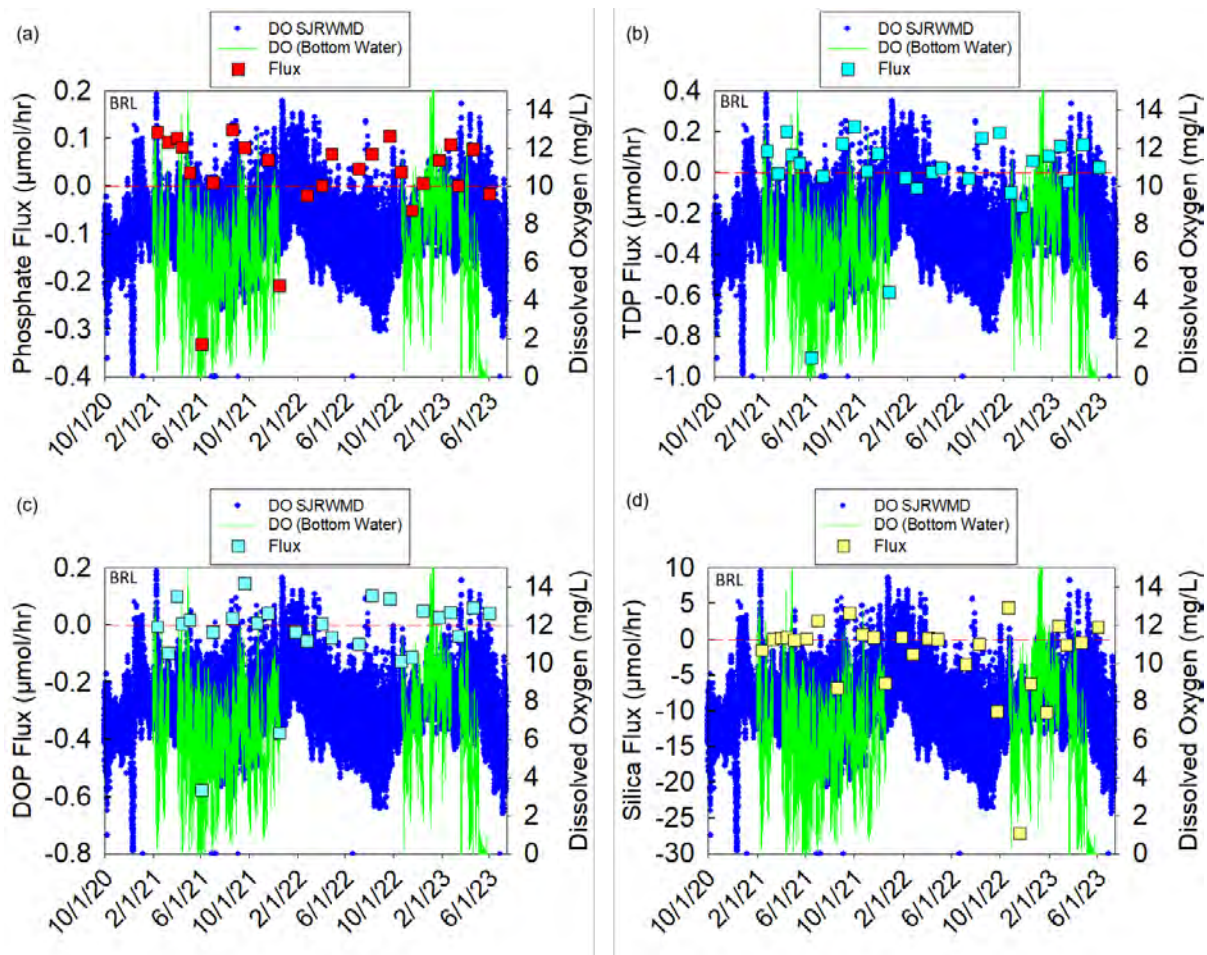
Figure 22. Water column fluxes of (a) PO4, (b) TDP, (c) DOP and (d) SiO2. Green and blue dotted lines show DO in the region at mid water depths (SJRWMD site IRLB04) and in bottom water at the inflow site.

3.4.2 *Water Column Ratios and Fluxes of Oxygen (O):N and N:P*

Overall, data for water column recycling from Phases 2 and 3 of this study indicate that inflow of seawater would bring water with lower rates of dark respiration (approximately 30% lower O_2 consumption) into the BRL, thereby increasing resilience to hypoxia while also decreasing the rate of nutrient recycling in the water column. Because rates of nitrogen recycling were 4 to 5 times higher and rates of P recycling were 2 times lower in lagoon water compared to seawater from Port Canaveral, higher N:P ratios were identified for recycling in lagoon water. Based on data from this study, the water column recycling ratio of DIN:SRP for Port water was 30.7 ± 6.4 relative to the DIN:SRP recycling ratio for lagoon water at 15 ± 11.44 in BRL. As expected, ratios for recycling of TDN:TDP were higher at 58.6 ± 17.2 in the Port and 98.7 ± 6.6 in lagoon water during the complete study. These rates were highly variable, responding to changes in water quality. Nevertheless, these recycling ratios act to stabilize ratios of N to P in the water column and followed patterns for ratios observed for the standing stock of nutrients as discussed in **Section 3.3.2**. Based on these data and consistent with global processes, water column recycling acts to buffer against changes to the relative abundance of N to P and helps to sustain algal communities over time. In addition to exchanging dissolved nutrients, restoration efforts such as ocean inflow would exchange particles, altering water column processes and respiration. In the

case of inflow, inputs of seawater to the lagoon would decrease ratios of N:P in the water column and through rates of recycling. Based on processes related to differences in particles this would likely lead to a lower N:P ratio of the standing stock of nutrients in the lagoon over time.

Table 10. Molar ratios of TDN:TDP and DIN:DIP in seawater from port Canaveral and in BRL.

	TDN:TDP (existing)	TDN:TDP (flux)	DIN:DIP (existing)	DIN:DIP (flux)
Port	58.6 ± 17.2	9.9 ± 17.8	30.7 ± 6.4	4.1 ± 15.2
BRL	98.7 ± 6.6	66.7 ± 100	15 ± 11.44	21.8 ± 21

3.4.3 Importance of Benthic–pelagic coupling (fluxes)

Benthic fluxes of N and P from muck are estimated to contribute more than 30% of the annual N and P loading to the IRL (Gao et al., 2009, Tetra Tech 2023, Fox and Trefry 2018). These estimates are based only on fluxes from fine–grained, organic–rich sediments locally referred to as "muck." Because sand covers at least 90% of the lagoon bottom, non–trivial fluxes from sand need to be considered when evaluating the importance of internal nutrient sources and geochemical nutrient cycling within the lagoon. To evaluate the importance of these geochemical processes towards regulating nutrient concentrations in lagoon water, residence times for nutrients were calculated using benthic nutrient fluxes, long–term average nutrient concentrations in lagoon water and an average lagoon depth of 1.5 meters. Data from this study serve as a baseline from which the importance of sandy sediments as both a source and sink of nutrients can be evaluated. Although this study focused on sandy sediments, non–trivial fluxes from muck would be influenced by changes to temperature, salinity, and DO. For example, Fox and Trefry (2018) reported a 7 to 10% increase in benthic fluxes of N and P from fine–grained organic rich sediments "muck" per 1°C increase in lagoon temperature. Lagoon–wide, this equates to a decrease of approximately 40 tons of N per year from muck if lagoon temperature decreased by 1°C.

3.4.4 Benthic Fluxes

During this study, including Phase 1, no significant trends for benthic nutrient fluxes versus the composition of sandy sediments (e.g., sediment OM content) were identified (**Figure 23**). This contrasts an established pattern where sediment water and OM content are strongly correlated with benthic fluxes from fine–grained, organic–rich sediments, "muck," throughout the IRL (Fox and Trefry 2018). The absence of a trend for sandy sediments is likely at least partially related to (1) more dependence of sandy sediments on conditions in overlying water, including variations in the supply of OM and DO and (2) potential groundwater seepage into the lagoon through water–permeable sandy sediments (Pandit, Heck, Berber, Al-Taliby, & Mamoua, 2017). During Phases 2 and 3, benthic chambers were focused along the eastern shoreline of the BRL in the proposed area of inflow with chambers also deployed in the reference/control area. The approach during Phases 2 and 3 provided a detailed temporal evaluation of fluxes at the proposed inflow site.
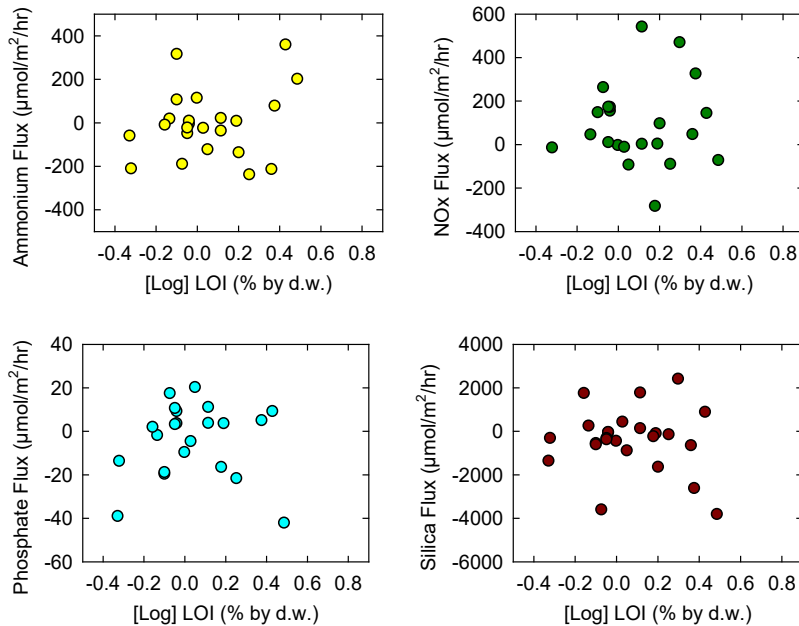
Figure 23. Benthic fluxes of (a) NH$_4$, (b), NO$_x$, (c) PO$_4$, and (d) SiO$_2$ versus OM content as log[LOI] for Phase 1 sampling

Collectively, median ± standard deviation SOD (oxygen flux into sediments) for sandy sediments during Phases 2 and 3 (including data from other projects) was –2500 ± 1400 µmoles/m^2/hr (median ± SE 2,400 ± 200 µmoles/m^2/hr, n = 54) for sediment collected at the inflow site. SOD at the inflow location between 2020 and 2023 averaged –2500 ± 1500 µmoles/m2/hr (median = –2400 ± 200 µmoles/m2/hr, n = 54). Consistent with trends for concentrations of dissolved nutrients in overlying water, SOD decreased from an average at –2963 ± 1174 in 2021 to –2477 ± 1677 in 2022 and –2163 ± 1194 so far in 2023. Overall, concentrations of DO in bottom water and rates of oxygen consumption varied together with lower bottom water DO identified during periods with higher oxygen demand (more negative SOD), except when DO in bottom water approached zero and there was no oxygen to be consumed (i.e., December 2020,

Figure 24). This pattern is consistent with temperature related trend for (1) the solubility of dissolved oxygen and (2) bacterial metabolism. For example, at a salinity of 25, a reasonable average for the IRL, DO solubility increases from 6.4 mg/L at 32°C during summer months to 8.7 mg/L at 15°C during winter an annual range of about 2.3 mg/L. At the same time, bacterial metabolism increases by approximately 4–fold as temperature increases from 15° to 32°C. Overall, values for sandy sediment in the IRL and BRL fit nicely within a range of values previously reported for estuaries around the world, at –200 to –7,000 µmoles/m^2/hr (Boynton et al., 2018). Oxygen demand of muddy sediments were higher and more variable at –5,700 ± 4,600 µmoles/m^2/hr (n = 8); however, muddy sediments were investigated during cooler months and average fluxes from muddy sediments almost certainly underestimate annual average values where SOD as high as –9,000 µmoles/m^2/hr were measured during summer months.
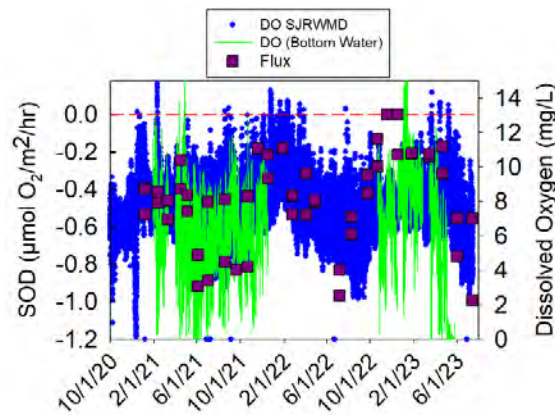
Figure 24. Sediment Oxygen Demand (SOD) over time at the inflow site. Blue and green lines show DO in mg/L at mid water depth (SJRWMD sensor IRLB04) and in bottom water, respectively.

Table 11. Median ± standard error for benthic fluxes from sandy and muddy sediments in µmoles/m^2/hour for lagoon wide sampling of sandy sediments during Phase 1 (lagoon wide sand) and high-resolution sampling at the proposed inflow and reference sites during Phase 2.

Sediment	Oxygen	NH$_4$	NOx	DIN	PO$_4$	TDP	DOP
Lagoon sand	−3,200 ± 900	90 ± 60	150 ± 150	260 ± 170	4.1 ± 8.1	−0.6	−4.7 ± 4.9
Inflow Site	−2,400 ± 200	88 ± 268	44 ± 628	14 ± 687	1 ± 12	6 ± 24	4 ± 20
Muck	−4,300 ± 2,500	580 ± 460	−180 ± 200	400	12 ± 18	20 ± 23	8.8 ± 6.6

Table 12. Average ± standard deviation for sediment oxygen demand plus benthic fluxes of ammonium (NH4), nitrate + nitrite (NOx), total dissolved nitrogen (TDN), dissolved inorganic nitrogen (DIN) and dissolved organic nitrogen (DON) in µmol/m2/hr.

Year	O2 (µmol/m2/hr)	NH4 (µmol/m2/hr)	NOx (µmol/m2/hr)	TDN (µmol/m2/hr)	DIN (µmol/m2/hr)	DON (µmol/m2/hr)
All	−2458 ± 1514	88 ± 268	44 ± 628	165 ± 2853	14 ± 687	152 ± 2500
2023	−2163 ± 1194	−10 ± 112	−124 ± 237	−245 ± 947	−141 ± 211	−101 ± 823
2022	−2477 ± 1677	20 ± 142	−130 ± 159	−385 ± 1473	−163 ± 253	−221 ± 1341
2021	−2963 ± 1174	125 ± 288	177 ± 833	991 ± 3882	284 ± 922	707 ± 3447

Table 13. Average ± standard deviation for benthic phosphate (PO4), total dissolved phosphorus (TDP), dissolved organic phosphorus (DOP) and silica in µmol/m2/hr.

Year	PO4 (µmol/m2/hr)	TDP (µmol/m2/hr)	DOP (µmol/m2/hr)	Silica (µmol/m2/hr)
All	1 ± 12	6 ± 24	4 ± 20	426 ± 1164
2023	0.07 ± 13	−3 ± 19	−5 ± 10	468 ± 1065
2022	−0.81 ± 10	8 ± 20	9 ± 16	821 ± 1566
2021	0.09 ± 12	8 ± 27	8 ± 22	195 ± 660

During Phase 1 (2019 and 2020), median ± standard deviation N fluxes varied among areas with sandy versus muddy sediments. Lagoon wide, DIN was released from sandy sediments (median ± SE = 260 ± 170 µmoles/m^2/hr, 32 tons/km^2/year) primarily as NO$_x$ (63% of DIN, 150 ± 150 µmoles/m^2/hr, 20 tons N/km^2/year), and NH$_4$ accounted for 37% of the DIN efflux from sandy sediments at 90 ± 60 µmoles/m^2/hr (11 tons N/km^2/year). During 2021 through 2023 (Phases 2 and 3), benthic fluxes of dissolved nutrients followed patterns for SOD with highest fluxes during 2021 with lower and even negative fluxes during 2022 and 2023 (**Table 11, Table 12**, and **Table 13**). In 2021 DIN efflux was 284 ± 992 µmoles/m^2/hr (approximately 35 tons/km^2/year from sandy sediments) and nitrate accounted for 58% of the DIN efflux. During 2022 (complete year) DIN fluxes had decreased and were negative, removing −163 ± 253 µmoles/m^2/hr (−20 tons N/km^2/year) with a large negative nitrate flux and a slightly positive ammonium flux (). So far in 2023 the median DIN flux is negative −141 ± 211 µmoles/m^2/hr (−17 tons/km2/year) with negative fluxes of both nitrate and ammonium. The uptake of ammonium during the first half of 2023 is consistent with temperature related trends where during and following cooler months with less bacterial respiration ammonium fluxes are lowest. These data are consistent with lower sediment oxygen demand, lower pelagic respiration, and improved water quality in the region so far this year that though feedback loops connect benthic and pelagic processes. Greater availability of oxygen in surface sediments promotes nitrification that is (1) less inhibited by sulfides (2) promoted by oxygen and conditions that support nitrifying bacteria as discussed in detail in UWFs Phase 3 final report. Perhaps counterintuitive, although nitrification makes nitrate from ammonium, it can promote denitrification and removal of nitrate (negative flux) as nitrification is often the limiting step in nitrogen removal from marine environments. These data demonstrate the value of healthy sediments as a sink for nutrients. In healthy coastal systems geochemical processes in sediments remove a large fraction of nutrients before discharge to the coastal ocean (Nixon et al., 1996).
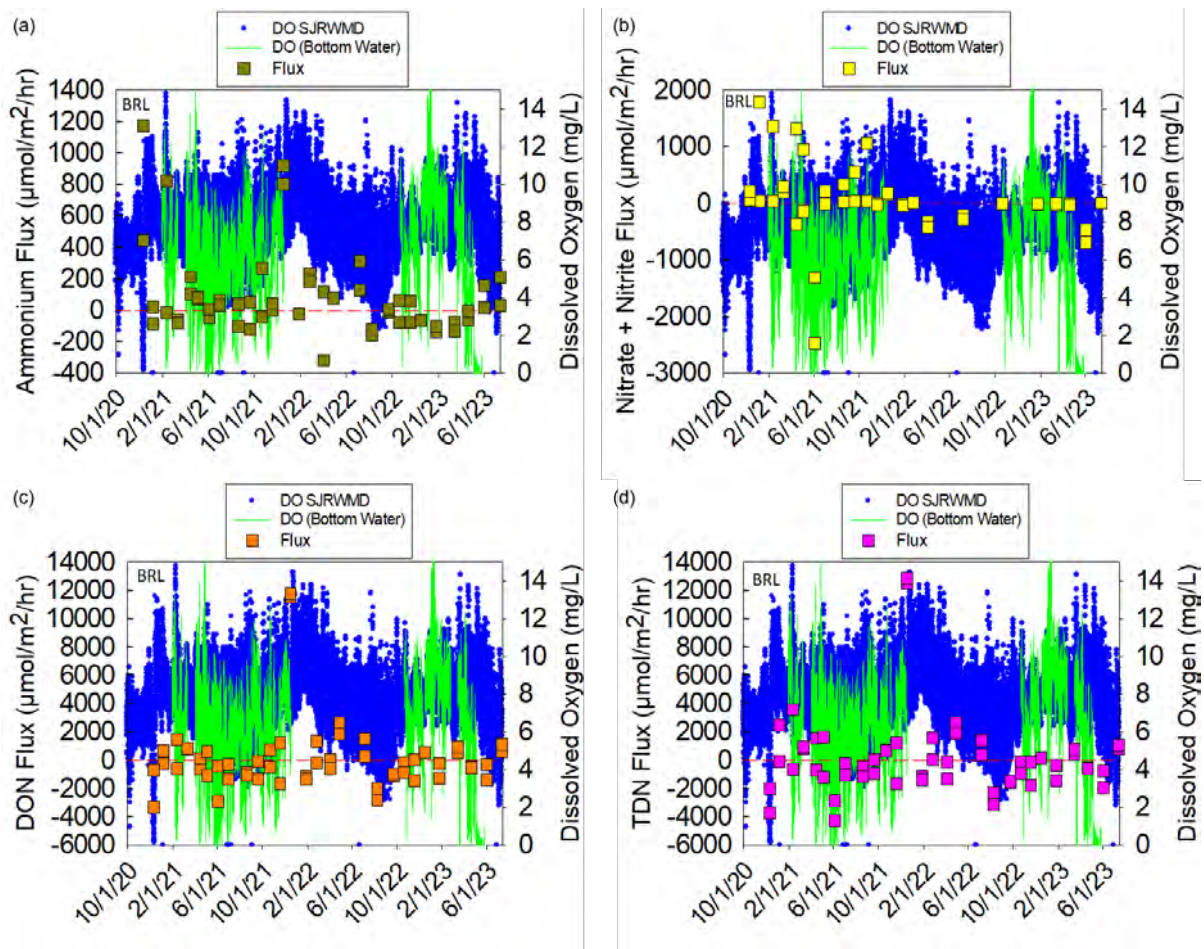
Figure 25. Benthic fluxes of (a) NH₄, (b) NOₓ, (c) DON and (d) TDN. Green and blue dotted lines show DO in the region at mid water depths (SJRWMD site IRLB04) and in bottom water at the inflow site.

During Phase 1 (2019 and 2020), fluxes of DON were highly variable with median DON fluxes directed out of sediments for a median TDN flux from sandy sites at 290 ± 430 µmoles/m^2/hr (35 tons N/km^2/year). During Phases 2 and 3 (2021 to 2023) at the inflow site, DON fluxes were highly variable and typically directed into sediments from overlying water with a median at -277 ± 334 µmoles/m^2/hr (**Figure 25**). The collective DIN + DON fluxes yielded TDN fluxes at -200 ± 381 µmoles/m^2/hr (-24 tons/km^2/year) consistent with values reported for sandy sediments in other estuaries from around the world (Boynton et al., 2018).

Different outcomes from Phase 1 versus Phases 2 and 3 demonstrate the large spatial and temporal variability in nutrient fluxes as a function of water and sediment quality along with the susceptibility of sediment and water column processes to changing environmental conditions. For example, previous studies have identified moderate post–bloom organic enrichment of sediment to stimulate denitrification and thereby N removal; however, over enrichment of OM and oxygen depletion can suppress nitrifying bacteria, favoring production of NH₄ over nitrate, helping to sustain eutrophic conditions (a positive feedback loop) (Bartoli et al., 2021). Overall, sandy sediments (this study) represented both a source and a sink for N where small changes to fluxes can have dramatic impacts on nitrogen supply or removal from the lagoon. The negative TDN flux during 2023 is consistent with a general downward trend in TDN in the northern BRL between

2021 and 2023). The decreased flux and lower concentrations are consistent with strong benthic–pelagic coupling and feedback in shallow coastal systems (Burdidge, 2012; Rodil et al., 2020). With continued sampling during the pilot study, we hope to better resolve these differences that are critical to understanding nitrogen in this system. We feel fortunate to have this dataset during a time with changing sediment and water quality and these data demonstrate the need and power of long-term monitoring.

At muddy (muck) sites investigated during Phase 2, fluxes of NO_x were directed from the water into sediments (–5 ± 19 μmoles/m^2/hr; –0.5 tons N/km^2/year), consistent with the use of nitrate as an oxidizing agent for the decomposition of OM in suboxic/anaerobic sediments. Releases of DIN from muddy sediments were virtually 100% NH_4 at a median of 580 ± 460 μmoles/m^2/hr (71 tons N/km^2/year), >2–fold higher than DIN fluxes from sandy sediments and positive relative to on average negative TDN fluxes identified for sandy sediments. Based on these data, muddy sediments represented a significant source of reduced N to overlying water (approximately 70 tons/km^2/year). When applied to the surface area of muck discussed in **Section 3.5.6,** we get approximately 400–500 tons N entering the lagoon per year from muck, consistent with data obtained using other methodologies from the Brevard County Save Our Indian River Lagoon Project Plan 2023 Update. In contrast, healthy sandy sediments were either a sink or a source of dissolved nitrogen as a function of changes to water and sediment quality.
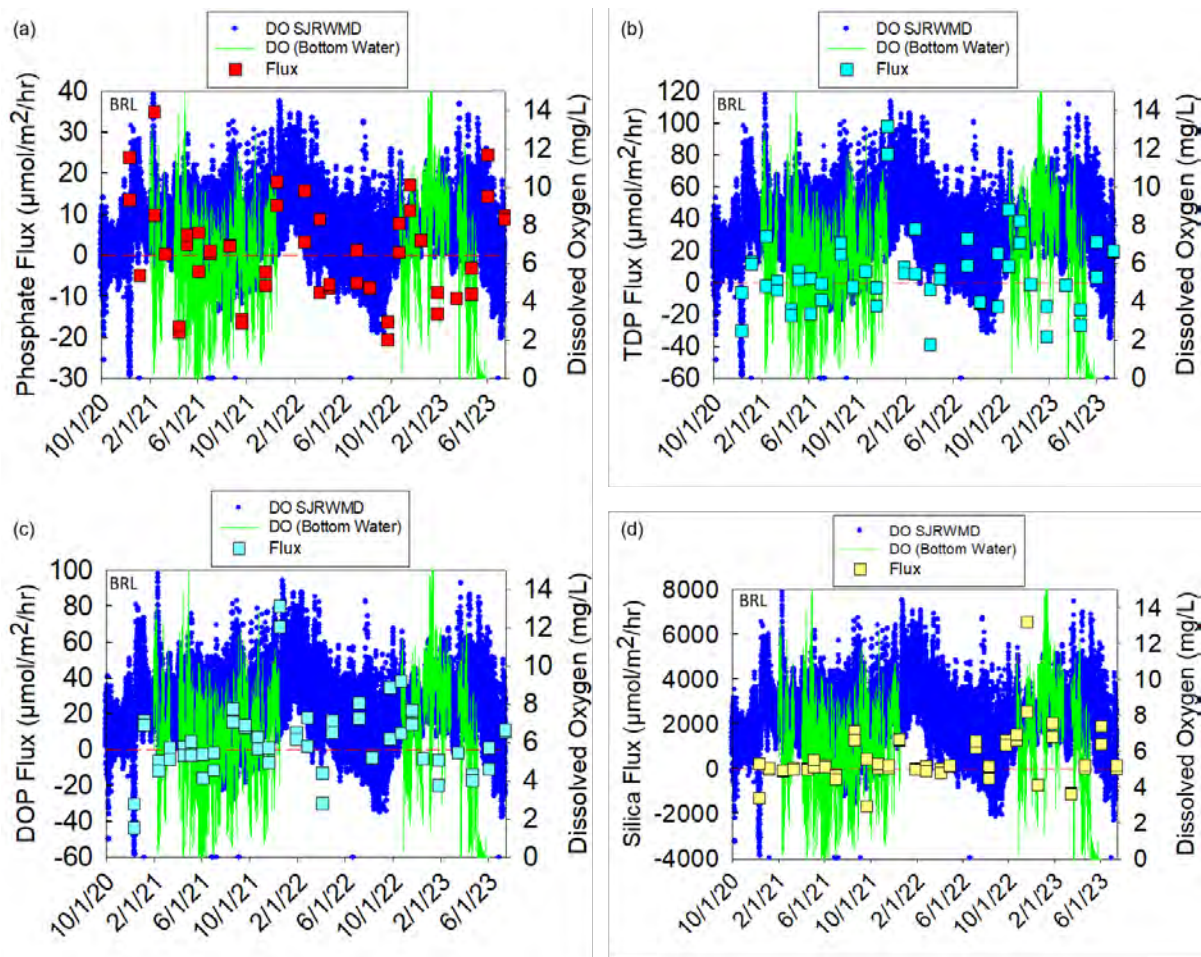
Note: Green and blue dotted lines show DO in the region at mid water depths (SJRWMD site IRLB04) and in bottom water at the inflow site.

Figure 26. Benthic fluxes of (a) PO$_4$, (b) TDP, (c) DOP and (d) SiO$_2$

Consistent with results for nitrogen, distinct spatial and temporal variations were observed. During Phase 1, at sandy sites through the lagoon, the median ± standard error PO$_4$ flux was 4.1 ± 8.1 µmoles/m^2/hr (1.1 ton/km^2/year). During Phases 2 and 3 at the inflow and reference sites, PO$_4$ fluxes were lower at 0.6 ± 1.7 µmoles/m^2/hr (0.16 tons/km^2/year) and −5.9 ± 3.8 µmoles/m^2/hr (−1.6 tons/km^2/year), respectively. Wide ranges of values for P fluxes are expected because P fluxes vary as a result of bacterial decomposition and concentration gradients, but also due to changing redox conditions in sediments and overlying water. As sediments and water become oxidized, P is scavenged by oxidized iron and aluminum while simultaneously aerobic decomposition of sediment OM can promote enhanced releases of P. Under anaerobic conditions, bacterial metabolism of OM slows; however, PO$_4$ can be released from reduced sediments, temporarily increasing fluxes (Cowan and Boynton 1996; Boynton et al., 2018). Data presented here show this change where sediments switch from a sink to a source of PO$_4$ (e.g., **Figure 26**). For example, during sampling in December 2020, bottom water DO at the inflow site was hypoxic at 1.3–1.5 mg/L and P fluxes were very high and directed out of sediments (18.8 ± 5.2 µmoles/m^2/hr, **Figure 26**). A similar, high P flux was identified in February 2021 (22 ± 12 µmoles/m^2/hr) immediately following a hypoxic event the night before.

During Phase 1 (2019 and 2020) lagoon–wide DOP fluxes were highly variable but on average directed into sandy sediments at –4.7 ± 4.9 µmoles/m^2/hr, consistent with mineralization of DOM and a concentration gradient driving fluxes into sediments. During Phases 2 and 3 (2021–2023) fluxes of DOP were 1.5 ± 2.5 µmoles/m^2/hr. Based on these collective datasets, the net TDP flux was directed from sediments into overlying water.

At muddy sites, the median PO$_4$ flux was 12 ± 18 µmoles/m^2/hr (3.3 tons/km^2/year). Higher PO$_4$ fluxes in muddy/anaerobic sediments from the IRL are consistent with data previously reported for other estuaries (e.g., Cowan and Boynton 1996). Fluxes of DOP were also directed out of sediments at 8.8 ± 6.6 µmoles/m^2/hr (2.4 tons/km^2/year). Overall TDP fluxes were directed out of muddy sediments and the net flux of P was large and positive.

Collectively, these data yielded trends in nutrient fluxes that were at least partially explained by changes to temperature and DO of bottom water. For example, during oxic conditions, sandy sediments were often a sink for P (e.g., **Figure 26**); however, during or shortly following periods of hypoxia or anoxia, sandy sediments were a source of P to overlying water. At the same time, during oxic conditions, sandy sediments promoted lower fluxes of ammonium (NH$_4$) and during periods of hypoxia, sandy sediments were more frequently a large source of reduced N (NH$_4$) (**Figure 25**). Pulses of bioavailable P can support algal growth and fluxes of reduced N during periods of hypoxia, preferentially support small, fast–growing algae like picocyanobacteria including *Aureoumbra lagunensis* (Lui et al., 2001).

3.4.5 Turnover Times

Benthic nutrient and oxygen fluxes plus existing nutrient concentrations in IRL were used to estimate residence (turnover) times for nutrients, based on water column processes and benthic fluxes. Residence times indicate the theoretical amount of time required for all nutrients in the water column to be either re–generated (positive flux) or consumed (negative flux). If other nutrient sources were to be included (external sources including tributaries, runoff etc.), residence times for nutrients would decrease. Relatively short residence times for nutrients (e.g., hours to weeks) relative to water (months to years) indicate that water column processes and benthic–pelagic coupling help to maintain nutrient concentrations over time. As the relative input of nutrients from internal (water column respiration and benthic fluxes) versus external loading increases, the system becomes less dependent on external loading to sustain eutrophication and algal blooms. Following the 2011 superbloom, the frequency and intensity of algal blooms are less predictable based on external loading. Instead, changes to internal nutrient cycling are likely responsible for a switch to a new, algal dominated, stable state or "regime" (Phlips et al., 2021). As the eutrophic state progresses, restoration strategies need to address both external and internal nutrient loading (Kemp et al., 2009). Restoring balance between freshwater inputs and seawater exchanges using managed inflow is one method that would help to address these internal processes. Exchanges would help to immediately decrease water column recycling at the inflow site by up to 5–fold for nitrogen and 2–fold for phosphorus based on respiration in the BRL versus Port Canaveral.

Residence times based on benthic fluxes alone were calculated using data from this study. Using an average lagoon depth of 1.5 m, each 1 m^2 section of lagoon contains 1.5 m^3 or 1,500 L of water (1 m$_{Length}$ x 1 m$_{width}$ x 1.5 m$_{depth}$ = 1.5 m^3 = 1,500 L; **Figure 27**). Nutrient concentrations (µmoles/L) times volume (1,500 L) yields the total standing stock of nutrients (µmoles) in each 1 m^2 section of the lagoon. The total quantity of nutrients was then divided by fluxes (µmoles/m^2/hr) to yield residence times in hours.
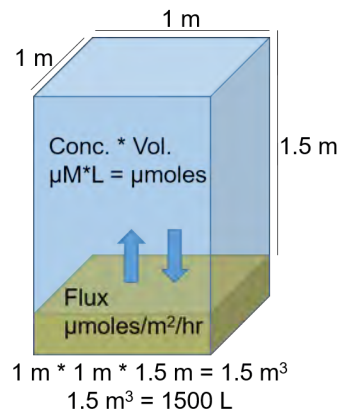
Figure 27. Conceptual diagram showing a 1 m^2 column of water and sediments from the IRL using an average depth of 1.5 m.

Overall (2019 to 2023), turnover times for nutrients varied from hours to days. In sandy sediments at the inflow site, the residence time for NH$_4$ was approximately 80 hours based on average nutrient concentrations during this study (e.g., 4.5 µmol NH$_4$–N/L in the lagoon) times 1,500 L/m^2 of lagoon (**Figure 27**) = 6,750 µmol N/m^2. At with a benthic flux at 88 µmol N/m^2/hr the residence time for ammonium nitrogen is approximately 3 days (**Table 11** and **Table 12**). In contrast, using only particulate (water column) fluxes, pelagic recycling could turn over the complete pool of NH$_4$ in approximately 113 hours or 4.7 days (4.5 µM / 0.04 µmol/L/hr = 113; **Table 14**) for a combined turnover time for nitrogen of just over 2 days (approximately 46 hours). Based on these data, pelagic (water column) respiration accounted for approximately 40% of the NH$_4$ recycling in the lagoon (**Table 14.**). Taking into account temporal changes in BRL the sediment and water column turnover times increased from 2021 to 2023 consistent with decreased nutrient concentrations and generally improved water quality.

Overall, NOx fluxes (44 ± 628 µmol/m2/hr;) from sandy sediments were about half of NH$_4$ fluxes and concentrations of NOx in BRL water were 10 times lower than concentration of NH$_4$ yielding turnover times based on sediment fluxes ranging from approximately 10 to 20 hours. Rapid recycling of NOx in the water column (1.2 ± 0.7 µM/hr; **Table 14**) coupled with low concentrations (0.41 µM) yielded a turnover time in water of less than one hour. Based on these data, water column processes accounted for 95% of NOx recycling in the lagoon (**Table 14**). Turnover times for NH$_4$ and NO$_x$ from muck were 20 hours and 10 hours, respectively, where muck acted as a major source of NH$_4$ (approximately 70 tons/km^2/year) and a sink for NOx (approximately -22 tons/km^2/year). Because NO$_x$ fluxes into sediments are balanced by increased NH$_4$ fluxes from sediments, the NH$_4$ flux accounted for NO$_x$ with regards to turnover of all the N in the water column. Based on these data, NH$_4$ could replace all the dissolved N in the water column overlying muck in approximately 13 days (300 hours). When water column processes are included, this decreases to less than 3 days demonstrating the relative importance of water column processes.

Turnover times for PO$_4$ from sandy sediments averaged approximately 375 hours, or 15 days, compared to only 14 hours for areas with muck sediments (**Table 14**). To cycle the complete pool of dissolved P, it would take 500 to 1,100 hours, or 20 to 50 days, for sandy sediments and 60 hours, or 2 to 3 days, for muck. Water column processes appeared to be much more important compared to sediments for P recycling and water column processes cycled the complete pool of TDP in just 6 to 7 hours and in the adjacent Port, TDP was recycled in only approximately 10 hours (). Due to rapid recycling in the water column, in areas with sandy sediments, benthic fluxes

accounted for only 0.1% of the total recycling; in muddy areas, sediments accounted for only 1% of the total phosphorus recycling. Although sediments accounted for a small fraction of the overall recycling, sediment–water exchanges are involved in the long-term storage of P whereas water column processes reflect algal and bacterial recycling into new biomass. The very short recycling time for P is consistent with P limitation in this area of the lagoon.

Due to the large temporal and spatial variability in DO throughout the lagoon, turnover times for oxygen were highly variable. Using the 5–year average DO concentration, 7.4 mg/L, equal to 100% saturation at 20 PSU and 25˚C, then the median turnover time based on SOD alone (not including water) ranged from approximately 140 hours for sandy sites in the inflow and reference areas to 80 hours for mucky sites (e.g., 7.4 mg/L / 32 mg/mmol * 1,000 µmol/mmol = 231 µmoles/L * 1,500L/m^2 of lagoon = 347,000 µmoles/m^2 divided by 2,400 µmoles/m^2/hr at sandy sites = 110 hours). When pelagic respiration (–1.4 ± 0.16 mg/L/hr) and SOD are considered together, turnover times based on a 1.5–m deep water column were approximately 40 hours for sandy sites and 26 hours for muddy sites. Overall, sediments accounted for 27% and 32% of the total oxygen demand for areas containing sand and muck, respectively (assuming 1.5 m average depth, sandy sediments shown in **Table 6**). These short turnover times are consistent with observed nighttime (dark) decreases in DO observed throughout the lagoon in continuous monitoring networks (e.g., Figure 42.). The Florida Tech network of bottom water DO sensors (**Section 3.5.5**) captures the importance of sediments towards overall oxygen consumption and nutrient recycling.

Table 14. Turnover times calculated using nutrient recycling in the water column and benthic fluxes, nutrient concentration in the water column, and an average depth of 1.5 m based on conceptual diagram in Figure 27.

Sediment	Oxygen (hours)	NH$_4$ (hours)	NOx (hours)	DIN to replace TDN (hours)	PO$_4$ (hours)
Water Column	62	113	<1	60	7
Inflow Sand	170	80	9	–	375
Lagoon Wide Sand	110	140	10	700	120
Muck	80	20	10*	460	10
Water + Sand	30	80	<1	60	9
Sediment/Total	26%	55%	5%	–	0.1%

*removal by sediments

Despite the importance of benthic–pelagic coupling and short residence times for nutrients in shallow coastal systems, improved water quality that could result from artificial inflow would likely modify geochemical processes, possibly increasing or decreasing benthic fluxes into overlying water and changing residence times for nutrients. To address some of these potential changes, laboratory incubation experiments were carried out for water and sediments to investigate how changes to temperature, salinity, and DO might influence geochemical nutrient cycling in the lagoon. In addition to geochemical processes, changes to temperature, salinity and DO could influence benthic faunal communities to favor species with different tolerances to hypoxia, or favor species with differing salinity tolerances. Nevertheless, the large fraction of total nutrient cycling that occurs in the water column suggest that direct exchanges of water and particles would likely have large and direct impacts on nutrient cycling in the lagoon.

3.5 Laboratory Experiments

3.5.1 Phosphorus sorption

To evaluate chronic impacts of hypoxia that could be mitigated or prevented from progressing by enhanced ocean inflow, sediments were collected and evaluated from 8 sites throughout the lagoon. Laboratory sorption experiments were carried out to investigate how the sorption capacity of sediments (S_{max}) has changed since these same sites were evaluated in 2001 prior to a regime shift that occurred in 2010 (Pant and Reddy, 2001; Phlips et al., 2021). Changes to the sorption capacity of sediments alter how sediments respond to hypoxic events and how efficiently sediments sequester phosphorus, effectively removing it from the system through burial in sediments. In samples collected from within 5m of 2001 coordinates, the sediment composition was in many cases different from 2001, with for example TOC ranging from 39% to 720% of 2001 values with medians at 0.28% in 2001 versus 0.71% in 2022 to 2023. Higher average OM and TOC contents are consistent with smaller particle sizes and a larger surface area to volume ratio of current sediments. An increase in OM content and decrease in grain size should lead to an increase in sorption capacities while also changing the native sorbed concentrations. Separately, higher OM contents increase the potential for mineralization and release of P from these sediments independent of sorption or desorption of exchangeable inorganic phosphorus. Changing grain size and composition of IRL sediments has been previously reported with increasing abundance and thicknesses of fine–grained, organic–rich sediments. For example, Trefry and Trocine (2011) found muck thicknesses to be 67% greater in 2006 to 20007 compared to the same sites in 1989 with layers >1m in thickness found at 22 sites in 2006 to 20007 compared to only 1 site in 1989 (Trefry and Trocine, 2011).

Table 15. 2022–23 Aerobic

Site ID	Smax	EPC	So	Kd	k	Kf	Pr	LOI OM(%)	TOC
1	98.6	0.01	2.7	212.8	2.23	44.5	0.92	1.77	0.59
2	90.6	0.09	9.1	96.9	1.45	33.9	0.92	2.53	0.84
4	71.3	0.54	5.4	11.0	0.15	8.8	0.76	1.50	0.50
5	45.4	0.19	2.2	10.6	0.23	6.8	0.71	0.57	0.19
8	227.4	0.06	8.5	217.4	1.02	130.9	0.97	4.53	1.51
11	90.0	0.03	4.9	152.5	1.75	47.2	0.97	5.63	1.88
13	74.2	0.15	26.4	230.7	2.17	38.2	0.76	-	-
15	95.8	0.01	2.7	222.9	2.13	48.2	0.95	2.13	0.71

Table 16. 2001 Aerobic

Site ID	Smax	EPC	So	Kd	k	Kf	Pr (%)	TOC
1	222.2	0.01	1.5	190.8	6.43	616	99%	0.69
2	67.1	0.01	0.6	82.6	0.59	29.3	92%	0.735
4	85.5	0.19	2.9	15.9	0.16	9.8	92%	0.199
5	64.1	0.01	0.4	26.1	0.36	8.9	85%	0.284
8	108.7	0.08	1.2	15.2	0.15	9.6	96%	0.211
11	500	0.01	4.3	346.6	4	1467	99%	4.79
13	31.2	0.06	1.3	21.1	0.32	5.8	82%	0.237
15	67.6	0.08	1.6	18.6	0.23	9.2	89%	0.145
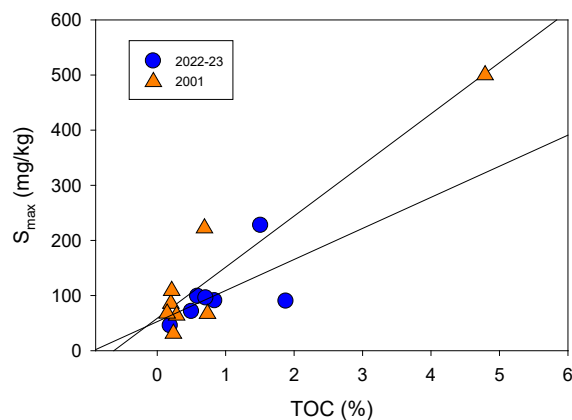
Figure 28. Total organic carbon (calculated from LOI) versus S_{max}.

With increasing spatial extent of fine–grained, organic–rich sediments in IRL, sediment oxygen demand and nutrient fluxes have likely increased as discussed as in **Section 3.4.4** above. With increased respiration and internal nutrient loading, coastal systems are more likely to experience hypoxia (e.g., Kemp et al., 2005, 2009). This is demonstrated in IRL by lower DO concentrations in bottom water overlying deposits of fine–grained, organic–rich sediments compared to sandy sediments (e.g., **Figure 38**). With relatively higher respiration and SOD as OM contents increase, IRL and BRL experience frequent diurnal and episodic hypoxia as discussed below in **Section 3.5.5**. Although most hypoxic events are short in duration (a few days or less) the effects of chronic diel and episodic hypoxia may significantly alter the phosphorus sorption and sequestration capacity of sediments.

Short term changes in sediment associated with hypoxia, reversibly release phosphate as Fe(III) is reduced to Fe(II) by suboxic bacterial metabolism leading to large positive fluxes. As sediments and water become re–oxidized, P is scavenged by Fe(III) oxyhydroxides decreasing fluxes. During hypoxic events, some reduced iron (Fe(II)) can irreversibly bind HS^- to form FeS, thereby decreasing the capacity of sediments to reuptake P. Over time the cumulative effects of hypoxia can decrease the capacity of sediments to sequester phosphorus leading to higher concentrations remaining in the water column. Independent of sorption of inorganic phosphorus, mineralization of OM leads to benthic fluxes where greater oxygen availability can increase flux from decomposing OM complicating interpretations of phosphate flux versus DO.

Because phosphorus is either buried in sediments or discharged to the coastal ocean, it is likely that sediment phosphate concentrations increase over time with the accumulation of OM while the capacity of sediments to sorb inorganic phosphorus simultaneously decreases. In 2001 Pant and Reddy reported and an average sorption capacity (S_{max}) for aerobic sediments at 133 mg/kg with an average initial sorbed concentration at 1.6 mg/kg. In 2022 to 2023 the average sorption capacity was 99 with an average initially sorbed concentration at 7.7 mg/kg. These changes are at least partially the result of changing sediment OM contents and grain size (e.g., **Figure 28**); however, they also reflect the long–term impacts of hypoxia on lagoon sediments. In 2022–23 the equilibrium phosphorus concentration averaged 0.13 mg/L (aerobic) and 0.18 mg/L (anaerobic) compared to 0.05 mg/L (aerobic) and 0.75 mg/L (anaerobic) in 2001. Higher aerobic EPC and lower anaerobic EPC in 2023 are consistent with greater OM and P contents of sediments combined with a loss of sorption capacity over time. As a result, higher EPC in 2022 to 2023 helps to maintain higher porewater P concentrations and larger overall fluxes; however, the event scale exchange (episodic hypoxia) of P is likely more limited.

Table 17. 2022–23 Anaerobic

Site ID	Smax	EPC	So	Kd	k	Kf	Pr	LOI OM (%)	TOC
1	90.0	0.02	1.9	88.1	1.09	36.9	0.94	1.77	0.59
2	126.6	0.09	6.4	72.4	0.74	36.5	0.94	2.53	0.84
4	100.1	0.21	9.1	51.3	0.51	26.0	0.90	1.50	0.50
5	66.0	0.50	1.9	3.8	0.06	4.0	0.68	0.57	0.19
8	121.5	0.11	5.3	38.3	0.41	26.3	0.94	4.53	1.51
11	–	–	–	–	–	–	–	5.63	1.88
13	–	–	–	–	–	–	–	–	–
15	76.7	0.13	1.7	27.5	0.36	12.1	0.96	2.13	0.71

Table 18. 2001 Anaerobic

Site ID	Smax	EPC	So	Kd	k	Kf	Pr (%)	TOC
1	*nd*	3.74	8.6	2.3	*nd*	*nd*	50%	0.69
2	30.8	0.14	2	14.7	0.61	10.2	90%	0.735
4	42.2	0.28	1.5	5.5	0.16	4.6	84%	0.199
5	24.6	0.36	5.4	14.8	0.71	9	86%	0.284
8	27.5	0.18	3.1	17.6	0.72	10.1	93%	0.211
11	74.6	1.57	22.5	14.4	0.03	14.7	70%	4.79
13	13.7	0.21	0.6	2.7	0.23	1.7	71%	0.237
15	24.1	0.13	1.3	9.9	0.44	6.4	87%	0.145

The higher EPC in 2023 reflects higher concentrations in overlying water compared to pre 2010 and is consistent with concentrations measured in porewater resulting from increased sediment OM contents. The increased EPC and native sorbed concentrations in 2023 compared to 2001 would support and sustain higher P fluxes, concentrations in overlying water and increased water column respiration and recycling as discussed above. In addition, the lower sorption capacity in

2023 would limit the ability of sediments to uptake future phosphorus inputs without increasing water column concentrations.

These changes reflect increased OM content of sediments since 2001. With strong benthic–pelagic coupling, settling of suspended particles and algae often associated with the senescence of algal blooms contributes to the accumulation OM plus N and P in sediments. Based on water column respiration from high turbidity and particle loads in BRL versus Port Canaveral, increased exchange of lagoon and seawater would decrease turbidity and respiration in BRL helping to mitigate further accumulation of OM. At the same time, more stable dissolved oxygen concentrations could promote mineralization of OM already present in organic–rich sediments. For example, in short term laboratory experiments to increase bioturbation and bio irrigation of fine–grained, organic–rich sediments, benthic fluxes were increased resulting from enhanced mineralization of OM from organic rich sediments. In contrast, in healthy, sandy sediment, increased bio–irrigation is known to increase the depth of aerobic sediments to promote nitrification, the limiting step in nitrogen removal, and phosphorus sorption (Hale et al., 2016; Wrede et al., 2017). Due to tight benthic pelagic coupling in shallow estuaries as outlined above, decreased water column respiration is likely to improve sediment quality.

3.5.2 Water Column; Dark, Laboratory Conditions

Geochemical responses to changes in water quality that could result from enhanced ocean inflow were evaluated through a series of laboratory incubation experiments. These experiments were carried out to stimulate changes in lagoon temperature, salinity, and DO that could occur as a result of inflow. These data also provide insight into how nutrient cycling may respond to other processes including warming temperatures and enhanced rainfall. With respect to ocean inflow, the most likely results would be a small decrease in lagoon temperature, an increase in salinity, and more stable DO as discussed above. Consistent with data for temperature and DO, changes to water column salinity were used to isolate responses of sediments; however, intrinsic changes to particles during salinity adjustments confound interpretation of responses within the water column; as a result, no discussion for changes to water column salinity is included here.

No significant trends for N or P were identified for water column fluxes as a function of temperature, salinity, or DO (**Table 19**, **Table 20**, **Table 21**, **Table 22, Figure 29,** and **Figure 30**).
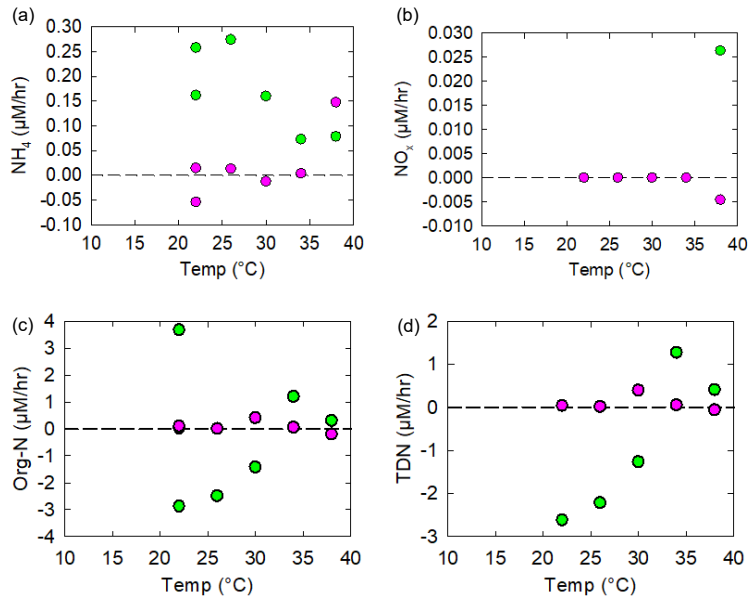
Figure 29. Water column fluxes from laboratory incubations in µM/hr versus temperature for (a) NH₄, (b) NOₓ, (c) organic N and (d) TDN. Green dots show incubations from time 0–2 hours, pink dots show incubations from 2–18 hours.
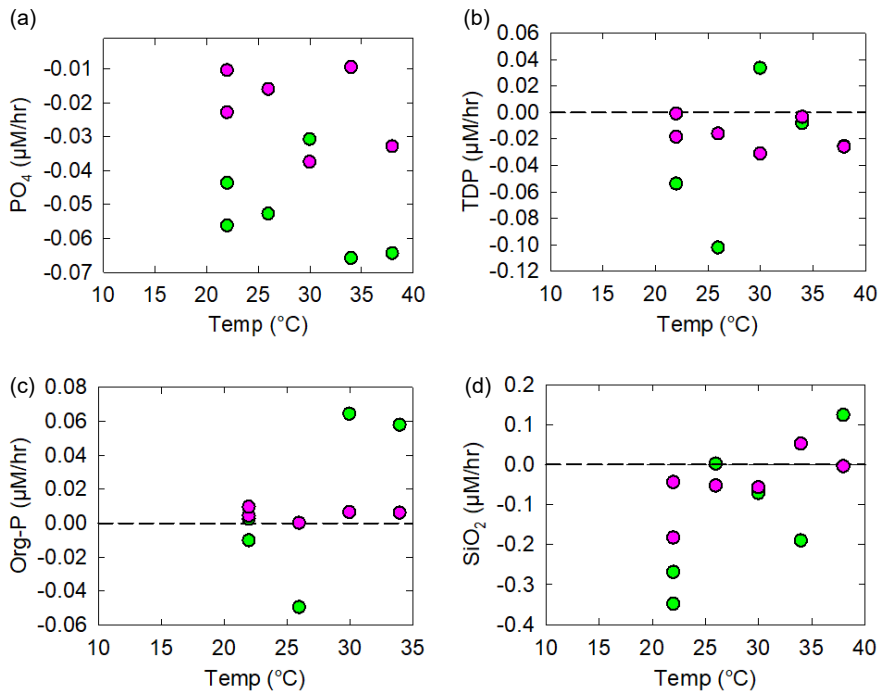
Figure 30. Laboratory incu ... **hr versus temperature (°C)**
for (a) PO₄, (b) TDP, (c) org ... **how incubations from time**
0–2 hours, ... **2–18 hours.**

Table 19. Coefficient of determination (R^2), probability values (p) and equations for water column fluxes (dark) versus temperature (0–2 hours).

Plot	R^{2*}	P–value*	Equation
TDN and Temp	0.007	0.874	–
NH_4 and Temp	0.617	0.064	–
NO_x and Temp	0.490	0.122	–
DIN and Temp	0.548	0.093	–
DON and Temp	0.011	0.841	–
PO_4 and Temp	0.185	0.395	–
TDP and Temp	0.248	0.315	–
DOP and Temp	0.425	0.161	–
Silica and Temp	0.520	0.106	–
H^+ and Temp	0.001	0.944	–
DIN:SRP and Temp	0.490	0.122	–
TDN:TDP and Temp	0.154	0.442	–

Table 20. Coefficient of determination (R^2), probability values (p) and equations for water column fluxes (dark) versus temperature (2–18 hours).

Plot	R^{2*}	P–value*	Equation
TDN vs. Temp	0.004	0.908	–
NH_4 vs. Temp	0.524	0.104	–
NO_x vs. Temp	0.490	0.122	–
DIN vs. Temp	0.522	0.105	–
DON vs. Temp	0.085	0.575	–
PO_4 vs. Temp	0.140	0.464	–
TDP vs. Temp	0.110	0.521	–
DOP vs. Temp	0.017	0.807	–
Silica vs. Temp	0.510	0.111	–
H^+ vs. Temp	0.838	**0.010**	**H^+(nmol/hr) = –0.005[°C] + 0.17**
DIN:SRP vs. Temp	0.491	0.121	–
TDN:TDP vs. Temp	0.151	0.446	–
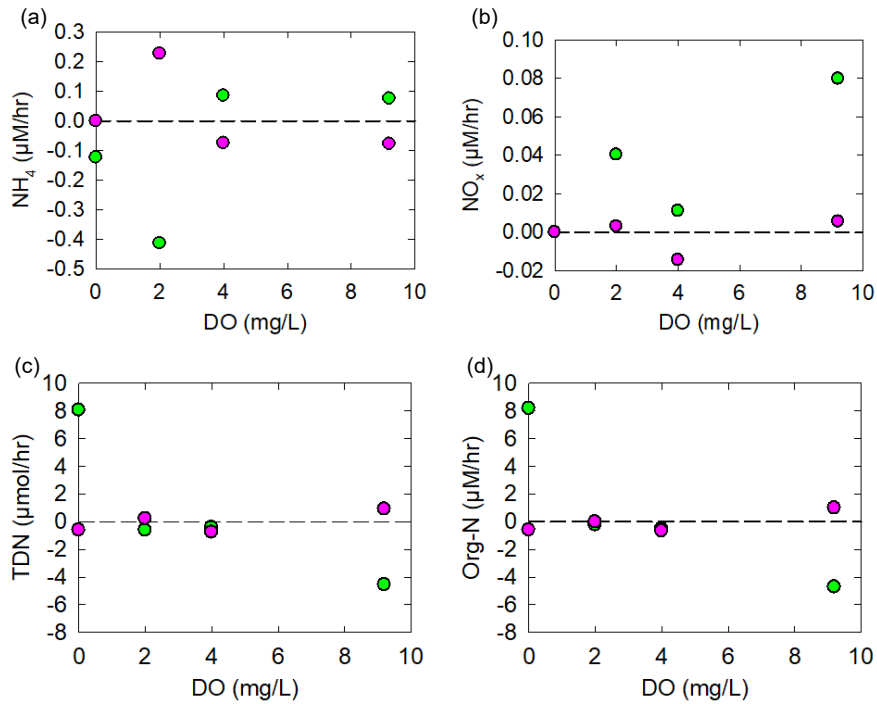
Figure 31. Water column fluxes from laboratory incubations in µM/hr versus DO for (a) NH₄, (b) NOₓ, (c) TDN, and (d) organic N. Green dots show incubations from time 0–2 hours, pink dots show incubations from 2–18 hours.
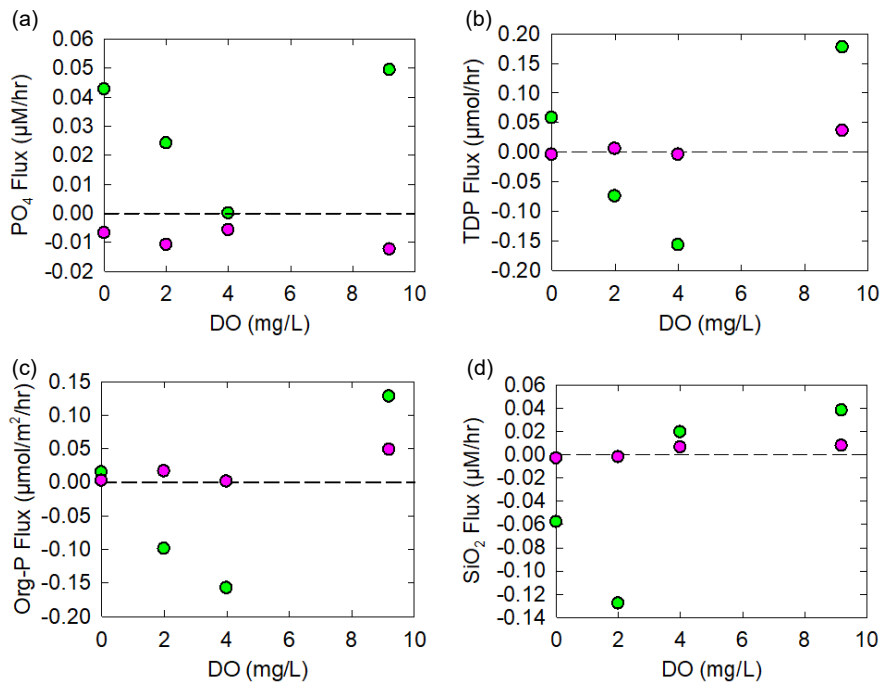
Figure 32. Laboratory incubation water column fluxes in µM/hr versus DO for (a) PO₄, (b) TDP, (c) organic P, and (d) SiO₂. Green dots show incubations from time 0–2 hours, pink

dots show incubations from 2–18 hours. Other colors show data from Phase 1 experiments.

Table 21. Coefficient of determination (R^2), probability values (*p*) and equations for water column fluxes (dark) versus DO (0–2 hours).

Plot	R^{2*}	P–value*	Equation
TDN vs. DO	0.741	0.139	–
NH$_4$ vs. DO	0.349	0.409	–
NO$_x$ vs. DO	0.726	0.148	–
DIN vs. DO	0.493	0.298	–
DON vs. DO	0.770	0.123	–
PO$_4$ vs. DO	0.054	0.767	–
TDP vs. DO	0.232	0.519	–
DOP vs. DO	0.271	0.479	–
Silica vs. DO	0.533	0.270	–
H$^+$ vs. DO	0.873	0.066	–
DIN:SRP vs. DO	0.001	0.976	–
TDN:TDP vs. DO	0.610	0.219	–

Table 22. Coefficient of determination (R^2), probability values (*p*) and equations for water column fluxes (dark) versus DO (2–18 hours).

| Plot	R^2	P–value	Equation
TDN vs. DO	0.526	0.274	–
NH$_4$ vs. DO	0.243	0.507	–
NO$_x$ vs. DO	0.041	0.799	–
DIN vs. DO	0.219	0.532	–
DON vs. DO	0.680	0.175	–
PO$_4$ vs. DO	0.365	0.396	–
TDP vs. DO	0.778	0.118	–
DOP vs. DO	0.733	0.144	–
Silica vs. DO	0.774	0.120	–
H$^+$ vs. DO	0.120	0.653	–
DIN:SRP vs. DO	0.152	0.610	–
TDN:TDP vs. DO	0.245	0.505	–

3.5.3 Laboratory Experiments (Sandy Sediments)

To estimate how changes to temperature, salinity, and DO may influence geochemical processes within sediments, laboratory experiments with sandy sediments were carried out with temperatures ranging from 13˚C to 32˚C, salinities ranging from 0 to 34 PSU, and DO ranging from 0% (0 mg/L) to 100% (about 9 mg/L). Wide ranges of values for temperature, salinity and DO were investigated to resolve changes among large natural variability while also controlling other variables. Using equations from statistically significant trends, responses to small changes in temperature, salinity, or DO over large areas of the lagoon can be modeled as discussed below in **Section 3.5.4**. During Phase 2, incubations were carried out with multiple sampling intervals to investigate immediate responses to changes in temperature, salinity, or DO (0–2 hours) and responses after the initial change (2–18 hours). Water column processes were tracked separately (discussed above **Section 3.4.1**) and subtracted from sediment fluxes allowing for sediment and water column processes to be evaluated independently.

3.5.3.1 Temperature

Collectively, during Phases 1 and 2, temperature was adjusted between 13 and 38°C (±0.2°C) using recirculating water baths to simulate the maximum annual range of lagoon temperatures, including extreme heat and cold events. Sediments cores from the IRL were returned to the laboratory and slowly adjusted to the desired temperature within 2 hours of collection. After reaching the desired temperature, cores were allowed to equilibrate for at least 1 hour before overlying water was drained and replaced with new water from the collection site. Once temperature was stable for at least 1 hour, start samples (time 0) were collected and cores were stirred using air diffusers to maintain DO at 100%. Diffusers were installed in such a way as to prevent the buildup of concentration gradients at the sediment–water interface without causing resuspension. Samples were then collected at 2 and 18 hours after starting incubations.
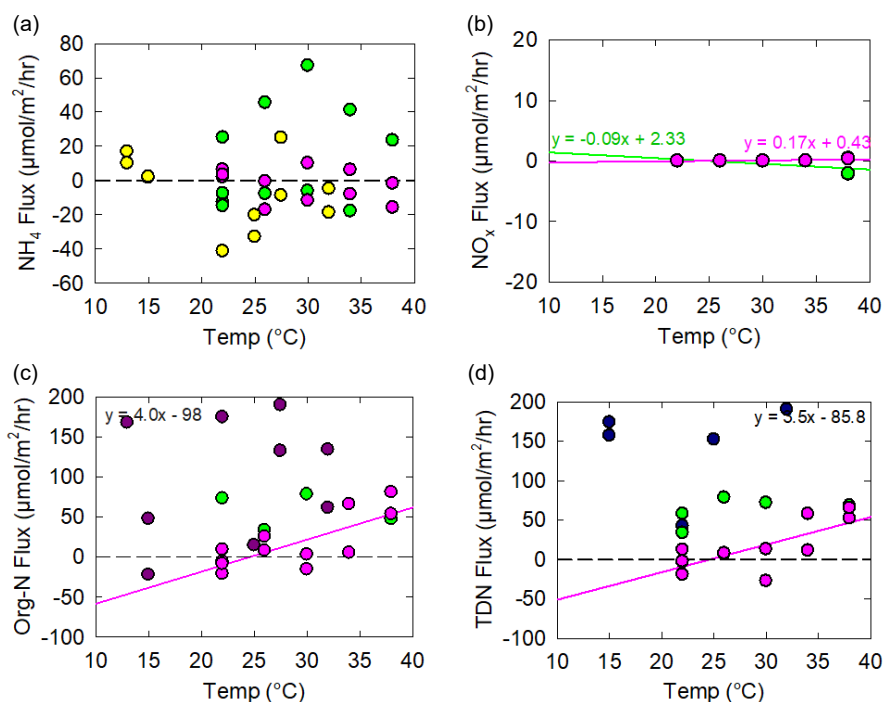
Figure 33. Fluxes from laboratory incubations (sandy sediment) in µmoles/m^2/hour versus sediment temperature for (a) NH$_4$, (b) NO$_x$, (c) organic N, and (d) TDN. Green dots show incubations from time 0–2 hours, pink dots show incubations from 2–18 hours. Other colors show data from Phase 1 experiments.

Significant positive correlations were identified for TDN (TDN flux [µmoles/m^2/hr] = 3.5 * [˚C] – 85.8, p = 0.006, r = 0.55; **Figure 33d**; **Table 24**), NO$_x$ (NO$_x$ flux [µmoles/m^2/hr] = 0.17 * [˚C] – 0.43, p = 0.012, r = 0.49; **Figure 33b**; **Table 24**), and DON (DON flux [µmoles/m^2/hr] = 4.0 * [˚C] – 98, p = 0.005, r = 0.57; **Figure 33c**; **Table 24**) from sandy sediments versus sediment temperature. Overall, NO$_x$ fluxes were positively correlated with temperature but accounted for only a small (<1%) fraction of the TDN. TDN increased by 3.5 µmoles/m^2/hr (0.4 tons/km^2/yr) per °C, virtually all as organic N with sediments switching from a sink for N at temperatures below 25°C to a source of N into overlying water at temperatures above 25°C (**Figure 33**).

Table 23. Coefficient of determination (R^2), probability values (p) and equations for benthic fluxes versus temperature (0–2 hours).

Plot	R^{2*}	P–value*	Equation
TDN vs. Temp	0.008	0.778	–
NH_4 vs. Temp	0.275	0.080	–
NO_x vs. Temp	0.490	**0.025**	Y=–0.09x+2.33
DIN vs. Temp	0.267	0.086	–
DON vs. Temp	0.028	0.603	–
PO_4 vs. Temp	0.317	0.057	–
TDP vs. Temp	0.081	0.371	–
DOP vs. Temp	0.248	0.100	–
Silica vs. Temp	0.417	**0.023**	Y=27.0x–868
H^+ vs. Temp	0.096	0.328	–
DIN:SRP vs. Temp	0.058	0.452	–
TDN:TDP vs. Temp	0.142	0.227	–

Table 24. Coefficient of determination (R^2), probability values (p) and equations for benthic fluxes versus temperature (2–18 hours).

Plot	R^{2*}	P–value*	Equation
TDN vs. Temp	0.550	**0.006**	Y=3.5x–85.8
NH_4 vs. Temp	0.130	0.249	–
NO_x vs. Temp	0.488	**0.012**	Y=0.17x–0.43
DIN vs. Temp	0.123	0.264	–
DON vs. Temp	0.567	**0.005**	Y=4.0x–98
PO_4 vs. Temp	0.001	0.915	–
TDP vs. Temp	0.184	0.164	–
DOP vs. Temp	0.624	**0.002**	Y=0.12x–4.1
Silica vs. Temp	0.682	**0.001**	Y=14.9x–513
H^+ vs. Temp	0.022	0.647	–
DIN:SRP vs. Temp	0.0001	0.978	–
TDN:TDP vs. Temp	0.0767	0.384	–

Based on data from Phase 1, fluxes of dissolved PO_4 from sandy sediments were positively correlated with temperature (PO_4 flux [µmoles/m^2/hr] = 0.58 * [˚C] – 7.6, p = 0.04, r = 0.63) and increased from near 0 µmoles/m^2/hr at 13˚C to 5 to 10 µmoles/m^2/hr at 32˚C. During Phase 2, a significant positive correlation was identified for DOP versus temperature (DOP flux [µmoles/m^2/hr] = 0.12 * [˚C] – 4.1, p = 0.002, r = 0.62; **Figure 34c**, **Table 24**) and SiO_2 fluxes were positively correlated with sediment temperature increasing by 14.9 µM/m^2/hr per ˚C (SiO_2 flux [µmoles/m^2/hr] = 14.9 * [˚C] – 513, p = 0.01, r = 0.68; **Figure 34d**, **Table 24**).
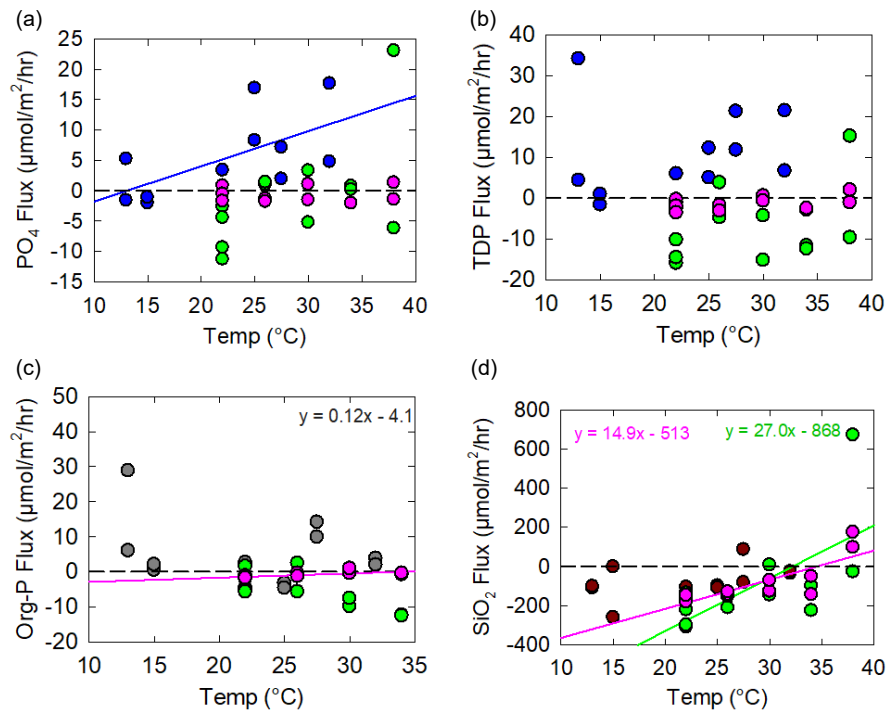
Figure 34. Laboratory incubation fluxes (sandy sediments) in μmoles/m2/hour versus sediment temperature for (a) PO4, (b) TDP, (c) organic P, (d) SiO2. Green dots show incubations from time 0–2 hours, pink dots show incubations from 2–18 hours. Other colors show data from Phase 1 experiments.

Based on significant positive correlations between sediment temperature and NO_x, DON, TDN, PO_4, DOP, and SiO_2 fluxes, a decrease in water temperature that could result from inflow would decrease inputs of these nutrients into the lagoon. For example, a 1°C decrease in lagoon temperature would decrease PO_4 fluxes from sandy sediments by about 0.16 tons/km^2/year (0.58 μmoles/m^2/hr per °C) or about 15% from the current median at 4.1 μmoles/m^2/hr (1.1 ton/km^2/year). Although lagoon–wide changes to temperature are likely to be small, small changes applied to large areas of the lagoon could have significant impacts on nutrient loading. Decreased inputs of these nutrients due to restoration of ecosystem services could be of more significance than decreased concentrations due to dilution by seawater mitigating impacts of flushing on the coastal ocean as discussed in **Section 3.5.4**.

3.5.3.2 Salinity

Laboratory experiments were carried out to evaluate potential uptake or releases of nutrients associated with changes to salinity of overlying water. These experiments were carried out in water baths at 22°C (laboratory temperature) and chambers were stirred using diffused air to maintain oxygen at 100% saturation. Before each experiment, overlying water was drained from cores and replaced with a mixture of either site water plus deionized water (decreased salinity) or with site water and added sea salt (higher salinity). Once overlying water was exchanged, cores were allowed to equilibrate for at least one hour before sampling.
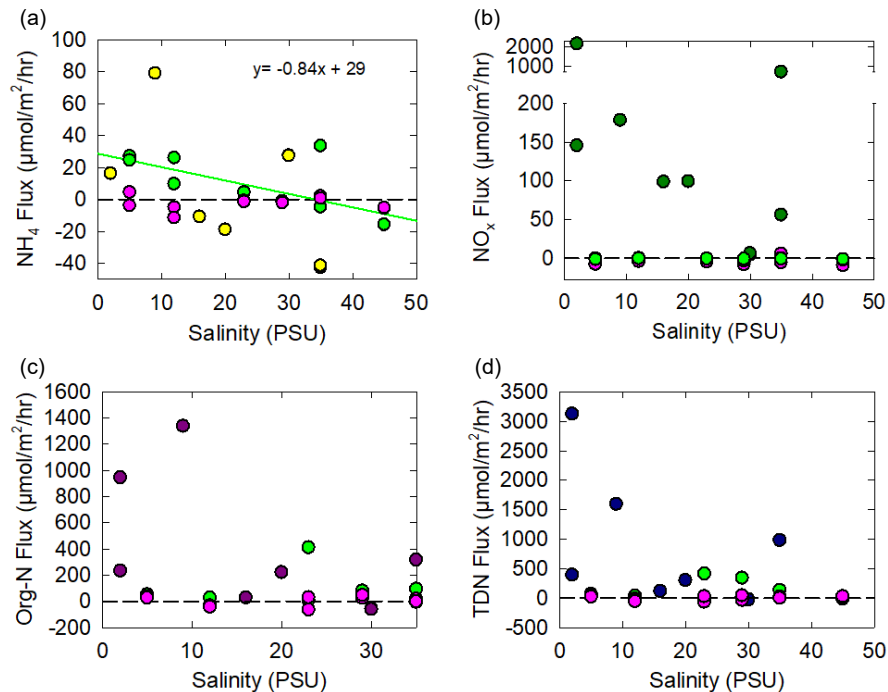
Figure 35. Laboratory incubation fluxes (sandy sediment) in µmoles/m²/hour versus salinity for (a) NH₄, (b) NOₓ, (c) organic N, and (d) TDN. Green dots show incubations from time 0–2 hours, pink dots show incubations from 2–18 hours. Other colors show data from Phase 1 experiments.

During Phase 1, a significant correlation was identified for NO_x (flux (µmoles/m²/hr) = –4.7 * [PSU] + 180) with a decrease in NO_x flux of 4.7 µmoles/m²/hr (about 0.6 tons/km²/hr) per PSU or about 3% per PSU from the median of 150 µmoles/m²/hr (–20 tons N/km²/year) for sandy sites throughout the lagoon (**Figure 35b**). This trend likely represented short–term equilibrium processes during the shorter duration experiments carried out during Phase 1. This same trend was not identified during Phase 2, likely because there was very little NO_x present in any of the cores. During Phase 2, a significant correlation was identified for NH_4 flux versus salinity (NH_4 flux (µmoles/m²/hr) = –0.84 [PSU] + 29) during the initial incubation period where NH_4 flux decreased by 0.84 µmoles/m²/hr per PSU) (**Figure 35a, Table 25**). This equates to a decrease of approximately 1% per PSU from the median of 90 µmoles/m²/hr (11 tons N/km²/year) for sandy sites throughout the lagoon. These trends for small changes to N fluxes observed shortly after changes to salinity likely reflect lower concentrations in overlying water for diluted (lower salinity) samples. The absence of tends over the longer incubation periods (2 to 18 hours) suggest that small changes to salinity alone are not likely to influence geochemical N cycling over the long term.
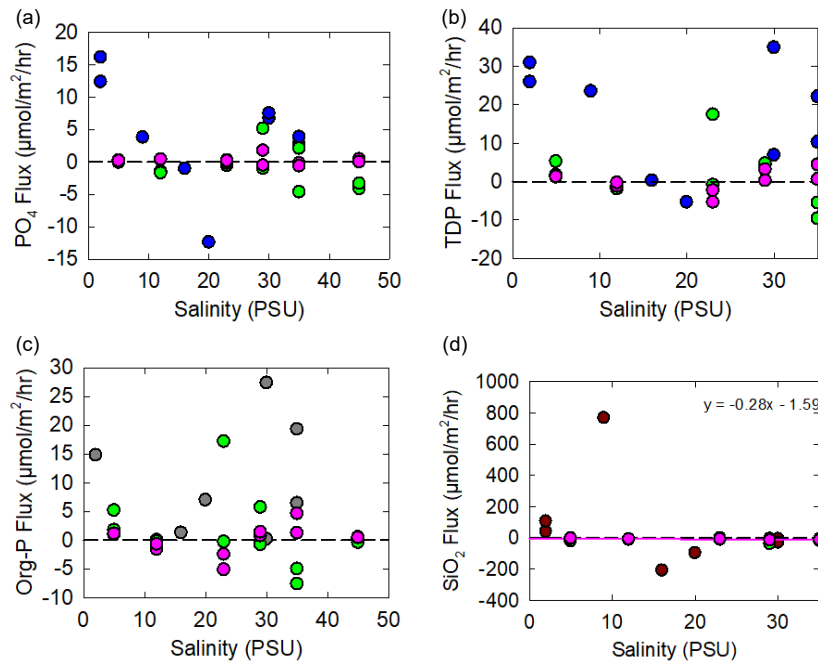
Figure 36. Results fron[...]ents showing fluxes in µmoles/m²/hour versus the s[...] PO₄, (b) TDP, (c) organic P, and (d) SiO₂. Green dots[...]2 hours, pink dots show incubations from 2–18 h[...]om Phase 1 experiments.

Table 25. Coefficient of d[...]lues (*p*) and equations for benth[...]ours).

P[...]			Equation
TDN vs. S[...]			–
NH₄ vs. Sa[...]			–0.84x+29
NOₓ vs. Salinity	0.036	0.553	–
DIN vs. Salinity	0.005	0.822	–
DON vs. Salinity	0.0001	0.978	–
PO₄ vs. Salinity	0.080	0.373	–
TDP vs. Salinity	0.137	0.237	–
DOP vs. Salinity	0.086	0.356	–
Silica vs. Salinity	0.092	0.339	–
H⁺ vs. Salinity	0.201	0.144	–
DIN:SRP vs. Salinity	0.076	0.386	–
TDN:TDP vs. Salinity	0.022	0.649	–

Table 26. Coefficient of determination (R^2), probability values (*p*) and equations for benthic fluxes versus salinity (2–18 hours).

Plot	R^{2*}	P–value*	Equation
TDN vs. Salinity	0.032	0.576	–
NH₄ vs. Salinity	0.009	0.773	–
NOₓ vs. Salinity	0.151	0.212	–
DIN vs. Salinity	0.012	0.733	–
DON vs. Salinity	0.061	0.437	–
PO₄ vs. Salinity	0.019	0.670	–

Plot	R²*	P–value*	Equation
TDP vs. Salinity	0.040	0.532	–
DOP vs. Salinity	0.059	0.447	–
Silica vs. Salinity	0.657	**0.001**	Y=–0.28x–1.59
H⁺ vs. Salinity	0.500	**0.010**	Y=2.65x–97
DIN:SRP vs. Salinity	0.236	0.120	–
TDN:TDP vs. Salinity	0.031	0.583	–

No significant trends were identified for fluxes of dissolved PO_4 versus salinity during any of the Phase 1 or Phase 2 experiments (**Figure 36; Table 25** and **Table 26.**). These data suggest that no significant long–term changes to N or P cycling are expected based on changes to salinity. A similar study of N and P exchanges along a salinity gradient in the Florida Everglades found no correlation between fluxes of N or P and salinity while investigating how restored flow to the everglades may influence nutrient cycling (Owens et al., 2021).

3.5.3.3   DO
Even though DO is not a conservative property of seawater, it is one of the water quality variables likely to change with enhanced ocean water exchange, and it is arguably one of the most important variables controlling nutrient cycling, infauna, epifauna, fish populations, and overall lagoon health. Changes to DO would likely result from (1) a change in the solubility of oxygen due to changing temperature and salinity, plus (2) inflow of lower turbidity seawater with lower respiration, and (3) higher density seawater and enhanced circulation that could mix deep areas currently prone to stagnation and low DO events. To manipulate DO concentrations in the laboratory, cores were place in temperature stable water baths (22°C laboratory temperature) and continuously bubbled using mixed gases (air and nitrogen) to maintain DO concentrations between 0% (0 mg/L) and 100% saturation (7 to 8 mg/L).
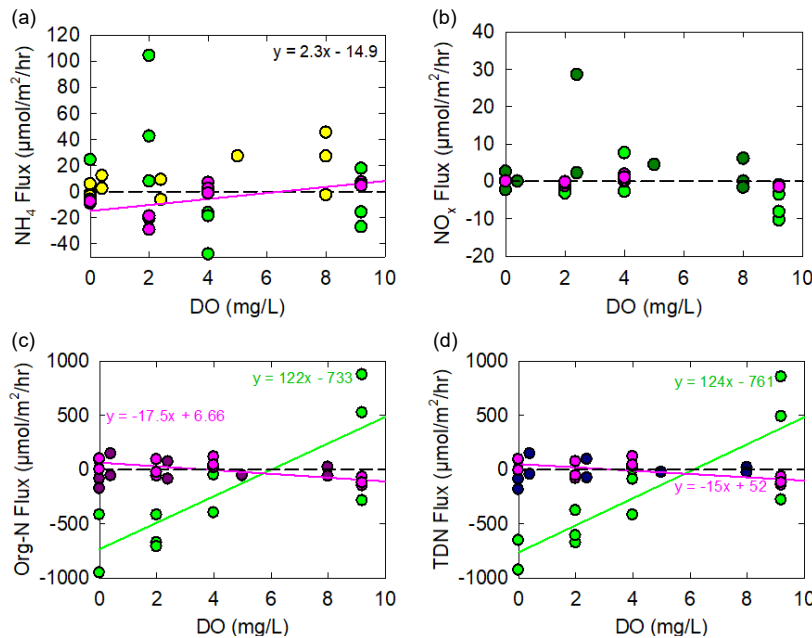
Figure 37. Results from laboratory incubation experiments showing fluxes in μmoles/m²/hour versus bottom water DO concentrations (mg/L) for (a) NH₄, (b) NOₓ, (c) organic N, and (d) TDN versus the salinity of overlying water. Note: Green dots show incubations from time 0–2 hours, pink dots show incubations from 2 to 18 hours. Other colors show data from Phase 1 experiments.

Consistent with trends observed for in–situ benthic chambers, significant positive correlations were identified for organic and total N versus concentrations of DO in bottom water (DON flux [µmoles/m^2/hr] = 122 * [mg/'] – 733, p = 0.003, r = 0.63; TDN flux (µmoles/m^2/hr) = 124 * [mg/L] – 761, p = 0.002, r = 0.69; **Table 27**, **Figure 37**). In both the field and in the laboratory, sediments switched from a sink of organic and total N to a source, as DO concentrations increased above approximately 6 to 8 mg/L. These data show an approximately 15 tons/km^2/year increase in TDN fluxes, almost all as organic N, per mg/L increase in DO. This result is likely tied to the relationship between SOD and bottom water DO, where greater oxygen consumption (respiration and nutrient cycling) by sediments yielded lower bottom water DO concentrations. In other words, higher rates of decomposition in sediments yielded higher fluxes of organic and total N. In the laboratory, following an initial pulse of organic N and TDN, aerobic sediments were a net sink for organic N and TDN (–82 ± 89 µmoles/m^2/hr) and anaerobic sediments were sometimes a source of organic N and TDN to overlying water (119 ± 240 µmoles/m^2/hr) (**Figure 37**), with a significant negative correlation (–15 µmoles/m^2/hr per mg/L) identified between TDN flux and DO over the 2–18 hour incubation (**Figure 37**; **Table 27**, **Table 28**).
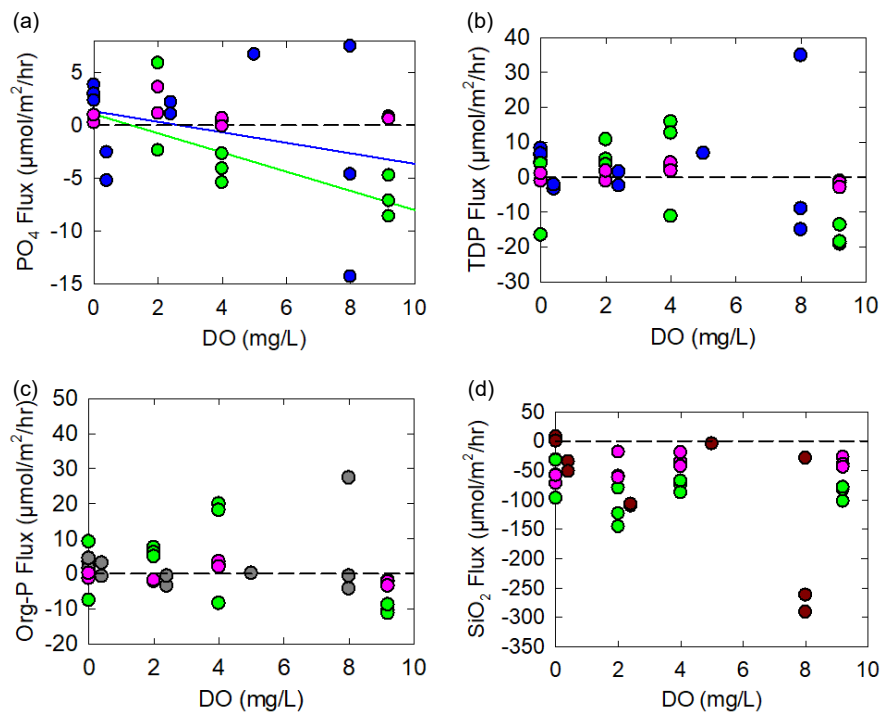
Figure 38. Results from laboratory incubation experiments showing fluxes in µmoles/m^2/hour versus bottom water DO concentrations (mg/L) for (a) PO$_4$, (b) organic P, (c) TDP, and (d) SiO$_2$ plus (e) molar ratios of DIN to SRP versus sediment temperature.

Fluxes of dissolved PO$_4$ decreased at higher concentrations of bottom water DO (PO$_4$ flux [µmoles/m^2/hr] = –0.9 * [mg/L] + 1.6, p = 0.03, r = 0.50; **Figure 38**, **Table 27**). These observations were consistent with data from the field study, where PO$_4$ fluxes from hypoxic sediments were typically higher and positive from anaerobic sediments (19 ± 11 µmoles/m^2/hr in December 2020 and February 2021), compared to a negative median flux (–4.4 ± 7.3 µmoles/m^2/hr) under aerobic conditions during all other sampling events (**Figure 38a** and **Figure 26a**). Laboratory incubations with multiple sample intervals captured changes to nutrient cycling that resulted from the initial

change and dump of P and longer–term sampling captured the more stable fluxes at new DO concentrations. Variable responses as identified during different experimental periods are consistently identified in the literature (e.g., Foster and Fulweiler 2019), mostly due to the complexities of the N and P cycles as discussed earlier.

Table 27. Coefficient of determination (R^2), probability values (p) and equations for benthic fluxes versus DO (0–2 hours).

Plot	R^{2*}	P–value*	Equation
TDN and DO	0.686	**0.002**	Y=124x–761
NH_4 and DO	0.021	0.673	–
NO_x and DO	0.368	0.048	
DIN and DO	0.014	0.730	–
DON and DO	0.633	**0.003**	Y=122x–733
PO_4 and DO	0.500	**0.033**	Y=–0.9x+1.06
TDP and DO	0.279	0.095	–
DOP and DO	0.252	0.116	–
Silica and DO	0.0001	0.978	–
H^+ and DO	0.007	0.802	–
DIN:SRP and DO	0.016	0.709	–
TDN:TDP and DO	0.165	0.215	–

Table 28. Coefficient of determination (R^2), probability values (p) and equations for benthic fluxes versus DO (2–18 hours).

Plot	R^2	P–value	Equation
TDN and DO	0.371	**0.047**	Y=–15x+52
NH_4 and DO	0.420	**0.031**	Y=2.3x–14.9
NO_x and DO	0.174	0.202	–
DIN and DO	0.370	**0.047**	–
DON and DO	0.474	**0.019**	Y=–17.5x+66.6
PO_4 and DO	0.042	0.545	–
TDP and DO	0.146	0.247	–
DOP and DO	0.077	0.409	–
Silica and DO	0.214	0.152	–
H^+ and DO	0.064	0.454	–
DIN:SRP and DO	0.453	**0.023**	Y=2.8x–15.0
TDN:TDP and DO	0.429	**0.029**	Y=11.4x–32.0

3.5.3.4 Infauna

As discussed above, previous studies have identified feedback interactions where oxygen sensitive biogeochemistry, food–webs and habitat quality interact to influence nutrient and algal dynamics that regulate oxygen levels and nutrient fluxes. With previous studies suggesting that suspension feeding bivalves could control phytoplankton growth, restoration of filter feeders and seagrass has been proposed as a mechanism to reduce hypoxia in in shallow coastal systems (e.g., Prins et al., 1998; Dame and Olenin, 2005; Kemp et al., 2009). Weather restored or naturally recruiting, benthic faunal communities contribute towards bioturbation, biogeochemical cycling, and the burying of pollutants into the sediment (Wrede 2016; Rius 2018). Bioturbation and bio–irrigation can increase the thickness of the oxic sediment layer allowing for a more viable surface area for nitrogen–fixing bacteria and phosphorus sorption (An and Gardner 2002). With fewer infauna, ecosystems are less able to remove nutrients as efficiently whereby hypoxia tends to be

more prevalent in areas with decreased benthic faunal abundance (Kemp et al., 2009; Wrede 2016). In IRL, Fuller et al. (2021) reported lower abundance and diversity of infauna in areas with higher OM contents. Another infauna study compared the three basins: IRL, BRL, and Mosquito Lagoon (Lunt et al. 2021). The main Indian River Lagoon basin had a species composition 84.92% different than that of the BRL basin. The reasons for this were unknown, but it was hypothesized to be due to longer water residence time and different sediment compositions of the Banana River (Lunt et al. 2021). The Banana River basin was also shown to have decreased species richness, with more diverse infauna communities being more effective at cycling nutrients (Bricker et al., 2007).

To explore the bioturbation potential of the specific species documented in BRL, we focused on species with over 1,000 individuals identified in BRL during the 2021 study (**Table 29**; Lunt et al., 2021). The burrowing and feeding behavior of these species were identified for their potential to contribute towards bioturbation or bio–irrigation. Burrowing behaviors that were considered the most effective at bioturbating were structure building and upward conveyor (**Table 29**). Structure building burrowing species have been found to have a large effect on increasing the oxic layer, but this behavior's effectiveness varied depending on the type of structure the organism built (Schenone 2019). In addition to burrowing behavior, each species was identified as marine, brackish, or freshwater in an effort to better understand how changing salinity that may result from enhanced circulation could impact these species. Although specific salinity tolerance were not identified, most of the most common BRL species examined were identified as marine, with few identified as brackish. This preliminary data suggest that BRL species are best suited for marine salinities. This effort is the first step in evaluating how changes to habitat quality might influence benthic fluxes.

In our short–term experiment supplementing fine–grained, organic–rich sediments with additional infauna (*Macoma* spp.), bio irrigation of sediments increased benthic fluxes of TDN and TDP. This result was likely related to enhanced mineralization of organic matter from the organic rich sediments. Although not the expected result, this demonstrated one potential benefit of decreased sediment organic contents, while illustrating the complexity of geochemical, food–web and habitat interactions. Future experiments repeating this experiment in sandy sediments expect to quantify enhanced nutrient removal, where enhanced bio–irrigation in sandy sediments increases the surface area of sediments available to nitrifying bacterial and for phosphorus sorption as has been observed in previous studies (e.g., Xi and Zhang, 2023). The Macoma clam species used in our experiment is also a filter feeder and does not have a highly effective burrowing behavior (Schenone 2019). This experiment will be performed again, and the species will be selected based on potential for bio irrigation and in sandy sediments.

Table 29. Common infauna species found in BRL

Species	Phylum	Burrowing Behavior	Feeding Behavior	Reference	Salinity Tolerance
Cylindroleberididae	Arthropoda	biodiffuser	suspension feeder	Syme 2007, Lindqvist 2016	marine
Hargeria rapax	Arthropoda	structure building	deposit feeder	Myers 1971, Heard, R.W. and G. Anderson 2009	marine
Parastarte triquetra	Mollusca	biodiffuser	suspension feeder	Conrad,1841	marine
Mulinia lateralis	Mollusca	biodiffuser	suspension feeder	Say, 1822	marine
Phascolion sp.	Annelida	upward conveyor	deposit feeder	Murina 1984	marine
Oxyurostylis smithi	Arthropoda	biodiffuser	deposit feeder	Myers 1977	marine, brackish
Ampelisca abdita	Arthropoda	structure building	suspension/ deposit feeder	Lippsom & Lippsom 1997, Cohen and Carlton 1995	marine
Kinbergonuphis sp.	Annelida	structure building	scavenger/deposit feeder	Fauchauld & Jumars 1986	marine, brackish, fresh
Pectinaria gouldii	Annelida	structure building	deposit feeder	Castanedo et al 2012, Hsieh & Simon 1990	marine
Cerapus sp.	Arthropoda	structure building	suspension feeder	Barnard et al 1991	marine
Polydora sp.	Annelida	biodiffuser	suspension feeder	Castanedo et al 2010	marine
Cyclaspis varians	Arthropoda	upward conveyor	deposit feeder	larsen and rogers 2015	marine
Ericthonius brasiliensis	Arthropoda	structure building	suspension feeder	Sotka et al 1998, Myers & Lowry 2003	marine
Clymenella mucosa	Annelida	structure building	deposit feeder	Fauchauld & Jumars 1977, Andrews 1891	marine
Streblospio benedicti	Annelida	structure building	suspension feeder	Dauer et al 2003, Carlton 2007	marine, fresh
Gemma	Mollusca	biodiffuser	suspension feeder	Sellmer 1967	marine
Nereididae	Annelida	upward conveyor	deposit feeder/ suspension feeder	Fauchauld & Jumars 1977	marine, brackish, fresh, terrestrial
Capitellidae	Annelida	upward conveyor	deposit feeder	Castanedo et al 2012	marine

3.5.4   Summary of Laboratory Experiment Results

Water column processes play a major role in overall nutrient recycling; however, no significant correlations were identified between water column nutrient fluxes and changes to temperature, salinity, or DO (**Section 3.5.2**). Although no changes were observed in response to variations in temperature, salinity, or DO, mixing seawater with differing turnover times into lagoon water would, in and of itself, decrease rates of nutrient recycling in the area of inflow as discussed in **Section 3.4.1**. During Phase 2, significant positive correlations were identified for NO_x, TDN, PO_4, DOP, and SiO_2 versus sediment temperature (**Table 24**), indicating that lower temperature could decrease internal loading (inputs) of these nutrients into the IRL. Significant positive correlations were identified between DO and both DON and TDN (**Table 27**); however, after initial releases, significant negative correlations were identified between DON and TDN and DO and a positive correlation between ammonium and DO (**Table 28**).

Overall, N and P responded to changes in temperature and DO, but not salinity. Using equations from statistically significant relationships, quantities of nutrients that could be removed or prevented from entering the lagoon in response to changes in temperature or DO were calculated using data from this study. Because these responses are scalable depending on the magnitude of change to temperature or DO and the area of lagoon that experiences various levels of change (km^2), results are presented per °C and per mg/L per km^2 (**Table 30**).

Table 30. Expected changes to fluxes of N and P resulting from an increase in temperature of 1°C and an increase in DO of 1 mg/L.

	Change in N flux / °C	Change in P flux / °C
Water	–	–
Sediment	0.4 tons/km^2/year/°C	0.16 tons/km^2/year/°C
	Change in N flux / mg*L^{-1}	**Change in P flux / mg*L^{-1}**
Water	–	–
Sediment	1.8 tons/km^2/year/mg*L^{-1}	–0.9 µmoles/m^2/hr (0.24 tons/km^2/year/mg*L^{-1})

Using a simple mixing model for temperature, a current residence time for water in the northern lagoon (50% exchange approximately 300 days and complete exchange approximately 2 years, Smith 1993; FDEP 2013), inflow of seawater at 0.5 m^3/sec, and a difference in temperature in the lagoon and in Port Canaveral of (approximately 0.5°C), the average change in lagoon temperature over various spatial scales with inflow (new equilibrium temperatures) was calculated and used to estimate decreases in N and P loading from sandy sediments. Changes in temperature assume that heating is proportional to ratios of lagoon water and Port water with associated particles and color (i.e., clearer water absorbs less heat). Even though the change in temperature would be greater if mixing occurred over a smaller area, small changes over larger areas would have more impact on decreasing fluxes and internal nutrient loading. For example, if mixing from the pilot study (0.5 m^3/sec) occurred over 5 km^2, we calculated that 0.6 tons of N and 0.3 tons of P would be prevented from entering the lagoon each year based on a decrease in lagoon temperature of 0.23°C over 5 km^2 and decreased fluxes (e.g., 0.4 tons N/km^2/year/°C * 0.23°C * 5 km^2 = 0.6). If mixing occurred throughout the entire 170 km^2 of the BRL, we estimate that 1.6 tons of N and 0.7 tons of P would be prevented from entering the lagoon each year based on a 0.02°C decrease in lagoon temperature over 170 km^2. Based on modeling of inflow in the corresponding engineering and modeling report (Task 1), mixing after the startup period is expected to be confined to the study area, with limited impacts throughout the BRL. Based on these data and calculations, the

quantity of nutrients removed via changes to benthic fluxes is expected to be greater than the net quantity of nutrients that would be discharged to the coastal ocean. Additional benefits are expected based on increased DO concentrations; however, these improvements are less easily modeled. Nevertheless, these data suggest that a pilot inflow project would yield net removal of N and P from the combined lagoon–ocean system, where decreased nutrient concentrations resulting from changes to internal cycling are expected to exceed changes to resulting from direct exchanges of water.

Although trends used here were statistically significant, varying responses over different time intervals and large natural variability resulted in lower than expected statistical power. For this reason, we use caution when extrapolating these small changes over large areas as presented here and plan to focus future efforts in developing trends. Our recommendation is to carry out additional focused sampling to better link field and laboratory results thereby improving power of these outcomes.

In addition to short term changes that would result from lower lagoon temperatures or increased and stabilized DO concentrations, decreased respiration of seawater would mitigate hypoxia and could prevent future sediments from deteriorating and losing sorption / sequestration capacity for phosphorus through the formation of FeS. The 2.6–fold increase in equilibrium phosphorus concentrations and 30% decrease in sorption capacity in 2023 compared to 2001 helps to sustain higher benthic phosphorus fluxes and concentrations in overlying water.

Overall, laboratory experiments carried out to estimate the potential impacts of pumping on geochemical nutrient cycling showed that potential lower lagoon temperatures and higher DO lead to significant decreases in benthic fluxes for N and P. These observations suggest that geochemical responses to inflow would contribute to decreasing nutrient concentrations within the IRL, mitigating discharges to the coastal ocean. Over the long term, decreased respiration and settling of algal biomass would help to mitigate hypoxia allowing future sediments to maintain higher sorption / sequestration potential. Data obtained during this study illustrate the importance of DO in the IRL towards regulating fluxes, cycling and sequestration of dissolved nutrients. To track hypoxia and estimate the spatial extent of these processes, beginning with this project, Florida Tech established a network of DO sensors to aid in modeling efforts and to better understand benthic–pelagic coupling in this system.

3.5.5 Bottom Water DO

Due to the dependence of biogeochemical nutrient cycling on DO, it is not possible to accurately model nutrient fluxes, turnover times, or nutrient concentrations without a detailed picture of DO in the lagoon. To assist modeling efforts, long–term datasets for DO concentrations from the IRL and BRL were obtained for surface water from SJRWMD (**Figure 39**). Most existing sensors record DO at fixed depths, often in the middle of the water column, and can miss events that are restricted to the near bottom. For example, sensors referenced in this study had average depths during 2019 to 2023 of approximately 0.5 to 1.5 m (SJRWMD). Overall data for DO from these sensors showed annual trends relatively consistent with variations in DO solubility. For example, at a salinity of 25, a reasonable average for the IRL, DO solubility increases from 6.4 mg/L at 32°C to 8.7 mg/L at 15°C, an annual range of 2.3 mg/L (). In addition to this expected range in DO (at 100%), values sometimes fell below saturation during summer with some instances of hypoxia (<2 mg/L) recorded by existing sensors located in the middle of the water column (e.g., cyan line, **Figure 39**). During winter months, DO in bottom water at sandy sites typically tracked patters for DO at 0.5 to 1.5 m (**Figure 39**); however, during summer months, bottom water DO

was often lower and less stable, especially following peaks in DO concentrations (pink line, **Figure 39**).
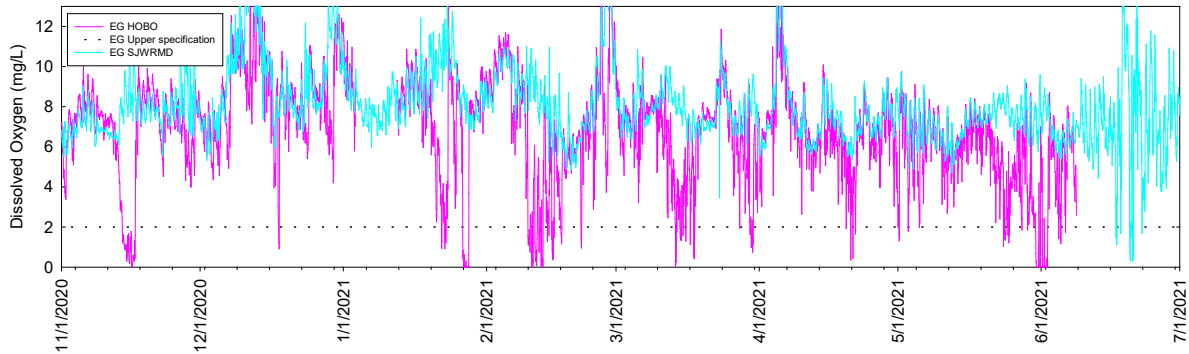
Figure 39. Concentrations of DO (mg/L) in the IRL near Eau Gallie in bottom water (<10 cm above the bottom; cyan line) and at mid–depths ~1–1.5m (pink line) with the dashed black line at 2 mg/L indicating hypoxic conditions.
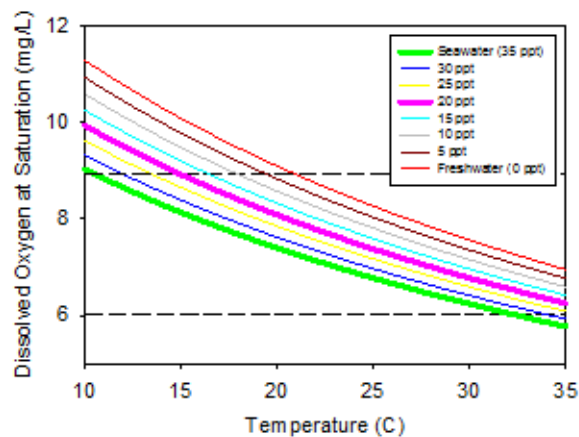
Figure 40. DO (mg/L) at saturation (100%) versus temperature for seawater at 35 PSU, freshwater at 0 PSU and at 5 PSU intervals.

During Phase 1, sensors deployed in the BRL near the reference/control location showed large differences for DO in bottom water overlying mud (muck) versus sand, although the sensors are only about 200–m apart (**Figure 39**). These data are consistent with SOD differences among substrates from –2,400 µmoles/m^2/hr for sandy sites (inflow site) and –4,300 µmoles/m^2/hr for muddy sites (during winter months).
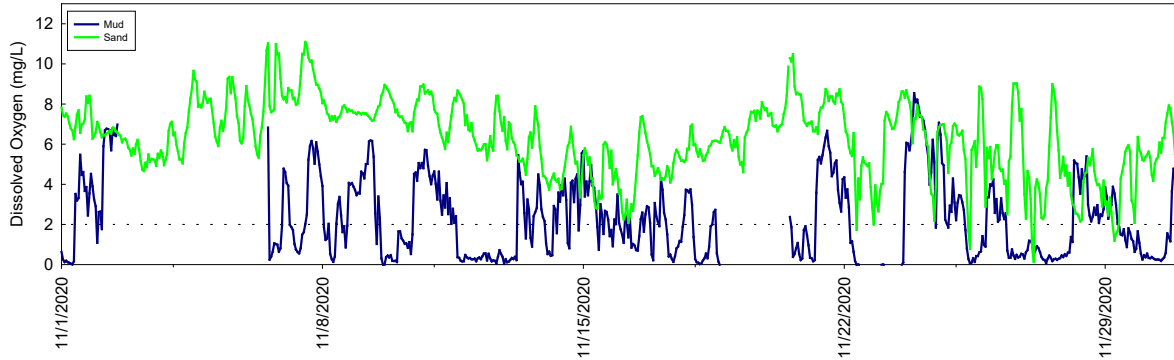
Figure 41. Bottom water DO at sites near the lagoon reference area at sites containing muck (blue line) and sand (green line) with the dashed black line at 2 mg/L indicating hypoxic conditions.

In Port Canaveral, concentrations of DO followed patterns similar to those observed in the adjacent lagoon (**Figure 42**); however, diurnal fluctuation in the Port were much less than those observed in the lagoon. For example, DO in the lagoon varied by up to 4 to 6 mg/L on a daily basis (dark yellow line on **Figure 42**), relative to diurnal variations of only 1 to 2 mg/L in Port Canaveral (dark yellow line **Figure 42**). These trends follow patterns for respiration with higher respiration and more rapid changes to DO in BRL compared to Port Canaveral.
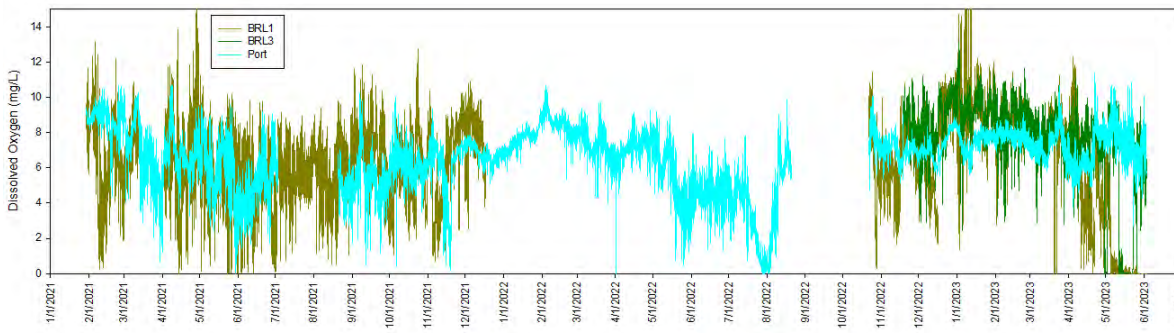
Figure 42. DO in the BRL in the area of inflow and in Port Canaveral

Temporal and spatial differences in bottom water DO, such as the examples shown above, can drive spatial and temporal changes, where sediments alternate between sinks and sources of nutrients (**Section 3.3** and **Section 3.4**). Changes to DO in bottom water led to changes in concentrations and the relative abundance of bioavailable N and P with implications to algal community composition and density as discussed throughout this report. As a result, data for bottom water DO are essential to improving lagoon modeling, not only for this project but for any generalized nutrient loading or HAB models (**Figure 43**).
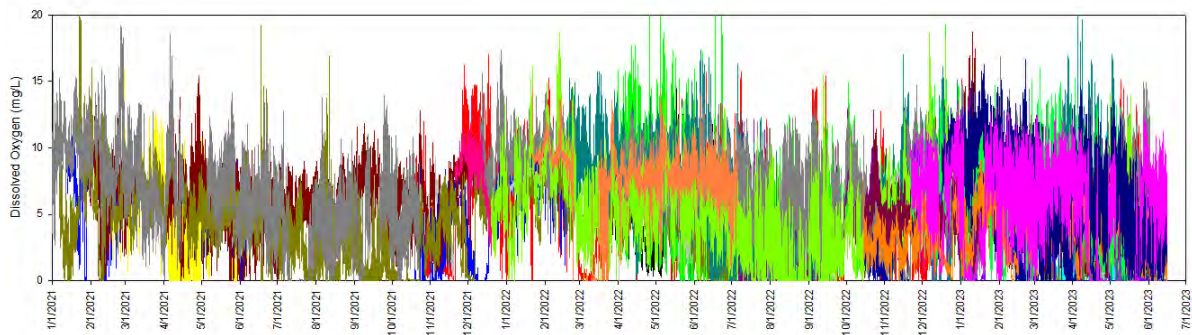
Figure 43. Plot showing all data for bottom water DO obtained during this study (includes data from other projects).

3.5.6 Known Muck Distribution

N and P loading from muck deposits are calculated and modeled based on estimates for the current surface area of muck present in the lagoon at a given time. Despite coving only an estimated <10% of the lagoon bottom, muck is a significant source of N and P to overlying water while also acting as a large sink for dissolved oxygen (Fox and Trefry 2018). To assist in modeling efforts and to better resolve the relative importance of muck versus sand, data for known muck deposits in the IRL have been synthesized into a single map (e.g., **Figure 44**).
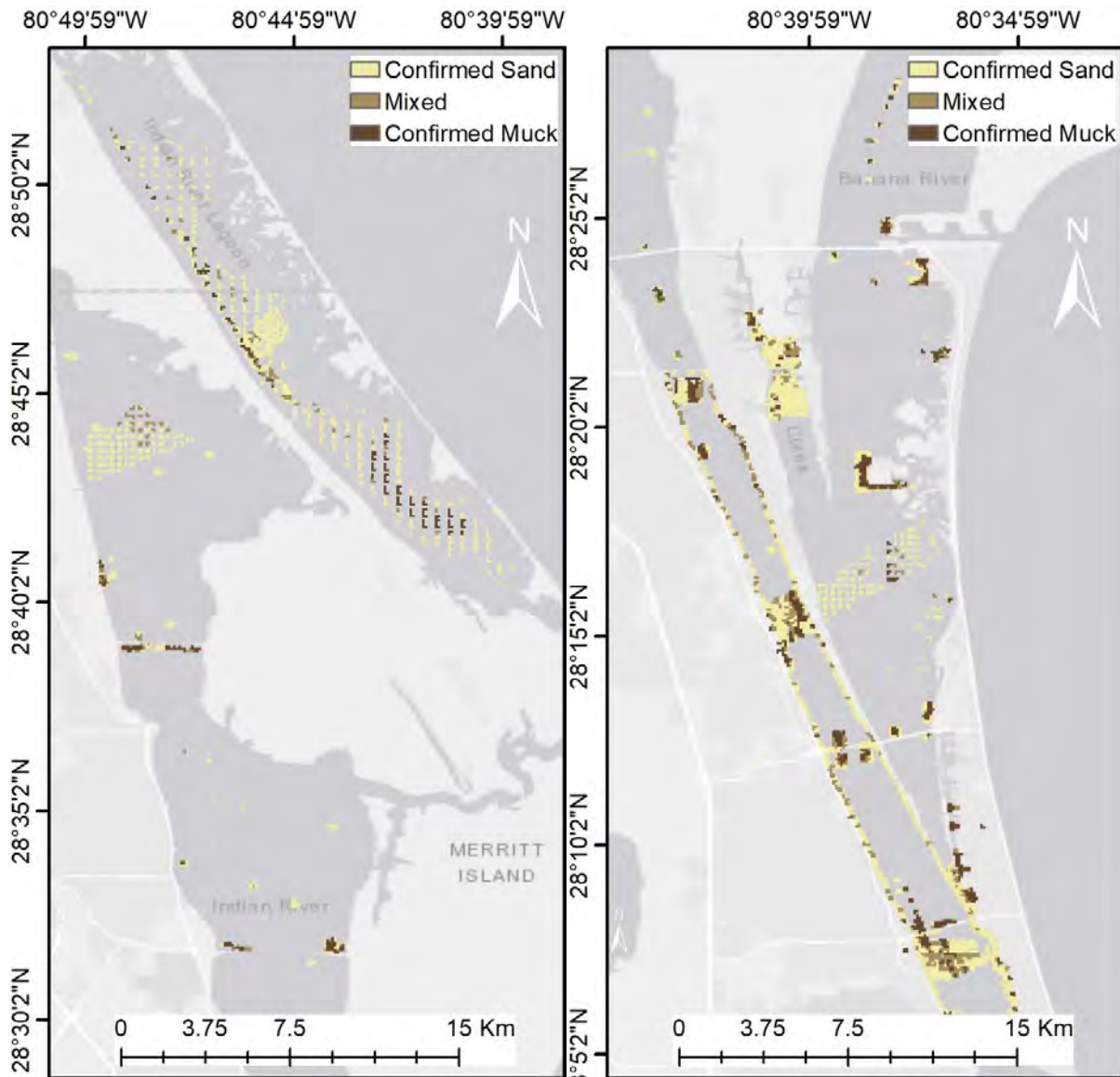
Figure 44. Map the northern IRL, Mosquito Lagoon, and BRL showing locations of confirmed sand, mixed sand and muck, and confirmed muck with 100 m spatial resolution.

This years–long effort has yielded numerous contoured plots showing detailed distributions of muck in discrete deposits; however, for a larger, lagoon–wide map, contouring often misrepresents areas where muck is present and changes in thickness have not been identified. In other words, contouring does not allow for unbiased inclusion of individual data points and can be misleading when conducted over large areas. With input from computer modelers, the lagoon–wide map was approached as a gridded raster where each cell contains a value signifying known sand, known muck (probe penetration), or something in–between only where data are available. Although the resolution could change from region to region based on the resolution of available data, this initial synthetic map uses a 100 m (approximately 300 ft) grid pattern showing only areas where data is present (**Figure 44**).

3.6 Summary and Conclusions

A shift in the IRL system from a seagrass dominated stable state to an algal dominated state has been referenced as a "regime" shift beginning in 2010 (Phlips et al., 2021). This sudden shift coincided with the loss of biomass and fish kills associated with extreme low temperatures during winter 2009/2010, reaching <4°C in the IRL. Prior to these events, algal blooms followed general patterns related to external nutrient loading; however, since 2010 occurrences of algal blooms are less predictable based on external factors. Since 2010 Internal processes, geochemical nutrient cycling of material already in the system, likely contributes to and fuels subsequent blooms. Similar changes have been reported in other estuaries with systems becoming less able to assimilate external nutrient loads without experiencing hypoxia and amplified effects of eutrophication (e.g., Kemp et al., 2005; Buskey et al., 1996, 1997). Eutrophication driven hypoxia promotes a series of self–reinforcing feedback loops that helps to sustain eutrophication and hypoxia with geochemical processes helping to maintain either stable state or regime. Historically, few data are available to describe the spatial extent of hypoxia in IRL or BRL; however, data from three phases of this study kicked off a broader monitoring network that has increased our understanding of hypoxia in this system, most recently in August 2023 capturing an increase in DO associated with a bloom of *P. bahamense* followed by a crash in the bloom and DO leading to a fish kill that was not captured with other nearby sensors higher in the water column. Based on data from this study, diurnal and episodic bottom water hypoxia events are a regular occurrence in the IRL and BRL. Although most are short in duration (a few days or less) the effects of chronic diel and episodic hypoxia may significantly alter nutrient cycling. Concurrently with the 2010 regime shift, concentrations of dissolved phosphorus in IRL increased without any known corresponding increase in external loading (Phlips et al., 2021). This increase in dissolved phosphate is likely related to the chronic impacts of hypoxia, with sulfide produced in anerobic sediments irreversibly binding iron and aluminum oxides. This hypoxia driven, geochemical change in sediment composition has decrease the capacity of sediments to sequester phosphorus from 133 mg P/kg of sediments reported in 2001, compared to only 99 mg P/kg of sediments in 2022 to 2023 at the same sites. This and related changes likely contributed to the sudden 1.65 to 2.3–fold increase in dissolved phosphorus after major hypoxic events and fish kills that occurred in 2010 (Phlips et al., 2021). In 2023, the average sorption capacity was 99 mg P/kg of sediments compared to 133 mg P/kg of sediments for the same sites in 2001. With respect to nitrogen, chronic impacts of hypoxia or lower dissolved oxygen concentrations would decrease the thickness of the surface oxidizing layer of sediments, decreasing the surface area occupied by nitrifying bacteria (also contributing to increased dissolved phosphate in the water column). We began to evaluate how changes to habitat quality such as increased or stabilized temperature, salinity, and DO may influence bioturbating species, another layer of potential benefits of inflow.

In eutrophic systems, HAB events contribute to occurrences of hypoxia and anoxia, where even short hypoxic or anoxic events can promote loss of ecosystem services including coupled nitrification–denitrification thereby decreasing the removal of N from the system as inert N gas and decreasing the quantity of P that is sequestered in sediments. Loss of these ecosystem services over time and space create positive feedback loops sustaining eutrophication and hypoxia. Distinct differences in the ability of poorly flushed versus well flushed estuaries to cope with eutrophication have been observed throughout the literature, where poorly flushed estuaries with long residence times, like the IRL, more readily retain nutrients to promote algal blooms, loss of seagrass beds, hypoxia, and loss of ecosystem services (Twilley et al., 1999; Defne and Ganju 2015; Kemp et al., 1992; Twilley et al., 1999). Within this conceptual framework, impacts of enhanced inflow of seawater into the IRL were evaluated for its potential to (1) directly decrease nutrient concentrations and (2) promote water column and sediment processes that would help

to restore ecosystem services to remove or prevent N and P from entering the lagoon and (3) buffer against extreme and low salinity and temperature events.

Overall, temperatures in Port Canaveral and the coastal Atlantic Ocean were moderate relative to more variable and extreme temperatures in the lagoon. During winter months water in port Canaveral experienced fewer extreme cold events and during summer months average temperatures ranged from approximately 0.5 to 3°C higher in BRL. On all occasions, salinity was higher in Port Canaveral than in the lagoon, leading to distinct densities among the lagoon (1,007–1,016 kg/m^3) and Port (1,018–1,028 kg/m^3) water masses. These data indicate that inflow of seawater and a mixed water mass would favor circulation of bottom water, on average raising salinity and helping to stabilize concentrations of dissolved oxygen at the sediment–water interface.

Overall, concentrations of TDN and TDP were lowest at offshore sites (8 ± 2.4 µM TDN, 0.15 ± 0.05 µM TDP); nevertheless, concentrations in Port Canaveral (36 ± 12 µM TDN, 0.56 ± 0.22 µM TDP) were approximately 3–fold 2–fold lower than concentration in the BRL at the inflow site (107 ± 30 µM TDN, 1.2 ± 0.6 µM TDP). This small pilot project would have little impact at the lagoon scale; however, changes at the inflow site would facilitate a scientifically sound scaled study of inflow in a well–defined area while preserving reference/control sites and also mitigating risk of adverse impacts to the broader lagoon. Data from the pilot study could then be used to determine the scale of a full–sized project necessary to achieve desired improvement to water quality.

Biogeochemical responses of the water column and sediments to short term changes in temperature, salinity, DO and infauna were investigated using a combination of field and laboratory experiments. Laboratory experiment also investigated long–term impacts of hypoxia on the sediments ability to sorb and sequester phosphorus. Sediment and water column incubations in the field were used to establish current rates of nutrient fluxes and cycling from sandy sediments and water in the lagoon and to serve a baseline to evaluate changes over time.

Despite no significant changes, lower rates of recycling in the proposed inflow water from Port Canaveral and lower N:P ratios (DIN:SRP 34 in the lagoon, 37 in Port Canaveral; TDN:TDP 109 in the lagoon, 82 in Port Canaveral) would, when mixed, help to slow recycling and promote lower N:P ratios in the new, mixed water mass. Lower concentrations and ratios of N:P would help to promote beneficial photosynthesizers. In laboratory incubation experiments, significant positive correlations were identified between benthic fluxes of NO_x, TDN, PO_4, DOP, and SiO_2 versus sediment temperature. Collectively, these data show that lowering lagoon temperatures, a likely result of inflow, would help to reduce inputs of both N and P to the lagoon. Based on a simple mixing model, the pilot project could prevent 1.6 and 0.7 of N and P from entering the lagoon each year based on lower lagoon temperatures.

Overall, based on laboratory experiments of geochemistry (independent of infauna), no long–term changes in nutrient cycling are expected based on modest changes to salinity that would result from inflow. Nevertheless, stabilized, and higher salinities would favor historically bioturbating and bio irrigating species such as *M. Mercinaria* that help to move oxygen from overlying water into sediments. Therefore, increasing and stabilizing salinity could promote geochemical nutrient cycling though feedback interactions of habitats, food–webs, and biogeochemistry (Kemp et al., 2009). We began to investigate this relationship in BRL; however, longer term studies in sandy sediments will be required to quantify these complex interactions and potential benefits of inflow.

Finally, in both field measurements and laboratory experiments, low DO promoted release of PO_4 and NH_4, both known to promote HABs. In contrast, higher, stable concentrations of DO promoted

removal of PO$_4$ while also promoting fluxes of nitrate over NH$_4$, both changes that support beneficial photosynthesizers. Based on these data and trends, lower lagoon temperatures and higher and stabilized bottom water DO expect to result from inflow would support lower nutrient concentrations and ratios promoting species of nutrients that are more favorable to beneficial photosynthesizers.

Concentrations of DO in bottom water (<10 cm above the bottom) followed general seasonal patterns observed at mid–depths reported by other existing monitoring networks; however, bottom water experienced frequent periods of hypoxia or anoxia, likely due to proximity to sediments responsible for 20 to 50% of the total respiration. These new data are essential towards improving lagoon models used in this study and other generalized nutrient loading or HAB models. Other notable observations from our growing network of bottom water DO sensors was lower concentrations of DO overlying muck deposits relative to concentrations in bottom water overlying directly adjacent sand. On an annual scale, concentrations of DO in Port Canaveral tracked concentrations in lagoon water, both lagoon and seawater varying in response to changes in solubility over time. Despite similarities in long–term trends, diurnal fluctuations in Port Canaveral were much less that those in the lagoon, due mostly to 30% lower rates of dark respiration in Port Canaveral and almost monthly instances of hypoxia observed in lagoon were not observed in Port Canaveral.

3.7 Next Steps

To date, this project has greatly improved our understanding of nutrient cycling in the IRL system, especially in sandy sediment and in the water column. These data are useful not only to modeling possible impacts of inflow, but for HAB and for generalized nutrient load modeling, especially as we look to addressing changes to temperature and rainfall associated with changing climatic patterns. Despite knowledge gained during this study, the lagoon is dynamic and with this temporally limited dataset, it is not possible to isolate natural, seasonal patterns from event scale occurrences, something that would be more feasible in the near future if this work is continued to evaluate the pilot project (1 to 2 years). Data to date have demonstrated the importance of processes in sandy sediments and on particles and have yielded wide ranges of values for these critical processes. Phase 3 allowed us to evaluate these processes over multiple years coinciding with localized improvements to water quality. Continuing this biogeochemical evaluation would help to resolve event scale variability versus seasonal trends and improve statistical power of trends identified to date. Additional data obtained during the pilot project would improve confidence in extrapolated models. Due to the importance of bottom water DO towards cycling of both N and P, we hope to find long–term support for this network of quality–controlled bottom water sensors. We view these collective datasets as tools that will help managers select restoration projects based on potential to restore natural cycling of N or P to make efficient use of taxpayer dollars. To continue the specific study of inflow and in response to results to date, we plan to expand our investigation of changes in oxygen and nutrient cycling in sediments with restored infauna communities. Preliminary data obtained as part of this study indicated that biota influence geochemistry; however, restoring infauna to organic–rich sediments promoted mineralization of OM that overshadowed benefits of oxidized surface sediments. We plan to repeat and improve these experiments in sandy sediments that are more representative of the lagoon bottom. We propose these next steps to take place before and alongside the proposed pilot inflow project that will move water from the coastal Atlantic Ocean into the lagoon. Overall, data to date support a limited test of inflow as part of a multifaceted approach to lagoon restoration.

4 References

Abell, G.C. J., A.T. Revill, C. Smith, A.P. Bissett, J.K. Volkman, and S.S. Robert. 2010. Archaeal ammonia oxidizers and *nirS*–Type denitrifiers dominate sediment nitrifying and denitrifying populations in a subtropical macrotidal estuary. *The ISME Journal* 4(2):286–300.

American Society of Civil Engineers. (2017). Chapter 2: Combinations of Loads. In *Minimum design loads and associated criteria for buildings and other structures (ASCE/SEI 7–16)* (pp. 7–9). essay.

Babcock, K.K., F. Cesbron, W.F. Patterson, S.B. Garner, L.A. Waidner, and J.M. Caffrey. 2020. Changing biogeochemistry and invertebrate community composition at newly deployed artificial reefs in the northeast Gulf of Mexico. *Estuaries and Coasts* 43:680–92.

Boynton, W. R., Ceballos, M. A. C., Bailey, E. M., Hodgkins, C. L. S., Humphrey, J. L., and Testa, J. M. (2017) Oxygen and nutrient exchanges at the sediment–water interface: a Global synthesis and critique of estuarine and coastal data. *Estuar. Coasts*. doi: 10.1007/s12237–017–0274–5.

Edwards, M., Johns, D. G., Leterme, S. C., Svendsen, E., and Richardson, A. J. (2006). Regional climate change and harmful algal blooms in the north–east Atlantic. Limnol. Oceanogr. 1, 820–829. doi: 10.4319/lo.2006.51.2.0820

FDEP . 2013. Banana River Lagoon Basin Management Action Plan. Retrieved from https://floridadep.gov/sites/default/files/banana–river–lagoon–bmap.pdf.

Fox, A.L., Trefry, J.H., Trocine, R.P., Fox, S.L., Voelker, J.E., 2017. Determining the Effectiveness of Muck Removal on Sediment and Water Quality in the Indian River Lagoon. Project Report Submitted to Brevard County Natural Resources Management Department.

Heiri, O., Lotter, A. F., and Lemcke, G. (2001). Loss on ignition as a method for estimating organic and carbonate content in sediments: reproducibility and comparability of results. *J. Paleolimnol.* 25, 101–110.

Holmes, R.M., A. Aminot, R. Kérouel, B.A. Hooker and B.J. Peterson. 1999. A simple and precise method for measuring ammonium in marine and freshwater ecosystems. *Canadian Journal of Fisheries and Aquatic Sciences* 56:1801–1808.

Listopad, C. 2015. Spatial Watershed Iterative Loading (SWIL) Model Methodology Report; Updated for SWIL 3.0. Final Report submitted to Brevard County Natural Resources Management Office by Applied Ecology, Inc.

Parsons, T. R., Y. Maita, and C. M. Lalli. 1984. A manual of chemical and biological methods for seawater analysis. Pergamon Press.

Schnetger, B., and C. Lehners. 2014. Determination of nitrate plus nitrite in small volume marine water samples using vanadium (III) chloride as a reduction agent. *Marine Chemistry* 160: 91–98.

Smith, C.J., D.B. Nedwell, L.F. Dong, and A.M. Osborn. 2007. Diversity and abundance of nitrate reductase genes (*narG* and *napA*), nitrite reductase genes (*nirS* and *nrfA*), and their transcripts in estuarine sediments. *Applied and Environmental Microbiology* 73(11):3612–22.

Trefry, J.H., Johnson, K.B., Fox, A.L., and Ma, X. 2019. Optimizing Selection of Sites for Environmental Dredging in the Indian River Lagoon System. Project Report Submitted to Brevard County Natural Resources Management Department.

U.S. Army Corps of Engineers. (2001). *Unified Facilities Criteria (Ufc): Military harbors and coastal facilities*.

U.S. Army Corps of Engineers. (2002). *Coastal Engineering Manual*.

U.S. Department of Transportation, Federal Highway Administration. (1983). *Structural Design Manual for improved inlets and culverts*.

Waidner, L.A., and D.L. Kirchman. 2007. Aerobic anoxygenic phototrophic bacteria attached to particles in turbid waters of the Delaware and Chesapeake estuaries. *Applied and Environmental Microbiology* 73(12):3936–44.

Welshmeyer, N.A. 1994. Fluorometric analysis of chlorophyll *a* in the presence of chlorophyll and pheopigments. *Limnology and Oceanography* 39:1985–1992.

Westerink, J.J., R.A. Luettich and R.L. Kolar, 1996, ADCIRC an advanced finite element model for coastal ocean circulation, Proceedings, The Third Asian Pacific Conference on Computational Mechanics, 16–18 September, Seoul, Korea.

Zarillo, G.A. Listopad, C., 2016. Indian River Lagoon Hydrodynamic and Water Quality Model Quality Assurance Plan: Year 1 Final Report Prepared for Brevard County and the Florida Department of Environmental Protection.

Zarillo, G.A. and Listopad, C. 2020. Hydrologic and Water Quality Model for Management and Forecasting within Brevard County Waters of the Indian River Lagoon. Final Project Report to Brevard County Natural Resources Management Department. 128pp.

Appendix D   Task 3 – UWF Geochemistry Report

Restore Lagoon Inflow Research (Phase 3) Final Report University of West Florida: Geochemistry
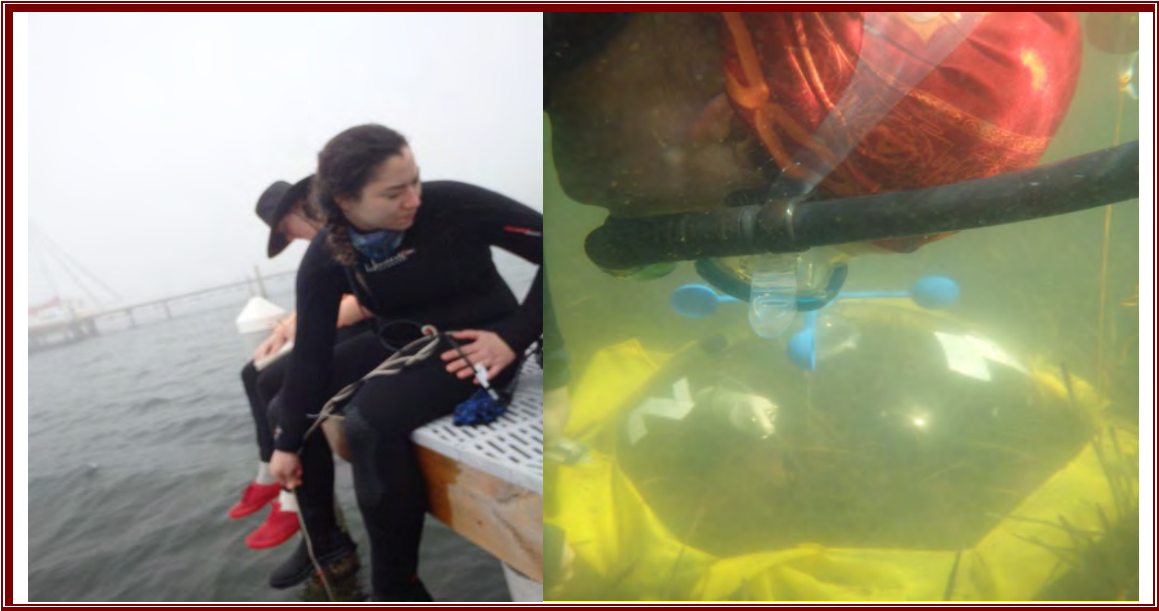
PREPARED FOR

Florida Institute of Technology
150 West University Boulevard
Melbourne, FL 32091

PREPARED BY

Jane Caffrey, Wade Jeffrey & Lisa Waidner
University of West Florida
11000 University Parkway
Pensacola, FL 32515

July 2023

Acknowledgements

Highlights

- Aerobic nitrogen-cycling microbes were on average nearly five times more abundant in Santa Rosa Sound (SRS) than Indian River Lagoon (IRL) sediments, indicating the potential for more rapid nitrogen removal in SRS sediments than in the IRL.

- Anaerobic ammonia producing microbes that can exacerbate the effects of eutrophication were on average two times more common relative to aerobic nitrogen-cycling microbes in the IRL than in the SRS.

- Salinity in the Banana River section of IRL normally falls within the known tolerances for two dominant seagrass species, *Halodule wrightii* and *Syringodium filiorme.* Extended periods of high salinity (> 35 ppt) between 2011-2014 and low salinity in the 1990s and following the 2004 hurricane season (< 10 ppt) exceeded ranges for optimal productivity.

- The amount of light available to support seagrass growth is higher in SRS than IRL. Analysis from this study and the literature point to the need to decrease light attenuation (increasing bottom light availability) in IRL to allow seagrasses to recover.

- Despite enhanced inflow, Destin Harbor bottom waters experience episodic hypoxia likely due to high nutrient loads, water column respiration, and sediment decomposition in this organic poor system. High chlorophyll-a concentrations below the pycnocline indicate substantial nutrients and light availability, which is likely driving water column and sediment decomposition reducing oxygen concentrations in the water column.

Table of Contents

List of Figures

List of Tables

List of Acronyms

amoA	gene encoding alpha subunit of ammonia monooxidase
AOA	Ammonium oxidizing Archaea containing *amoA*
AOB	Ammonium oxidizing Bacteria containing *amoA*
AOO	ammonium oxidizing organisms (AOA+AOB)
bp	base pair
CBA	Choctawhatchee Basin Alliance
Chla/gws	Chlorophyl a per gram wet sediment
Cm	centimeter
Ct value	PCR cycle in which dsDNA fluorescence crosses the threshold value
CV%	Coefficient of Variation
DIP	Dissolved Inorganic Phosphate
DNA	Deoxyribonucleic Acid
DNRA-organisms	Prokaryotes capable of dissimilatory nitrate reduction to ammonium

DO	Dissolved Oxygen
dsDNA	Double-stranded DNA
Fe2+	Dissolved Reduced Iron
Gws	Grams wet sediment
IRL	Indian River Lagoon
IWR	Impaired Waters Rule
Kd	Light Attenuation
m	meter
m^2	square meter
mg	milligrams
mL	milliliters
ng/ul	nanograms per microliter
NH4+	Ammonium
Nm	*Nanometer*
nrfA	Gene Encoding Nitrite Reductase
PCL	Port Canaveral Lagoon
PNR	Pelican National Wildlife Refuge
ppt	parts per thousand
qPCR	quantitative Polymerase Chain Reaction
RLI	Restore Lagoon Inflow
rRNA	Ribosomal Ribonucleic Acid
S2-	Dissolved Sulfide
SD	Standard Deviation
S.E.	Standard Error
SJRWMD	St Johns River Water Management District
SRS	Santa Rosa Sound
ssDNA	single-stranded
SYBR-Green	dsDNA binding fluorescent dye
TD	Touchdown
µM	micro moles
UWF	University of West Florida

1 Task Summary

University of West Florida (UWF) activities in support of the Restore Lagoon Inflow (RLI) project provide broader interpretation and context for the Phase 2 and 3 RLI project results, specifically those addressing how improved inflow may assist in remediation of the Indian River Lagoon (IRL). Our overall goal was to provide insight on the potential impact of increased inflow of oceanic water on the abundances of key prokaryotes that affect sediment biogeochemistry and how this would contribute to improved water quality. Results from prior RLI research suggested that nitrogen and phosphorus were being recycled by prokaryotes rather than removed through coupled nitrification-denitrification. Enhanced inflow of oxygenated water from the Atlantic Ocean to IRL has the potential to reduce water residence time and enhance this nitrogen removal process. This in turn could reduce harmful algal blooms and improve conditions for seagrasses. The analysis of existing water quality data in this report provides useful information to Statewide Surface Water and Estuarine Management Plans, assists the nascent Estuary Programs in the Florida Panhandle and assesses the applicability of enhanced water circulation to other sites. Water clarity and phytoplankton blooms were the major stressors on existing beds of *Halodule wrightii*, *Syringodium filiforme, Ruppia maritima,* and *Thalassia testudinum* with Banana River Lagoon being particularly impacted (Provancha et al.. 1999, Morris et al., 2022; Lapointe et al., 2020).

Eutrophication in the IRL negatively impacts dissolved oxygen (DO) levels and seagrasses. Destin Harbor has been used as a model to design the RLI project, but a detailed examination of the long-term effects of how the pumping system in Destin Harbor affects water quality has not been conducted. UWF goals also included analyses of these data to provide useful information for the RLI project. UWF efforts focused on three major tasks: (1) evaluating existing water quality data from Destin Harbor, (2) assessing fluctuations in communities that affect nitrogen cycling and IRL water quality by measuring abundances of key microbial groups performing nitrification and dissimilatory nitrate reduction to ammonium, and (3) evaluating existing IRL water quality monitoring data for conditions outside seagrass tolerances of salinity and DO. For the microbial community work, we examined sediments from IRL sites, as well as shallow and deep seagrass reference sites in the Florida Panhandle in Santa Rosa Sound (SRS) to compare with the IRL reference site. Specifically, this work addresses the question of inflow in monthly sampling performed in the IRL impacted and reference sites, tying in data with the Florida Panhandle site, and establishing the specific link between inflow and water quality data. This work will provide key information about the links between sediment biogeochemistry, microbial communities and seagrasses.

1.1 Specific Objectives

- Quantify abundance of key nitrogen transforming prokaryotes using quantitative polymerase chain reaction (qPCR) at sites of sediment/water nutrient flux in IRL. Samples were collected during monthly IRL benthic chamber deployments. Sediment samples were also analyzed for chlorophyll a.
- Assessment of microbial and biogeochemical responses from Florida Panhandle reference sites. Benthic fluxes and porewater nutrients were measured in a shallow seagrass site colonized by *Halodule wrightii* and a deeper site colonized by *Thalassia testudinum*.
- Review and assessment of existing Destin Harbor water quality data and how operation of the Destin pumping system affects water quality.
- Review salinity and light attenuation, key factors limiting seagrass growth and restoration, from existing water quality monitoring data in the Banana River and compare to tolerances of *Halodule wrightii* and *Syringodium filiforme,* the two dominant species in the IRL.

1.2 Study Area

The primary reference study area was SRS in the Florida Panhandle. SRS is a lagoonal system similar to IRL with a barrier island separating it from the coastal ocean. SRS has a similar morphometry to the Banana River segment of the IRL (**Table 1**), but somewhat lower salinity and light attenuation values that are about 1/3 of the IRL. In contrast, Destin Harbor is much smaller, has no seagrasses, and light attenuation about half that if the IRL. SRS still has healthy seagrass beds (Byron et al., 2018) while the Banana River has seen significant declines (Morris et al., 2018). Grab samples from four locations (**Figure 1**) were collected from Destin Harbor for water quality and sediment characteristics: chlorophyll a, water and organic content in October 2022. Two of these locations (sites A and C, **Figure 1**) have been consistently sampled for water quality by the Florida Department of Environmental Protection and Choctawhatchee Basin Alliance (CBA). These two locations are in the main channel of the harbor while sites D and E are near the pumping system (**Table 2**).

Two seagrass beds were sampled in SRS, a shallow (approximately 0.6 meter [m]) bed of *Halodule wrightii* and a deeper (approximately 1.2 m) bed of *Thalassia testudinum* (**Figure 2**, **Table 2**) in September 2022, November 2022 and April 2023. Summer diel hypoxia has been observed at this location (Caffrey, unpublished data), which is also the site of other studies conducted by UWF. Because of the close proximity of these sites, single water samples were collected halfway between them for nutrient and chlorophyll analysis. We also collected from the IRL sites Port Canaveral Lagoon (PCL) and Slick in March 2023 in conjunction with Austin Fox. IRL sediment samples from PCL, Slick, Sampson, and Pelican National Wildlife Refuge (PNR) were provided by Austin Fox for analysis of microbial communities and chlorophyll a.

Table 1. Characteristics of Banana River in Indian River Lagoon, Destin Harbor, and Santa Rosa Sound.

Parameter	Banana River	Destin Harbor	Santa Rosa Sound
Length (km)	62	4	60
Width (km)	2-5	0.05-0.4	0.5-3
Depth (m)	2	~2	2.8
Light attenuation (m^{-1})	1.5	0.84	0.5
Average Salinity	29	25	22
Seagrass species – dominant (other present)	*Halodule wrightii* (*Syringodium filiorme, Ruppia maritima* and *Halophila sp.*)	none	*Halodule wrightii* and *Thalassia testudinum* (*Ruppia maritima*)

Figure 1. Location of Destin Harbor sampling locations and inset map showing study area. Site locations: A – DH@ AJ; B – CBA Ft. Walton Beach – 9 & Old Pass Lagoon West; C - CBA Ft. Walton Beach – 10, CBA 10 & Old Pass Lagoon East; D – SC 1C; E – SC 1D
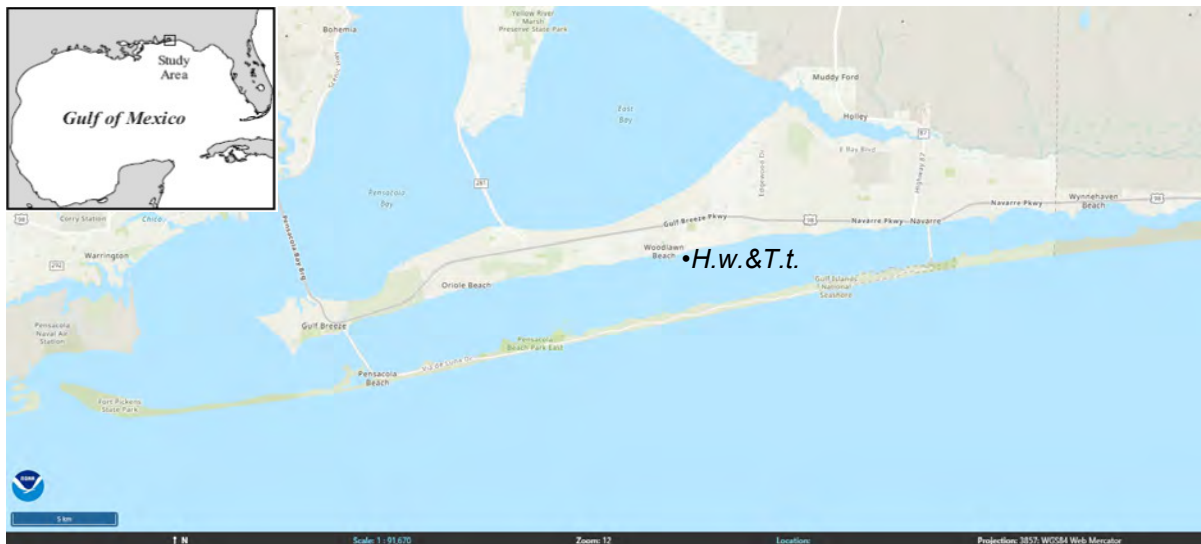
Figure 2. Location of Santa Rosa Sound sampling sites in *Halodule wrightii* (H.w.) bed and *Thalassia testudinum* (T.t.) bed. Inset map of Gulf of Mexico shown.

Table 2. Latitude and Longitude of Sample Sites

Location	Latitude	Longitude
Indian River Lagoon		
PCL (Port Canaveral Lagoon)	28.40713	-80.6385
Slick (Route 520)	28.35714	-80.6289
Samson (Samson Island Nature Park)	28.18161	-80.6139
PNR (Pelican Island National Wildlife Refuge)	27.97627	-80.5307
Destin Harbor		
DH@AJ	30.39189	-86.50919
CBA10	30.38903	-86.49228
SC1C	30.38668	-86.48829
SC1D	30.38629	-86.48523
Santa Rosa Sound		
Halodule wrightii bed	30.38787	-86.98744
Thalassia testudinum bed	30.38763	-86.98740

1.3 Approach

1.3.1 Background

To characterize the dynamics of microbial nutrient cycling we targeted the key nitrogen processes nitrification and dissimilatory reduction of nitrate to ammonium (DNRA) were targeted (Figure 3). The two major groups of nitrifiers are ammonium oxidizing archaea and beta-proteobacteria. Nitrification only occurs when molecular oxygen is present and provides nitrate to denitrifying prokaryotes. This is the dominant pathway removing nitrogen in estuaries when water column nitrate concentrations are low as they are in the IRL. Conversely, dissimilatory nitrate reduction to ammonium is an anaerobic process that recycles nitrogen in the system, exacerbating effects of eutrophication. Enumeration of abundances of these key prokaryotes directly relates to benthic chamber and sediment geochemistry measurements collected in the IRL and to the seagrass reference sites in SRS. We also believe that measurements of benthic chlorophyll a will also be useful because benthic primary producers may enhance uptake of nutrients when light reaches the bottom. Benthic microalgae and seagrasses also produce oxygen and increase the depth of oxygen penetration into sediments, enhancing the potential for nitrification.
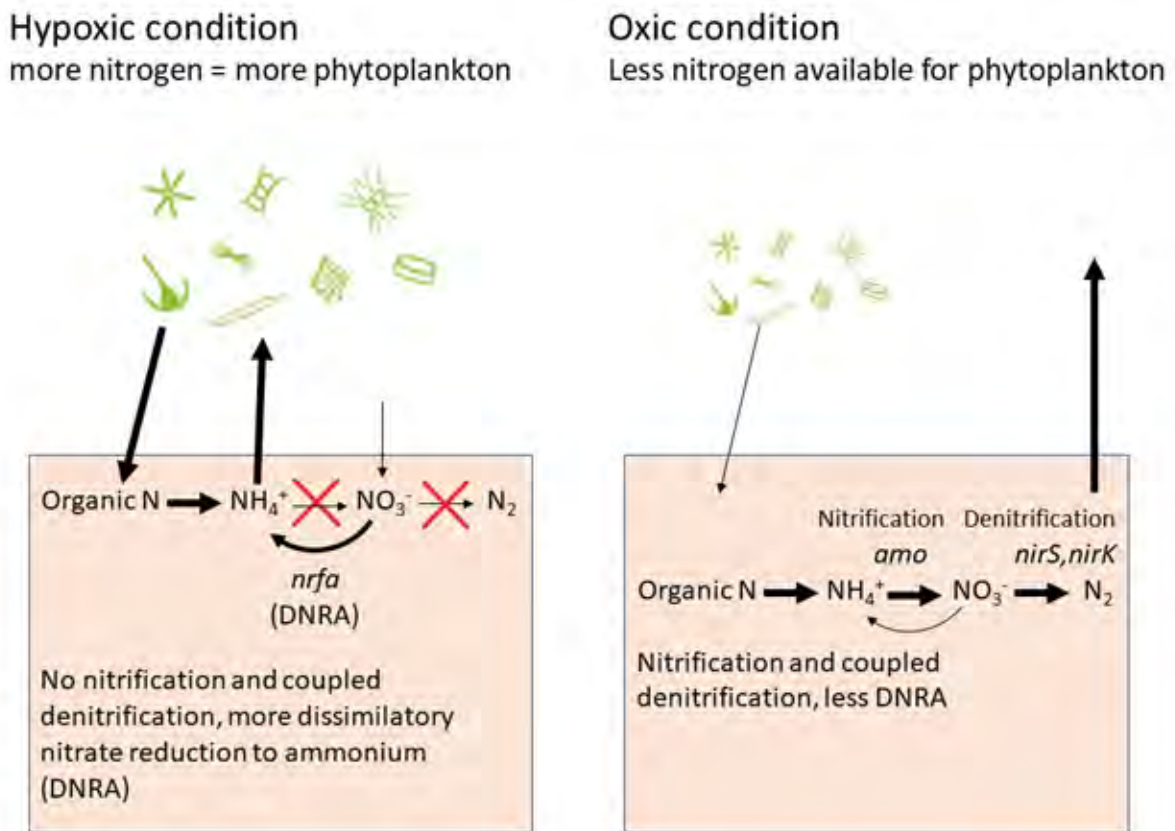
Figure 3. Conceptual model of key nitrogen transformation and genes under hypoxic and oxic conditions that are the focus of UWF research activities.

Nitrifying prokaryotes were measured with two gene encoding alpha subunit of ammonia monooxidase (*amoA*) targets: archaeal *amoA* (AOA) and bacterial *amoA* (AOB), since the first step, ammonium oxidation, is often the rate limiting set in the process. Prokaryotes capable of DNRA were enumerated with the gene encoding nitrite reductase (*nrfA*) gene. The relative abundances of these target genes were normalized to total bacteria or total prokaryotes since different sediment types may have different microbial abundances. Total prokaryote abundances

were enumerated with prokaryotic ribosomal ribonucleic acid (rRNA) marker genes for bacteria and archaea (BACT1 16S rRNA for Bacteria, Arch-Group I 16S rRNA for Thaumarchaeota 16S rRNA). Polymerase chain reaction (PCR) conditions for all targets (gene encoding alpha subunit of ammonia monooxidase [*amoA*] and prokaryote marker genes) were already established at UWF (Babcock et al., 2020), but conditions were again tested and optimized with current qPCR chemistry available for this study's sediment samples. DNRA bacteria enumeration required optimization of *nrfA* qPCR conditions and testing.

Benthic fluxes of nutrients (ammonium, nitrate+nitrite, dissolved inorganic phosphate) and DO in Florida Panhandle reference sites were measured with sediment domes. During flux experiments, sediments were collected next to domes for qPCR analysis, benthic chlorophyll, sediment porewater, water content, and organic content. Benthic flux experiments were done in September, November, and April.

1.3.2   Sediment Sampling

Sediment samples from four Destin Harbor locations were obtained using a 0.1 square meter (m^2) Ponar Grab that was lowered slowly from an anchored boat until it hit the bottom. Any standing water was poured off prior to sample collection. Surface sediments were subsampled and placed in 50 milliliter (mL) centrifuge tubes and stored on ice at 4 degrees Celsius (°C), in the dark for transport to the laboratory. Subsamples for chlorophyll a, water, and organic content analyses were made in the lab. Sediment samples from SRS were collected using either syringe cores or polycarbonate cores (5 centimeter [cm] internal diameter). The top 2 cm from syringe cores were extruded in the field after removing overlying water into whirl pack bags. They were stored on ice at 4°C, in the dark for transport to the laboratory where they were frozen until extraction for deoxyribonucleic acid (DNA). Polycarbonate cores were stored in a cooler and extruded in the laboratory for chlorophyll a analysis, potential nitrification experiments, water, and organic matter content. Large, living roots and rhizomes were removed from sediments before analysis.

1.3.3   Benthic oxygen and nutrient fluxes

Methods used in this study were developed following guidelines in Boynton et al. (2018) and used in both IRL and SRS deployments. Light and dark benthic domes were used to determine fluxes of dissolved oxygen and nutrients from sediments. MiniDOT™ oxygen sensors were deployed inside domes and sampled every 5 minutes. Incubation duration was 4 hours for SRS and 2 hours in IRL. During each deployment, water samples from domes were collected at 0, 2, and 4 hours in SRS and 0, 1, and 2 hours in IRL using a syringe. Mixing of domes occurred with an anemometer as in Cesbron et al. (2019). Dissolved oxygen fluxes in the light domes are a measure of net primary production (gross primary production – community respiration) while dark domes are a measure of community respiration.

1.3.4   Water Column measurements

Water quality parameters (temperature, salinity, dissolved oxygen, pH and turbidity) were recorded with a YSI multimeter in SRS, Destin Harbor, and IRL. In addition, a Seabird was used at the DH@AJ and CBA 10 stations to measure conductivity, temperature, dissolved oxygen, colored dissolved organic matter, and chlorophyll fluorescence with depth. Light levels were measured at depth using LiCor 4PI quantum sensor for calculation of light attenuation (Kd).

$$I_z = I_0 e^{-Kd*z}$$

where I is irradiance in µmoles/m^2/s, z is depth in m, and Kd is light attenuation coefficient in /m.

Grab water samples were collected and analyzed for dissolved nutrients (nitrate+nitrite, nitrite, ammonium, and dissolved inorganic phosphate) and chlorophyll a. Water was filtered through GF/F filters (nominal pore size 0.7 μm) for dissolved nutrients. The filter which had 60 mL of water filtered through it was preserved for chlorophyll a analysis. Samples were held on ice and then stored at 4°C until analysis.

1.3.5 Enumerating Prokaryote Functional Groups

Sediment DNA was extracted from 52 sediment samples (0 to 2 cm depth) using the manufacturer's suggested protocol in use of the soil microbial DNA miniprep kit from ZymoBIOMICS (cat# D4300T). DNA quality and concentration were assessed with spectrophotometry (NanoDrop® ND-1000 UV-Vis Spectrophotometer, Thermo). For qPCR analyses, aliquots of each of the DNA samples were diluted to 5 nanograms per microliter (ng/uL). Throughout the course of the study, only one sediment sample was collected from the PNR site.

All sediment DNA samples were assessed for basic quality spectrophotometry (Nanodrop) prior to testing with well-established (BACT1 16S rRNA) qPCR assays to further validate lack of inhibitors in the DNA samples. There was no statistical trend in higher or lower yields between or among sites, although yields in the samples processed earliest in the project (September SRS reference site samples) were lowest (**Table 3**). The low yields in these samples were likely due to protocol development at the time of sediment processing. The range of DNA yield from all sites and seasons was as expected, from 1.6 to 11 nanogram (ng) DNA per milligram (mg) of sediment.

DNA samples were next evaluated for use in bacterial 16S rRNA gene quantitative PCR to enumerate total bacteria as previously described (Waidner and Kirchman, 2007; Suzuki et al. 2000). Bacterial 16S rRNA gene copies were calculated from standard curves in each qPCR plate, with standard DNA comprised of *E. coli* K12 strain, containing 7 copies of the 16S rRNA gene per chromosome. Since *E. coli* also has a *nrfA* gene (1 copy of the *nrfA* gene per chromosome), the standard DNA used for bacterial 16S rRNA gene was also used for the *nrfA* assay (see below). Total bacteria were enumerated with the BACT1 primer pair that was originally developed and described with use of TaqMan probe by Suzuki et al. (2000) and later adapted for use in double-stranded DNA (dsDNA) binding fluorescent dye (SYBR-Green)-based (not TaqMan-based) reactions as previously described (Waidner and Kirchman 2007, Babcock et al. 2020). The BACT1 primer pair targets the bacterial 16S rRNA gene, and gene copies are calculated from the *E. coli* genomic DNA standard curve. With the newest SYBR-Green-based qPCR chemistry available, the bacterial 16S rRNA assay was validated and tested again for sensitivity specificity and lack of non-specific amplification (Figure 4). Shown in the top panel are representative amplicons from qPCR with samples #1-23. Standard DNA qPCRs are marked with "J" sample names. The values below "J" names represent known quantities of the standard DNA in each qPCR. The relevant sizes of bands in the DNA size standards are indicated (200 and 75 base pair [bp]). In the bottom panel, an example standard curve with *E. coli* genomic DNA is shown.

Table 3. Sediment DNA yields and amounts used in qPCR. For each site and date, the mean and range of associated amount of sediment (mg) used in each qPCR is provided, shown as DNA equivalent amount of sediment used per qPCR. For site abbreviations, see Table 2.

Site, Month	DNA equivalent mg sed per qPCR[1]				DNA yield (ng) per mg of sediment	
	Min	Max	Mean	n	Mean	Standard Deviation (SD)
PCL, July	1.4	2.0	1.7	2	4.52	1.09
PCL, Aug[2]	0.7	1.6	1.1	2	4.63	n/a
PCL, Sept	1.2	3.9	2.5	2	4.11	3.08
SRS Hw, Sept[3]	3.0	3.6	3.2	3	2.33	0.20
SRS Tt, Sept[3]	2.9	4.7	4.0	3	1.96	0.54
PCL, Oct	3.0	3.6	3.3	2	2.30	0.28
PCL, Nov	1.5	2.1	1.8	2	4.19	0.98
Slick, Nov	1.3	1.9	1.6	2	4.96	1.41
SRS Hw, Nov[3]	1.4	3.3	2.5	3	3.39	1.65
SRS Tt, Nov	1.6	3.0	2.4	4	3.36	0.98
PCL, Dec	2.5	3.9	3.2	2	2.45	0.78
PCL, Jan	2.4	2.5	2.5	2	3.06	0.13
Samson, Jan	2.3	3.2	2.7	2	2.79	0.58
PNR, Feb			2.0	1	3.72	n/a
PCL, AF Ch, Mar[4]	1.1	2.4	1.7	2	5.06	2.72
Slick, AF Ch, Mar[4]	1.0	1.2	1.1	2	6.84	0.85
PCL, JC Dome Mar[4]	1.3	1.5	1.4	4	5.44	0.21
Slick, JC Dome Mar[4]	1.0	2.4	1.6	4	5.24	1.81
SRS Hw, Apr	1.9	3.4	2.5	4	3.13	0.74
SRS Tt, Apr	1.4	2.5	1.9	4	4.21	0.93

[1] DNA Amount of sediment (mg) used in qPCR calculated from the DNA equivalent, 7.5 ng, used in each well of qPCR. The overall mean of sediment mg used per qPCR was 3.9 +/- 1.6 (n=51).

[2] One DNA yield (11.09 ng DNA per mg sediment) was excluded from the calculation for this site/month and the overall mean, due to uncertainty in the amount of sediment used for the DNA extraction. However, both PCL August 2023 DNA samples were tested in all qPCR assays.

[3] Four sediment samples collected; three DNA samples were of sufficient quality or quantity for qPCR use.

[4] In this table, UWF and Florida Tech joint activities at PCL and Slick during the March 2023 work are broken out by two different types of *in situ* rate determination: AF Ch, Austin Fox Chamber method (n=2 at each site); JC Dome, Jane Caffrey dome method (n=4 at each site).
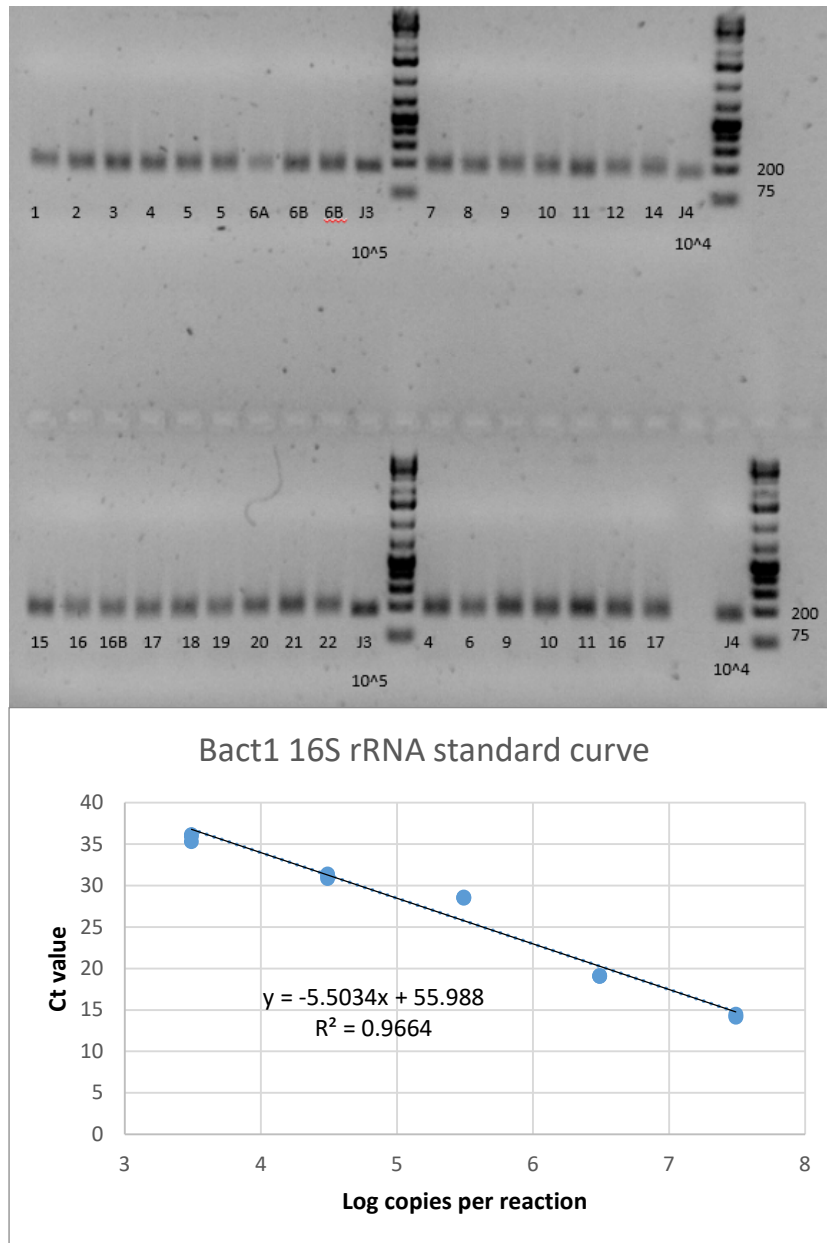
Figure 4. Representative quality of amplicons from BACT1-16S rRNA qPCR on standard DNA and IRL project sample DNA preparations.

Protocol development and validation of qPCR for all gene targets included delta-PCR cycle in which dsDNA fluorescence crosses the threshold value (Ct) analyses of DNA dilution series, melt curve analyses, and gel electrophoresis evaluations of the qPCR products generated. However, we also extensively evaluated two different Archaea primer pairs and qPCR conditions, for enumerating 16S rRNA genes of the types of sediment Archaea that would contain *amoA.* Two Archaea 16S rRNA gene primer pairs were tested with representative sediment DNA samples. The general Archaea primer pair ("universal") and the Group I Archaea primer pair (Archaea GpIArch1334F - GpIArch1551R, Thaumarchaeota group) were tested on the same DNA preparations for assessing sensitivity and specificity for the Archaea in the project sediment samples (**Figure 5 and Table 4**). Both Archaeal 16S rRNA gene primer pairs were originally developed and described with use of TaqMan probe by Suzuki et al. (2000), and here were further tested and evaluated for use in SYBR-Green-based qPCR.

Initial test reactions of Archaeal 16S rRNA primer pairs were conducted using samples with known low Ct values from qPCR for the AOA gene. For both Archaeal 16S rRNA primer pairs, 40 cycles with an annealing temperature of 56°C was used. Three different IRL project DNA samples: #16 (November 2022 SRS reference site, *Halodule* bed), #48 (April 2023 SRS reference site, *Halodule* bed), and #50 (a duplicate sediment sample from April 2023 *Halodule* bed in SRS) were part of this test. After qPCR, three replicate wells for each condition were combined resulting in 60 uL total, and 35 uL of this mixture was subjected to electrophoresis in 2.2% agarose. A single concentration (16A, 5.0 ng/uL) was tested in the plate with both primer pairs, shown in the middle row between ladder lanes (Figure 5). Additionally, for each sample (#16, 48 and 50), a serial dilution of initial template DNA was made and used in qPCR (25.0, 2.5, 0.25 and 0.025 ng/uL). The qPCR on each of the three-dilution series are shown as DNA #, 25 through 0.025 (Figure 5). The top row and first half of the middle row contain dilution series for the "universal" Archaea 16S rRNA primer pair, and the second half of the middle row and the entire bottom row contain for the Group I primer pair. Of all no-template control (NTC) wells in the plate, none crossed the threshold and hence obtained values of "undetermined;" but a combined NTC for each primer pair was run on the gel (bottom row, last two lanes).

Further testing and optimization of one or both of these archaeal 16S rRNA gene primer pairs in qPCR was done by assessing Ct values obtained in qPCR (**Table 4**). For each sample (#16, 48, and 50), as shown in **Figure 5**, four different DNA dilutions (25, 2.5, 0.25, and 0.025 ng/uL) were tested The mean and standard deviation (SD) for the Ct values were recorded from three wells for each DNA preparation and concentration. The dCt series represents the delta-Ct value for each of the sample dilution series, where 100% efficiency would be approximately 3.5. Detection in qPCR with the Group I pair was sensitive, with a signal resulting from DNA concentrations as low as 0.025 ng per uL (0.0375 ng DNA per reaction) (**Table 4**). The Group I primer pair provided a greater dynamic range and more representative values of actual sediment Archaea ribosomal RNA genes than the "universal" Archaea 16S rRNA gene primer pair. Therefore, for all archaea gene copies reported, Archaea were enumerated using the Group I primer pair, and relative abundances were calculated using the dCt method (Livak and Schmittgen, 2001).
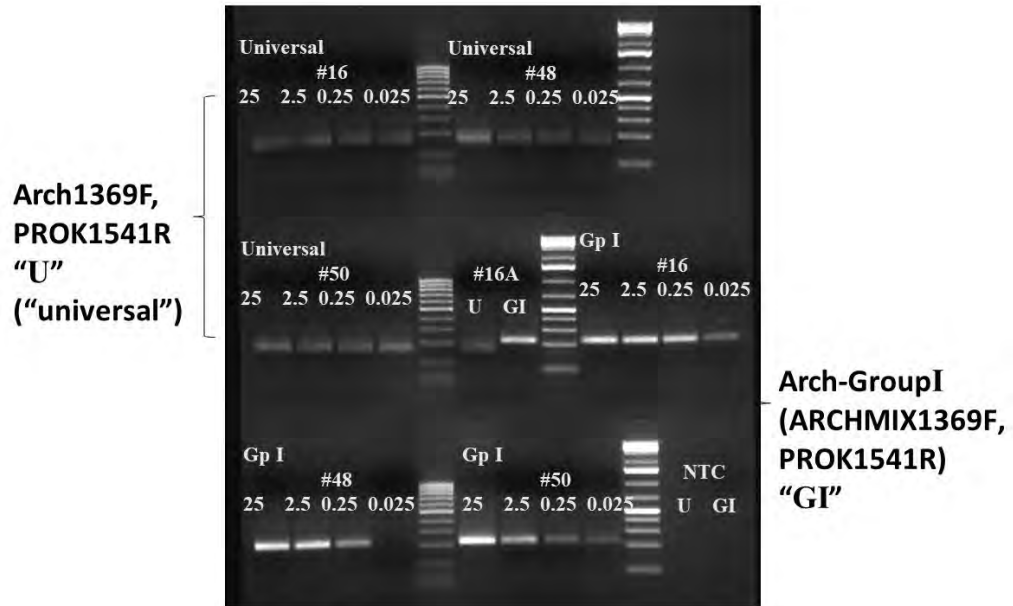
Figure 5. Gel electropherogram of Archaeal 16S rRNA genes generated in qPCR.

Table 4. Summary of Archaea 16S rRNA Ct values obtained from representative IRL sediment DNA samples in dilution series tests.

Target (Primer Pair)	Sample Name	DNA concentration (ng/uL)	Ct Mean	SD	Ct CV%	dCt series	Mean dCt for series
"Universal" Archaea 16S rRNA (ARCH-1369F & PROK-1541R	16	25	20.86	0.15	0.70	2.94	3.44
		2.5	23.80	0.21	0.90	3.58	
		0.25	27.37	0.21	0.75	3.80	
		0.025	31.17	0.63	2.02		
	48	25	21.21	0.20	0.93	2.60	3.38
		2.5	23.81	0.14	0.60	3.73	
		0.25	27.54	0.21	0.76	3.81	
		0.025	31.35	0.24	0.77		
	50	25	20.16	0.35	1.75	3.24	3.64
		2.5	23.40	0.05	0.23	3.49	
		0.25	26.89	0.04	0.15	4.18	
		0.025	31.07	0.62	1.99		
	NTC	0	UND	n/a	n/a		
Archaea Group I, Thaumarchaeota (Arch-1334F & Arch-1551R)	16	25	23.96	0.68	2.85	3.00	3.08
		2.5	26.96	0.47	1.73	4.72	
		0.25	31.68	2.47	7.80	1.54	
		0.025	33.22	0.04	0.14		
	48	25	24.02	0.27	1.12	2.90	3.26
		2.5	26.92	0.24	0.90	3.63	
		0.25	30.54	1.17	3.83	n/a	
		0.025	UND	n/a	n/a		
	50	25	25.18	0.38	1.52	2.74	2.34
		2.5	27.91	0.48	1.71	2.50	
		0.25	30.41	0.01	0.02	1.80	
		0.025	32.206	0.000	0.00		
	NTC	0	UND	n/a	n/a		

Protocol development and validation of qPCR for AOO and *nrfA*-bacteria was similarly performed, again for optimization of qPCR using the newest version of the SYBR-Green-based chemistry. For AOO, two gene targets were enumerated in qPCR: AOA and AOB. The expected amplicon of AOA enumerated with primer pair originally described by Meinhardt et al. (2015) was validated in a multiple sequence alignment and confirmed by gel electrophoresis of the final products. This primer pair and new SYBR-Green conditions were highly specific for AOA environmental DNA samples, as assessed by both gel electrophoresis and post-qPCR melt-curve analyses (not shown). AOA optimal conditions were finalized with annealing at 56 °C, and detection of dsDNA fluorescence at both 56°C annealing and 72°C extension steps (**Table 5**).

AOB was enumerated with primer pair described for use in qPCR by Caffrey et al. (2007), and originally designed as described in Rotthauwe et al. (1997), for Forward primer; and in Hornek et al. (2006) (**Table 5**). Conditions were modified and tested on several project sediment DNA samples, one with DNA at the normal concentration used in qPCR (5 ng/uL) and also 10-fold diluted (0.5 ng/uL), for testing specificity and sensitivity of the assay. Sizes of AOB qPCR products were as expected and previously reported, and lack of non-specific amplification evident by gel electrophoresis results were validated by the melt curve analysis. Ct values resulting from qPCR on a dilution series of a DNA sample with known ammonium oxidation activity were expected (not shown).

As with bacterial 16S rRNA gene qPCR, the *nrfA* qPCR also used standard curves using *E. coli* genomic DNA. The dynamic range of amplification was tested with genomic DNA known to contain *nrfA* (*E. coli*, strain K12). Relative abundances of DNRA of total bacteria were calculated given that *E. coli* strain K12 contains 7 copies of 16S rRNA and 1 copy of the *nrfA* gene for every chromosome molecule. Although the dynamic range of amplification with *E. coli* DNA was validated in qPCR with dual hot-start SYBR-Green based qPCR conditions, additional improvements were needed, to further reduce non-specific amplification, increase sensitivity, and improve the dynamic range possible in qPCR with sediment DNA samples. For *nrfA* qPCR protocol development, test DNAs included selected IRL samples as well as a DNA sample, from our University of Maine colleague, extracted from sediment that had previously been validated to contain activity of both DNRA and *amoA* prokaryotes (not shown). Primer concentrations tested included our standard (8 nanometer [nM] each primer) protocol, as well as 100 nM by Mohan et al. (2004), with several additional concentrations in between (12.5, 25, and 50 nM, not shown). The highest tested primer concentration (100 nM) was required to achieve sensitivity for *nrfA*.

The optimal *nrfA* qPCR conditions were then chosen for various primer pairs, amending numbers and extent of touchdown (TD) cycles, as well as adjusted total number of qPCR cycles. Altered TD protocols using the Mohan et al. (2004) *nrfA* primer pairs were developed to optimize the conditions for current SYBR-Green qPCR chemistry. The Mohan et al. (2004) primer pairs F2 & 7R1 (amplicon 231 bp) and 7F3 & 7R1 (133 bp) were first tested as originally described by the authors, with 60 cycles total (30 TD, 30 at 45 ºC annealing). Test templates included two from the IRL sediment DNA samples (PCL -#2; 3/15/2023; and 520 Slick #2; 3/15/2023), *E. coli* genomic DNA dilution series, and a dilution series of the University of Maine test sample DNA.

The best *nrfA* primer pair was 7F3&7R1. Adjustments to the qPCR TD protocol for qPCR with 7F3&7R1were based on findings as previously described for a different gene (Kesanopoulos et al. 2005). The final, best, set of cycling conditions for *nrfA* are outlined in **Table 5**. Briefly, the best *nrfA* qPCR conditions included a 20-cycle TD stage of, starting with 60 ºC annealing, decreasing by 0.5 ºC per cycle, ending with an annealing temperature of 50 ºC. The second stage used 50 ºC annealing for a further 35 cycles. Fluorescence values and resulting Ct values for obtaining abundances were from the second stage, where fluorescence was measured at the 72 ºC extension step. This improved protocol was used for all 52 IRL project sediment DNA samples, and final amplicon quality was assessed by both gel electrophoresis of the qPCR product as well

as melt curves of both standard and experimental DNA. The final set of *nrfA* qPCR conditions with the new TD qPCR protocol resulted in high sensitivity, where all 52 sediment DNA samples contained detectable *nrfA* gene copies, ranging from approximately 1 x 10^4 to 6 x 10^5 copies per reaction, corresponding to an average approximately 7 x 10^4 *nrfA* copies per ng of DNA per reaction.

Table 5 lists the best assay parameters for each of the target groups: Archaeal and Bacterial *amoA* genes (AOA and AOB, respectively), *nrfA* for DNRA organisms, bacterial 16S rRNA (BACT1), and Group-I-Archaeal (Thaumarchaeota) 16S rRNA. Conditions for the "universal" Archaea 16S rRNA gene, the primer pair that was tested but not used for IRL qPCR, is also provided in the Table. All methods used were tested and/or re-optimized for use in qPCR with the currently available SYBR-Green master mixes. Final enumeration of each of the target genes used 1.5 uL of DNA (7.5 ng total) in a total 20 uL reaction volume. The SYBR-Green master mix used in qPCR for all genes except *nrfA* was ThermoFisher Scientific Applied Biosystems™ PowerTrack™ SYBR™ Green Master Mix (cat #A46109). The mix used for *nrfA* was ThermoFisher Scientific Applied Biosystems™ PowerUp™ SYBR™ Green Master Mix (cat # A25918). The PowerTrack™ Mix contains an antibody-bound polymerase to enable hot-start reaction, while the PowerUp™ Mix contains two different enzyme suppression mechanisms (Dual-Lock™ Taq DNA polymerase) to enable highly specific hot-start reactions. Both master mixes use carboxy-X-rhodamine as the reference dye, and both also contain an enzyme Uracil-DNA glycosylase for carry-over cross-contamination reduction enabled by initial incubations at either room temperature or 50 °C, followed by heat-inactivation of the Uracil-DNA glycosylase at 95 °C during the initial hot-start incubation >90 °C. All qPCR master mixes also contain deoxyuridine phosphate in the nucleotide mixes to incorporate the nucleotide uracil into all dsDNA generation for subsequent degradation by Uracil-DNA glycosylase.

Table 5. Basic qPCR parameters for target groups enumerated in the study.

Group (Gene)	Conc. (nM)[1]	Primer name	Size (bp)[2]	Primer seq. [3]	Primer(s) references	Cycling Parameters [4]
Ammonium oxidation (nitrifiers), *amoA* gene encoding alpha subunit of ammonia oxidase							
Archaeal *amoA* (AOA)	8	Gen AOAF	135	ATAGAGCCTCAAGTA GGAAAGTTCTA	Meinhardt et al. (2015)	1X UDG, 50°C, 2 min 1X HS, 95°C, 10 min 40X cycles + 1X Melt: 95°C, 15 sec
		Gen AOAR		CCAAGCGGCCATCCA GCTGTATGTCC		**56°C, 20 sec*** **72°C, 20 sec***
Bacterial *amoA* (AOB)	8	amoA-F	530	GGGGTTTCTACTGGTGGT	Caffrey et al. (2007), Rotthauwe et al. (1997)	1X UDG, 50°C, 2 min 1X HS, 95°C, 5 min 40X cycles + 1X Melt: 95°C, 15 sec
		amoA-R		CCCCTCBGSAAAVCCTTCTTC	Caffrey et al. (2007), Hornek et al. (2006)	56°C, 20 sec **72°C, 20 sec***
DNRA, *nrfA* gene encoding nitrite reductase							
nitrite reductase *nrfA*	100	7F3	133	ATGYTNAARGCNCAR CAYCC	Mohan et al. (2004)	1X UDG, 50°C, 2 min 1X HS, 95°C, 4 min 20X TD cycles: 95°C, 15 sec 60°C (-0.5°C/cycle), 15 sec **72°C, 15 sec*** 35X fixed annealing cycles: 95°C, 15 sec 50°C (-0.5°C/cycle), 15 sec **72°C, 45 sec*** 1X Melt
		7R1		TWNGGCATRTGRCARTC		

Group (Gene)	Conc. (nM)[1]	Primer name	Size (bp)[2]	Primer seq. [3]	Primer(s) references	Cycling Parameters[4]
16S rRNA, Archaea ("general")	8	ARCH MIX 1369F	193	CGGTGAATAYGCCCCTGC	Suzuki et al. (2000), Babcock et al (2020)	1X UDG, 50°C, 2 min 1X HS, 95°C, 5 min 40X cycles + 1X Melt: 95°C, 15 sec 56°C, 45 sec **72°C, 45 sec***
		PROK 1541R		AAGGAGGTGATCCRGCCGCA		
16S rRNA, Archaea Group I (Thaum.)	8	ARCH GI-1334F	243	AGATGGGTACTGAGACACGGAC	Suzuki et al. (2000), Babcock et al (2020)	1X UDG, 50°C, 2 min 1X HS, 95°C, 5 min 40X cycles + 1X Melt: 95°C, 15 sec 56°C, 45 sec **72°C, 45 sec***
		ARCH GI-1554R		CTGTAGGCCCAATAATCATCCT		
16S rRNA, Bacteria, BACT1 primer pair	8	BACT 1369F	193	CGGTGAATACGTTCYCGG	Suzuki et al. (2000), Babcock et al (2020), Waidner and Kirchman (2007)	1X UDG, 50°C, 2 min 1X HS, 95°C, 5 min 37X cycles + 1X Melt: 95°C, 5 sec **60°C, 30 sec***
		PROK 1541R		AAGGAGGTGATCCRGCCGCA		

[1] Final concentration of each primer in the qPCR.

[2] Size of amplicon (PCR product), in base pairs;

[3] Non-standard DNA letters indicate mixed sequence at that location, as per IUPAC degeneracy nucleotide codes.

[4] UDG, step at which the uracil deglycosylase enzyme is active at 50 °C, for degradation of previously-generated amplicons with qPCR mixes containing dUTG nucleotide bases; HS, hotstart enzyme activation, which disables a heat-labile antibody bound to the polymerase; * and **bold, step in the cycle** at which the program turned on the laser detection of dsDNA fluorescence; Melt, for all runs, after indicated number of cycles, one stage dissociation curve and melt curve analysis cycle was run, as per the standard protocol in the ThermoFisher Applied Biosystems QuantStudio 3 system.

1.3.6 *Potential nitrification experiments*

Potential nitrification was measured is described in Henriksen et al. (1981) where approximately 2 grams of sediment and 50 mL of filtered site water were placed in a 50 mL centrifuge tube. Ammonium chloride was added to provide a final concentration of 0.5 millimole. Samples were incubated in the dark at ambient temperatures on a shaker table. Water was collected at 0 and 24 hours for nitrite and nitrate+nitrite analysis. Experiments were conducted at both seagrass sites in SRS in September, November, and April and at PCL and Slick IRL sites in March.

1.3.7 Laboratory Analysis

Ammonium was analyzed using the Holmes et al. (1999) fluorometric method. Detection limit was 0.03 micro moles (µM). The Parsons et al. (1984) spectrophotometric method was used for the analysis of nitrite and dissolved inorganic phosphate (DIP) concentrations which had detection limits of 0.1 µM and 0.05 µM, respectively. Nitrate+nitrite was analyzed using vanadium reduction on a spectrophotometer as in Schnetger & Lehners (2014) with detection limits of 0.2 µM. Filters for chlorophyll a were extracted with 90% acetone overnight and read on a fluorometer as in Welschmeyer (1994) and have a detection limit of 0.14 µg/L.

1.3.8 Data sources and analysis

Water quality data between 2000 and 2020 from the CBA and Florida Department of Environmental Protection Impaired Waters Rule (IWR) databases were analyzed for Destin Harbor sites and bottom dissolved oxygen concentrations are reported below. Salinity, water, and secchi disk depth data from the St. Johns River Water Management District (SJRWMD) between January 1987 and April 2022 were analyzed. Where secchi disk depth was less than the water depth, Kd was calculated using the following equation.

$$Kd = 1.4/secchi\ depth$$

1.4 Results

1.4.1 Comparison of water quality between Destin Harbor, Santa Rosa Sound and Indian River Lagoon - Banana River

Plans for a pumping system to improve water quality in Destin Harbor were discussed in the 1988 Destin Harbor Management Plan (Landers-Atkins Planners, Inc. 1987). This report describes an extended fish kill in 1982 and subsequent concerns about poor water quality. A pumping system was installed in 1992 with a goal to have dissolved oxygen levels greater than 5 mg/L (Michael Burgess, City of Destin Engineer, pers. Comm.). According to Mr. Burgess, the pump was run for 8 hours/day at high tide and repairs to this system were required about every 12-18 months. Problems with reliability and repairs were noted in 1996 (Lipnicky 1996). In 2004, the system was replaced (NWFDN 2005). In March 2019, a new schedule of pumping operations was established with pumping for 6 hours every day between March 1 and October 31 on outgoing tides (Burgess, pers. comm). Pumping every other day for several hours occurs between November and April. Between May and November 2021, the pump was out of operation. Additional problems also occurred between July and August 2022.

Choctawhatchee Basin Alliance sampling in Destin Harbor was temporally more comprehensive than the IWR sampling (Bottom water dissolved oxygen concentration in Destin Harbor from Choctawhatchee Basin Alliance sampling (upper panel) and Impaired Waters Rule database (**Figure 6**). Bottom water dissolved oxygen was often low at CBA FL Walton Beach-10 between May and October. Old Pass E was the same location as the CBA FL Walton Beach-10 site and showed similar patterns. The Old Pass W and CBA Ft Walton Beach 9 sites were at the same location and closer to Destin Pass than Old Pass E. IWR data had lower bottom water dissolved oxygen values in 2013 and 2014 than the CBA sampling (**Figure 6**). There were 198 values out of 446 sampling events that were below the target 5 mg/L between March 1 and October 31 at these two sampling locations. Not surprisingly, in the cooler months between November 1 and February 28, only 26 out of 183 values were less than 5 mg/L.
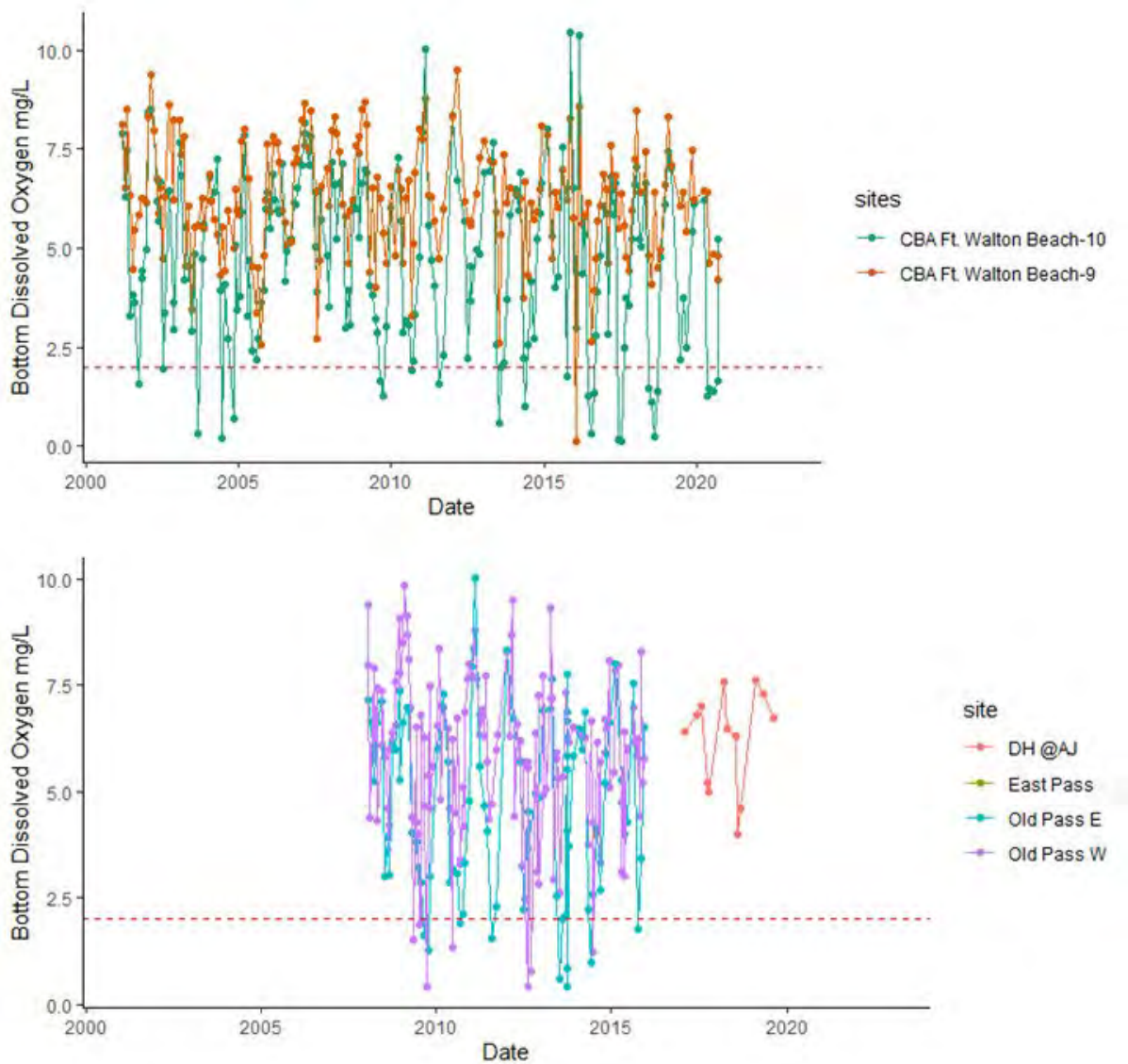
Figure 6. Bottom water dissolved oxygen concentration in Destin Harbor from Choctawhatchee Basin Alliance sampling (upper panel) and Impaired Waters Rule database (lower panel).

Sampling by UWF during October 2022 revealed stratification between the surface and bottom layers and the depth of the pycnocline was between 1.5 - 2 m (**Figure 7**). Dissolved oxygen levels were similar between surface and bottom at 3 of the sampling locations. However, at CBA-10 (the same sample location as CBA FL Walton Beach-10 and Old Pass E), dissolved oxygen concentrations declined below the pycnocline to about 5 mg/L (**Figure 7**). Chlorophyll a fluorescence values, a measure of chlorophyll a biomass, increased with depth particularly at site CBA-10. Bottom water chlorophyll values were also high, 10.4 µg/L, at this site (**Table 6**). Bottom water ammonium and DIP concentrations were higher than surface concentrations at this site and SC-1D. Similar patterns were observed in turbidity and TSS concentrations at these two stations. Nitrate+nitrite concentrations were at or below detection limits (< 0.2 µM) at all locations. Light

attenuation ranged from 0.37 to 0.58 /m with the lowest values near the mouth at site DH @AJ (**Table 6**).
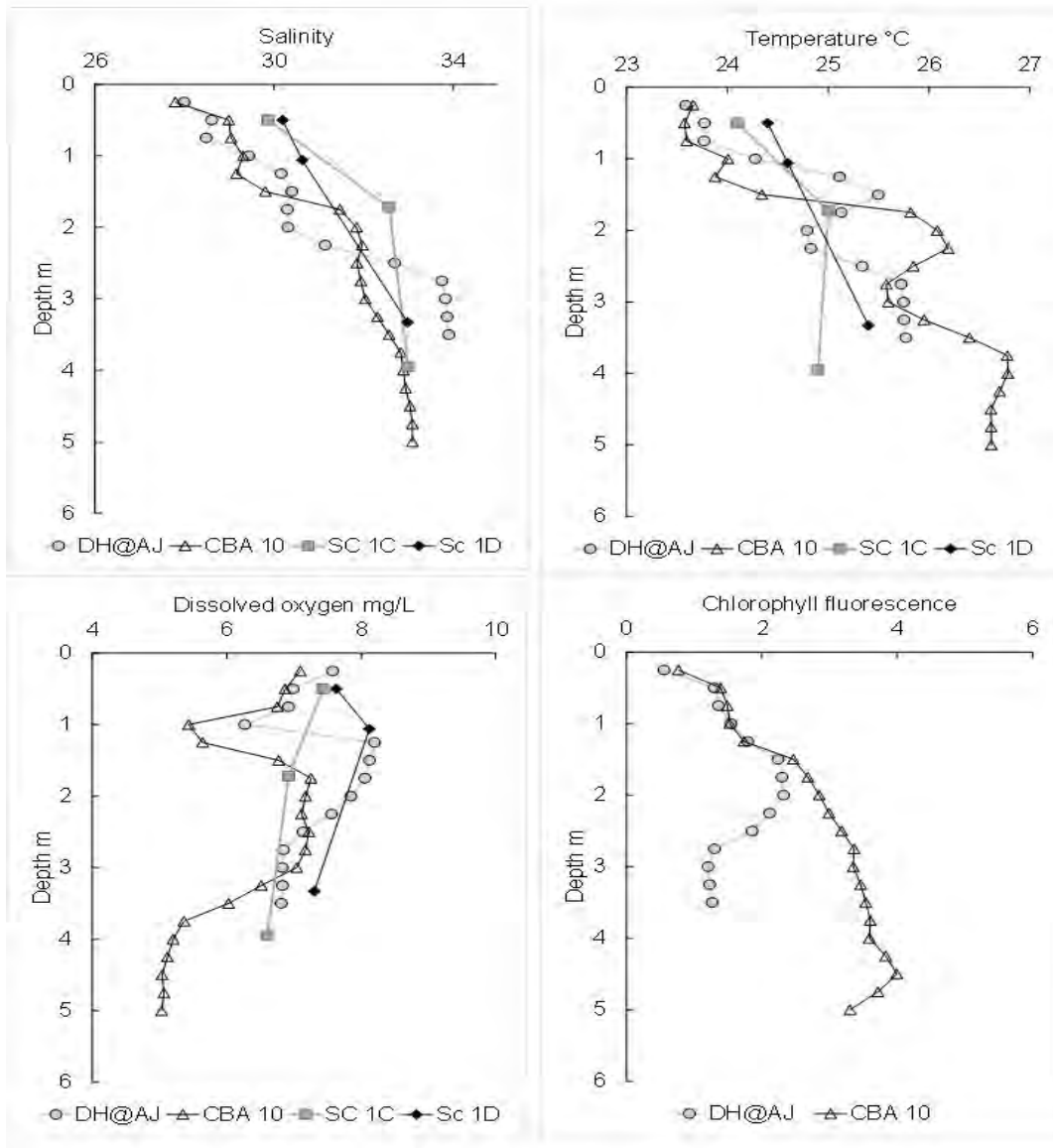
Figure 7. Depth profiles of salinity (upper left), temperature (upper right), dissolved oxygen (bottom left) and chlorophyll fluorescence (bottom right) in Destin Harbor in October 2022.

Table 5. Water column characteristics from Santa Rosa Sound, Destin Harbor and Indian River Lagoon.

Location (Layer S-surface, B-bottom)	Date	Salinity	Kd /m	Chlorophyll a µg/L	Nitrate+ nitrite µM	Ammonium µM	DIP µM	TSS mg/L
Santa Rosa Sound								
Seagrass (S)	9/21/22	23.7	0.68	2.21	<0.2	0.07	0.16	14.5
Seagrass (S)	11/2/22	26	0.29	0.61	<0.2	0.67	0.27	14.5
Seagrass (S)	4/4/22	24.4	0.45	1.47	0.62	0.52	0.08	11.60
Destin Harbor								
DH@AJ (S)	10/5/22	29.89	0.37	1.91	<0.2	0.21	0.12	36.00
DH@AJ (B)	10/5/22	34.62		2.8	<0.2	0.34	<0.05	5.50
CBA-10 (S)	10/5/22	29.55	0.53	1.43	<0.2	0.09	0.16	9
CBA-10 (B)	10/5/22	33.8		10.43	<0.2	0.45	0.42	26.00
SC-1C (S)	10/5/22	29.86	0.43	2.62	<0.2	0.30	0.37	14
SC-1C (B)	10/5/22	32.99		2.52	<0.2	0.61	0.17	17
SC-1D (S)	10/5/22	30.19	0.58	3.52	<0.2	0.13	0.26	5.5
SC-1D (B)	10/5/22	32.98		8.72	<0.2	0.30	0.29	9
Indian River Lagoon								
Slick (S)	3/15/23	18.54	0.62	5.65	<0.2	0.18	0.13	18.00
PCL (S)	3/15/23	18.88	3.27	4.02	<0.2	0.12	0.17	20.00

Salinity in Santa Rosa Sound seagrass bed ranged from 19.7 to 26 (**Table 6**, Bowman in prep.). Periodic low concentrations of dissolved oxygen (<5 mg/L) were observed at night and dawn, while concentration in the afternoon usually exceeded saturation (Bowman in prep., Caffrey, unpublished data). Nitrate+nitrite, ammonium and DIP concentrations were often low, less than 1 µM (**Table 6**). Water column chlorophyll a values ranged from 0.6 to 7.7 µg/L (**Table 6**). Sediments were easily resuspended at this location resulting in TSS concentrations above 60 mg/L (Bowman in prep., Caffrey et al. 2023).

Productivity and survival of seagrasses are influenced by a variety of factors. Salinity, temperature, light availability and nutrients all interact with each species having different requirements. *Halodule wrightii* is considered a pioneer species with a broad salinity tolerance (10-35 PSU) and an ability to survive extended periods of 5 PSU (Biber, 2022; Lirman & Cropper, 2003). *Syringodium filiforme* has a narrower range, having higher leaf productivity between 15 and 25 PSU (Lirman and Cropper 2003). *Ruppia maritima*, which is also present in IRL, has a wide salinity tolerance, ranging from 0 to 70 ppt (Kantrud, 1991), but can be negatively impacted by repeated salinity changes (La Peyre and Rowe, 2003)" Long-term monitoring of salinity in the Banana River region of IRL suggest that salinities are usually within these ranges (**Figure 8**). Salinity outside of the 10 to 25 range occurred in the mid-1990s when some salinity values were below 10 (**Figure 8**). In the early 2010s, there were several years with 6-10 months of salinity above 35 (**Figure 8**).

Minimum light requirements for *H. wrightii* are less than for *S. filiforme*, 20% and 23% average surface irradiance, respectively (Lee et al., 2007). When light attenuation is high, less light is available for seagrasses. In March 2023, light attenuation at site Slick was 0.62 /m but 3.27 /m at PCL. In a 2 m water column, this translates into 29% of surface irradiance at the bottom at the Slick site. However, in a 2 m water column at PCL, the bottom would only see 0.14% of surface irradiance, far below the requirements for seagrasses. Lapointe et al. (2020) reported average light attenuation values of 0.7 /m during the dry season and 2.8/m during the wet season. These were consistent with long term measurements by SJWMD in Banana River (**Figure 8**) and a 15-year trend in decreasing secchi disk depth (SJWMD 2022). Increasing chlorophyll a, color and turbidity contribute to the increased light attenuation which decreases habitat availability for seagrasses. Chlorophyll a values during our March 2023 trip were 4.0 and 5.6 µg/L at the PCL and Slick sampling locations, respectively. These values are lower than the 15-year median value of 12.1 µg/L from the SJWMD (SJWMD 2022).

Figure 8. Salinity (upper panel) and light attenuation (lower panel) in Banana River between January 1987 and April 2022 from St Johns River Water Management District (downloaded 8/24/22). Red dashed lines indicate minimum and maximum salinity tolerances for H. wright.

1.4.2 Sediment biogeochemistry

All locations in the Florida Panhandle had sandy, low organic matter sediments (**Table 7**). The depth layers (0-2, 2-4, 4-6 cm) all had similar water and organic matter contents at the shallow *Halodule* and deep *Thalassia* sites during each sampling trip (data not shown). Destin Harbor was similar to the two Santa Rosa Sound sites in water content but had a much lower organic matter content. This was likely due to the presence of small roots and detritus from the seagrass beds in the Santa Rosa Sound samples which were not present in Destin Harbor.

Table 6. Water and organic matter content from sediment samples (0-6 cm). Santa Rosa Sound samples collected in September 2022, November 2022 and April 2023. Destin Harbor samples collected in October 2022. Average + S.E.

Location	Site	Water content %	Organic matter content %
Santa Rosa Sound	*T. testudinum* bed	72.7 + 1.0	3.84 + 0.62
Santa Rosa Sound	*H. wrightii*	75.8 + 1.5	3.40 + 0.46
Choctawhatchee Bay	Destin Harbor	73.8 + 2.7	0.39 + 0.26

Porewater ammonium and DIP concentrations were always higher than concentrations in the overlying water. Porewater DIP ranged from 1 to 7 µM, increasing with depth at the *Halodule* site and IRL sites (**Figure 9**). DIP at the *Thalassia* site was similar among depth layers with the highest concentrations in November and lowest in April, which is the start of the growing season. *Halodule* DIP concentrations were also low in April compared to other dates. Ammonium concentrations were highest at IRL sites, increasing from 35 µM in the 0-2 cm layer to 60 µM at 4-6 cm. Concentrations in the *Halodule* bed were less than 20 µM, similar to those in the *Thalassia* bed except for November at the 2-4 cm layer which was 30 µM (**Figure 9**). These values are consistent with previous work in Santa Rosa Sound (Presley and Caffrey, 2021; Rothfus, 2022).
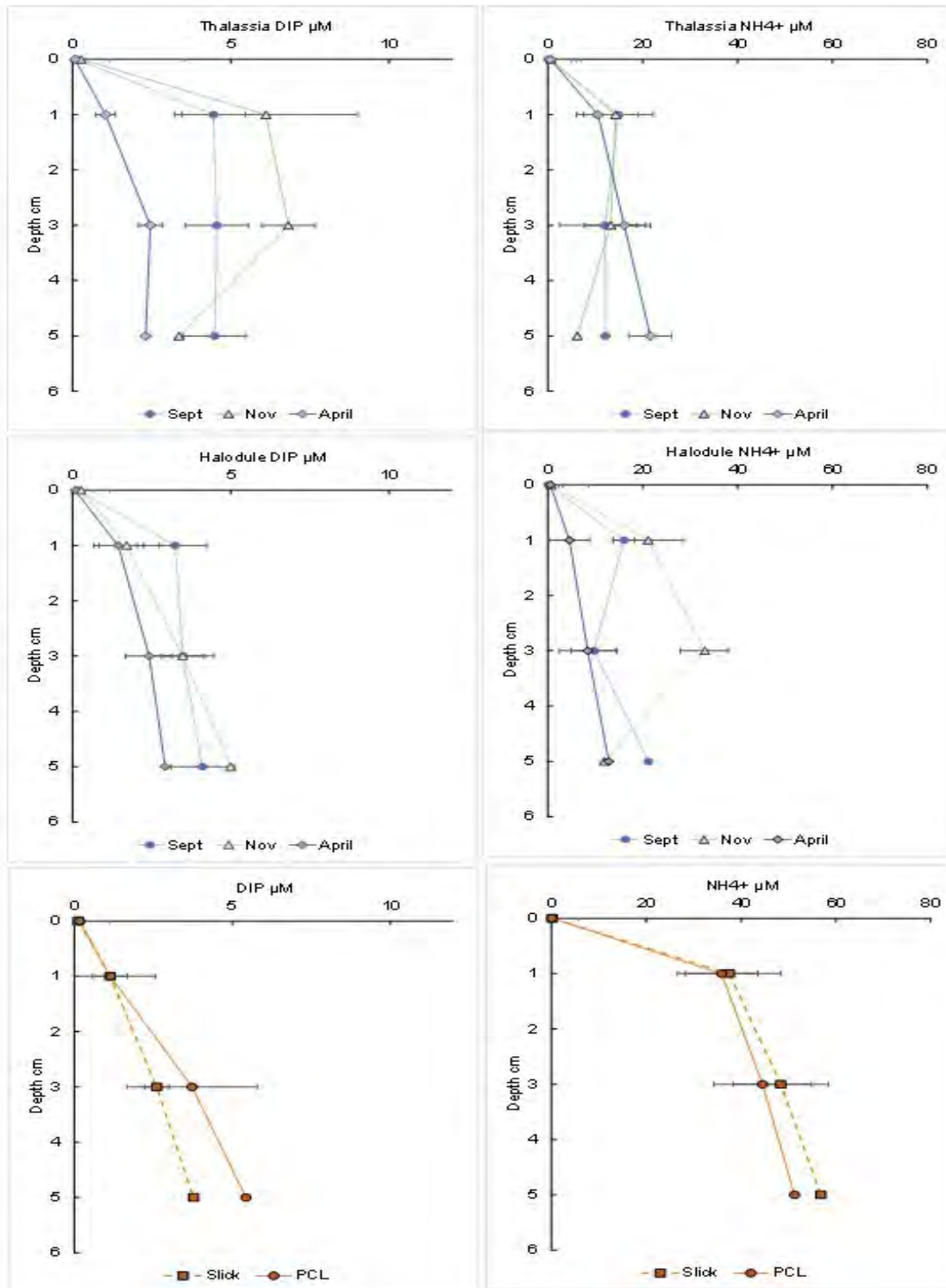
Figure 9. Porewater profiles of dissolved inorganic phosphate (DIP) and ammonium (NH4+) with depth in sediment. Value at 0 cm is overlying water value. Mean + S.E.

Replicate porewater sulfide concentrations were highly variable in the *Halodule* and *Thalassia* beds (**Figure 10**). The coefficient of variation among quadruplicate samples ranged from 7% to 65%. Concentrations were higher in *Thalassia* than *Halodule* or IRL sites and were similar among depth layers. In contrast, sulfide concentrations increased with depth at the other two locations except for in September at the *Halodule* site (**Figure 10**). Concentrations were similar to previous studies in Santa Rosa Sound (Presley and Caffrey, 2021; Rothfus, 2022). Porewater Fe2+ concentrations were higher in *Thalassia* and *Halodule* beds than IRL sites, particularly in September (**Figure 10**). Concentrations from SRS were similar to previous studies (Rothfus, 2022).
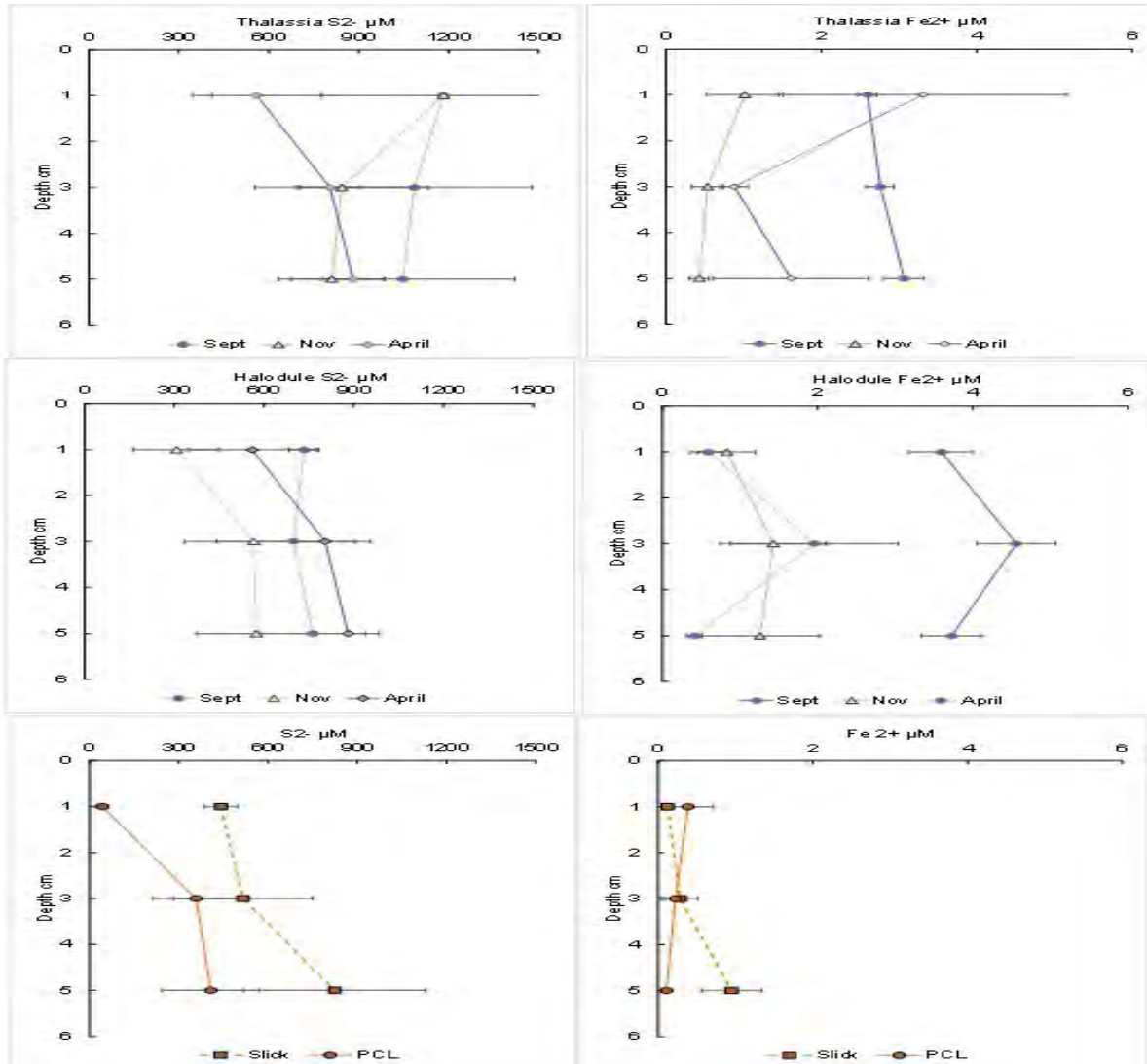
Figure 10. Porewater profiles of dissolved sulfide (S2-) and iron (Fe2+) with depth in sediment. Mean + S.E.

Benthic chlorophyll a concentrations were similar in both seagrass beds, between 2 and 4 µg chla/gws (**Figure 11**). Concentrations were somewhat higher in the Thalassia beds than Halodule in September and November. Sites in Destin Harbor were slightly lower at 2.7 µg chla/gws or less. The PCL, Slick and PNR sites were in the same range as Santa Rosa Sound, except for the PCL site in March which was 5.8 µg chla/gws. The highest benthic chlorophyll, 9.2 µg chla/gws, occurred at the IRL Samson in January. Samson was also higher than the PCL site in March and June, although variability between duplicates was high.
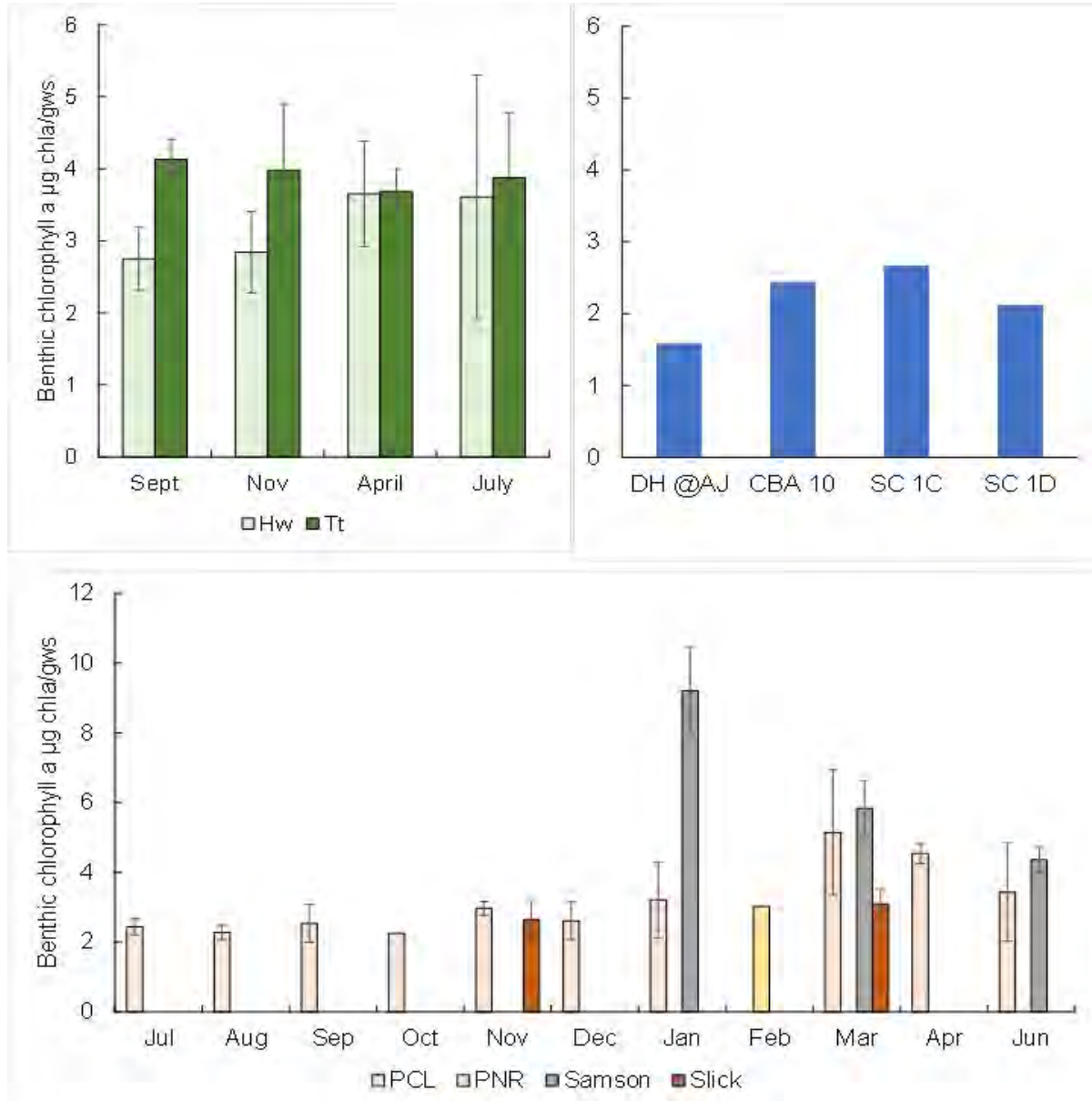
Figure 11. Benthic chlorophyll a concentrations in Santa Rosa Sound (top left), Destin Harbor (top right) and Indian River Lagoon (Bottom panel) between July 2022 and July 2023. Destin Harbor samples from October 2022. Mean + S.D.

Four measurements from dark benthic domes could not be used due to exchange between the dome and surrounding water as the tide changed during the incubation, lifting up the domes from the sediment. Because of this no dark flux measurements from *Halodule* were available for November. It was not an issue in the clear domes which were less buoyant.

Oxygen consumption in Santa Rosa Sound ranged from -7919 to -1304 µmol/m2/h with higher consumption in *Halodule* beds than *Thalassia* (**Figure 12**). These are comparable to the fluxes measured at PCL and Slick in March 2023 (**Table 8**), but lower than those measured in mixed *Halodule* and *Thalassia* beds in Big Lagoon (part of the Pensacola Bay system) in 2011 (Hester et al. 2016). Net community production was also higher in *Halodule* beds than *Thalassia* (**Figure 12**). Higher net community production occurred at the Slick site than the PCL site. Lower light attenuation at Slick could have been responsible for the greater production by benthic microalgae.

Ammonium fluxes were higher in dark chambers than light where uptake often occurred, particularly in *Halodule* beds in September. A similar pattern was observed at PCL and Slick sites in March (**Table 8**). At Slick, uptake occurred in both light and dark domes, but those in the dark had lower uptake. This pattern is consistent with nutrient uptake by seagrasses or benthic microalgae. Nitrate+nitrite fluxes were very low since concentrations were usually at detection limits. Uptake of nitrate+nitrite in the *Halodule* bed occurred in both September and April. Nitrate+nitrite uptake occurred at both IRL sites. DIP fluxes were also near zero except for one high dark chamber value from *Halodule*. There were no consistent differences in nitrate+nitrite or DIP fluxes between light and dark domes from Santa Rosa Sound or Indian River Lagoon.
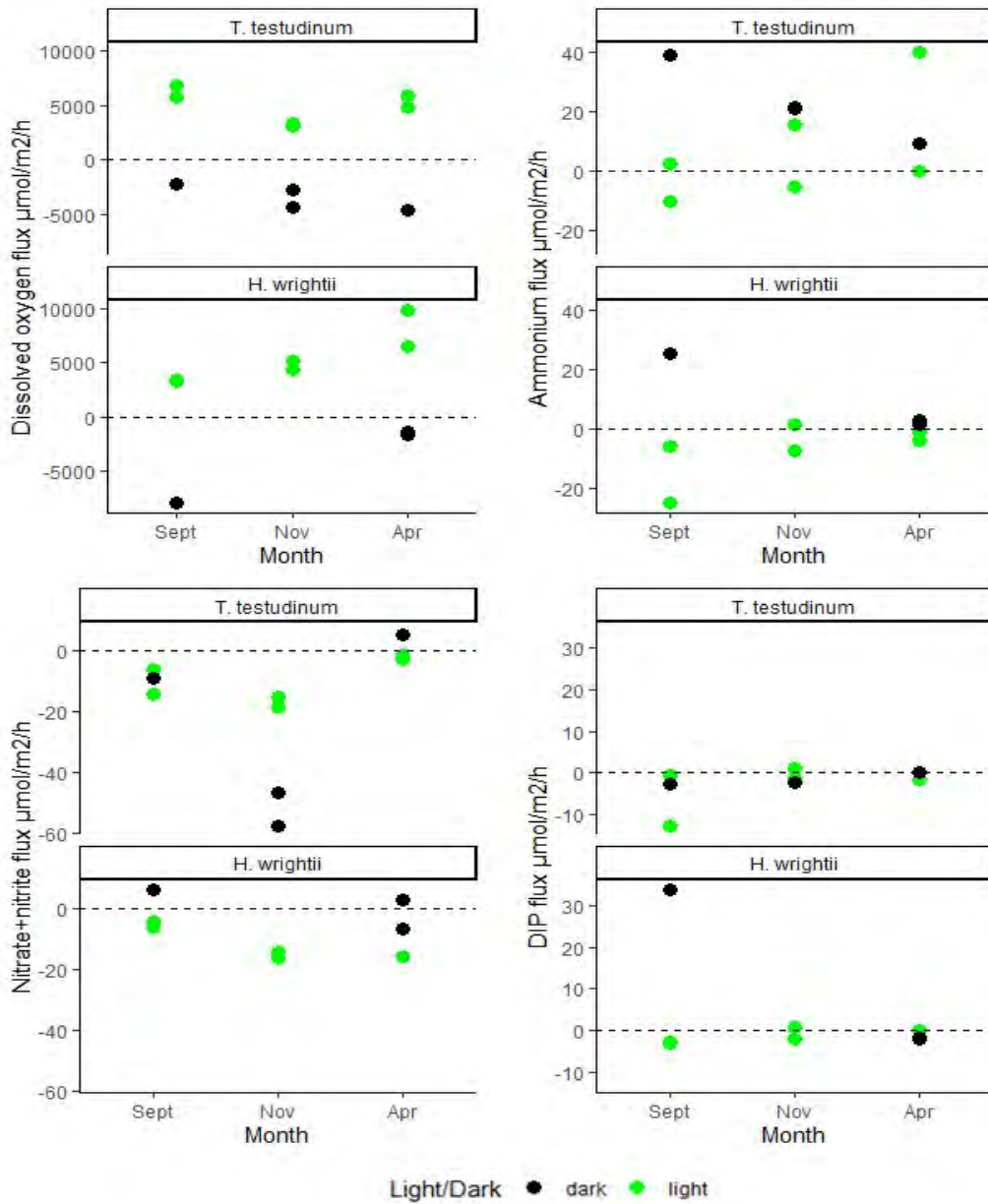
Figure 12. Benthic fluxes of oxygen, ammonium, nitrate+nitrite and dissolved inorganic phosphate (DIP) in Santa Rosa Sound seagrass beds in September 2022, November 2022 and April 2023 from light and dark domes.

Table 8. Benthic fluxes of oxygen, ammonium, nitrate+nitrite and dissolved inorganic phosphate (DIP) From Slick and PCL in Indian River Lagoon in March 2023

Location	Light/Dark	DO flux µmol/m2/h	NH4+ flux µmol/m2/h	NO3-+NO2- flux µmol/m2/h	DIP flux µmol/m2/h
Slick	Light	1785 + 111	-41.3 + 0.7	-6.1 + 17.2	-3.0 + 16.2
Slick	Dark	-2391 + 2527	-23.7 + 6.7	-12.2 + 8.6	-1.2 + 0.0
PCL	Light	160 + 133	-0.3 + 4.0	-14.8 + 20.9	0.0 + 5.8
PCL	Dark	-1676 + 654	12.1 + 4.6	-0.8 + 1.0	0.6 + 0.6

Potential nitrification rates were highest in the *Thalassia* bed in September. Rates were also high in the PCL site in March (**Figure 13**). There were no differences between the first (ammonium oxidation) and second (nitrite oxidation) steps in nitrification. While nitrite oxidizers can be more prone to inhibition by sulfide or low oxygen levels (Ward 2008), there was no evidence of that in these incubations. Low or negative rates of potential nitrification may have occurred due to uptake of nitrate and/or nitrite by living plant roots present in sediment over the course of the incubation.
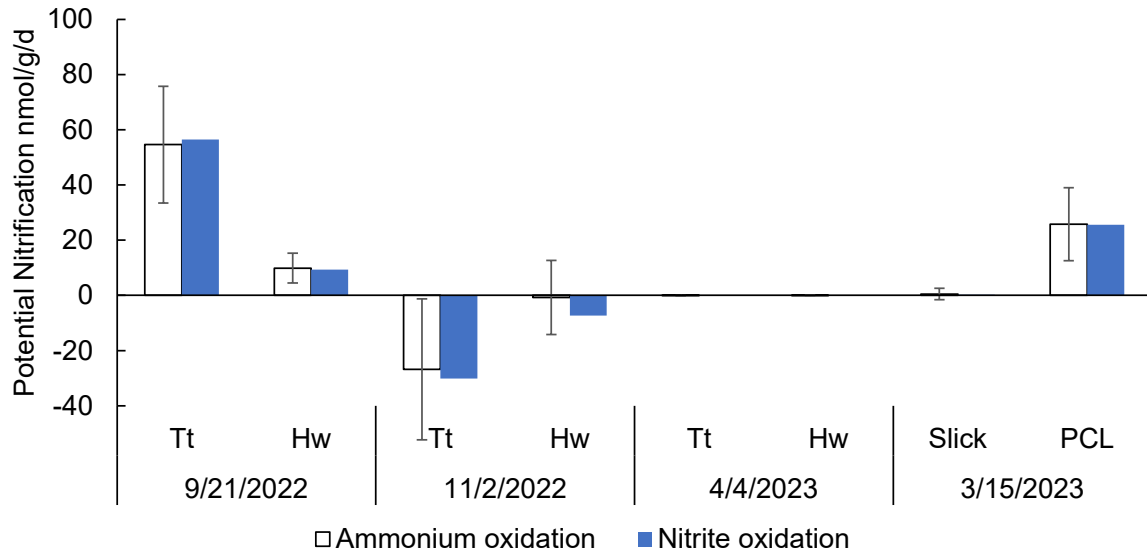
Figure 13. Potential nitrification rates from Thalassia testudinum (Tt) and Halodule wrightii (Hw) beds in Santa Rosa Sound from September, November and April and from Indian River Lagoon sites Slick and PCL in March.

1.4.3 Abundance of prokaryotes capable of dissimilatory nitrate reduction to ammonium *(DNRA)* and nitrification

The relative abundances of prokaryotes capable of nitrification (AOO, ammonium oxidizing organisms) or capable of DNRA were determined in sediment samples of the IRL study sites and of the SRS Panhandle reference site. AOO were enumerated by measuring levels of the *amoA* gene, which encodes the first important enzyme in the nitrification pathway; and DNRA bacteria were enumerated using the *nrfA* gene. We would expect sediments from impacted sites during periods of hypoxia to contain higher abundances of *nrfA* and conversely, sediments with more oxygen to have higher abundances of *amoA* (**Figure 3**). In all sediments examined throughout the study, we observed a general pattern of higher DNRA bacteria from the SRS reference sites than from the IRL sites. Additionally, there was also an overall higher abundance of AOO in the SRS sites than in the IRL sediments. There was a seasonal component to changes in abundance of AOO at the Port Canaveral site in the IRL. At all sites overall, there were fewer prokaryotes containing the *amoA* genes than DNRA bacteria. Together, these data suggest both types of prokaryotes with nitrogen-cycling functional genes are more abundant in the SRS sediments than in IRL sediments, and nitrogen compounds in the SRS sediments may be more rapidly recycled than those in the IRL.

The yields in all samples were sufficient to perform qPCR for highest sensitivity for all genes (**Table 9**). Coefficient of variation among triplicate wells for all assays were generally low, with average CV% for *nrfA,* bacterial and archael 16S rRNA of ~16, 4, and 1%, respectively (**Table 9**, bottom). Ranges of gene copies from dominant organisms throughout the study sample set were as expected. Total prokaryotes in two domains (Archaea, Bacteria) were enumerated with primer pairs as first described (Suzuki et al. 2000) but amended to work with SYBR-Green based qPCR assays as previously described (Babcock et al. 2020; Waidner and Kirchman 2007). The dynamic range of bacterial 16S rRNA assays ranged from 416 copies to 4.2×10^7 copies of the target gene.

Total bacteria using the "universal" BACT1 primer pair were quite abundant throughout, from 3.4×10^4 to 5.2×10^5, averaging ~3×10^5 copies per ng of DNA. Similarly, Archaea Group I (Thaumarchaeota, those that are known to contain *amoA* in their genomes) were highly abundant, with an average copy number per ng of DNA of ~2.5×10^6. Bacteria containing *nrfA* (those capable of DNRA processes) were also very abundant throughout the study; none of the 52 samples tested contained undetectable amounts of *nrfA* genes. The average *nrfA* gene copy abundance normalized to ng of DNA was ~7×10^4, suggesting DNRA bacteria comprised a significant proportion of total bacteria in all sediment samples collected. **Table 9** provides minimum, maximum and mean gene copies for 52 DNA samples from IRL and SRS sediment samples. Coefficient of variation (CV%) values are for triplicate wells for each of the 52 samples.

Table 7. Range of calculated copies of nrfA and BACT1- or Arch-Group I 16S rRNA in sediment DNA samples.

Ranges and Means	Gene					
	nrfA		Bacteria 16S rRNA		Archaea Group I 16S rRNA	
	Rxn[1]	ng DNA[2]	Rxn[1]	ng DNA[2]	Rxn[1]	ng DNA[2]
Min	9.90E+03	3.30E+03	2.53E+05	3.37E+04	1.32E+06	1.76E+05
Max	6.13E+05	2.04E+05	3.91E+06	5.21E+05	2.57E+08	3.43E+07
Mean	2.09E+05	6.97E+04	2.35E+06	3.14E+05	1.88E+07	2.51E+06
CV%						
Range	0.5 - 38.4		0.7 – 17.4		0.18 – 3.73	
Mean	15.9		4.4		1.24	

[1] Copies of gene in each qPCR reaction well; [2] Copies normalized to nanogram (ng) DNA.

In the SRS Panhandle reference sites and the four IRL sites, *nrfA*-containing bacteria were present in all samples (**Table 10 and Figure 14**). However, the range of *nrfA* bacteria abundances was 4 to 65% of total bacteria (**Table 9**). In both SRS reference seagrass beds, relative abundance of DNRA bacteria decreased in November compared to the other two months (**Figure 14**), but this was likely not significant because of within-site variability (core to core DNA sediment sample variability). Overall, at the SRS sites, DNRA bacteria comprised on average 32 ± 14 and 25 ± 14% of bacteria in the *Halodule* and *Thalassia* beds, respectively (**Table 10**). In contrast, the mean abundances in the IRL PCL and Slick sites were slightly lower than those of the SRS reference sites. At PCL, DNRA comprised 20 ± 8.5% of bacteria with similar abundances at the Slick site, 14 ± 8%. At the PCL site (**Figure 14**, bottom), there was no obvious seasonal component in relative abundance in DNRA bacteria. Within-month comparison of abundances between the Slick and PCL sites (dark maroon bars and light pink bars, respectively, **Figure 14**) showed no consistent differences in DNRA sediment bacteria. Abundances in samples from the Sampson site (January) and Pelican National Wildlife Refuge site (PNR, February) were similar to those observed at the PCL site (peach and grey bars, **Figure 14**). There were also no differences between FIT and UWF samples collected at IRL sites in March.

Table 8. Percentages of bacteria containing the *nrfA* gene in 52 sediment DNA samples from the IRL sites and the Santa Rosa Sound (SRS) reference sites.

Sample Collection Date	Location[1]	Bacteria containing the *nrfA* gene as a percentage of total bacteria		
		Mean	**SD**	**n**
7/7/2022	PCL	27	18	2
8/9/2022	PCL	25	17	2
9/23/2022	PCL	19	8.1	2
9/21/2022	SRS Hw	46	17	3
9/21/2022	SRS Tt	32	1.1	3
10/21/2022	PCL	25	3.5	2
11/18/2022	PCL	10	3.4	2
11/2/2022	SRS Hw	22	5.5	3
11/2/2022	SRS Tt	17	11	4
11/21/2022	Slick	22	3.6	2
12/16/2022	PCL	23	2.7	2
1/25/2023	PCL	18	2.3	2
2/6/2023	PNR	15	n/a	1
1/13/2023	SAMSON	13	6.6	2
3/15/2023	PCL, AF Ch[1]	17	10	2
3/15/2023	Slick, AF Ch[1]	11	5.3	2
3/15/2023	PCL, JC Dome[1]	20	6.8	4
3/15/2023	Slick, JC Dome[1]	11	8.9	4
4/4/2023	SRS Hw	29	10	4
4/4/2023	SRS Tt	27	20	4
3/15/2023	PCL, All (n=6)[1]	19	7.0	6
3/15/2023	Slick, All (n=6)[1]	11	7.3	6
Study-wide means (+/- SD) per site				
SRS Hw		32	14	10
SRS Tt		25	14	11
PCL		20	8.5	20
Slick		14	8.0	8
PNR		15	n/a	1
Sampson		13	6.6	2

[1] Site abbreviations are provided in **Table 2**. Lines with SRS Panhandle reference site data are shaded grey.

[2] Descriptions of the six March 2023 samples collected at each PCL and Slick sites are given in **Table 3**. For showing overall mean during March 2023 in **Figure 14**, data from all 6 samples collected from both chamber and dome methods were also combined to obtain an overall mean of dome (n=4) and chamber (n=2) methods.
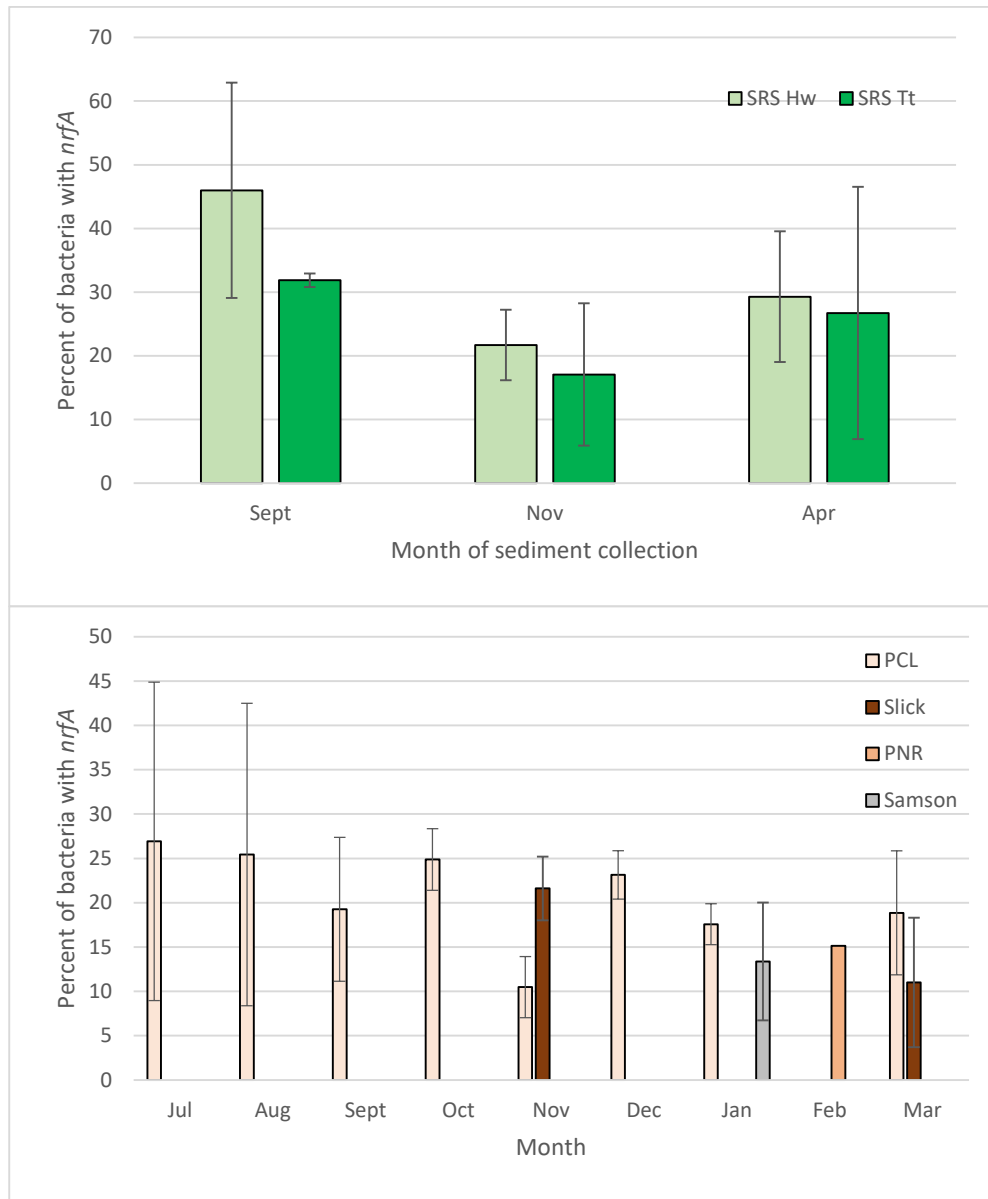
Figure 14. Percentages of total bacteria that contain the *nrfA* gene, by site and month of sediment collection.

Ammonium oxidizers (the first step in nitrification) from Archaea, Bacteria, or both, were detected in all samples. In contrast to DNRA organisms, there were fewer prokaryotes containing the *amoA* genes. While DNRA comprised >60% of bacteria in some samples, the highest percentage of prokaryotes with the nitrifying capability (having the *amoA* gene) was 55%, obtained from one SRS *Halodule* sample collected in September 2022. Two additional samples contained relatively high abundances of nitrifiers, and both were also from SRS *Halodule beds* in November and April at 46% and 24%, respectively. These few samples, however, were the exceptions. Overall, the average percentage of prokaryotes at all sites was only 5%, a value approximately 25% that obtained for the overall DNRA relative abundance throughout the study (where *nrfA* organisms comprised ~22% of total bacteria on average).

Additionally, spatial variability (core-to-core comparison within the same site on the same date) was high so there were no consistent differences between the SRS reference sites and the IRL sites (**Table 10**). In the SRS *Halodule* and *Thalassia* beds, the study-wide means were 12 $\pm$ 13 and 9 $\pm$ 15, respectively. The overall abundances of PCL and Slick sites were lower than in the SRS sites ~2 and 3%, respectively (**Table 10**). The percentage of total ammonium-oxidizing organisms (AOO) that were attributed to AOB (Bacteria *amoA*) varied from <1% to >99%. This ratio was somewhat site-specific; the mean overall AOB/AOO in the SRS-Hw (n=10) and SRS-Tt (n=11) samples were 95 and 86%, respectively. In contrast, the AOO in the PCL (n=20) and Slick (n=8) sites were more dominated by Archaeal *amoA,* where the mean AOB/AOO were 15 and 17%, respectively.

In contrast to the seasonal patterns seen with DNRA organism relative abundances, there was no decrease in *amoA* prokaryotes in the winter at either SRS reference site. Also, in contrast to DNRA patterns in the PCL, there was a seasonal pattern in *amoA* prokaryotes in the PCL site (**Figure 15**). Please note, in the March 2023 joint activities by UWF and Florida Tech personnel, the sediment samples collected from both methods (Caffrey Dome and Fox Chamber) at both PCL and Slick sites were combined in the bars shown in the bottom panel of **Figure 15** (n=6 samples at each PCL and Slick sites).

Relative abundances of AOA+AOB prokaryotes at the PCL site decreased from approximately 4-5% in July and August as the waters cooled, with a study-wide minimum range at this site from <1 to approximately 1% between October to January. Relative abundances were also low in March (approximately 1.5 and ~2.5% at PCL and Slick, respectively, **Table 10**).

Table 9. Percentages of total prokaryotes containing the *amoA* gene in 52 sediment DNA samples from the IRL sites and the Santa Rosa Sound (SRS) reference sites. Means (+/- SD) for each site and collection date are provided.

Sample Collection Date	Location	Prokaryotes containing the amoA gene as a percentage of total prokaryotes		
		Mean	SD	n
7/7/2022	PCL	3.9	4.0	2
8/9/2022	PCL	4.8	1.7	2
9/23/2022	PCL	2.7	3.0	2
9/21/2022	SRS Hw	5.6	2.7	3
9/21/2022	SRS Tt	23	28	3
10/21/2022	PCL	0.8	0.3	2
11/18/2022	PCL	0.6	0.1	2
11/2/2022	SRS Hw	20	23	3
11/2/2022	SRS Tt	3.0	1.5	4
11/21/2022	Slick	3.1	0.5	2
12/16/2022	PCL	1.1	0.6	2
1/25/2023	PCL	0.6	0.5	2
2/6/2023	PNR	15	n/a	1
1/13/2023	SAMSON	1.0	0.8	2
3/15/2023	PCL, AF Ch[1]	0.8	0.1	2
3/15/2023	Slick, AF Ch[1]	2.6	0.5	2
3/15/2023	PCL, JC Dome[1]	1.9	1.4	4
3/15/2023	Slick, JC Dome[1]	2.4	1.3	4
4/4/2023	SRS Hw	11	9	4
4/4/2023	SRS Tt	3.7	2.1	4
3/15/2023	PCL, All (n=6)[1]	1.5	1.2	6
3/15/2023	Slick, All (n=6)[1]	2.5	1.0	6
Study-wide means, SD and number of samples per site				
SRS Hw		12	13	10
SRS Tt		8.7	15	11
PCL		1.9	2.0	20
Slick		2.6	0.9	8
PNR		1.7	n/a	1
Sampson		1.0	0.8	2

[1] Overall mean during March 2023 includes data from all 6 samples collected from both chamber and dome methods. Mean of dome (n=4) and chamber (n=2) methods is reported.
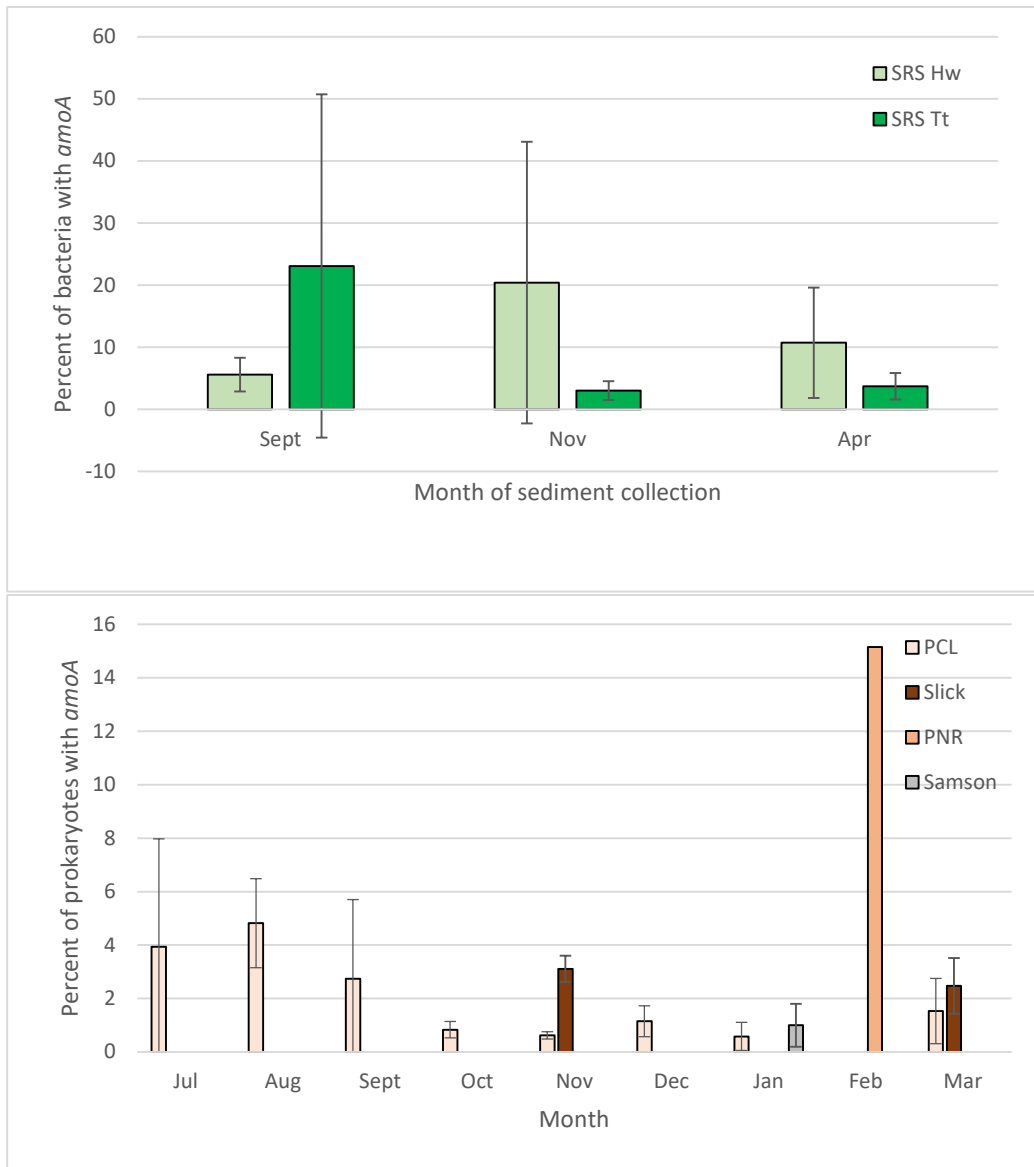
Figure 15. Percentages of total prokaryotes containing the *amoA* gene, by site and month of sediment collection.

1.5 Conclusion

- Methods for quantification of key nitrogen transforming microbes were optimized for IRL and SRS sediments.

- Relative abundances of aerobic nitrifying microbes at the Port Canaveral site had a seasonal component, while abundances of anaerobic ammonia producing microbes remained high throughout the year.

- At SRS reference sites, relative abundances of ammonia producing microbes were lowest in late fall/winter, but there was no seasonal pattern in relative abundances of aerobic nitrifying bacteria.

- Aerobic nitrogen-cycling microbes were on average nearly 5x more abundant in SRS than IRL sediments, indicating more rapid nitrogen removal in SRS sediments than in the IRL.

- Anaerobic ammonia producing microbes that can exacerbate the effects of eutrophication were on average 2 times more common relative to aerobic nitrogen-cycling microbes in the IRL than in the SRS.

- Sediment oxygen and nutrient fluxes were similar between SRS and IRL reference sites.

- Salinity in the Banana River section of IRL normally falls within the known tolerances for two dominant seagrass species, *Halodule wrightii* and *Syringodium filiorme.* Extended periods of high salinity (> 35 ppt) between 2011-2014 and low salinity in the 1990s and following the 2004 hurricane season (< 10 ppt) exceeded optimal conditions for productivity.

- The amount of light available to support seagrass growth is higher in SRS than IRL. Analysis from this study and the literature point to the need to decrease light attenuation (increasing bottom light availability) in IRL to allow seagrasses to recover.

- Despite enhanced inflow, Destin Harbor bottom waters experience episodic hypoxia likely due to high nutrient loads, water column respiration, and sediment decomposition in this organic poor system. High chlorophyll a concentrations below the pycnocline indicate substantial nutrients and light availability, which is likely driving water column and sediment decomposition reducing oxygen concentrations in the water column.

1.6 Next Steps

DNA samples from IRL sediments collected in the 2023 growing season (April to June 2023) as well as recently collected (July 2023) sediment samples from the Panhandle reference (SRS) sites will be processed for DNA extraction and qPCR using the standardized protocols developed for this project. Samples will be analyzed from benthic flux and potential nitrification experiments conducted in July 2023. These results will be combined with existing data to examine relationships among water quality parameters, sediment characteristics and relative abundances of DNRA-organisms and AOO for publication in a peer reviewed journal.

2   References

Babcock, K. K., F. Cesbron, W.F. Patterson, S.B. Garner, L.A. Waidner, and J.M. Caffrey. (2020). Changing Biogeochemistry and Invertebrate Community Composition at Newly Deployed Artificial Reefs in the Northeast Gulf of Mexico. Estuaries and Coasts, 43(4), 680–692. https://doi.org/10.1007/s12237-020-00713-4

Biber, P. (2022). Prolonged low salinity tolerance in Halodule wrightii Asch. Aquatic Botany, 178, 103498. https://doi.org/10.1016/j.aquabot.2022.103498

Bowman, L.T. in prep. Seasonal variation of epiphyte abundance and nitrogen fixation rates of two seagrass species in the Pensacola Bay System. Master's thesis. University of West Florida.

Boynton, W.R., M.A.C.Ceballos, E.M. Bailey, C.L.S. Hodgkins, J.L. Humphrey, and J.M. Testa. (2018). Oxygen and Nutrient Exchanges at the Sediment-Water Interface: A Global Synthesis and Critique of Estuarine and Coastal Data. Estuaries and Coasts, 41(2), 301–333. https://doi.org/10.1007/s12237-017-0275-5

Caffrey, J.M. R. O'Conner, C. Verlinde, B. Albrecht, M. Harvey, and I. Orrantia. 2023. Citizen Science Seagrass Monitoring Report 2022. Center for Environmental Diagnostics and Bioremediation. University of West Florida. https://ircommons.uwf.edu/esploro/outputs/99380176397306600

Caffrey, J.M., N. Bano, K. Kalanetra, and J.T. Hollibaugh. (2007). Ammonia oxidation and ammonia-oxidizing bacteria and archaea from estuaries with differing histories of hypoxia. The ISME Journal, 1(7), 660–662. https://doi.org/10.1038/ismej.2007.79

Cesbron, F., M.C. Murrell, M.E. Hagy, W.H. Jeffrey, W.F. Patterson, and J.M. Caffrey. (2019). Patterns in phytoplankton and benthic production on the shallow continental shelf in the northeastern Gulf of Mexico. Continental Shelf Research, 179, 105–114. https://doi.org/10.1016/j.csr.2019.04.003

Henriksen, K., J.I. Hansen, and T.H. Blackburn. (1981). Rates of nitrification, distribution of nitrifying bacteria and nitrate fluxes in different types of sediment from Danish waters. Marine Biology, 61, 299–304.

Hester, C. M., H.M. Smith, M.E. Head, H. Langsten, S. Linder, E. Manor, J. Norman, L. Sartory, and J.M. Caffrey. (2016). Comparing productivity and biogeochemistry of native and transplanted thalassia testudinum and halodule beaudettei in big Lagoon, Florida, USA. Gulf of Mexico Science, 1, 14–25.

Holmes, R. M., A. Aminot, R. Kerouel, B.A. Hooker, and B.J. Petersen, B. J. (1999). A simple and precise method for measuring ammonium in marine and freshwater ecosystems. Can. J. Fish. Aquat. Sci, 56, 1801–1808.

Hornek, R., A. Pommerening-Röser, H-P. Koops, A.H. Farnleitner, N. Kreuzinger, A. Kirschner, and R.L. Mach. (2006). Primers containing universal bases reduce multiple amoA gene specific DGGE band patterns when analysing the diversity of beta-ammonia oxidizers in the environment. Journal of Microbiological Methods, 66(1), 147–155. https://doi.org/10.1016/j.mimet.2005.11.001

Kesanopoulos, K., G. Tzanakaki, S. Levidiotou, C. Blackwell, J. Kremastinou, J. (2005). Evaluation of touch-down real-time PCR based on SYBR Green I fluorescent dye for the detection of Neisseria meningitidis in clinical samples. FEMS Immunology and Medical Microbiology, 43(3), 419–424. https://doi.org/10.1016/j.femsim.2004.10.011

Landers-Atkins Planners, Inc. (1987). Destin Harbor Management Plan, City of Destin, Florida. September 8, 1987. DER Contract No. CM-176.

Lapointe, B. E., L.W. Herren, R.A. Brewton, and P.K. Alderman. (2020). Nutrient over-enrichment and light limitation of seagrass communities in the Indian River Lagoon, an urbanized subtropical estuary. Science of The Total Environment, 699, 134068. https://doi.org/10.1016/j.scitotenv.2019.134068

Lee, K.-S., S.R. Park, and Y.K. Kim. (2007). Effects of irradiance, temperature, and nutrients on growth dynamics of seagrasses: A review. Journal of Experimental Marine Biology and Ecology, 350(1–2), 144–175. https://doi.org/10.1016/j.jembe.2007.06.016

Lirman, D., and W.P. Cropper. (2003). The influence of salinity on seagrass growth, survivorship, and distribution within Biscayne Bay, Florida: Field, experimental, and modeling studies. Estuaries, 26(1), 131–141. https://doi.org/10.1007/BF02691700

Lipnicky, C.D. (1996) Council Ponders Pump System. Northwest Florida Daily News, December 7, 1996. 379494590. U.S. Southeast Newsstream. https://login.ezproxy.lib.uwf.edu/login?url=https://www.proquest.com/newspapers/council-ponders-pump-system/docview/379494590/se-2?accountid=14787

Livak, K. J., and T.D. Schmittgen. (2001). Analysis of relative gene expression data using real-time quantitative PCR and the 2(-Delta C(T)) Method. Methods (San Diego, Calif.), 25(4), 402–408. https://doi.org/10.1006/meth.2001.1262

Meinhardt, K. A., A. Bertagnolli, M.W. Pannu, S.E. Strand, S.L. Brown, D.A. Stahl. (2015). Evaluation of revised polymerase chain reaction primers for more inclusive quantification of ammonia-oxidizing archaea and bacteria. Environmental Microbiology Reports, 7(2), 354–363. https://doi.org/10.1111/1758-2229.12259

Mohan, S. B., M. Schmid, M. Jetten, and J. Cole. (2004). Detection and widespread distribution of the nrfA gene encoding nitrite reduction to ammonia, a short circuit in the biological nitrogen cycle that competes with denitrification. FEMS Microbiology Ecology, 49(3), 433–443. https://doi.org/10.1016/j.femsec.2004.04.012

Morris, L, L. Hall, R. Chamberlain, and C. Jacoby. (2018). Summary report for the Northern Indian River Lagoon. In Seagrass Integrated Mapping and Monitoring Program. Mapping and Monitoring Report No. 3. Editors. L.A Yarbro and P.R. Carlson Jr. Technical Report 17, Version 3. 2018. Florida Fish and Wildlife Conservation Commission. Fish and Wildlife Research Institute. DOI10.13140/RG.2.2.12366.05445

Morris, L.J., L.M. Hall, C.A. Jacoby, R.H. Chamberlain, M.D. Hanisak, J.D. Miller, and R.W. Virnstein. (2022). Seagrass in a Changing Estuary, the Indian River Lagoon, Florida, United States. Frontiers in Marine Science, 8, 789818. https://doi.org/10.3389/fmars.2021.789818

Northwest Florida Daily News (NWFDN). BRIEFS LOCAL" June 3, 2005. 379430140. U.S. Southeast Newsstream.

Parsons, T. R., Y. Maita, and C.M. Lalli. (1984). A manual of chemical and biological methods for seawater analysis. Pergamon Press.

Presley, R., and J.M. Caffrey. (2021). Nitrogen Fixation in Subtropical Seagrass Sediments: Seasonal Patterns in Activity in Santa Rosa Sound, Florida, USA. Journal of Marine Science and Engineering, 9(7), Article 7. https://doi.org/10.3390/jmse9070766

Rothfus, M. J. (2022). Sediment Biogeochemistry Response to Stingray Bioturbation in Halodule wrightii [M.S., The University of West Florida]. https://www.proquest.com/docview/2705870638/abstract/E5CEF9B91D0B4DD1PQ/1

Rotthauwe, J. H., K.P. Witzel, and W. Liesack. (1997). The ammonia monooxygenase structural gene amoA as a functional marker: Molecular fine-scale analysis of natural ammonia-oxidizing populations. Applied and Environmental Microbiology, 63(12), 4704–4712. https://www.ncbi.nlm.nih.gov/pmc/articles/PMC168793/

Schnetger, B., and C. Lehners. (2014). Determination of nitrate plus nitrite in small volume marine water samples using vanadium(III)chloride as a reduction agent. Marine Chemistry, 160, 91–98. https://doi.org/10.1016/j.marchem.2014.01.010

St. Johns River Water Management District (SJRWMD) 2022. 2022 Status and Trends Report. https://www.sjrwmd.com/data/water-quality/#status-trends

Suzuki, M. T., L.T. Taylor, and E.F. DeLong. (2000). Quantitative Analysis of Small-Subunit rRNA Genes in Mixed Microbial Populations via 5′-Nuclease Assays. Applied and Environmental Microbiology, 66(11), 4605–4614. https://doi.org/10.1128/AEM.66.11.4605-4614.2000

Waidner, L. A., and D.L. Kirchman. (2007). Aerobic anoxygenic phototrophic bacteria attached to particles in turbid waters of the Delaware and Chesapeake estuaries. Applied and Environmental Microbiology, 73(12), 3936–3944. https://doi.org/10.1128/AEM.00592-07

Ward, B. B. (2008). Nitrification in Marine Systems. In Nitrogen in the Marine Environment, edited by D. C. Capone, D. A. Bronk, M. R. Mulholland, and E. J. Carpenter, 199–261. Amsterdam: Elsevier.

Welschmeyer, N. A. (1994). Fluorometric analysis of chlorophyll a in the presence of chlorophyll b and pheopigments. Limnology and Oceanography, 39(8), 1985–1992. https://doi.org/10.4319/lo.1994.39.8.1985

Appendix E   Task 4 – Brevard Zoo Biology Report

Restore Lagoon Inflow Research (Phase 3)
Final Report
Brevard Zoo

PREPARED FOR

Florida Institute of Technology
150 West University Boulevard
Melbourne, FL 32091

FLORIDA TECH

PREPARED BY

Olivia Escandell
Brevard Zoo
8225 North Wickham Rd
Melbourne, FL 32940

July 2023

Acknowledgements

Highlights

- Total seagrass cover ranged from 0.1% to 3.88% at Banana River North sites and from 0% to 0.5% at Banana River South sites

- Seagrass cover increased at Banana River North sites from spring 2021 to summer 2023 but no significant change in cover was observed at Banana River South sites.

- Some sampling locations which once boasted dense seagrass beds, were devoid of seagrass throughout the study period.

- Drift algae and rooted macroalgae (*Caulerpa prolifera*) coverage was seasonal and highest in summer 2023 (15.6 - 24.6%).

- Improvements to water quality in the Banana River lagoon are necessary to expand seagrass cover and restore this essential benthic habitat.

Project Staffing (includes part-time and full-time project staff)

Staff – Ashley Rearden, Olivia Escandell, Adam Klingenberg, Tyler Provoncha, Hope Leonard, Virginia Wine, Kelsey Koonce, Amber Santoso, Liam Corcoran

Volunteers – Caroline Muscat, Erin Cassidy

Table of Contents

Table of Figures

List of Acronyms

cm	centimerters
m	meters
m^2	square meters

1   Introduction

The Banana River of the Indian River Lagoon supports seagrass and rooted macro-algae beds which provide critical habitat to lagoon life. In an effort to establish baseline benthic habitat conditions prior to lagoon inflow piloting, seagrass and other submerged aquatic vegetation were surveyed at sites in the northern and southern Banana River Lagoon during three phases between fall 2019 and summer 2023.

1.1   Approach

Phase 3 sampling locations were selected in two general areas of the Indian River Lagoon: Banana River North and Banana River South. Banana River North sites lay nearest the proposed inflow site at Port Canaveral and Banana River South was chosen to represent baseline controls away from the treatment site. An additional site in Vero Beach was sampled during Phase 1 of the project as part of an assessment of candidate inflow sites. Six locations in the Banana River Lagoon were sampled during Phase 1, 2, and 3 of the Restore Lagoon Inflow Project. Six additional shallow, sandy sites consistent with historic seagrass habitat conditions were selected on the eastern shoreline of the Banana River Lagoon to sample in spring and summer 2023 to strengthen sample size.

At each location, a 100 meter (m) long transect was surveyed with standard methods used to evaluate seagrass in the Indian River Lagoon (Virnstein and Morris, 1996; Morris et al., 2001). The transect lines were run perpendicular to shore and a 1 square meter (m^2) quadrat with 100 equal cells was used to collect the following every 10 m along the transect: seagrass visual % cover (estimated coverage upon imagining the seagrass crowded into corner of quadrat at a high density), seagrass % occurrence (proportion of 100 quadrat cells having at least 1 blade of seagrass), seagrass shoot density, seagrass canopy height, drift algae % occurrence (proportion of 100 quadrat cells that contain any drift algae), drift algae biomass (scale of 0 to 5), drift algae canopy height, rooted macro algae visual % cover (estimated coverage upon imagining the rooted macro algae crowded into corner of quadrat at a high density), and rooted macro algae % occurrence (proportion of 100 quadrat cells that contain any rooted macro algae). Sampling occurred twice at each site between March and June 2023.
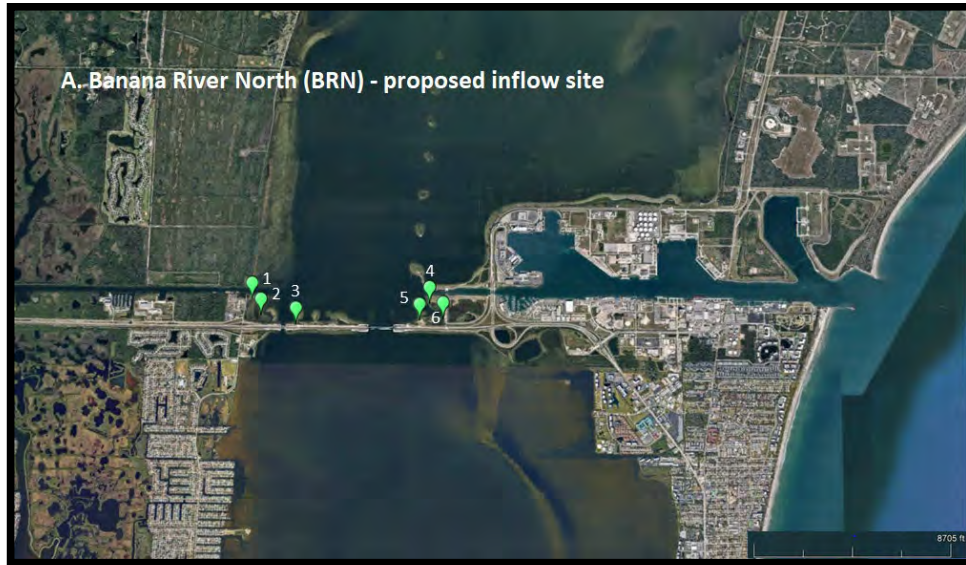
Figure 1. Banana River North submerged aquatic vegetation sampling sites shown in green, numbered 1-6 (n=6).


Figure 2. Banana River South submerged aquatic vegetation sampling sites shown in green, numbered 7-12 (n=6).

1.2 Results

1.2.1 Submerged Aquatic Vegetation Results for Phase 3

Seagrass presence varied across all sites and when present, was mostly sparse. Two species of seagrass were observed in sampling, Widgeon grass (*Ruppia maritima*) and Cuban shoalgrass (*Halodule wrightii*) (Figure 4 and 5). No seagrass was observed in 2023 at five of the sampling sites: the three westernmost sites in Banana River North (transects #4, #5, #6) and the two southernmost sites in the west portion of Banana River South (transects #11 and #12).

Mean total seagrass visual percent cover was highest at the sites in Banana River North during both sampling events (1.1% in spring and 2.5% in summer). *R. maritima* was the only seagrass species observed at sites in Banana River South, while both *R. maritima* and *H. wrightii* were observed at the easternmost sites in Banana River North. *R. maritima* made up 86% of observed total seagrass cover in Banana River North in spring. In summer, mean cover increased for both *R. maritima* and *H. wrightii* in Banana River North (0.96% to 1.23% and 0.15% to 1.28%, respectively), shifting species composition more evenly between the two. Mean seagrass cover at Banana River South sites fell from 0.62% to 0.31% in summer 2023 (Figure 3).
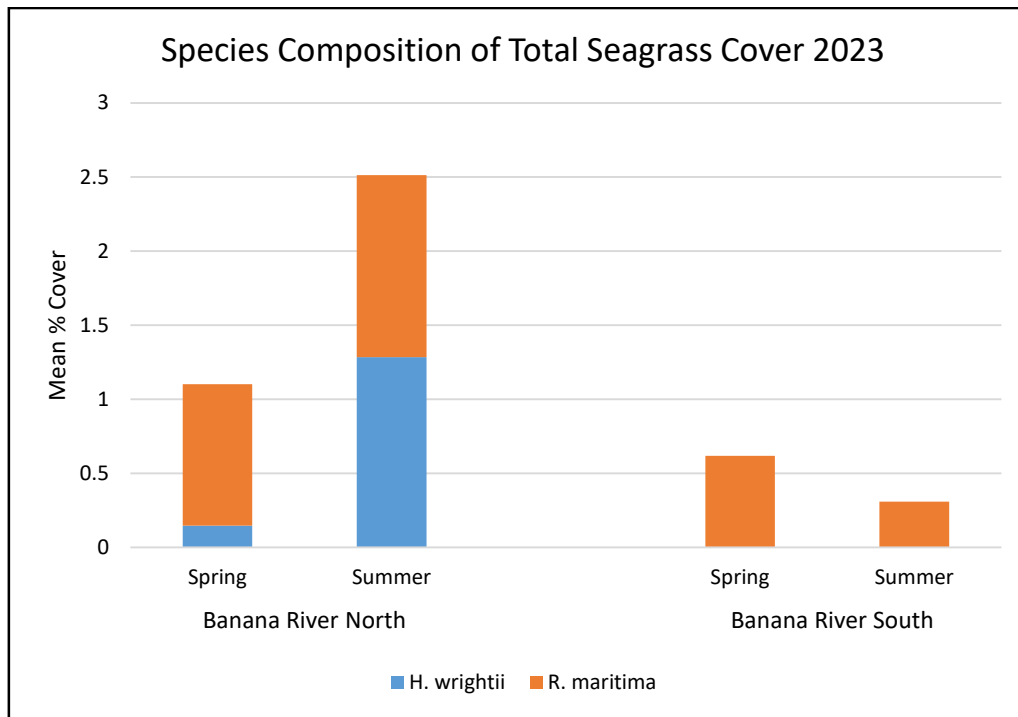
Figure 3. Species composition of mean total visual percent seagrass cover for Banana River North and Banana River South sites spring and summer 2023. Observed species of seagrasses include *Ruppia maritima* and *Halodule wrightii*.

During both monitoring events, patchy seagrass occurred throughout the length of the transect when present (Figure 7 and 8). However, patches of *R. maritima* occurred 0 to 100 m from shore while *H. wrightii* was only observed between 0 and 70 m from shore with the densest patches (9-29%) occurring in shallow depths only 10 to 20 m from shore. Epiphyte biomass on seagrass remained low across all sites through both sampling events (0.3 in spring and 0.27 in summer on a 0 to 5 scale). Mean canopy height for *H. wrightii* rose from 9.1 centimeters (cm) to 13 cm

between spring and summer at sites in Banana River North. Mean canopy height for *R. maritima* rose from 6.5 cm to 6.9 cm between both seasons in Banana River North and from 4.9 cm to 13.6 cm in Banana River South. Maximum canopy height sampled for *R. maritima* in Banana River South was 48 cm with branching formation and flowering observed (Figure 5).

Unrooted drift algae species and rooted macroalgae *Caulerpa prolifera* were observed at each sampling site and cover for both increased in summer sampling (Figure 6). Species of drift algae observed included *Gracilaria spp.*, *Chaetomporpha spp.*, and *Trichosolen spp*. Percent occurrence of drift algae ranged from 0 to 96% across sites and mean percent occurrence was highest at Banana River South sites in summer when mean percent occurrence increased from 1.7% to 25.92%. (Figure 9 and 10). *C. prolifera* formed dense patches at many sites and percent covers observed ranged from 0 to 100%. Mean percent cover of *C. prolifera* remained stable in Banana River North sites between spring and summer (15.5% to 15.6%) while percent cover increased from 16.3% to 24.6% in Banana River South sites (Figure 11 and 12).
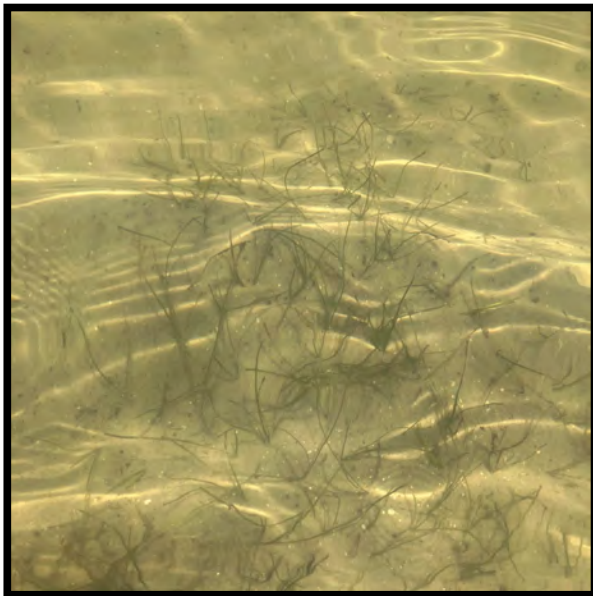
Figure 4. Cuban shoalgrass or *Halodule wrightii* near transect #1 in Banana River North.

Figure 5. Branching form of Widgeon grass or *Ruppia maritima* growing in a dense patch of rooted macro algae *Caulerpa prolifera* near transect #1 in Banana River North.
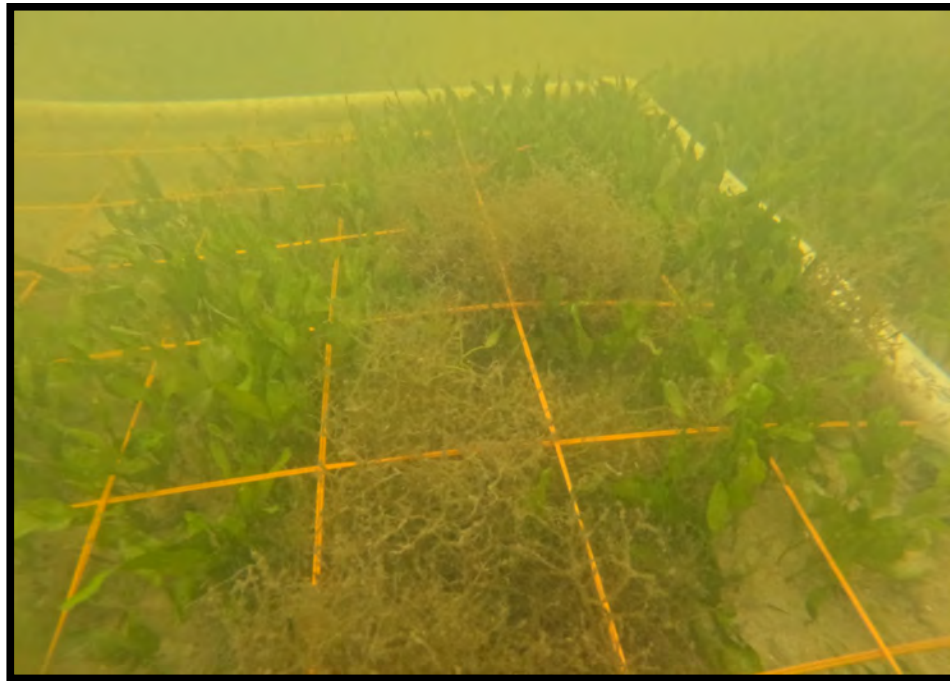
Figure 6. Rooted macro algae (*Caulerpa prolifera)* and drift algae (*Gracilaria spp.*) near transect #7 in Banana River South.
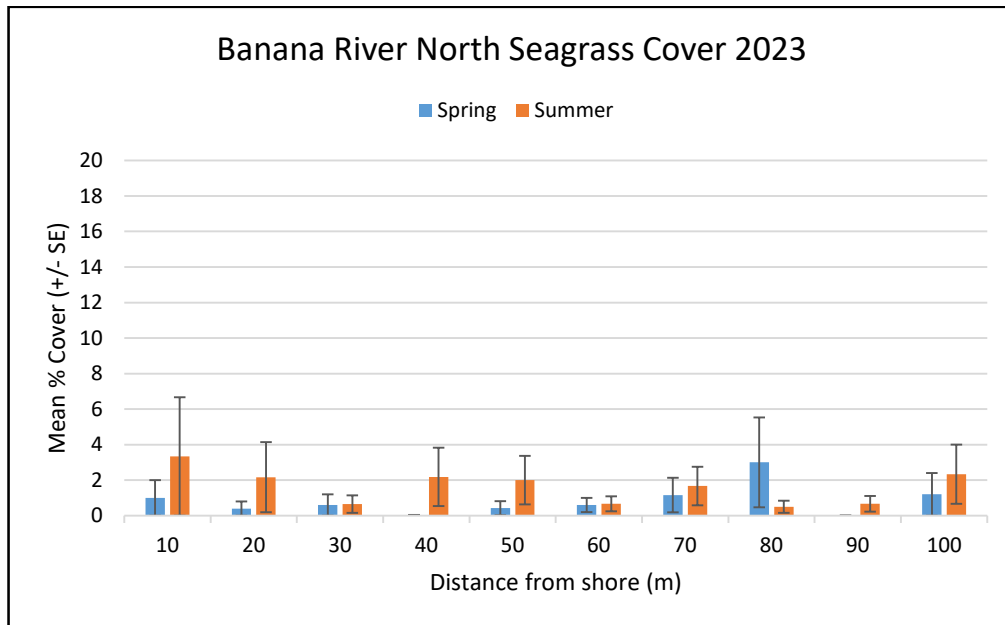
Figure 7. Mean total seagrass visual percent cover for Banana River North sites spring and summer 2023.
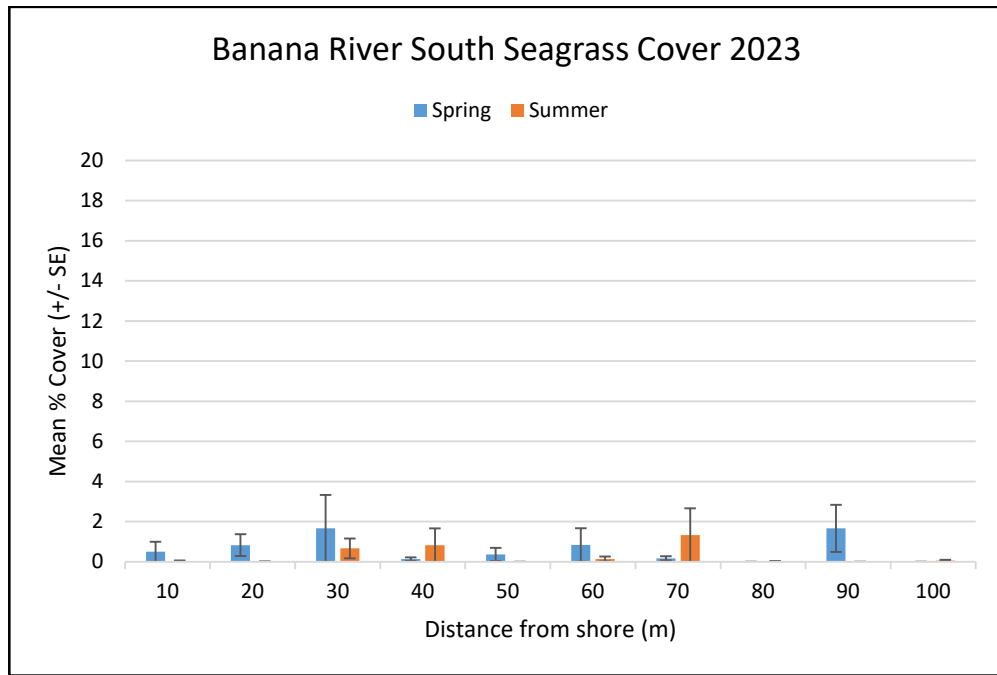
Figure 8. Mean total seagrass visual percent cover for Banana River South sites spring and summer 2023.
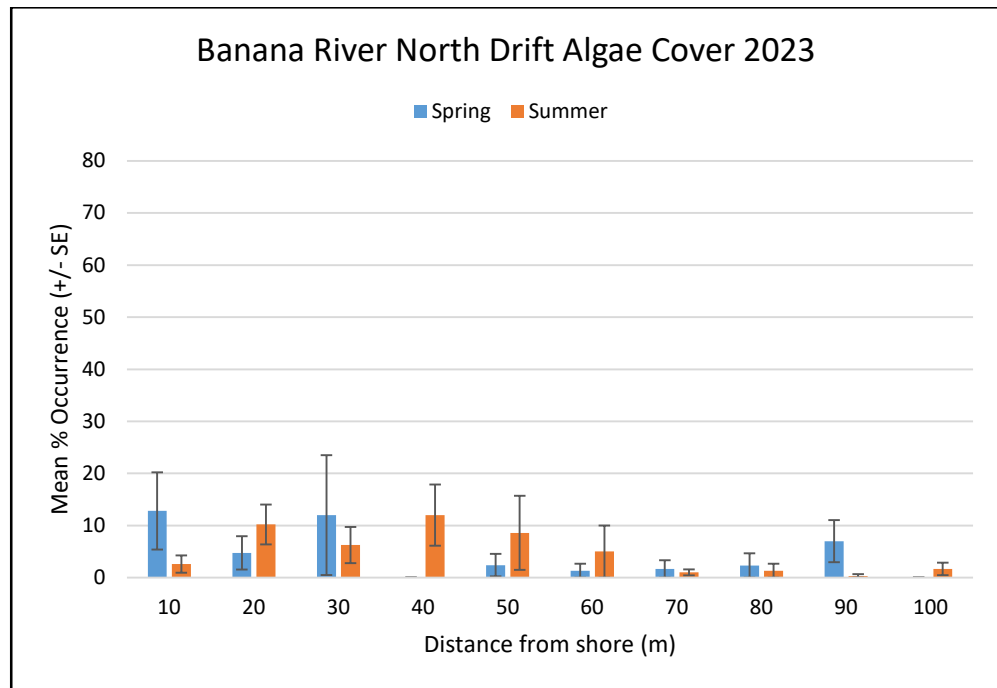
Figure 9. Mean percent occurrence of drift algae for Banana River North sites spring and summer 2023.
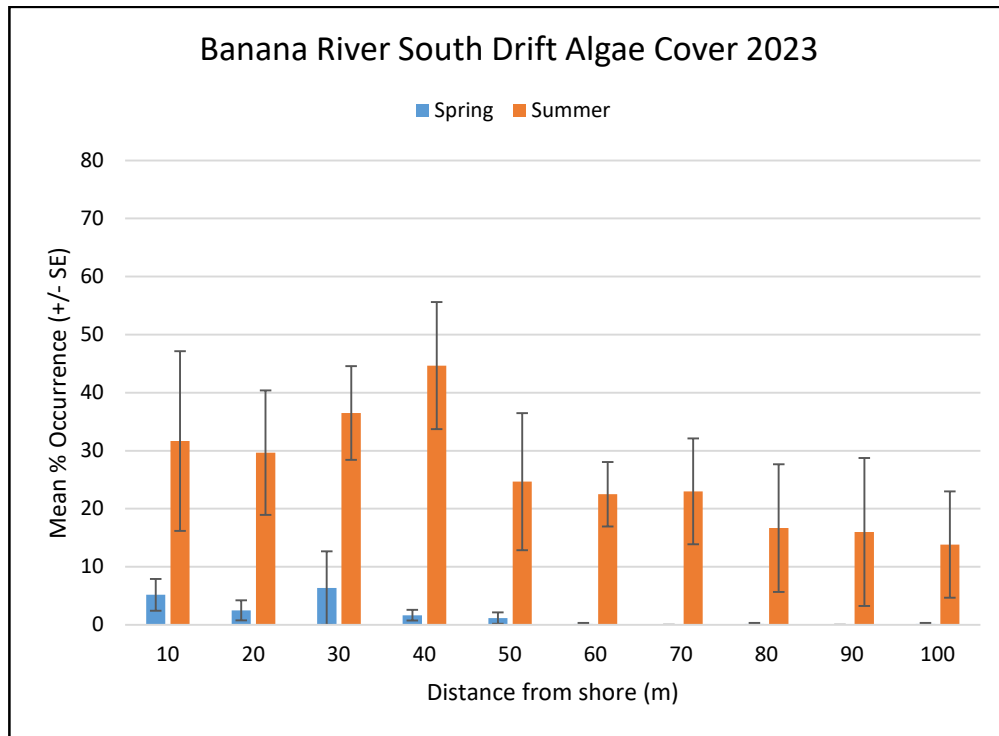
Figure 10. Mean percent occurrence of drift algae for Banana River South sites spring and summer 2023.
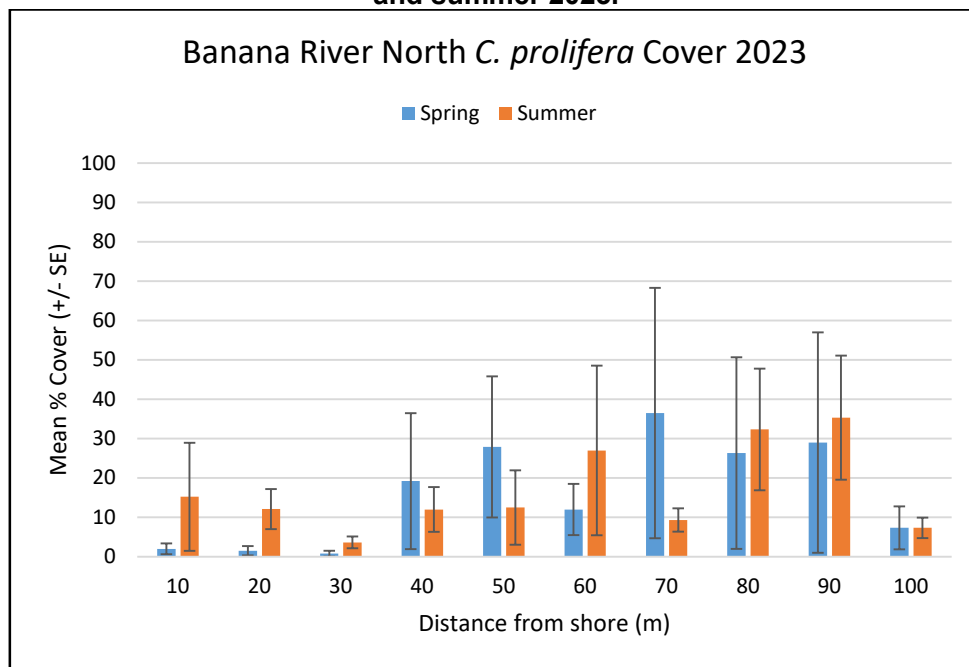
Figure 11. Mean visual percent cover of *Caulerpa prolifera* for Banana River North sites in spring and summer 2023.
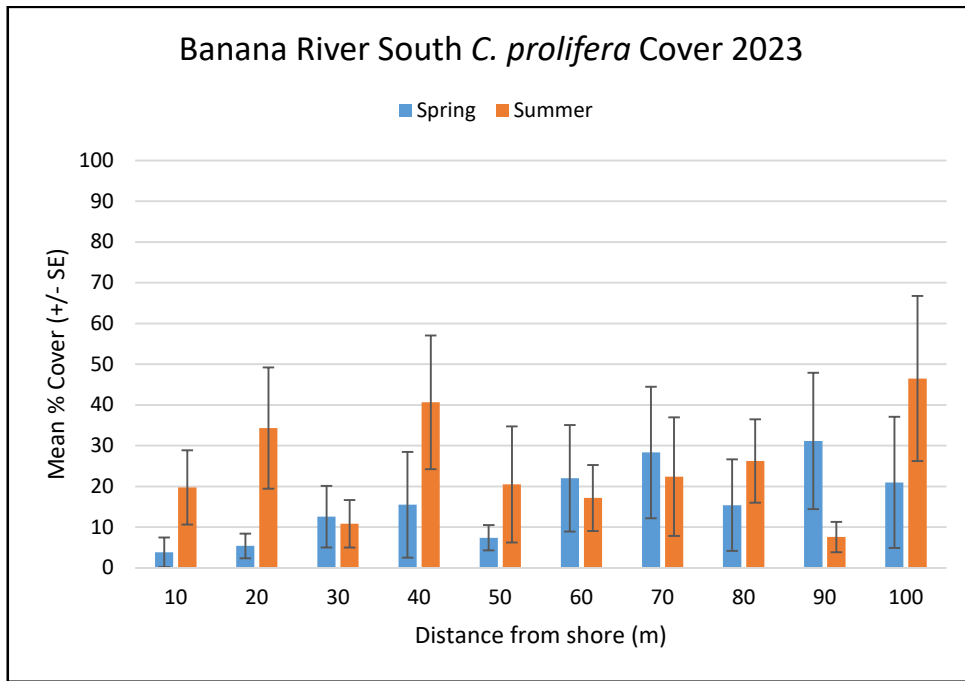
Figure 12. Mean visual percent cover of *Caulerpa prolifera* for Banana River South sites in spring and summer 2023.

1.2.2 Seagrass Results for Phases 1 through 3

Of the six sites surveyed continuously during all three project phases (transects #1, #2, #3, #7, #8, and #9), mean total visual seagrass cover was highest at Banana River North sites in summer 2023. Total seagrass cover ranged from 0.1% to 3.88% at Banana River North sites and 0% to 0.5% at Banana River South sites (Figure 13 and 14). Banana River North experienced positive growth in mean total visual seagrass cover from March 2021 to summer 2023. Mean total visual seagrass cover was more stable at the Banana River South sites throughout the three phases and did not mimic the growth trend observed at Banana River North sites in the latter half of the project.

Drift algae and *C. prolifera* cover were dynamic throughout the study in both Banana River North and Banana River South. Trends in drift algae cover at Banana River North and Banana River South sites were similar, with peaks in winter 2020 and summer 2021, until summer of 2023 when mean drift algae cover reached its highest point at Banana River South (34.1%) while mean cover in Banana River North stayed relatively low (4.6%). Cycles of *C. prolifera* cover at Banana River North and Banana River South sites did not trend as closely as drift algae cover, reaching peaks in different seasons. The highest mean percent cover of *C. prolifera* occurred in Banana River South sites in spring 2020 (27%).

Additional results from Phase 1 and 2 sampling can be found in previous reports (Eble et al. 2021, Shelton et al. 2020).
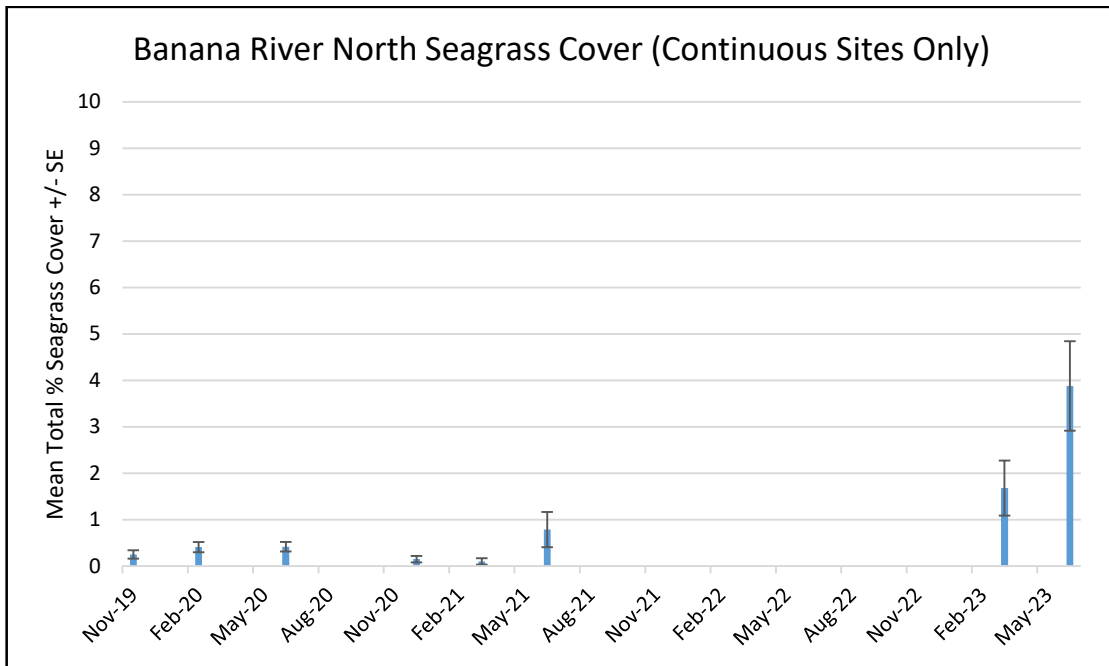
Figure 13. Mean total visual percent cover of seagrass of Banana River North sites surveyed fall 2019 to summer 2023 (transects #1, #2, and #3 only).
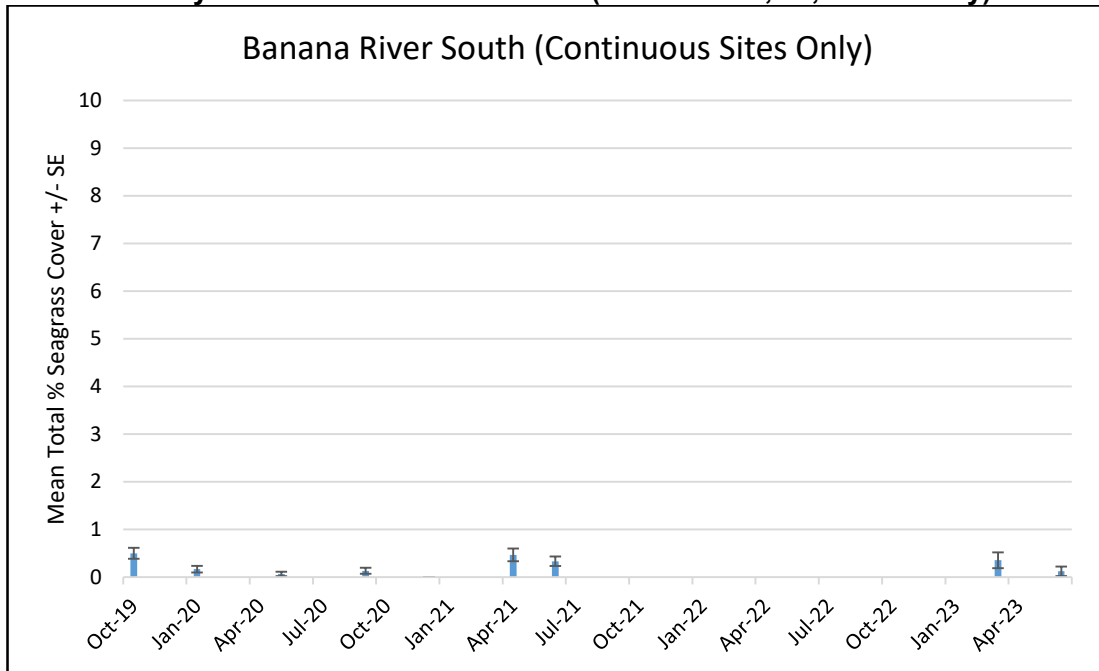

Figure 14. Mean total visual percent cover of seagrass of Banana River South sites surveyed fall 2019 to summer 2023 (transects #7, #8, #9 only).

1.3 Conclusion

Since 2011, the Indian River Lagoon has lost approximately 58% of seagrass coverage (Morris et al. 2022). These losses are evident in current seagrass conditions of the Banana River Lagoon as seagrass coverage was low at most sampling locations throughout the study. Some sampling locations which once boasted dense seagrass beds, were devoid of seagrass throughout the study period. Additionally, coverage of other submerged aquatic vegetation including drift algae species and rooted macroalgae species *Caulerpa prolifera* were inconsistent and ephemeral through the study. Without established seagrass beds or stable macroalgae communities, the Banana River Lagoon lacks essential benthic habitat and will continue to suffer from nutrient resuspension as algae and seagrass populations go through cycles of growth and collapse.

In Phase 3, sites in Banana River North exhibited increases in seagrass cover and species composition that may be consistent with signs of recovery of seagrass populations, but water quality conditions remain dynamic in the area. Several months of reduced water clarity brought on by nutrient pollution driven algae blooms could reverse progress. Improvements to water quality in the Banana River lagoon are necessary to expand seagrass cover and restore benthic habitat.

2   References

Eble, J.A, et al. 2021. Restore Lagoon Inflow Research Project Phase 2 Project Summary. Florida Department of Education. https://www.fit.edu/media/site-specific/wwwfitedu/indian-river-lagoon/documents/irlri-research/Final-Phase-2-Final-Project-Report_091521.pdf

Morris, L.J., Hall, L.M., Jacoby, C.A., Chamberlain, R.H., Hanisak, D.M., Miller, J.D., Virnstein, R.W. 2022. Seagrass in a Changing Estuary, the Indian River Lagoon, Florida, United States. https://doi.org/10.3389/fmars.2021.789818

Morris, L.J., Hall, L.M., Virnstein, R.W. 2001. Field guide for fixed seagrass transect monitoring in the Indian River Lagoon. St. Johns River Water Management District, Palatka, Florida.

Shelton, et al. 2020. Restore Lagoon Inflow Research Project Phase 1 Project Summary. Florida Department of Education. https://www.fit.edu/media/site-specific/wwwfitedu/indian-river-lagoon/documents/State-of-Florida-Restore-Lagoon-Inflow-Research-Phase-1-Full-Report-2020.pdf

Virnstein, R.W., Morris, L.J. 1996. Seagrass preservation and restoration: A diagnostic plan for the Indian River Lagoon. SJRWMD, Tech. Memorandum No. 14, Palatka, Florida.

Appendix F   Task 4 – FWC Biology Report

Restore Lagoon Inflow Research (Phase 3) Final Report
Florida Fish and Wildlife Conservation Commission, Florida Fish and Wildlife Research Institute

Acknowledgements

Project Staffing (includes part-time and full-time project staff)

Non-faculty –   Richard Paperno
                Autumn Biddle
                Shelby Casali
                Jessica Schieber
                Shawna Landers
                Drew Mertzlufft

Highlights

- Fish in the proposed inflow area was more diverse than the control site (30 vs. 23 taxa).

- The difference in fish abundance was a result of the greater number of Bay Anchovies (*Anchoa mitchilli*) collected at the inflow sites (n = 29,623) versus the control sites (n = 2,134).

Table of Contents

List of Figures

List of Tables

List of Appendicies

List of Acronyms

BR	Banana River
$^\circ$C	Degrees Celsius
CV	Coefficient of Variation of the Mean
DO	Dissolved Oxygen
FIM	Fisheries-Independent Monitoring Program
Florida Tech	Florida Institute of Technology
FWC-FWRI	Florida Fish and Wildlife Conservation Commission, Florida Fish and Wildlife Research Institute
IRL	Indian River Lagoon
km	kilometer
m	meter
mm	millimeter
PPM	Parts Per Million
PVC	Polyvinyl Chloride
SL	Standard Length
SRS	Stratified-Random Sampling

1   Introduction

Prolonged algal blooms have had a substantial negative impact on the seagrass beds in much of the Indian River Lagoon (IRL). In late 2010 and early 2011, an unusually large phytoplankton "superbloom" and subsequent loss of seagrass occurred throughout much of the IRL, which prompted a multi- agency effort to understand and monitor the impacts of these changes to the lagoon ecosystem (IRL 2011 Consortium, 2012; Phlips et al, 2015). The Florida Institute of Technology (Florida Tech) received funding from the Florida Legislature in 2020 for the first phase of the Restore Lagoon Inflow Project, which was designed to examine the viability of a permanent ocean inflow system as a tool to assist with stabilizing and restoring the IRL (Johnson et al., 2020). Phase 1 of the project involved modelling responses of the physical and biological components of the central portion of the Banana River (BR) to the project, Phase II involved designing a system to pump ocean water into the system, and Phase III will involve a pilot project in the Banana River basin of the IRL to test the design. To quantify the scale of the impact to the BR nekton community (Phase 1), quantitative sampling data are needed from the test site and from a suitable control site within the basin.

The nekton community of the BR basin was sampled by the Florida Fish and Wildlife Conservation Commission, Florida Fish and Wildlife Research Institute's (FWC-FWRI) Fisheries-Independent Monitoring Program (FIM) between 1990 until 2016 (Tremain and Adams, 1995; Paperno et al., 2016; FWC-FWRI, 2017), after which budgetary restrictions resulted in these efforts being discontinued. As a result of the reduction in effort from this basin, the status of the small-bodied nekton community in the BR has been largely undocumented over the past several years.

The objective of this sampling project was to provide a current account of nekton abundance and species richness in close proximity of the proposed Restore Lagoon Inflow Project and at a control site approximately 12.5 kilometers (km) south in the BR **(Figure 1)**, that will function as a baseline to evaluate future changes that may occur under pilot project conditions.
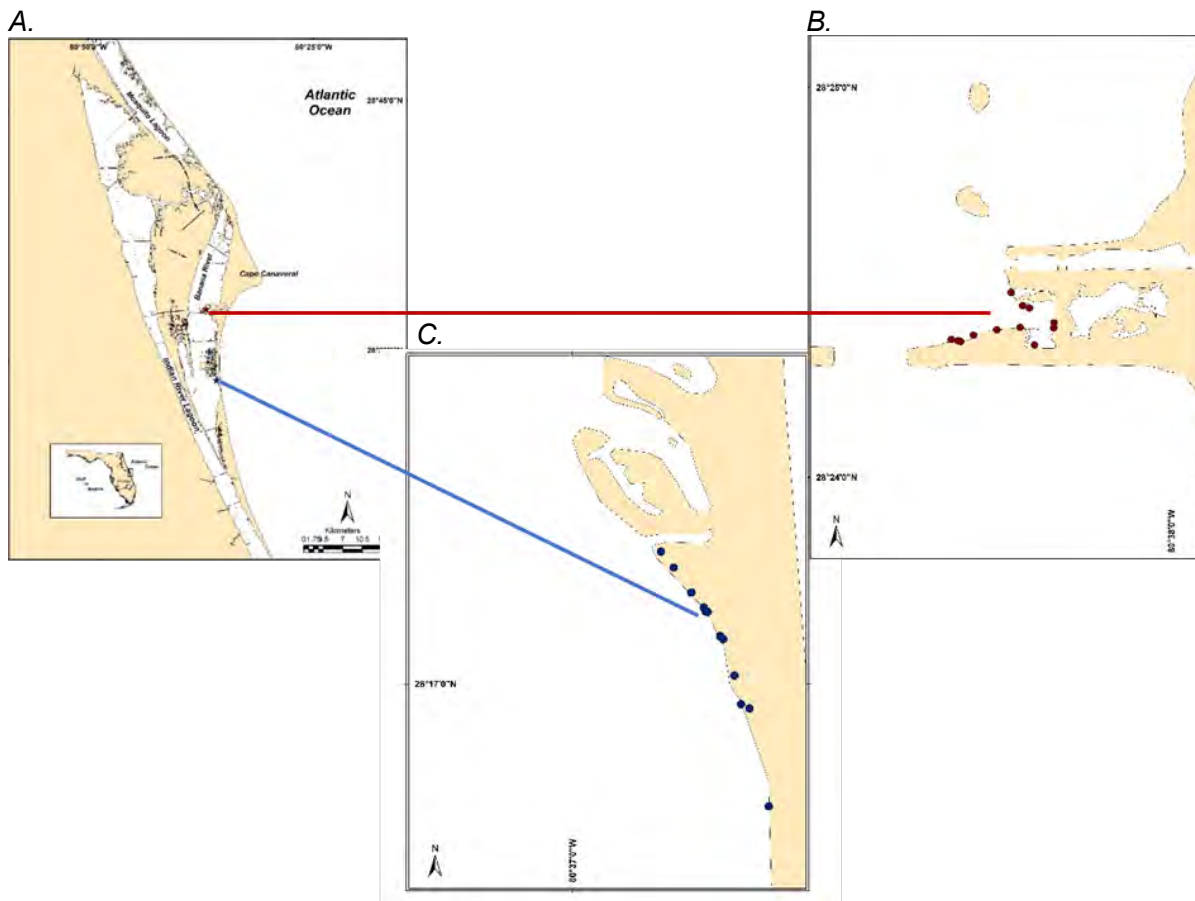
Figure 1. Map of Banana River (Map A.), location of study sites within Banana River (Maps B. and C) in Brevard County, FL. Red circles=21.3-m shore seines at the inflow site; Blue circles = 21.3-m shore seines at the control site.

1.1 Approach

Beginning in March 2023 and continuing through June 2023, stratified-random sampling (SRS) was conducted to provide comprehensive abundance and distribution data on fishes that occur at two sites in the BR. Sampling events occurred in March, May, and June 2023 and consisted of eight randomly selected 21.3-meter (m) seine stations split evenly between the proposed inflow site near Cape Canaveral in the BR and a control site located approximately 12.5 km south in the BR (**Table 1, Figure 1**). All sampling was conducted during daytime hours (one hour after sunrise to one hour before sunset). Environmental data consisting of standardized FIM water quality parameters including water temperature in degees celcius (°C), salinity in parts per thousand (ppt), conductivity, pH, and dissolved oxygen (DO) in parts per mipllion (ppm) were recorded with a YSI multiprobe instrumen); comprehensive habitat characteristics (e.g., seagrass coverage, shore type, substrate composition); and physical parameters such as current, tidal conditions, and water clarity were recorded for each sample (FWC-FWRI, 2023). The sample work-up technique was standardized for all collected samples. All fish and selected invertebrates (i.e., stone crabs, Penaeid shrimp, horseshoe crabs, cannonball jellyfish, and Callinectes crabs) captured in net collections were identified to the lowest practical taxonomic level, counted, and measured (standard length [SL] for teleosts, disk width for rays, carapace width for crabs, post-

orbital head length for shrimp). During each sampling event, representative samples of each taxon were returned to the laboratory for quality control purposes; fish not identified to the lowest taxonomic level in the field were returned to the laboratory for further identification. Detailed explanations of the standard sample work-up and processing for data collection are described in the FIM program's Procedure Manual (FWC-FWRI, 2023).

Mean water quality data were plotted to examine changes in the physical environment between the areas during the four-month sampling period. Data were pooled and summarized for the overall project for all taxa. Data were also summarized separately for taxa of recreational or commercial importance ('Selected Taxa'; Appendix-1). In addition, data were summarized by site (inflow and control) for the 2023 sampling period.

The taxonomic nomenclature in this report follows the American Fisheries Society's Common and Scientific Names of Fishes (Page et al. 2013). Certain taxa were not identified to species because of the possibility of hybridization (e.g., Menhaden, Brevoortia spp., and Silversides, Menidia spp.; Dahlberg 1970; Middaugh et al. 1986) or because they were indistinguishable based on morphological or meristic characteristics at small juvenile sizes (e.g., Mojarras, Eucinostomus spp. < 40 milimeters (mm) SL; Matheson 1983). These aggregated species were treated as a single species for reporting purposes and determination of species richness. Common names are reported in the text the first time a species is referenced and in Appendices.

Table 1. Sample effort within each area.

Area	21.3-m seine	Total
Inflow site	Three sampling events (4 shore seines)	12
Control site	Three sampling events (4 shore seines)	12
Total Hauls	8	24

1.1.1 GEAR DESCRIPTION: 21.3-m seine

The 21.3-m (70 feet) seine is made of 1/8-inch #35 knotless nylon stiff material Delta mesh with #7 (or comparable) finish. The net is exactly 70 feet long and six feet high with 6 feet by 6 feet by 6 feet bag placed in the center. The top and bottom lines are 1/8-inch 450-pound test braided nylon. The sponge floats are SB4 (3 inches diameter by 1½ inch long with a ½ inch hole) and spaced at 8 inches on center along the wings and front of bag. The float spacing along the sides and back of the bag are every 12 inches on center. The bottom line is leaded with #13, 1.3 ounce leads (1 inch long, 3/8 inch hole) spaced every 6 inches on center on the main net (wings) and front of the bag. The leads are spaced every 12 inches on center along the sides and back of the bag. The top and bottom braided nylon lines extend 2 to 3 feet beyond the net, so they can be tied to polyvinyl chloride (PVC) poles for fishing (there should be a 12-inch gap between the mesh and the seine poles once the top and bottom lines are tied off).
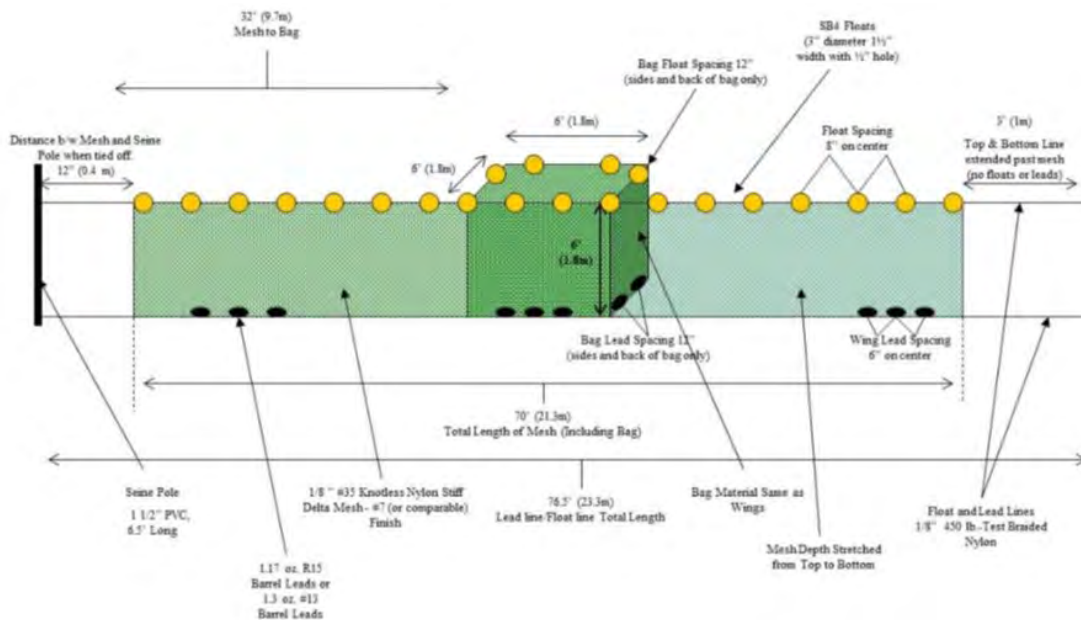
Figure 2. Schematic of 21.3-m seine configuration.

1.2 Results

During 2023 sampling, water quality parameters varied slightly between the inflow and control sites in the Banana River (**Table 2**). Within each sampling area the measured parameters displayed typical seasonal variation over the course of the four-month sampling period (Figure 3). Mean water temperature varied little between areas, exhibiting slight warming through spring; ranging from a low of 23.9 ºC during the start of the sampling in March to a high of 28.9 ºC at the end of the project in June. The cooler temperatures were found at the inflow sites while the warmer temperatures were recorded at the control sites. Mean salinity values varied little between the sites or through the sampling period, ranging from 18.2 ppt during March at the control sites to 20.7 ppt during June, also around the control sites. Mean DO values were above 4.0 ppm during the entire sampling period. Mean values ranged between 4.4 ppm to 7.1 ppm, with the lowest mean DO values observed during May from the control sites (**Table 2; Figure 3**). Water clarity

varied little between sites, ranging from a low of 0.8 m at the inflow sites to a high of 1.3 m at the control sites.

Table 2. Summary of physical parameters by sampling event collected in Banana River during 2023.

Area		Sampling Event	Temperature (º C)	Salinity (ppt)	DO (ppm)	Water Clarity (m)
Banana River	Inflow site	March	23.9 ± 0.31	18.8 ± 0.05	6.9 ± 0.13	0.8 ± 0.42
		May	28.3 ± 0.39	19.5 ± 0.09	7.1 ± 1.03	0.9 ± 0.29
		June	28.6 ± 0.05	19.5 ± 0.0	5.0 ± 0.33	1.2 ± 0.23
		N=12	26.9 ± 2.23	19.2 ± 0.34	6.3 ± 1.15	1.0 ± 0.35
	Control site	March	24.9 ± 0.31	18.2 ± 0.05	6.8 ± 0.88	1.0 ± 0.22
		May	28.0 ± 0.16	19.5 ± 0.12	4.4 ± 0.78	1.3 ± 0.23
		June	29.3 ± 0.08	20.7 ± 0.12	7.0 ± 0.23	1.1 ± 0.22
		N=12	27.4 ± 1.91	19.4 ± 1.05	6.1 ± 1.39	1.1 ± 0.25
Pooled totals		N=24	27.1 ± 2.07	19.3 ± 0.78	6.2 ± 1.26	1.0 ± 0.31

All mean values are ± standard deviation
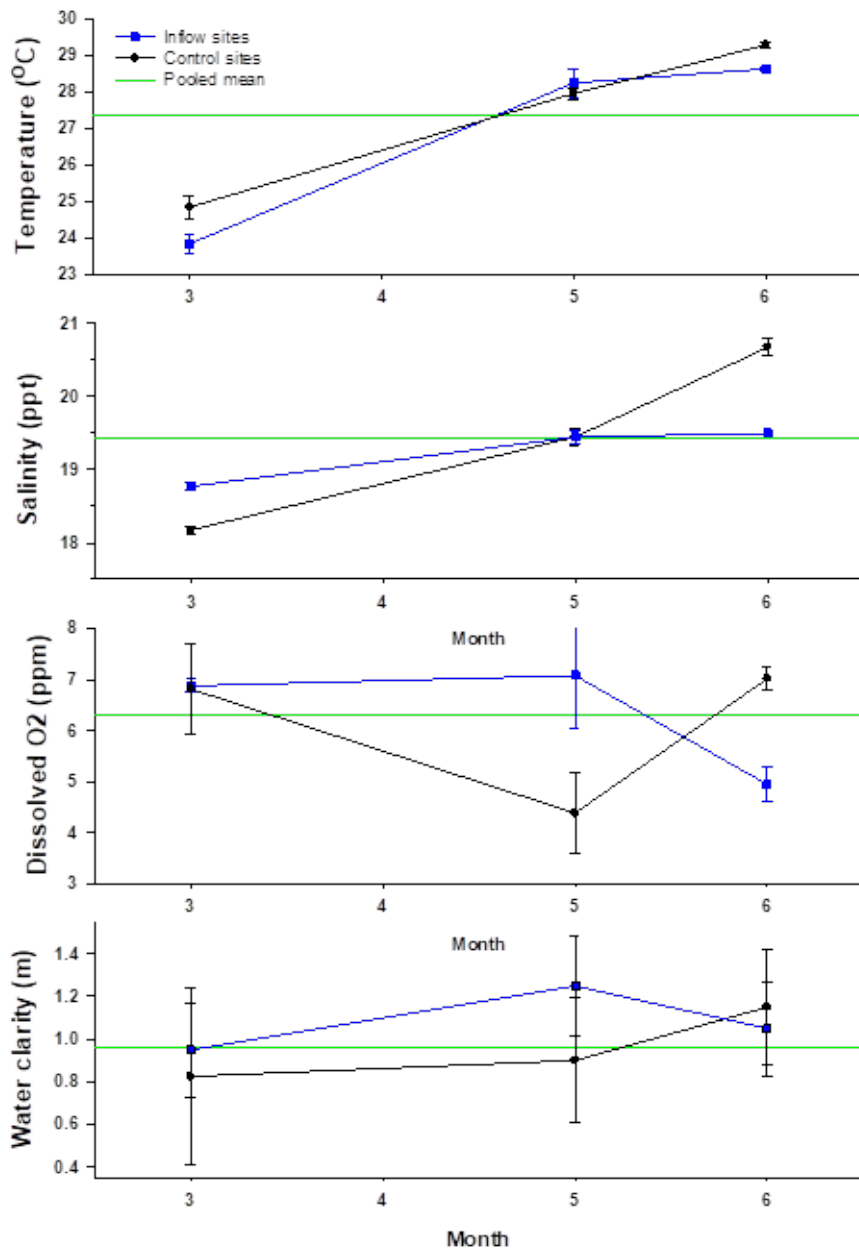
Figure 3. Mean water quality measurements measured from the Central Banana River during 2023. Blue squares= inflow sites; Black circles= control sites; Green line represents the pooled mean.

Table 3. Summary of catch and effort data for central Banana River stratified-random sampling, 2023.

| Area | 21.3-m bay seine | |
	Animals	Hauls
Inflow	31,557	12
Control	2,362	12
Totals	33,919	24

1.2.1 Stratified-Random Sampling

A total of 33,919 animals, which included 38 taxa of fishes and 3 taxa of selected invertebrates, were collected from 24 Banana River SRS samples (Table 3; Appendix 2). Bay Anchovy, *Anchoa mitchilli* (n = 31,757) was the most abundant taxon collected, accounting for 93.6% of the total catch (**Table 4**). Spot, *Leiostomus xanthurus* (n = 472), *Brevoortia* spp. (n = 287), and *Menidia* spp. (n = 2,409) were the next most abundant taxa collected, accounting for an additional 3.1% of the total catch. Thirteen Selected Taxa (n = 1,161) composed 3.4% of the total catch (**Table 5**). *Leiostomus xanthurus* (n = 472), *Brevoortia* spp. (n = 287), and Atlantic Croaker, *Micropogonias undulatus* (n = 266) were the most abundant Selected Taxa, representing 88.2% of the Selected Taxa (3.0% of the total catch).

Table 4. Catch statistics for 10 dominant taxa collected in 24 21.3-m seine samples during Banana River stratified-random sampling during 2023. Percent (%) is the percent of the total catch represented by that taxon; the percentage of samples in which that taxon was collected; the coefficient of variation of the mean (CV). Taxa are ranked in order of decreasing mean catch-per-unit-effort.

Species	Number		% Occur	Catch-per-unit-effort (animals/100m²)				Standard Length (mm)			
	No.	%		Mean	Stderr	CV	Max	Mean	Stderr	Min	Max
Anchoa mitchilli	31,757	93.6	52.2	986.24	759.19	369.17	17,517.86	44	0.03	27	57
Leiostomus xanthurus	472	1.4	39.1	14.66	8.47	277.18	169.29	24	0.58	13	70
Brevoortia spp.	287	0.9	13.0	8.91	5.59	300.61	115.71	37	0.47	27	92
Menidia spp.	283	0.8	65.2	8.79	2.52	137.58	40.71	34	0.43	18	72
Micropogonias undulatus	266	0.8	8.7	8.26	6.89	400.05	156.43	38	0.78	9	58
Eucinostomus spp.	247	0.7	52.2	7.67	3.38	211.19	62.86	23	0.38	14	38
Membras martinica	151	0.5	13.0	4.69	4.47	456.74	102.86	59	1.56	28	97
Mugil curema	87	0.3	39.1	2.70	1.24	219.59	20.00	36	3.37	17	135
Harengula jaguana	68	0.2	17.4	2.11	1.74	394.77	40.00	38	0.65	29	50
Lucania parva	53	0.2	26.1	1.65	1.42	414.48	32.86	23	0.40	18	30
Subtotal	33,671	99.3	.	.	.	.	.	.	.	9	135
Totals	33,919	100	.	1,009.49	739.92	359.07	17,851.43	.	.	3	394

Table 5. Catch statistics for Selected Taxa collected in 24 21.3-m seine samples during Banana River stratified-random sampling during 2023. Percent (%) is the percent of the total catch represented by that taxon; percent occurrence (% Occur) is the percentage of samples in which that taxon was collected; CV is the coefficient of variation of the mean. Taxa are ranked in order of decreasing mean catch-per-unit-effort.

Species	Number		% Occur	Catch-per-unit-effort (animals/100m²)				Standard Length (mm)			
	No.	%		Mean	Stderr	CV	Max	Mean	Stderr	Min	Max
Leiostomus xanthurus	472	1.4	39.1	14.66	8.47	277.18	169.29	24	0.58	13	70
Brevoortia spp.	287	0.9	13.0	8.91	5.59	300.61	115.71	37	0.47	27	92
Micropogonias undulatus	266	0.8	8.7	8.26	6.89	400.05	156.43	38	0.78	9	58
Mugil curema	87	0.3	39.1	2.70	1.24	219.59	20.00	36	3.37	17	135
Farfantepenaeus spp.	26	0.1	21.7	0.81	0.50	298.57	10.71	8	0.46	3	14
Callinectes sapidus	6	<0.1	17.4	0.19	0.10	264.00	2.14	121	16.82	46	165
Archosargus probatocephalus	6	<0.1	13.0	0.19	0.10	264.00	1.43	46	10.88	18	86
Sciaenops ocellatus	4	<0.1	13.0	0.12	0.07	282.34	1.43	202	62.86	61	365
Mugil cephalus	3	<0.1	4.3	0.09	0.09	479.58	2.14	154	87.19	57	328
Farfantepenaeus aztecus	2	<0.1	8.7	0.06	0.04	331.32	0.71	18	1.00	17	19
Cynoscion nebulosus	1	<0.1	4.3	0.03	0.03	479.58	0.71	394	.	394	394
Pogonias cromis	1	<0.1	4.3	0.03	0.03	479.58	0.71	266	.	266	266
Mugil trichodon	1	<0.1	4.3	0.03	0.03	479.58	0.71	54	.	54	54
Totals	1,162	3.4	.	34.58	16.2	229.53	324.29	.	.	3	394

1.2.2 Inflow Sites

21.3-m Seines. A total of 31,557 fishes and selected invertebrates which included 30 taxa of fishes and 3 taxa of selected invertebrates, were collected in 12 samples from this site during the study period (**Table 3**, Appendix 2). *Anchoa mitchilli* (n = 29,623) was the most numerous species collected, representing 93.9% of the total 21.3-m seine catch at this site (**Table 6**). The two next most abundant taxa, *L. xanthurus* (n = 472) and Brevoortia spp. (n = 287) accounted for an additional 2.4% of the total catch at this site. The taxa most frequently caught at the inflow sites were *Eucinostomus* spp. (100% occurrence), followed by *A. mitchilli*, *L. xanthurus*, and *Menidia* spp. (all at 75.0% occurrence).

A total of 13 Selected Taxa (n=1,158 animals) were collected, representing 3.7% of the total 21.3-m seine catch at the inflow sites (**Table 7**). *Leiostomus xanthurus* (n = 472), *Brevoortia* spp. (n = 287), and *M. undulatus* (n = 266) were the most abundant Selected Taxa, representing 3.2% of the total inflow site catch (88.5% of the Selected Taxa). The Selected Taxa most frequently caught at the inflow sites were *L. xanthurus* (75.0% occurrence) and White Mullet, *Mugil curema* (66.7% occurrence).

Table 6. Catch statistics for 10 dominant taxa collected in 12 Lagoon inflow site 21.3-m bay seine samples during Banana River stratified-random sampling during 2023. Percent (%) is the percent of the total catch represented by that taxon; percent occurrence (% Occur) is the percentage of samples in which that taxon was collected; CV is the coefficient of variation of the mean. Taxa are ranked in order of decreasing mean catch-per-unit-effort.

Species	Number		% Occur	Catch-per-unit-effort (animals/100m²)				Standard Length (mm)			
	No.	%		Mean	Stderr	CV	Max	Mean	Stderr	Min	Max
Anchoa mitchilli	29,623	93.9	75.0	1,763.27	1,441.84	283.26	17,517.86	44	0.03	27	57
Leiostomus xanthurus	472	1.5	75.0	28.10	15.52	191.34	169.29	24	0.58	13	70
Brevoortia spp.	287	0.9	25.0	17.08	10.34	209.72	115.71	37	0.47	27	92
Micropogonias undulatus	266	0.8	16.7	15.83	13.08	286.20	156.43	38	0.78	9	58
Eucinostomus spp.	247	0.8	100.0	14.70	5.86	138.07	62.86	23	0.38	14	38
Menidia spp.	194	0.6	75.0	11.55	4.18	125.35	40.71	34	0.43	18	72
Membras martinica	151	0.5	25.0	8.99	8.54	329.18	102.86	59	1.56	28	97
Mugil curema	86	0.3	66.7	5.12	2.18	147.53	20.00	36	3.37	17	135
Harengula jaguana	68	0.2	33.3	4.05	3.30	282.19	40.00	38	0.65	29	50
Farfantepenaeus spp.	26	0.1	41.7	1.55	0.93	208.12	10.71	8	0.46	3	14
Subtotal	**31,420**	**99.6**	.	.	.	.	.	.	.	**3**	**135**
Totals	**31,557**	**100**	.	**1,878.39**	**1461.31**	**269.49**	**17,851.43**	.	.	**3**	**394**

Table 7. Catch statistics for Selected Taxa collected in 12 Lagoon inflow site 21.3-m bay seine samples during Banana River stratified-random sampling during 2023. Percent (%) is the percent of the total catch represented by that taxon; percent occurrence (% Occur) is the percentage of samples in which that taxon was collected; CV is the coefficient of variation of the mean. Taxa are ranked in order of decreasing mean catch-per-unit-effort.

Species	Number		% Occur	Catch-per-unit-effort (animals/100m²)				Standard Length (mm)			
	No.	%		Mean	Stderr	CV	Max	Mean	Stderr	Min	Max
Leiostomus xanthurus	472	1.5	75.0	28.10	15.52	191.34	169.29	24	0.58	13	70
Brevoortia spp.	287	0.9	25.0	17.08	10.34	209.72	115.71	37	0.47	27	92
Micropogonias undulatus	266	0.8	16.7	15.83	13.08	286.2	156.43	38	0.78	9	58
Mugil curema	86	0.3	66.7	5.12	2.18	147.53	20.00	36	3.37	17	135
Farfantepenaeus spp.	26	0.1	41.7	1.55	0.93	208.12	10.71	8	0.46	3	14
Callinectes sapidus	6	<0.1	33.3	0.36	0.19	180.91	2.14	121	16.82	46	165
Archosargus probatocephalus	6	<0.1	25.0	0.36	0.19	180.91	1.43	46	10.88	18	86
Mugil cephalus	3	<0.1	8.3	0.18	0.18	346.41	2.14	154	87.19	57	328
Farfantepenaeus aztecus	2	<0.1	16.7	0.12	0.08	233.55	0.71	18	1.00	17	19
Cynoscion nebulosus	1	<0.1	8.3	0.06	0.06	346.41	0.71	394	.	394	394
Pogonias cromis	1	<0.1	8.3	0.06	0.06	346.41	0.71	266	.	266	266
Sciaenops ocellatus	1	<0.1	8.3	0.06	0.06	346.41	0.71	365	.	365	365
Mugil trichodon	1	<0.1	8.3	0.06	0.06	346.41	0.71	54	.	54	54
Totals	1,158	3.7	100	68.93	29.72	149.38	324.29	.	.	3	394

1.2.3 Control Sites

21.3-m Seines. A total of 2,362 animals, which included 23 taxa of fishes and 0 taxa of selected invertebrates, were collected in 12 samples from this site during the study period (Table 3; Appendix 2). *Anchoa mitchilli* (n = 2,134) was the most numerous taxa collected, accounted for 90.4% of the total catch at this site (**Table 8**). The two next most abundant taxa, *Menidia* spp. (n = 89) and Rainwater killifish, *Lucania parva* (n = 48), accounted for an additional 5.8% of the catch at this site. The taxa most frequently caught at the control sites were *Menidia* spp. and Goldspotted Killifish, *Floridichthys carpio* (both at 54.5% occurrence).

A total of two Selected Taxa (n = 4 animals) were collected, representing 0.2% of the total catch at the control sites (**Table 9**). Red Drum, *Sciaenops ocellatus* (n = 3) and a single *M. curema* were the only Selected Taxa collected at control sites.

Table 8. Catch statistics for 10 dominant taxa collected in 12 Control site 21.3-m bay seine samples during Banana River stratified-random sampling during 2023. Percent (%) is the percent of the total catch represented by that taxon; percent occurrence (% Occur) is the percentage of samples in which that taxon was collected; CV is the coefficient of variation of the mean. Taxa are ranked in order of decreasing mean catch-per-unit-effort.

Species	Number		% Occur	Catch-per-unit-effort (animals/100m²)				Standard Length (mm)			
	No.	%		Mean	Stderr	CV	Max	Mean	Stderr	Min	Max
Anchoa mitchilli	2,134	90.4	27.3	138.57	137.43	328.93	1512.86	44	0.03	27	57
Menidia spp.	89	3.8	54.5	5.78	2.56	146.91	27.86	34	0.43	18	72
Lucania parva	48	2.0	27.3	3.12	2.98	316.59	32.86	23	0.40	18	30
Eucinostomus harengulus	15	0.6	45.5	0.97	0.46	158.21	5.00	56	3.35	40	110
Floridichthys carpio	14	0.6	54.5	0.91	0.35	127.13	3.57	41	2.44	15	65
Strongylura notata	11	0.5	36.4	0.71	0.41	189.74	4.29	198	23.15	75	320
Microgobius gulosus	11	0.5	9.1	0.71	0.71	331.66	7.86	32	1.09	24	45
Eucinostomus jonesii	6	0.3	27.3	0.39	0.22	189.88	2.14	63	4.04	52	78
Syngnathus scovelli	6	0.3	27.3	0.39	0.26	222.49	2.86	47	8.69	25	85
Oligoplites saurus	5	0.2	27.3	0.32	0.18	180.44	1.43	23	1.36	19	27
Subtotal	**2,339**	**99.0**	.	.	.	.	.	.	.	**15**	**320**
Totals	**2,362**	**100**	.	**140.6**	**129.34**	**318.68**	**1562.86**	.	.	**3**	**394**

Table 9. Catch statistics for Selected Taxa collected in 12 Control site 21.3-m bay seine samples during Banana River stratified-random sampling during 2023. Percent (%) is the percent of the total catch represented by that taxon; percent occurrence (% Occur) is the percentage of samples in which that taxon was collected; CV is the coefficient of variation of the mean. Taxa are ranked in order of decreasing mean catch-per-unit-effort.

Species	Number		% Occur	Catch-per-unit-effort (animals/100m²)				Standard Length (mm)			
	No.	%		Mean	Stderr	CV	Max	Mean	Stderr	Min	Max
Scienops ocellatus	3	0.1	18.2	0.19	0.14	237.11	1.43	249	59.03	172	365
Mugil curema	1	<0.1	9.1	0.06	0.06	331.66	0.71	96	.	96	96
Totals	**4**	**0.2**	**27.3**	**0.24**	**0.13**	**195.40**	**1.43**	**.**	**.**	**96**	**365**

1.3 Conclusion

This report summarizes data collected from two areas within the central BR with an objective of providing a current account of nekton abundance and species richness in close proximity of the proposed Restore Lagoon Inflow Project and at a control site approximately 12.5 km south in the BR. The communities at both sites were found to be typical of historic communities described for the area. The proposed inflow area was more diverse than the control site (30 v 23 taxa). The difference in overall number of animals collected at each area was a result of the greater number of A. mitchilli that were collected at the inflow sites (n = 29,623) versus the control sites (n = 2,134). The collection of fisheries community data in the BR provide a baseline database from which changes in estuarine health (i.e., loss of seagrass) and restoration efforts may be evaluated for this area of the Indian River Lagoon.

2   References

FWC-FWRI. 2017. Fisheries-Independent Monitoring Program 2016 Data Summary Report. Florida Fish and Wildlife Research Institute. St. Petersburg, Florida.

FWC-FWRI. 2023. Fisheries-Independent Monitoring Program Procedure Manual. Florida Fish and Wildlife Research Institute. St. Petersburg, Florida

IRL 2011 Consortium. 2012. Indian River Lagoon 2011: Superbloom plan of investigation. Prepared by SJRWMD, 27pp.

Johnson, K.B., Turingan, R.G., Eble, J., Shenker, J., and Blanchard, J.R. 2020. Restore Lagoon Inflow Research Project (Phase 1) Task 2, Biological Monitoring.

Matheson, R.E., Jr. 1983. Taxonomic studies of the Eucinostomus argenteus complex (Pisces: Gerreidae). Ph.D. Dissertation, Texas A&M University, College Station. 195 p.

Middaugh, D.P., M.J. Hemmer, and Y.L. Rose. 1986. Laboratory spawning cues in Menidia beryllina and Menidia peninsulae (Pisces: Atherinidae) with notes on survival and growth of larvae at different salinities. Environmental Biology of Fishes 15:107-117.

Paperno, R., D.H. Adams, and A.P. Sebastian. 2016. Indian River Lagoon Enhanced Fisheries Monitoring and Phytoplankton Bloom Impact Evaluation. Final Report to the SJRWMD Contract 27574 Prepared by FWC-FWRI, 43 pp.

Phlips, E.J., S. Badylak, M.A. Lasi, R. Chamberlain, W.C. Green, L.M. Hall, J.A Hart, J.C. Lockwood, J.D. Miller, L.J. Morris, and J.S. Steward. 2015. From red tides to green and Brown tides: Bloom dynamics in a restricted subtropical lagoon shifting climatic conditions. Estuaries and Coasts 38:886-904.Matheson, R.E., Jr. 1983. Taxonomic studies of the Eucinostomus argenteus complex (Pisces: Gerreidae). Ph.D. Diss., Texas A&M University, College Station, 195 pp.

Page, L.M., H. Espinosa-Pérez, L.T. Findley, C.R. Gilbert, R.N. Lea, N.E. Mandrak, R.L. Mayden, and J.S. Nelson. 2013. Common and scientific names of fishes from the United States, Canada, and Mexico. Seventh Edition. American Fisheries Society Special Publication 34. 243 pp.

Tremain, D.M. and D.H. Adams. 1995 Seasonal variation in species diversity, abundance, and composition of fish communities in the northern Indian River Lagoon, Florida. Bulletin of Marine Science 57:171–192.

3. Appendices

Appendix 1. Animals designated as Selected Taxa because of their commercial or recreational importance.

SCIENTIFIC NAME	COMMON NAME	SCIENTIFIC NAME	COMMON NAME
Acanthocybium solanderi	Wahoo	*Centropomus pectinatus*	Tarpon Snook
Albula sp.cf.vulpes	Unnamed Bonefish	*Centropomus undecimalis*	Common Snook
Albula goreensis	Channel Bonefish	*Centropristis ocyurus*	Bank Sea Bass
Albula spp.[1]	Bonefish	*Centropristis philadelphica*	Rock Sea Bass
Albula vulpes	Bonefish	*Centropristis striata*	Black Sea Bass
Alectis ciliaris	African Pompano	*Cephalopholis cruentata*	Graysby
Alphestes afer	Mutton Hamlet	*Cephalopholis fulva*	Coney
Alopias vulpinus	Common Thresher	*Coryphaena equiselis*	Pompano Dolphinfish
Apsilus dentatus	Black Snapper	*Coryphaena hippurus*	Dolphinfish
Archosargus probatocephalus	Sheepshead	*Cynoscion arenarius*	Sand Seatrout
Argopecten gibbus[2]	Atlantic Calico Scallop	*Cynoscion complex*[3]	*C. regalis* x *C. arenarius*
Argopecten irradians[2]	Bay Scallop	*Cynoscion nebulosus*	Spotted Seatrout
Balistes capriscus	Gray Triggerfish	*Cynoscion nothus*	Silver Seatrout
Brevoortia spp.[1,2]	Menhaden	*Cynoscion regalis*	Atlantic Weakfish
Calamus arctifrons[2]	Grass Porgy	*Dermatolepis inermis*	Marbled Grouper
Calamus bajonado[2]	Jolthead Porgy	*Diplectrum formosum*[2]	Sand Perch
Calamus calamus[2]	Saucereye Porgy	*Elops saurus*	Ladyfish
Calamus leucosteus[2]	Whitebone Porgy	*Elops smithi*	Malacho
Calamus nodosus[2]	Knobbed Porgy	*Epinephelus adscensionis*	Rock Hind
Calamus penna[2]	Sheepshead Porgy	*Epinephelus drummondhayi*	Speckled Hind
Calamus proridens[2]	Littlehead Porgy	*Epinephelus guttatus*	Red Hind
Calamus spp.[1,2]	Porgies	*Epinephelus itajara*	Goliath Grouper
Callinectes sapidus[2]	Blue Crab	*Epinephelus morio*	Red Grouper
Caranx crysos	Blue Runner	*Epinephelus striatus*	Nassau Grouper
Caranx hippos	Crevalle Jack	*Etelis oculatus*	Queen Snapper
Carcharhinus acronotus	Blacknose Shark	*Euthynnus alletteratus*	Little Tunny
Carcharhinus brevipinna	Spinner Shark	*Farfantepenaeus aztecus*[2]	Brown Shrimp
Carcharhinus falciformis	Silky Shark	*Farfantepenaeus brasiliensis*[2]	Caribbean Brown Shrimp
Carcharhinus leucas	Bull Shark	*Farfantepenaeus duorarum*[2]	Pink Shrimp

SCIENTIFIC NAME	COMMON NAME	SCIENTIFIC NAME	COMMON NAME
Carcharhinus isodon	Finetooth Shark	*Farfantepenaeus spp.*[1,2]	Shrimp
Carcharhinus limbatus	Blacktip Shark	*Galeocerdo cuvier*	Tiger Shark
Carcharhinus longimanus	Oceanic Whitetip Shark	*Ginglymostoma cirratum*	Nurse Shark
Carcharhinus obscurus	Dusky Shark	*Haemulon album*[2]	Margate
Carcharhinus plumbeus	Sandbar Shark	*Haemulon aurolineatum*[2]	Tomtate
Caulolatilus chrysops	Goldface Tilefish	*Haemulon flavolineatum*[2]	French Grunt
Caulolatilus cyanops	Blackline Tilefish	*Haemulon macrostomum*[2]	Spanish Grunt
Caulolatilus intermedius	Anchor Tilefish	*Haemulon melanurum*[2]	Cottonwick
Caulolatilus microps	Blueline Tilefish	*Haemulon parra*[2]	Sailors Choice
Centropomus ensiferus	Swordspine Snook	*Haemulon plumierii*	White Grunt
Centropomus mexicanus	Largescale Fat Snook	*Haemulon sciurus*[2]	Bluestriped Grunt
Centropomus parallelus	Smallscale Fat Snook	*Hyporthodus flavolimbatus*	Yellowedge Grouper
Hyporthodus mystacinus	Misty Grouper	*Mycteroperca phenax*	Scamp
Hyporthodus nigritus	Warsaw Grouper	*Mycteroperca tigris*	Tiger Grouper
Hyporthodus niveatus	Snowy Grouper	*Mycteroperca venenosa*	Yellowfin Grouper
Istiophorus platypterus	Sailfish	*Negaprion brevirostris*	Lemon Shark
Isurus oxyrinchus	Shortfin Mako	*Ocyurus chrysurus*	Yellowtail Snapper
Katsuwonus pelamis	Skipjack Tuna	*Pagrus pagrus*	Red Porgy
Lachnolaimus maximus	Hogfish	*Panulirus argus*	Spiny Lobster
Lamna nasus	Porbeagle	*Paralichthys albigutta*	Gulf Flounder
Leiostomus xanthurus	Spot	*Paralichthys dentatus*	Summer Flounder
Litopenaeus setiferus[2]	White Shrimp	*Paralichthys lethostigma*	Southern Flounder
Lobotes surinamensis	Tripletail	*Paralichthys oblongus*	Fourspot Flounder
Lopholatilus chamaeleonticeps	Tilefish	*Paralichthys squamilentus*	Broad Flounder
Lutjanus analis	Mutton Snapper	*Paranthias furcifer*	Creole-fish
Lutjanus apodus	Schoolmaster	*Pogonias cromis*	Black Drum
Lutjanus buccanella	Blackfin Snapper	*Pomatomus saltatrix*	Bluefish
Lutjanus campechanus	Red Snapper	*Prionace glauca*	Blue Shark
Lutjanus cyanopterus	Cubera Snapper	*Pristipomoides aquilonaris*	Wenchman
Lutjanus griseus	Gray Snapper	*Pseudupeneus maculatus*[2]	Spotted Goatfish
Lutjanus jocu	Dog Snapper	*Pterois spp.*[1]	Lionfish
Lutjanus mahogoni	Mahogany Snapper	*Rachycentron canadum*	Cobia

SCIENTIFIC NAME	COMMON NAME	SCIENTIFIC NAME	COMMON NAME
Lutjanus synagris	Lane Snapper	*Rhizoprionodon terraenovae*	Atlantic Sharpnose Shark
Lutjanus vivanus	Silk Snapper	*Rhomboplites aurorubens*	Vermilion Snapper
Malacanthus plumieri	Sand Tilefish	*Sciaenops ocellatus*	Red Drum
Megalops atlanticus	Tarpon	*Scomberomorus cavalla*	King Mackerel
Menippe spp.[1,2]	Stone Crab	*Scomberomorus maculatus*	Spanish Mackerel
Menticirrhus americanus	Southern Kingfish	*Scomberomorus regalis*	Cero
Menticirrhus littoralis	Gulf Kingfish	*Seriola dumerili*	Greater Amberjack
Menticirrhus saxatilis	Northern Kingfish	*Seriola fasciata*	Lesser Amberjack
Micropogonias undulatus	Atlantic Croaker	*Seriola rivoliana*	Almaco Jack
Mugil cephalus	Striped Mullet	*Seriola zonata*	Banded Rudderfish
Mugil curema	White Mullet	*Sphyraena barracuda*	Great Barracuda
Mugil liza	Liza	*Sphyrna tiburo*	Bonnethead
Mugil rubrioculus	Redeye Mullet	*Thunnus albacares*	Yellowfin Tuna
Mugil trichodon	Fantail Mullet	*Thunnus atlanticus*	Blackfin Tuna
Mulloidichthys martinicus[2]	Yellow Goatfish	*Thunnus obesus*	Bigeye Tuna
Mullus auratus[2]	Red Goatfish	*Thunnus thynnus*	Bluefin Tuna
Mustelus spp.[1]	Smooth Dogfish	*Trachinotus carolinus*	Florida Pompano
Mycteroperca bonaci	Black Grouper	*Trachinotus falcatus*	Permit
Mycteroperca interstitialis	Yellowmouth Grouper	*Trachinotus goodei*	Palometa
Mycteroperca microlepis	Gag	*Upeneus parvus*[2]	Dwarf Goatfish

[1]   Commercially important, but frequently not identified to species (added 06/03). See Procedure 6.1

[2]   Do not need to measure 40. Measure appropriate length in accordance with Procedure 6.1.

[3]   Hybridization on Atlantic coast makes positive identification to species difficult or impossible (added to selected species list on 06/03).

Appendix 2. Seasonal summary of species collected at Inflow and Control sites during central Banana River stratified-random sampling during 2023. Effort, or total number of hauls, is labeled 'E'. Taxa are arranged alphabetically.

Species		Month						Site		Totals
		March		May		June				
		Inflow	Control	Inflow	Control	Inflow	Control	Inflow	Control	
		E=4	E=4	E=4	E=4	E=4	E=4	E=12	E=12	E=24
Achirus lineatus	Lined Sole	3	2	.	.	.	.	3	2	5
Anchoa mitchilli	Bay Anchovy	99	.	28,010	4	1,514	2,130	29,623	2,134	31,757
Archosargus probatocephalus	Sheepshead	2	.	2	.	2	.	6	.	6
Ariopsis felis	Hardhead Catfish	.	.	.	.	2	.	2	.	2
Bairdiella chrysoura	Silver Perch	.	.	11	.	.	2	11	2	13
***Brevoortia* spp.**	Menhaden	125	.	162	.	.	.	287	.	287
Callinectes sapidus	Blue Crab	1	.	4	.	1	.	6	.	6
Chasmodes saburrae	Florida Blenny	.	1	.	.	.	2	.	3	3
Chilomycterus schoepfii	Striped Burrfish	.	2	.	.	.	.	.	2	2
Cynoscion nebulosus	Spotted Seatrout	.	.	1	.	.	.	1	.	1
Dasyatis sabina	Atlantic Stingray	.	1	3	1	1	.	4	2	6
Diapterus auratus	Irish Pompano	1	.	.	.	8	1	9	1	10
Eucinostomus gula	Silver Jenny	1	.	1	.	1	1	3	1	4
Eucinostomus harengulus	Tidewater Mojarra	4	12	6	2	8	1	18	15	33
Eucinostomus jonesii	Slender Mojarra	.	4	.	2	.	.	.	6	6
Eucinostomus spp.	Juvenile *Eucinostomus*	45	.	179	.	23	.	247	.	247
Eugerres plumieri	Striped Mojarra	.	1	.	.	.	.	.	1	1
Farfantepenaeus aztecus	Brown Shrimp	1	.	1	.	.	.	2	.	2
***Farfantepenaeus* spp.**	Commercial Shrimps	17	.	9	.	.	.	26	.	26
Floridichthys carpio	Goldspotted Killifish	12	5	.	4	1	5	13	14	27
Gobiesox strumosus	Skilletfish	.	1	.	.	.	1	.	2	2
Gobiosoma robustum	Code Goby	5	1	2	.	.	.	7	1	8
Harengula jaguana	Scaled Sardine	.	.	12	.	56	.	68	.	68
Lagodon rhomboides	Pinfish	2	.	7	.	.	.	9	.	9
Leiostomus xanthurus	Spot	397	.	71	.	4	.	472	.	472
Lucania parva	Rainwater Killifish	4	2	1	.	.	46	5	48	53
Membras martinica	Rough Silverside	1	.	6	.	144	.	151	.	151

Species		Month						Site		Totals
		March		May		June				
		Inflow	Control	Inflow	Control	Inflow	Control	Inflow	Control	
		E=4	E=4	E=4	E=4	E=4	E=4	E=12	E=12	E=24
Menidia spp.	Silversides	94	20	51	53	49	16	194	89	283
Microgobius gulosus	Clown Goby	14	.	3	.	1	11	18	11	29
Micropogonias undulatus	Atlantic Croaker	47		219	.	.		266	.	266
Mugil cephalus	Striped Mullet	.		3		.		3	.	3
Mugil curema	White Mullet	38	1	30	.	18	.	86	1	87
Oligoplites saurus	Leatherjacket	.	.	.	1	6	4	.	5	5
Opisthonema oglinum	Atlantic Thread Herring	3		3		.		6	.	6
Orthopristis chrysoptera	Pigfish	.		1		.		6	.	6
Pogonias cromis	Black Drum	1	.	.	.	.	.	1	.	1
Sciaenops ocellatus	Red Drum	1	.	.	.	.	3	1	3	4
Sphoeroides testudineus	Checkered Puffer	1		.		2		1	.	1
Strongylura notata	Redfin Needlefish	.	3	.	7	6	1	3	11	14
Syngnathus scovelli	Gulf Pipefish	.	6	3	.	.	.	.	6	6
Totals		919	62	28,799	74	1,839	2,226	31,557	2,362	33,919
Mugil trichodon	Fantail Mullet	.		1		.		1	.	1

Economically important taxa are highlighted in bold.

Appendix G   Task 4 – Florida International University Biology Report

Restore Lagoon Inflow Research (Phase 3)
Task 4 Biological Monitoring
Final Report
Florida International University

PREPARED FOR

Florida Institute of Technology
150 West University Boulevard
Melbourne, FL 32091

PREPARED BY

Jesse R. Blanchard

Earth and Environment

Acknowledgements

I would like to thank the Department of Education for supporting this important work, as well as the broader community of stakeholders and politicians who make this possible. I would also like to thank Florida Fish and Wildlife Conservation Commission's Fish and Wildlife Research Institute for collecting and curating the incredible resource that is the Fisheries Independent Monitoring data presented herein, as well as for the permission to use it.

Project Staffing

Faculty – Jesse Blanchard

Highlights

- Temperature and salinity frequency of occurrences for 11 species of interest (SoI) are described for the Banana River over a 22-year period using Florida Fish and Wildlife Commission (FWC) monitoring data.
- Targeted literature reviews are provided for the 11 SoI to describe known temperature and salinity limits.
- Annual spatiotemporal distribution of 11 SoI densities were mapped and rasterized.
- The BRL environment is mapped with respect to salinity, temperature and shoreline type using FWC monitoring data.
- Generated species tolerance data and rasterized occurrence and environmental outputs are critical inputs required to support future habitat suitability modelling.
- Enhanced inflow from an offshore source could potentially mitigate negative impacts from severe heat and cold events, which are expected to become more frequent with human-induced climate change.
- SoI are likely to be relatively unaffected by net changes to salinity and temperature predicted with inflow; however, negative impacts are expected if rates of change exceed species' response capacity.

Table of Contents

List of Figures

List of Tables

List of Acronyms

BRL	Banana River Lagoon
°C	Degrees Celsius
FWC	Florida Fish and Wildlife Conservation Commission
HSM	Habitat Suitability Model
IRL	Indian River Lagoon
RLI	Restore Lagoon Inflow
SoI	Species of Interest

1   Introduction

The Restore Lagoon Inflow (RLI) project proposes increasing oceanic inflow to the Banana River Lagoon (BRL) to improve overall water quality and reduce impacts from reoccurring harmful algal bloom outbreaks. As the BRL is currently a low flow system (FL.Tech. 2020) with a mean observed salinity of 23.29±0.07 ppt and temperature of 25.55 degrees Celsius (°C) ±0.04 (Table 2), the introduction of oceanic water is likely to increase salinity, decrease temperature, increase dissolved oxygen, increase the pH and decrease turbidity (FL.Tech. 2020, Blanchard et al. 2021). Each of these are known to be important factors in fish health. As such, in Phase I of the RLI project the Fish Team sought to identify which of these factors would be most influential on Indian River Lagoon (IRL) fishes and generally describe the fish communities of the BRL and two other proposed inflow sites (Johnson et al. 2020). Phase II developed predictive models to forecast the potential community level responses of the BRL fishes, as well as population level responses of the key species of interest (SoI, Blanchard et al. 2021). While the bulk of the broader RLI Phase III work focused on permitting and engineering, see other sections of this report for details, there are still several pending questions regarding how fishes may respond to enhanced inflow. One of the key needs for evaluating fish responses to the RLI proposal is habitat suitability modelling, which all previous Fish Team efforts have been laying the groundwork for. With that goal in mind, a feasible next step was to establish the environmental envelopes for two of the most influential abiotic factors of interest and prepare the geographic informational system infrastructure necessary to facilitate the construction of habitat suitability models (HSMs) in a future stage.

For Phase III, the goal was to investigate thermal and halotolerances, with available data, through complimentary literature review and data explorations to describe the relationships between key SoI, temperature and salinity. For each species I had 2 guiding questions: 1) What are the known temperature and salinity relationships described in the literature for this species and 2) What temperatures and salinities is this species typically found in in the BRL?

Fish physiology and temperature

Most fish are poikilothermic, they rely on their aquatic environment to regulate their body temperature (Helfman et al. 1997). This makes them particularly sensitive to temperature fluctuations. Many will actively seek temperatures that optimize their metabolism, and actively avoid temperatures outside this preferred range. Rapidly onset and/or prolonged deviations outside a fish's preferred temperature range can have a series of consequences (Helfman et al. 1997). This has been well exemplified in recent decades by the numerous extreme weather events Florida has experienced. Famously, the 2010 cold snap was the most extreme in terms of severity of cold, duration of cold, and biological impact from 1927-2012 analyzed by Boucek & Rehage (2014). During this period, several non-native fishes were extirpated from the shallow estuarine drainages of Taylor Slough in Everglades National Park (Rehage et al. 2016). Massive fish kills due to the rapid change of temperature during this event led to a complete restructuring of Florida's fisheries (Santos et al. 2016). However, we also saw that the broader native estuarine fish community was fairly resistant and highly resilient (Rehage et al. 2016), which likely speaks to the nature of the estuarine environment itself being defined by changing conditions. Those that evolved to live in estuaries have compensatory mechanisms at work to deal with these changing conditions.

Estuaries fluctuate on hourly, daily, monthly and annual scales due to, for example, influxes of freshwater following a rainstorm, influxes of saltwater during high tide, increases in water temperature over the course of the day in shallow regions, decreases of water temperature with

tidal inflows or rain, seasonal changes, etc. (FL.Tech. 2020). As water temperature increases, oxygen solubility decreases (i.e., Henrys law, see Henry 1803) leading to Bohr effects (see Riggs, 1988), protein disfunction, and slowed biochemical reactions (Helfman et al. 1997). To survive this, estuarine fishes must have compensatory mechanisms in place to cope with such fluctuations. These mechanistic responses can be behavioral (e.g., moving to more favorable conditions, see Coutant 1985) or physiological in nature (e.g., adjusting the unsaturated to saturated fatty acid ratio of cell membranes, Helfman et al. 1997) and may vary between evolutionarily independent lineages. It is currently unclear how frequently the fishes of the BRL interact with those in the rest of the IRL or offshore community. We know some species, such as Red Drum (Sciaenops ocellatus), have some limited genetic mixing outside the BRL, but a majority of the population spawn locally (Reyier et al. 2011). The inverse is true for the confamilial Spotted Seatrout and Black Drum (Reyier et al. 2020). Bay Anchovies, however, have been described as both estuarine and oceanic spawners (Zastrow et al. 1991, Jung and Houde 2004). In the cases of locally restricted spawning, the limited genetic mixing may lead to the evolution of exacerbated or novel physiological or even behavioral mechanisms for coping with estuarine conditions and significantly different environmental tolerances. For example, Atlantic coast Sheepshead management plans are now recommended to treat them as multiple separate stocks due to their spatial ranges and genetic differences, with significantly different environmental envelopes (Adams et al. 2018, Gutierrez et al. 2023). While we can draw general inferences about the biology and physiology of BRL fishes from the broader literature and observed spatiotemporal distributions, it must be done with this cautionary caveat in mind. There is also the reality that, while the physiological capacity to adapt to changing temperatures is inherent in most estuarine fishes, all of the mechanisms they use for this require time to work. The rate of changing temperature is often more important than the degree of change itself. The general 'rule of thumb' in fish husbandry is to limit the change to 1°C per day to limit stress. However, the exact limit of any given species is likely to be population specific, derived from a combination of individual and evolutionary history (Chung and Strawn 1994) and requires dedicated study of the target stock to fully understand. For a clear understanding of the thermal tolerances of the fishes of the BRL, dedicated physiology studies of representative species are needed (see Brown et al., 2022; Langston et al., 2010; Schofield et al., 2007, 2010; Schofield & Huge, 2008; Schofield & Kline, 2018 for examples).

Fish physiology and salinity

Fish halotolerance is largely a result of any given species' osmoregulatory mechanism and efficiency. In short, they maintain hyperosmotic, isosmotic, or hypoosmotic body fluids through a combination of renal regulation and exchanges across the gill membranes or gut tissues (Kültz 2015). Many estuarine species are able to resist deleterious effects of changes to salinity, if given time to do so. The general 'rule of thumb' used in the aquaculture industry is to limit the rate of change to 1 ppt/hour to avoid osmotic stress; however, this is likely a conservative estimate erring on the side of caution. This caution is warranted because osmotic shock due to excess (hyperosmotic) or insufficient (hypoosmotic) intracellular ionic concentrations compared to the ambient water conditions can be severe. Hyperosmotic shock dehydrates the cells, inducing frantic movements and often visible levels of pain accompanying altered cortisol levels, eventually leading to lethargy, loss of equilibrium and death. Hypoosmotic shock conversely overhydrates the cells leading to bloating, possible cell rupture, lethargy, loss of equilibrium and eventually death (Helfman et al. 1997, McGuire et al. 2010, Kültz 2015). However, acclimation and acclimatization, limiting the rate of salinity change to give time for osmoregulatory mechanisms to work accordingly, can prevent this. Indeed, many of Florida's

estuarine fishes are euryhaline (Gunter 1956), using both freshwater and saltwater environments over the course of their life cycles, or even over the course of a single month (e.g., Massie et al., 2020; Reyier et al., 2011, 2020). However, not all can do this and even the euryhaline species have a maximum rate at which they can adjust, and many species' euryhalinity is ontogenetic in nature, not indicative of their entire life history (e.g., Black Drum, see Murphy and Taylor 1989). Unfortunately, very little information exists on the rate of tolerable change for most fishes. Importantly, this osmotic shock risk is not limited to concerns over salinity, but all aqueous ions. The rapid reductions of nitrogen species targeted by RLI inflow also have the potential to induce osmotic shock as BRL fishes have acclimatized to high nutrient conditions and would need to acclimate to lower levels over time. Such studies would be needed to fully understand the rate of environmental change that BRL fishes can acclimate to and what can be expected.

2 Approach

2.1.1 Species selection

Species selection began with the Species of Interest (SoI) used in the RLI Phase II report: Bay Anchovy, *Anchoa mitchilli*, Sheepshead, *Archosargus probatocephalus*, Spotted Seatrout, *Cynoscion nebulosus*, Pinfish, *Lagodon rhomboides*, Gray Snapper, *Lutjanus griseus*, Black Drum, *Pogonias cromis*, Red Drum, *Sciaenops ocellatus* and Gulf Pipefish, *Syngnathus scovelli*. Please see the RLI Phase 2 Final Report section 4.3.1.1 for information on how and why those species were chosen (Blanchard et al. 2021). From here, the 20 most abundant fishes in the BRL as described in the RLI Phase I final report (Johnson et al. 2020) were considered, selecting species which have ecological significance not necessarily captured in the previous listing (e.g., trophic position, feeding strategy, life history, etc.). This led to the inclusion of Tidewater Mojarra, *Eucinostomus harengulus*, Spot, *Leiostomus xanthurus*, Thread herring, *Opisthonema oglinum* and Striped Mullet, *Mugil cephalus*. The Mojarra and Herring are commonly used as baitfish, colloquially called 'greenies' and 'saw-bellies'. There are active fisheries for them in several regions of the state and both are pelagic low-trophic level predators, with Mojarra primarily targeting small crustaceans (Chi-Espínola et al. 2018) and Herring being more zooplanktivorous ram filter feeders (Finucane and Vaught 1986, Smith 1994). Spot are culled recreationally, though mainly for bait, and there are limited commercial fisheries for them around the state. They are smaller bodied, low trophic level, con-familials of the recreationally important drums already in the list (McCall and Fleeger 1993, Johnson et al. 2013). Striped Mullet are popular baitfish culled by recreational net collections as table fair and bait. They are benthivorous, low trophic level fish that form large schools and have a well-documented migration which provides substantial economic value to Florida (Whitfield et al. 2012). For several of these species, there were other analogous options (e.g., *Eucinostomus gula* instead of *Eucinostomus harengulus*, *Bairdiella chrysoura* instead of *Leiostomus xanthurus*, etc.). In such an instance, the 'tie' was broken by selecting the more common species in the BRL area, as described in the Phase 1 report (Johnson et al. 2020).

2.1.2 What are the known temperature and salinity relationships described in the literature for this species?

This question was addressed with a limited and constrained literature review, focused exclusively on this subject. While few studies have been conducted to quantify the exact thermal or halotolerance of the SoIs, I recorded the conditions within which each species was observed, reviewed aquacultural notes on their rearing and survivorship under different conditions, and reviewed management plan documentation when available. As this was a task-specific, constrained, literature review, the majority of literature on the SoI was excluded. The reader is

cautioned from interpreting this report as a comprehensive treatise of knowledge on these species.

2.1.3 What temperatures and salinities are this species typically found in in the BR?

To investigate this question, Florida Fish and Wildlife Conservation Commission's (FWC's) Fish and Wildlife Research Institute's (FWRI's) Fisheries Independent Monitoring (FIM) Program's IRL data (henceforth referred to as FWC data) was used to assess BRL fish occurrence with respect to water temperature and salinity, using a model-based approach similar to Phases I & II (Johnson et al. 2020, Blanchard et al. 2021). These data encompass all fish records collected in the upper IRL by FIM from 1996-2018; however, because the RLI project is currently focused on the BRL pilot pumping project, and our Phase I work identified that the BRL fish community operates differently than other regions in the IRL (FL.Tech. 2020), the current effort was focused exclusively on the FWC data's 'Zone E', which only includes the BRL. This work also focuses exclusively on the gear types used in previous RLI Phases, for consistency and accuracy (Johnson et al. 2020, Blanchard et al. 2021). However, as before, each gear type will be presented separately for all analytics as each has necessarily different biases associated with the method making direct comparison between them inappropriate. The one exception to this is with respect to the mapping of fish density. The FIM sampling protocol provides a stratified random sample distribution for each gear type, and each gear is designed to target a different life history stage of the generalized fish, making combined spatiotemporal representations of the data appropriate. Density, $\frac{\text{Fish}}{\text{m}^3}$, was calculated from the raw count data in the FWC data according to the equations in Table 1. Outlier samples were defined as those that were more than 1 standard deviation from the median density and were removed prior to analysis.

Table 1. General description of gear types and abundance to density conversion equations. Please see the FWRI-FWC-FIM procedural manual for full technical design specifications of each gear type and usage methodologies.

Gear	Description	Density equation used	Justification
20	21.3 m center bag seine- beach set	$\dfrac{\text{\# of fish}}{\text{Pi} * (\frac{21.3}{2})^2 / 4}$	¼ cylinder
160	183 m center bag seine-beach set	$\dfrac{\text{\# of fish}}{\text{Pi} * (\frac{183}{2})^2 / 2}$	½ cylinder
300	Otter trawl-straight tow	$\dfrac{\text{\# of fish}}{1.2 * 6.1 * \text{Distance towed}}$	Rectangle pulled a set distance
301	Otter trawl-arc tow	$\dfrac{\text{\# of fish}}{1.2 * 6.1 * \text{Distance towed}}$	Rectangle pulled a set distance

For each gear and SoI combination, 4 plots were generated in R Studio (R Core Team 2020), including: 1) a histogram of the frequency of occurrence of the SoI at observed temperatures, 2) the raw density of the SoI at the observed temperature, 3) a histogram of the frequency of occurrence of the SoI at observed salinity, and 4) the raw density of the SoI at the observed salinity. The relationship between density and temperature, or salinity, was also calculated and

critical statistics provided on the relevant plot. A frequency of occurrence of 0.05 or greater in the histograms was considered the threshold for a 'normal' range, whereas values outside that range were assumed to be temporary or stressful conditions, or generally abnormal for the species. While our Phase II study focused on generating models describing the relationship between abundance and environmental parameters, here the response variable was density. Both provide different, but valuable insight.

A set of temporally explicit rasters of environmental conditions encountered within the FWC data, regardless of species collected, as well as rasters containing the combination of spatiotemporally explicit occurrences of each SoI with respect to those environmental parameters were also provided. While this geospatial analysis is not complete enough to draw direct conclusions from, it was deemed a feasible way to make progress toward the next necessary step in the RLI investigations, Habitat Suitability Models (HSM), with the time provided. However, they do provide a way to qualitatively visualize the described relationships.

2.2 Results

2.2.1 Banana River Environment

The observed temperatures of the BRL in the FWC data ranged from 6.30-40 °C with a mean of 25.05+-0.04 (**Figure 2, Figure 3**). The observed salinity of the BRL in the FWC data ranged from 0-47.80 ppt with a mean of 23.29+-0.07 ppt (**Figure 4, Figure 5**). Substantial seasonal variation can be expected as well, as described in the RLI Phase I report (Johnson et al. 2020).

Observed BRL shorelines were dominated by mangroves, with some artificial shores near Patrick Space Force Base, Kennedy Space Center, Port Canaveral, and the neighborhoods along the southern reaches (**Figure 6**). For a detailed accounting of the shoreline delineations, please reference the Florida Department of Environmental Protection report (Fl. DEP 2016). For a detailed discussion on the status and history of the benthic, seagrass, habitat in BR, please see Morris et al. 2021.
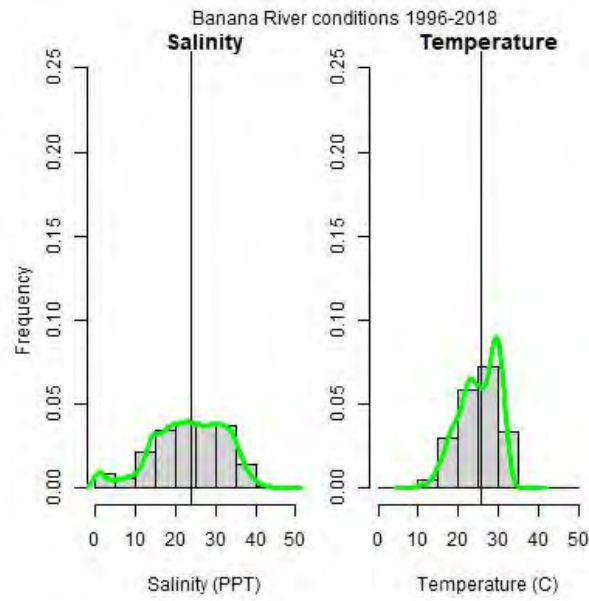
Figure 1. Histograms of the salinity and temperature observed in the BR, FWC data zone E, from 1996-2018. The median is marked by a vertical line and a smoothed line of the values is shown in green.
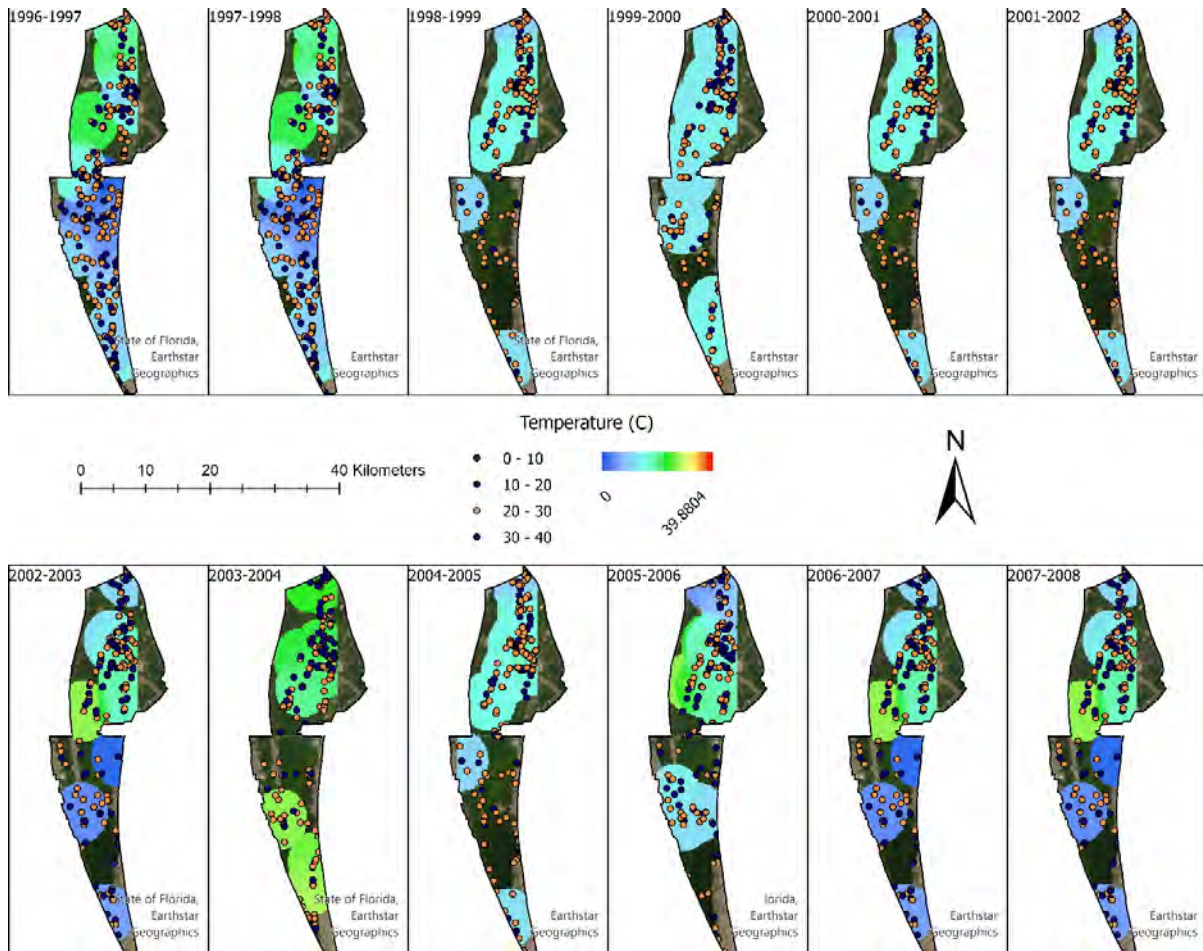
Figure 2. Annual BRL temperature readings taken at the time of fish sampling from 1996-2008, with values differentiated by colored dots, as well as an inverse distance weighting extrapolated temperature surfaces derived from those values. When multiple records occurred for the same location within a single year, the mean value is presented.
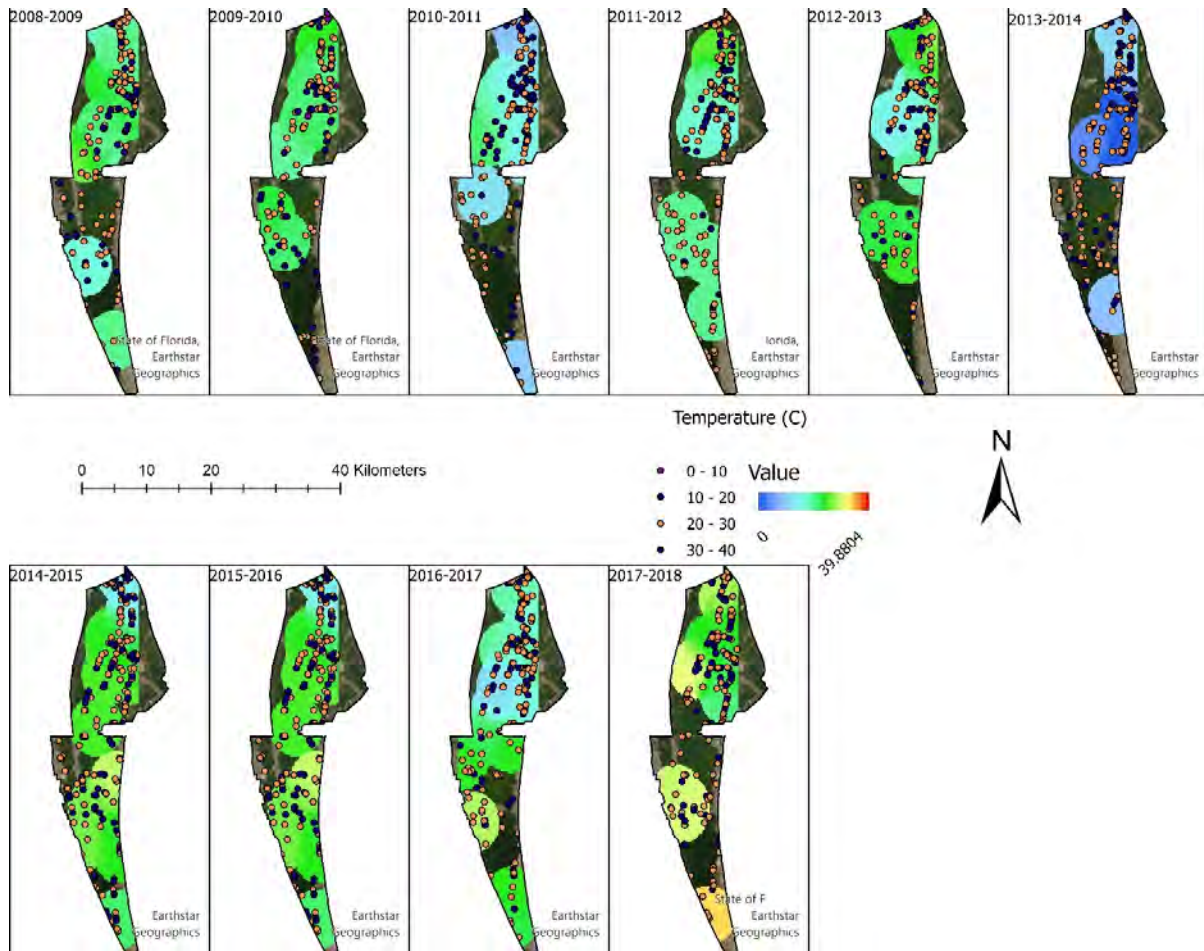
Figure 3. Annual BRL temperature readings taken at the time of fish sampling from 2008-2018, with values differentiated by colored dots, as well as an inverse distance weighting extrapolated temperature surfaces derived from those values. When multiple records occurred for the same location within a single year, the mean value is presented.
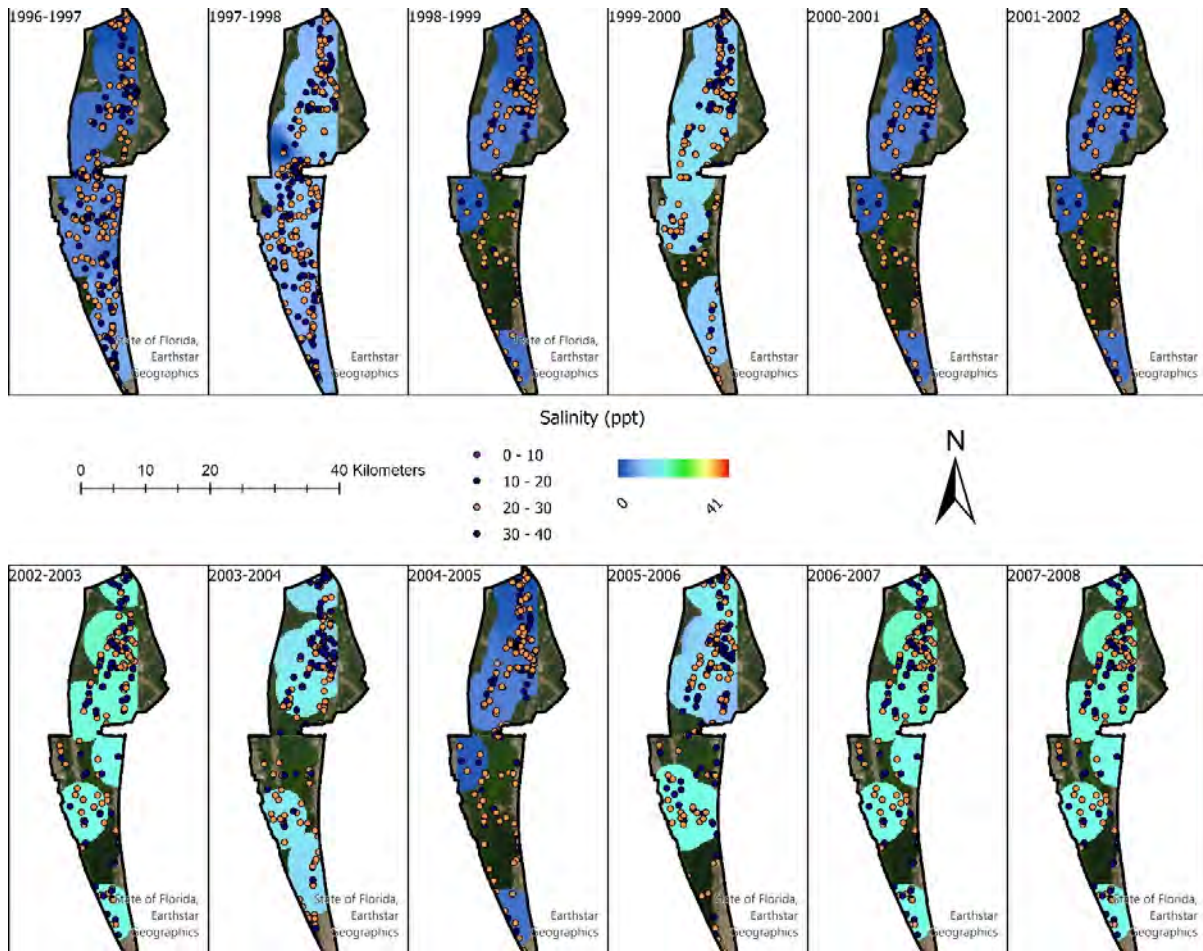
Figure 4. Annual BRL salinity readings taken at the time of fish sampling from 1996-2008, with values differentiated by colored dots, as well as an inverse distance weighting extrapolated temperature surfaces derived from those values. When multiple records occurred for the same location within a single year, the mean value is presented.
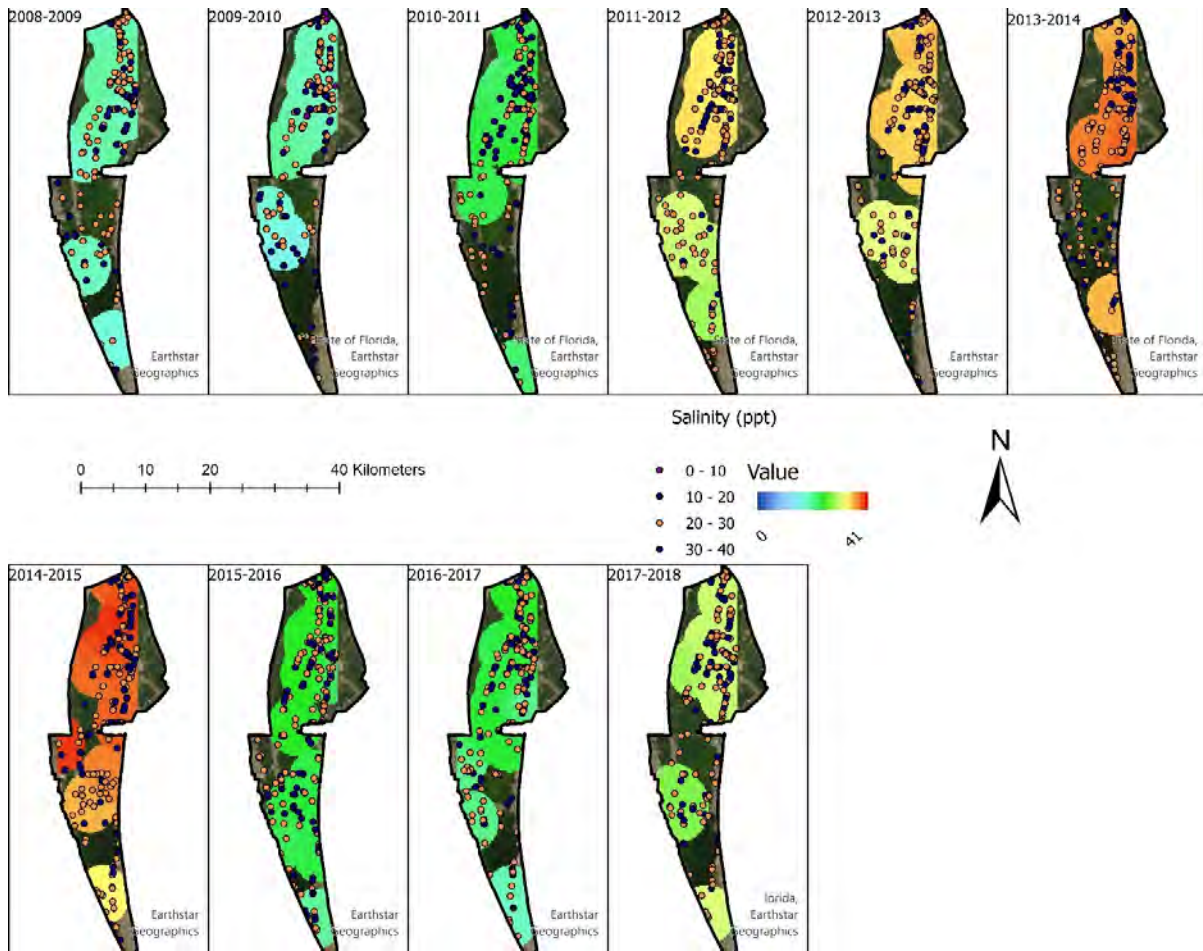
Figure 5. Annual BRL salinity readings taken at the time of fish sampling from 2008-2018, with values differentiated by colored dots, as well as an extrapolated, through inverse distance weighting, temperature surfaces derived from those values. When multiple records occurred for the same location within a single year, the mean value is presented.
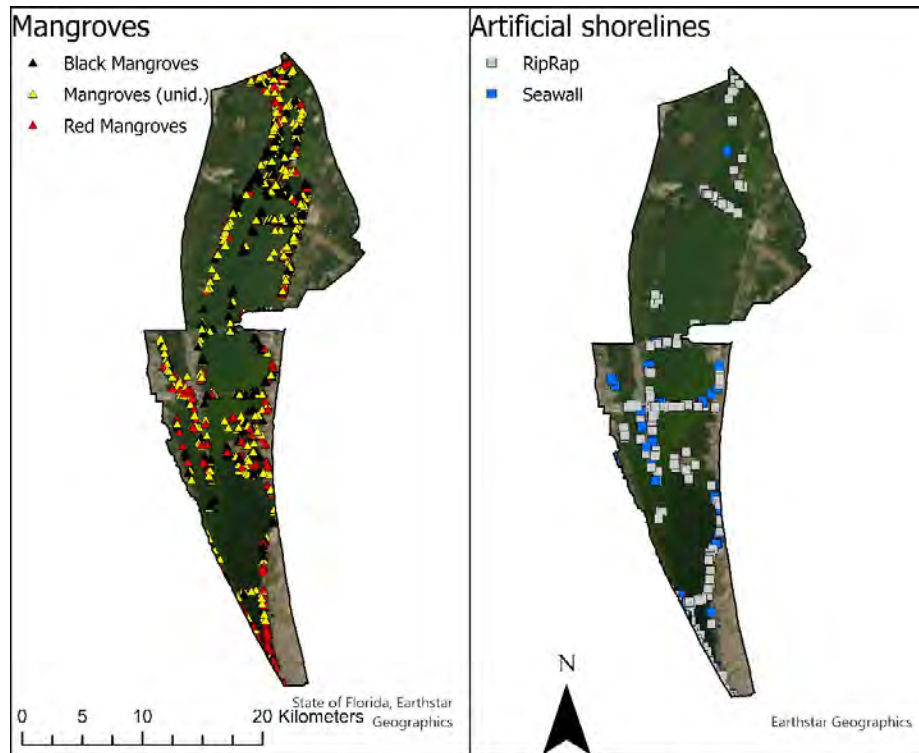
Figure 6. Banana River shorelines as observed in the FWC data at the time of fish collections, focusing on the mangrove (left) and artificial (right) shoreline types as these dominate this ecosystem. Note that all years are presented here in one snapshot as they do not represent consistent repeated measures of every site. This is meant as a general guide to facilitate discussion below but should not be interpreted as reliable shoreline survey data. Please see Fl DEP 2016 for a more detailed and nuanced discussion of the BRL shoreline.

2.2.2 *Anchoa mitchilli- Bay Anchovy*

There were 5040, 3, 249 and 255 usable occurrences in gears 20, 160, 300, and 301, respectively. All Bay Anchovies were found in temperatures between 9.6 °C and 34 °C with only gear 20 presenting a weak but significant positive relationship between density and temperature for this species (P<0.001, adjusted R^2=0.007). The mean temperature observed was 25.51±0.33 °C, 24.59±0.32 °C, and 24.88±0.33 °C for gears 20, 300, and 301, respectively. Bay Anchovies were found in nearly the full range of salinities in the BR, 0.20 to 47.80 ppt with a mean of 25.52±0.10 ppt, 22.21±0.45 ppt, and 27.07±0.36 ppt in gears 20, 300, and 301 respectively, but the majority were found in salinities from 10 to 35 ppt (**Figure 6, Table 3, Table 4**). This species has a tendency to move in large schools and as such can be very patchy in distribution; however, the region of BRL North of Port Canaveral appears to provide the most reliable occurrences (**Figure 7, Figure 8**).

Figure 7. A four paneled figure for gears 20 (top left), 160 (top right), 300 (bottom left) and 301 (bottom right). Each panel contains four figures: a histogram of observed temperatures for this species, with the median denoted by a vertical line and a smoothed representation of the data in green (top left), a similar histogram showing observed salinities for this species (top right), a scatterplot of density versus temperature for this species with a green line of best fits representing and statistics for the linear model of this relationship (bottom left), and a similar scatterplot of density versus salinity (bottom right). Note that no data are presented if there were less than 25 occurrences of this species for any given gear type.

Figure 8. Annual *Anchoa mitchilli* BRL densities (fish/m³), 1996-2008.
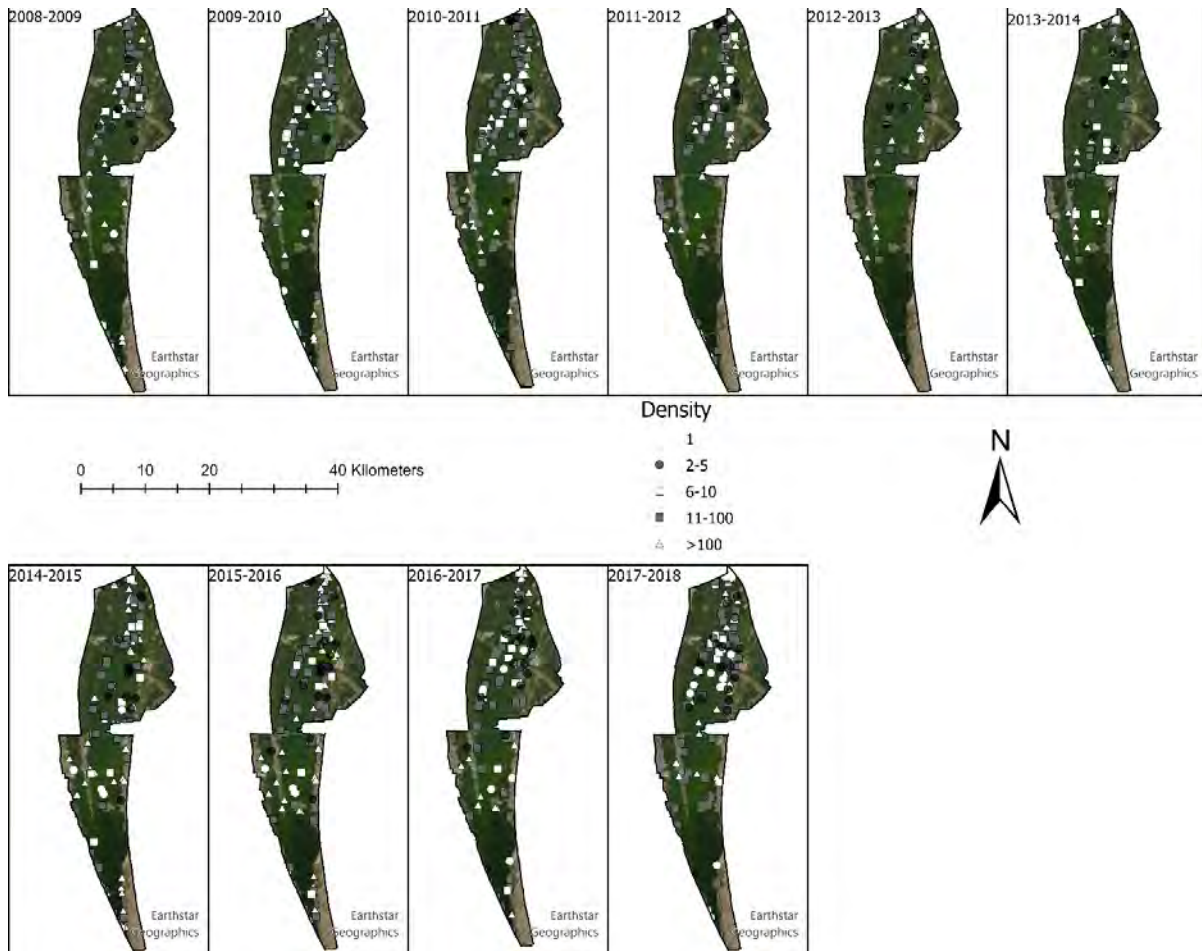
Figure 9. Annual *Anchoa mitchilli* BRL densities (fish/m^3), 2008-2018.

2.2.2.1 Bay Anchovy literature review

This species was listed by Gunter (1956) as a euryhaline fish, which was defined at the time as 'a fish which has been recorded from both fresh-water and pure sea water by competent reporters. The other works regarding this species generally refer to them as being found in fresh to hypersaline waters (Castro and Cowen 1991) and 20 to 30 °C (Jung & Houde, 2004). By all accounts, this species was found to have limited to no significant relationships with temperature or salinity. Rather, they were most heavily influenced by dissolved oxygen and rainfall, presumably through its impact on prey availability (Castro and Cowen 1991, Castillo-Rivera et al. 1994, Jung and Houde 2004, Castillo-Rivera 2013). Notably, similarly weak environmental forcing for this species in the BRL were reported in RLI Phase's I and II (Johnson et al. 2020, Blanchard et al. 2021), and herein (**Table 2, Table 3, Table 4, Figure 2**).

2.2.2.2 Bay Anchovy summary

By all accounts, this is a euryhaline species which engages in significant seasonal migrations and is more responsive to prey pulsing than direct environmental conditions (Bay et al. 1987, Castro and Cowen 1991, Castillo-Rivera et al. 1994, Jung and Houde 2004). Within the BRL, they are generally found in the 10 to 30 °C range, and at any salinity in excess of 10 ppt (**Table 2, Table 3, Table 4, Figure 2**). These conditions broadly reflect the BRL itself (**Figure 1, Table 2**), suggesting little to no selectivity of temperature or salinity conditions in this species. However,

Gunter (1956) did point out that the rate of water condition change which this species can endure had not yet been determined. This appears to still be true. It was also noted that the primary habitat descriptor of this species was the prevalence of submerged vegetation (Castro and Cowen 1991), which is also a restoration target for the broader IRL restoration community and may outweigh the importance of changing abiotic conditions for this species.

Regarding the implications of enhanced inflow on this species, there are a few open questions that still need to be answered. First, it is not yet known what rate of change this species can endure before experiencing thermal or osmotic stress (Gunter 1956). Second, RLI Phase 1 engineering models suggested that temperatures would decrease, and salinities would increase under pumping (FL.Tech. 2020). While this expected change is not to a degree that would be deemed stressful for this species, the most pressing question for this species with regards to the RLI proposal is: What is the daily expected rate of change in water conditions under pumping conditions? Finally, the information presented here lays out the necessary framework for inferring preferred habitat and provides the necessary resources for habitat suitability assessments as a component of the proposed pilot inflow project. The biggest pending question for this, and all fishes in the IRL with respect to the RLI proposal is: How will habitat suitability change under proposed pumping scenarios?

2.2.3 *Archosargus probatocephalus- Sheepshead*

There were 1184, 2808, 92, and 165 usable occurrences in gears 20, 160, 300, and 301, respectively. All Sheepshead were found in temperatures between 7.1 °C and 35 °C with gears 20 and 160 presenting weak but significant positive relationship between density and temperature for this species (P<0.013, adjusted R^2=0.004; P<=0.001, adjusted R^2=0.013, respectively; **Figure 9**). The mean temperature observed was 26.97±0.12 °C, 25.89±0.09 °C, 25.72±0.41 °C and 26.46±0.30 °C for gears 20, 160, 300, and 301, respectively. Sheepshead were found in nearly the full range of salinities in the BRL, 0.20 to 47.60 ppt with a mean of 28.66±0.21 ppt, 26.20±0.13 ppt, 28.29±0.68 ppt, and 30.11±0.43 ppt in gears 20, 160, 300, and 301, respectively, but the majority were found in salinities from 10 to 40 ppt (**Figure 9, Table 3, Table 4**). Significant, weak, positive relationships were found between salinity and density for this species in gears 20 (P=0,021, adjusted R^2=0.004), 160 (P<=0.001, adjusted R^2=0.009), and 300 (P=0.004, adjusted R^2=0.076). Sheepshead were rarely encountered in high densities, with the northern BRL providing the most consistent occurrences (**Figure 10, Figure 11**).
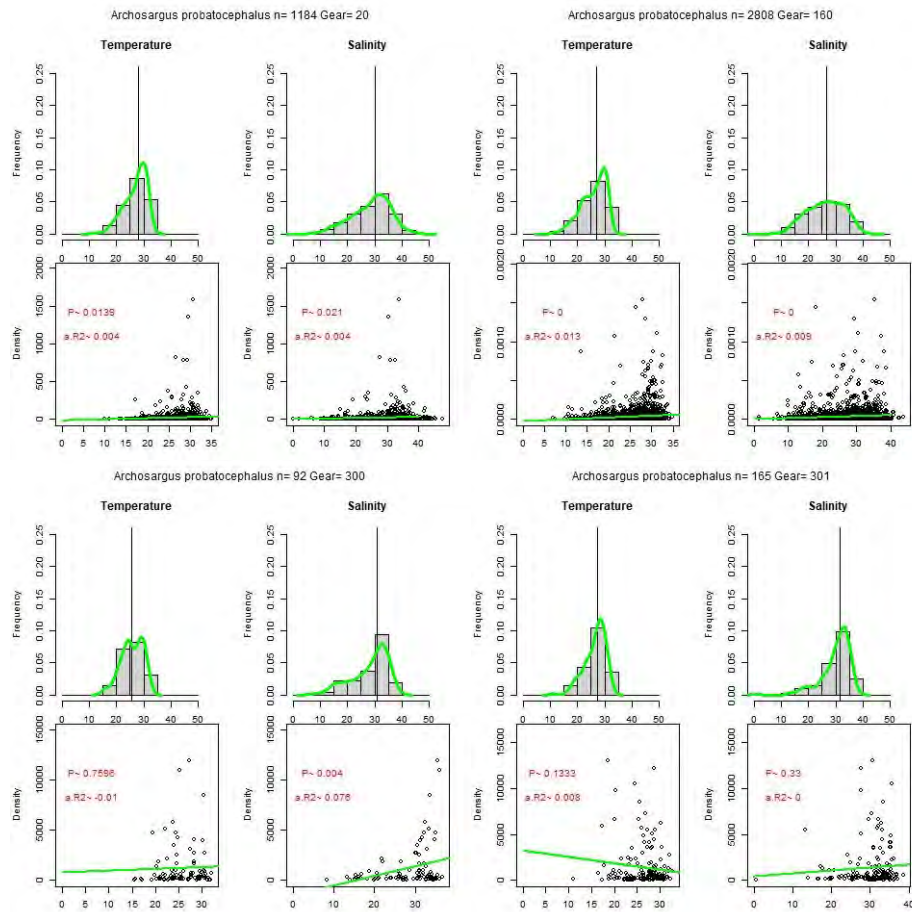
Figure 10. A four paneled figure for gears 20 (top left), 160 (top right), 300 (bottom left) and 301 (bottom right). Each panel contains four figures: a histogram of observed temperatures for this species, with the median denoted by a vertical line and a smoothed representation of the data in green (top left), a similar histogram showing observed salinities for this species (top right), a scatterplot of density versus temperature for this species with a green line of best fits representing and statistics for the linear model of this relationship (bottom left), and a similar scatterplot of density versus salinity (bottom right). Note that no data are presented if there were less than 25 occurrences of this species for any given gear type.

Figure 11. Annual *Archosargus probatocephalus* BRL densities (fish/m³), 1996-2008.
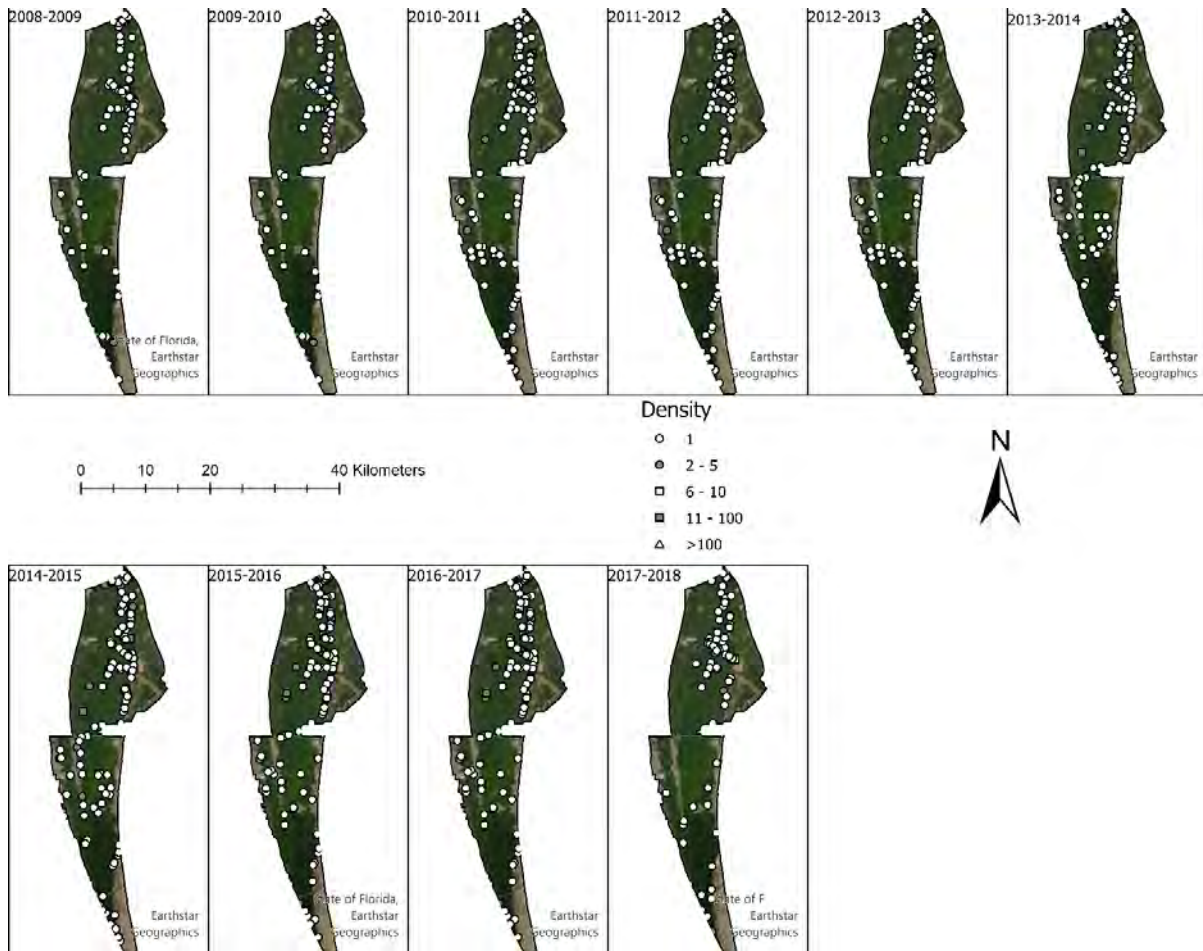
Figure 12. Annual *Archosargus probatocephalus* BRL densities (fish/m^3), 2008-2018.

2.2.3.1 Sheepshead literature review

Generally regarded as a euryhaline species (Gunter 1956), Sheepshead are typically found in a full range of estuarine and marine salinities (Tucker and Barbera 1987, Tolley et al. 2005, Dutka-Gianelli et al. 2011, Bell and McDonough 2015, Adams et al. 2018, Golden and Froeschke 2023, Gutierrez et al. 2023). As they undergo ontogenetic habitat shifts, their observed relationship with salinity shifts, but their distribution seems to be more heavily related to habitat structure rather than the abiotic conditions typical of a Florida estuary (Bell and McDonough 2015, Golden and Froeschke 2023, Gutierrez et al. 2023). However, as a popular sportfish and a desirable food fish, they have been studied in aquacultural settings to identify their physiological relationship with temperature and salinity. Sheepshead will survive, with no visible signs of stress, in salinities ranging from 10 to 45 ppt, and have been noted to spawn as salinities increase from low to high, generally spawning as salinity approaches 33 to 35 ppt (Tucker and Barbera 1987, Merino Contreras 2018, Patetta 2022). Larvae tend to be more marine, but once they gain directional capacity, they begin migrating inshore seeking areas with suitable habitat structure, such as mangrove shorelines, oyster reefs, or otherwise dense structure (Gutierrez et al. 2023). Regarding temperature, this species prefers stable conditions more typical of a marine environment, 21 to 26 °C with a maximum captive condition achieved at 23 °C and will abandon estuaries as temperatures fluctuate or decrease (Tucker and Barbera 1987). In two estuaries

surrounding the Gulf of Mexico, estuarine emigration occurred as temperatures approached 12 °C and 21 °C, respectively (David Heil 2017). However, they are tolerant of pulsed cold conditions, with a lower lethal limit of 3 to 8 °C depending on life history stage (Patetta 2022). Their observed critical maximum temperature, the maximum temperature from which recovery is unlikely due to severe physiological stress and/or physical damage, has been measured to range from 33 to 38 °C, depending on life history stage (Patetta 2022), with their skin collagen denaturing at 34 °C (Ogawa et al. 2003).

Overall, the reviewed literature agrees that this is a warmer water euryhaline fish that seems to value stability of conditions over the values themselves and will actively migrate seeking preferable conditions. Notably, a study observing how various species responded to the opening of a new canal in Northern Brazil found that many of the euryhaline fishes, including Sheepshead, left the area while conditions fluctuate (Saad et al. 2002). However, this study did not have a long-term monitoring component to indicate if this was a permanent or temporary change.

2.2.3.2 Sheepshead summary

The abiotic conditions experienced by Sheepshead in the BRL align well with those found in the literature, existing in the full range of estuarine and marine salinities in excess of 10 ppt, and rarely in temperatures below 10 °C (**Figure 10**). They tend to be in the highest and most consistent densities in the northern BRL (**Figure 11, Figure 12**). This species is well known for migrating away from adverse conditions, particularly with respect to lowering temperatures or fluctuating salinities, moving offshore to presumably find more stable conditions (Bell and McDonough 2015, David Heil 2017, Adams et al. 2018, Gutierrez et al. 2023). They are among the few to have well defined physiological limits, with a lower lethal temperature of 3 to 8 °C, and a maximum thermal limit of 33 to 38 °C depending on life history stage (Patetta 2022), with severe physical damage expected at temperatures exceeding 34 °C (Ogawa et al. 2003). While this upper temperature is above normal conditions for the BRL, it is not outside the observed range (**Figure 1**). Presumably, Sheepshead would emigrate offshore in search of more stable, cooler, conditions in the event of a heat wave, if possible. However, their movement in response to pulse and press abiotic changes in the BRL area is currently not described in detail, though Tremain et al. (2004) did show Sheepshead in the IRL do undergo long distance migrations. The introduction of the cooler water from offshore, through the RLI proposal, would likely serve to mitigate many of large swings in conditions currently typical of the system. Such a change may be beneficial to Sheepshead in the long term, though we might expect them to emigrate from the area for an undeterminable amount of time while conditions changed, as was observed following a Brazilian canal opening (Saad et al. 2002).

Regarding the RLI proposal, there are several pending questions for this species which must be addressed. Introducing water from an offshore source could 'stabilize' the conditions to a degree, providing a buffer against such pulse disturbances (FL.Tech. 2020), as was seen in South Florida's 2010 cold snap where deeper water changed slower, providing a thermal refuge for species that would otherwise have been killed (Hallac et al. 2010, Rehage et al. 2016). However, typical seasonal changes are important for spawning and movement of Sheepshead movement regimes (Tucker and Barbera 1987, Dutka-Gianelli and Murie 2001, David Heil 2017, Adams et al. 2018), making it imperative that seasonal fluctuations in abiotic conditions still persist while habitat restoration activities continue. As such, pending questions for this species with regards to the RLI proposal are: 1) What is the daily expected rate of change in water conditions under each pumping scenario, 2) What rate of change can Sheepshead acclimate to, and 3) How will habitat suitability change under each pumping scenario, for each life history stage of this species?

2.2.4 Cynoscion nebulosus- Spotted Seatrout

There were 2637, 1440, 212, and 135 usable occurrences in gears 20, 160, 300, and 301, respectively. All Spotted Seatrout were found in temperatures between 6.3 °C and 40 °C with no significant relationship detected between density and temperature for this species. The mean temperatures observed were 28.20±0.08 °C, 24.32±0.14 °C, 28.16±0.29 °C and 29.27±0.28 °C for gears 20, 160, 300, and 301, respectively. The majority of Spotted Seatrout were found in the 15 to 35 °C range. They were also found in nearly the full range of salinities in the BRL, 0.20 to 42.60 ppt with a mean of 24.95±0.14 ppt, 25.16±0.16 ppt, 21.40±0.47 ppt, and 26.92±0.55 ppt in gears 20, 160, 300, and 301, respectively, but the majority were found in salinities from 10 to 40 ppt (**Table 2, Table 3, Table 4, Figure 4**). A significant, weak, positive relationship was found between salinity and density in gear 160 (P=0.002, adjusted R^2=0.006). As adults, this genus tends to occur in low densities; however, the BRL has been suggested as a local spawning site due to the high densities of juvenile Spotted Seatrout in the northern and central BRL early in the dataset. Those high densities appear to be increasingly rare in the later portions of the data (**Figure 13, Figure 14**). As Spotted Seatrout are known to rely on seagrass in early life history stages when their densities are highest (Flaherty-Walia et al. 2015, Moulton et al. 2017), and the BRL has lost significant amounts of seagrass since the 2011 Super Bloom (Kamerosky et al. 2015, Morris et al. 2021, 2022), this perceived change may be the result of changes in the community itself.
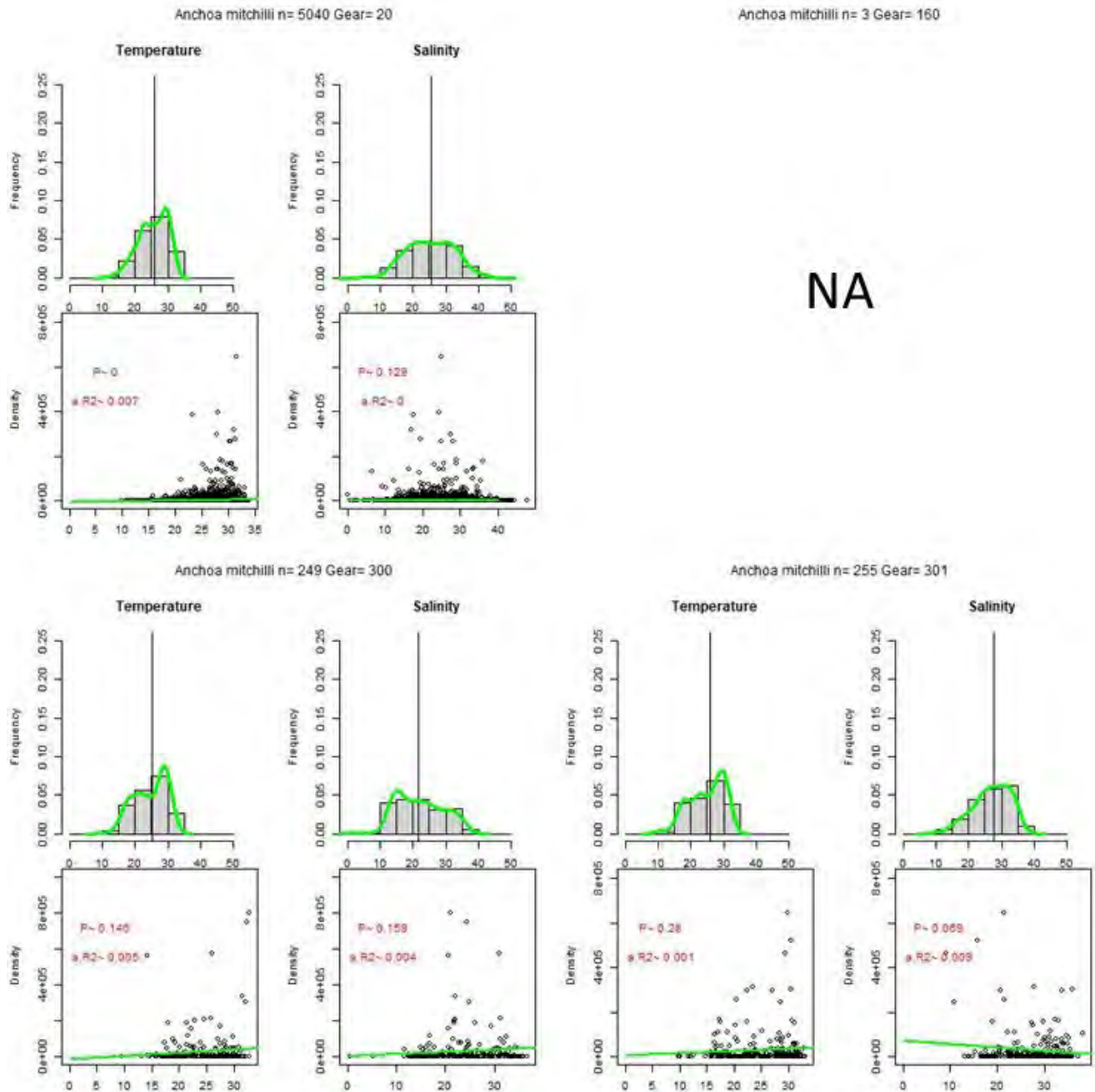
Figure 13. A four paneled figure for gears 20 (top left), 160 (top right), 300 (bottom left) and 301 (bottom right). Each panel contains four figures: a histogram of observed temperatures for this species, with the median denoted by a vertical line and a smoothed representation of the data in green (top left), a similar histogram showing observed salinities for this species (top right), a scatterplot of density versus temperature for this species with a green line of best fits representing and statistics for the linear model of this relationship (bottom left), and a similar scatterplot of density versus salinity (bottom right). Note that no data are presented if there were less than 25 occurrences of this species for any given gear type.

Figure 14. Annual *Cynoscion nebulosus* BRL densities (fish/m^3), 1996-2018.
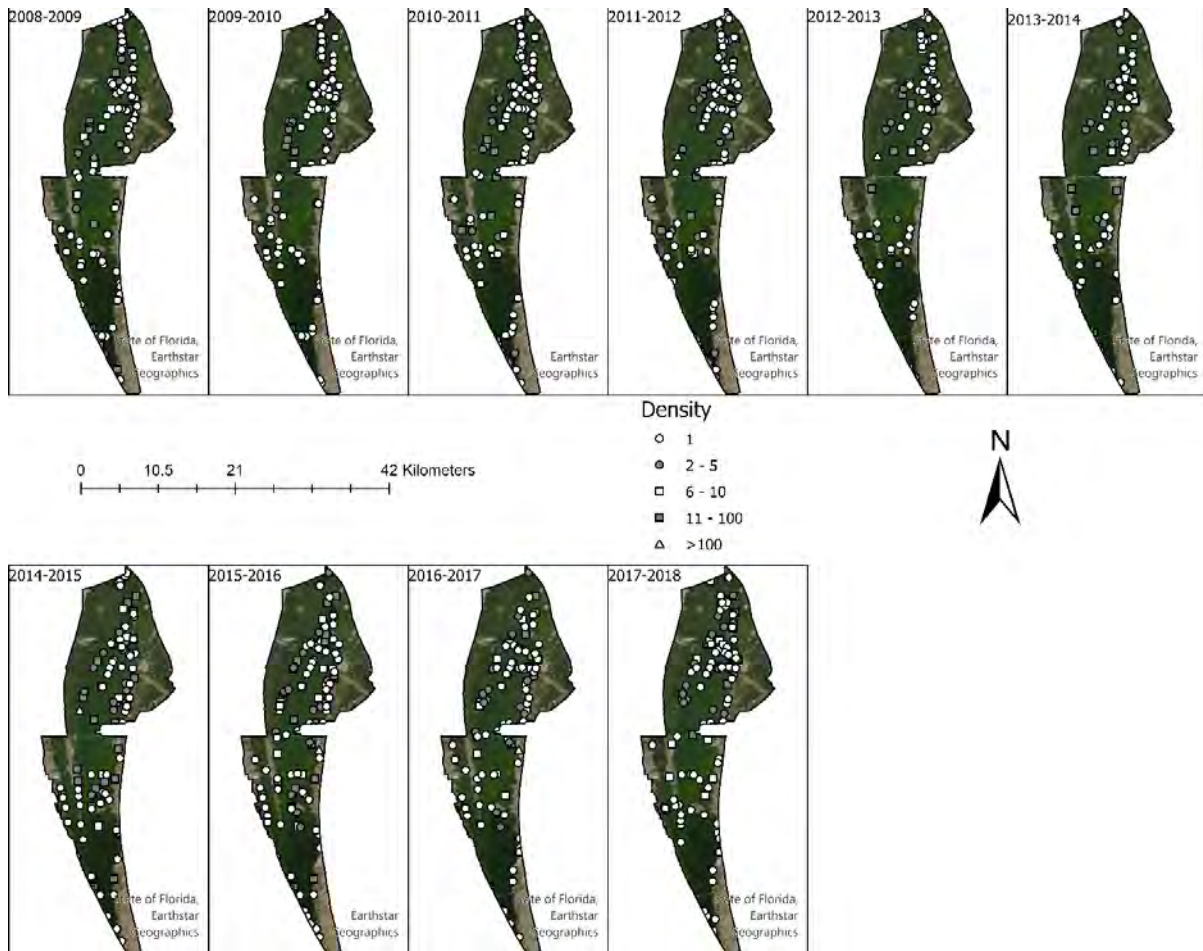
Figure 15. Annual *Cynoscion nebulosus*. BRL densities (fish/m³), 2008-2018.

2.2.4.1 Spotted Seatrout literature review

Spotted Seatrout are a euryhaline sportfish (Gunter 1956) with a complex life history, heavily linked to the prevalence of submerged vegetation as larvae and juveniles and moving to more open waters as they age (Moody 1950, Saucier and Baltz 1993, Kucera et al. 2002, Anweiler 2013). They are generally found in estuarine to marine salinities, 14 to 40 ppt (Colura 1974, Rutherford et al. 1989, Kucera et al. 2002), though there is evidence of microevolution of different halotolerances and thermal tolerances within this species along their latitudinal range (Kucera et al. 2002, Song and McDowell 2021). In general, studies have found that this species has a greater thermal tolerance in higher salinity waters and grow faster in hypersaline conditions when compared to hyposaline growth rates (Kucera et al. 2002, Song et al. 2019, Song and McDowell 2021). They are also highly tolerant to accumulated cold stress, with an accumulated lower lethal temperature in the 2 to 4 °C range. However, if the cold persists for 10 days or more, they struggle below 5 °C (Ellis et al. 2017). Also, in the condition of a rapid cooling event, in excess of 1 °C/day, they show signs of cold stress at much warmer temperatures, similar to the levels of cold stress exhibited at an extreme cooling rate of 1 °C / 10 minutes (Anweiler 2013, Ellis et al. 2017). Fluctuating conditions during cooling, or reducing salinity, also induce stress more quickly. In one study, fluctuating conditions induced loss of equilibrium and acute mortality in less than 130 hours 2 °C warmer than the accumulated lower lethal limit (Anweiler 2013). The rate of decline in that

study was an average of 2.5 °C/hour. It is also important to note that the rate of temperature and salinity change has been identified as a key method for signaling spawning preparations in females, and changes to water conditions alter the timing and periodicity of spawning in this species (Colura 1974, Brown-Peterson et al. 2002, Blaylock et al. 2021). Ambient water conditions are also highly influential on larval growth, with most larvae failing to metamorphose in water temperatures below 24 °C but succeeding in 28 °C in one study (Colura 1974).

2.2.4.2 Spotted Seatrout Summary

The Spotted Seatrout is, by all literary accounts (see above) and by observation (**Figure 13**, **Table 2, Table 3, Table 4**), a euryhaline species with a complex life history heavily tied to environmental cues. They are known to emigrate in and out of the study area, despite a high site fidelity (Reyier et al. 2020), likely linked to reproductive behavior induced by environmental changes (Moody 1950, Kilma and Tabb 1959, Colura 1974, Rutherford et al. 1989, Saucier and Baltz 1993, Brown-Peterson et al. 2002, Kucera et al. 2002). They have a well-defined, though spatially variable, lower thermal limit of approximately 2 °C (Anweiler 2013, Ellis et al. 2017), preferring temperatures in the 20 to 30 °C range (**Figure 13**, Colura 1974, Brown-Peterson et al. 2002) with steady, slow, rates of change (Anweiler 2013, Ellis et al. 2017).

With regards to the RLI proposal, the introduction of cool seawater from an offshore source will likely have a few notable negative impacts on this species. First, a targeted restoration goal is the restoration of the seagrasses which have been lost, in part, due to the eutrophication induced recurrent severe algal blooms (Morris and Virnstein 2004, Morris et al. 2021, 2022). While RLI represents many different actions and changes to the system, at its core it is aimed at expediting biochemical processes to remove algae bloom feeding nutrients from the system while reducing the amount of benthic muck (FL. Tech 2020). This is proposed to be done by introducing water from offshore at some as of yet undetermined rate which would reduce and stabilize water temperatures, reduce and stabilize salinity, and introduce oxygen to the system to fuel the processes (FL. Tech 2020, Blanchard et al. 2021). The rate of these changes will be crucial to understand, as this species has been clearly shown to be sensitive to fluctuating conditions both in the pulse and press form, with a higher tolerance for presses at or below 1 °C-day of change (Anweiler 2013, Ellis et al. 2017). The increased stability of the conditions will likely have a more nuanced effect on the Spotted Seatrout. The rapidly fluctuating conditions of shallow water estuaries could be problematic if pulse disturbances occur at a 'bad time' (Ellis et al. 2017), and climate variability is expected to continue to increase throughout the Anthropocene with significant impacts on sensitive biological communities (Brander 2010, Boucek and Rehage 2014, Rehage and Blanchard 2016, Rehage et al. 2016, Santos et al. 2016). Introducing water from offshore could 'stabilize' the conditions to a degree, providing a buffer against such pulse disturbances (FL.Tech. 2020), as was seen in South Florida's 2010 cold snap where deeper water changed slower, providing a thermal refuge for species that would otherwise have been killed (Hallac et al. 2010, Rehage et al. 2016). However, typical seasonal changes and seagrass habitat restoration being important for spawning and growth (Moody 1950, Rutherford et al. 1989, Saucier and Baltz 1993, Brown-Peterson et al. 2002) as well as Spotted Seatrout movement regimes (Reyier et al. 2020), making it imperative that seasonal fluctuations in abiotic conditions still persist, and other habitat restoration activities continue. As such, pending questions for this species with regards to the RLI proposal are: 1) What is the daily expected rate of change in water conditions under each pumping scenario, 2) How will RLI impact seagrass restoration, and at what rate, and 3) How will habitat suitability change under each pumping scenario, for each life history stage of this species?

2.2.5 *Eucinostomus harengulus- Tidewater Mojarra*

There were 2365, 1893, 83, and 117 usable occurrences in gears 20, 160, 300, and 301, respectively. Tidewater Mojarra were found in temperatures between 9 °C and 40 °C with weak significant positive relationships detected between density and temperature with gear 20 ($P<=0.001$, adjusted $R^2=0.022$) and 300($P=0.050$, adjusted $R^2=0.040$). The mean temperatures observed were 26.80±0.09 °C, 25.88±0.11 °C, 25.19±0.55 °C, and 27.20±0.46 °C for gears 20, 160, 300, and 301, respectively. The majority were found in the 15 to 35 °C range. With regards to salinity, while they were noted in lower salinities, ranging from 1.15 to 46.40 ppt, they were primarily found in marine conditions, primarily in the 15 to 40 ppt bins, with a mean of 27.35±0.14 ppt, 25.87±0.15 ppt, 29.17±0.76 ppt, and 28.30±0.56 ppt in gears 20, 160, 300, and 301, respectively (**Table 3, Table 4, Figure 5**). Significant, weak, positive relationships existed between salinity and density in gear 160 ($P=0.002$, adjusted $R^2=0.005$) and gear 300 ($P=0.041$, adjusted $R^2=0.039$). The highest densities of this species are regularly found surrounding Port Canaveral, and in the northern BRL (**Figure 16, Figure 17**).

Figure 16. A four paneled figure for gears 20 (top left), 160 (top right), 300 (bottom left) and 301 (bottom right). Each panel contains four figures: a histogram of observed temperatures for this species, with the median denoted by a vertical line and a smoothed representation of the data in green (top left), a similar histogram showing observed salinities for this species (top right), a scatterplot of density versus temperature for this species with a green line of best fits representing and statistics for the linear model of this relationship (bottom left), and a similar scatterplot of density versus salinity (bottom right). Note that no data are presented if there were less than 25 occurrences of this species for any given gear type.

Figure 17. Annual *Eucinostomus harengulus* BRL densities (fish/m³), 1996-2008.
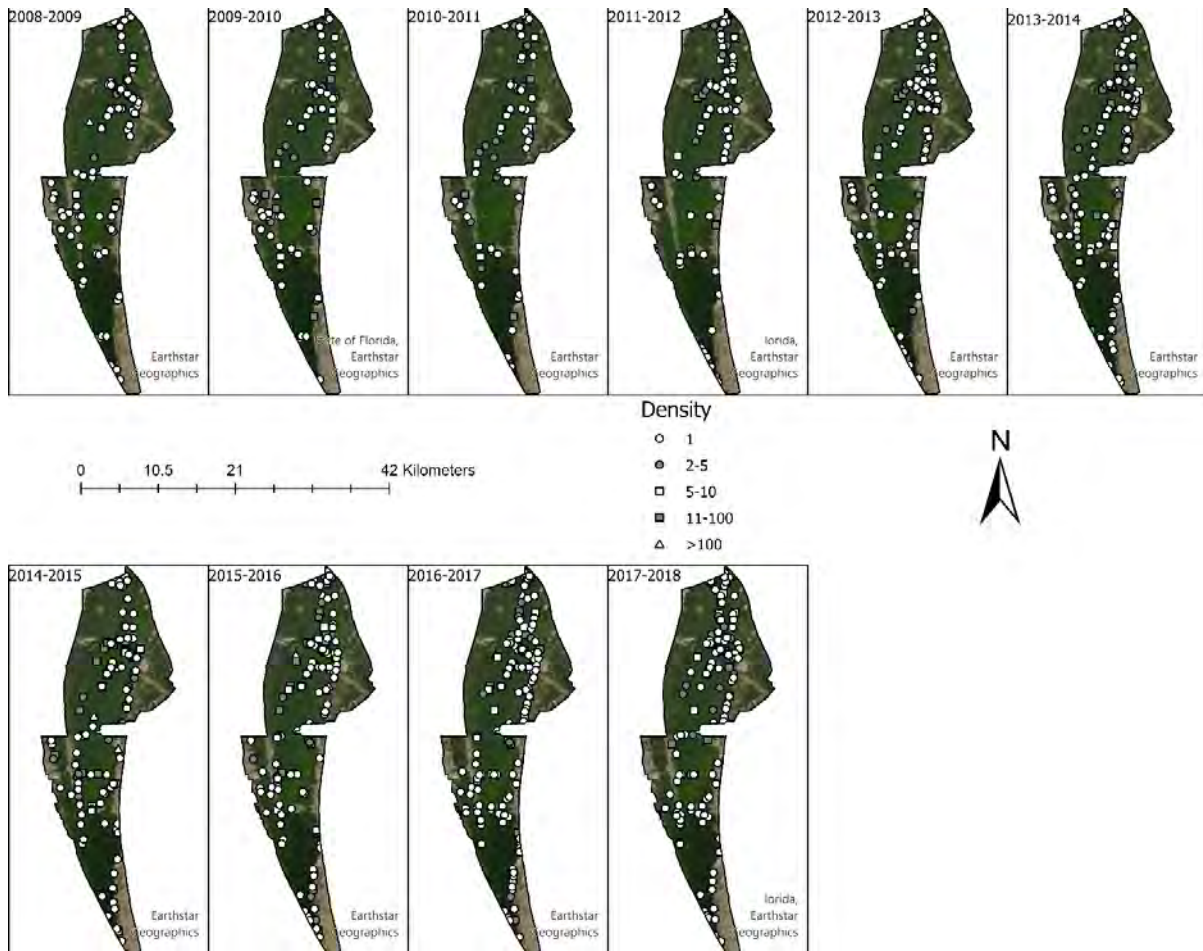
Figure 18. Annual Eucinostomus harengulus BRL densities (fish/m3), 2008-2018.

2.2.5.1 Tidewater Mojarra literature review

Comparatively little focused work has been done on this species' physiology individually, with most studies focusing on either their taxonomic identification to clarify common mis-identifications with Eucinostomus argenteus (e.g. Matheson and Mceachran 1984), or with them as a component of a broader fish community (e.g. Sogard' et al. 1989, Vega-Cendejas et al. 1997a, Paperno and Brodie 2004, Stevens et al. 2013). In general, Tidewater Mojarra are noted in oligohaline (Ley et al. 1999, Stevens et al. 2013), mesohaline (Ley et al. 1999, Powell et al. 2002) and hyperhaline (Ley et al. 1999, Chi-Espínola et al. 2018) fish communities, suggesting a euryhaline status, and are often discussed as being best defined as associated with the seagrass-mangrove nearshore community (Poulakis et al. 2003). In Florida's estuaries they are largely transient with a strong seasonal pattern of abundance which varies by basin. Along the Alafia River they were most abundant in the Fall and Winter with significant associations to freshwater flow rates, in salinities ranging from 0 to 25 ppt (Greenwood et al. 2007). In the Sebastian River, and adjacent portions of the IRL, they were most abundant in the Spring with very few observed in the Fall, and they ordinated along a temperature and salinity axis (Paperno and Brodie 2004). Notably, they are recorded as victims of cold-kills near Merritt Island, in the RLI focal area, in 1985 and 1983, where temperatures were in the 0 16 °C range (Provancha et al. 1986).

2.2.5.2 Tidewater Mojarra summary

Compared to the other species in this report, Tidewater Mojarra have received little dedicated attention to their physiology. They are reported in oligohaline, mesohaline, and hyperhaline (Ley et al. 1999, Powell et al. 2002, Stevens et al. 2013, Chi-Espínola et al. 2018) communities suggesting that they are euryhaline, as is seen in the BRL (**Figure 16, Table 2, Table 3, Table 4**). Regarding temperature, they appear to prefer cooler temperatures, in the 20 to 30 °C range. As they were observed being killed in cold snaps in the 0 to 16 °C range, and are rarely observed in the BRL below 15 °C (**Figure *16*,**Provancha et al. 1986), I would hypothesize that their thermal minimum is around 10 °C, though this would need dedicated physiology experiments to confirm. However, their low incidence at colder temperatures could also be a function of their transient nature in the BR, being most abundant in the spring and are rare in the colder months (Paperno and Brodie 2004). Unfortunately, no data were found to indicate the rate of change which this species can tolerate, how they respond to pulsed versus press changes to conditions, their detailed tolerances to salinity or temperature, or the environmental determinants of their spatially variable transience. We know that they are typically found along seagrass-mangrove shorelines, but habitat suitability still needs to be determined.

Overall, we know surprisingly little about the physiology of this species in the BRL beyond their broader ecology. This report provides data to infer some temperature and salinity information, but dedicated study would be needed to understand 1) the rate of change this species can endure, 2) the thermal limits of this species, and 3) the determinants of habitat suitability for this species, and how they will change under different RLI pumping scenarios.

2.2.6 *Lagodon rhomboides- Pinfish*

There were 2955, 3135, 285, and 464 usable occurrences in gears 20, 160, 300, and 301, respectively. Pinfish were found in temperatures between 6.7 °C and 35 °C with weak significant positive relationships detected between density and temperature with gear 20 (P=0.040, adjusted R^2=0.001) and 160(P<=0.001, adjusted R^2=0.016). The mean temperatures observed were 25.69±0.09 °C, 25.94±0.08 °C, 24.43±0.26 °C and 24.93±0.22 °C for gears 20, 160, 300, and 301, respectively. The majority were found in the 15 to 35 °C range. With regards to salinity, while they were noted in lower salinities, ranging from 7.30 to 47.80 ppt, they were primarily found in marine conditions, the 15 to 40 ppt bins, with a mean of 29.25±0.13 ppt, 25.96±0.12 ppt, 28.81±0.39 ppt, and 30.00±0.22 ppt in gears 20, 160, 300, and 301, respectively. Significant, weak, positive relationships existed between salinity and density in gear 20 (P=0.001, adjusted R^2=0.003) and gear 160 (P<=0.001, adjusted R^2=0.018 (**Table 2, Table 3, Table 4, Figure 6**). This species is widespread throughout the BRL, but has had a notable decline in density and abundance over the last decade (**Figure 19, Figure 20**, Blanchard et al. 2021).
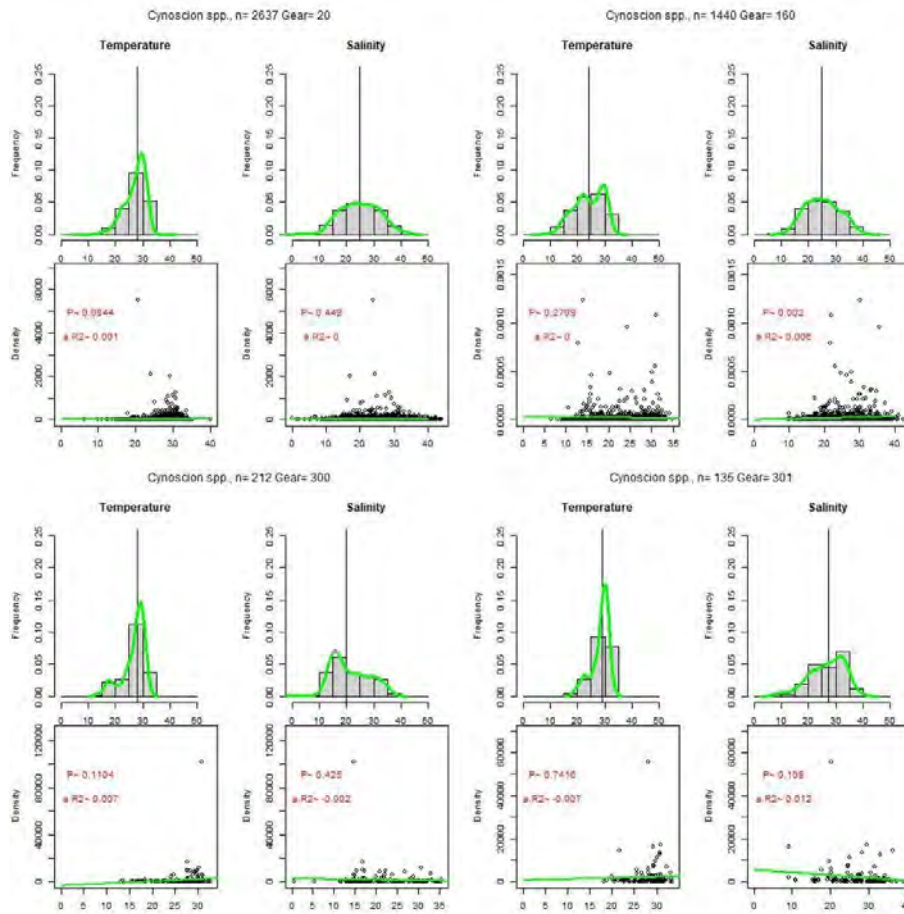
Figure 19. A four paneled figure for gears 20 (top left), 160 (top right), 300 (bottom left), and 301 (bottom right). Each panel contains four figures: a histogram of observed temperatures for this species, with the median denoted by a vertical line and a smoothed representation of the data in green (top left), a similar histogram showing observed salinities for this species (top right), a scatterplot of density versus temperature for this species with a green line of best fits representing and statistics for the linear model of this relationship (bottom left), and a similar scatterplot of density versus salinity (bottom right). Note that no data are presented if there were less than 25 occurrences of this species for any given gear type.

Figure 20. Annual *Lagodon rhomboides* BRL densities (fish/m^3), 1996-2008.
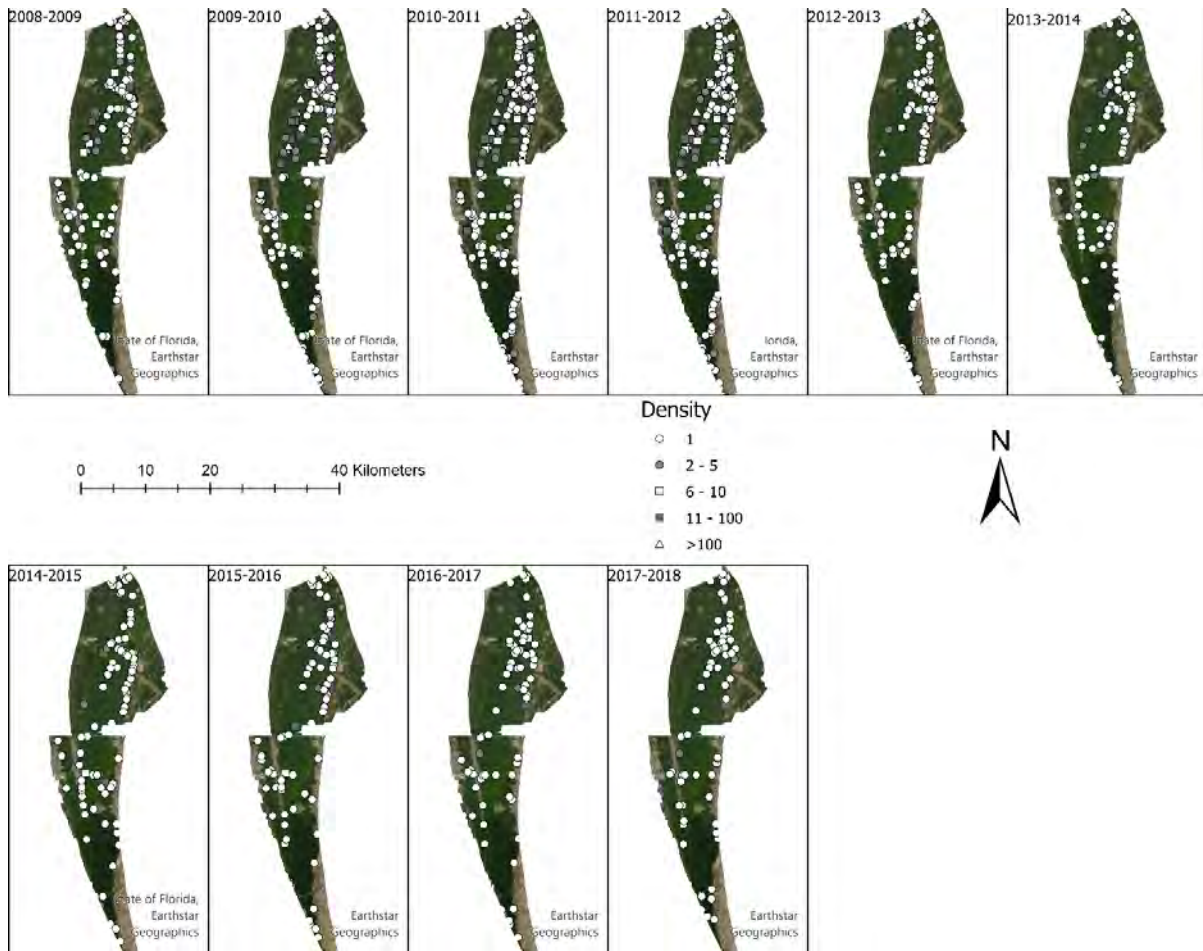
Figure 21. Annual *Lagodon rhomboides* BRL densities (fish/m³), 2008-2018.

2.2.6.1 Pinfish literature review

Pinfish are a euryhaline species (Gunter 1956) that is widely noted as being particularly temperature tolerant for a warm-temperate fish (Darcy 1985). They have been observed in salinities ranging from 0 to 43.8% (Darcy 1985), with growth rate maximized in warm waters with salinities in the 15 to 30 ppt range but have significantly reduced survival at 60 ppt (Shervette et al. 2007). Rapid changes to salinity can be lethal (Darcy 1985). The maximum critical temperature for this species has been experimentally determined to be in the 31 to 38 °C range, depending on salinity (Patetta 2022), and they have been observed actively avoiding temperatures in excess of 35 °C (Darcy 1985). Their lower thermal limit has been described as more variable, dependent on the acclimation and acclimatization history of the animals, as well as the dynamism of their exposure (Darcy 1985, Bennett and Judd 1992). In rapid transitions the measured loss of equilibrium temperature is in the 3.5 to 7.5 °C range, some as high as 10.6 °C depending on salinity. With slower transitions, their lower thermal limit was measured at 3.4 °C (Bennett and Judd 1992). In the wild, fishes have been observed being killed by 10.6 °C waters, as well as surviving, all be it with loss of equilibrium, at 5 °C (Darcy 1985). Densities tend to be highest in estuaries with access to oceanic inflow, access to the broader pool of their planktonic larval recruitment pool (Chacin et al. 2016), and with contiguous beds of submerged aquatic vegetation (Chacin et al. 2016, Santos et al. 2018) for which they have particularly high site fidelity (Potthoff and Allen 2003). Once settled, their home range is typically less than 10 m in SAV (Potthoff and

Allen 2003) except when they migrate offshore during colder months (Darcy 1985, Gelwick et al. 2001), and their growth rate is largely dependent on the interaction between temperature, salinity, and pollutants (White and Angelovic 1973, Darcy 1985).

2.2.6.2 Pinfish summary
Pinfish in the BRL largely align with what is described in the literature, occurring in the BRL's full suite of salinities, with highest densities at higher brackish salinities (15-30 ppt). No pinfish were observed above 35 °C, corroborating observations from the literature, and they were largely absent in colder waters, below 10 °C, which approach their thermal limits. While noted as a particularly hardy species, commonly used in pollutant effect testing, and historically quite abundant, this species' numbers have been declining in the IRL in recent years. (**Figure 23, Figure 24**, Blanchard et al. 2021) This is thought to be due to the significant reductions in submerged aquatic vegetation and pollution, but this is a still a subject of active study (Douglas Adams, personal communication).

Regarding the RLI proposal, Pinfish are largely unaffected by normal environmental changes and will actively relocate to find preferable conditions when possible. However, they have been noted to be sensitive to rapid changes to the environment, though that critical rate of change they can tolerate is still unknown. Their spatial growth rates are typically determined by interactions with the abiotic environment, growing fastest at moderate salinities in warm-temperate waters, but their density and distribution is most heavily influenced by the presence of contiguous submerged vegetation meadows and the distance to a propagule source (i.e., distance to an inlet). An understanding of how the RLI proposal will impact submerged vegetation and propagule pressure, the number of pre-settlement larvae entering the system, is needed. As such, the pending questions for Pinfish with regards to the RLI program are: 1) What is the rate of change which they can endure with minimal stress, within the projected range of conditions, 2) What rate of environmental change can be expected under each pumping scenario, and 3) How will habitat suitability, particularly in terms of submerged vegetation availability, change in response to the RLI proposal and over what time scale?

2.2.7 *Leiostomus xanthurus*- Spot

There were 1399, 1314, 86, and 114 usable occurrences in gears 20, 160, 300, and 301, respectively. Spot were found in temperatures between 8.50 °C and 33.90 °C with weak significant positive relationships detected between density and temperature with gear 20 (P<=0.001, adjusted R^2=0.010) and 160(P=0.001, adjusted R^2=0.007). The mean temperatures observed were 22.95±0.13 °C, 26.74±0.11 °C, 24.07±0.57 °C and 23.92±0.51 °C for gears 20, 160, 300, and 301, respectively. The majority were found in the 15 to 35 °C range. With regards to salinity, while they were noted in lower salinities, ranging from 4.80 to 47.80 ppt, they were primarily found in marine conditions, 15 to 40 ppt bins, with a mean of 28.22±0.19 ppt, 27.62±0.17 ppt, 25.65±0.89 ppt, and 30.53±0.45 ppt in gears 20, 160, 300, and 301, respectively. Significant, weak, positive relationships existed between salinity and density in gear 160 (P<=0.001, adjusted R^2=0.010; **Table 2, Table 3, Table 4, Figure 7**). The highest densities of this species have historically occurred in the Northern BRL (**Figure 22, Figure 23**).
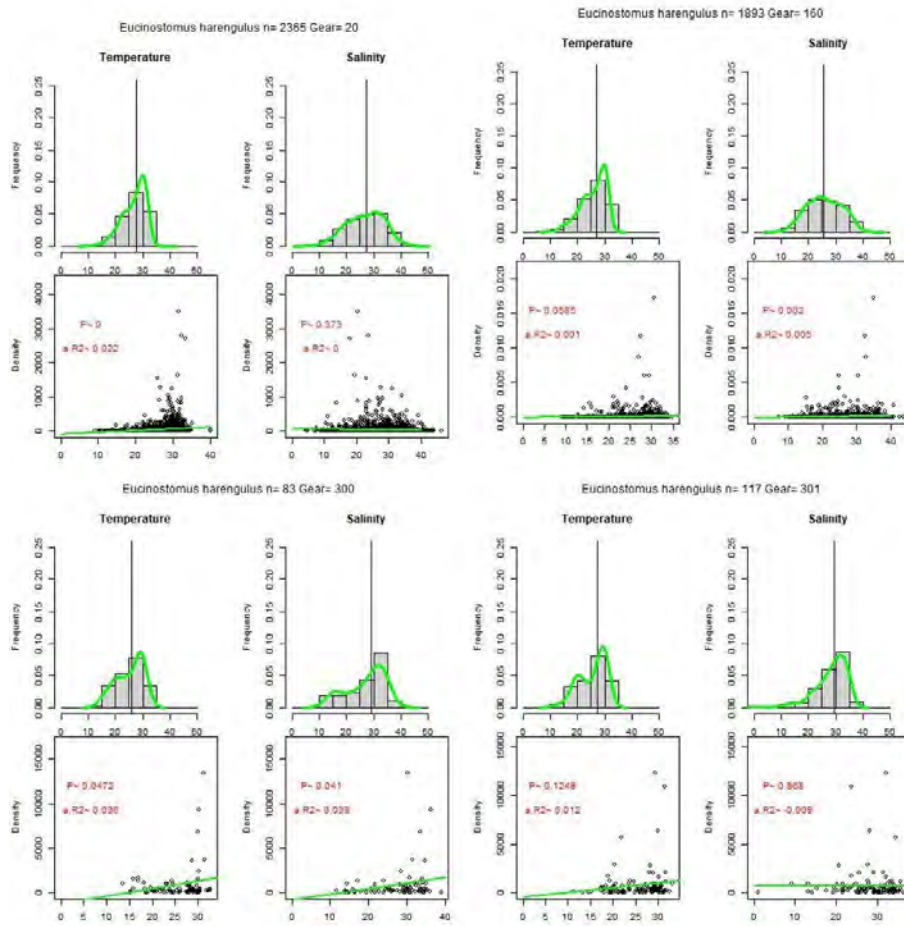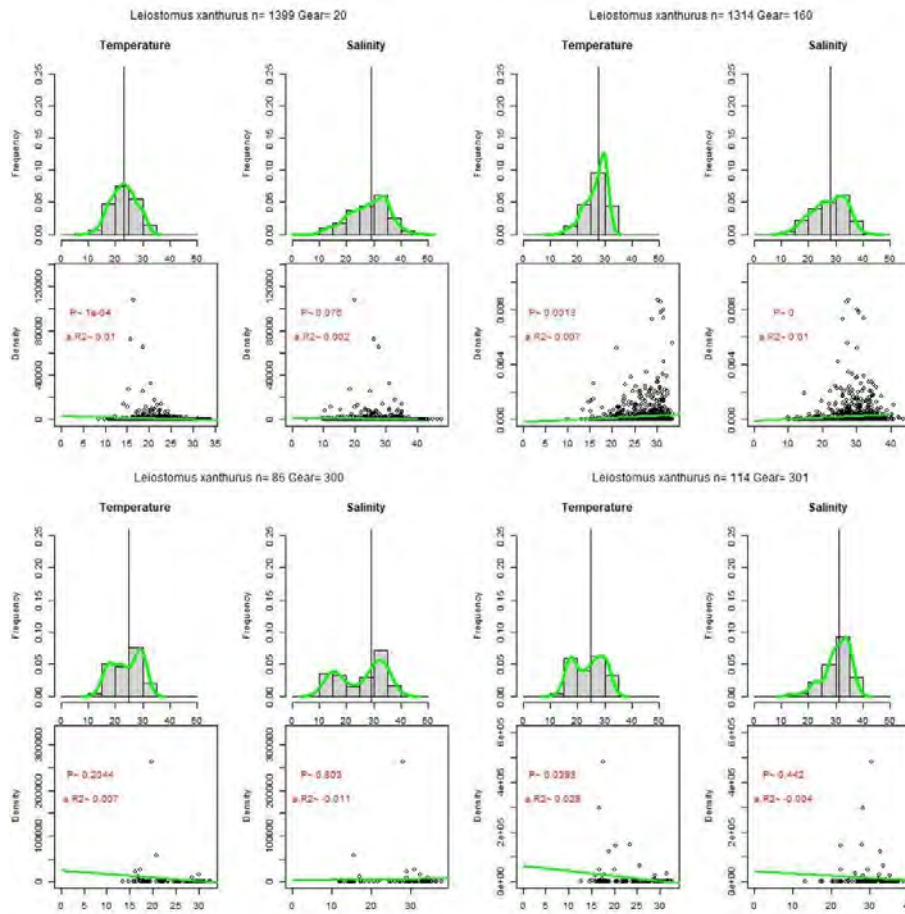
Figure 22. A four paneled figure for gears 20 (top left), 160 (top right), 300 (bottom left) and 301 (bottom right). Each panel contains four figures: a histogram of observed temperatures for this species, with the median denoted by a vertical line and a smoothed representation of the data in green (top left), a similar histogram showing observed salinities for this species (top right), a scatterplot of density versus temperature for this species with a green line of best fits representing and statistics for the linear model of this relationship (bottom left), and a similar scatterplot of density versus salinity (bottom right). Note that no data are presented if there were less than 25 occurrences of this species for any given gear type.
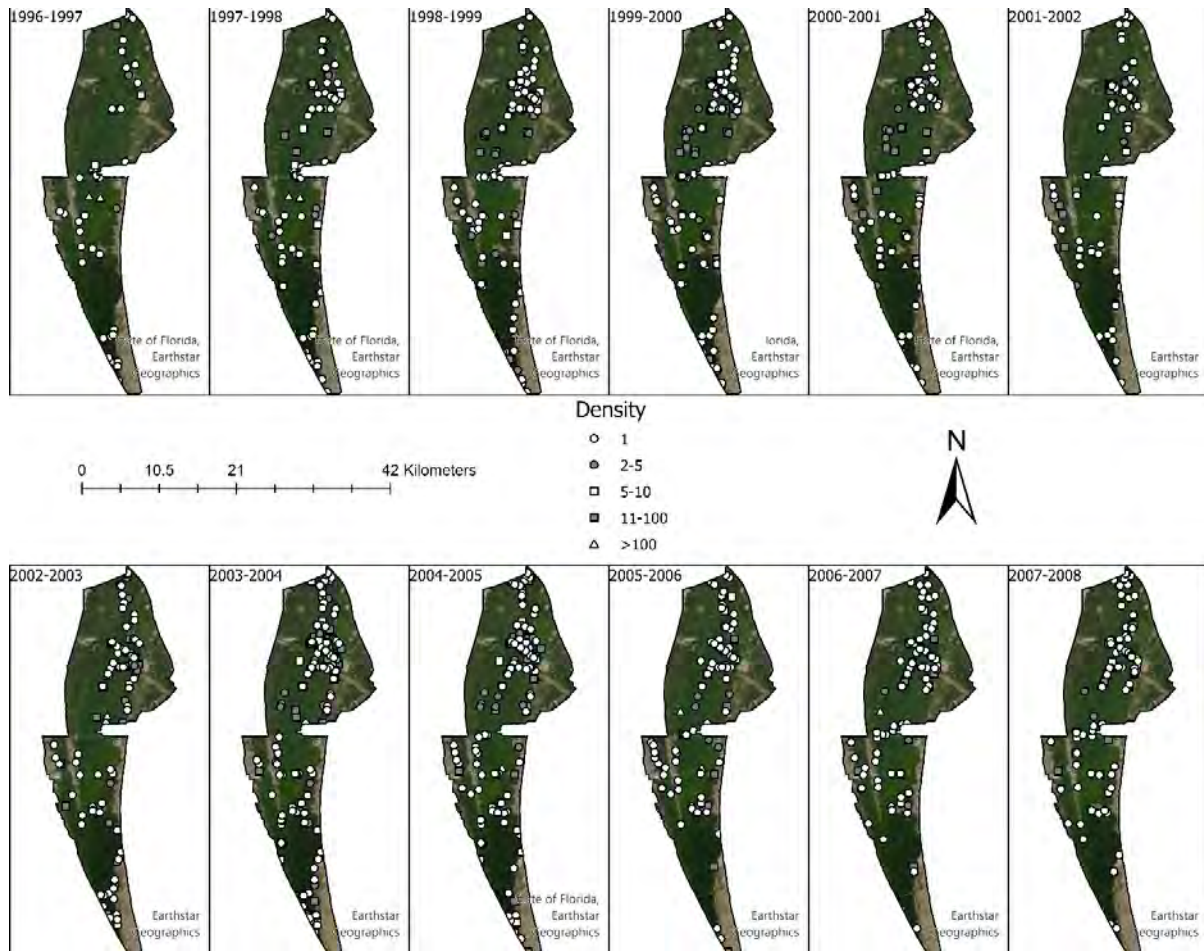
Figure 23. Annual *Leiostomus xanthurus* BRL densities (fish/m³), 1996-2008.
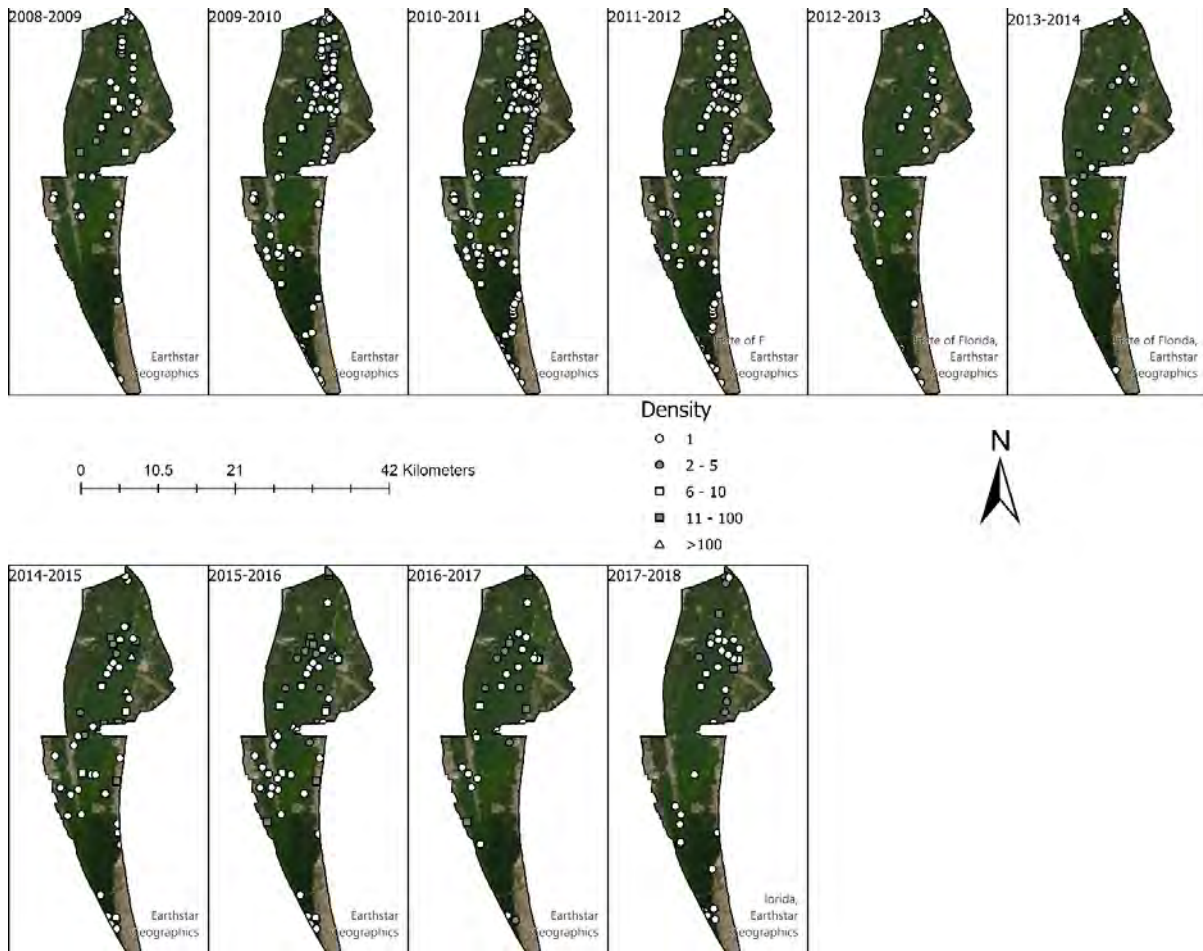
Figure 24. Annual *Leiostomus xanthurus* BRL densities (fish/m³), 2008-2018.

2.2.7.1 Spot literature review

Spot are a marine fish which utilize estuaries on a seasonal basis, though some do remain resident in warm estuaries (Weinstein and Walters 1981). Their eggs require temperatures in excess of 14 °C to develop, but juveniles can tolerate temperatures from 10 to 37 °C, with 37 being the lethal thermal limit for pre-settlement larvae (Hall et al. 1989). As juveniles they tend to be slightly more tolerant of different salinity and temperature conditions, but generally speaking this species can tolerate temperatures as low as 1.2 °C for very short periods and will not usually show signs of distress until temperatures exceed 35.5 °C (Hodson et al. 1961, Bridges 1971, Hartwell and Hoss 1979, Hall et al. 1989). However, the temperature to which they are acclimated to significantly alters these values (Hodson et al. 1961, Bridges 1971, Hartwell and Hoss 1979, Hall et al. 1989, Marcek et al. 2019), with lower acclimation temperatures reducing the boundary for which thermal stress can be expected to 28 °C when acclimated to 10 °C (Hartwell and Hoss 1979). Their metabolic scope also tends to increase as acclimation temperatures increase from 10 to 30 °C (Marcek et al. 2019). Spot can tolerate any salinity above 2 ppt (Hall et al. 1989), and can be found in oligohaline, polyhaline, and mesohaline conditions, but will typically be found in more marine waters and higher mortality rates were observed in polyhaline marshes than mesohaline estuaries (Weinstein and Walters 1981). One study noted exceptionally high mortality rates in oligohaline marshes during high freshwater inflow events (Weinstein and Walters 1981),

and others noted they are more capable of responding favorably to rapid increases in salinity than decreases (Moser and Gerry 1989, Moser and Miller 1994).

2.2.7.2   Spot summary

Spot are a nearly euryhaline species, requiring only trace amounts of salt (Hall et al. 1989), and are able to tolerate the full suite of temperature conditions presented by the BRL, except for the most extreme heat (Bridges 1971, Hartwell and Hoss 1979, Hall et al. 1989). However, their metabolic processes seem to be optimized in the 20 to 30 °C range as evidenced by their densities and published metabolic scope surfaces (Marcek et al. 2019). Much attention has been given to this species as the larvae and juveniles are easily entrained in coolant pumps despite exclusionary efforts, as would presumably be the case with RLI related equipment. The possibility of physical damage notwithstanding, it has been generally accepted that this would not pose physiological harm to the animals so long as the recipient conditions are not more than 10 °C different from the source (Bridges 1971). Moderate fluctuations to temperature and salinity are well tolerated by this species, and they appear more capable of utilizing modified environments than other similar fishes (Govonil et al. 1986, Moser and Gerry 1989, Marcek et al. 2019). The RLI proposal would likely result in an increase in salinity and a decrease in temperature (FL.Tech. 2020), both directions of change are well tolerated by this species depending on the rate of that change (Hartwell and Hoss 1979, Moser and Miller 1994). However, we do not yet have a good understanding of what rate of change can be tolerated and what rate of change to expect from the RLI proposal at various inflow levels.

Regarding the RLI proposal, it is then necessary to address the following questions with respect to this species, to better evaluate the proposal: 1) What is the rate of change in abiotic conditions expected from each pumping scenario for the RLI proposal, 2) What rate of change can Spot tolerate from BRL conditions to the eventual new conditions, and 3) How will habitat suitability change for this species under each pumping scenario?

2.2.8   *Lutjanus griseus*- Gray Snapper

There were 473, 725, 50, and 153 usable occurrences in gears 20, 160, 300, and 301, respectively. Gray Snapper were found in temperatures between 7.50 °C and 34.95 °C with weak significant positive relationships detected between density and temperature with gear 20 (P=0.003, adjusted R^2=0.017) and 160 (P=0.029, adjusted R^2=0.005). The mean temperatures observed were 27.81±0.17 °C 27.88±0.14 °C, 27.89±0.45 °C and 27.75±0.32 °C for gears 20, 160, 300, and 301, respectively. The majority were found in warmer waters, in the 20 to 35 °C range. With regards to salinity, they were primarily found in marine conditions, in the 15 to 35 ppt bins, ranging from 0.2 to 43.50 ppt with a mean of 26.91±0.31 ppt, 25.58±0.24 ppt, 27.87±0.84 ppt, and 27.23±0.43 ppt in gears 20, 160, 300, and 301, respectively. Significant, weak, positive relationships existed between salinity and density in gear 160 (P<=0.001, adjusted R^2=0.019; **Table 2, Table 3, Table 4, Figure 8**). While this species is not widespread in the BRL, it is most reliably encountered in the Northern BRL. Notably, the existing cove targeted for the RLI pilot pumping project appears to have been a reliable location for encountering this species since 2008 (**Figure 25, Figure 26**).
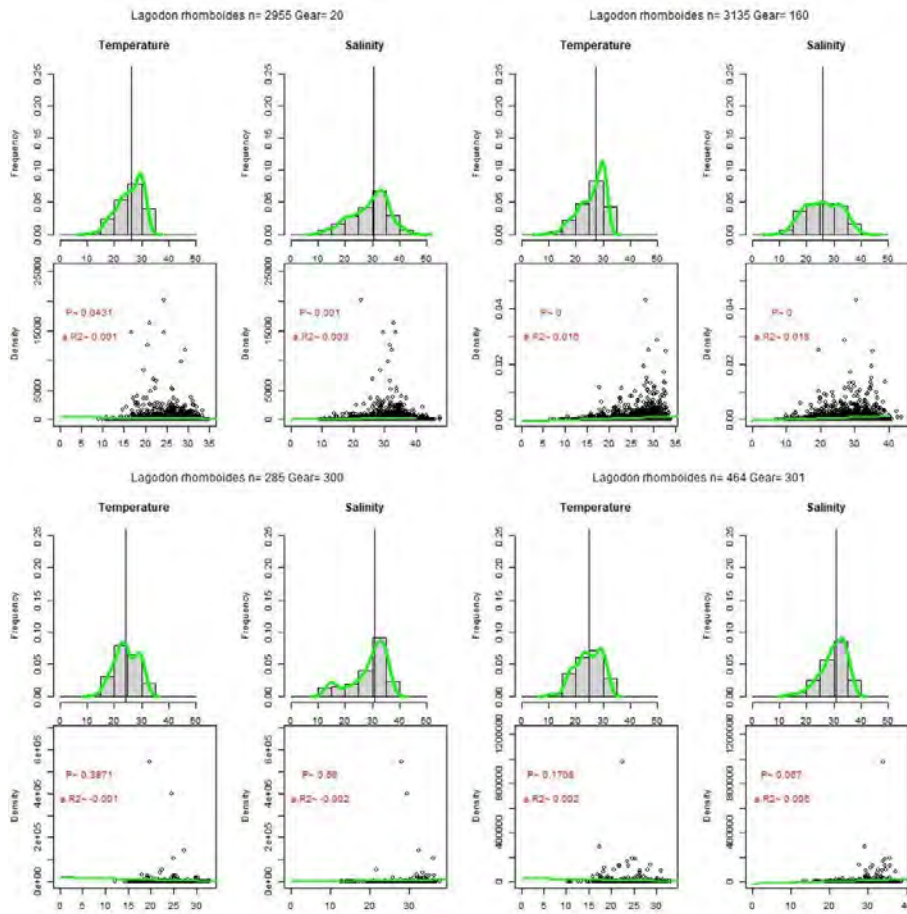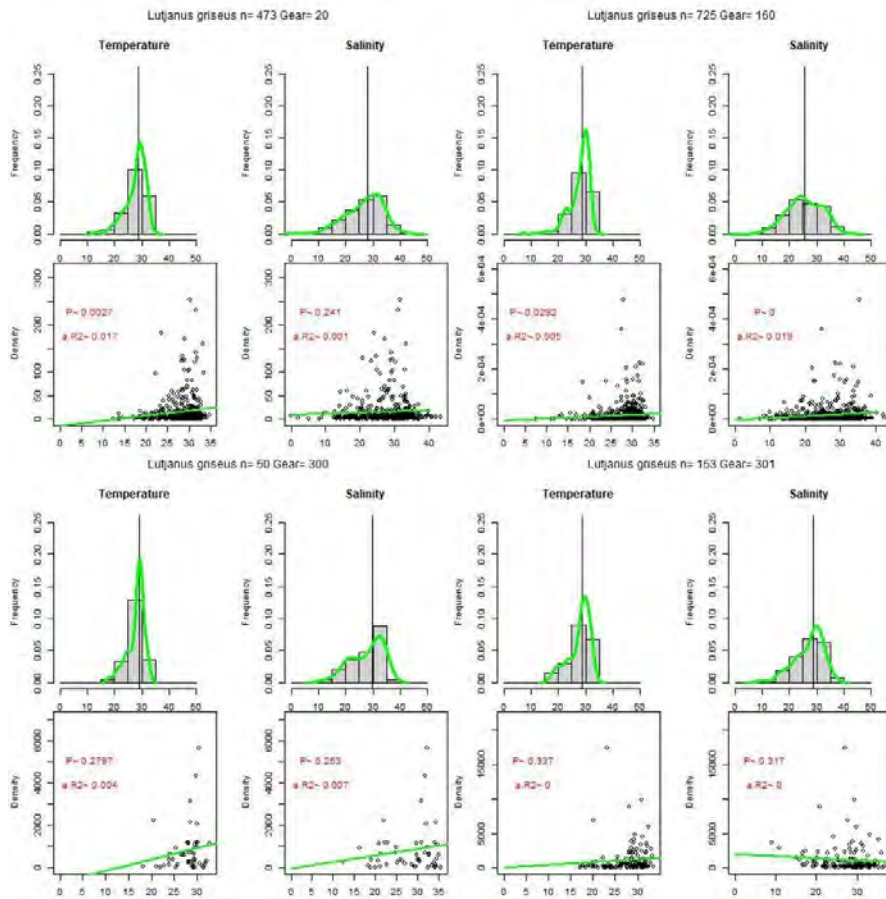
Figure 25. A four paneled figure for gears 20 (top left), 160 (top right), 300 (bottom left) and 301 (bottom right). Each panel contains four figures: a histogram of observed temperatures for this species, with the median denoted by a vertical line and a smoothed representation of the data in green (top left), a similar histogram showing observed salinities for this species (top right), a scatterplot of density versus temperature for this species with a green line of best fits representing and statistics for the linear model of this relationship (bottom left), and a similar scatterplot of density versus salinity (bottom right). Note that no data are presented if there were less than 25 occurrences of this species for any given gear type.
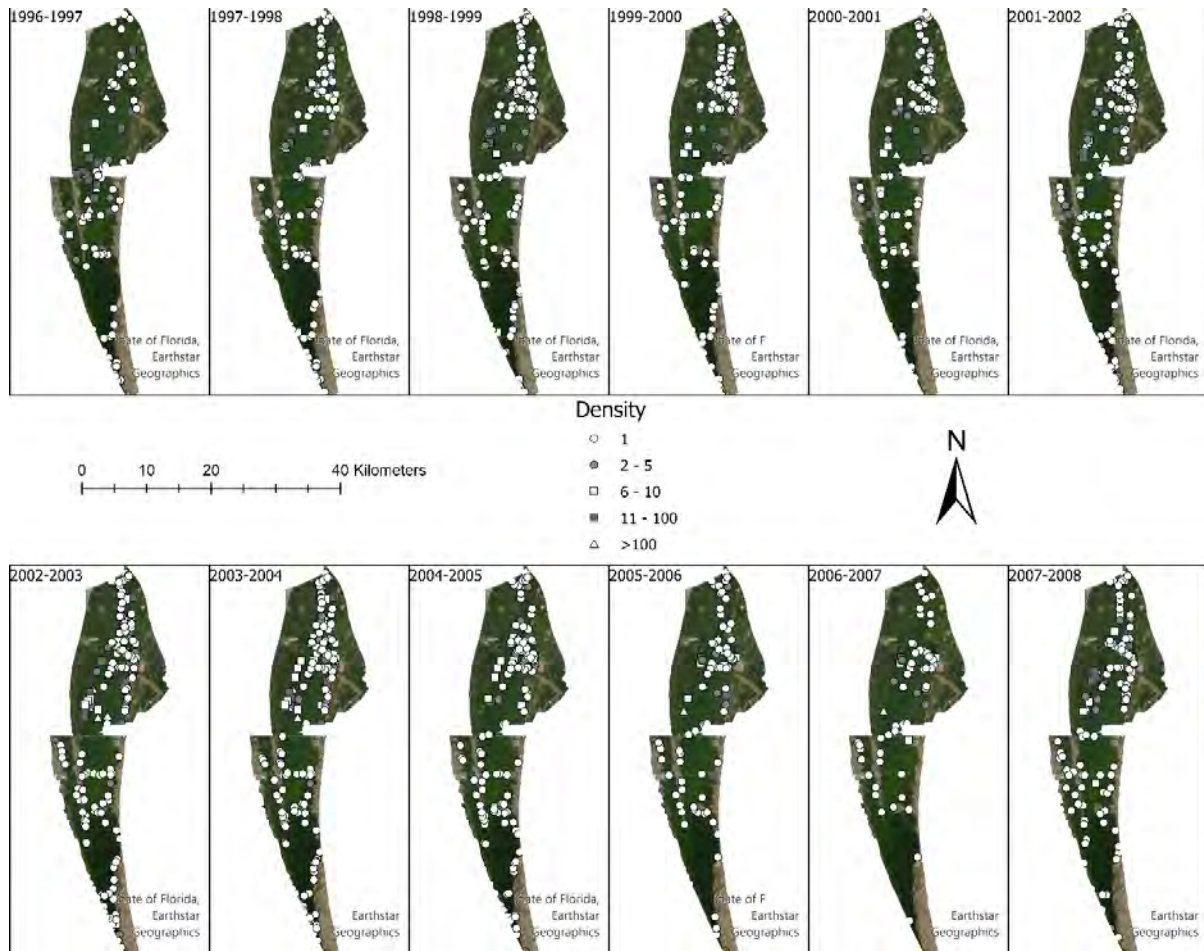
Figure 26. Annual *Lutjanus griseus* BRL densities (fish/m³), 1996-2008.
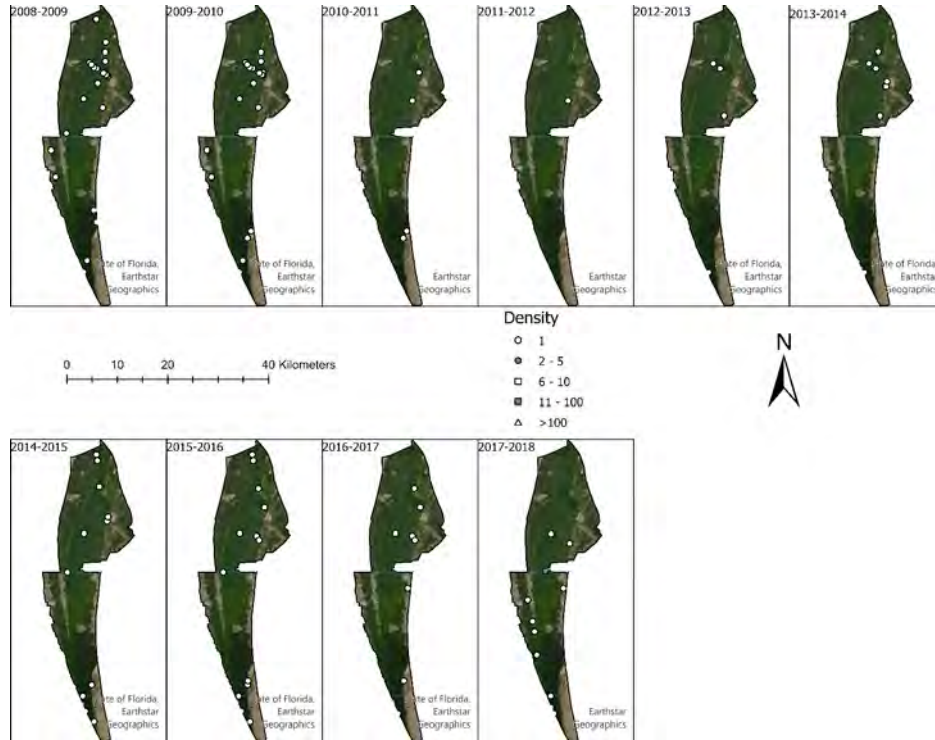
Figure 27. Annual *Lutjanus griseus* BRL densities (fish/m³), 2008-2018.

2.2.8.1 Gray Snapper literature review

The Gray Snapper is a euryhaline (Gunter 1956) sportfish found throughout Florida's waters. They have a well-defined ontogenetic habitat use pattern of spawning offshore, then juveniles moving into estuaries and tracking freshwater inflow gradients to find suitable settlement sites inside mangroves and seagrasses. As they grow, they are physically excluded from the structural refuges and move to patrol the fringes or other structures (Wuenschel et al. 2012, Hare et al. 2012, Golden and Froeschke 2023). As they near the time for spawning runs, they will cluster near inlets and acclimate to oceanic salinities before moving offshore (Golden and Froeschke 2023). As such, they can be found in nearly all naturally occurring salinities, except they were noted as undergoing physiological stress in salinities below 5 ppt and above 50 ppt (Serrano 2008, Serrano et al. 2010, 2011). Their growth rate is negatively related to salinity within that tolerable range, 5 to 45 ppt, an effect which interacts with a positive relationship between growth rate and temperature in similarly tolerable thermal regimes, 18 to 33 °C (Wuenschel et al. 2004). No experimentally derived physiological tolerances were found in this targeted literature review.

2.2.8.2 Gray Snapper summary

Gray Snapper are a hardy species that supports a popular fishery. Throughout their complex life history, they utilize many of the habitats available within the IRL, as well as the marine environment offshore. They show no signs of physiological stress in temperatures between 18 and 33 °C in experimental settings and have been rarely seen outside that range in the BRL. Similarly with salinity, the range within which no physiological stress was detected is 5 to 45 ppt, and in the BRL they were rarely observed below 10 ppt and the BRL itself rarely exceeds 40 ppt. There was no strong observed relationship between temperature or salinity in these data, which would agree with the broad tolerances described in the literature, and it is likely that they are more closely linked to habitat changes, such as changes to seagrass or mangrove availability and connectivity to offshore waters for spawning. In Phase 2 of the RLI project, we described similarly weak forcing of temperature and salinity for this species but could predict abundance of Gray Snapper using dissolved oxygen. I would hypothesize that the true impacts of RLI on Gray Snapper will be seen most readily in the behavioral responses of Gray Snapper to changing oxygen concentrations and mangrove availability. If seagrasses return to the BRL in sufficient densities, I expect Gray Snapper to be found utilizing them as well. However, we do not currently have a working understanding on the complex relationship between Gray Snapper and the consequences of inflow on water quality and habitat structure. Specifically, we need a detailed understanding of 1) the behavioral responses of Gray Snapper to changes in water quality in the BR, 2) the rate of changing environmental conditions which this species can tolerate, 3) the rate of changing temperature, salinity and dissolved oxygen distributions we expect the BRL to experience under each pumping scenario, and 4) how habitat suitability of the BRL will change under each pumping scenario.

2.2.9 Mugil cephalus- Striped Mullet

There were 1379, 4033, 2, and 1 usable occurrences of Striped Mullet in gears 20, 160, 300, and 301, respectively. As such, gears 300 and 301 were deemed data deficient and excluded from analysis. Striped Mullet were found in temperatures between 6.70 °C and 37.40 °C with weak significant positive relationships detected between density and temperature with gear 20 ($P<=0.001$, adjusted $R^2=0.017$). The mean temperatures observed were 22.41±0.14 °C, and 24.91±0.08 °C for gears 20 and 160, respectively. The majority were found in the 15 to 35 °C range, with over 50% in the 20 to 30 °C range. With regards to salinity, they were primarily found in most BRL conditions, ranging from 1.50 to 44.10 ppt, but over 60% were found in the 20 to 35 ppt range. Mean salinities were 25.41±0.19 ppt and 25.42±0.1 ppt in gears 20 and 160,

respectively. A significant, weak, positive relationships existed between salinity and density in gear 20 (P<=0.001, adjusted R^2=0.003; **Table 2, Table 3, Table 4, Figure 9**). This species is fairly widespread throughout the BRL.
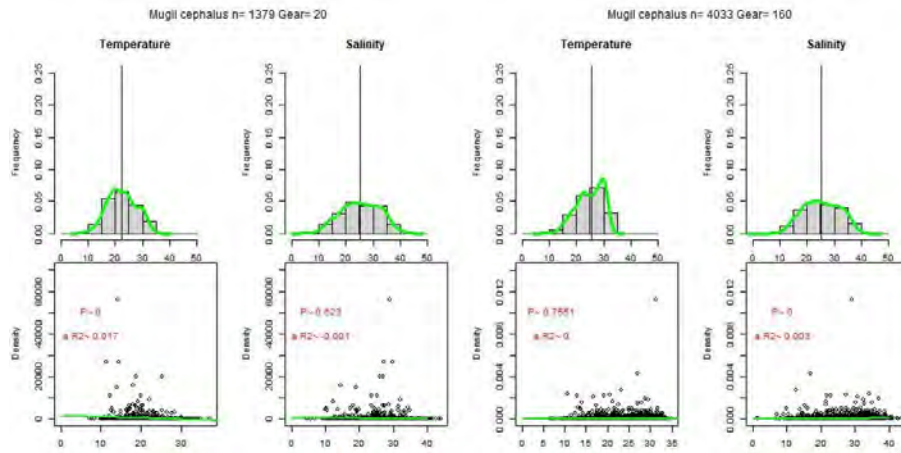
Figure 28. A two paneled figure for gears 20 (left), 160 (right). Note that gears 300 and 301 did not have enough occurrences to support analyses for this species. Each panel contains four figures: a histogram of observed temperatures for this species, with the median denoted by a vertical line and a smoothed representation of the data in green (top left), a similar histogram showing observed salinities for this species (top right), a scatterplot of density versus temperature for this species with a green line of best fits representing and statistics for the linear model of this relationship (bottom left), and a similar scatterplot of density versus salinity (bottom right).
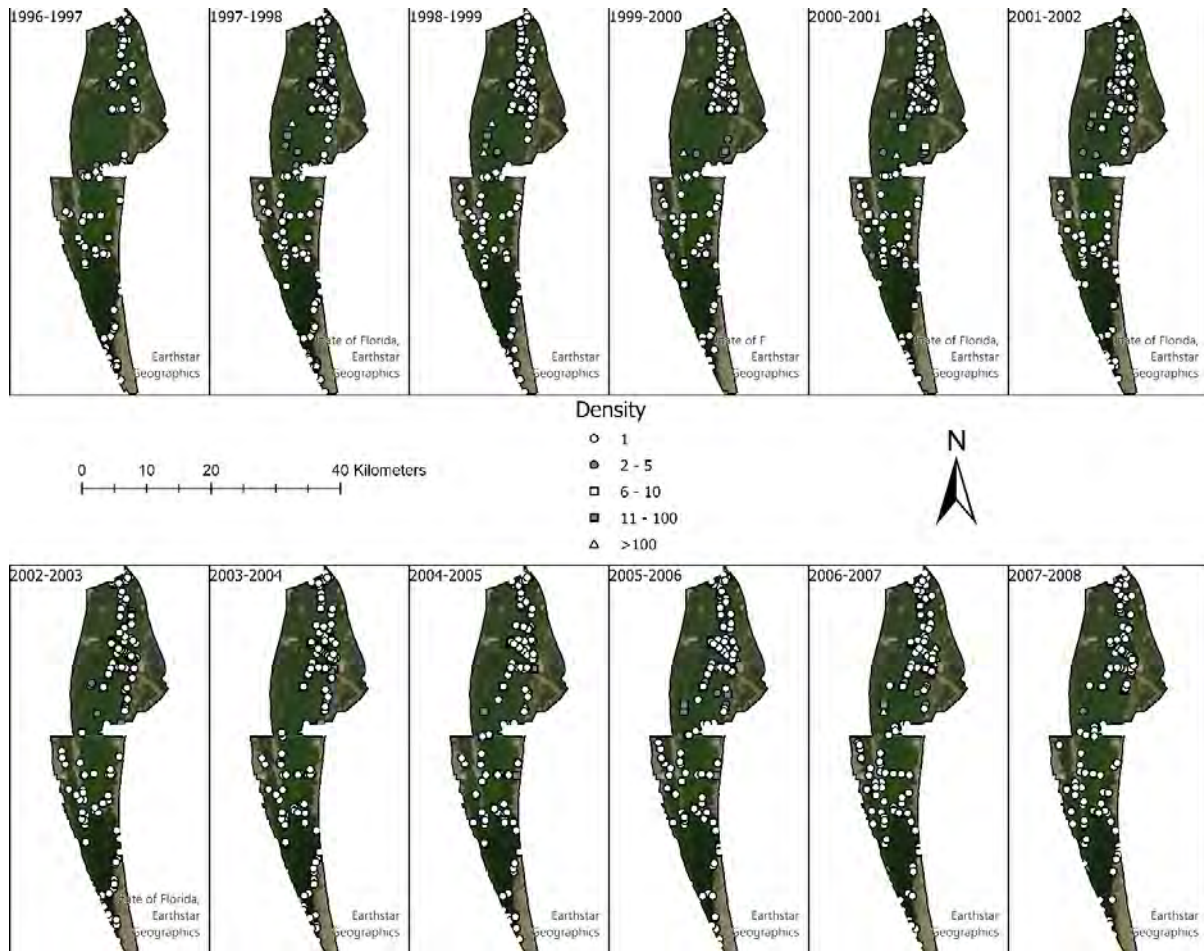
Figure 29. Annual *Mugil cephalus* densities (fish/m³), 1996-2008.
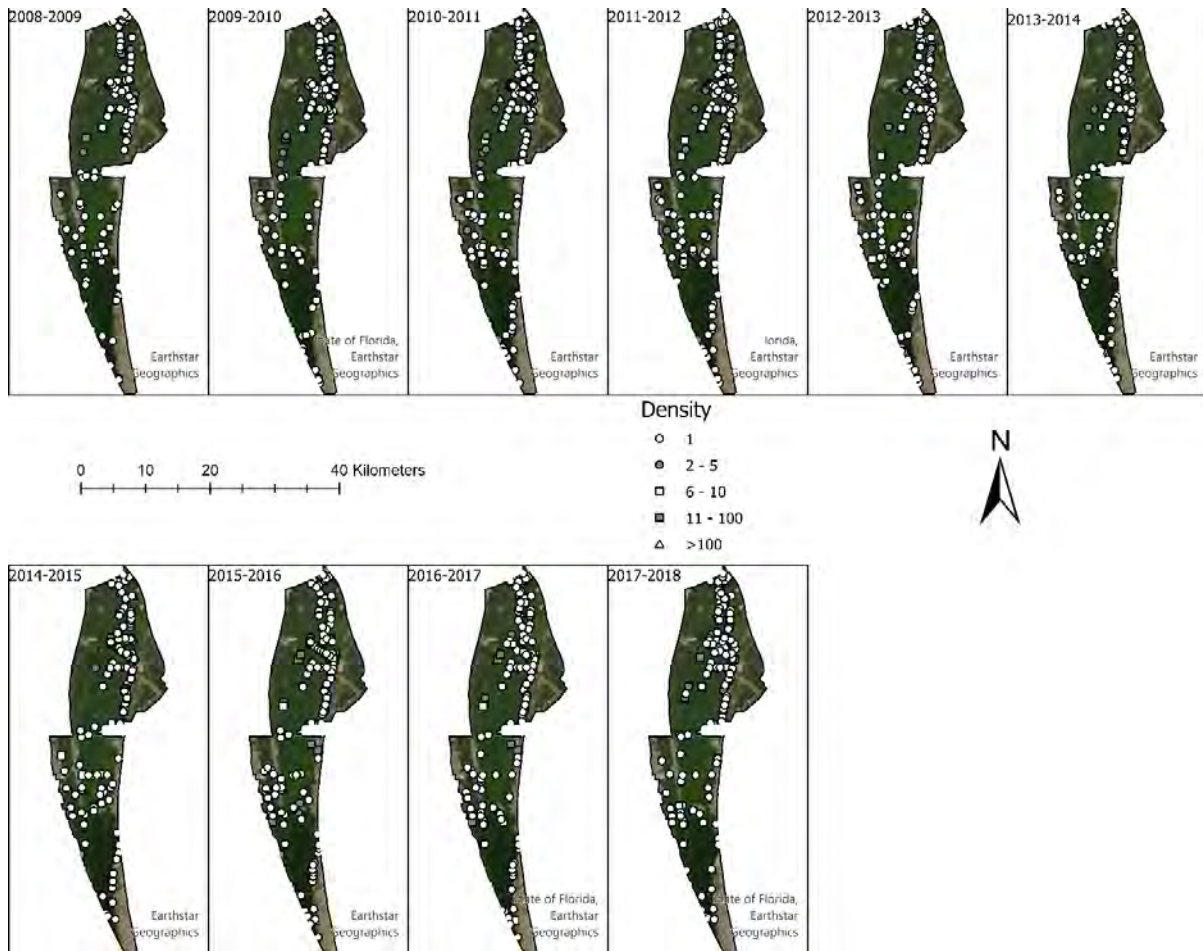
Figure 30. Annual *Mugil cephalus* densities (fish/m^3), 1996-2008.

2.2.9.1 Striped Mullet literature review

A comprehensive, at the time of publication, review on the status of knowledge of Striped, also known as gray or flathead, mullet was prepared by Whitfield et al. in 2012. I would reference the reader to this document for a more comprehensive treatise on this than can be provided here. Here, I will provide only a brief summary. Striped mullet are likely the most truly euryhaline species discussed here. Noted in the list of euryhaline fishes by Gunter (1956), their extreme halotolerance was perhaps best demonstrated by Hotos & Vlahos (1998) who documented no signs of visible stress or mortality while increasing salinity, in 5 ppt increments, from 20 ppt to 126 ppt, far exceeding natural salinities in the BRL. However, Striped Mullet do show signs of biochemical and haematological stress at lower salinities, with a clear negative relationship between various stress indicators and salinity (Marais 1978, Khériji et al. 2003, Fazio et al. 2013). Although, these studies were almost exclusively conducted on young adults. Cardona (2000) notes that juveniles and post-metamorphosis larvae tend to favor freshwater and oligohaline areas, while the adults stayed mainly in polyhaline areas.

Far less attention has been given to the temperature tolerance of this species (Chung and Strawn 1994, Whitfield et al. 2012). Most studies seem to focus on aquaculture system optimization. In general, all studies reviewed here maintained Striped Mullet in the 13 to 33 °C range (Nordlie 1976, Marais 1978, Khériji et al. 2003, Whitfield et al. 2012, Fazio et al. 2013). Higher

temperatures seem to induce a degree of physiological stress, with a positive relationship between oxygen consumption and temperature (Marais 1978, Khériji et al. 2003), as well as most hematological indicators of stress (Nordlie 1976, Fazio et al. 2013).

2.2.9.2 Striped Mullet summary

Striped Mullet are a ubiquitous low trophic level species across many Atlantic estuaries, migrating in very large schools with clearly defined *ontogenetic* shifts in habitat use (Whitfield et al. 2012). They are likely the most euryhaline species discussed here, able to tolerate salinities from 0 to 126 ppt with seemingly rapid rates of change, 5 ppt / 3 days in one study (Hotos and Vlahos 1998). However, they appear to be more tolerant of high salinities as adults than they are of low salinities, yet they prefer low salinities during development (Marais 1978, Hotos and Vlahos 1998, Cardona 2000). In the BRL, they seem to largely favor higher salinities (**Figure 28**), but it is worth noting here that the BRL does not offer many oligohaline environments (**Figure 4, Figure 5**) that the juveniles prefer (Cardona 2000). Little work has been done to describe their thermal limitations, but all published studies reviewed here, and by Whitfield et al. (2012), maintained or observed Striped Mullet in 13 to 33 °C waters, which aligns well with their observed occurrences in the BRL (**Figure 28**).

Regarding the RLI proposal, I see no reason for concern over Striped Mullet regarding temperature or salinity effects. Increased inflow is projected to increase salinities and decrease temperatures (FL.Tech. 2020), both of which favor reduced stress for this species (Marais 1978, Khériji et al. 2003, Fazio et al. 2013). While no thermal limits or rate of change studies were found, the aquaculture literature demonstrates extreme adaptability in this species (See Whitfield et al. 2012 for a comprehensive discussion of the physiological mechanisms this species uses to adapt to environmental change). However, their habitat use patterns are highly context dependent and ontogenetically variable (Cardona 2000, Whitfield et al. 2012), requiring further investigation into the BRL specific patterns of habitat use and habitat suitability, and migration patterns, for Striped Mullet.

2.2.10 *Opisthonema oglinum*- Thread Herring

There were 372, 512, 10, and 9 usable occurrences of Striped Mullet in gears 20, 160, 300, and 301, respectively. As such, gears 300 and 301 were deemed data deficient and excluded from analysis. Thread Herring were found in temperatures between 8.80 °C and 33.70 °C with weak significant positive relationships detected between density and temperature with gear 160 (P<=0.022, adjusted R^2=0.008). The mean temperatures observed were 28.14±0.16 °C, and 26.51±0.18 °C for gears 20 and 160, respectively. The majority were found in the 20 to 35 °C range, with over 50% in the 25 to 30 °C bin. With regards to salinity, they were primarily found in most BRL conditions ranging from 0.20 to 43.87 ppt with most spread fairly evenly across the 15-40 ppt bins. Mean salinities were 27.63±0.35 ppt and 26.04±0.27 ppt in gears 20 and 160, respectively. A significant, weak, positive relationship existed between salinity and density in gear 20 (P=0.046, adjusted R^2=0.008; **Table 2, Table 3, Table 4, Figure 10**). This species shows no particular spatial bias in occurrences from 1996-2018 (**Figure 31, Figure 32**).
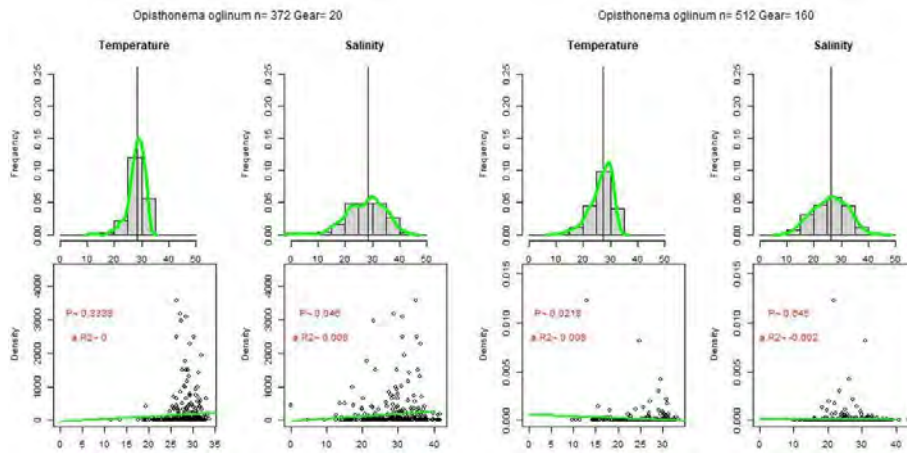
Figure 31. A two paneled figure for gears 20 (left) and 160 (right). Note that gears 300 and 301 did not have enough occurrences to support analyses for this species. Each panel contains four figures: a histogram of observed temperatures for this species, with the median denoted by a vertical line and a smoothed representation of the data in green (top left), a similar histogram showing observed salinities for this species (top right), a scatterplot of density versus temperature for this species with a green line of best fits representing and statistics for the linear model of this relationship (bottom left), and a similar scatterplot of density versus salinity (bottom right).
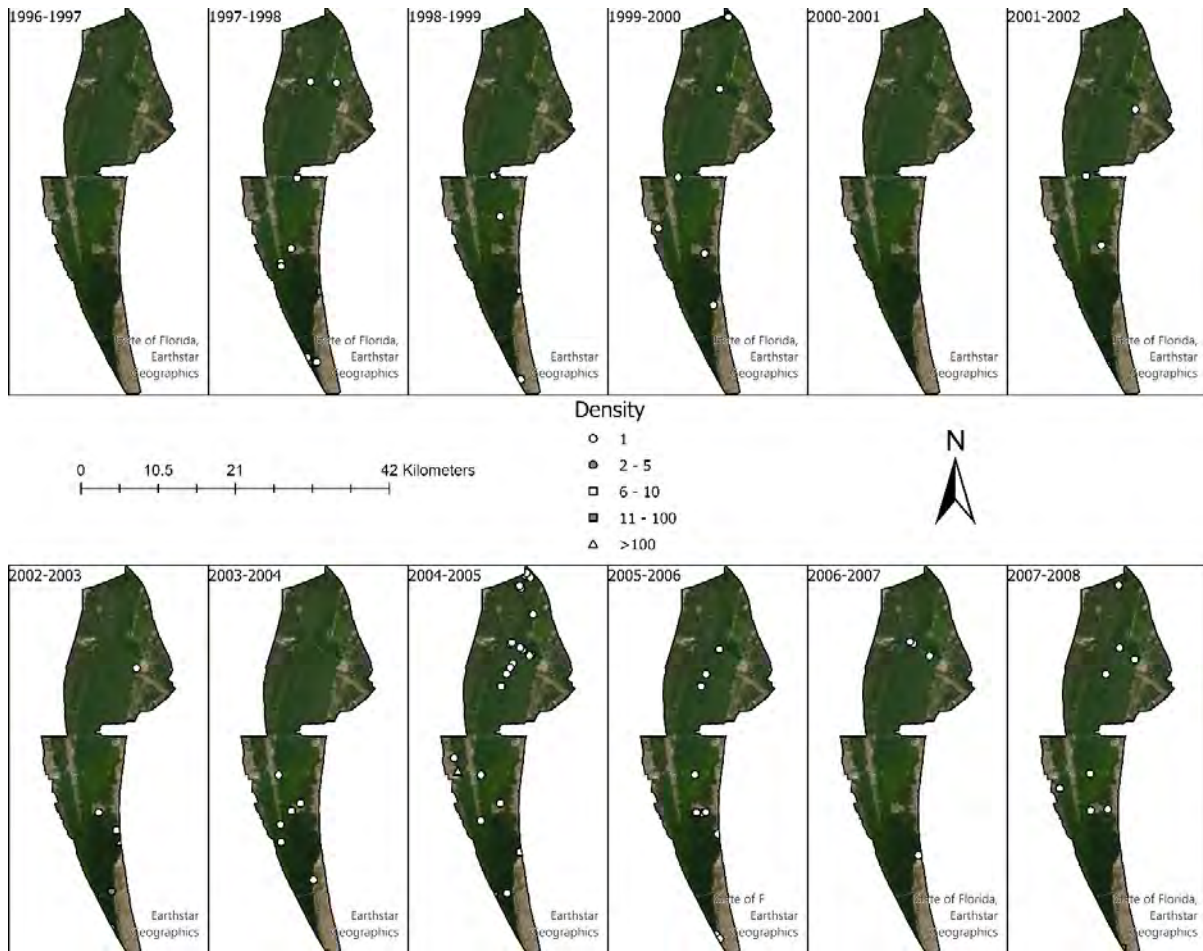
Figure 32. Annual *Opisthonema oglinum* densities (fish/m³), 1996-2008.
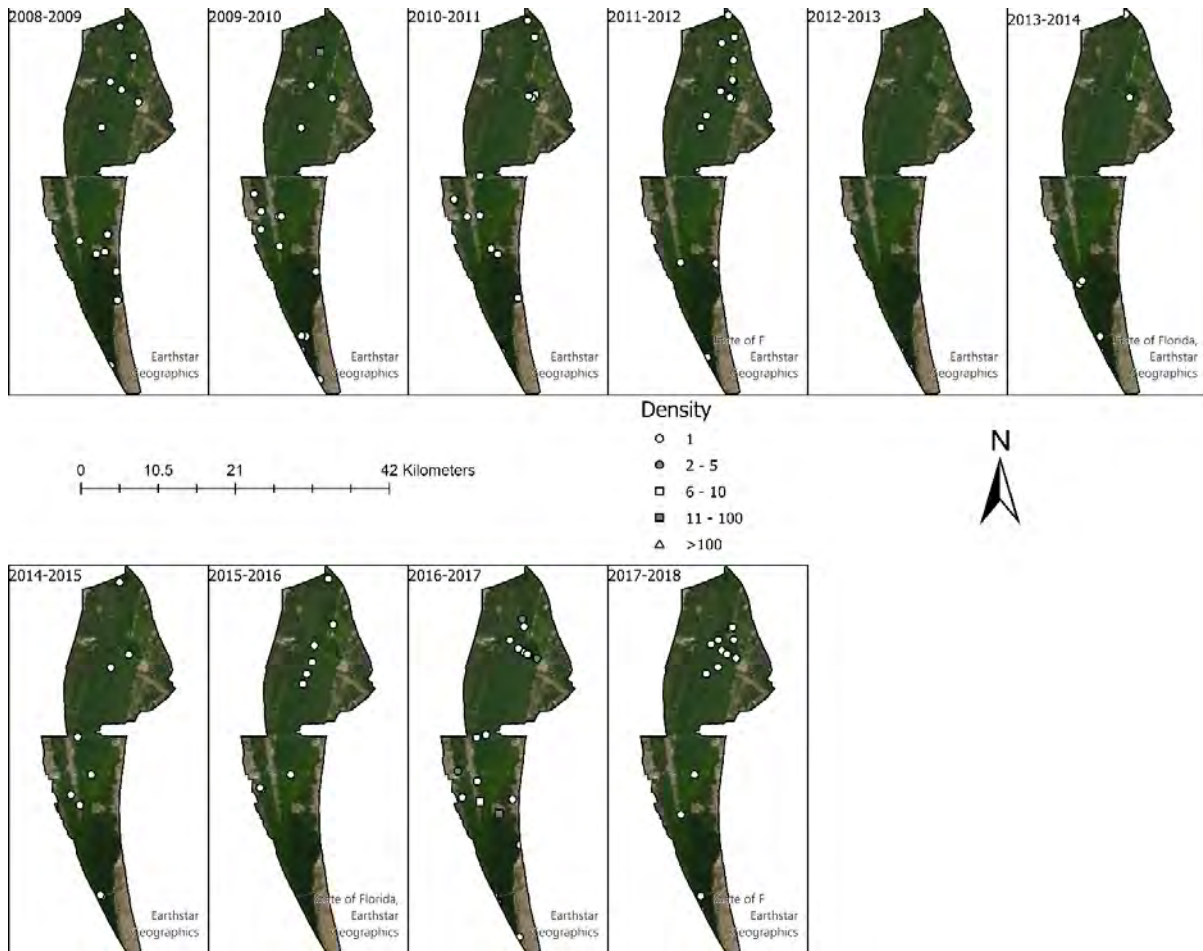
Figure 33. Annual *Opisthonema oglinum* densities (fish/m^3), 2008-2018.

2.2.10.1 Thread Herring literature review
Thread Herring are a commercially sought after species as a food fish, as bait during their autumnal migrations past Florida, and they are regularly referenced as important prey for Atlantic predators (Richards and Palko 1969, Richards et al. 1974, Houde 1977, Finucane and Vaught 1986, Smith 1994). Looking specifically for information on their salinity and thermal tolerances returned 8 usable references, which all reported the same general description of the species. Thread Herring are a tropical-subtropical fish preferring warm, blue waters and high salinity (Finucane and Vaught 1986, Smith 1994, Vega-Cendejas et al. 1997b). They do undergo an ontogenetic shift in habitat use, changing from a primarily estuarine larval-juvenile stage to the more marine adults. However, even as their habitat use changes, both adults and juveniles are found to have peak abundances in the 25-30 °C range (Finucane and Vaught 1986). A commercial fishing report notes their catches were highest in a slightly broader range, suggesting to fish in waters in the 15-32 °C range but targeting a mean temperature of 24 °C (Kinnear and Fuss Jr. 1971). With that said, juveniles do appear to be less tolerant of colder temperatures, with captive rearing notes suggesting a loss of equilibrium and general cold stress setting in at temperatures below 28 °C, documenting mass juvenile mortality with a temperature change in excess of 6 °C in one day (Richards and Palko 1969). Spawning for this species typically occurs offshore in warm, 22.5-30 °C, high salinity, 34-36.8 ppt, waters with stable conditions fluctuating less than 1 ppt/day and when isotherms are too deep to impact the process (Houde 1977).

Outside of spawning, the salinity preference for these species appears to be marine, with all studies reporting salinities in excess of 20 ppt being the norm, though they can be observed in salinities as low as 5 ppt on rare occasions, and the highest abundances occurring at salinities in the 25-35 ppt range (Richards and Palko 1969, Kinnear and Fuss Jr. 1971, Houde 1977, Finucane and Vaught 1986).

2.2.10.2 Thread Herring summary

Thread Herring are universally reported as preferring warm, 20-30 °C clear, high salinity, 20-35 ppt, waters regardless of their ontogenetic stage. The limited research focusing on the physiology of this species suggests they are also attuned to fluctuations in water temperatures, perhaps more so than the actual temperature and salinity itself, as their spawning requiring very stable water conditions and temperature fluctuations are lethal to the estuarine larvae. These literary observations align well with what was observed in the Banana BRL fishes, which saw peak abundances on the higher end of the spectrum for BRL (**Table 2**), in the 20-30 °C, 15-40 ppt range (**Table 3, Table 4, Figure 10**).

Regarding the implications of RLI on this species, there are a few open questions that still need to be answered. First, it is not yet known what rate of change this species can endure before experiencing thermal or osmotic stress, only that they are particularly sensitive to fluctuations in early life stages, which begs the question: What rate of change in water conditions can this species endure as larvae and juveniles? Second, RLI Phase 1 models suggested that temperatures would decrease, and salinities would increase under pumping. While this expected change is not to a degree that would be deemed stressful for this species, we still need a clear understanding of: What is the daily expected rate of change in water conditions under pumping conditions? Finally, the information presented here lays out the necessary framework for inferring preferred habitat, and provides the necessary inputs to calculate habitat suitability, but falls short of predicting changes in habitat suitability. The biggest pending question for this, and all fishes in the IRL with respect to the RLI proposal is: How will habitat suitability change under each pumping scenario?

2.2.11 Pogonias cromis- Black Drum

There were 115, 908, 0, and 1 usable occurrences of Black Drum in gears 20, 160, 300, and 301, respectively. As such, gears 300 and 301 were deemed data deficient and excluded from analysis. Black Drum were found in temperatures between 8.85 °C and 34.25 °C with no significant relationships detected between density and temperature. The mean temperatures observed were 26.44±0.42 °C, and 25.94±0.15 °C for gears 20 and 160, respectively. The majority were found in the 15-35 °C range favoring the warmer end of the range, with over 80% in the 20 to 35 °C bin and approximately 40% in 25 to 30 °C waters. With regards to salinity, they were found in most BRL conditions. Their observations ranged from 0.20 to 43.87 ppt with most spread fairly evenly across the 15 to 40 ppt bins. Mean salinities were 26.58±0.71 ppt and 26.07±0.23 ppt in gears 20 and 160, respectively. A significant, weak, positive relationship existed between salinity and density in gear 160 ($P<=0.001$, adjusted $R^2=0.026$; **Table 2, Table 3, Table 4, Figure 10**). The majority of occurrences of this species occur in the Northern BRL (**Figure 34, Figure 35**).
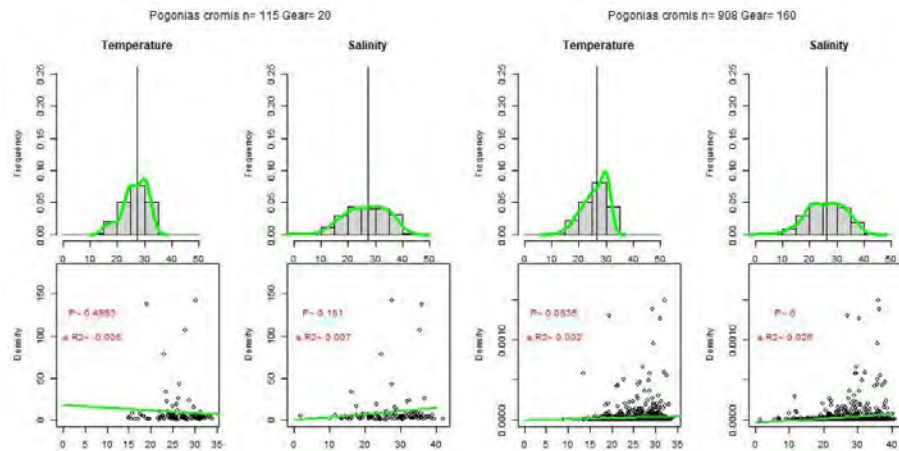
Figure 34. A two paneled figure for gears 20 (left) and 160 (right). Note that gears 300 and 301 did not have enough occurrences to support analyses for this species. Each panel contains four figures: a histogram of observed temperatures for this species, with the median denoted by a vertical line and a smoothed representation of the data in green (top left), a similar histogram showing observed salinities for this species (top right), a scatterplot of density versus temperature for this species with a green line of best fits representing and statistics for the linear model of this relationship (bottom left), and a similar scatterplot of density versus salinity (bottom right).
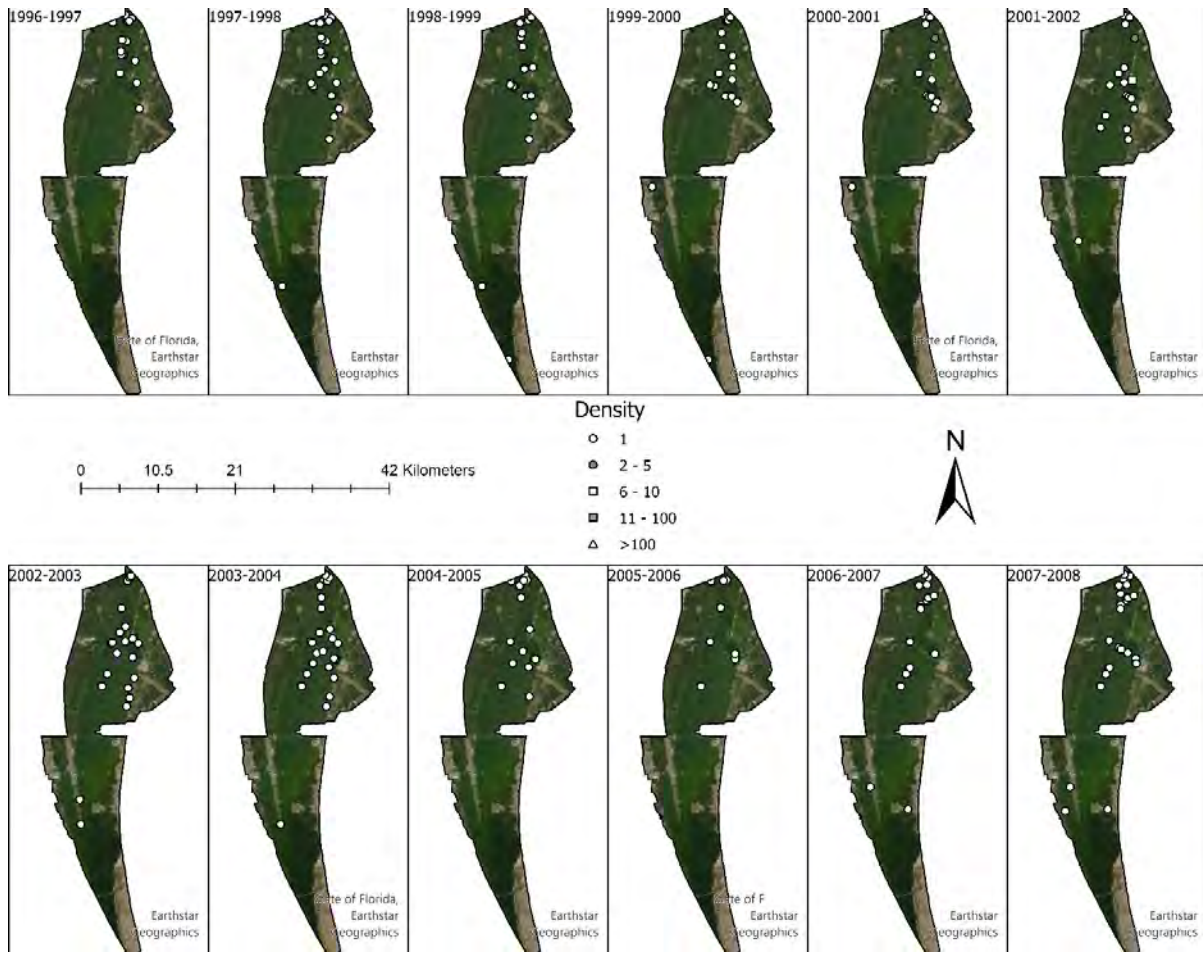
Figure 35. Annual *Pogonias cromis* densities (fish/m^3), 1996-2008.
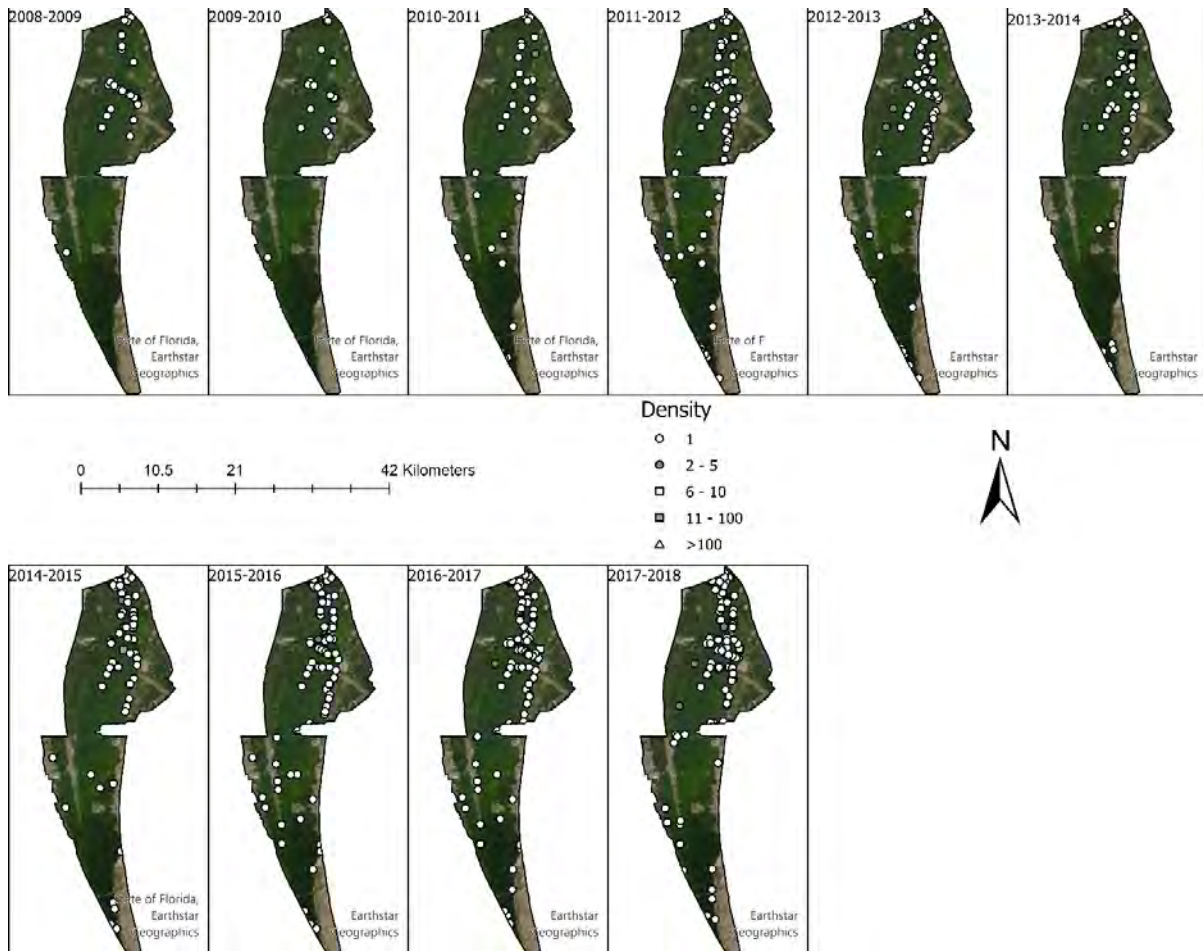
Figure 36. Annual *Pogonias cromis* densities (fish/m^3), 2008-2018.

2.2.11.1 Black Drum literature review.

Black Drum are a large, popular, euryhaline sportfish that favor structured substrata adjacent to unvegetated mud flats (Gunter 1956, Silverman 1979, Mcneese 2021). They have received much attention in the literature as a potential aquaculture species for both food as well as stock enhancement. They have been found to prefer lower salinity, including full freshwaters, as post-settlement larvae and juveniles, moving to higher salinity, often hypersaline, areas as adults (Chamberlain and Strawn 1977, Silverman 1979, Alshuth and Gilmore 1995, Mcneese 2021). Their tolerance limits for salt and temperature have not been well documented, seemingly largely because attempts to do so have failed to elicit lethal responses. One study seeking to quantify upper thermal limits of several fishes in submerged cages showed that Black Drum were the only fish in the study, a list which includes several of the species in this report, which did not die within four days at temperatures 40 °C (Chamberlain and Strawn 1977). However, Black Drum skin collagen begins breaking down at 34 to `35.8 °C (Ogawa et al. 2003), suggesting that persisting in hot water for a prolonged period would cause severe damage. Their lower thermal limit is likely near 3 °C based on two cold kill events documented in Texas in the late 1920's and 1960's (Silverman 1979), but I did not find studies which sought to

formally quantify lower thermal limits. Aquacultural operations typically incubate Black Drum eggs at 20 °C and 27% salinity, which optimizes their survival, and rapid changes to temperature are avoided as they can cause larval mortality (Frisbie 1961, Alshuth and Gilmore 1995).

2.2.11.2 Black Drum summary

Black Drum are one of the largest members of the drum family, and a particularly popular recreational sportfish (Richards 1973, Silverman 1979, Adriance et al. 2019). Their life history involves a cycle of offshore spawning, tidal ingress of larvae which settle in lower salinity areas with structural refugia (e.g., mangroves, seagrass beds) then, as they grow, they move to higher salinity structured areas with adjacent unvegetated flats they can forage in (Silverman 1979, Mcneese 2021). Within the BRL they seem to prefer the 20 to 30 °C range (**Figure 37**), which would align well with the standards of animal husbandry for this species (Alshuth and Gilmore 1995). They also occur within the full range of salinities above 10 ppt which were observed. Their absence below 10 ppt is likely more due to sampling effect than an intolerance of oligohaline conditions, as larvae and juveniles tend to prefer these conditions (Silverman 1979, Adriance et al. 2019, Mcneese 2021). While they are a particularly hardy fish (Bayly 1972, Olsen 2014), they are susceptible to rapid changes in conditions both as juvenile and adults (Frisbie 1961, Silverman 1979). Unfortunately, we do not have a clear understanding of what rate of change they can endure, and how they will respond to changing conditions. A concerted effort to understand their movement and behavioral ecology in and around the BRL has led to the general understanding that while they are not a highly mobile species in the BRL, they can and will leave an area for various reasons, including but not limited to spawning and likely environmental changes (Reyier et al. 2020). While these efforts are valuable, they do not provide the data resolution necessary to quantify habitat suitability within the BRL.

Regarding the RLI proposal, the expected net change of temperature and salinity are unlikely to significantly impact on Black Drum. However, we have limited understanding of the rate at which this change will take place, or what rate of change the fish can tolerate. We also do not have a clear understanding of the spatial or temporal habitat suitability of the BRL for Black Drum today, or how that will change over time. The data presented here provide the majority of what will be needed to support that effort, but further study is needed to complete the task. As such, the pending questions for Black Drum with respect to the RLI proposal are: 1) What rate of change in environmental parameters is expected under each pumping scenario, 2) What rate of change can this species tolerate, and 3) How will habitat suitability change for this species under each pumping scenario?

2.2.12 *Sciaenops ocellatus*- Red Drum

There were 1234, 2248, 17, and 45 usable occurrences of Red Drum in gears 20, 160, 300, and 301, respectively. As such, gear 300 was deemed data deficient and excluded from analysis. Red Drum were found in temperatures between 7.50 °C and 34.25 °C with significant positive relationships detected between density and temperature for gears 160 (P=0.002, adjusted R^2=0.004) and 301 (P<=0.001, adjusted R^2=0.233). The mean temperatures observed were 22.48±0.13 °C, 25.40±0.10 °C, and 20.76±0.51 °C for gears 20, 160, and 301, respectively with the majority found in the 15 to 30 °C range. Regarding salinity, Red Drum favored brackish-marine conditions, with records ranging from 1.60 to 43.87 ppt, with means of 24.78±0.19, 25.26±0.14 and 25.09±1.82 ppt (gears 20, 160, and 301, respectively) and primarily spread between the 15 to 35 ppt bins. A significant positive relationship existed between salinity and density in gear 160 (P<=0.001, adjusted R^2=0.019) and a significant negative relationship existed in gear 301 (P=0.006, adjusted R^2=0.142; **Table 2, Table 3, Table 4, Figure 12**). The majority of occurrences

for this species took place in the Northern BRL, though they can be found throughout (**Figure 37, Figure 38**).
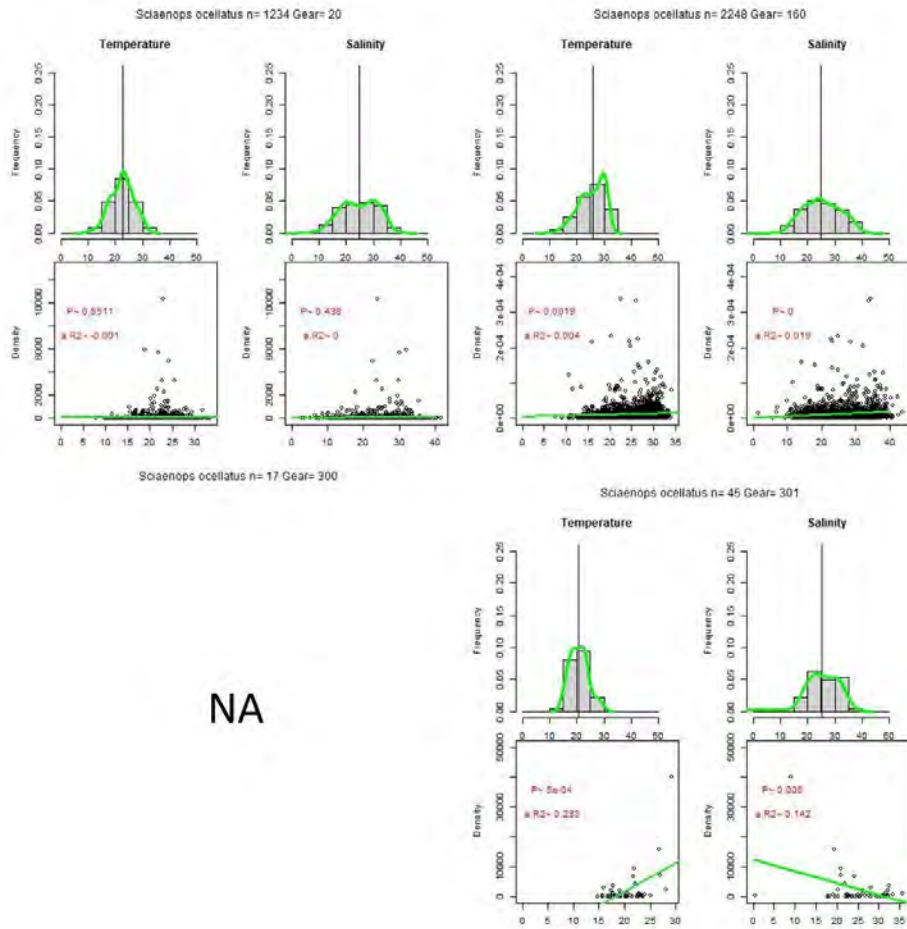
Figure 37. A three paneled figure for gears 20 (top left), 160 (top right) and 301 (bottom right). Note that gears 300 did not have enough occurrences to support analyses for this species. Each panel contains four figures: a histogram of observed temperatures for this species, with the median denoted by a vertical line and a smoothed representation of the data in green (top left), a similar histogram showing observed salinities for this species (top right), a scatterplot of density versus temperature for this species with a green line of best fits representing and statistics for the linear model of this relationship (bottom left), and a similar scatterplot of density versus salinity (bottom right).
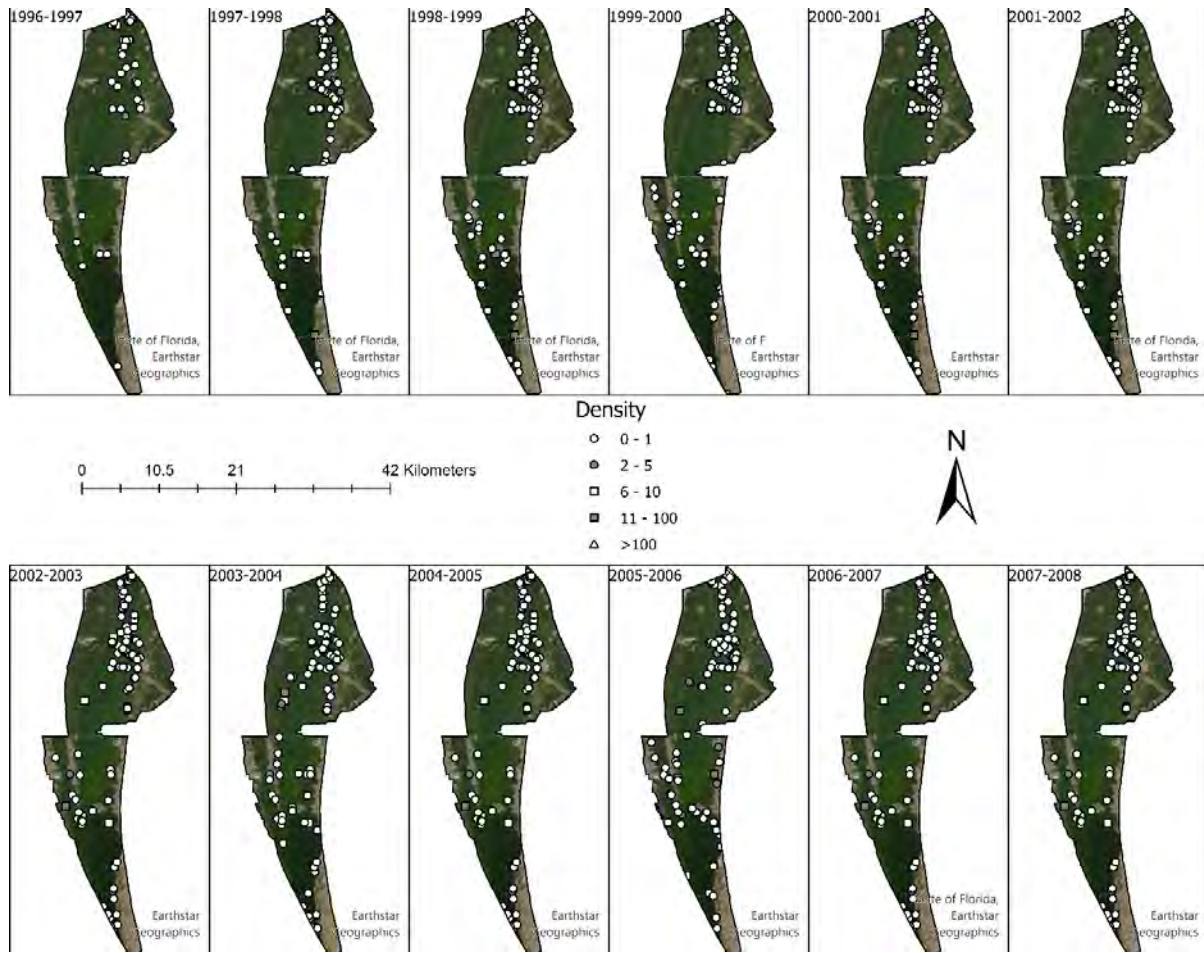
Figure 38. Annual *Sciaenops ocellatus* densities (fish/m³), 1996-2008.
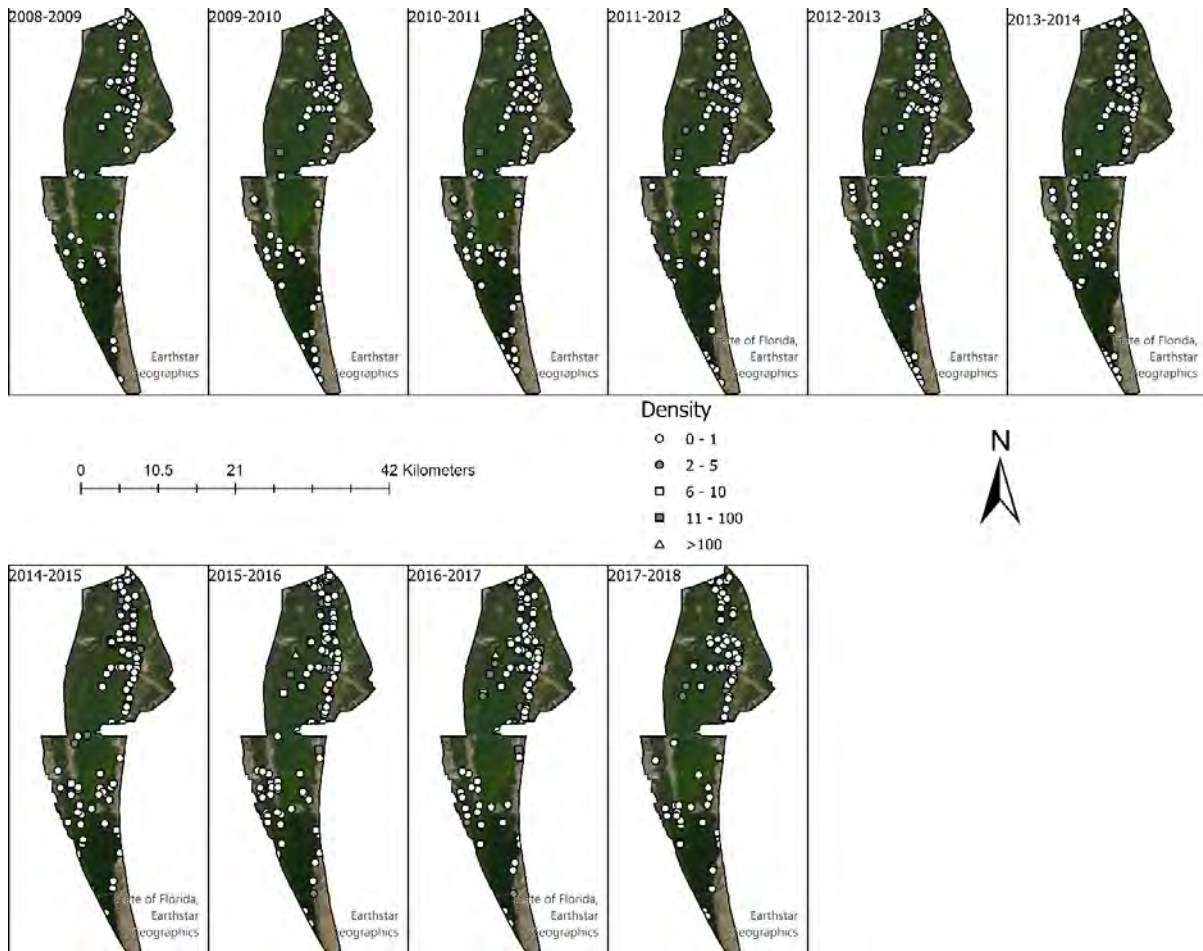
Figure 39. Annual *Sciaenops ocellatus* densities (fish/m³), 2008-2018.

2.2.12.1 Red Drum literature review

Red Drum are an exceptionally popular euryhaline sportfish that have a broad range of physiological tolerances (Gunter 1956). They have been observed and captively held in salinities ranging from 0 to 60 ppt (Craig et al. 1995, Ern and Esbaugh 2018). Aquacultural operations typically keep them at or around 27 °C as this optimizes their growth rate (Craig et al. 1995). The upper thermal tolerance of Red Drum varies slightly by source population and acclimation but is in the 29 to 35 °C range (Ward et al. 1993). Their lower lethal thermal limit depends heavily on their diet and general condition. In one study, captive fingerlings fed high quality food had a lower lethal thermal limit of 3.9 °C, whereas lower quality food fed fish died at 9.4 °C, with a dynamic reduction of temperature of 1 °C per day (Craig et al. 1995). However, field derived stocks used in a different study showed a lower lethal thermal limit of 1.6 °C (Ward et al. 1993). Shock halotolerance studies also noted that this species will undergo significant stress when rapidly transitioned from 35 ppt to 10 ppt but saw limited mortality and found that their osmoregulatory capacity under these conditions was not a limiting factor for survival due to compensatory mechanisms which are potentially unique to the species. When Red Drum were acclimated from 35 to 10 ppt over the course of 14 days, in the same study, they exhibited far fewer signs of stress and had no mortality (Ern and Esbaugh 2018). It is also worth noting that the RLI proposal would increase salinities and decrease temperatures in the BRL while reducing nitrogen species densities. Wise and Tomasso (Wise and Tomasso 1989) found that Red Drum are particularly

sensitive to nitrogen toxicity, and lower salinities increased the effects of acute nitrite toxicity on juvenile Red Drum.

Red Drum summary

Red Drum are one of the most popular recreation sportfish in Florida, and the BRL population is well known internationally as historically among the best places to fish for them as the Kennedy Space Center effectively serves as a marine protected area, which exports record-sized fishes into the fishable areas (Johnson et al. 1999). They are capable estuarine predators with a highly efficient osmoregulatory capacity which makes them able to survive, all be it with substantial physical stress, dramatic changes to water conditions (Ern and Esbaugh 2018). In captivity they can be housed in anything from freshwater to hypersaline conditions (Ward et al. 1993, Craig et al. 1995, Ern and Esbaugh 2018), though their ability to tolerate nitrogenous wastes is reduced with lower salinity (Wise and Tomasso 1989). Their lower thermal limit ranges from 1.6 °C to nearly 10 °C depending on their diet, with no noted impact of salinity on this relationship (Craig et al. 1995). Their thermal maximum; however, is dependent on the temperature they were acclimated to before the onset of thermal stress, with reports setting their upper thermal limit in the 29 to 35 °C range (Ward et al. 1993, Ern and Esbaugh 2018). Their distribution within the BRL would seem to corroborate these observations, with the Red Drum being observed in that fairly narrow temperature range of approximately 10 to 35 °C across the full range of salinities above 10 ppt experienced in the BRL (**Figure 37**). There are concerns however that the lack of suitable habitat in the BRL since the crash of the seagrass populations (see Morris et al. 2022 for a discussion of this) will translate to reduced larval settlement or retention. While no significant decline in the population has been noted here, or in Phase 2 abundance assessments (Blanchard et al. 2021), ongoing efforts are investigating if the size frequency distribution of this stock has changed over time (Blanchard & Turingan, in progress).

Regarding the RLI proposal, the anticipated net changes from the introduction of seawater into the BRL are unlikely to exceed the physiological limits of this particularly hardy species. However, we do not yet know how habitat suitability will change for this species in the BRL, or how their behavior may change in response to increased inflow. We do know that they will emigrate out of the BRL both through Cape Canaveral and into other portions of the IRL, but the triggers for these emigrations are unknown. Similarly, we currently only have a coarse understanding of their habitat use patterns within the BRL, insufficient for determining how the habitat suitability for this species will change. As such, the pending necessary questions for this species are 1) What determines habitat suitability for Red Drum in the BR, and 2) How will it change with the RLI proposal?

2.2.13 Syngnathus scovelli- Gulf Pipefish

There were 3459, 2, 429, and 396 usable occurrences of Gulf Pipefish in gears 20, 160, 300, and 301, respectively. As such, gear 160 was deemed data deficient and excluded from analysis. Gulf Pipefish were found in temperatures between 7.40 °C and 35.30 °C with a significant positive relationship detected between density and temperature for gears 20 (P<=0.001, adjusted R^2=0.010). The mean temperatures observed were 24.68±0.08 °C, 24.44±0.23 °C, and 25.53±0.25 °C for gears 20, 300, and 301, respectively with the majority found in the 15 to 30 °C

range and over 60% of occurrences in the 20 to 30 °C range. Regarding salinity, Gulf Pipefish occurred in waters ranging from 1.60 to 47.67 ppt, with means of 26.11±0.13, 23.51±0.37 and 28.71±0.28 (gears 20, 300, and 301, respectively) and fairly evenly spread throughout the 10 to 40 ppt bins. No significant relationship was detected between Gulf Pipefish densities and salinity (**Table 2, Table 3, Table 4, Figure 13**). There has been a substantial contraction of the range within which this species can be found in the BRL. Formerly widespread throughout, they are now restricted to the Northern BRL (**Figure 40, Figure 41**) due to the significant habitat loss and other changes to the ecosystem (Adams et al. 2022).
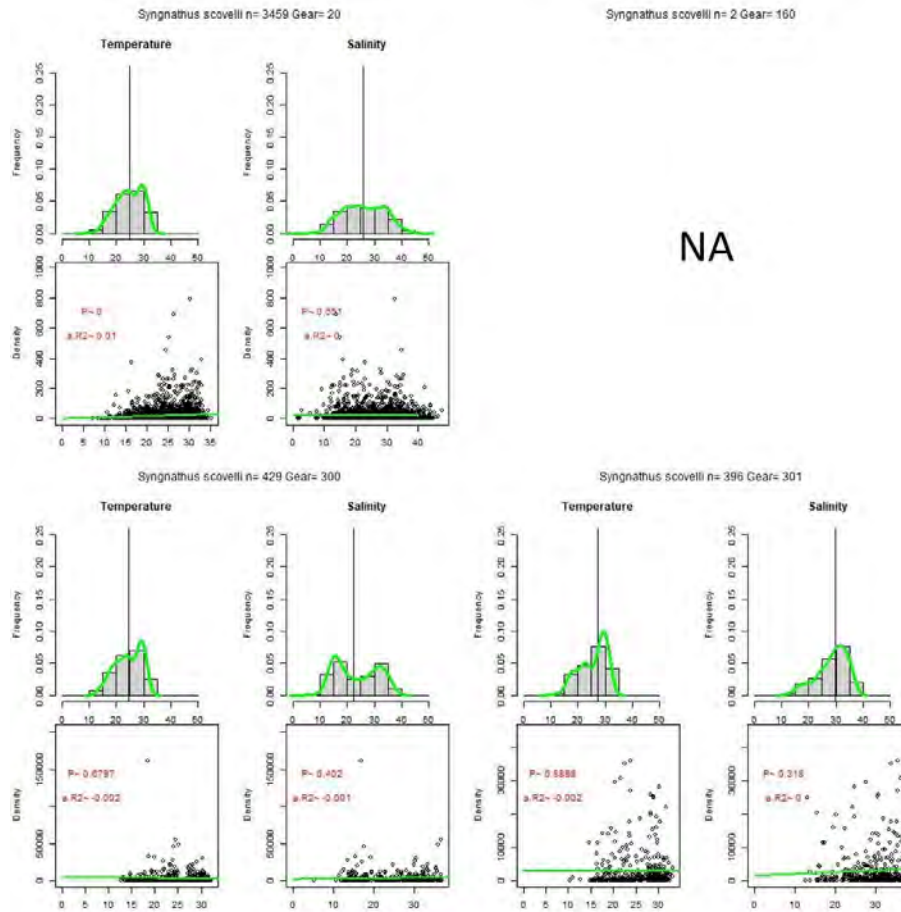
Figure 40. A three paneled figure for gears 20 (top left), 300 (bottom left) and 301 (bottom right). Note that gear 160 did not have enough occurrences to support analyses for this species. Each panel contains four figures: a histogram of observed temperatures for this species, with the median denoted by a vertical line and a smoothed representation of the data in green (top left), a similar histogram showing observed salinities for this species (top right), a scatterplot of density versus temperature for this species with a green line of best fits representing and statistics for the linear model of this relationship (bottom left), and a similar scatterplot of density versus salinity (bottom right).
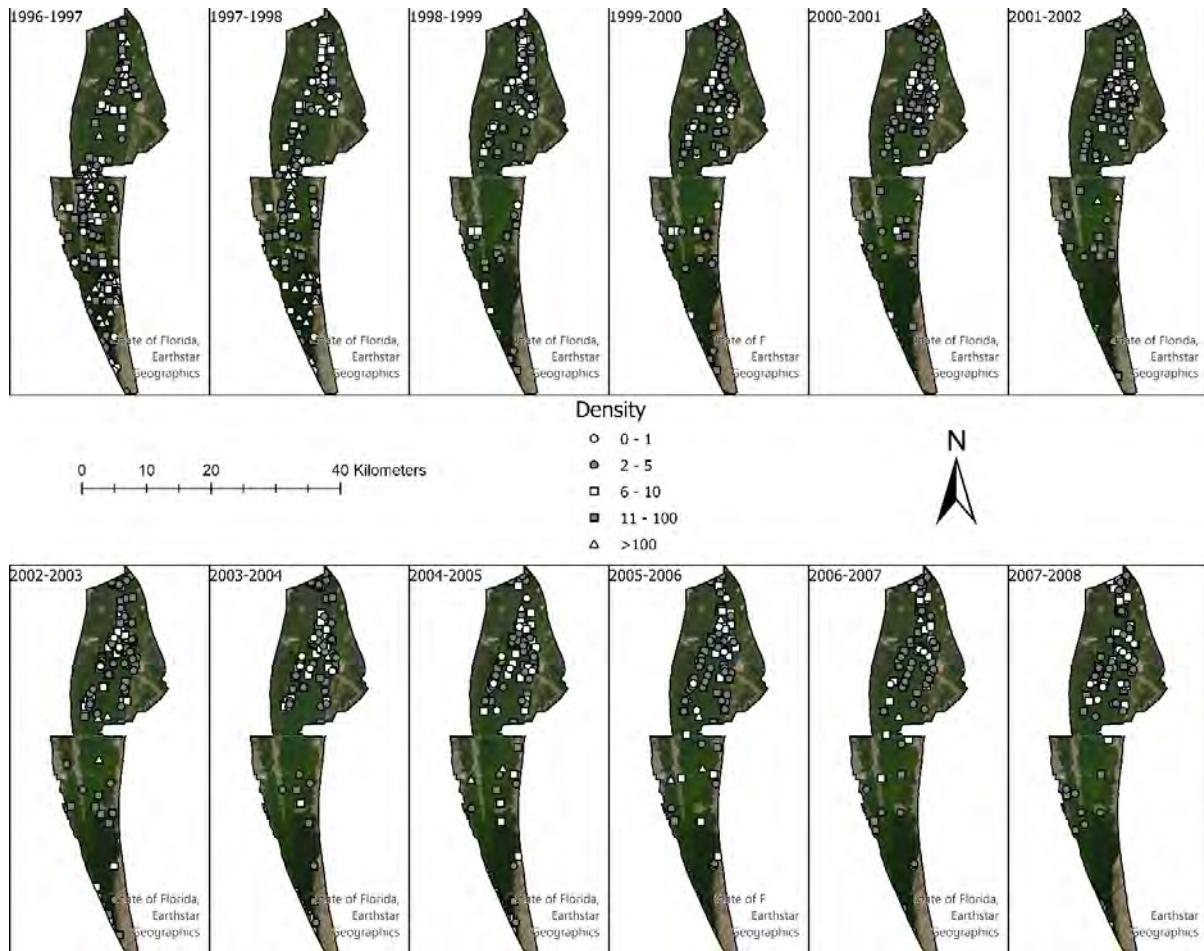
Figure 41. Annual *Syngnathus scovelli* densities (fish/m^3), 1996-2008.
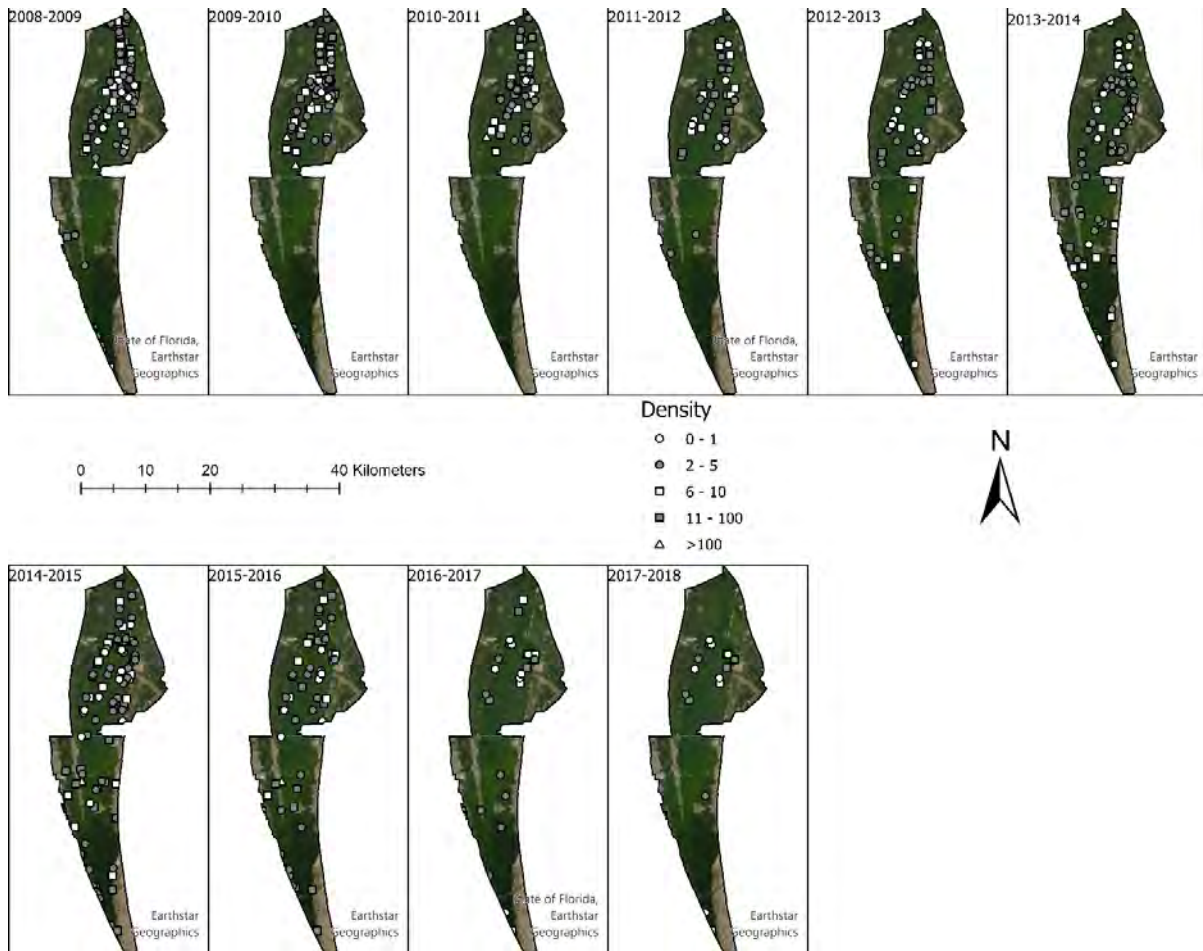
Figure 42. Annual *Syngnathus scovelli* densities (fish/m^3), 2008-2018.

2.2.13.1 Gulf Pipefish literature review

The Gulf Pipefish is a euryhaline fish (Gunter 1956), being the only member of its genus capable of reproduction in freshwater (Kuiter 2003) it has been observed in both freshwater and hypersaline conditions (Joseph 1957, Dalton Brown 1972, Bolland and Boeticher 2005, Krejci 2012). They are tolerant of most BRL conditions, with a minimum lethal temperature approximated at 10 °C , and a maximum temperature of approximately 35 °C (Gasparini and Teixeira n.d., Joseph 1957, Bolland and Boeticher 2005). They are capable of limiting the incidence of osmotic stress during reproduction through active osmoregulation of the brood pouch, though there is likely a metabolic cost to this regulation in direct proportion to the difference between brood pouch conditions, maintained at 0 to 10ppt, and the external environment (Partridge et al. 2007). Conversely, temperature is a significant indicator of their reproductive condition and success, explaining more than 50% of the variance in gonadosomatic indices, a measure of individual reproductive state, in one study (Bolland and Boeticher 2005). However, despite their relative insensitivity to abiotic conditions, Gulf Pipefish populations are heavily tied to habitat structure. Particularly to submerged vegetation, pollution, human disturbance (Bolland and Boeticher 2005, Adams et al. 2022), and the behavioral impacts of predator presence (Krejci 2012). Due to their high reliance on community structure, Gulf Pipefish are now considered an indicator species for IRL and BRL health. Their numbers have significantly declined in recent years (Adams et al. 2022).

2.2.13.2 Gulf Pipefish summary

The Gulf Pipefish is an indicator species of estuarine health, and their populations in the IRL have significantly declined in concert with habitat degradation since the late 1990's (Adams et al. 2022), supporting the notion that the IRL is at risk of collapse (Adams et al. 2019). While they are relatively insensitive to most abiotic conditions of their environment (Joseph 1957, Bolland and Boeticher 2005), they are highly sensitive to changes in the submerged vegetation, including floating drift algae, pollution (Bolland and Boeticher 2005, Adams et al. 2022), and community structure (Krejci 2012). Of the abiotic conditions that influence them, temperature is the most significant (**Figure 40**, (Dalton Brown 1972, Bolland and Boeticher 2005, Adams et al. 2022) being most often found in the BRL at temperatures between 10 and 35 °C (**Figure 40**).

With regards to the RLI proposal, Gulf Pipefish are likely to be relatively unaffected by the net changes to salinity and temperature produced. However, the rate at which those changes occur, and the rate of change which these fish can accommodate, and if a pulse or press change is more impactful, are currently unknown. To that point, it is also worth recognizing that this species is rarely found in temperatures exceeding 35 °C. In spring 2023, at the time of writing this report, Florida experienced a severe marine heat wave (Stillman 2023, NOAA 2023). The author conducted a haphazard visual survey of the mangrove fringes along the eastern coast of the BRL, near Port Canaveral, to observe how the fish were behaving in the BRL as water temperatures were well beyond the levels indicated as normal herein. Generally speaking, most fishes observed appeared lethargic and sticking to the shaded, deeper waters, as is expected. A large predator presence, mostly Bottlenose Dolphins, were slowly gathering the few fishes that left the mangroves. The only Gulf Pipefish observed was dead and floating, with no visible signs of damage, emaciation, or disease (**Figure 43**). There was an algae bloom present, likely Pyrodinium sp. based on personal observation, but it did not appear to be causing direct stress.

Figure 43. Gulf Pipefish found dead and floating in the BRL on 7/14/2023 at approximately 28.40202, -80.6226371.

While it cannot be stated with any degree of certainty that this was a heat-related death, few alternate hypotheses are forthcoming. A projected consequence of the RLI proposal is a reduction and stabilizing of BRL temperatures (FL.Tech. 2020), potentially mitigating some of the consequences of severe heat and severe cold events which are likely to become more frequent and severe as the Anthropocene progresses (IPCC 2012, 2018). However, there are still the same general suite of pending questions for this species as there have been for the majority in this report: 1) What rate of change is expected in the BRL in response to each pumping scenario, 2) What rate of change can Gulf Pipefish acclimate to, and 3) How will habitat suitability change in the near and long terms in response to each RLI scenario? The work presented here, and in the previous two RLI reports (Johnson et al. 2020, Blanchard et al. 2021) establishes a base from which these questions can be addressed, but a concerted effort needs to be made to build on this base to fully understand the implications of the proposed system alterations. As this species is an indicator of ecosystem health, addressing these questions will help establish the total system impact of RLI, as well as offer a potential after action monitoring target.

Table 2. Observed abiotic conditions for the Banana River and each species of interest for each gear type from 1996-2018 in the FWC data. T represents temperature, S represents salinity. The P and Adj R² presented are in reference to the linear model between fish density and temperature or salinity. NS denotes where the relationship was not statistically significant, and any specie-gear combination that had less than 25 observations was left blank to indicate it being data deficient.

Species	Gear	# of fish	Min. T.obs	Max T.obs	Mean T.	T. sem	P	Adj. R2	Min. S.obs	Max S.obs	Mean S.	S. sem	P	Adj. R²
Banana River			6.30	40.00	25.55	0.04			0.00	47.80	25.52	0.07		
Anchoa mitchilli	20	5040	9.90	34.00	25.51	0.33	<=0.001	0.007	0.20	47.80	23.29	0.10	NS	NS
	160	3												
	300	249	9.67	32.90	24.59	0.32	NS	NS	0.60	36.70	22.21	0.45	NS	NS
	301	255	9.90	33.05	24.88	0.33	NS	NS	0.20	47.60	28.66	0.21	0.020	0.004
Archosargus probatocephalus	20	1184	9.95	35.00	26.97	0.12	0.013	0.004	0.60	36.30	27.07	0.36	NS	NS
	160	2808	7.10	34.95	25.89	0.09	<=0.001	0.013	1.50	43.87	26.20	0.13	<=0.001	0.009
	300	92	15.50	32.03	25.72	0.41	NS	NS	8.40	36.70	28.29	0.68	0.004	0.076
	301	165	11.07	32.75	26.46	0.30	NS	NS	0.55	38.67	30.11	0.43	NS	NS
Cynoscion nebulosus	20	2637	6.30	40.00	28.20	0.08	NS	NS	0.20	35.00	24.95	0.14	NS	NS
	160	1440	6.70	34.95	24.32	0.14	NS	NS	9.70	42.60	25.16	0.16	0.002	0.006
	300	212	13.20	32.77	28.16	0.29	NS	NS	0.60	35.63	21.40	0.76	0.040	0.040
	301	135	18.25	33.60	29.27	0.28	NS	NS	9.13	39.10	26.92	0.55	NS	NS
Eucinostomus harengulus	20	2365	9.00	40.00	26.80	0.09	<=0.001	0.022	4.40	46.40	27.35	0.14	NS	NS
	160	1893	9.10	34.95	25.88	0.11	NS	NS	7.50	43.87	25.87	0.15	0.002	0.005
	300	83	13.60	32.77	25.19	0.55	0.050	0.040	11.72	39.00	29.17	0.76	0.040	0.040
	301	117	11.23	33.20	27.20	0.46	NS	NS	1.15	35.40	28.30	0.56	NS	NS
Lagodon rhomboides	20	2955	9.10	35.00	25.69	0.09	0.040	0.001	9.40	47.80	29.25	0.13	0.001	0.003
	160	3135	6.70	34.00	25.94	0.08	<=0.001	0.016	7.30	43.87	25.96	0.12	<=0.001	0.018
	300	285	12.15	32.90	24.43	0.26	NS	NS	12.80	37.80	28.81	0.39	NS	NS
	301	464	10.40	33.20	24.93	0.22	NS	NS	13.17	38.67	30.00	0.22	NS	NS
Leiostomus xanthurus	20	1399	8.50	33.90	22.95	0.13	<=0.001	0.010	4.80	47.80	28.22	0.19	NS	NS
	160	1314	10.00	33.55	26.74	0.11	0.001	0.007	10.00	43.87	27.62	0.17	<=0.001	0.010
	300	86	13.45	32.50	24.07	0.57	NS	NS	12.10	37.80	25.65	0.89	NS	NS
	301	114	12.67	32.75	23.92	0.51	0.039	0.029	13.23	38.67	30.53	0.45	NS	NS

Restore Lagoon Inflow Research (Phase 3)
Final Report

Species	Gear	# of fish	Min. T.obs	Max T.obs	Mean T.	T. sem	P	Adj. R2	Min. S.obs	Max S.obs	Mean S.	S. sem	P	Adj. R²
Lutjanus griseus	20	473	12.40	34.80	27.81	0.17	0.003	0.017	0.20	43.50	26.91	0.31	NS	NS
	160	725	7.50	34.95	27.88	0.14	0.029	0.005	1.60	42.60	25.58	0.24	<=0.001	0.019
	300	50	18.10	32.77	27.89	0.45	NS	NS	12.43	35.55	27.87	0.84	NS	NS
	301	153	17.10	33.60	27.75	0.32	NS	NS	9.13	36.70	27.23	0.43	NS	NS
Mugil cephalus	20	1379	7.2	37.40	22.47	0.14	<=0.001	0.017	4.65	44.10	25.41	0.19	NS	NS
	160	4033	6.70	34.95	24.91	0.08	NS	NS	1.50	43.87	25.42	0.11	<=0.001	0.003
	300	2												
	301	0												
Opisthonema oglinum	20	372	11.50	33.70	28.14	0.16	NS	NS	0.20	41.80	27.63	0.35	0.046	0.008
	160	512	9.75	33.50	26.51	0.18	0.022	0.008	10.00	43.87	26.04	0.27	NS	NS
	300													
	301													
Pogonias cromis	20	115	14.80	33.90	26.44	0.42	NS	NS	2.00	42.00	26.58	0.71	NS	NS
	160	908	8.85	34.25	25.94	0.15	NS	NS	1.50	43.87	26.07	0.23	<=0.001	0.026
	300	0												
	301	1												
Sciaenops ocellatus	20	1234	7.80	33.55	22.48	0.13	NS	NS	2.80	41.70	24.78	0.19	NS	NS
	160	2248	7.50	34.25	25.40	0.10	0.002	0.004	1.60	43.87	25.26	0.14	<=0.001	0.019
	300													
	301													
Syngnathus scovelli	20	3459	7.40	35.30	24.68	0.08	<=0.001	0.010	1.60	47.60	26.11	0.13	NS	NS
	160	2												
	300	429	12.70	32.23	24.44	0.23	NS	NS	5.28	36.93	23.51	0.37	NS	NS
	301	396	10.40	33.20	25.53	0.25	NS	NS	12.70	37.10	28.71	0.28	NS	NS

Table 3. Frequency of occurrences of each species of interest-gear type combination within each temperature bin. Cells with more than 5% of the occurrences are highlighted in light gray, those with less than 5% of the occurrences are blocked in dark gray.

Species	Gear	# of fish	0-5 °C	5-10 °C	10-15 °C	15-20 °C	20-25 °C	25-30 °C	30-35 °C	35-40 °C
Anchoa mitchilli	20	5040	0.00%	0.05%	1.35%	11.30%	30.75%	39.25%	17.30%	0.00%
	160	3	0.00%	0.00%	0.00%	0.00%	33.33%	33.33%	33.33%	0.00%
	300	249	0.00%	0.40%	2.41%	18.47%	28.11%	37.35%	13.25%	0.00%
	301	255	0.00%	0.78%	1.57%	20.39%	23.14%	34.51%	19.61%	0.00%
Archosargus probatocephalus	20	1184	0.00%	0.08%	0.59%	6.59%	22.47%	43.16%	27.11%	0.00%
	160	2808	0.00%	0.11%	1.75%	10.15%	26.35%	40.71%	20.94%	0.00%
	300	92	0.00%	0.00%	0.00%	7.61%	35.87%	41.30%	15.22%	0.00%
	301	165	0.00%	0.00%	0.61%	7.27%	21.82%	52.12%	18.18%	0.00%
Cynoscion nebulosus	20	2637	0.00%	0.08%	0.30%	5.23%	20.40%	47.71%	26.17%	0.11%
	160	1440	0.00%	0.35%	5.56%	18.40%	29.03%	31.32%	15.35%	0.00%
	300	212	0.00%	0.00%	0.94%	10.85%	13.21%	56.13%	18.87%	0.00%
	301	135	0.00%	0.00%	0.00%	2.22%	13.33%	45.93%	38.52%	0.00%
Eucinostomus harengulus	20	2365	0.00%	0.08%	1.06%	7.15%	23.38%	41.48%	26.77%	0.08%
	160	1893	0.00%	0.21%	2.38%	10.04%	25.99%	40.20%	21.18%	0.00%
	300	83	0.00%	0.00%	1.20%	16.87%	26.51%	38.55%	16.87%	0.00%
	301	117	0.00%	0.00%	2.56%	16.24%	20.51%	40.17%	20.51%	0.00%
Lagodon rhomboides	20	2955	0.00%	0.07%	1.52%	12.18%	26.77%	39.76%	19.70%	0.00%
	160	3135	0.00%	0.19%	1.85%	11.20%	23.76%	41.82%	21.18%	0.00%
	300	285	0.00%	0.00%	1.05%	15.79%	39.65%	32.98%	10.53%	0.00%
	301	464	0.00%	0.00%	1.72%	18.10%	30.82%	35.56%	13.79%	0.00%
Leiostomus xanthurus	20	1399	0.00%	0.21%	3.86%	23.95%	37.60%	27.31%	7.08%	0.00%
	160	1314	0.00%	0.08%	0.61%	6.39%	22.68%	48.02%	22.22%	0.00%
	300	86	0.00%	0.00%	2.33%	25.58%	23.26%	38.37%	10.47%	0.00%
	301	114	0.00%	0.00%	1.75%	29.82%	20.18%	31.58%	16.67%	0.00%
Lutjanus griseus	20	473	0.00%	0.00%	1.06%	3.59%	16.07%	49.68%	29.60%	0.00%
	160	725	0.00%	0.14%	0.83%	2.21%	15.86%	48.00%	32.97%	0.00%

Restore Lagoon Inflow Research (Phase 3)
Final Report

Species	Gear	# of fish	0-5 °C	5-10 °C	10-15 °C	15-20 °C	20-25 °C	25-30 °C	30-35 °C	35-40 °C
	300	50	0.00%	0.00%	0.00%	2.00%	16.00%	64.00%	18.00%	0.00%
	301	153	0.00%	0.00%	0.00%	7.19%	15.03%	44.44%	33.33%	0.00%
Mugil cephalus	20	1379	0.00%	0.51%	6.96%	27.56%	32.78%	22.41%	9.72%	0.07%
	160	4033	0.00%	0.22%	2.78%	15.15%	29.51%	35.71%	16.64%	0.00%
	300	2								
	301	0								
Opisthonema oglinum	20	372	0.00%	0.00%	0.54%	1.34%	10.75%	59.41%	27.96%	0.00%
	160	512	0.00%	0.20%	1.56%	5.86%	22.46%	49.61%	20.31%	0.00%
	300	10								
	301	9								
Pogonias cromis	20	115	0.00%	0.00%	0.87%	10.43%	25.22%	38.26%	25.22%	0.00%
	160	908	0.00%	0.11%	1.65%	11.01%	25.22%	40.53%	21.48%	0.00%
	300	0								
	301	1								
Sciaenops ocellatus	20	1234	0.00%	0.49%	4.29%	24.23%	42.63%	24.39%	3.97%	0.00%
	160	2248	0.00%	0.13%	2.49%	12.37%	28.20%	37.94%	18.86%	0.00%
	300	17								
	301	45	0.00%	0.00%	2.22%	40.00%	46.67%	11.11%	0.00%	0.00%
Syngnathus scovelli	20	3459	0.00%	0.14%	2.63%	16.94%	30.90%	33.13%	16.22%	0.03%
	160	2								
	300	429	0.00%	0.00%	3.50%	17.48%	31.47%	34.73%	12.82%	0.00%
	301	396	0.00%	0.00%	1.26%	16.67%	23.23%	38.13%	20.71%	0.00%

Table 4. Frequency of occurrences of each species of interest-gear type combination within each salinity bin. Cells with more than 5% of the occurrences are highlighted in light gray, those with less than 5% of the occurrences are blocked in dark gray.

Species	Gear	# of fish	0-5 ppt	5-10 ppt	10-15 ppt	15-20 ppt	20-25 ppt	25-30 ppt	30-35 ppt	35-40 ppt	40-44 ppt	45-50 ppt
Anchoa mitchilli	20	5040	0.20%	0.60%	6.50%	17.60%	23.15%	22.15%	21.00%	7.40%	1.40%	0.00%
	160	3										
	300	249	0.40%	0.40%	20.08%	22.49%	22.09%	15.26%	16.47%	2.81%	0.00%	0.00%
	301	255	0.00%	0.39%	2.75%	9.80%	21.96%	29.02%	31.37%	4.71%	0.00%	0.00%
Archosargus probatocephalus	20	1184	0.17%	0.84%	3.72%	8.70%	15.29%	21.71%	31.25%	15.46%	2.70%	0.17%
	160	2808	0.07%	0.43%	5.41%	15.35%	21.12%	24.93%	22.83%	9.44%	0.43%	0.00%
	300	92	0.00%	1.09%	2.17%	10.87%	10.87%	18.48%	46.74%	9.78%	0.00%	0.00%
	301	165	0.61%	0.00%	1.21%	4.85%	7.27%	24.24%	49.09%	12.73%	0.00%	0.00%
Cynoscion nebulosus	20	2637	0.23%	0.61%	7.24%	18.66%	23.59%	23.25%	18.28%	6.83%	1.33%	0.00%
	160	1440	0.00%	0.21%	4.10%	20.00%	26.32%	25.21%	17.64%	6.18%	0.35%	0.00%
	300	212	0.47%	0.47%	18.87%	30.66%	17.92%	16.04%	13.68%	1.89%	0.00%	0.00%
	301	135	0.00%	1.48%	1.48%	9.63%	24.44%	22.22%	34.81%	5.93%	0.00%	0.00%
Eucinostomus harengulus	20	2365	0.13%	0.51%	4.02%	13.32%	20.68%	24.40%	25.03%	10.19%	1.69%	0.04%
	160	1893	0.00%	0.16%	3.91%	16.90%	25.25%	24.62%	20.66%	8.19%	0.32%	0.00%
	300	83	0.00%	0.00%	9.64%	9.64%	12.05%	21.69%	42.17%	4.82%	0.00%	0.00%
	301	117	0.85%	0.85%	2.56%	3.42%	14.53%	29.91%	43.59%	4.27%	0.00%	0.00%
Lagodon rhomboides	20	2955	0.00%	0.14%	3.38%	8.32%	14.42%	20.95%	33.91%	14.99%	3.72%	0.17%
	160	3135	0.00%	0.19%	3.80%	17.99%	23.13%	23.76%	22.55%	8.20%	0.38%	0.00%
	300	285	0.00%	0.00%	6.32%	7.37%	9.47%	20.00%	45.26%	11.58%	0.00%	0.00%
	301	464	0.00%	0.00%	0.65%	2.80%	12.50%	28.66%	42.46%	12.93%	0.00%	0.00%
Leiostomus xanthurus	20	1399	0.07%	0.21%	4.72%	8.79%	18.66%	22.02%	30.38%	12.22%	2.72%	0.21%
	160	1314	0.00%	0.15%	2.44%	11.19%	20.32%	24.81%	30.44%	10.05%	0.61%	0.00%
	300	86	0.00%	0.00%	17.44%	16.28%	6.98%	15.12%	36.05%	8.14%	0.00%	0.00%
	301	114	0.00%	0.00%	0.88%	1.75%	2.80%	11.40%	24.56%	46.49%	14.91%	0.00%
Lutjanus griseus	20	473	0.42%	0.85%	4.86%	10.99%	18.39%	26.64%	30.02%	6.98%	0.85%	0.00%
	160	725	0.14%	0.69%	4.83%	15.17%	27.03%	24.14%	21.66%	5.93%	0.41%	0.00%

Species	Gear	# of fish	0-5 ppt	5-10 ppt	10-15 ppt	15-20 ppt	20-25 ppt	25-30 ppt	30-35 ppt	35-40 ppt	40-44 ppt	45-50 ppt
Mugil cephalus	300	50	0.00%	0.00%	2.00%	10.00%	18.00%	24.00%	44.00%	2.00%	0.00%	0.00%
	301	153	0.00%	0.65%	0.65%	9.80%	20.26%	33.99%	31.37%	3.27%	0.00%	0.00%
	20	1379	0.22%	0.65%	7.69%	15.88%	24.22%	21.75%	21.54%	7.03%	1.02%	0.00%
	160	4033	0.05%	0.27%	5.73%	18.35%	24.52%	22.56%	20.31%	7.86%	0.35%	0.00%
	300	2										
	301	0										
Opisthonema oglinum	20	372	0.54%	0.27%	2.15%	8.33%	24.73%	24.46%	24.46%	13.44%	1.61%	0.00%
	160	512	0.00%	0.20%	3.71%	15.43%	23.05%	28.91%	22.46%	5.86%	0.39%	0.00%
	300	10										
	301	9										
Pogonias cromis	20	115	0.87%	0.00%	6.09%	14.78%	21.74%	20.00%	20.00%	15.65%	0.87%	0.00%
	160	908	0.22%	0.88%	4.63%	14.76%	23.79%	24.56%	20.70%	9.91%	0.55%	0.00%
	300	0										
	301	1										
Sciaenops ocellatus	20	1234	0.16%	1.13%	6.48%	19.85%	22.61%	23.50%	21.72%	4.29%	0.24%	0.00%
	160	2248	0.04%	0.31%	6.09%	18.59%	25.09%	23.13%	17.57%	8.67%	0.49%	0.00%
	300	17										
	301	45	2.22%	2.22%	0.00%	11.11%	31.11%	24.44%	26.67%	2.22%	0.00%	0.00%
Syngnathus scovelli	20	3459	0.12%	0.43%	7.55%	16.97%	21.19%	19.57%	21.02%	10.90%	2.17%	0.09%
	160	2										
	300	429	0.00%	0.23%	16.55%	26.34%	12.35%	14.69%	24.48%	5.36%	0.00%	0.00%
	301	396	0.00%	0.00%	1.01%	8.84%	13.38%	28.54%	38.13%	10.10%	0.00%	0.00%

2.3 Conclusion

In Phase 1 of the RLI effort, the fish team sought to identify key SoI for further study and identify the key abiotic factors that are of the highest importance to those species which may be impacted by the proposed increase in oceanic inflow within the 3 defined regions of interest. Following that effort, the broader RLI team identified the BRL as the most viable candidate location for a pilot study, so the remainder of fish efforts were focused there. In Phase 2, the fish team quantified the relationships of each SoI with their abiotic environment, developed predictive models of species-specific abundance and projected the potential impact of different pumping scenarios on each species. The biggest takeaway from the fish team's second year of effort is there is a paucity of information on the physiological tolerances of SoI within the BR, or more broadly, highlighting the need to quantify broader habitat suitability changes rather than only projecting static responses to abiotic shifts. However, the needs of the RLI effort dictated that biological research be paused moving in to the third phase to focus on permitting, which is described elsewhere in this volume. However, given the vital importance of understanding fish responses to the RLI proposal, this limited and constrained study was developed to 1) advance our understanding of the models produced in Phase 2, and 2) lay the groundwork for that next phase of research: habitat suitability modelling.

For this Phase 3 effort the SoI list was expanded from eight to eleven species to represent a broader ecological context. As this effort is descriptive in nature, no specific conclusions can be reached at this time. Rather, this report provides two valuable deliverables. 1) The identification of critical unknowns which will guide future research questions to be answered during or in advance of any pilot project. 2) A large portion of the data-infrastructure needed to build species specific habitat suitability models.

Rather, this effort represents a substantial step toward the most critical component of the RLI fish work, which would be the development of habitat suitability models. These models require an understanding of the environmental envelope, range of tolerances, of a species as well as their spatiotemporal distribution in the target area with respect to the abiotic features of interest, in the form of Geographic Information Systems compatible rasters. This report provides those data and input features. The models will also require input from the external predictive models developed in Phase 2.

2.3.1 Critical unknowns

This report discusses several critical unknowns with respect to each of the eleven SoI examined. While data on physiological tolerances and habitat use varies among species, there was an emergent recurrent theme in the data gaps described above.

1. **What is the rate of environmental change anticipated by the proposed pumping scenarios?**

   Estuarine fishes are used to environmental change. It is a normal part of their daily lives in the IRL. They can adapt to changes within their environmental envelopes, and many will emigrate if conditions warrant. However, their adaptive mechanisms take time to respond. If the rate of change exceeds their responsive capacity, it results in quantifiable levels of stress and can result in fish kills similar to what is seen during a harmful algal bloom induced hypoxia event, cold snap, or heat wave. Inflow pumping ramp-up speeds must be below the level which would induce a fish kill. *To determine what pumping schedule (ramp-up speeds and final pumping rates) are both safe and effective, we need to understand the spatially explicit rate of environmental change to be expected under proposed pumping scenarios.*

2. What rate of environmental change can BRL fishes tolerate?

The mechanism behind a fish's adaptive capacity, its efficacy, and their ability to endure stresses to that system are highly species specific. In many cases, they are population specific. For several of the SoI described above, this information is known, or at least can be approximated with a reasonable degree of confidence. However, data gaps exist for the majority of species and the literature review presented above highlighted this need. *To determine a safe pumping schedule, we need to understand the rate of change which can be tolerated by BRL fishes.*

3. How will habitat suitability change in the BRL under each pumping scenario?

At its core, the proposal to increase inflow to the BRL to facilitate biochemical processes to reduce resident pollution levels and restore water quality is an effort to restore the suitability of the BRL habitats to resident species. The RLI Fish Team's efforts to date, including this report, have been building the necessary infrastructure to model habitat suitability changes anticipated in response to each proposed inflow scenario. With this report, we now have the analytical infrastructure necessary to produce these projections. However, we have also learned that the story of how BRL fishes will respond to increased inflow is likely as much behavioral as it is physiological. Some data exist regarding the movement ecology of fishes in the BR, as summarized in the Phase 2 report, but it is not at the resolution we would need to inform habitat suitability model development. *Moving forward, to improve assessment of inflow impacts to the BRL and IRL overall, we need to better understand the behavioral component of fish responses to changing water quality conditions. This information will inform habitat suitability modeling to address the core question regarding the fish response to the RLI proposal: How will habitat suitability for each SoI change under each pumping scenario?*

2.3.2 Habitat suitability modelling infrastructure

Perhaps the most valuable product of this effort is the infrastructure produced to develop the required habitat suitability model development. HSMs seek to model species' habitat use based on the complex interactions of the abiotic and biotic factors influencing their spatiotemporal distribution. HSMs require:

1. Environmental rasters describing the abiotic environment (**Figure 2, Figure 3, Figure 4, Figure 5** and **Figure 6**).
2. Spatiotemporal distribution rasters describing the density distribution of the SoI in space and time (**Figure 8, Figure 9, Figure 11, Figure 12, Figure 14, Figure 15, Figure 17, Figure 18, Figure 20, Figure 21, Figure 23, Figure 24, Figure 26, Figure 27, Figure 29, Figure 30, Figure 32, Figure 33, Figure 35, Figure 36, Figure 38, Figure 39, Figure 41,** and **Figure 42**).
3. An understanding of the regionally specific, and more global, environmental envelopes of each SoI, which are described with the above literature reviews and by: **Figure 7, Figure 10, Figure 13, Figure 16, Figure 19, Figure 22, Figure 25, Figure 28, Figure *31*, Figure 34, Figure 37,** and **Figure 40**.
4. Mechanistic predictive models of how the habitat will change under each pumping scenario. These are provided by the biogeochemical and hydrodynamic modelling teams, as described in other sections of this volume.
5. Predictive abundance models for each SoI within the region of interest. These were provided in the Fish Team's RLI Phase 2 report.

6. Detailed behavioral response and habitat use data during analogous environmental change for a representative sample of the SoI. The development of this final necessary data input is proposed for the next phase of this research, in concert with the proposed pilot project.

3 References

Adams, D. H., A. Sebastian, and R. Paperno. 2022. Population decline of Gulf pipefish (Syngnathus scovelli) in a subtropical estuary: ecosystem changes and habitat loss. Marine Biodiversity:52–57.

Adams, D. H., D. M. Tremain, R. Paperno, and C. Sonne. 2019. Florida lagoon at risk of ecosystem collapse. Science 365:991–992.

Adams, G. D., R. T. Leaf, J. C. Ballenger, S. A. Arnott, and C. J. McDonough. 2018. Spatial variability in the growth of Sheepshead (Archosargus probatocephalus) in the Southeast US: Implications for assessment and management. Fisheries Research 206:35–43.

Adriance, J., K. Chapiesky, and J. Isaacs. 2019. Louisiana Black Drum.

Alshuth, S., and R. G. Gilmore. 1995. EGG AND EARLY LARVAL CHARACTERISTICS OF POGONIAS CROMIS, BAIRDIELLA CHRYSOURA AND CYNOSCION NEBULOSUS (PISCES: SCIAENIDAE), FROM THE INDIAN RIVER LAGOON, FLORIDA. International Council for the Exploration of the Sea. Conference Manuscript 50.

Anweiler, K. 2013, May. Low-temperature tolerance of juvenile Spotted Seatrout, Cynoscion nebulosus, in South Carolina. Thesis, College of Charleston.

Bay, B., F. Author, J. C. Leak, E. D. Houde, J. C. Leak1, and E. D. Houde2. 1987. Cohort growth and survival of bay anchovy Anchoa mitchilli larvae in Cohort growth and survival of bay anchovy Anchoa mitchilli larvae in Biscayne Bay Florida. Source: Marine Ecology Progress Series 37:109–122.

Bayly, I. A. E. 1972. SALINITY TOLERANCE AND OSMOTIC BEHAVIOR OF ANIMALS IN ATHALASSIC SALINE AND MARINE HYPERSALINE WATERS.

Bell, M., and C. McDonough. 2015. Sheepshead, Archosargus probatocephalus.

Bennett, W. A., and F. W. Judd. 1992. Comparison of Methods for Determining Low Temperature Tolerance: Experiments with Pinfish, Lagodon rhomboides. Copeia 1992:1059–1065.

Blanchard, J., J. Eble, K. Johnson, R. Turingan, R. Weaver, G. Zarillo, M. Shelton, and M. Frick. 2021. Restore Lagoon Inflow Research (Phase 2). Melbourne, FL.

Blaylock, R., E. Saillant, A. Apeitos, D. Abrego, P. Cason, and R. Vega. 2021, June 1. The status of spotted seatrout (Cynoscion nebulosus) as a technologically feasible species for U.S. marine aquaculture. Blackwell Publishing Inc.

Bolland, J., and A. Boeticher. 2005. Population Structure and Reproductive Characteristics of the Gulf Pipefish, Syngnathus scovelli, in Mobile Bay, Alabama.

Boucek, R. E., and J. S. Rehage. 2014. Climate extremes drive changes in functional community structure. Global Change Biology 20:1821–31.

Brander, K. 2010. Impacts of climate change on fisheries. Journal of Marine Systems 79:389–402.

Bridges, D. W. 1971, January. The Critical Thermal Maximum of Juvenile Spot Leiostomus xanthurus Lacepede. Thesis, North Carolina State University, Raleigh, North Carolina.

Brown, M., R. Robins, and P. Schofield. 2022. Risk assessment of chanchita Cichlasoma dimerus (Heckel, 1840), a newly identified non-native cichlid fish in Florida. Management of Biological Invasions 13:435–448.

Brown-Peterson, N. J., M. S. Peterson, D. L. Nieland, M. D. Murphy, R. G. Taylor, and J. R. Warren. 2002. Reproductive biology of female spotted seatrout, Cynoscion nebulosus, in the Gulf of Mexico: differences among estuaries? Page Environmental Biology of Fishes.

Cardona, L. 2000. Effects of salinity on the habitat selection and growth performance of Mediterranean flathead grey mullet Mugil cephalus (Osteichthyes, Mugilidae). Estuarine, Coastal and Shelf Science 50:727–737.

Castillo-Rivera, M. 2013. Influence of Rainfall Pattern in the Seasonal Variation of Fish Abundance in a Tropical Estuary with Restricted Marine Communication. Journal of Water Resource and Protection 05:311–319.

Castillo-Rivera, M., G. Moreno, and R. Iniestra. 1994. Spatial, Seasonal, and Diel Variation in Abundance of the Bay Anchovy, Anchoa mitchilli (Teleostei: Engraulidae), in a Tropical Coastal Lagoon of Mexico. Source: The Southwestern Naturalist 39:263–268.

Castro, L. R., and R. K. Cowen. 1991. Environmental factors affecting the early life history of bay anchovy Anchoa mitchilli in Great South Bay, New York. MARINE ECOLOGY PROGRESS SERIES Mar. Ecol. Prog. Ser 76:235–247.

Chacin, D. H., T. S. Switzer, C. H. Ainsworth, and C. D. Stallings. 2016. Long-term analysis of spatio-temporal patterns in population dynamics and demography of juvenile Pinfish (Lagodon rhomboides). Estuarine, Coastal and Shelf Science 183:52–61.

Chamberlain, G., and K. Strawn. 1977. SUBMERGED CAGE CULTURE OF FISH IN SUPERSATURATED THERMAL EFFLUENT. Proceedings of the annual meeting - World Mariculture Society 8:625–645.

Chi-Espínola, A. A., M. E. Vega-Cendejas, and W. G. Canto-Maza. 2018. Feeding habits of the mojarras (Gerreidae) population in the hyperhaline lagoon system of ría Lagartos, Yucatan, Mexico. Latin American Journal of Aquatic Research 46:810–819.

Chung, K. S., and K. Strawn. 1994. What factors influence the thermal tolerance of estuarine animals? Interpretation of multiple regression analyses. Rev. Biol. Trop. 42:365–370.

Colura, R. L. 1974. INDUCED SPAWNING OF THE SPOTTED SEATROUT, Cynoscion nebulosus (CUVIER). Proceedings of the annual meeting - World Mariculture Society 5:319–330.

Coutant, C. C. 1985. Striped Bass, Temperature, and Dissolved Oxygen: A Speculative Hypothesis for Environmental Risk. Transactions of the American Fisheries Society 114:31–61.

Craig, S. R., W. H. Neill, and D. M. Gatlin. 1995. Effects of dietary lipid and environmental salinity on growth, body composition, and cold tolerance of juvenile red drum (Sciaenops ocellatus). Fish Physiology and Biochemistry 14:49–61.

Dalton Brown, J. 1972. A COMPARATIVE LIFE HISTORY STUDY OF FOUR SPECIES OF PIPEFISHES (FAMILY SYNGNATHIDAE) IN FLORIDA. Dissertation, University of Florida.

Darcy, G. H. 1985. Synopsis of biological data on Pinfish, Lagodon rhomboides (Pisces: Sparidae). FAO Fisheries Synopsis No. 141. NOAA Technical Report NMFS 23.

David Heil, A. 2017, July 19. Life history, diet, and reproductive dynamics of the sheepshead (Archosargus probatocephalus) in the Northeastern Gulf of Mexico. Master of Science Thesis, Florida State University , Tallahassee, FL.

Dutka-Gianelli, J., and D. J. Murie. 2001. AGE AND GROWTH OF SHEEPSHEAD, ARCHOSARGUS PROBATOCEPHALUS (PISCES: SPARIDAE), FROM THE NORTHWEST COAST OF FLORIDA. Page BULLETIN OF MARINE SCIENCE.

Dutka-Gianelli, J., R. Taylor, E. Nagid, J. Whittington, and K. Johnson. 2011. Habitat Utilization and Resource Partitioning of Apex Predators in Coastal Rivers of Southeast Florida. Page Library.

Ellis, T. A., J. A. Buckel, J. E. Hightower, and S. J. Poland. 2017. Relating cold tolerance to winterkill for spotted seatrout at its northern latitudinal limits. Journal of Experimental Marine Biology and Ecology 490:42–51.

Ern, R., and A. J. Esbaugh. 2018. Effects of salinity and hypoxia-induced hyperventilation on oxygen consumption and cost of osmoregulation in the estuarine red drum (Sciaenops ocellatus). Comparative Biochemistry and Physiology -Part A : Molecular and Integrative Physiology 222:52–59.

Fazio, F., S. Marafioti, F. Arfuso, G. Piccione, and C. Faggio. 2013. Influence of different salinity on haematological and biochemical parameters of the widely cultured mullet, Mugil cephalus. Marine and Freshwater Behaviour and Physiology 46:211–218.

Finucane, J. H., and R. N. Vaught. 1986. Species profile of the Atlantic thread herring Opisthonema oglinum (Lesueur 1818). Page NOAA Technical Memorandum NMFS-SEFC-182.

Fl. DEP. 2016. Indian River Lagoon Aquatic Preserves System Management Plan. Tallahassee, FL.

Flaherty-Walia, K. E., R. E. Matheson, and R. Paperno. 2015. Juvenile Spotted Seatrout (Cynoscion nebulosus) Habitat Use in an Eastern Gulf of Mexico Estuary: The Effects of Seagrass Bed Architecture, Seagrass Species Composition, and Varying Degrees of Freshwater Influence. Estuaries and Coasts 38:353–366.

McCall, J. N., and J. W. Fleeger. 1993. Recognition and utilization of prey aggregations by juvenile spot (Leiostomus xanthurus Lacepede). Journal of experimental marine biology and ecology 174.1:121–134.

FL.Tech. 2020. Restore Lagoon Inflow Research (Phase 1) Summary Report.

Frisbie, C. M. 1961. Young Black Drum, Pogonias cromis, in Tidal Fresh and Brackish Waters, Especially in the Chesapeake and Delaware Bay Areas. Chesapeake Science 2:94.

Gasparini, J. L., and R. L. Teixeira. (n.d.). REPRODUCTIVE ASPECTS OF THE GULF PIPEFISH, Syngnathus scovelli (TELEOSTEI: SYNGNATHIDAE), FROM SOUTHEASTERN BRAZIL. Page Rev. Brasil. Biol.

Gelwick, F. P., S. Akin, D. A. Arrington, and K. O. Winemiller. 2001. Fish Assemblage Structure in Relation to Environmental Variation in a Texas Gulf Coastal Wetland. Page Estuarine Research Federation Estuaries.

Golden, Z., and B. F. Froeschke. 2023. Comparison of Ecological Niches Between Two Important Recreational and Commercial Fisheries. PhD Dissertation Honors Program, The University of Tampa.

Govonil, J. J., P. B. Ortner, F. Al-yamani, and L. C. Hill. 1986. Selective feeding of spot , Leiostomus xanthurus , and Atlantic croaker , Micropogonias undulatus , larvae in the northern Gulf of Mexico 28:175–183.

Greenwood, M. F. D., R. E. Matheson, R. H. McMichael, and T. C. MacDonald. 2007. Community structure of shoreline nekton in the estuarine portion of the Alafia River, Florida: Differences along a salinity gradient and inflow-related changes. Estuarine, Coastal and Shelf Science 74:223–238.

Gunter, G. 1956. A Revised List of Euryhaline Fishes of North and Middle America. Source: The American Midland Naturalist 56:345–354.

Gutierrez, E. M., J. D. Plumlee, D. G. Bolser, B. E. Erisman, and R. J. D. Wells. 2023. Regional Variation in Feeding Patterns of Sheepshead (Archosargus probatocephalus) in the Northwest Gulf of Mexico. Fishes 8.

Hall, L. H. Jr., S. J. Bushong, S. A. Fischer, and J. A. Sullivan. 1989. A synthesis of water quality and contaminants data for the Spot, Leiostomus xanthurus. Shady Side, Maryland.

Hallac, D., J. Kline, J. Sadle, S. Bass, T. Ziegler, and S. Snow. 2010. Preliminary effects of the January 2010 cold weather on flora and fauna in Everglades National Park.

Hare, J. A., M. J. Wuenschel, and M. E. Kimball. 2012. Projecting Range Limits with Coupled Thermal Tolerance - Climate Change Models: An Example Based on Gray Snapper (Lutjanus griseus) along the U.S. East Coast. PLoS ONE 7.

Hartwell, S. I., and D. E. Hoss. 1979. Thermal Shock Resistance of Spot (Leiostomus xanthurus) after Acclimation to Constant or Cycling Temperature. Transactions of the American Fisheries Society 108:397–400.

Helfman, G. S., B. B. Collette, and D. E. Facey. 1997. The Diversity of Fishes. 1st edition. Wiley-Blackwell.

Henry, W. 1803. Experiments on the quantity of gases absorbed by water, at different temperatures, and under different pressures. Philosophical Transactions of the Royal Society of London 93:29–43.

Hodson, R. G., R. G. Fechhelm, and R. J. Monroe. 1961. Upper Temperature Tolerance of Spot, Leiostomus xanthurus, from the Cape Fear River Estuary, North Carolina. Estuaries 4:345–356.

Hotos, G. N., and N. Vlahos. 1998. Salinity tolerance of Mugil cephalus and Chelon labrosus Pisces: Mugilidae fry in experimental conditions. Aquaculture 167:329–338.

Houde, E. D. 1977. Abundance and potential yield of the Atlantic Thread Herring, Opisthonema oglinum, and aspects of its early life history in the Eastern Gulf of Mexico. Fishery Bulletin 75:493–512.

IPCC. 2012. Managing the risks of extreme events and disasters to advance climate change adaptation: special report of the intergovernmental panel on climate change. Page (C. B. Field, V. Barros, T. F. Stocker, D. Qin, D. J. Dokken, K. L. Ebi, M. D. Mastrandrea, K. J. Mach, G. K. Plattner, S. K. Allen, M. Tignor, and P. M. Midgley, Eds.). Cambridge University Press, Cambridge, UK & New York, NY, USA.

IPCC. 2018. Special Report on Global Warming of 1.5oC.

Johnson, D. R., N. A. Funicelli, and J. A. Bohnsack. 1999. Effectiveness of an Existing Estuarine No-Take Fish Sanctuary within the Kennedy Space Center, Florida. North American Journal of Fisheries Management 19:436–453.

Johnson, J. C., S. Arnott, T. Advisor, B. Roumillat, D. Whitaker, J. Ballenger, C. Mcdonough, and A. T. Mccandless. 2013. QUANTIFICATION OF LIFE HISTORY PARAMETERS IN SOUTH CAROLINA SPOT (Leiostomus xanthurus) at THE GRADUATE SCHOOL OF THE COLLEGE OF CHARLESTON.

Johnson, K. B., R. G. Turingan, J. Eble, J. Shenker, and J. R. Blanchard. 2020. Restore Lagoon Inflow Research Project (Phase 1) Task 2, Biological Monitoring. Melbourne, FL.

Joseph, E. B. 1957. A study of the systematics and life history of the Gulf Pipefish, Syngnathus scovelli (Evermann and Kendall). Doctoral Dissertation, Florida State University.

Jung, S. ;, and E. D. Houde. 2004. Recruitment and spawning-stock biomass distribution of bay anchovy (Anchoa mitchilli) in Chesapeake Bay. Fishery Bulletin 102:63–77.

Kamerosky, A., H. J. Cho, and L. Morris. 2015. Monitoring of the 2011 super algal bloom in Indian River Lagoon, FL, USA, Using MERIS. Remote Sensing 7:1441–1460.

Khériji, S., M. El Cafsi, W. Masmoudi, J. D. Castell, and M. S. Romdhane. 2003. Salinity and temperature effects on the lipid composition of mullet sea fry (Mugil cephalus, Linne, 1758) *. Aquaculture international 11:571–582.

Kilma, E. F., and D. C. Tabb. 1959. A contribution to the Biology of the Spotted Weakfish, Cynoscion nebulosus, (Cuvier) from northwest Florida, with a Description of the Fishery. Florida Board Conservation Marine Lab Tech. Ser. No. 30.

Kinnear, B. S., and C. M. Fuss Jr. 1971. Thread herring distribution off Florida's West Coast. Fisheries Review 33:27–39.

Krejci, S. E. 2012. HABITAT PREFERENCES AND THE EFFECTS OF SEAGRASS DENSITY ON POPULATION DEMOGRAPHICS AND FEEDING ECOLOGY OF PIPEFISH IN THE INDIAN RIVER LAGOON, FL. Dissertation, Florida Institute of Technology , Melbourne, Fl.

Kucera, C. J., C. K. Faulk, and G. J. Holt. 2002. The effect of parental acclimation to spawning salinity on the survival of larval Cynoscion nebulosus. Journal of Fish Biology 61:726–738.

Kuiter, R. H. 2003. American Gulf Pipefish Sygnathus scovelli. Pages 196–196 Seahorses, Pipefishes and their relatives, a comprehensive guide to Syngnathiformes. Revised Edition.

Kültz, D. 2015, June 1. Physiological mechanisms used by fish to cope with salinity stress. Company of Biologists Ltd.

Langston, J. N., P. J. Schofield, J. E. Hill, and W. F. Loftus. 2010. Salinity Tolerance of the African Jewelfish Hemichromis letourneuxi, a Non-native Cichlid in South Florida (USA). Copeia 3:475–480.

Ley, J. A., C. C. Mcivor, and C. L. Montague. 1999. Fishes in Mangrove Prop-root Habitats of Northeastern Florida Bay: Distinct Assemblages across an Estuarine Gradient. Estuarine, Coastal and Shelf Science 48.

Marais, J. F. K. 1978. Routine Oxygen Consumption of Mugil cephalus, Liza dumerili and L. richardsoni at Different Temperatures and Salinities. Marine Biology 50:9–16.

Marcek, B. J., R. W. Brill, and M. C. Fabrizio. 2019. Metabolic scope and hypoxia tolerance of Atlantic croaker (Micropogonias undulatus Linnaeus, 1766) and spot (Leiostomus xanthurus Lacepède, 1802), with insights into the effects of acute temperature change. Journal of Experimental Marine Biology and Ecology 516:150–158.

Massie, J. A., B. A. Strickland, R. O. Santos, J. Hernandez, N. Viadero, R. E. Boucek, H. Willoughby, M. R. Heithaus, and J. S. Rehage. 2020. Going Downriver: Patterns and Cues in Hurricane-Driven Movements of Common Snook in a Subtropical Coastal River. Estuaries and Coasts 43:1158–1173.

Matheson, R. E., and J. D. Mceachran. 1984. Taxonomic Studies of the Eucinostomus argenteus Complex (Pisces: Gerreidae): Preliminary Studies of External Morphology. Copeia 18:893–902.

McGuire, A., N. Aluru, A. Takemura, R. Weil, J. M. Wilson, and M. M. Vijayan. 2010. Hyperosmotic shock adaptation by cortisol involves upregulation of branchial osmotic stress transcription factor 1 gene expression in Mozambique Tilapia. General and Comparative Endocrinology 165:321–329.

Mcneese, H. C. 2021, May. COMPARISON OF ENDOHELMINTH PARASITES IN BLACK DRUM (POGONIAS CROMIS) AND RED DRUM (SCIAENOPS OCELLATUS) FROM THE SABINE LAKE ESTUARY. Master of Science Thesis, Sam Houston State University.

Merino Contreras, M. de la L. 2018. Aclimatación en cautiverio del sargo Archosargus probatocephalus (Perciformes: Sparidae). Ecosistemas y Recursos Agropecuarios 5:511–521.

Moody, W. D. 1950. A STUDY OF THE NATURAL HISTORY OF THE SPOTTED TROUT CYNOSCION NEBULOSUS, IN THE CEDAR KEY, FLORIDA, AREA. Quarterly Journal of the Florida Academy of Sciences 12:147–171.

Morris, L. J., L. M. Hall, C. A. Jacoby, R. H. Chamberlain, M. D. Hanisak, J. D. Miller, and R. W. Virnstein. 2022. Seagrass in a Changing Estuary, the Indian River Lagoon, Florida, United States. Frontiers in Marine Science 8.

Morris, L. J., L. M. Hall, J. D. Miller, M. A. Lasi, R. H. Chamberlain, R. W. Virnstein, and C. A. Jacoby. 2021. Diversity and distribution of seagrasses as related to salinity, temperature, and availability of light in the Indian River Lagoon, Florida. Source: Florida Scientist 84:119–137.

Morris, L. J., and R. W. Virnstein. 2004. The Demise and Recovery of Seagrass in the Northern Indian River Lagoon, Florida. Page Estuarine Research Federation Estuaries.

Moser, M. L., and L. R. Gerry. 1989. Differential Effects of Salinity Changes on Two Estuarine Fishes, Leiostomus xanthurus and Micropogonias undulatus.

Moser, M. L., and J. M. Miller. 1994. Effects of salinity fluctuation on routine metabolism of juvenile spot, Leiostomus xanthurus. Journal of Fish Biology 45:335–340.

Moulton, D. L., M. A. Dance, J. A. Williams, M. Z. Sluis, G. W. Stunz, and J. R. Rooker. 2017. Habitat Partitioning and Seasonal Movement of Red Drum and Spotted Seatrout. Estuaries and Coasts 40:905–916.

Murphy, M., and R. Taylor. 1989. Reproduction and growth of black drum Pogonias cromis in northeast Florida.

NOAA. 2023, July 14. The ongoing marine heat waves in U.S. waters, explained. https://www.noaa.gov/news/ongoing-marine-heat-waves-in-us-waters-explained.

Nordlie, F. G. 1976. Influence of environmental temperature on plasma ionic and osmotic concentrations in Mugil cephalus Lin. Comparative Biochemistry and Physiology Part A: Physiology 55:379–381.

Ogawa, M., M. W. Moody, R. J. Portier, J. Bell, M. A. Schexnayder, and J. N. Losso. 2003. Biochemical Properties of Black Drum and Sheepshead Seabream Skin Collagen. Journal of Agricultural and Food Chemistry 51:8088–8092.

Olsen, Z. T. 2014. Potential impacts of extreme salinity and surface temperature events on population dynamics of black drum, pogonias cromis, in the upper Laguna Madre, Texas. Gulf of Mexico Science 32:60–68.

Paperno, R., and R. B. Brodie. 2004. Effects of environmental variables upon the spatial and temporal structure of a fish community in a small, freshwater tributary of the Indian River Lagoon, Florida. Estuarine, Coastal and Shelf Science 61:229–241.

Partridge, C., J. Shardo, and A. Boettcher. 2007. Osmoregulatory role of the brood pouch in the euryhaline Gulf pipefish, Syngnathus scovelli. Comparative Biochemistry and Physiology - A Molecular and Integrative Physiology 147:556–561.

Patetta, N. 2022, April 27. Linking thermal tolerances to estuarine residency of NC fish species. Senior Honors Thesis, The University of North Carolina, Chapel Hill.

Potthoff, M. T., and D. M. Allen. 2003. Site fidelity, home range, and tidal migrations of juvenile pinfish, Lagodon rhomboides, in salt marsh creeks. Environmental Biology of Fishes 67:231–240.

Poulakis, G. R., D. A. Blewett, and M. E. Mitchell. 2003. The effects of season and proximity to fringing mangroves on seagrass-associated fish communities in Charlotte Harbor, Florida. Gulf of Mexico Science 21:171–184.

Powell, A. B. ;, M. W. ; Lacroix, and R. T. Cheshire. 2002. An evaluation of Northern Florida Bay as a nursery area for red drum, Sciaenops ocellatus, and other juvenile and small resident fishes. Item Type monograph.

Provancha, M. J., P. A. Schmalzer, and C. R. Hall. 1986. EFFECTS OF THE DECEMBER 1983 AND JANUARY 1985 FREEZING AIR TEMPERATURES ON SELECT AQUATIC POIKILOTHERMS AND PLANT SPECIES OF MERRITT ISLAND, FLORIDA. Source: Florida Scientist 49:199–212.

R Core Team. 2020. The R Stats Package. R Core Team.

Rehage, J. S., and J. R. Blanchard. 2016. What Can We Expect from Climate Change for Species Invasions? Fisheries 41:405–407.

Rehage, J. S., J. R. Blanchard, R. E. Boucek, J. J. Lorenz, and M. Robinson. 2016. Knocking back invasions: variable resistance and resilience to multiple cold spells in native vs nonnative fishes. Ecosphere 7:1–13.

Reyier, E. A., R. H. Lowers, D. M. Scheidt, and D. H. Adams. 2011. Movement patterns of adult red drum, Sciaenops ocellatus, in shallow Florida lagoons as inferred through autonomous acoustic telemetry. Environmental Biology of Fishes 90:343–360.

Reyier, E. A., D. M. Scheidt, E. D. Stolen, R. H. Lowers, K. G. Holloway-Adkins, and B. J. Ahr. 2020. Residency and dispersal of three sportfish species from a coastal marine reserve: Insights from a regional-scale acoustic telemetry network. Global Ecology and Conservation 23:e01057.

Richards, C. E. 1973. Age, Growth and Distribution of the Black Drum (Pogonias cromis) in Virginia. Transactions of the American Fisheries Society 102:584–590.

Richards, W. J., R. V. Miller, and E. D. Houde. 1974. Egg and larval development of the Atlantic Thread Herring, Opishtonem oglinum. Fishery bulletin 72:1123–1136.

Richards, W. J., and B. J. Palko. 1969. Methods Used to Rear the Thread Herring, *Opisthonema oglinum*, from Fertilized Eggs. Transactions of the American Fisheries Society 98:527–529.

Riggs, A. F. 1988. The Bohr Effect. Ann. Rev. Physiol 50:181–204.

Rutherford, E. S., J. T. Tilmant, E. B. Thue, and T. W. Schmidt. 1989. FISHERY HARVEST AND POPULATION DYNAMICS OF SPOTTED SEATROUT , CYNOSCION NEBULOSUS , IN FLORIDA BAY AND ADJACENT WATERS. Bulletin of Marine Science 44:108–125.

Saad, A. M., A. C. Beaumord, and E. P. Caramaschi. 2002. Effects of artificial canal openings on fish community structure of Imboassica Coastal Lagoon, Rio deJaneiro, Brazil. Journal of Coastal Research SI 36:634–639.

Santos, R. O., D. Lirman, S. J. Pittman, and J. E. Serafy. 2018. Spatial patterns of seagrasses and salinity regimes interact to structure marine faunal assemblages in a subtropical bay. Marine Ecology Progress Series 594:21–38.

Santos, R. O., J. S. Rehage, R. Boucek, and J. Osborne. 2016. Shift in recreational fishing catches as a function of an extreme cold event. Ecosphere 7:1–16.

Saucier, M. H., and D. M. Baltz. 1993. Spawning site selection by spotted seatrout, *Cynoscion nebulosus*, and black drum, *Pogonias cromis*, in Louisiana. Environmental Biology of Fishes 36:257–272.

Schofield, P. J., and D. H. Huge. 2008. Low-temperature tolerance of two non-native fishes (*Hoplosternum littorale* [Hancock 1828], *Cichlasoma bimaculatum* [Linnaeus 1758]) established in Florida. Florida Scientist 74:73–83.

Schofield, P. J., and J. L. Kline. 2018. Lower Lethal Temperatures for Nonnative Freshwater Fishes in Everglades National Park, Florida. North American Journal of Fisheries Management.

Schofield, P. J., W. F. Loftus, and M. E. Brown. 2007. Hypoxia tolerance of two centrarchid sunfishes and an introduced cichlid from karstic Everglades wetlands of southern Florida, U.S.A. Journal of Fish Biology 71:87–99.

Schofield, P. J., W. F. Loftus, R. M. Kobza, M. I. Cook, and D. H. Slone. 2010. Tolerance of nonindigenous cichlid fishes (*Cichlasoma urophthalmus*, *Hemichromis letourneuxi*) to low temperature: laboratory and field experiments in south Florida. Biological Invasions 12:2441–2457.

Serrano, X., M. Grosell, and J. E. Serafy. 2010. Salinity selection and preference of the grey snapper *Lutjanus griseus*: Field and laboratory observations. Journal of Fish Biology 76:1592–1608.

Serrano, X. M. 2008, August. Ecophysiology of the Gray Snapper (*Lutjanus griseus*): Salinity Effects on Abundance, Physiology and Behavior. Master of Science Thesis, University of Miami, Coral Gables, FL.

Serrano, X., J. Serafy, and M. Grosell. 2011. Osmoregulatory capabilities of the gray snapper, Lutjanus griseus: Salinity challenges and field observations. Marine and Freshwater Behaviour and Physiology 44:185–196.

Shervette, V. R., N. Ibarra, and F. Gelwick. 2007. Influences of salinity on growth and survival of juvenile pinfish Lagodon rhomboides (Linnaeus). Environmental Biology of Fishes 78:125–134.

Silverman, M. J. 1979. Biological and Fisheries Data on black drum, Pogonias cromis (Linnaeus).

Smith, J. W. 1994. Biology and Fishery for Atlantic Thread Herring, Opisthonema oglinum, along the North Carolina Coast. Marine Fisheries Review 56:1–7.

Sogard', S. M., G. V. N. Powell, and J. G. Holmquist. 1989. Utilization by fishes of shallow, seagrass-covered banks in Florida Bay: 1. Species composition and spatial heterogeneity. Environmental Biology of Fishes 24:53–65.

Song, J., R. W. Brill, and J. R. McDowell. 2019. Plasticity in standard and maximum aerobic metabolic rates in two populations of an estuarine dependent teleost, spotted seatrout (Cynoscion nebulosus). Biology 8.

Song, J., and J. R. McDowell. 2021. Comparative transcriptomics of spotted seatrout (Cynoscion nebulosus) populations to cold and heat stress. Ecology and Evolution 11:1352–1367.

Stevens, P. W., M. F. D. Greenwood, and D. A. Blewett. 2013. Fish Assemblages in the Oligohaline Stretch of a Southwest Florida River during Periods of Extreme Freshwater Inflow Variation. Transactions of the American Fisheries Society 142:1644–1658.

Stillman, D. 2023, July 10. Florida ocean temperatures at "downright shocking" levels. The Washington Post.

Tolley, G. S., A. K. Volety, and M. Savarese. 2005. Influence of salinity on the habitat use of oyster reefs in three Southwest Florida estuaries. Journal of Shellfish Research 24:127–137.

Tremain, D. M., C. W. Harnden, and D. H. Adams. 2004. Multidirectional movements of sportfish species between an estuarine no-take zone and surrounding waters of the Indian River Lagoon, Florida. Fishery Bulletin 102:533–544.

Tucker, J. W., and P. A. Barbera. 1987. Laboratory Spawning of Sheepshead. The Progressive Fish-Culturist 49:229–230.

Vega-Cendejas, M. E., G. Mexicano-Cintora, and A. M. Arce. 1997a. Biology of the thread herring Opisthonema oglinum (Pisces: Clupeidae) from a beach seine fishery of the Campeche Bank, Mexico. Fisheries Research 30:117–126.

Vega-Cendejas, M. E., G. Mexicano-Cintora, and A. M. Arce. 1997b. Biology of the thread herring Opisthonema oglinum (Pisces: Clupeidae) from a beach seine fishery of the Campeche Bank, Mexico. Fisheries Research 30:117–126.

Ward, R., I. R. Blandon, T. L. King, and T. L. Beitinger. 1993. Comparisons of Critical Thermal Maxima and Minima of Juvenile Red Drum (Sciaenops ocellatus) from Texas and North Carolina. Northeast Gulf Science 13.

Weinstein, M. P., and M. P. Walters. 1981. Growth, Survival and Production in Young-of-Year Populations of Leiostomus xanthurus Lacepede Residing in Tidal Creeks. Estuaries 4:185–197.

White, J. C. JR., and J. W. Angelovic. 1973. Interactions of chromic gamma radiation, salinity, and temperature on the morphology of post-larval Pinfish, Lagodon rhomboides. Pages 199–217 Proceedings of A Workshop on Egg, Larval, and Juvenile Stages of Fish In Atlantic Coast Estuaries.

Whitfield, A. K., J. Panfili, and J. D. Durand. 2012. A global review of the cosmopolitan flathead mullet Mugil cephalus Linnaeus 1758 (Teleostei: Mugilidae), with emphasis on the biology, genetics, ecology and fisheries aspects of this apparent species complex. Reviews in Fish Biology and Fisheries 22:641–681.

Wise, D. J., and J. R. Tomasso. 1989. Acute Toxicity of Nitrite to Red Drum Sciaenops ocellatus: Effect of Salinity. Journal of the World Aquaculture Society 20:193–198.

Wuenschel, M. J., J. A. Hare, M. E. Kimball, and K. W. Able. 2012. Evaluating juvenile thermal tolerance as a constraint on adult range of gray snapper (Lutjanus griseus): A combined laboratory, field and modeling approach. Journal of Experimental Marine Biology and Ecology 436–437:19–27.

Wuenschel, M. J., A. R. Jugovich, and J. A. Hare. 2004. Effect of temperature and salinity on the energetics of juvenile gray snapper (Lutjanus griseus): Implications for nursery habitat value. Journal of Experimental Marine Biology and Ecology 312:333–347.

Zastrow, C. E., E. D. Houde, and L. G. Morin. 1991. Spawning, fecundity, hatch-date frequency and young-of-the-year growth of bay anchovy Anchoa mitchilli in mid-Chesapeake Bay. Page Source: Marine Ecology Progress Series.

Appendix H   Task 4 – HSWRI Biology Report

Restore Lagoon Inflow Research (Phase 3) Final Report Hubbs-SeaWorld Research Institute

Assessing nutritional condition in common bottlenose dolphins (*Tursiops truncatus truncatus*) inhabiting the northern Indian River Lagoon

PREPARED FOR

Florida Institute of Technology
150 West University Boulevard
Melbourne, FL 32091

PREPARED BY

Wendy Noke Durden
4020 S. Hwy A1A
Melbourne Beach, FL

July 2023

Acknowledgements

We are grateful for the volunteers and interns who contributed to data collection and management. This study would not have been possible without their perseverance, talent, and dedication. We would also like to thank staff from 321-Boats for their assistance.

Project Staffing (includes part-time and full-time project staff)

Non-faculty – Wendy Noke Durden, Teresa Jablonski, Agatha Fabry

Volunteers – Solaris Coton, Becky Nichols, Arianna Petrovia, Missa Kes, Nichole Nebel, Alina Rodriguez, Margarita Morales, Jessica Provenzano, Victoria Shalaby

Highlights

- Five vessel-based dolphin surveys were conducted in the Northern Indian River Lagoon (Banana River and northern Indian River) in the summer of 2023 to assess the nutritional condition of the dolphin community inhabiting the area.

- 77 groups (sightings) were encountered, and 233 distinct dolphins were identified.

- 22,498 images were reviewed to assess nutritional condition. Body index was assessed for 155 marked adult dolphins.

- 93% of dolphins presented in a compromised nutritional condition (68%-underweight, 25%-emaciated).

- Compared to prior evaluations (2013, 2016) the dolphin community appears to be increasingly nutritionally stressed, although the influence of variance between surveys should be considered.

Table of Contents

List of Figures

List of Tables

List of Acronyms

CBD	Could not be determined
IRL	Indian River Lagoon
HSWRI	Hubbs Sea World Research Institute
UME	Unusual Mortality Event

1 Introduction

Evaluating the nutritional condition of free-swimming dolphins can provide valuable information regarding the health of the individuals as well as the population as a whole (Hart et al. 2013; Joblon et al. 2014). Assessing the health of bottlenose dolphins inhabiting the Indian River Lagoon (IRL) is particularly important as this dolphin stock has been described as an immune compromised population (Bossart et al. 2007) and has been subjected to four Unusual Mortalities Events (UMEs) (2001, 2008, 2013) including a morbillivirus epidemic (2013-2015) (NOAA 2015).

In light of these reoccurring events, establishing baseline information on nutritional condition for the IRL dolphin population is critical to interpreting significant changes during subsequent UMEs. Furthermore, as efforts are made to improve water quality within the region, it will be imperative to have an accurate understanding of dolphin health before and after extensive restorative efforts are employed. The evaluation of lateral photographs of free-swimming bottlenose dolphins can provide consistent data on nutritional condition between seasons or even between years. Previous evaluation of IRL dolphin nutritional condition (2016) indicated that the majority of dolphins in this region (75%) are not in adequate nutritional condition (59% underweight; 16% emaciated). The intent of this study was to collect and utilize images of bottlenose dolphins to evaluate nutritional condition and other indicators of dolphin health (epidermal lesions) for animals inhabiting the northern IRL (northern Indian River and Banana River).

Figure 2. The Indian River Lagoon study area. Dolphin surveys were conducted in the Northern Indian River (N of Eau Gallie Causeway) and Banana River (excluding the restricted area within the dashed ellipse).

Bottlenose dolphin survey efforts

The IRL has historically been divided into six segments based on hydrodynamics and geographic features for purposes of characterization and management (U.S. EPA, 1996). Photo-identification efforts for this study focused on the northern portions of the IRL. Sub-basins included the northern Indian River (north of Eau Gallie Causeway) and Banana River, excluding the restricted areas (Figure 1), as this dolphin community is known to utilize both basins. The nutritional condition of dolphins in this area is of particular interest as they have been heavily impacted in prior UMEs (2001, 2008, 2013; 2013-2015). Likewise, this area has low water exchange rates and long residence periods (Smith 1993) resulting in nutrient accumulation (Lapointe et al. 2020), phytoplankton blooms (Phlips et al. 2021), and sea grass depletion (Morris et al. 2022). Since seagrass provides critical habitat for prey consumed by estuarine dolphins (Barros and Wells 1998), significant changes to the ecosystem could further jeopardize IRL dolphin health. As an apex predator, the health of IRL dolphins may also reflect the health of the IRL ecosystem. Significant restoration and mitigation efforts are underway to improve IRL ecosystem health. Vessel-based capture-recapture surveys were conducted in the study area between 19 June 2023

and 27 June 2023. Replicates of each sub-basin were conducted within seven days to allow population mixing. Each survey (complete replicate) was completed in one day under optimal conditions with a Beaufort Sea State $\leq$3 (conditions = glassy to crests of some large wavelets breaking). Vessels were staffed with a minimum of three researchers to search along predetermined track lines. To minimize capture heterogeneity, the survey design utilized both depth contour lines and alternating saw-tooth transects (Durden et al. 2021). Dorsal fins of all dolphins within each group were photographed using a Canon EOS digital camera with a 100-400 millimeter telephoto lens. A group was defined as all dolphins within 100 meters with the same general heading and behavior (Wells and Scott 1987). Calves were defined as swimming in adult echelon and <75% of the size of the adult. Animals not identified as calves were considered "adults."

Photographic Analyses and Body Condition Scoring

Dorsal fin image analyses followed established protocols (Mazzoil et al. 2004) and were matched to an existing photo-identification catalog. Matches were accepted only if at least two experienced personnel agreed. To ensure that dolphins were not evaluated twice (unrecognized dolphins resighted), only animals with marked (identifiable) dorsal fins were included in analyses. Likewise, dorsal fins were compared between sub-basins within each complete replicate (northern Indian River, Banana River) to ensure that animals were only evaluated once. To avoid biasing data with age-related features that may resemble an underweight body condition, calves (including marked calves) were excluded from analyses. A standardized body condition index was utilized as in prior assessment of IRL dolphins (Fair et al. 2006, Table 1). All images of each individual (head, body and peduncle regions) were reviewed to facilitate body condition evaluation. The post-nuchal region is recognized as the key area that loses fat reserves in a nutritionally compromised dolphin and can reliably predict poor body condition (Gryzbek 2013). However, since movement can temporarily alter the degree of convexity or concavity of a dolphin's post-nuchal fat pad or cause the misleading appearance of fat rolls on the neck, only straight-line body position images were utilized for scoring. Photographic analyses of body condition of free-swimming dolphins can be subjective and extreme care was taken to be conservative when evaluating photographs. From our prior work, we found that assigning body condition based on one criterion (excluding the post-nuchal depression), may over-estimate the number of dolphins that are underweight. The epaxial musculature and transverse processes are often difficult to evaluate since the animal may be diving or otherwise contorted when exposing the transverse processes, and the epaxial musculature is often obscured by lighting and may appear slightly depressed in some photographs and flat in others. For these reasons, individuals were evaluated conservatively by utilizing the presence of two or more criteria with an emphasis on the post-nuchal criterion (only acceptable single criterion) to most accurately determine body condition.

Prototype images for ideal, underweight, and emaciated body conditions are presented (Figure 2). Based on these criteria, dolphin nutritional condition was binned into ideal, underweight, or emaciated categories and the percentage of each was further evaluated by sub-basin and age class (adult females with and without dependent calves). In circumstances where more than one indicator of body condition was not available, the body condition was scored as could not be determined (CBD). Consistent scoring was conducted to enable comparisons with prior evaluations (2008, 2013, 2016).

Table 5. Body condition index score based on weight loss observable from photographs of dolphins.

Body Condition Score		1	2	3	4	5
Body Area	**Description**	**Emaciated**	**Underweight**	**Ideal**	**Overweight**	**Obese**
Head	Nuchal crest	depressed	slightly depressed	flat	slight mid-dorsal indentation	mid-dorsal indentation
Head	Cervical region (lateral)	concave	mild concavity	flat	broad	broad
Head	Prominent facial bones	exposed	slightly exposed	not observed	not observed	not observed
Head	Ear os	exposed	no dimpling	slight dimpling	dimpled	significantly dimpled
Head	Chin skin folds	not present	not present	not present	present	present
Body	Epaxial muscle definition	concave	slightly concave	flat	convex	convex
Body	Dorsal ridge of scapula	exposed	slightly exposed	not observed	not observed	not observed
Body	Ribs	exposed	slightly exposed	not observed	not observed	not observed
Tail	Transverse processes	exposed	slightly exposed	not observed	not observed	not observed

Bi-lateral striping was a previously undefined abnormality that has only been documented in the northern and central portion of the Indian River Lagoon (Titcomb et al. 2020). Since the anomaly may be related to significant weight gain/loss (like stretch marks in humans) (Titcomb et al. 2020), we thoroughly evaluated each individual for presence of striping and examined the influence of sub-basin and age class (adults with and without dependent calves).

Epidermal conditions and anomalies

Epidermal lesions may serve as indicators of cetacean population health and can signify a compromised environment (Van Bressem et al. 2009; Reif et al. 2009; Sanino et al. 2014). The presence and prevalence of epidermal conditions (lesions/anomalies) can provide useful baseline information. Images were thoroughly evaluated for the presence of epidermal disease/anomalies (adjusting contrast/exposure where necessary). If images were not of sufficient quality (poor contrast, lacking excellent focus) or sufficient portions of the animal's body were not exposed during the sighting, epidermal lesions were scored as CBD. When epidermal conditions were detected, cases were further grouped based on previously published literature (Harzen and Brunnick 1997; Bertulli et al. 2012; Sanino et al. 2014; Vilela et al. 2016; Herr et al. 2020) or, in correspondence with prior Hubbs Sea World Research Institute (HSWRI) stranding histological evidence (HSWRI unpublished data). Groupings included: 1) pox-like lesions, 2) paracoccidioidomycosis, 3) ulcerated lesions, 4) raised cutaneous lumps, 5) suspected algal sheen, and 6) other unspecified lesions without classification (Figure 3).

1.1 Results

Field Effort

Between 19 June and 27 June 2023, five vessel-based surveys were conducted over three days to enable two replicate surveys of the northern Indian River and Banana River (40 h). A total of 77 dolphin groups (sightings) were encountered, containing 393 individuals. A total of 194 dolphins were sighted in the Banana River (97 ± 26.70 per survey) and 199 dolphins in the northern Indian River (99.5 ± 0.71 per survey). Average group size was 5.17 ± 5.57. Photographs were sorted by standardized methods, matched to an existing catalog, and evaluated for nutritional condition. A total of 233 identifiable dolphins were identified.

Evaluation of nutritional condition

Available images were reviewed for each individual to further evaluate nutritional condition (total of 22,498 images). Calves, unmarked individuals, and those for which images did not enable thorough evaluation (post-nuchal or > 2 criteria) were excluded. A total of 155 marked dolphins (80%) were evaluated for nutritional condition (88 northern Indian River, 67 Banana River), while 39 marked adults were excluded as images were insufficient to accurately determine body condition (20%).

Most animals (68%) presented in underweight nutritional condition (106/155), 25% were emaciated (38/155), and only 7% of adult animals sighted were in ideal body condition (11/155) (Table 2). Body condition exhibited little variation by sub-basin (Table 2). Females with dependent calves presented in emaciated nutritional condition (13/35; 37.14%) more frequently than other marked adults (25/120, 20.83%) and were less likely to be in ideal condition (2.86%) compared to their adult counterparts (8.33 %) (Table 3). Adults without dependent calves presented more commonly in underweight or in ideal nutritional condition, compared to adults with calves (Table 3).

Lateral striping presence

We found evidence of lateral striping in 15.5 % of the animals evaluated (24/155). The presence of lateral striping was more prevalent in the northern Indian River (18/91; 19.78%) compared to the Banana River (8/77; 10.39%). Lateral striping was slightly more common in adult females with dependent calves (20%; 7/35) than adults not accompanied by dependent calves (15%; 17/120).

Epidermal conditions

A total of 227 identifiable individuals were evaluated for epidermal conditions. For 68.8% of individuals, photographs enabled a thorough assessment (*n*=154). Epidermal conditions (disease/anomalies) were present in all evaluated cases. For 40.26% of these animals, more than one epidermal condition was present. Pox-like lesions and suspected algal sheens were present in 66.23% of evaluated individuals (Table 4). Other skin conditions were underrepresented in the population (Table 4).

1.2 Conclusion

We found the overwhelming majority of IRL dolphins presented in decreased nutritional condition (underweight or emaciated). Prior evaluation of IRL dolphin nutritional condition has shown variance in the number of animals presenting in ideal (2008: 15%; 2013: 31%; 2016: 24%),

underweight (2008: 50%; 2013: 64%; 2016: 59%) and emaciated (2008: 35%; 2013: 5%; 2016: 15%) nutritional condition (Table 5). Our results (ideal: 7%, underweight: 68%, emaciated: 25%) were comparable to prior studies. However, the percentage of animals presenting in less-than-ideal condition (93%), was staggering and unprecedented. It is important to recognize the factors that may have influenced this variation. Assessments in 2008 and 2013 were conducted during UME years, with 2008 data collected just prior to the UME, and 2013 data collected towards the end of the UME. During these years, the surge of mortalities may have influenced the percent of emaciated animals remaining in the population. Data from 2016 most closely matched the current data set (non-UME data collection year), however data were collected year-round and a mean for all seasons presented. Isolating nutritional condition in summer 2016 revealed 87% of the animals were in non-ideal body condition (25% emaciated, 62% underweight, 13% ideal) (Durden et al. unpublished data), more closely aligning with our results. Nevertheless, our findings clearly indicate that dolphins inhabiting the northern Indian River Lagoon present in a compromised nutritional state.

Female dolphins with dependent calves were more commonly found in poor body condition (emaciated) than adult animals without calves. This finding is similar to other studies which have found cetaceans with dependent calves present in decreased body condition compared to cohorts without dependent calves (Bradford et al. 2012; Pettis et al. 2004). Underweight female nutritional condition may be attributed to spring-summer parturition, as bimodal IRL calving peaks have been reported (Urian et al., 1996; Stolen, 1998; Howells et al., 2008). Seasonality may also play a role in nutritional condition. Blubber thickness evaluation in stranded IRL dolphins has found decreased thickness in summer months (Durden et al. unpublished data). Similarly, blubber thickness in Sarasota Bay dolphins is reported to decrease by about 39% from the winter to the summer (Meagher et al. 2009). Therefore, it is feasible that seasonal decreases in blubber may contribute to the appearance of the post-nuchal depression and prominence of the skeletal structure in IRL dolphins.

The prevalence of dolphins that are in poor nutritional condition and the infrequent observation of dolphins in adequate nutritional condition within the IRL is concerning. Baseline data from other regions are needed to assess nutritional condition in other dolphin populations to ascertain if our results are endemic to the immune compromised dolphin population (Bossart 2007) inhabiting this compromised ecosystem. While we took extreme care to conservatively evaluate each individual and utilized multiple criteria, it is important to note that evaluations can be influenced by glare, lighting, image angle, and body contortions. Since dolphins inhabiting the lagoon are clearly nutritionally compromised, future studies should take advantage of emerging technologies (Unmanned Aircraft Systems imaging) that can incorporate photogrammetry to enhance our ability to evaluate health and body condition (Christie et al. 2022, Durban et al. 2021, Cheney et al. 2022).

Epidermal conditions were extremely common in IRL dolphins, with the most common finding being pox-like lesions and suspected algal sheens. While conducting survey efforts, we observed dolphins swimming through several phytoplankton blooms. In a prior survey (2016), we found that 33.85% of individuals presented a suspected algae sheen. The drastic increase during the current survey (66.23%) may have been associated with active blooms. HSWRI is actively working with a collaborator to culture and isolate similar specimens from stranded IRL dolphins to enable species identification. Histological findings to date indicate that the suspected algae can penetrate the epidermis (HSWRI unpublished data). While direct comparisons of the prevalence of epidermal conditions in other cetacean populations is difficult due to differences in categorization, other regions have also reported high rates of cetacean skin disorders (85-81% respectively; Harzen and Brunnick 1997; Sanino et al. 2014). IRL dolphin findings were also comparable to

several sites along the northwestern Atlantic where one third of dolphins presented with more than one lesion type (Hart et al. 2012). Future studies should evaluate not only the prevalence in individuals, but the severity (a few focal lesions vs. diffuse lesion presence). Diffuse lesions coupled with emaciation may indicate significant underlying health issues and could be a prelude to mortality.

The presence of lateral striping in these animals appears to be confined to the IRL as it has not been documented in other regions. Furthermore, it is interesting that lateral striping predominantly occurs in dolphins inhabiting the northern portions of the lagoon (UME area) and is only very rarely documented in the southern regions (1.2% of cases; Titcomb et al. 2020). We found lateral striping was slightly more prevalent in females with dependent calves, corresponding with prior study results that found this condition predominantly in reproductive females (Titcomb et al. 2020). As lateral striping occurs predominantly in the portion of the lagoon with declining water quality and is hypothesized to be related to sudden weight loss (Titcomb et al. 2020), it could serve as an indicator of declining health in future studies.

As a largely enclosed micro-tidal estuary, the IRL is susceptible to terrestrial pollutants (Smith 1993, 2001). In recent years, the lagoon has undergone several large-scale ecosystem changes including catastrophic seagrass loss associated with declining water quality and nutrient accumulation (Sigua et al. 2000; Morris et al. 2022). Since seagrass provides critical habitat for prey consumed by estuarine dolphins (Barros and Wells 1998), significant changes to the ecosystem could further jeopardize the health of the vulnerable IRL dolphin population. As large apex predators, IRL dolphin health may reflect the health of the IRL ecosystem as a whole. Ultimately, we found that the vast majority of IRL dolphins present in decreased nutritional condition with epidermal lesions. Significant restoration efforts are underway to improve IRL ecosystem health. These data will serve as baseline data to evaluate if future mitigation efforts result in improved health of dolphins residing in the northern IRL.

Figure 3. Body condition prototypes: A. ideal, B. underweight, C. emaciated.

Figure 4. Epidermal conditions observed in Indian River Lagoon dolphins: (A) pox-like lesions (dashed oval), (B) suspected algal sheen (dashed ovals), (C) paracoccidioidomycosis (formerly lacaziosis) like lesions (dashed oval), D) ulcerated lesions (arrows indicate), (E) example of unspecified lesions without classification (dashed oval), (F) example of unspecified lesions without classification (dashed oval), (G) raised cutaneous lesions (dashed oval), and (H) lateral striping example (arrows indicate).

Table 6. Summary of the nutritional condition of IRL dolphins in the northern Indian River and Banana River during summer 2023 (evaluated by photographic images). The percentage of each nutritional condition type per sub-basin is presented.

Nutritional condition	northern Indian River	%	Banana River	%	Total	%
Ideal	7	7.95	4	5.97	11	7.10
Underweight	58	65.91	48	71.64	106	68.39
Emaciated	23	26.14	15	22.39	38	24.52
Total number evaluated	88		67		155	

Table 7. Summary of the nutritional condition of IRL dolphins in the northern Indian River and Banana River during summer 2023 (evaluated by photographic images). The percentage of each nutritional condition type per age class (adult with and without dependent calves) is presented.

Nutritional condition	Adult females with dependent calves	%	Adults without dependent calves	%	Total	%
Ideal	1	2.86	10	8.33	11	7.10
Underweight	21	60.00	85	70.83	106	68.39
Emaciated	13	37.14	25	20.83	38	24.52
Total number evaluated	35		120		155	

Table 8. Evaluation of the presence of epidermal conditions in dolphins inhabiting the northern Indian River Lagoon during summer 2023. Total evaluated is the number of cases where photographs allowed for a thorough evaluation. Conditions were grouped and the percentage of individuals that exhibited each condition in each sub-basin is presented.

Epidermal condition	Northern Indian River	%	Banana River	%	Total	%
Pox-like	58	70.73	44	61.11	102	66.23
Algal sheen	51	62.20	51	70.83	102	66.23
>1 epidermal condition	35	42.68	27	37.50	62	40.26
Paracoccidioidomycosis like	1	1.22	1	1.39	2	1.30
Ulcerated lesions	0	0.00	1	1.39	1	0.65
Raised cutaneous lumps	0	0.00	2	2.78	2	1.30
Other unspecified lesions	5	6.10	1	1.39	6	3.90
Total evaluated	82		72		154	

Table 9. Comparison of Indian River Lagoon dolphin nutritional condition. Evaluation years include UME years (2008 and 2013) and non-UME years (2016 and 2023).

Year of survey effort	% ideal	% underweight	% emaciated	Comments
2008	15	50	35	June 2008; *n* = 20 animals evaluated in the northern Indian River, and Banana River (Mazzoil et al. 2008)
2013	31	64	5	August-December 2013; *n* = 337 individuals evaluated in the northern Indian River and Banana River
2016	25	59	16	August 2016- May 2017; *n* = 340 individuals evaluated in the northern Indian River, Banana River and Mosquito Lagoon
2023	7	68	25	June 2023; *n* = 155 individuals evaluated in the northern Indian River and Banana River

2 References

Barros, N.B. and R.S. Wells. 1998. Prey and feeding patterns of resident bottlenose dolphins (Tursiops truncatus) in Sarasota Bay, Florida. *Journal of Mammalogy* 79:1045–1059.

Bechdel, S.E., M. Mazzoil, E. Murdoch, E.M. Howells, J.S. Reif, S.D. McCulloch et al. 2009. Prevalence and impacts of motorized vessels on bottlenose dolphins (*Tursiops truncatus*) in the Indian River Lagoon, Florida. *Aquatic Mammals*; 35(3): 367-37.

Bertulli, C.G., A. Cecchetti, M.F. Van Bressem, and K.V. Waerebeek. 2012. Skin disorders in common minke whales and white-beaked dolphins off Iceland, a photographic assessment. *Journal of Marine Animals and Their Ecology* 5(2): 29-40.

Bossart, G.D. 2007. Emerging diseases in marine mammals: from dolphins to manatees. *Microbe*, 2: 544-547. doi: 10.1128/microbe.2.544.1

Bradford, A.L., D.W. Weller, A.E. Punt, Y.V. Ivashchenko, A.M. Burdin, G.R. Vanblaricom, and R.L. Brownell, Jr. 2012. Leaner leviathans: body condition variation in a critically endangered whale population. *Journal of Mammalogy* 93:251-266.

Cheney, B.J., J. Dale, P.M. Thompson, and N.J. Quick. 2022. Spy in the sky: a method to identify pregnant small cetaceans. *Remote Sensing in Ecology and Conservation* 8: 492-505.

Christie, A.I., A.P. Colefax, and D. Cagnazzi. 2022. Feasibility of using small UAVs to derive morphometric measurements of Australian snubfin (*Orcaella heinsohni*) and humpback (*Sousa sahulensis*) dolphins. *Remote Sensing* 14: 21

Durban, J.W., H. Fearbch, A. Paredes, L.S. Hickmott, and D.J. Le Roi. 2021. Size and body condition of sympatric killer whale ecotypes around the Antarctic Peninsula. *Marine Progress Series* 677: 209-217.

Durden, W.N., M.K. Stolen, D.H. Adams, and E.D. Stolen. 2007. Mercury and selenium concentrations in stranded bottlenose dolphins from the Indian River Lagoon system, Florida. *Bulletin of Marine Science*; 81(1): 37-54.

Durden, W.N., J. St. Leger, M. Stolen, T. Mazza, and C. Londono. 2009. Lacaziosis in bottlenose dolphins (*Tursiops truncatus*) in the Indian River Lagoon, Florida, USA. *Journal of Wildlife Diseases*, 45: 849-856. doi: 10.7589/0090-3558-45.3.849.

Durden W.N., E. D. Stolen, T. Jablonski, L. Moreland, E. Howells, A. Sleeman, M. Denny, G. Biedenback, M. Mazzoil. 2021. Robust design capture-recapture analysis of abundance and demographic parameters of Indian River Lagoon common bottlenose dolphins (*Tursiops truncatus truncatus*). *PLoS One* 16: e0250657

Environmental Protection Agency (EPA). 1996. The Indian River Lagoon Comprehensive Conservation & Management Plan. www.onelagoon.org/wp-content/uploads/irl_1996_ccmp.pdf. Accessed August 2022.

Fair, P.A., J.D. Adams, E. Zolman, S.D. McCulloch, J.D. Goldstein, M.E. Murdoch, R. Varela, L. Hansen, F. Townsend, J. Kucklick, C. Bryan, S. Christopher, R. Pugh, and G.D. Bossart. 2006.

Protocols for Conducting Dolphin Capture-Release Health Assessment Studies. NOAA Technical Memorandum NOS NCCOS 49. 83 pp.

Gryzbek, M.K. 2013. A visual body condition index for bottlenose dolphins (*Tursiops truncatus*). Msc. Thesis. University of Florida.

Joblon, M.J., M.A. Pokras, B. Morse, C.T. Harry, K.S. Rose, S.M. Sharp, M.E. Niemeyer, K.M. Patchett, B. Sharp, and M. Moore. 2014. Body condition scoring system for delphinids based on short-beaked common dolphins (*Delphinus delphis*). *Journal of Marine Animals and their Ecology*. 7(2): 5-13.

Hart, L.B., D.S. Rotstein, R.S. Wells, J. Allen, A. Barleycorn, B. Balmer, S.M. Lane, T. Speakman, E.S. Zolman, M. Stolen, W. McFee, T.K. Goldstein, and L.H. Schwacke. 2012. Skin lesions on common bottlenose dolphins (*Tursiops truncatus*) from three sites in the northwest Atlantic, USA. *PlosOne*, 7(3): e33081.

Hart, L.B., R.S. Wells, and L.H. Schwacke. 2013. Reference ranges for body condition in wild bottlenose dolphins, *Tursiops truncatus*. *Aquatic Biology* 18(1): 63-68.

Harzen, S. and B.J. Brunnick. 1997. Skin disorders in bottlenose dolphins (*Tursiops truncatus*), resident in the Sado estuary, Portugal. Aquatic Mammals, 21 (1): 59-68.

Herr, H., P. Burkhardt-Holm, K. Heyer, U. Siebert, and J. Selling. 2020. Injuries, malformations, and epidermal conditions in cetaceans of the Strait of Gibraltar. *Aquatic Mammals*, 46(2): 215-235.

Howells, E., J.S. Reif, M. Mazzoil, M.E. Murdoch, S.E. Bechdel, S. Ziemann, et al. 2008. Using photo-analysis of dolphin mother-calf pairs to determine reproductive rates in the Indian River Lagoon, Florida. Florida Marine Mammal Health Conference III. Marineland, FL, April 22-25

Lapointe, B.E., L.W. Herren, R.A. Brewton, and P.K. Alderman. 2020. Nutrient over enrichment and light limitation of seagrass communities in the Indian River Lagoon, an urbanized subtropical estuary. *Science of the Total Environment* 699:134068.

Mazzoil, M., S.D. McCulloch, R.H. Defran, R. H., and E. Murdoch. 2004. Use of digital photography and analysis of dorsal fins for photo-identification of bottlenose dolphins. *Aquatic Mammals* 30:209-2019.

Mazzoil, M., J.S. Reif, P. Fair, and G.D. Bossart. 2008. 2008 Indian River Lagoon Unusual Mortality Event Report to the Working Group re: Dolphin Body Condition. Technical Report.

Meagher, E.M., W.A McLellan, A. J. Westgate, R.S. Wells, J.E. Blum, and D.A. Pabst. 2009. Seasonal patterns of heat loss in wild bottlenose dolphins (*Tursiops truncatus*). *Journal of Comparative Physiological Biology* 178: 529-543.

Morris, L.J., L.M. Hall, C.A. Jacoby, R.H. Chamberlain, M.D. Hanisak, J.D. Miller, and R.W Virnstein. 2022. Seagrass in a changing estuary, the Indian River Lagoon, Florida, United States. *Frontiers in Marine Science* 8:789818.

Murdoch, M.E., J.S. Reif, M. Mazzoil, S.D. McCulloch, P.A. Fair, and G.D. Bossart. Lobomycosis in bottlenose dolphins (*Tursiops truncatus*) from the Indian River Lagoon, Florida: Estimation of

prevalence, temporal trends and spatial distribution. 2008. *EcoHealth*, 5(3) 289-297; doi: 10.1007/s10393-008-0187-8.

National Oceanic and Atmospheric Administration (NOAA) Fisheries. 2015. *Marine mammal stock assessment reports (SARs) by species/stock. Bottlenose dolphin (Tursiops truncatus): Indian River Lagoon estuarine system stock*. NOAA Fisheries Office of Protected Resources. https://media.fisheries.noaa.gov/dam-migration/f2015_bodoirl_508.pdf.

Noke, W.D. and D.K. Odell. Interactions between the Indian River Lagoon blue crab fishery and the bottlenose dolphin *Tursiops truncatus*. *Marine Mammal Science*, 2002; 18: 819-832.

Pettis, H., R. Rolland, P. Hamilton, S. Brault, A. Knowlton, and S. Kraus. 2004. Visual health assessment of North Atlantic right whales (*Eubalaena glacialis*) using photographs. *Canadian Journal of Zoology* 82:8-19.

Phlips EJ, Badyalk S, Nelson NG, Hall LM, Jacoby CA, Lasi MA, Lockwood JC, Miller JD. 2021. Cyclical patterns and a regime shift in the character of phytoplankton blooms in a restricted sub-tropical lagoon, Indian River Lagoon, Florida, United States. *Front Mar Sci* 8:730934.

Reif, J.S., M.M. Peden-Adams, T.A. Romano, C.D. Rice, P.A. Fair, and G.D. Bossart. 2009. Immune dysfunction in Atlantic bottlenose dolphins (*Tursiops truncatus*) with lobomycosis. *Medical Mycology* 47:125-135.

Sanino, G.P., M.F. Van Bressem, K. Van Waerebeek, and N. Pozo. 2014. Skin disorders of coastal dolphins at Añihué Reserve, Chilean Patagonia: a matter of concern. *Boletin del Museo Nacional de Historia Natural*, Chile, 63: 127-157.

Sigua, G.C., J.S. Steward, and W.A. Tweedale. 2000. Water quality monitoring and biological integrity assessment in the Indian River Lagoon, Florida: Status, trends and loadings (1988-1994). *Environmental Management* 25:199-209.

Smith, N.P. 1993. Tidal and nontidal flushing of Florida's Indian River Lagoon. *Estuaries* 16:739-746.

Smith, N.P. 2001. Seasonal-scale transport patterns in a multi-inlet coastal lagoon. *Estuarine Coastal and Shelf Science* 52:15-28.

Stolen, M.K. 1998. Age, growth, and mortality patterns of bottlenose dolphins from the east coast of Florida. Masters thesis. Univ. of Central Florida, Orlando, FL

Stolen, M., W.N. Durden, T. Mazza, N. Barros, and J. St. Leger. 2013. Effects of fishing gear on bottlenose dolphins (*Tursiops truncatus*) in the Indian River Lagoon system, Florida. *Marine Mammal Science*, doi: 10.1111/j.1748-7692.2012.00575.x.

Titcomb, E.M., J. Stevens, A. Sleeman, B. Nelson, L. Yrastorza, A,M. Schaefer, G.M. Bossart, J.S. Reif, and M. Mazzoil. 2020. Linear skin markings in common bottlenose dolphins (*Tursiops truncatus*) from the Indian River Lagoon, Florida. *Marine Mammal Science* 36:858-870.

Urian, K.W., D.A. Duffield, A.J. Read, R.S. Wells, and E.D. Shell. (1996) Seasonality of reproduction in bottlenose dolphins, *Tursiops truncatus*. *Journal of Mammalogy* 77, 394-403

Van Bressem, M.F., M.C. De O Santos, and J.F. Oshima. 2009. Skin diseases in Guiana dolphins (*Sotalia guianensis*) from the Paranagua estuary, Brazil: a possible indicator of a compromised environment. *Marine Environmental Research*, 67: 63-68.

Vilela, R., G.D. Bossart, J. St. Leger, L.M. Dalton, J.S. Reif, A.M. Schaefer, P.J. McCarthy, P.A. Fair, and L. Mendoza. 2016. Cutaneous granulomas in dolphins caused by novel uncultivated *Paracoccidiodes brasiliensis*. *Emerging Infectious Diseases*, 22(12): 2063-2069.

Wells, R.S., M.D. Scott, and A.B. Irvine. 1987. The social structure of free-ranging bottlenose dolphins. In: *Current mammalogy*, Genoways HH, editor. Plenum Press, New York, New York, pp. 247-305.

Appendix I   Task 4 – University of Florida Biology Report

Restore Lagoon Inflow Research (Phase 3)
Final Report
University of Florida
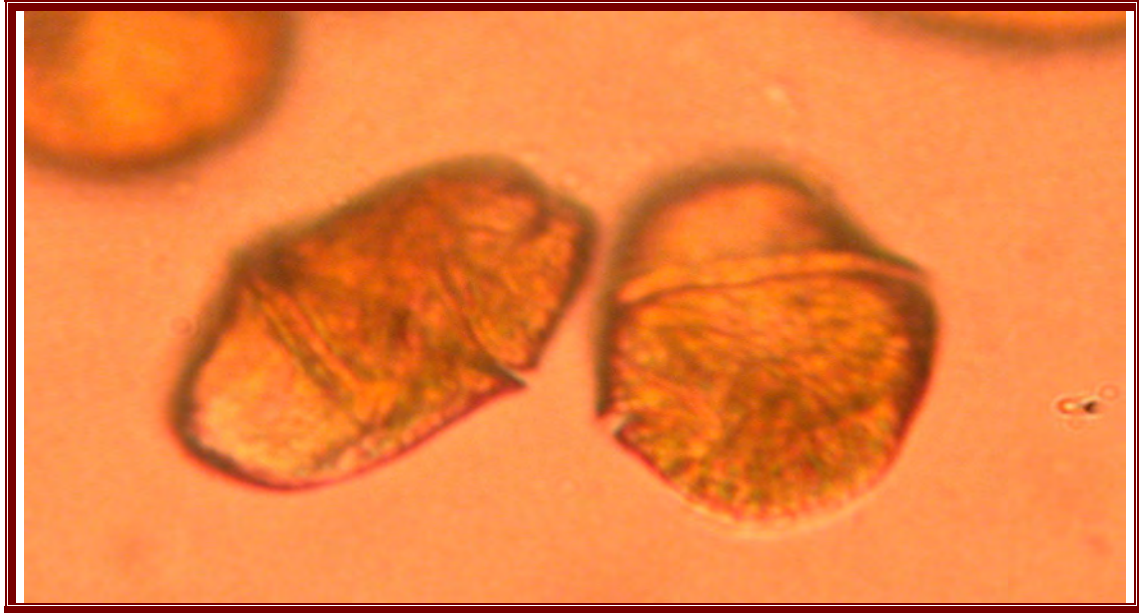
PREPARED FOR

Florida Institute of Technology
150 West University Boulevard
Melbourne, FL 32091

PREPARED BY

Edward Phlips
McCarty Hall, 1604 McCarty Dr #1008,
Gainesville, FL 32603

July 2023

Highlights

- Phytoplankton composition and biomass at the four sampling sites varied by month.

- The list of dominant species at the four sites over the study period contained many of the same elements. In any given month, Site 1 showed the greatest difference in composition relative to the other three sites, while site 3 and4 were the most closely aligned.

- In terms of numerical abundance, picoplanktonic cyanobacteria (including spherical forms and *Synechococcus* cf spp.) were always the highest at all four sites, followed by nanoplanktonic eukaryotes (including cryptophytes).

- Diatoms were observed in every sample collected over the study period, but largely at comparatively low biomass levels. Dinoflagellates were often the dominant taxa in terms of biomass in June and July.

- The results of this study provide information helpful for the design of monitoring programs associated with future management efforts aimed at mitigation of harmful algal blooms (HABs).

Table of Contents

List of Figures

List of Tables

List of Acronyms

|	
HAB	Harmful Algal Bloom
Mg	milligrams
mL	milliliter
L	Liter
μm	Micrometer

1   Introduction

The goal of this study was to examine spatial trends in the composition, abundance and biomass of phytoplankton in the northern Banana River estuary. The results of this study provide information helpful for the design of monitoring programs associated with future management efforts aimed at mitigation of harmful algal blooms (HABs). Four sampling sites were selected for the study, each representing key regions within the northern Banana River ecosystem.

1.1   Approach

Water samples were collected monthly from four sites in the northern Banana River lagoon (**Figure 1**) from February through June 2023. Samples were preserved with Lugol's. General phytoplankton abundance and composition was determined using the Utermöhl method (Utermöhl et al. 1958), as described in Badylak et al., (2014). Aliquots of sample water were settled in 19 millimeter diameter cylindrical chambers. Phytoplankton cells were identified and counted at 400× and 100× with a Leica phase contrast inverted microscope. At 400×, a minimum of 100 cells of a single taxon and 30 grids will be counted. If 100 cells were not counted by 30 grids, up to a maximum of 100 grids were counted until 100 cells of a single taxon will be reached. At 100×, a total bottom count was completed for taxa >30 micrometers (µm) in size.

Figure 1. Site Map

Picocyanobacteria abundances were determined using a Zeiss Axio compound microscope, using green and blue light excitation (Fahnenstiel & Carrick, 1992, Phlips et al., 1999). Samples were preserved with buffered glutaraldehyde. Subsamples of water were filtered onto 0.2 µm Nucleopore filters and mounted between a microscope slide and cover slip with immersion oil, and picoplankton counted at 1000x magnification.
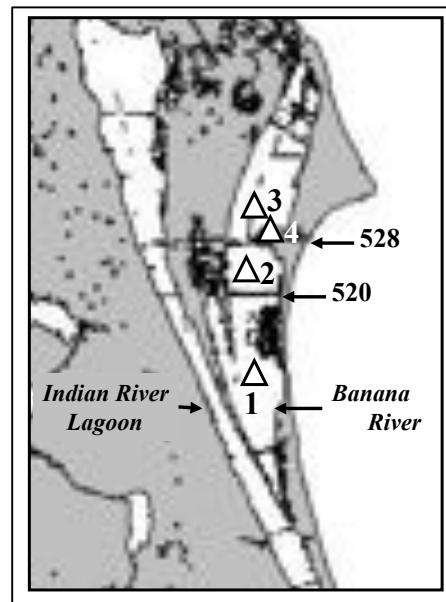
Count data was converted to phytoplankton biovolume, using the closest geometric shape method (Smayda 1978; Sun & Liu 2003). Phytoplankton carbon values (as milligrams [mg] of carbon per liter [L]$^{-1}$) were estimated by applying conversion factors for different taxonomic groups to biovolume estimates (expressed as µm^3 of a taxon in one mL]$^{-1}$): i.e., based on literature values Strathmann, 1967; Ahlgren, 1983; Sicko-Goad et al., 1984; Verity et al., 1992; Work et al., 2005).

1.2   Results

Phytoplankton composition and biomass at the four sampling sites varied by month (**Figure 2**). On February 28, all four sites had similar total biomass levels, ranging from 0.56 to 0.73 mg carbon L^{-1}. Site 1 was dominated by dinoflagellates, principally *Hermesinum adriaticum*. Sites 2-4 were dominated by picoplanktonic cyanobacteria, and nanoplanktonic eukaryotes, including cryptophytes, and other unspecified nano-eukaryotes.

On March 23, Site 1 had the lowest biomass, at 0.19 mg carbon L^{-1}, with a mixed assemblage of predominantly picoplanktonic cyanobacteria and nano-planktonic eukaryotes. Sites 2 to 4 had

biomass values from 0.42 to 0.59 mg carbon L^{-1}. Site 2 had mixed assemblage of dinoflagellates and picocyanobacteria, while Sites 3 and 4 were dominated by picoplanktonic cyanobacteria.

On April 19, Site 1 had the lowest biomass, at 0.21 mg carbon L^{-1}, dominated by dinoflagellates. Sites 2 to 4 had biomass values from 0.46 to 0.58 mg carbon L^{-1}, and all three were dominated by picoplanktonic cyanobacteria.

On May 23, Site 1 had the lowest biomass, at 0.19 mg carbon L^{-1}, , dominated by dinoflagellates. Site 2 had the highest biomass, at 1.62 mg carbon L^{-1}, dominated by dinoflagellates, principally the toxic species *Pyrodinium bahamense*. Site 3 had a total biomass of 0.59 mg carbon L^{-1}, also dominated by *P. bahamense*. Site 4 had a biomass of 0.38 mg carbon L^{-1}, with a mixed dominance of picoplanktonic cyanobacteria and dinoflagellates, including *P. bahamense*.

On June 21, all four sites had biomass values between 0.47 and 0.69 mg carbon L^{-1}. Biomass at Site 1 was dominated by cryptophytes and other nanoplanktonic eukaryotes. At Sites 2-4 the phytoplankton communities were dominated by dinoflagellates, predominantly *P. bahamense*.

In terms of total biomass levels and general phytoplankton group composition, Site 1 was the most distinct from the other three sites, with the lowest total biomass in three of the five sampling months, and significantly different composition in the two other months (Fig. 2). The other three sites had generally similar phytoplankton group composition, and total biomass, with the exception of Site 2 in May, which had a bloom (defined as > 1 mg carbon L^{-1}) of the toxic dinoflagellate *P. bahamense.* Historical records of phytoplankton composition in the Banana River, and broader Indian River Lagoon, show that *P. bahamense* has been the most prevalent bloom-forming dinoflagellate in this ecosystem at least since 1997 (Phlips et al. 2010, 2015, 2020, 2021).
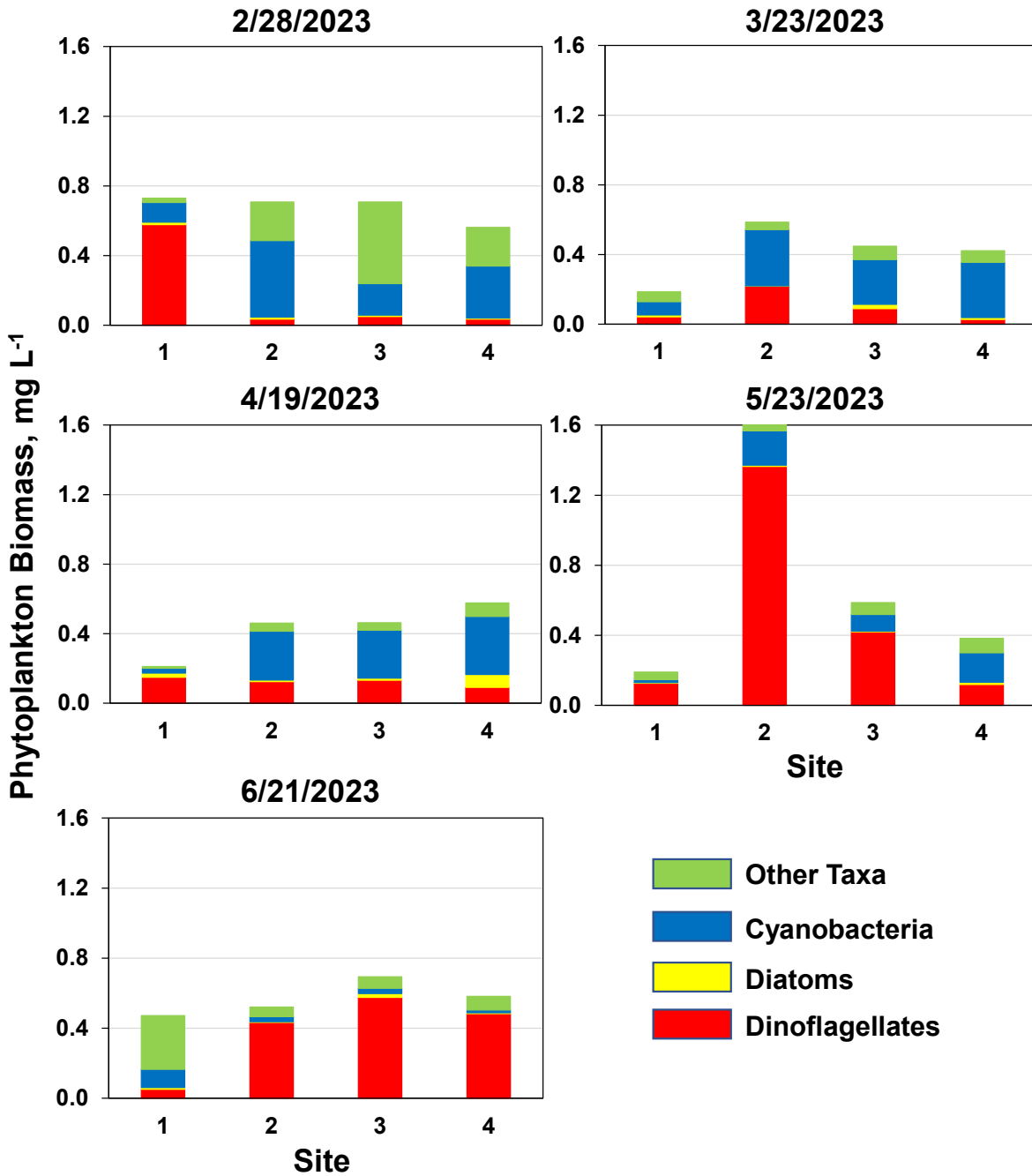
Figure 2. Phytoplankton biomass (mg carbon L-1) at the four sampling sites divided by major phytoplankton group, dinoflagellates (red), diatoms (yellow), cyanobacteria (blue), and other taxa (e.g., cryptophytes, chlorophytes, undefined nanoeukaryotes).

Table 1. Top-20 list of highest biomass observations for individual taxa, including frequency of occurrence in the list, highest biomass observed, and highest cell density.

Site 1 - Central Banana River - Buck Pt.			
Species	**Freq. in Top-20**	**Highest Biomass mg carbon/L**	**Highest Cell Density Cells x 10³/L**
Dinoflagellates			
Pyrodinium bahamense	3	0.085	14.6
Hermesinum adriaticum	1	0.531	1041.0
Gonyaulax polygramma	1	0.055	7.6
Gonyaulax sp.	1	0.032	14.2
Gymnoid sp. (< 15μ)	1	0.030	659.5
Pheopolykrikos hartmannii	1	0.017	1.0
Diatoms			
Rhizosolenia setigera	1	0.023	179.8
Cyanobacteria			
Spherical picocyanobacteria	3	0.107	606805.1
Cyanobium sp. cf	1	0.072	23160.5
Other Taxa			
Nanoplankton (2μ - 5μ)	3	0.059	18862.5
Cryptophyte (>5<15μ)	2	0.047	5123.4
Eutreptia sp (<30μ length)	1	0.196	604.6
Picoeukaryote (≤ 2μ)	1	0.021	43226.0

Site 2 - Between Highway 520 and 528			
Species	**Freq. in Top-20**	**Highest Biomass mg carbon/L**	**Highest Cell Density Cells x 10³/L**
Dinoflagellates			
Pyrodinium bahamense	3	1.257	214.8
Hermesinum adriaticum	1	0.170	332.7
Peridinium quinquecorne	1	0.064	60.5
Tripos fusus	1	0.029	4.8
Protoperidinium sp.	1	0.016	30.2
Cyanobacteria			
Spherical picocyanobacteria	4	0.388	2204879.2
Cyanobium sp. cf	2	0.120	38600.8
Synechococcus spp.	1	0.038	111170.4
Other Taxa			
Nanoplankton (2μ - 5μ)	3	0.118	38087.3
Cryptophyte (>5<15μ)	2	0.033	3597.1
Picoeukaryote (≤ 2μ)	1	0.102	210084.6

Site 3 - North of Highway 528			
Species	Freq. in Top-20	Highest Biomass mg carbon/L	Highest Cell Density Cells x 10^3/L
Dinoflagellates			
Pyrodinium bahamense	3	0.472	80.6
Peridinium quinquecorne	1	0.032	30.2
Diatoms			
Rhizosolenia setigera	1	0.034	280.0
Cyanobacteria			
Spherical picocyanobacteria	4	0.315	1787990.8
Cyanobium sp. cf	2	0.067	21616.4
Synechococcus spp.	2	0.042	120434.6
Other Taxa			
Nanoplankton (2μ - 5μ)	3	0.156	50178.5
Cryptophyte (>5<15μ)	3	0.047	5123.7
Picoeukaryote (≤ 2μ)	1	0.057	116377.8

Site 4 - Adjacent to Port Canaveral Basin			
Species	Freq. in Top-20	Highest Biomass mg carbon/L	Highest Cell Density Cells x 10^3/L
Dinoflagellates			
Pyrodinium bahamense	3	0.561	95.8
Gonyaulax sp.	1	0.047	20.8
Hermesinum adriaticum	1	0.022	42.6
Gonyaulax polygramma	1	0.017	2.4
Diatoms			
Coscinodiscus sp.	1	0.021	10.0
Cerataulina pelagica	1	0.018	100.8
Cyanobacteria			
Spherical picocyanobacteria	4	0.276	1565649.8
Cyanobium sp. cf	2	0.024	7720.2
Synechococcus spp.	1	0.026	74113.6
Other Taxa			
Cryptophyte (>5<15μ)	3	0.062	6711.1
Nanoplankton (2μ - 5μ)	2	0.457	146901.6

1.3 Conclusion

The dominant species observed in the four regions over the five-month study period were similar, as illustrated by the Top-20 list of highest biomass values for individual taxa (**Table 1**). In terms of numerical abundance, picoplanktonic cyanobacteria (including spherical forms and

Synechococcus cf spp.) were always the highest at all four sites throughout the period, followed by nanoplanktonic eukaryotes (including cryptophytes). Picoplanktonic cyanobacteria and nanoplanktonic eukaryotes were also major components of the Top-20 list in terms of biomass at all four sites. Dinoflagellates were the other group prominently represented on the Top-20 list, particularly the HAB species *P. bahamense*. Diatoms were observed in every sample collected over the study period, but largely at comparatively low biomass levels.

2   References

Ahlgren, G. (1983). Comparison of methods for estimation of phytoplankton carbon. *Arch. Hydrobiologia* 98, 489-508.

Badylak, S., Phlips, E. J., and Mathews, A. L. (2014). *Akashiwo sanguinea* (Dinophyceae) blooms in a sub-tropical estuary: An alga for all seasons. *Plankton Benthos Res.* 9. 1-9.

Phlips, E. J., Badylak, S., Christman, M. C., Lasi, M. A. (2010). Climatic trends and temporal patterns of phytoplankton composition, abundance and succession in the Indian River Lagoon, Florida, USA. *Estuaries Coasts* 33, 498-512.

Phlips, E. J., Badylak, S., Lasi, M., Chamberlain, R., Green, W., Hall, L., et al. (2015). From red tides to green and brown tides: Bloom dynamics in a restricted subtropical lagoon under shifting climatic conditions. *Estuaries Coasts* 38, 886-904.

Phlips, E. J., Badylak, S., Nelson, N., and Havens, K. (2020). Hurricanes, El Niño and harmful algal blooms in two sub-tropical Florida estuaries: Direct and indirect impacts. *Scientific Reports* 10, 1910. Doi.org/10.1038/s41598-020-58771-4

Phlips, E. J., Badylak, S., Nelson, N., Hall, L., Jacoby, C., Lasi, M., Lockwood, J., and Miller, J. (2021). Cyclical patterns and a regime shift in the character of phytoplankton blooms in a restricted sub-tropical lagoon, Indian River Lagoon, Florida, USA. *Frontiers Mar. Sci.* 8:730934. Doi.org/10.3389/fmars.2021.730934

Sicko-Goad, L. M., Schelske, C. L., and Stoermer, E. F. (1984). Estimation of intracellular carbon and silica content of diatoms from natural assemblages using morphometric techniques. *Limnol. Oceanogr*. 29, 1170-1178.

Smayda, T. J. (1978). "From phytoplankters to biomass" in *Phytoplankton Manual*, ed. A. Sournia (UNESCO, Paris), 273-279.

Strathmann, R. R. (1967). Estimating the organic carbon content of phytoplankton from cell volume or plasma volume. *Limnol. Oceanogr*. 12, 411-418.

Sun, J., and Liu, D. (2003). Geometric models for calculating cell biovolume and surface area for phytoplankton. *J. Plankton Res*. 25, 1331-1346.

Verity, P., Robertson, C. Y., Tronzo, C. R., Andrews, M. G., Nelson, J. R., and Stieracki, M. E. (1992). Relationships between cell volume and the carbon and nitrogen content of marine photosynthetic nanoplankton. *Limnol. Oceanogr*. 37, 1434-1446.

Work, K., Havens, K., Sharfstein, B., and East, T. (2005). How important is carbon to planktonic grazers in a turbid, subtropical lake? *J. Plankton Res*. 27, 357-372.